USE OF HEADED BARS AS SHEAR REINFORCEMENT

By

Rémy D. Lequesne, Matthew O'Reilly, David Darwin,
Andres Lepage, Abdalkader Al-Sabawy,
Eduardo Guillen, Donald Spradling

A Report on Research Sponsored by

Electric Power Research Institute

Structural Engineering and Engineering Materials
SM Report No. 126
January 2018
(Second Printing)

THE UNIVERSITY OF KANSAS CENTER FOR RESEARCH, INC.
2385 Irving Hill Road, Lawrence, Kansas 66045-7563

USE OF HEADED BARS AS SHEAR REINFORCEMENT

By

Rémy Lequesne

Matthew O'Reilly

David Darwin

Andres Lepage

Abdalkader Al-Sabawy

Eduardo Guillen

Donald Spradling

A Report on Research Sponsored by

Electric Power Research Institute

Structural Engineering and Engineering Materials

SM Report No. 126

THE UNIVERSITY OF KANSAS CENTER FOR RESEARCH, INC.

LAWRENCE, KANSAS

January 2018

(Second Printing)

SUMMARY OF REVISIONS (FEBRUARY 2019):

The following sections were modified to emphasize that the applicability of study findings is limited to reinforcing bar sizes similar to those used in this study.

Page i: Abstract
Page 72: Recommendations for headed transverse reinforcement
Page 80: Section 25.7.2 of proposed building code provisions
Page 82: Conclusion 2

Minor editorial changes were also made.

ABSTRACT

Thirty-nine beams with a shear span-to-depth ratio of 3 were tested with the goal of determining whether headed deformed bars can be used in reinforced concrete members in place of stirrups as shear reinforcement as well as whether shear reinforcement with yield strengths up to 80 ksi [550 MPa] may be used without problems related to strength or serviceability. Grade 60 and Grade 80 [Grade 420 and Grade 550] No. 3, No. 4, and No. 6 [No. 10, No. 13, and No. 16] headed bars and stirrups were used as transverse reinforcement, and were spaced between one-quarter and one-half of the member effective depth. The shear strength of members reinforced with U stirrups and crossties was compared with the strength of matching specimens reinforced with headed bars as shear reinforcement. Stirrups were anchored around longitudinal bars, as required by ACI 318-14. Headed bars were anchored using one of three details: (1) engaged with longitudinal bars, that is, with the bearing face of the head in contact with a longitudinal bar; (2) not engaged with longitudinal reinforcement, with the headed bar outside of the longitudinal reinforcement and close to the side of the member; and (3) not engaged with longitudinal reinforcement, with the headed bar inside of the longitudinal reinforcement and at least 4 in. from the side of the member. Member depths ranged from 12 to 48 in. [310 to 1220 mm] with widths of 24 and 42 in. [620 and 1070 mm]. Test specimens were designed to represent beams, walls, and mat foundations. Modifications to the ACI 318-14 Code are proposed, which will in turn impact the design of nuclear power plants worldwide through changes in ACI 349-13 and ACI 359-13.

The results show that members with adequately anchored headed deformed bars have shear strengths that are equivalent to members with stirrups. Adequate anchorage of headed bars is provided if (1) No. 4 [No. 13] and smaller headed bars engage longitudinal reinforcement with the bearing face of the head in contact with a longitudinal bar or (2) No. 6 [No. 19] and smaller headed bars are placed inside longitudinal reinforcement with side cover to the headed bar of at least six bar diameters.. Placing headed bars outside of longitudinal reinforcement and close to the side of a member may result in reduced shear strength. Grade 80 [Grade 550] shear reinforcement provides the same strength and similar serviceability as Grade 60 [Grade 420] shear reinforcement.

Keywords: cracking (fracturing); headed bars; high-strength reinforcement; reinforced concrete; shear strength; stirrups

ACKNOWLEDGEMENTS

Support for this research was provided by the Electric Power Research Institute. Material support for the study was provided by Commercial Metals Company, Gerdau Corporation, Headed Reinforcement Corp., LENTON® products from Pentair®, MMFX Technologies Corporation, Nucor Corporation, Dayton Superior, and Midwest Concrete Materials. Thanks are due to Ken Barry, Mark Ruis, and David Scott who provided project oversight for the Advanced Nuclear Technology Program of the Electric Power Research Institute. The report was reviewed by Sam Johnson and David Scott the Electric Power Research Institute.

TABLE OF CONTENTS

LIST OF FIGURES

LIST OF TABLES

CHAPTER 1: INTRODUCTION

1.1 GENERAL

The behavior of reinforced concrete members in shear is a well-studied phenomenon. Shear failures in concrete are brittle and sudden; shear reinforcement is therefore frequently required in design to ensure this failure mode does not occur. The current provisions in the ACI Building Code, however, require that shear reinforcement be provided in the form of stirrups, ties, hoops, welded wire reinforcement, or spiral reinforcement, all of which require significant amounts of time to fabricate and place in the field. Furthermore, with the exception of welded wire reinforcement, an upper limit of 60,000 psi [420 MPa] is imposed when calculating the contribution of shear reinforcement to shear strength. These two limitations can increase construction time, congestion, and cost.

The use of bars with headed mechanical anchors (heads) at both ends as shear reinforcement in place of traditional hooked stirrups can be advantageous in construction. This is especially true in applications where large bars (e.g., No. 7 to No. 11 [No. 22 to No. 36]) are used as shear reinforcement because threading hooked bars through a reinforcement cage, which is relatively easy to do with small bars, can become prohibitively difficult with large bars.

Further reductions in construction time may be realized if smaller amounts of higher-strength reinforcement are allowed to be used as shear reinforcement. Use of Grade 80 [Grade 550] steel in place of Grade 60 [Grade 420] steel would not only allow a reduction in the total weight of steel, but would also allow greater spacing between reinforcing bars when shear demand is high and an otherwise tight spacing would be required. However, it is important to ensure that the use of a higher yield strength does not adversely affect serviceability, which is typically judged based on the width of shear cracks.

This project focused on characterizing the behavior of reinforced concrete beams, mat foundations, and walls with headed bars as shear reinforcement with the goal of improving the economy and ease of construction of nuclear power plants, as well as conventional buildings, both in the U.S, and internationally. Use of Grade 60 and 80 [Grade 420 and 550] headed bars was evaluated at various spacings in beams of varying depth, width, concrete compressive strength,

and longitudinal reinforcement ratio. Headed bars were used with the heads engaging (outside and in contact with) the longitudinal reinforcement or not engaging the longitudinal reinforcement to determine if such engagement is necessary for adequate behavior. Beams with Grade 60 [Grade 420] stirrups were used as a control. Based on the results of this study, design provisions are proposed for use of Grade 80 [Grade 550] and headed bars as shear reinforcement.

1.2 BACKGROUND

The shear strength of reinforced concrete members is generally taken as the sum of two components – the shear strength attributed to the concrete (V_c) and the shear strength attributed to shear reinforcement (V_s). The factors affecting each of these components are described next. See Appendix A for notation and conversion factors.

1.2.1 Shear Strength of Reinforced Concrete Members without Shear Reinforcement

The shear strength of slender reinforced concrete members without shear reinforcement is limited by the tensile strength of concrete. It can be shown with Mohr's circle that a state of pure shear is equivalent to equal tensile and compressive stresses applied at an angle of 45 degrees to the axis of the beam; the presence of flexural stresses changes this angle, but does not eliminate the tensile stress (Figure 1.1). When this tensile stress exceeds the tensile capacity (cracking stress) of the concrete, an inclined crack will form (Figure 1.2). This crack can form at mid-depth as a web-shear crack, or in conjunction with flexural cracks propagating from the tension face of the beam as a flexural-shear crack.

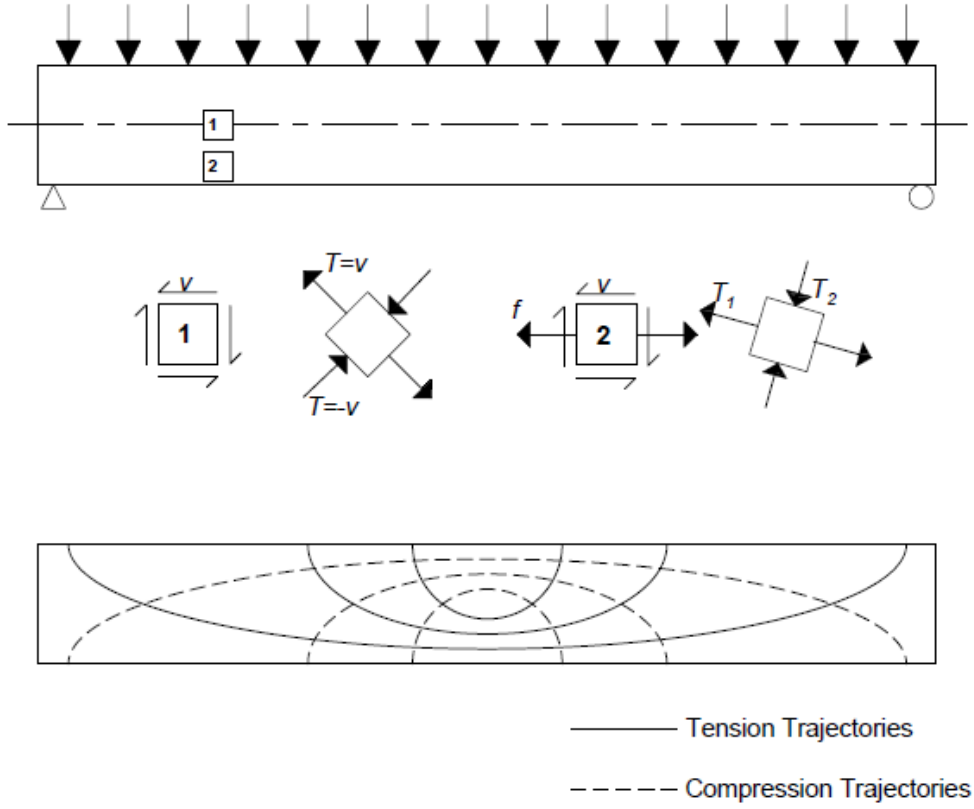

Figure 1.1: Development of diagonal tensile stresses in a beam under shear (figure after (Darwin et al. 2016))

Figure 1.2: Inclined cracks in a reinforced concrete beam

After cracking, vertical equilibrium can be maintained at a cracked section because of three mechanisms of shear transfer. The first is the force in the uncracked concrete in the compression region of the beam, V_{cz}. This force generally accounts for the majority of the shear capacity in a cracked concrete beam without transverse reinforcement. The second is aggregate interlock across the cracked section. When the crack width remains narrow, it is possible to transmit forces across the surface of the crack. These interlock forces (V_i) can account for up to one-third of the total shear force in concrete members without transverse reinforcement (Darwin et al. 2016). The third is dowel action of the longitudinal reinforcement across the crack; these forces (V_d) are typically small. These forces (V_{cz}, V_i, and $V_{d,}$) are shown in Figure 1.3 for an arbitrarily loaded beam in which a diagonal tension crack has formed.

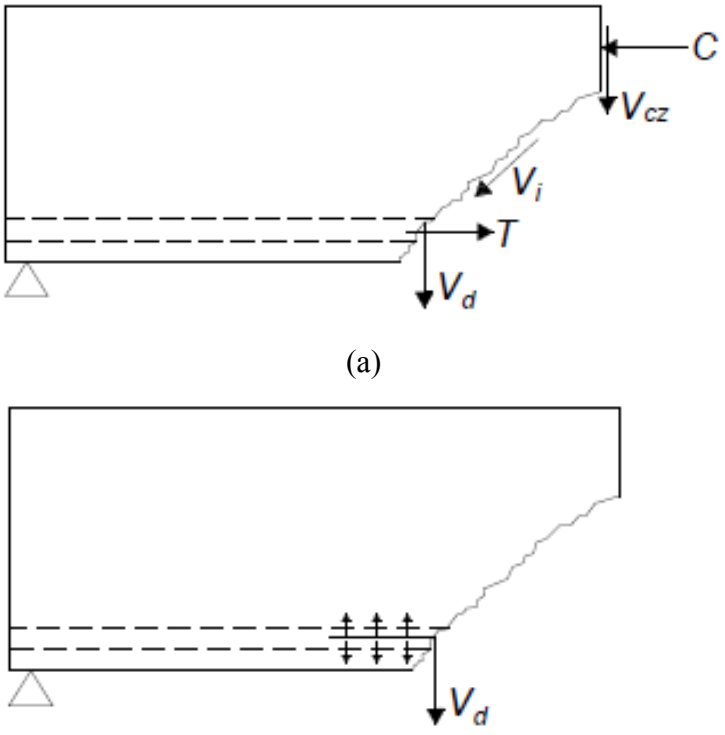

Figure 1.3: Forces at a diagonal crack in a beam without shear reinforcement (figure after (Darwin et al. 2016))

As the shear demand on the beam increases, the crack width increases (decreasing V_i) and the crack propagates further into the compression region of the beam, increasing the shear force on the uncracked concrete (V_{cz}). When the shear demand exceeds the capacity of these components, a shear failure occurs, often in a sudden and explosive manner.

1.2.1.1 Factors Influencing Shear Strength of Reinforced Concrete Members without Shear Reinforcement

Shear Span-to-Depth Ratio

The shear span (a_v) is defined in ACI 318-14 as the distance from the center of a concentrated load to either (a) the face of the support for continuous or cantilevered members, or (b) the center of the support for simply supported members. The shear span-to-depth ratio is the ratio of a_v to the effective beam depth (d). The shear span-to-depth ratio has a significant impact on shear strength and the mechanism of resistance to imposed shear forces. For a_v/d less than 1 (deep beams), a compressive strut forms that directly transfers shear from the point of load application to the support, resulting in high member shear strength. The shear strength decreases rapidly as a_v/d increases from 1 to 2; in this range, the direct strut becomes less effective at transferring shear directly to the support. As the shear span-to-depth ratio continues to increase, the shear strength continues to decrease (though less rapidly). This is shown in Figure 1.4a, which compares maximum shear stress with a_v/d for 784 tests (Reineck et al. 2013) with a_v/d greater than 2.4. As a_v/d increases, the failure mode shifts from crushing in the compression region to opening of a diagonal tension crack through the compression zone (Taub and Neville 1960a, Taub and Neville 1960b).

Member Dimensions

Increasing the depth of a member decreases the maximum shear stress a member can carry (Kani 1967). This is shown in Figure 1.4b, which compares the maximum shear stress with the effective beam depth d using the same database as Figure 1.4a. For very deep and lightly reinforced beams, current ACI 318 Code provisions (discussed in Section 1.4) can be unconservative (Collins

and Cuchma 1999). A study by Sherwood et al. (2006) found that the width of a member had little or no effect on the shear strength.

Longitudinal Reinforcement Ratio

Increasing the tensile reinforcement ratio (ρ_w, based on the area of the web) moderately increases the shear strength of slender reinforced concrete members, as shown in Figure 1.4c. The effect of the longitudinal reinforcement ratio is less pronounced in members with a_v/d less than approximately 1.5, because the shear transfer mechanism is different than in slender members.

The effect of compression reinforcement on shear strength is somewhat less clear. Although use of compression reinforcement tends to increase the resistance to shear within the compression zone, it also reduces the compression zone depth compared to a similar beam without compression reinforcement. Compression reinforcement is commonly neglected in calculations of beam shear strength.

Concrete Compressive Strength

The effect of the compressive strength of concrete on the shear strength of a member depends somewhat on a_v/d. For low values of a_v/d where the failure is controlled by crushing of the concrete, increasing compressive strength has a fairly significant impact on shear capacity. In more slender members, the effect of concrete compressive strength on shear strength is not strongly correlated (Figure 1.4d).

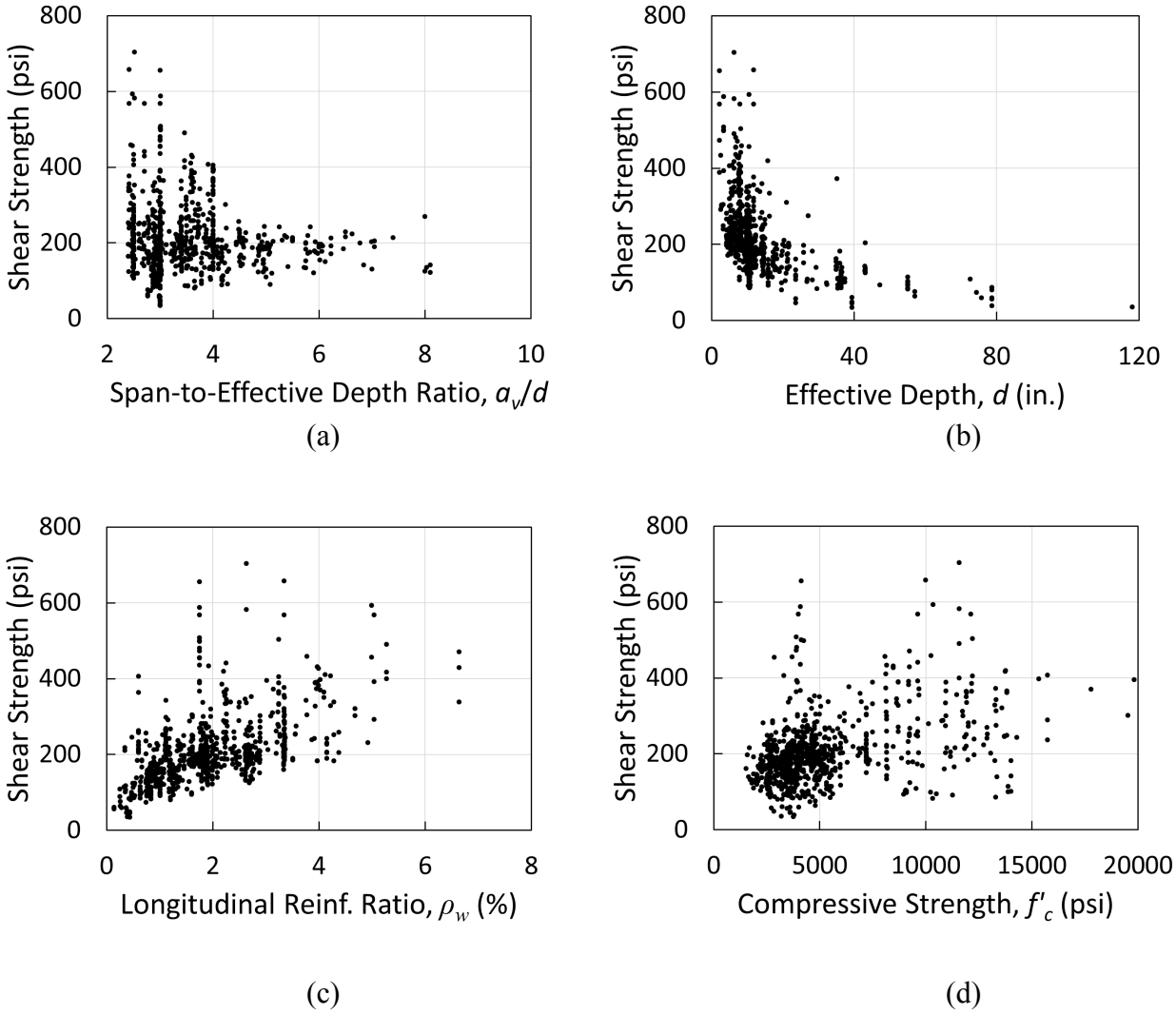

Figure 1.4: Maximum shear stress obtained in 784 tests of beams failing in shear plotted versus significant variables (database from (Reineck et al. 2013)) (1 psi = 6.9 kPa, 1 in. = 25.4 mm)

1.2.2 Shear Strength of Reinforced Concrete Members with Shear Reinforcement

The use of shear reinforcement in the form of stirrups, ties, hoops, welded wire reinforcement, or spiral reinforcement can greatly increase the shear strength of a reinforced concrete member. As shown in Figure 1.5, the contribution of transverse reinforcement to shear strength V_s can be taken as the sum of the forces in reinforcement intersected by the crack nA_vf_v, where n is the total number of stirrups (ties, etc.) intersected by the crack, A_v is the cross-sectional area of an individual stirrup, and f_v is the stress in the stirrup. In addition to the direct contribution

of the shear reinforcement, this reinforcement acts to stabilize the shear strength of the concrete itself. The presence of shear reinforcement delays propagation of inclined cracks, increasing V_{cz}, and reduces crack widths, increasing V_i. Furthermore, shear reinforcement is typically placed around the longitudinal reinforcement, providing restraint and increasing V_d. For simplicity, the contributions to shear strength from V_{cz}, V_i, and V_d are typically lumped into a single term (V_c) that represents the shear strength attributed to the concrete. The value of V_c is taken to be independent of the amount of transverse reinforcement.

In beams with shear reinforcement, failure is often preceded by yielding of the transverse reinforcement (at a stress of f_{yt}). For this reason, f_v is taken equal to f_y when calculating the nominal shear strength of a member.

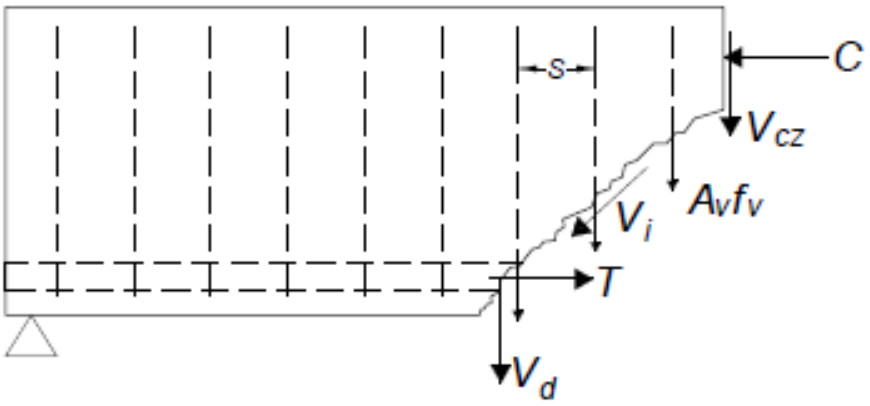

Figure 1.5: Forces at a diagonal crack in a reinforced concrete beam with shear reinforcement (figure after (Darwin et al. 2016))

1.2.2.1 Factors Influencing Shear Strength and Serviceability of Reinforced Concrete Members with Shear Reinforcement

All of the factors affecting the shear strength of reinforced concrete members without transverse reinforcement apply to members with transverse reinforcement. Their influence, however, is significantly reduced. The factors that specifically affect the contribution of reinforcement to the shear strength of a member are outlined below. Factors that affect serviceability are also addressed.

Shear Reinforcement Spacing

One significant factor controlling the shear strength of reinforced concrete members with transverse reinforcement is the amount of shear reinforcement crossed by the crack, which in turn is determined, in part, by the spacing (s) between layers of transverse reinforcement measured along the length of the beam. If shear reinforcement is spaced more than the effective depth (d) apart, it is possible that an inclined crack will form entirely between layers of transverse reinforcement, resulting in the member behaving as if transverse reinforcement was not present (Figure 1.6). This is because inclined cracks in beams, which typically form at an inclination close to 45 degrees, will span a length close to d along the beam. Shear reinforcement is, therefore, typically spaced at no greater than $d/2$ to ensure at least two stirrups will cross any inclined crack that forms. Some researchers have observed, however, that spacing transverse reinforcement at $d/2$ does not ensure that two stirrups will be crossed by an inclined crack (Loov 2002, Kuo et al. 2014). For example, for stirrups spaced at $d/2$, they argue that an inclined crack can barely miss a stirrup, intersect the next stirrup, and then again barely miss the third stirrup. Following this argument, for a given spacing (s), the number of stirrups (n) intersected by a crack inclined close to 45 degrees is $n = d/s\text{-}1$ (rounded up to the next integer). Decreasing s increases the amount of shear reinforcement intersected by the crack, increasing the shear strength of the member.

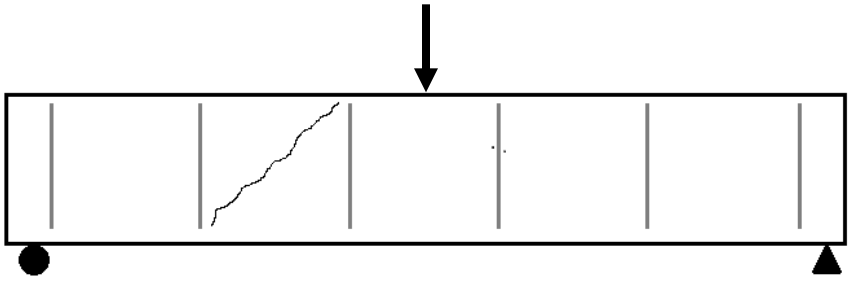

Figure 1.6: Inclined crack between widely-spaced transverse reinforcement

Shear Reinforcement Yield Strength

The nominal shear strength of a member is typically calculated by assuming that shear reinforcement crossing the inclined crack reaches its yield stress before the member fails in shear. It, therefore, follows that shear strength will increase with the yield strength of the shear

reinforcement. However, with the exception of welded-wire reinforcement, the use of a yield strength greater than 60 ksi [420 MPa] for calculating the contribution of transverse reinforcement to shear strength is not permitted by ACI 318-14. The primary concern with use of transverse reinforcement with a yield strength greater than 60 ksi [420 MPa] is crack width (a serviceability consideration) because smaller-size, higher-strength steel bars will exhibit greater strain at a given load (as the elastic modulus of reinforcing steel is insensitive to yield strength). Crack widths are usually compared with a value of 0.016 in. [0.40 mm], which was used as a basis for serviceability requirements in flexure in ACI Building Code editions prior to 1999 (more recent editions do not specifically address limiting crack width). The value of 0.016 in. [0.40 mm], in turn, was based on an expression developed by Gergely and Lutz (1968) for the "most probable maximum crack width," a value that Gergely and Lutz showed was exceeded by 31 to 98 percent of experimentally measured crack widths reported in the studies used to develop the equation.

Some previous research has addressed the validity of concerns dealing with the use of high-strength shear reinforcement. Sumpter, Rizkalla, and Zia (2009) tested nine beams with Grade 60 or 120 [Grade 420 or 830] shear reinforcement. Sumpter et al. found that the specimens with Grade 120 [Grade 830] steel as shear reinforcement exhibited greater shear strength than those with Grade 60 [Grade 420] reinforcement (although in the tests, the maximum stress in the transverse reinforcement was limited to approximately 80 ksi [550 MPa] by crushing of the beam compression zone). The specimens with high-strength steel reinforcement also exhibited narrower crack widths at service loads than those with Grade 60 [Grade 420] reinforcement, although the authors believed this was due to differences in the deformation patterns on the normal-strength and high-strength reinforcement.

Munikrishna et al. (2011) reported the results of 18 tests performed on nine 24-in. [610-mm] wide by 28-in. [710-mm] deep beams reinforced with Grade 60 [Grade 420] or Grade 100 [Grade 690] closed stirrups; where yield strength was defined based on the stress at a strain of 0.035. The beams were designed to obtain stresses in the stirrups of 60, 80, and 100 ksi [420, 550, and 690 MPa] at shear failure and to have similar shear capacities, regardless of reinforcement grade; therefore, fewer stirrups were used when a higher stress was targeted in the stirrups. All beams achieved at least the predicted shear strength. The strain measurements indicated that the

stirrups reached strains consistent with the design stress prior to beam failure by crushing of the compression zone. The specimens with a 100 ksi [690 MPa] stress in the stirrups exhibited slightly greater crack widths than the specimens with lower stresses in the stirrups, but the crack widths at estimated service loads (60% of nominal) were below 0.016 in. [0.40 mm].

Lee et al. (2011) tested 32 simply supported rectangular beams reinforced with high-strength stirrups. The beams had a transverse reinforcement ratio (ρ_t, equal to the cross-sectional area of an individual stirrup divided by the product of the spacing between stirrups and the width of the web of the beam) of either 0.3 or 0.5%, with f_{yt} between 55 and 109 ksi [380 and 750 MPa]. The longitudinal reinforcement ratio varied between 2.7% and 4.7% with f_y between 77 and 102 ksi [530 and 700 MPa]. Beam depths varied between 14 and 24 in. [360 and 610 mm]. The test results indicated that the shear strength increased almost linearly with an increase of $\rho_t f_{yt}$, where 23 out of the 32 tested beams experienced shear failure after yielding of the shear reinforcement. Crack width measurements near peak load indicated that for beams with the same spacing of stirrups (constant ρ_t) but different f_{yt}, the maximum crack widths of the beam with relatively greater f_{yt} was approximately the same as the crack width of the beam with lower f_{yt} because a larger number of diagonal cracks developed in the web of the beams with greater f_{yt}. Much like Munikrishna et al. (2011), Lee et al. observed that at 60% of the ultimate load, the average shear crack width for all test specimens was below 0.016 in. [0.40 mm]. Lee et al. also collected test data reported in the literature for 49 beams with $f_{yt} > 60$ ksi [420 MPa] that failed in shear prior to yielding of the longitudinal reinforcement. They observed that all beams with $f_{yt} < 102$ ksi [700 MPa] experienced failure after yielding of the shear reinforcement regardless of the compressive strength of the concrete, whereas the shear failure mode of the beams with $f_{yt} \geq 102$ ksi [700 MPa] was influenced by the compressive strength of the concrete.

Shear Reinforcement Anchorage

Shear reinforcement must have sufficient anchorage for the steel to develop its yield strength; otherwise, an anchorage failure may occur before reaching the calculated shear strength. ACI 318-14 requires that the ends of stirrups be bent in a standard hook with longitudinal reinforcement placed inside every bend to ensure that the stirrups are capable of reaching their

yield strength. Additional requirements apply when transverse reinforcement consists of No. 6 [No. 19] and greater bar sizes (full Code requirements are discussed in Section 1.4). Some researchers (Tompos and Frosch 2002) have argued that transverse reinforcement anchored in accordance with the ACI Building Code will not be fully effective when the tip of an inclined crack crosses the transverse reinforcement near the anchorage point. Munikrishna et al. (2011) suggested that stirrups with a yield strength of 100 ksi [690 MPa] should be anchored with at least 135-degree hooks to ensure adequate anchorage.

1.3 HEADED BARS AS SHEAR REINFORCEMENT

There is increasing interest in the use of headed deformed bars as shear reinforcement. These bars are straight deformed reinforcing bars fabricated with a headed mechanical anchor (head) at each end (Figure 1.7) and placed perpendicular to the longitudinal reinforcement in a reinforced concrete member (Figure 1.8). In accordance with ACI 318-14 and ASTM A970-16, the heads must have a bearing area (A_{brg}) equal to at least four times the area of the bar (A_b).

The use of headed deformed bars in place of conventional stirrups or ties presents several advantages during fabrication and construction, particularly in members with large transverse reinforcing bars (such as in large walls and foundations) because large bars require large hooks to ensure anchorage. Headed bars are more easily stored and handled on site due to their shape. Fabrication time for reinforced concrete members with headed bars in place of stirrups is also reduced. Headed bars, therefore, have the potential to significantly reduce the time and cost of reinforced concrete construction.

Figure 1.7: Headed deformed bar for use as shear reinforcement

Figure 1.8: Reinforcement cages with conventional stirrups (left) and headed bars (right) as shear reinforcement

Shear studs, which are permitted under the provisions of ACI 318-14 as shear reinforcement in two-way slabs, differ from headed deformed bars. Shear studs have smooth shafts, larger heads than typical of headed bars (equivalent to $A_{brg} \geq 9A_b$), and are often part of a stud rail assembly (ASTM A1044) (Figure 1.9). There have been some studies of beams with headed stud shear reinforcement, including that by Lubell, Bentz, and Collins (2009), who tested three beam specimens reinforced with headed shear studs. The specimens had high-strength Grade 150 [Grade 1035] flexural reinforcement with a longitudinal reinforcing ratio (ρ) of about 1% that experienced significantly higher longitudinal strains than typical in members containing conventional Grade 60 [Grade 420] flexural reinforcement. It was found that headed shear studs were capable of developing the yield strength of the studs despite large amounts of cracking at the top and bottom of the members. There are, however, concerns about the use of smooth studs in deeper members, as the lack of deformations along the shaft is likely to result in a smaller number of wide inclined cracks.

Figure 1.9: Stud rails used to increase the punching shear resistance of reinforced concrete slabs

Several researchers have investigated the use of deformed bars with heads as transverse (shear) reinforcement in slabs and beams. Zheng (1989), Monteleone (1993), Marzouk and Jiang (1997), and Jaeger and Marti (2009), using heads with bearing areas of 4.2 to 11.9, 19.7, and 16.9 to 21.1A_b, respectively, investigated the use of deformed headed transverse reinforcement in panels and slabs with thicknesses of 6 to 20 in. [150 to 510 mm]. Their results showed that headed deformed bars, most with significantly larger bearing areas than required for headed bars (ASTM A970-16), were effective as shear reinforcement when placed away from the edges of the member and when the heads have large net bearing areas. Dyken and Kepp (1988) tested three 20-in. [510-mm] deep I-beams with headed deformed shear reinforcement. Their specimens were constructed with high-strength concrete (13.8 ksi [95 MPa] cube strength) and headed bars with net bearing areas of approximately 8A_b that either engaged or did not engage the longitudinal reinforcement. Their limited results showed that headed deformed bars may be effective as shear reinforcement in high-strength concrete beams and may not need to engage longidutinal reinforcement, a requirement that is imposed by ACI 318-14 on hooked transverse reinforcement. Yoshida (2000) and Gayed and Ghali (2004) conducted additional tests on rectangular and I-shaped beams with headed deformed shear reinforcement and overall depths of 79 and 12 to 24 in. [2000 and 300 to 610 mm], respectively. Their results showed that headed deformed shear reinforcement results in slightly increased beam shear strength compared to beams with hooked stirrups. Gayed and Ghali

also showed that headed deformed bars may work with grades of steel greater than 60 ksi [420 MPa] (their yield stress was 87 ksi, or 600 MPa), but the net bearing area of the heads was approximately $9A_b$, much larger than conventional headed bars, and the longitudinal reinforcement ratio (ρ) in their specimens ranged from 3.5-7.6%, much higher than typically used in practice. Kim et al. (2004) tested beams with headed deformed bars under repeated cyclic loads, showing that headed deformed bars provide more sustained shear strength than hooked bars. However, the net bearing area of the heads was approximately $10A_b$, again larger than most commercially available heads. Tests of beams reported by Yang et al. (2010) were the first to include headed deformed bars placed near the side faces of the specimen without any reinforcement placed to confine the heads. Their results indicate that this detail may be permissible in normal strength (6 ksi, or 42 MPa) concrete, but the heads had a net bearing area near $9A_b$, larger than most commercially available heads. Finally, recent tests by Yang (2015) investigated the use of commercially available headed deformed bars in beams with depths of 18, 24, and 36 in. [460, 610, and 915 mm]. Their results indicate that headed deformed bars can be used as shear reinforcement, even when the net bearing area of the heads approaches the ACI 318-14 lower limit of $4A_b$. Their specimens had concrete compressive strengths near 5 ksi [35 MPa] and heads engaging the longitudinal reinforcement.

Although multiple studies have been conducted, several important questions remain unresolved. Among the tests of beams, Yang (2015) were the only ones to use commercially available heads with net bearing areas near the ACI 318-14 lower limit of $4A_b$. Their test program was limited to use of Grade 60 [Grade 420] reinforcement in 5 ksi [35 MPa] concrete, so the behavior of higher strength bars with the smaller heads in normal- and high-strength concrete has not be tested. Furthermore, the specimens tested by Yang (2015) exhibited large shear stresses at failure (typically greater than $5\sqrt{f_c'}$ psi, or $0.42\sqrt{f_c'}$ MPa), so the behavior of headed deformed shear reinforcement in more lightly reinforced members needs to be examined. There remain questions about whether headed shear reinforcement needs to engage longitudinal reinforcement and whether it can be used near the sides of a member. Regarding the former, only Dyken and Kepp (1988) considered whether headed deformed bars are effective as shear reinforcement when not engaging the longitudinal reinforcement, but their headed bars terminated in the center of wide

flanges that tend to provide confinement not present near the sides of members. Finally, the only study to investigate the behavior of headed shear reinforcement in members with large longitudinal reinforcement strain (Lubell, Bentz, and Collins 2009) used headed bars with smooth shafts and heads with large bearing areas ($9A_b$). Additional tests, therefore, are also needed to evaluate the behavior of headed deformed shear reinforcement in beams with yielding longitudinal reinforcement.

1.4 ACI BUILDING CODE (318-14) PROVISIONS

1.4.1 Shear Strength

Section 22.5.1.1 of ACI 318-14 defines the nominal shear strength of a reinforced concrete member (V_n) as the sum of contributions from the concrete (V_c) and the transverse reinforcement (V_s), as shown in Eq. (1.1).

$$V_n = V_c + V_s \tag{1.1}$$

For nonprestressed members without axial loads, V_c is calculated using either ACI 318-14 Eq. 22.5.5.1 or ACI 318-14 Table 22.5.5.1, presented in this report as Eq. (1.2) and Table 1.1, respectively.

$$V_c = 2\lambda\sqrt{f'_c}\,b_w d \tag{1.2}$$

Table 1.1: Detailed method for calculating V_c (ACI 318-14)

V_c		
Least of (a), (b), and (c)	$\left(1.9\lambda\sqrt{f'_c} + 2500\rho_w \frac{V_u d}{M_u}\right) b_w d$	(a)
	$\left(1.9\lambda\sqrt{f'_c} + 2500\rho_w\right) b_w d$	(b)
	$3.5\lambda\sqrt{f'_c}\,b_w d$	(c)

where f'_c is the specified concrete compressive strength (psi), ρ_w is the longitudinal reinforcement ratio in the web of the member, V_u and M_u are the factored shear and moment at a given section (kips and kip-in., respectively), d is the effective member depth (in.), b_w is the web

width (in.), and λ is a reduction factor for lightweight concrete (for normalweight concrete, $\lambda = 1.0$). Equation (1.2) provides a simple means of rapidly calculating the concrete contribution to shear strength and generally gives lower values for V_c than the equations listed in Table 1.1. Table 1.1 accounts for factors such as longitudinal reinforcement ratio and shear span-to-depth ratio (for a simply supported beam subjected to a concentrated load, the ratio of moment to shear M_u/V_u equals the shear span a_v).

The contribution to shear strength of any shear reinforcement (V_s) is given in Section 22.5.10.5.3 of ACI 318-14 and is shown as Eq. (1.3).

$$V_s = \frac{A_v f_{yt} d}{s} \tag{1.3}$$

where A_v is the effective area of all bar legs or wires in a stirrup at a given cross-section (in.^{2}), f_{yt} is the yield strength of the shear reinforcement (psi), and s is the center-to-center spacing between the transverse reinforcement (in.)

1.4.2 Code Requirements and Limitations

Concrete Compressive Strength

ACI 318-14 places an upper limit of 10,000 psi [69 MPa] on the nominal concrete compressive strength (expressed as a limit on $\sqrt{f'_c}$ of 100 psi [8.3 MPa]) when calculating the concrete contribution to shear strength (V_c). This restriction is in place because Eq. (1.2) was developed before testing had been conducted on members constructed with high-strength concrete. Subsequent tests of beams constructed with high-strength concrete indicate that Eq. (1.2) becomes less conservative when concrete strength exceeds 10,000 psi [69 MPa]. The limit on $\sqrt{f'_c}$ does not apply if at least the minimum shear reinforcement $A_{v,min}$ (described in the following) is provided.

Steel Yield Strength

ACI 318-14 has an upper limit of 60 ksi [420 MPa] on the nominal yield strength of the steel (80 ksi for welded wire reinforcement) when calculating V_s. This restriction was adopted

before any testing had been done on members reinforced with higher-strength reinforcement. The limit persists, in part, because of concerns related to control of inclined crack widths.

Requirements on Use of Shear Reinforcement

ACI 318-14 requires shear reinforcement to be used if the factored shear V_u exceeds the product of one-half of V_c and the strength reduction factor ϕ, as shown in Eq. (1.4).

$$V_u > 0.5\phi V_c \tag{1.4}$$

where ϕ is the strength reduction factor for shear, $\phi = 0.75$ (with some exceptions in seismic design).

Minimum Area of Shear Reinforcement

Where transverse reinforcement is required, ACI 318-14 requires the use of a minimum area of shear reinforcement $A_{v,min}$ equal to the greater of $0.75\sqrt{f'_c}b_w s/f_{yt}$ and $50b_w s/f_{yt}$. This restriction is in place to prevent sudden shear failures upon formation of an inclined crack.

Upper Limit on Shear Reinforcement

ACI 318-14 requires that concrete members be designed such that $V_s \le 8\sqrt{f'_c}b_w d$. This restriction is in place to prevent web-compression failures and limit inclined crack widths.

Maximum Spacing of Shear Reinforcement

ACI 318-14 limits the maximum spacing of shear reinforcement as outlined in Section 9.7.6.2 of the Code and as shown in Table 1.2. Where $V_s \le 4\sqrt{f'_c}b_w d$, this requirement is intended to ensure that any inclined crack crosses at least two stirrups. For higher shear stresses, the closer spacing of shear reinforcement is intended to provide more legs of transverse reinforcement crossing each crack and greater confinement to the concrete.

Table 1.2: Maximum spacing of shear reinforcement (ACI 318-14)

V_s	Maximum Spacing *s*, in. [mm]
$\leq 4\sqrt{f_c'}b_w d$	*d/2* or 24 in. [620 mm]
$> 4\sqrt{f_c'}b_w d$	*d/4* or 12 in. [310 mm]

Shear Reinforcement Detailing Requirements

ACI 318-14 allows the use of stirrups, ties, hoops, welded wire reinforcement, and spiral reinforcement as shear reinforcement. For stirrups, the reinforcement must be U-shaped or closed, extend a distance *d* from the extreme compression fiber of the beam, have a longitudinal bar or strand at each bend in the stirrup, and terminate at each end with a standard hook. Additional anchorage requirements are imposed when No. 6 [No. 19] and larger bars are used as shear reinforcement with $f_{yt} > 40{,}000$ psi [280 MPa]. Similar requirements are in place for other types of shear reinforcement and are outlined in Section 25.7 of ACI 318-14. These requirements are in place to ensure that the shear reinforcement is capable of developing its yield strength.

1.5 OBJECTIVE AND SCOPE

The objectives of this research are twofold: to determine whether headed bars may be used in place of stirrups as shear reinforcement and to determine whether shear reinforcement with yield strengths up to 80 ksi [550 MPa] may be used without problems related to either strength or serviceability.

The project was divided into three phases. Each phase included tests of simply supported beams subjected to a concentrated load at midspan with a shear span-to-depth ratio of 3. The goal of Phase 1 was to establish the feasibility of using high-strength headed bars as shear reinforcement. Seventeen beams with a depth of 36 in. [910 mm] and a width of 24 in. [610 mm] were tested with U stirrups, headed bars engaging the longitudinal reinforcement, and headed bars not engaging the longitudinal reinforcement. Nominal concrete strengths were 4 and 10 ksi [28 and 69 MPa], and Grade 60 and 80 [Grade 420 and 550] deformed steel bars were used as shear reinforcement. The aim of Phase 2 was to compare the effectiveness of headed and hooked shear

reinforcement in members with different depths and explore effects related to transverse reinforcing bar size and spacing. Twelve specimens with U stirrups or headed bars not engaging the longitudinal reinforcement were cast, with depths ranging from 12 to 48 in. [250 to 1220 mm] and an area of shear reinforcement at a given cross section ranging from 0.22 to 0.88 in.^{2} [140 to 570 mm^2]. Phase 3 was designed to evaluate the effectiveness of headed transverse bars in doubly reinforced and wider specimens (designed to simulate walls and deep slabs or mat foundations) and to compare the effectiveness of hooked and headed transverse reinforcement working under different longitudinal strain conditions (specimens were designed so that the longitudinal reinforcement strain at nominal shear strength varied among the specimens). Ten specimens with U stirrups or headed bars not engaging the longitudinal reinforcement were cast, with beam widths of 24 or 42 in. [610 or 1070 mm] and estimated longitudinal reinforcement strains at failure of 0.0010, 0.0018, and 0.018. Full specimen details are presented in Section 2; a summary of parameters is presented in Table 1.3.

Table 1.3: Summary of test parameters and scope of work

	Phase 1	Phase 2	Phase 3
Number of Specimens	17	12	10
Shear Reinforcement Details[1]	S, HE, HNE, HNE2	S, HNE2	S, HNE2
A_v, in.^{2} [mm^2]	0.40 [260]	0.22, 0.40, 0.80, 0.88 [140, 260, 520, 570]	0.40, 0.60, 0.80 [260, 390, 520]
f_{yt}, ksi [MPa]	60, 80 [420, 550]	80 [550]	60, 80 [420, 550]
f_c', ksi [MPa]	4, 10 [28, 69]	4, 10 [28, 69]	4 [28]
h, in. [mm]	36 [910]	12, 18, 48 [310, 460, 1220]	36 [910]
b, in. [mm]	24 [610]	24 [610]	24, 42 [610, 1070]
s	d/2, d/2.67	d/2, d/4	d/2
a/d	3.0	3.0	3.0

[1] S = U Stirrups, HE = Headed bars engaging the longitudinal reinforcement, HNE = Headed bars not engaging the longitudinal reinforcement and close (nominal side cover = 2 in. [50 mm]) to the side of the member, HNE2 = Headed bars not engaging the longitudinal reinforcement and more than 4 in. [100 mm] (5.6d_b) from the side of a member.

CHAPTER 2: EXPERIMENTAL WORK

2.1 SPECIMEN DESIGN

Specimens were designed to determine the suitability of high-strength steel and headed bars as shear reinforcement in reinforced concrete beams, walls, and mat foundations. As outlined in Section 1.5, the project was divided into three phases. The purpose of Phase 1 was to establish the feasibility of using high-strength steel and headed bars as shear reinforcement. All beams in Phase 1 had a width of 24 in. [610 mm], a depth of 36 in. [910 mm], and an effective depth of 31.5 in. [800 mm] (Table 2.1). Nominal concrete strengths of 4 and 10 ksi [28 and 69 MPa] were used. The reinforcement was either Grade 60 or 80 [Grade 420 or 550]. The Phase 1 specimens were organized into five groups. Within each group, the specimens were nominally identical except for the details of the transverse reinforcement (specimens within groups were cast simultaneously using concrete from the same trucks unless noted otherwise in Table 2.1). Four reinforcement details were investigated–conventional U-shaped hooked stirrups (S), headed bars placed so that the heads engaged the longitudinal reinforcement (HE), headed bars placed outside and not engaging the longitudinal reinforcement (HNE), and headed bars placed within, but not engaging, the longitudinal reinforcement (HNE2). In Phase 1, clear side cover was 1.5 in. [38 mm] for S specimens and 1.5 in. [38 mm] to the side of the head for HE and HNE specimens (resulting in approximately 2 in. [50 mm] clear to the bar). For Phase 1, HNE2 was only used for specimen P1S17, which was constructed after specimen P1S15 was tested and failed in an unexpected manner at a low shear force, as described in Chapter 3. Shear reinforcement using the HNE2 detail had a side cover to the bar of 5.75 in. [145 mm]. In Phases 2 and 3, side cover to the bar for specimens with the HNE2 detail ranged from 4.25 to 6 in. (105 to 150 mm), or between 5.6 and $14d_b$.

Table 2.1: Phase 1 specimen properties [a]

Specimen	Specimen Parameters [b]									Shear Reinforcement						
	h, in.	*d*, in.	*b*, in.	a/d	f_{yt} [c], ksi	f_{cm} [d], psi	$A_{b,}$ in.^{2}	ρ, %	ε_{long} [e]	Head / Hook Detail [f]	Bar Size, in.^{2}	*s*, in.	s, d	No. of Legs	$A_{v,}$ in.^{2}	$\rho_t f_{yt}$, psi
P1S1	36	31.5	24	3	69.8	4680	1.56	1.44	0.0016	S	0.20	16.0	d/2	2	0.40	72.7
P1S2	36	31.5	24	3	69.8	4540	1.56	1.44	0.0016	HE	0.20	16.0	d/2	2	0.40	72.7
P1S3	36	31.5	24	3	69.8	4570	1.56	1.44	0.0016	HNE	0.20	16.0	d/2	2	0.40	72.7
P1S4 [g]	36	31.5	24	3	69.8	4240	1.56	1.65	0.0016	S	0.20	12.0	*d*/2.625	2	0.40	96.9
P1S5 [g]	36	31.5	24	3	69.8	4360	1.56	1.65	0.0016	HE	0.20	12.0	*d*/2.625	2	0.40	96.9
P1S6 [g]	36	31.5	24	3	69.8	4310	1.56	1.65	0.0016	HNE	0.20	12.0	*d*/2.625	2	0.40	96.9
P1S7 [g]	36	31.5	24	3	85.0	4110	1.56	1.65	0.0016	S	0.20	16.0	d/2	2	0.40	88.5
P1S8 [h]	36	31.5	24	3	85.0	4130	1.56	1.65	0.0016	HE	0.20	16.0	d/2	2	0.40	88.5
P1S9 [h]	36	31.5	24	3	85.0	5260	1.56	1.65	0.0016	HNE	0.20	16.0	d/2	2	0.40	88.5
P1S10	36	31.5	24	3	85.0	4640	1.56	1.65	0.0018	S	0.20	12.0	*d*/2.625	2	0.40	118
P1S11	36	31.5	24	3	85.0	4730	1.56	1.65	0.0018	HE	0.20	12.0	*d*/2.625	2	0.40	118
P1S12	36	31.5	24	3	85.0	4790	1.56	1.65	0.0018	HNE	0.20	12.0	*d*/2.625	2	0.40	118
P1S13	36	31.5	24	3	85.0	11630	1.56	2.06	0.0017	S	0.20	16.0	d/2	2	0.40	88.5
P1S14	36	31.5	24	3	85.0	11400	1.56	2.06	0.0017	HE	0.20	16.0	d/2	2	0.40	88.5
P1S15	36	31.5	24	3	85.0	12080	1.56	2.06	0.0017	HNE	0.20	16.0	d/2	2	0.40	88.5
P1S16 [h]	36	31.5	24	3	85.0	9680	1.56	2.06	0.0017	HNE	0.20	16.0	d/2	2	0.40	88.5
P1S17 [h]	36	31.5	24	3	85.0	9960	1.56	2.06	0.0017	HNE2	0.20	16.0	d/2	2	0.40	88.5

[a] 1 in. = 25.4 mm, 1 in.^{2} = 645 mm^2, 1 ksi = 6.9 MPa, 1 psi = 0.0069 MPa

[b] As-built dimensions are reported in Appendix B

[c] Determined from tensile tests of reinforcing steel samples using the 0.2% offset method

[d] Measured from tests of 6 in. by 12 in. [150 mm by 300 mm] cylinders on the same day as the beam was tested

[e] Calculated with first principles based on the midspan moment associated with nominal shear strength (ACI 318-14) using nominal material properties

[f] See Figure 2.1

[g] P1S4 was cast with P1S7 and P1S8. P1S5 and P1S6 were cast together.

[h] P1S16 and P1S17 were cast together but separate from P1S13, P1S14, and P1S15.

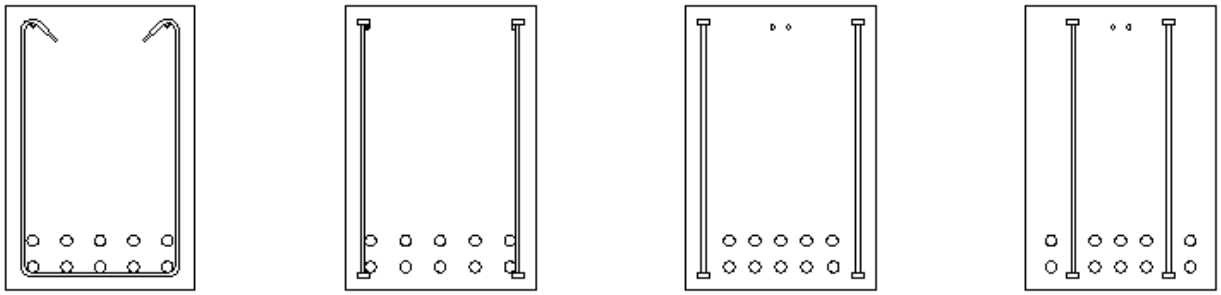

(a) (b) (c) (d)

Figure 2.1: Transverse reinforcement configurations: (a) conventional U-shaped hooked stirrup (S), (b) headed bars engaged (HE), (c) headed bars not engaged (HNE), (d) headed bars within longitudinal reinforcement not engaged (HNE2)

The purpose of Phase 2 was to compare the behavior of beams reinforced transversely with either hooked or headed transverse bars in beams of different depths and using different transverse reinforcing bar sizes and spacings. The Phase 2 specimens were organized into five groups. All beams in Phase 2 had a width of 24 in. [610 mm] and contained Grade 80 [Grade 550] transverse reinforcement (Table 2.2). Based on the results of Phase 1, two reinforcement configurations, S and HNE2, were investigated. Nominal concrete strengths of 4 and 10 ksi [28 and 89 MPa] were used. Beam depths of 12, 18, and 48 in. [310, 460, and 1220 mm] were investigated, using No. 3, No. 4, and No. 6 [No. 10, No. 13, and No. 19] bars as transverse reinforcement at spacings of $d/2$ and $d/4$. Skin reinforcement, required by ACI 318-14 for members with total depths exceeding 36 in. [910 mm], was not used on the 48-in. [1200-mm] deep beams to better simulate walls and foundations, which do not have skin reinforcement.

Table 2.2: Phase 2 specimen properties [a]

Specimen	Specimen Parameters [b]									Shear Reinforcement						
	h, in.	*d*, in.	*b*, in.	a/d	f_{yt} [c], ksi	f_{cm} [d], psi	$A_{b,}$ in.^{2}	ρ, %	ε_{long} [e]	Head/ Hook Detail [f]	Bar Size, in.^{2}	*s*, in.	*s*, d	No. of Legs	$A_{v,}$ in.^{2}	$\rho_t f_{yt}$, psi
P2S1	12	9.5	24	3	86.2	9710	0.79	2.43	0.0017	S	0.11	5.0	d/2	2	0.22	158
P2S2	12	9.5	24	3	86.2	9760	0.79	2.43	0.0017	HNE2	0.11	5.0	d/2	2	0.22	158
P2S3	18	14.5	24	3	86.2	10080	0.79	2.03	0.0017	S	0.11	7.5	d/2	2	0.22	105
P2S4	18	14.5	24	3	86.2	9760	0.79	2.03	0.0017	HNE2	0.11	7.5	d/2	2	0.22	105
P2S5	48	44.0	24	3	83.5	5630	1.56	1.21	0.0018	S	0.20	22.0	d/2	2	0.40	63
P2S6	48	44.0	24	3	83.5	5780	1.56	1.21	0.0018	HNE2	0.20	22.0	d/2	2	0.40	63
P2S7	48	43.75	24	3	82.7	9530	1.56	2.12	0.0019	S	0.44	22.0	d/2	2	0.88	138
P2S8	48	43.75	24	3	82.7	10410	1.56	2.12	0.0019	HNE2	0.44	22.0	d/2	2	0.88	138
P2S9	48	44.0	24	3	83.5	10440	1.56	2.12	0.0018	S	0.20	22.0	d/2	4	0.80	127
P2S10	48	44.0	24	3	83.5	11090	1.56	2.12	0.0018	HNE2	0.20	22.0	d/2	4	0.80	127
P2S11	48	44.0	24	3	83.5	9750	1.56	2.12	0.0018	S	0.20	11.0	d/4	2	0.40	127
P2S12	48	44.0	24	3	83.5	9750	1.56	2.12	0.0018	HNE2	0.20	11.0	d/4	2	0.40	127

[a] 1 in. = 25.4 mm, 1 in.^{2} = 645 mm^2, 1 ksi = 6.9 MPa, 1 psi = 0.0069 MPa

[b] As-built dimensions are reported in Appendix B

[c] Determined from tensile tests of reinforcing steel samples using the 0.2% offset method

[d] Measured from tests of 6 by 12 in. cylinders on the same day as the beam was tested

[e] Calculated with first principles based on the midspan moment associated with nominal shear strength (ACI 318-14) using nominal material properties

The purpose of Phase 3 was to compare the behavior of hooked and headed transverse reinforcement in the presence of varied longitudinal reinforcement strains and also in wide and doubly reinforced beams to better simulate walls and mat foundations. The Phase 3 specimens were organized into five groups. All beams in Phase 3 had a depth of 36 in. [910 mm] and No. 4 [No. 13] Grade 60 and 80 [Grade 420 and 550] transverse reinforcement spaced at *d*/2 (Table 2.3). Two reinforcement configurations–S and HNE2–were investigated. A nominal concrete strength of 4 ksi [28 MPa] was used. Beam widths of 24 and 42 in. [610 and 1070 mm] were used, with estimated longitudinal reinforcement strains ranging from 0.0010 to 0.018 when the beam reached nominal shear strength (as defined by ACI 318-14).

Table 2.3: Phase 3 specimen properties [a]

Specimen	Specimen Parameters [b]									Shear Reinforcement						
	h, in.	*d*, in.	*b*, in.	a/d	f_{yt}[c], ksi	f_{cm}[d], psi	A_b, in.^{2}	ρ, %	ε_{long} [e]	Head / Hook Detail[f]	Bar Size, in.^{2}	*s*, in.	*s*, d	No. of Legs	A_v, in.^{2}	$\rho_t f_{yt}$, psi
P3S1	36	33.25	42	3	66.3	4600	1.56	1.28	0.0019	S	0.20	16.0	d/2	4	0.80	78.9
P3S2	36	33.25	42	3	66.3	4360	1.56	1.28	0.0019	HNE2	0.20	16.0	d/2	4	0.80	78.9
P3S3	36	33.25	42	3	84.5	4040	1.56	1.28	0.0018	S	0.20	16.0	d/2	3	0.60	75.4
P3S4	36	33.25	42	3	84.5	4040	1.56	1.28	0.0018	HNE2	0.20	16.0	d/2	3	0.60	75.4
P3S5	36	32.0	24	3	84.5	5000	1.56	1.42	0.0017	S	0.20	16.0	d/2	2	0.40	88
P3S6	36	32.0	24	3	84.5	4810	1.56	1.42	0.0017	HNE2	0.20	16.0	d/2	2	0.40	88
P3S7	36	32.0	24	3	84.5	5060	1.56	2.44	0.0010	S	0.20	16.0	d/2	2	0.40	88
P3S8	36	32.0	24	3	84.5	5050	1.56	2.44	0.0010	HNE2	0.20	16.0	d/2	2	0.40	88
P3S9	36	32.0	24	3	84.5	4370	1.56	1.02	0.018	S	0.20	16.0	d/2	2	0.40	88
P3S10	36	32.0	24	3	84.5	4800	1.56	1.02	0.018	HNE2	0.20	16.0	d/2	2	0.40	88

[a] 1 in. = 25.4 mm, 1 in.^{2} = 645 mm^2, 1 ksi = 6.9 MPa, 1 psi = 0.0069 MPa

[b] As-built dimensions are reported in Appendix B

[c] Determined from tensile tests of reinforcing steel samples using the 0.2% offset method

[e] Calculated with first principles based on the midspan moment associated with nominal shear strength (ACI 318-14) using nominal material properties

All specimens were designed to promote failure in shear prior to yielding of the longitudinal reinforcement except specimens P3S9 and P3S10, in which a diagonal tension failure was expected to occur after yielding of the longitudinal reinforcement. Specimens from all phases were tested in a simply-supported condition with a span length equal to six times the effective depth of the beam (6*d*) and a shear-span to effective depth ratio of 3. The testing procedure and loading apparatus are described in Section 2.3. A shear-span to effective depth ratio of 3 was selected for all of the specimens because shear failures governed by diagonal tension can be achieved at this aspect ratio with relatively modest longitudinal reinforcement ratios.

In addition to the comparisons between hooked and headed shear reinforcement within each group, specimens within and across phases were designed to allow for the determination of the effect of numerous other variables. A list of the variables of interest and the specimens used to determine the effect of these variables on shear strength is given in Table 2.4.

Table 2.4: Specimen comparisons for isolating variables

Variable of Interest	Variable Value [a]	Specimens	Notes
Stirrup spacing, s	$d/2$	P1S1, P1S2, P1S3	-
	$d/2.625$	P1S4, P1S5, P1S6	
	$d/2$	P2S9, P2S10	-
	$d/4$	P2S11, P2S12	
Nominal yield strength of shear reinforcement, f_{yt}	Grade 60	P1S1, P1S2, P1S3	s held constant
	Grade 80	P1S7, P1S8, P1S9	
	Grade 60	P1S4, P1S5, P1S6	s held constant
	Grade 80	P1S10, P1S11, P1S12	
	Grade 60	P1S4, P1S5, P1S6	Nominal $\rho_t f_{yt}$ held constant
	Grade 80	P1S7, P1S8, P1S9	
	Grade 60	P3S1, P3S2	s held constant
	Grade 80	P3S3, P3S4	
Concrete compressive strength, f_c'	4,000 psi	P1S7, P1S8, P1S9	-
	10,000 psi	P1S13, P1S14, P1S15, P1S16, P1S17	
	4,000 psi	P2S5, P2S6	-
	10,000 psi	P2S9, P2S10	
Total beam depth, h	12 in.	P2S1, P2S2	-
	18 in.	P2S3, P2S4	
	36 in.	P1S13, P1S17	
	48 in.	P2S9, P2S10	
Transverse reinforcement size, amount	2 No 6. @ $d/2$	P2S7, P2S8	Similar $\rho_t f_{yt}$
	4 No. 4 @ $d/2$	P2S9, P2S10	
	2 No. 4 @ $d/2$	P2S11, P2S12	
Beam width, b_w	42 in.	P3S3, P3S4	-
	24 in.	P3S5, P3S6	
Compressive reinforment ratio, ρ'	1.42%	P3S5, P3S6	-
	0.05%	P1S7, P1S9	
Strain in longitudinal reinforcement, ε_{long}	0.001	P3S7, P3S8	-
	0.0017	P3S5, P3S6	
	0.018	P3S9, P3S10	

[a] 1 in. = 25.4 mm, 1 psi = 6.9 kPa, No. 4 = No. 13, No. 6 = No. 19

Specimens from Phase 1 and Phase 2 were designed so that the strain in the longitudinal reinforcement was estimated (using first principles for a cracked section) to be near to but less than the yield strain of Grade 60 [Grade 420] reinforcement (0.002). As discussed earlier, the

longitudinal reinforcement strain was intentionally varied in Phase 3. The beam longitudinal reinforcement consisted of No. 8 [No. 25] bars for specimens with a total depth *h* of 12 or 18 in. [310 or 460 mm]; all other specimens contained No. 11 [No. 36] bars as longitudinal reinforcement. In Phase 1, the longitudinal reinforcement was terminated beyond the simple supports with headed mechanical anchors. For Phases 2 and 3, a sufficient straight length of bar was provided beyond the supports to ensure that bond did not affect specimen behavior. Stirrups were placed at a 4-in. [100-mm] spacing at the ends of each beam (beyond the supports) to provide confinement to the ends of the longitudinal reinforcement; details of these stirrups are shown in Figure 2.2, with a side elevation view of a beam shown in Figure 2.3. Full cross section and elevation views for all specimens are shown in Appendix B.

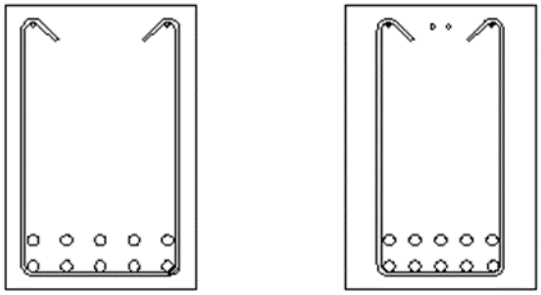

Figure 2.2: End stirrups for beams with (a) S, HE, and HNE2 detailing and (b) HNE detailing

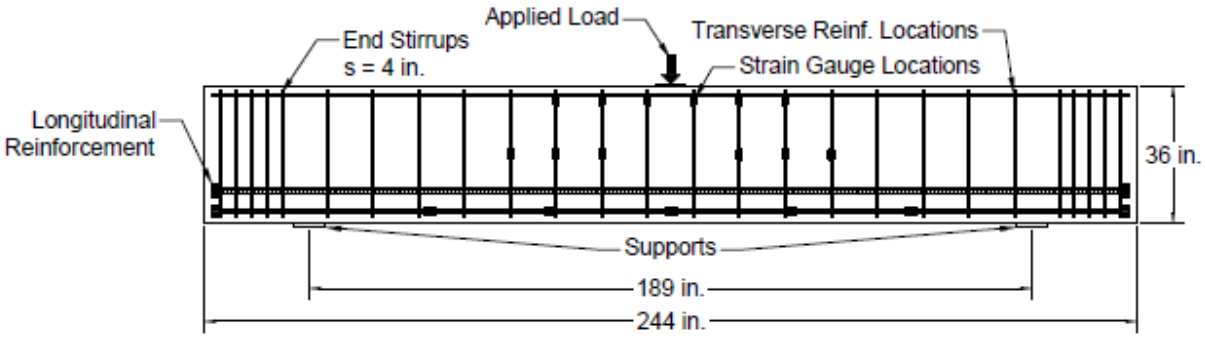

Figure 2.3: Side view showing reinforcement for specimens from Phase 1 with 12-in. [310-mm] transverse reinforcement spacing and strain gauge locations [1 in. = 25.4 mm]

Reinforcement cages were built and placed in plywood forms prior to casting (Figure 2.4). Between two and four specimens were cast at a time. Concrete was placed to minimize the effects of variation within a batch. The order of placement for a beam is shown in Figure 2.5. For placements where multiple concrete trucks were required, the bottom half of each beam in the placement was cast from the first truck followed immediately by the top half, cast from the second truck while the concrete in the bottom half was still plastic. In these cases, plastic concrete properties were measured and cylinders for measuring compressive strength were made for each truck. The concrete mixture proportions are provided in Section 2.2.1 and the plastic concrete properties for each batch are provided in Appendix C.

The concrete was consolidated using internal vibration after placement of the first layer of concrete and again after the forms were filled. After final consolidation, the beams were screeded, finished with a hand float, and covered with wet burlap for initial curing.

Figure 2.4: Reinforcement cages with conventional stirrups (left) and headed bars (right) as shear reinforcement

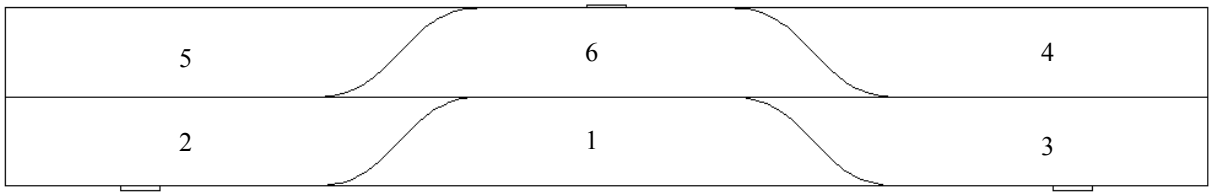

Figure 2.5: Side view of specimen showing placement order of fresh concrete

After completion of placement and finishing, the specimens and cylinders were cured in the same manner and stored in close proximity until testing. Starting three days after casting, cylinders from each truck were periodically tested in accordance with ASTM C39-17 to determine the concrete compressive strength (f_{cm}). When f_{cm} exceeded 2.5 ksi [17 MPa], the forms were removed from the specimens, and the concrete cylinders were removed from their molds. The specimens and cylinders completely covered with burlap and plastic and cured in the same manner.

For curing specimens with f_c' of 4 ksi [28 MPa], cylinders were placed on top of the specimens and then both were loosely covered with wet burlap and plastic. Periodic strength tests were performed until the compressive strength exceeded 3.6 ksi [25 MPa]. The plastic and burlap were then removed from the specimens and test cylinders. After one to two days of drying, the specimens were prepared for testing.

For curing specimens with f_c' of 10 ksi [69 MPa], both the beam specimens and cylinders were wrapped in wet (saturated) burlap, and tightly covered with plastic. Periodic strength tests were performed until the results indicated a concrete strength exceeding 9.0 ksi [62 MPa]. The burlap and plastic were then removed from the remaining cylinders and specimens to allow the concrete to dry prior to testing. For specimens P1S13, P1S14, and P1S15, the burlap and plastic were not removed until the compressive strength was approximately 11.0 ksi [76 MPa].

2.2 MATERIAL PROPERTIES

Specimens were cast using non-air-entrained ready-mix concrete with nominal compressive strengths of 4,000 and 10,000 psi [28 and 69 MPa]. Actual compressive strengths ranged from 4,110 to 5,780 psi [28.4 to 39.9 MPa] for specimens with a nominal compressive strength of 4,000 psi [28 MPa] and from 9,530 to 12,080 psi [65.8 to 83.4 MPa] for specimens

with a nominal compressive strength of 10,000 psi [69 MPa]. The concrete contained Type I/II portland cement, 0.75-in. [19-mm] maximum size crushed limestone, Kansas River sand, and for the 10,000 psi [69 MPa] mixture, a high-range water-reducing admixture. Pea gravel was incorporated in the Phase 1 specimens to improve the workability of the mixture; trial batching determined this was not necessary, and pea gravel was eliminated from the mixtures for Phases 2 and 3. Mixture proportions are listed in Table 2.5. Plastic concrete properties for each batch are given in Appendix C.

Table 2.5: Concrete mixture proportions

Material	Quantity (based on saturated-surface dry aggregate)				
	Phase 1		Phase 2		Phase 3
Design Compressive Strength	4000 psi [28 MPa]	10000 psi [69 MPa]	4000 psi [28 MPa]	10000 psi [69 MPa]	4000 psi [28 MPa]
Type I/II Cement, lb/yd^3 [kg/m^3]	600 [356]	750 [445]	600 [356]	750 [445]	600 [356]
Water, lb/yd^3 [kg/m^3]	324 [192]	199 [118]	324 [192]	218 [129]	324 [192]
Crushed Limestone, lb/yd^3 [kg/m^3]	1656 [982]	1800 [1067]	1236 [733]	1957 [1161]	1734 [1028]
Pea Gravel, lb/yd^3 [kg/m^3]	248 [147]	321 [190]	-	-	-
Kansas River Sand, lb/yd^3 [kg/m^3]	1111 [659]	1050 [623]	1734 [1028]	1255 [744]	1236 [733]
Estimated Air Content, %	1	1	1	1	1
High-Range Water-Reducer [a], oz (US) [L]	-	1051 [31.1]	-	831 [24.6]	-
w/c ratio	0.54	0.27	0.54	0.29	0.54

[a] ADVA 600

Grade 60 and 80 [Grade 420 and 550] deformed bars were used as shear reinforcement in the specimens in this study. For each phase, the same heat of each grade of steel was used for both conventional stirrups and headed shear reinforcement. Two tensile tests were performed for each bar size and grade. The average yield strength, tensile strength, uniform elongation, fracture elongation, and head dimensions for the reinforcement are shown in Table 2.6; plots of stress versus strain from tensile tests are provided in Appendix D.

Table 2.6: Steel reinforcement properties

	Bar Size	Grade	Sample Type[a]	Yield Stress[b] ksi [MPa]	Tensile Stress ksi [MPa]	Uniform Elong.[c] %	Fracture Elong.[d] %	Avg. Head Dia. in. [mm]	$\frac{A_{brg}}{A_b}$ [e]
Phase 1	No. 4 [No. 13]	60 [420]	T	69.8 [482]	105.1 [725]	10.0	10.0	1.38 [34.9]	6.42
	No. 4 [No. 13]	80 [550]	T	85.0 [587]	113.3 [782]	10.1	11.0	1.38 [34.9]	6.42
	No. 11 [No. 36]	80 [550]	L	88.9 [613]	120.4 [831]	9.6	– [f]	– [g]	– [g]
Phase 2	No. 3 [No. 10]	80 [550]	T	86.2 [595]	111.4 [769]	10.4	12.5	0.853 [21.7]	4.20
	No. 4 [No. 13]	80 [550]	T	83.5 [576]	108.7 [750]	9.8	14.8	1.143 [36.3]	4.13
	No. 6 [No. 19]	80 [550]	T	82.7 [571]	110.3 [761]	9.8	12.5	1.676 [42.6]	4.01
	No. 8 [No. 25]	80 [550]	L	86.0 [593]	117.3 [809]	10.1	10.9	– [g]	– [g]
	No. 11 [No. 36]	60 [420]	L	65.9 [455]	98.2 [678]	11.5	12.4	– [g]	– [g]
Phase 3	No. 4 [No. 13]	60 [420]	T	66.3 [457]	96.9 [669]	11.2	15.6	1.141 [29.0]	4.11
	No. 4 [No. 13]	80 [550]	T	84.5 [583]	115.1 [794]	8.6	16.4	1.141 [29.0]	4.11
	No. 11 [No. 36]	60 [420]	L	66.2 [457]	100.7 [695]	12.4	15.0	– [g]	– [g]

[a] T = Transverse reinforcement, L = Longitudinal Reinforcement
[b] Determined with 0.2% offset method
[c] Determined using the method described in Section 7.9.3.2 of ASTM E8/E8M-16a
[d] Data from mill certification
[e] Ratio of head bearing area (A_{brg}) to bar area (A_b) for headed transverse reinforcement
[f] Mill certification reported an erroneous value of 7.5%
[g] Not applicable

2.3 TEST PROCEDURE

2.3.1 Loading System

The majority of specimens were simply supported and subjected to a monotonically increasing point load at midspan using the loading system shown in Figure 2.6. Two specimens, P2S11 and P2S12, had a capacity greater than the loading configuration shown in Figure 2.6 was capable of applying; these specimens were tested using an alternate loading configuration, described in Section 2.3.1.1. Load was applied using four hydraulic jacks acting on a header beam via four load rods. The header beam was comprised of three members that were bolted together: a 10-ft [3.05-m] long HP18×204 beam and two 46-in. [1170-mm] long built-up members

constructed from back-to-back C15×33.9 channels welded to a 0.5 × 10 × 46 in. [13 × 255 × 1170 mm] plate at the top and bottom. A 3-in. [75-mm] gap was maintained between channel sections to allow the load rods to pass through the centroid of the built-up members. A 0.5 × 8 × 52 in. [13 × 200 × 1320 mm] plate was welded to the bottom side of the HP member where it contacted the specimen, resulting in an 8-in. [200-mm] wide bearing surface spanning the full width of the specimen. Gypsum cement was used between the bearing plate and the top of the specimen.

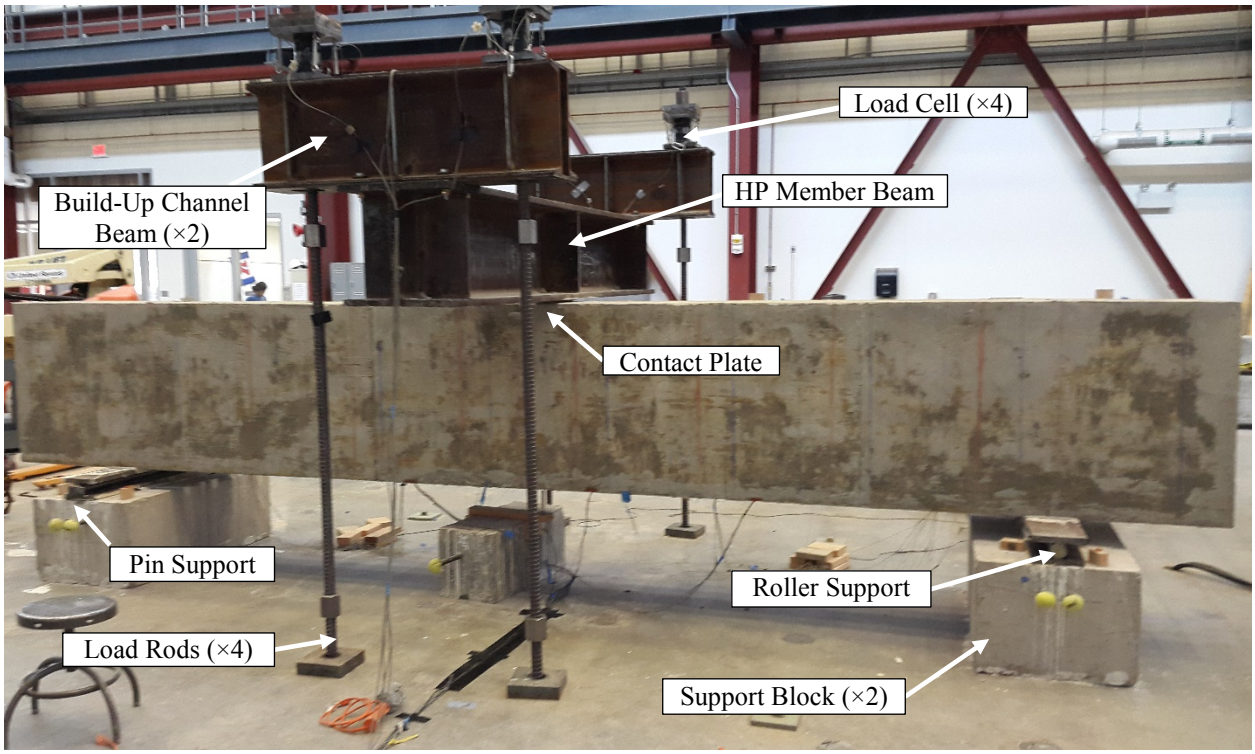

Figure 2.6: Test specimen and loading system, profile view

The beams were mounted on pin and roller supports on reinforced concrete support blocks. The pin and roller supports consisted of 1 × 8 × 52 in. [25 × 200 × 1320 mm] plates placed above and below a 2.75-in. [70-mm] diameter steel rod; at the pin support, the rod was welded to the bottom plate to restrict horizontal movement. During testing of the first ten specimens in Phase 1, the beams were placed directly on top of the steel supports without gypsum cement. A review of displacement data revealed that the beam displaced slightly (less than 0.1 in. [2.5 mm]) towards the support blocks during the first stages of loading. To mitigate settling at the contact areas during

loading, gypsum cement was used between the beam and the upper steel plate for subsequent testing. This change, however, did not affect the analysis because beam deflection is based on relative displacements, as described in Section 2.3.2.2.

For Phase 1, four 300,000-lb [1350-kN] capacity, double-acting, hydraulic jacks were mounted on the underside of the laboratory strong floor to apply downward force to the load rods. The rods passed through the strong floor and through slot holes cut into the top and bottom plates of the built-up sections located at the ends of the header beam. A hollow cylindrical load cell was placed at the top of each load rod to allow recording of the force from each jack. An end view of the loading system is shown in Figure 2.7. For Phase 2 and Phase 3, the hydraulic jacks were placed between the header beam and load cells on top of the specimen to simplify setup and assist in assuring an even load between the four jacks; the loading system was otherwise unchanged.

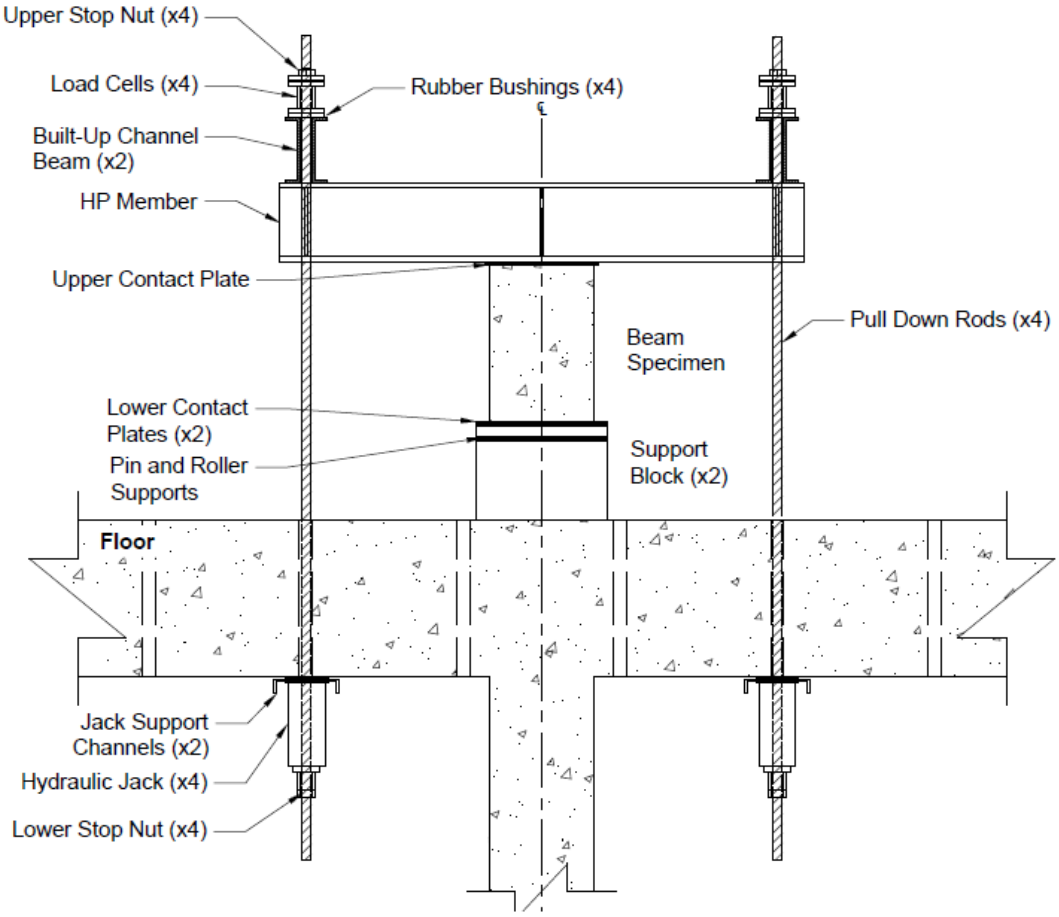

Figure 2.7: End view of loading system for Phase 1. For Phases 2 and 3, the hydraulic jacks were placed between built-up channel beams and load cells

2.3.1.1 Alternate Loading System

Two specimens, P2S11 and P2S12, had greater capacities than could be achieved with the configuration used for the other specimens. These specimens were tested using an alternate loading configuration, shown in Figure 2.8, designed to provide a distribution of forces on the beam similar to that provided by the original loading configuration. For these specimens, the header beam and loading system (Figure 2.6) was placed at one end of the specimen, the pin support was placed at the other end, and the roller support at midspan. A spreader beam (with no hydraulic jacks) was placed over the pin support and tied to the floor to prevent uplift of the beam. Load was applied via a downward force from the hydraulic jacks at the free end of the beam, effectively doubling the shear force that the loading system could apply while maintaining a similar (but inverted) shear and moment distribution throughout the beam. Due to laboratory constraints, the clear distance between the centerline of cross-beams above the specimen was not exactly 6*d* for these specimens. The center support was placed so that the distance between the center support and the loading point was 132 in. [3350 mm], or 3*d*, to be consistent with other specimens. External bracing, not shown in Figure 2.8, was placed along the 138 in. [3500 mm] span (left side in Figure 2.8) to force the shear failure to occur where the span was 3*d*.

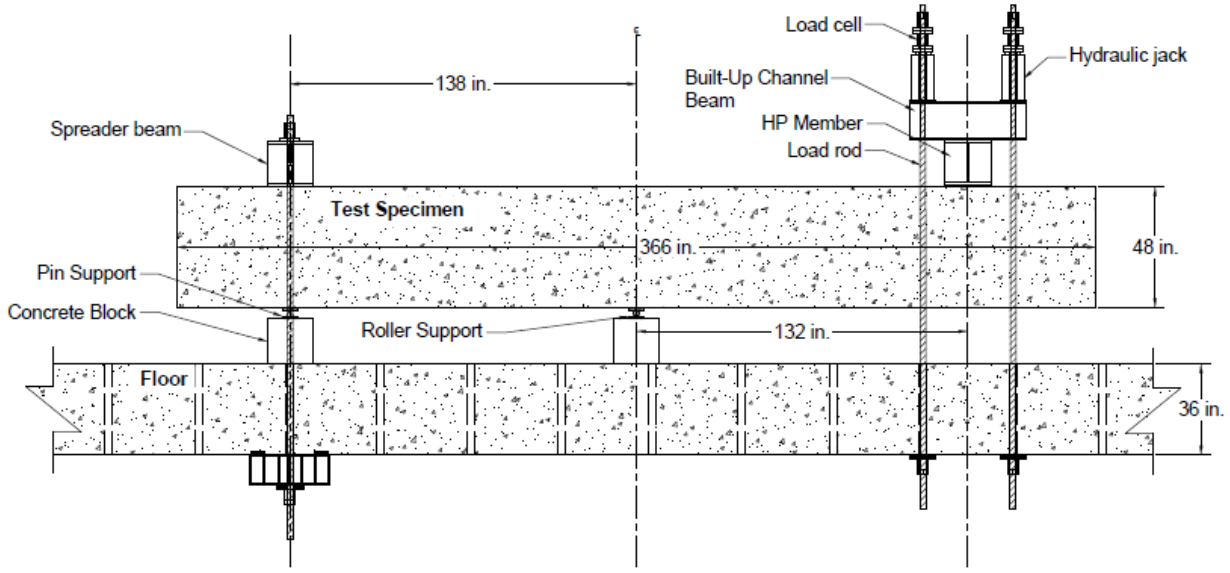

Figure 2.8: Alternate loading system for specimens P2S11 and P2S12 [1 in. = 25.4 mm]

2.3.2 Instrumentation

2.3.2.1 Strain Gauges

Strain gauges were applied to the longitudinal and transverse bars in the vicinity of the anticipated shear crack (Figure 2.9). A total of 17 strain gauges were applied to reinforcement in each specimen in Phases 1 and 2; 12 gauges (six on each side of the beam) at the top and mid-height of the transverse reinforcement in the region of the anticipated shear crack, and 5 gauges on the longitudinal reinforcement–one at midspan, and the other four spaced at distances of *d* and 2*d* from midspan. In addition to the 17 locations gauged in Phases 1 and 2, specimens in Phase 3 had four additional gauges on the transverse reinforcement near the bottom of the beam.

Strain gauges were identified according to location–SG and LG for gauges on the shear reinforcement and longitudinal reinforcement, respectively. Gauges on the shear reinforcement were numbered left-to-right according to the stirrup or headed bar they were on, with a "T" for gauges near the top of the reinforcement, an "M" for gauges at mid-height, and "B" for gauges near the bottom. Gauges on the longitudinal reinforcement were labeled with their distance from midspan, or an "M" for the midspan gauge.

Due to problems during testing, no strain data are available for the longitudinal reinforcement in specimens P1S16 and P1S17 and no strain data are available for specimen P2S11.

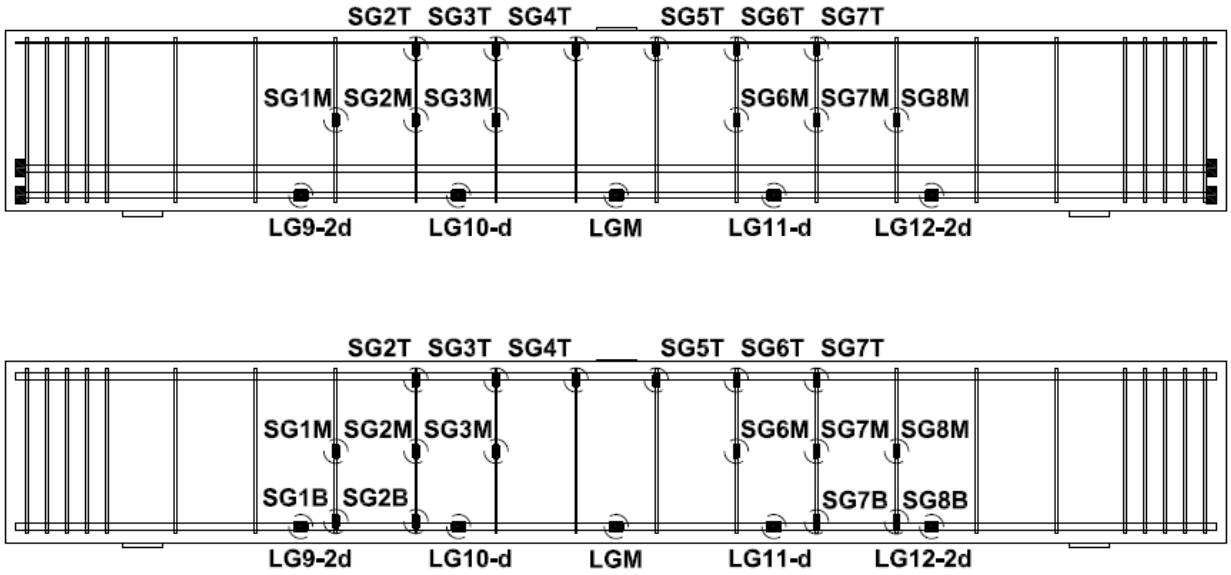

Figure 2.9: Strain gauge locations and naming convention (top: Phases 1 and 2; bottom: Phase 3)

2.3.2.2 Measurements of Displacement

An optical tracking system was used to record the position of optical tracking beacons (referred to as "markers") affixed to supports and in a grid pattern on one side of the specimen. Data from the system was then used to calculate beam deflection and rotation throughout each test. The system uses six infrared cameras to triangulate the position of each marker in three-dimensional space and records the position of each marker in x-y-z space throughout time. A total of 96 markers were placed in a 4 × 19 square grid pattern on the specimen, shown in Figures 2.10 and 2.11. The spacing between markers varied with the depth of the beam; marker spacings are given in Table 2.7. Six additional markers were used as stationary reference points–two on the beam, directly over the pin and roller supports (SM1 and SM2) and four on stationary support objects around the specimen (CTRL1–CTRL4). During testing, the camera system logged the three-dimensional location of each marker. The optical tracking system was mounted on the specimens on the face opposite the strain gauges, as shown in Figure 2.12. Cracks were marked, measured, and photographed on the side of the specimen with the strain gauges to avoid interfering with the optical tracking system.

The beam displacement at midspan was also tracked using a linear variable differential transformer (LVDT).

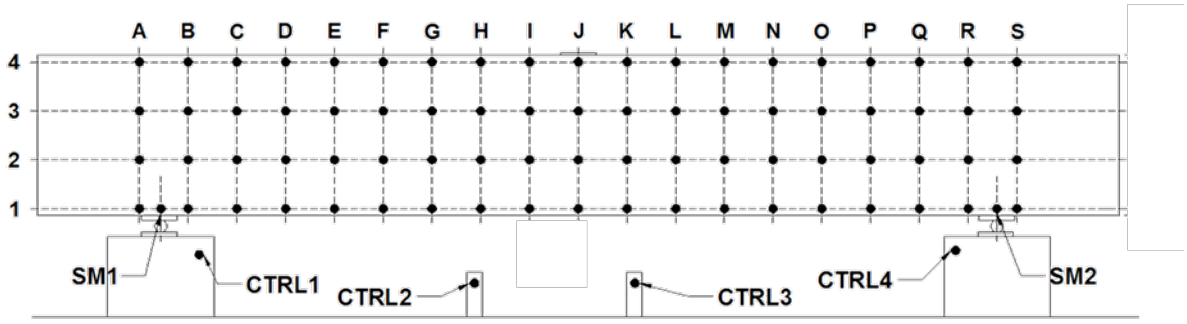

Figure 2.10: Optical tracking marker grid field positions and naming convention

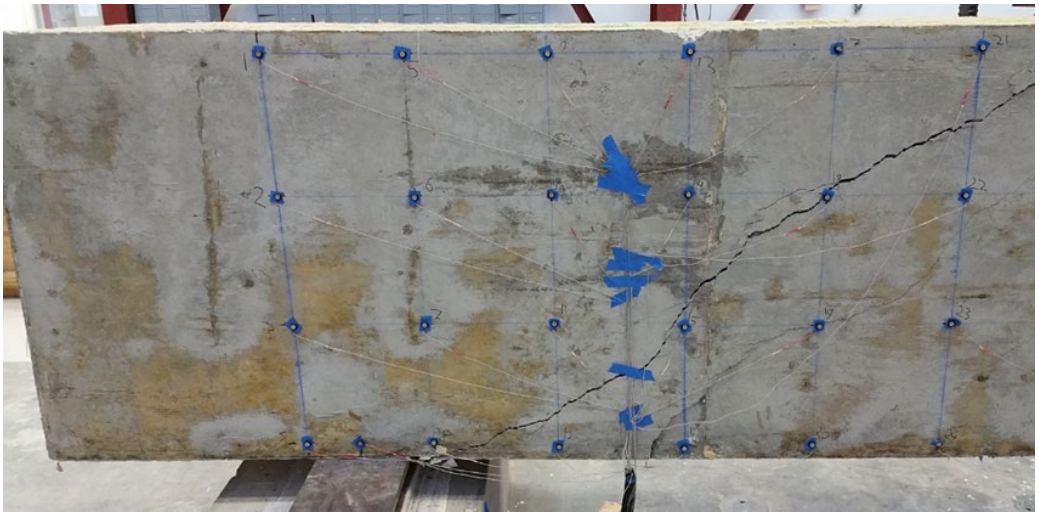

Figure 2.11: Optical tracking markers installed on a test specimen

Table 2.7: Grid spacing for optical tracking markers

Beam height, in. [mm]	Grid marker spacing, in. [mm]
12 [310]	3 × 3 [75 × 75]
18 [460]	5 × 5 [130 × 130]
36 [910]	11 × 11 [280 × 280]
48 [1220]	15 × 15 [380 × 380]

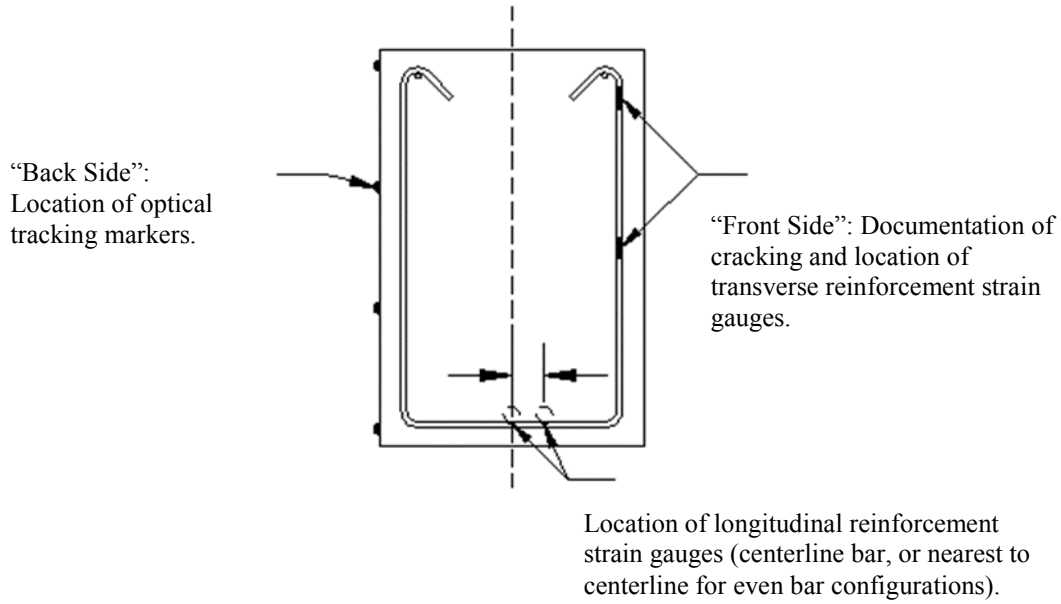

Figure 2.12: Relative placement of optical tracking markers and strain gauges

2.3.3 Loading Procedure

The specimens were loaded using four hydraulic jacks operated with a manual hydraulic pump. Force was applied monotonically in increments of 10 to 15% of the nominal strength of the specimen. The specimens were loaded slowly; each load increment took approximately 5 minutes to impose on the specimen. Between increments, loading was paused to mark cracks, measure crack widths, and take photographs. Crack marking occurred on the side of the beams that did not have optical tracking markers. The force on each of the four load cells was monitored and recorded using a data acquisition (DAQ) system. Once the force reached 80% of the nominal strength of a specimen, the specimen was loaded continuously until failure. After failure, the beams were photographed.

2.3.4 Alignment and Transformation of Recorded Data

Optical marker locations were collected using a second DAQ system. To align the datasets from the two DAQ systems, an event that was clearly identifiable in both datasets (specimen failure) was selected and assigned a common timestamp. Corrections were made to account for any irregular intervals of data collection.

To simplify the analysis of the optical marker locations, the original coordinate system {X, Y, Z}, which was a function of the location of the cameras, was transformed to a coordinate system coinciding with the plane of the side of specimen {X', Y', Z'}. In the final dataset, all markers on the face of the specimen (prior to loading the specimen) had Z' coordinates near zero, while markers within a single column or row had approximately the same X' or Y' coordinates, respectively (X' and Y' coordinates were not exactly equal within a given column or row because of minor variations in placement of the markers on the specimen).

CHAPTER 3: TEST RESULTS AND ANALYSIS

3.1 SPECIMEN BEHAVIOR

For all specimens, the first cracks observed were flexural cracks, oriented vertically and initiating from the tension face of the beam under the point load at midspan. As the load increased, new cracks developed further from midspan while existing cracks became inclined, propagating towards the point load, as shown in Figure 3.1. Failure consisted of approximately simultaneous splitting along an inclined crack and crushing/splitting of the compression zone near the point of load. This mode of failure was observed for all specimens, except specimen P1S15, including those exhibiting longitudinal bar yielding before failure (specimens P2S10 through P2S12, P3S9, and P3S10). Specimen P1S15 failed at an unexpectedly low load and in an unusual manner that included longitudinal cracks occurring on the top and bottom of the specimen along a vertical plane that contained the headed transverse reinforcement (see Section 3.2.1 for more detail). The unusual cracks were not observed in other specimens.

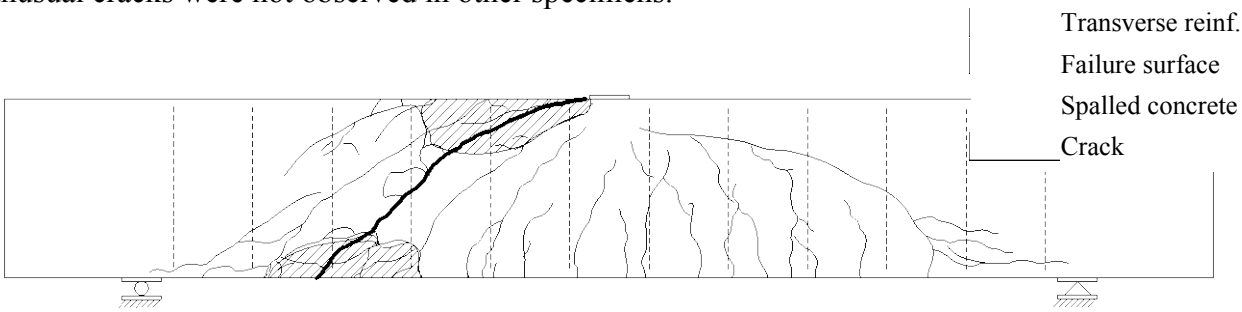

(a) Front side

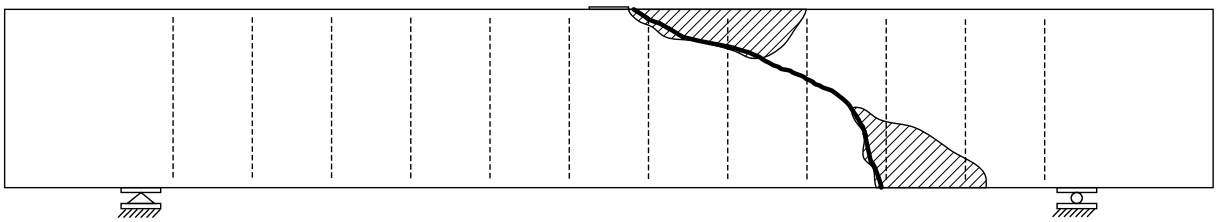

(b) Back side

Figure 3.1: Damage to specimen P1S1 with stirrups (S detail) (f_{ytm} = 69.8 ksi [482 MPa], h = 36 in. [910 mm])

3.2 SPECIMEN CRACKING AND DAMAGE

As described in Section 2, loading was paused at regular intervals to allow identification, measurement, and documentation of new cracks. Scaled drawings of the location and extent of cracking and other damage, like that shown in Figure 3.1 for specimen P1S1, were then created using geospatial mapping software based on photographs taken during and after testing. Specimen P1S1 had Grade 60 [Grade 420] stirrups spaced at $d/2$, a concrete compressive strength of 4680 psi [32.3 MPa], and a longitudinal reinforcement ratio of 1.44%. Figures showing cracking and damage are provided in Appendix E for all specimens. Each of these figures shows cracks that were identified during testing on the front face of the specimen, the location of the failure surface on both the front and back faces of the specimen, and the location of spalled or crushed concrete. The nominal location of transverse reinforcement is also shown.

Although the pattern of cracking was generally similar among specimens, some consistent differences occurred with respect to certain variables, especially the headed bar anchorage condition. For example, Figure 3.2 shows the cracking of specimens P1S14 and P1S16, which contained headed transverse reinforcement engaging and not engaging the longitudinal reinforcement, respectively (the specimens were otherwise nominally identical, except that the concrete compressive strengths on the day of testing (f_{cm}) were 11400 and 9680 psi [78.7 and 66.8 MPa] for specimens P1S14 and P1S16, respectively). Specimen P1S14 with the HE (head engaged) anchorage condition had a wider distribution of cracking throughout the span (and nearer to the supports) than specimen P1S16 with the HNE (head not engaged) anchorage condition. Although it is not clear why this occurred, similar differences occurred throughout Phase 1 between HE and HNE specimens – with the clear exception of specimen P1S17. For construction of specimen P1S17, the HNE detail used throughout Phase 1 was modified so that the transverse bars were further from the outside faces of the beam (see Figure 2.1(d) and Appendix B). Specimen P1S17 was otherwise nominally identical to specimen P1S16. Cracking of specimen P1S17, shown in Figure 3.3, closely resembled the cracking of specimens with the HE detail (such as specimen P1S14).

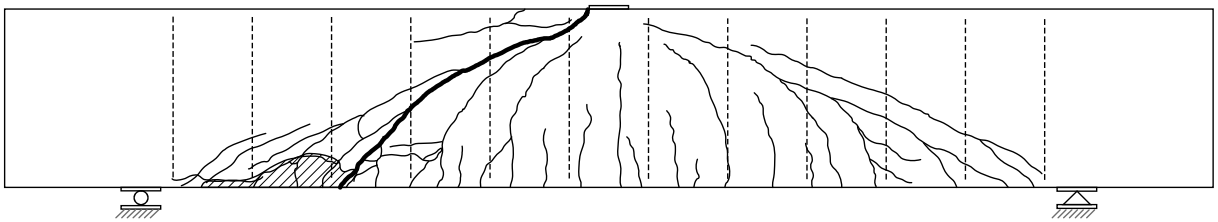

(a) Damage to specimen P1S14 with heads engaged (HE) (f_{ytm} = 85.0 ksi [587 MPa], h = 36 in. [910 mm])

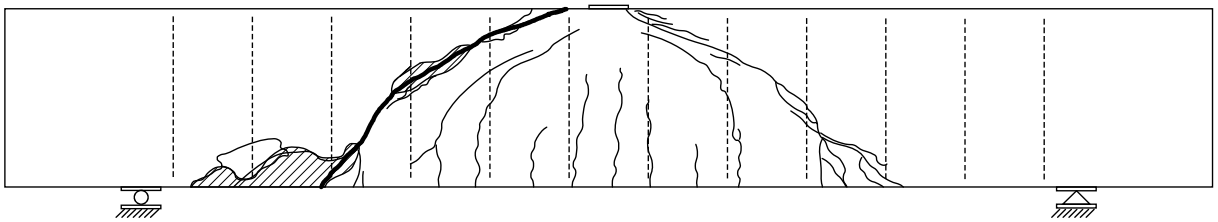

(b) Damage to specimen P1S16 with heads not engaged (HNE) (f_{ytm} = 85.0 ksi [587 MPa], h = 36 in. [910 mm])

Figure 3.2: Damage to specimens with different headed bar detailing

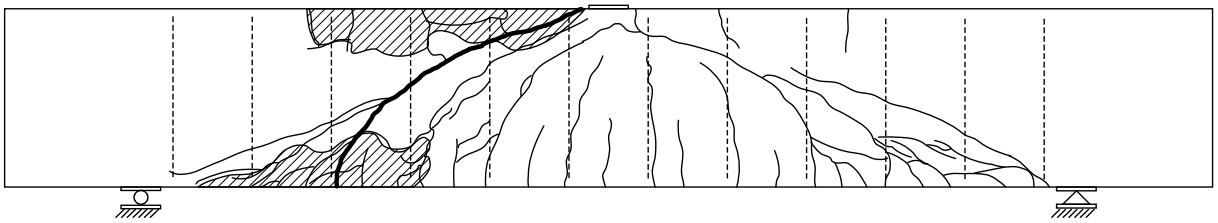

Figure 3.3: Damage to specimen P1S17 with the HNE2 detail (f_{ytm} = 85.0 ksi [587 MPa], h = 36 in. [910 mm])

The presence of compression reinforcement correlated with a difference in the amount of spalling associated with failure. For example, the extent of spalling after failure is shown in Figure 3.4 for specimens P1S7 and P3S5, which had longitudinal compression reinforcement ratios of 0.05 and 1.42%, respectively. The specimens were otherwise similar, with equivalent transverse reinforcement grade, spacing, and bar size, f_{cm} of 4110 and 5000 psi [28.4 and 34.5 MPa], and target longitudinal reinforcement strains of 0.0016 and 0.0017 at nominal shear strength. After failure, the compression zone of specimen P1S7 was extensively spalled while specimen P3S5 exhibited no spalling.

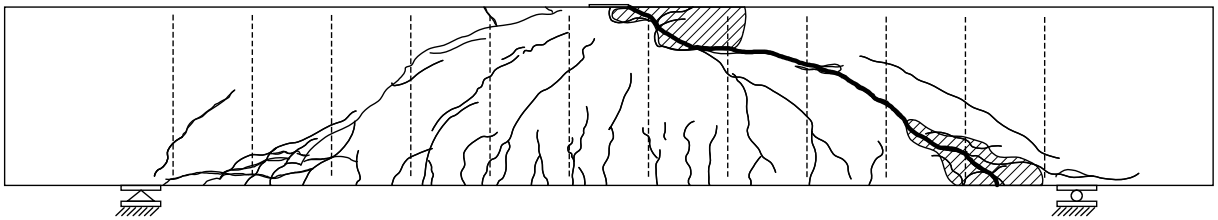

(a) Damage to specimen P1S7 with negligible compression reinforcement (ρ' = 0.05%, f_{ytm} = 85.0 ksi [587 MPa], S detail, h = 36 in. [910 mm])

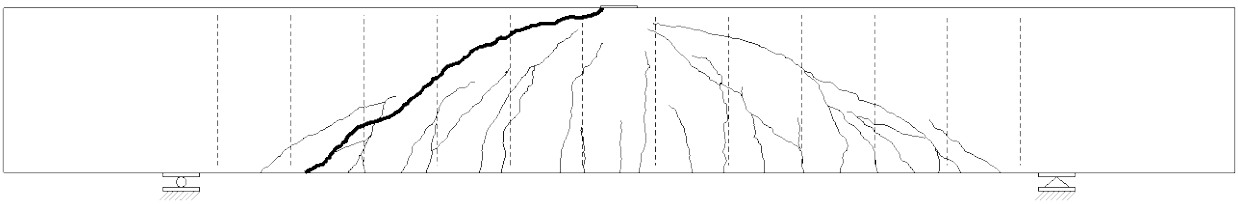

(b) Damage to specimen P3S5 with ρ' = 1.42% (f_{ytm} = 84.5 ksi [583 MPa], S detail, h = 36 in. [910 mm])

Figure 3.4: Damage to specimens with different amounts of compression reinforcement

3.2.1 Specimen P1S15

Specimen P1S15 exhibited unusual cracking at failure that warrants special attention. Although cracking on the sides of specimen P1S15, shown in Figure 3.5, was similar to that of other specimens with the HNE detail (Figure 3.2(b)), unusual cracking occurred on the top and bottom of the specimen, as shown in Figure 3.6. Unlike the other specimens in the study, where cracks on the bottom of the specimen were primarily transverse following failure, a longitudinal crack formed on the bottom of specimen P1S15, accompanied by another longitudinal crack on the top. These longitudinal cracks closely coincided with the vertical plane containing the headed transverse reinforcement, which was located outside of and did not engage the longitudinal reinforcement. Longitudinal cracking was not observed in other specimens with the HNE detail. As will be discussed in the following sections, specimen P1S15 also failed at an unexpectedly low strength. The unusual failure mode may explain the low strength.

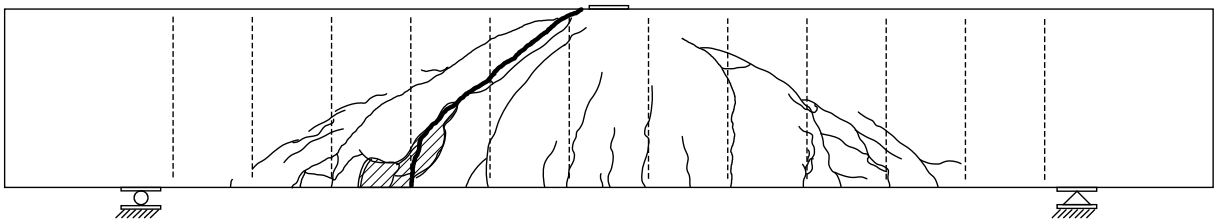

(a) Front side

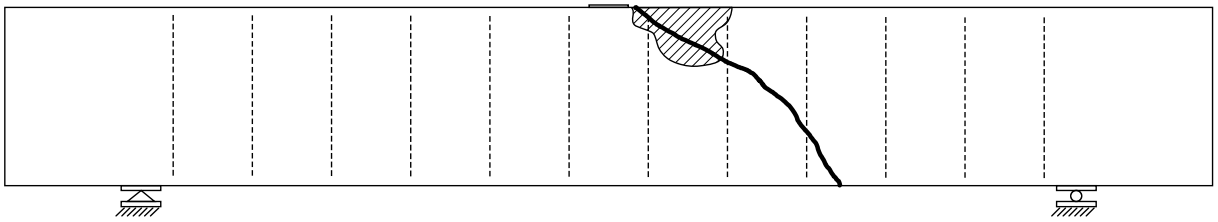

(b) Back side

Figure 3.5: Damage to specimen P1S15 (f_{ytm} = 85.0 ksi [587 MPa], h = 36 in. [910 mm], HNE detail)

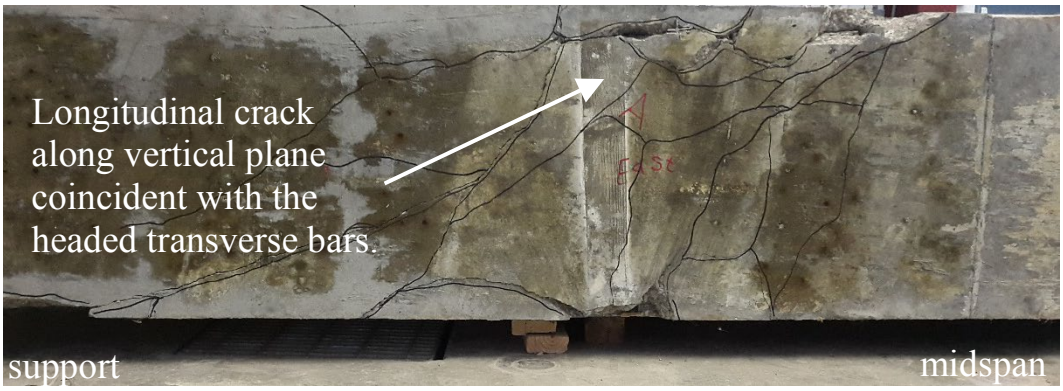

(a) Bottom of specimen

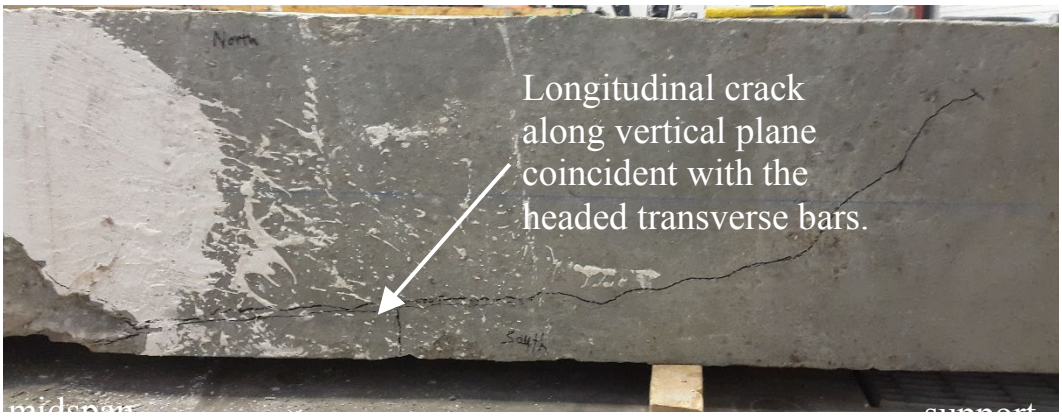

(b) Top of specimen

Figure 3.6: Damage observed on back side of specimen P1S15 (f_{ytm} = 85.0 ksi [587 MPa], h = 36 in. [910 mm], HNE detail)

3.3 Applied Load versus Deflection

Plots of applied load versus midspan deflection are provided in Appendix E for all specimens and in Figures 3.7 and 3.8 for specimens P1S4 through P1S9. The applied load in these plots is the sum of the forces recorded with the four individual load cells and does not include the weight of the loading frame or the self-weight of the specimen. Midspan deflection was calculated as the vertical displacement of markers located at midspan (column J in Figure 2.9) minus the average vertical displacement (settlement) of markers located directly over the supports (SM1 and SM2 in Figure 2.9). Where data from either SM1 or SM2 were unavailable, data from the available marker was used to represent the support settlement at both ends of the specimen.

As shown in Figures 3.7 and 3.8, the specimens exhibited an approximately bilinear response up to peak load. The initial (uncracked) stiffness of the specimens was sustained until flexural cracking began. After the formation of the initial cracks, the slope of the curve decreased and then remained stable until the load approached the peak value (the maximum applied load and the associated deflection are listed in Table 3.1). After the peak, the specimens exhibited brittle failure resulting in a loss in load.

The results in Figures 3.7 and 3.8 are for specimens designed to have the same nominal values of $\rho_t f_{yt}$ (83.3 psi [575 kPa]) but with either Grade 60 [Grade 420] (specimens P1S4 through P1S6 in Figure 3.7) or Grade 80 [Grade 550] (specimens P1S7 through P1S9 in Figure 3.8) transverse reinforcement. The actual values of $\rho_t f_{ytm}$ were 96.9 and 88.5 psi [669 and 610 kPa], respectively, based on the actual values of f_{ytm} of 68.8 and 85.0 ksi [475 and 587 MPa]. These specimens were otherwise similar (they had f_{cm} from 4110 to 5260 psi [28.4 to 36.3 MPa] and longitudinal reinforcement ratios of 1.65%). There is no consistently observable difference between the results plotted in Figures 3.7 and 3.8. This is generally true for all test results, that is, transverse reinforcement grade had no apparent effect on applied load versus midspan deflection results.

Figures 3.7 and 3.8 show results for specimens that contained stirrups (S), headed transverse bars engaging longitudinal reinforcement (HE), or headed transverse bars not engaging transverse reinforcement (HNE). These figures show no observable effect of transverse reinforcement anchorage condition on the applied load versus deflection data. Again, this is

consistent with observations for all test results: transverse reinforcement anchorage condition had no apparent effect on applied load versus midspan deflection results.

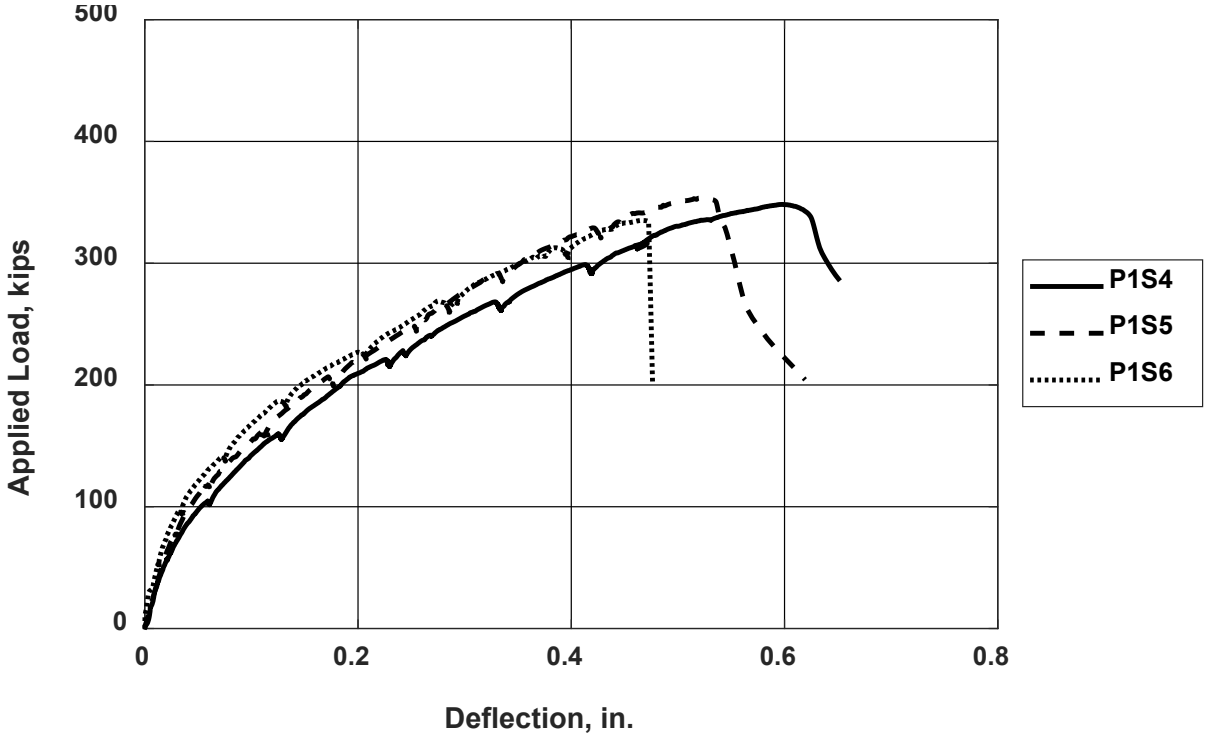

Figure 3.7: Applied load versus midspan deflection for specimens P1S4 through P1S6 (f_{ytm} = 69.8 ksi [482 MPa], $\rho_t f_{ytm}$ = 96.9 psi [669 kPa], h = 36 in. [910 mm], f_{cm} = 4240 to 4360 psi [29.3 to 30.1 MPa]) [1 in. = 25.4 mm, 1 kip = 4.45 kN]

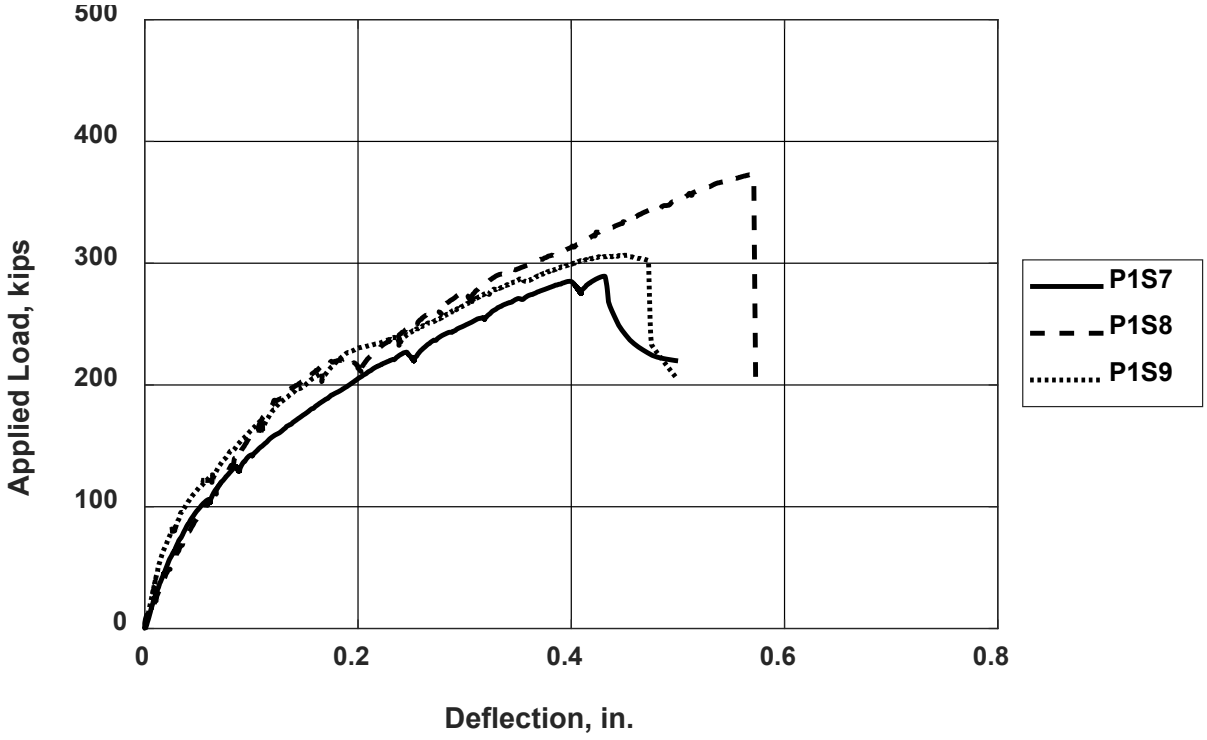

Figure 3.8: Applied load versus midspan deflection for specimens P1S7 through P1S9 (f_{ytm} = 85.0 ksi [587 MPa], $\rho_t f_{ytm}$ = 88.5 psi [610 kPa], h = 36 in. [910 mm], f_{cm} = 4110 to 5260 psi [28.4 to 36.3 MPa]) [1 in. = 25.4 mm, 1 kip = 4.45 kN]

As in Figures 3.7 and 3.8, plots of applied load versus midspan deflection in Appendix F show that specimens with similar overall depths and longitudinal reinforcement ratios exhibited similar overall behavior, as expected. The exception to this was specimen P1S15, which failed at a much lower force than similar specimens (see Section 3.2.1). Figure 3.9 shows applied load versus midspan deflection for specimens P1S13 through P1S17. Although the five specimens were nominally identical aside from the transverse reinforcement anchorage condition, the behavior of specimen P1S15 was clearly different. Specimen P1S15 began to exhibit lower stiffness than others in the group at an applied load of approximately 20 kips [90 kN], a difference that became more pronounced after flexural cracking began at approximately 125 kips [555 kN]. Specimen P1S15 failed in shear at an applied load of 276 kips [1230 kN], or approximately 60% of the average applied load at failure for other specimens in the group. It is not entirely clear why specimen P1S15 had such different behavior starting early in the test. Specimen P1S16, which was

nominally identical to specimen P1S15, exhibited a stiffness, cracking load, and peak strength similar to specimens P1S13, P1S14, and P1S17.

Table 3.1: Maximum applied load and deflection at peak

Specimen	P_{max}[a], kips [kN]	Δ_{max}[b], in. [mm]	Specimen	P_{max}[a], kips [kN]	Δ_{max}[b], in. [mm]
P1S1	275 [1223]	0.51 [13.0]	P2S4	217 [965]	0.25 [6.4]
P1S2	273 [1214]	0.50 [12.7]	P2S5	361 [1606]	–
P1S3	288 [1281]	0.56 [14.2]	P2S6	415 [1846]	0.87 [22.1]
P1S4	350 [1557]	0.60 [15.2]	P2S7	755 [3358]	0.92 [23.4]
P1S5	354 [1575]	0.53 [13.5]	P2S8	765 [3403]	0.95 [24.1]
P1S6	336 [1495]	0.47 [11.9]	P2S9	697 [3100]	0.77 [19.6]
P1S7	290 [1290]	0.43 [10.9]	P2S10	771 [3429]	0.90 [22.9]
P1S8	373 [1659]	0.57 [14.5]	P2S11	484 [2153][c]	1.17 [29.7][d]
P1S9	307 [1366]	0.45 [11.4]	P2S12	481 [2139][c]	1.47 [37.3][d]
P1S10	385 [1712]	0.62 [15.7]	P3S1	673 [2994]	0.76 [19.3]
P1S11	394 [1753]	0.61 [15.5]	P3S2	530 [2357]	0.49 [12.4]
P1S12	363 [1615]	0.61 [15.5]	P3S3	470 [2091]	0.52 [13.2]
P1S13	468 [2082]	0.57 [15.5]	P3S4	505 [2246]	0.64 [16.3]
P1S14	462 [2055]	0.53 [13.5]	P3S5	359 [1597]	0.53 [13.5]
P1S15	276 [1228]	0.26 [6.6]	P3S6	337 [1499]	0.55 [14.0]
P1S16	437 [1943]	0.49 [12.4]	P3S7	405 [1801]	0.47 [11.9]
P1S17	490 [2180]	0.57 [14.5]	P3S8	443 [1970]	0.53 [13.5]
P2S1	200 [890]	0.15 [3.8]	P3S9	263 [1170]	0.48 [12.2]
P2S2	172 [765]	0.10 [2.5]	P3S10	283 [1259]	0.59 15.0]
P2S3	243 [1081]	0.30 [7.6]			

[a] Maximum applied load (sum of load cell data, not including weight of fixtures and specimen)
[b] Deflection at maximum applied load
[c] Alternate loading system (Figure 3.10) was used
[d] Deflection was corrected for rotation over middle support, as described in Appendix F, to facilitate comparisons with other specimens

The behavior of specimen P1S15 motivated the use of an alternative HNE detail for specimen P1S17 wherein the side cover to the transverse reinforcement was increased (see Figure 2.1(d) and Appendix B). The side cover to the transverse bars in specimens P1S15 and P1S17 were 2.0 and 5.75 in. [50 and 145 mm], respectively. Given the behavior of specimen P1S17 (similar stiffness and marginally greater strength than other specimens within the group) and the observation that the cracking of specimen P1S17 was similar to that of beams with the S or HE

transverse reinforcement anchorage conditions (Section 3.2), the HNE2 detail was selected in place of the HE and HNE details for Phases 2 and 3 of this study.

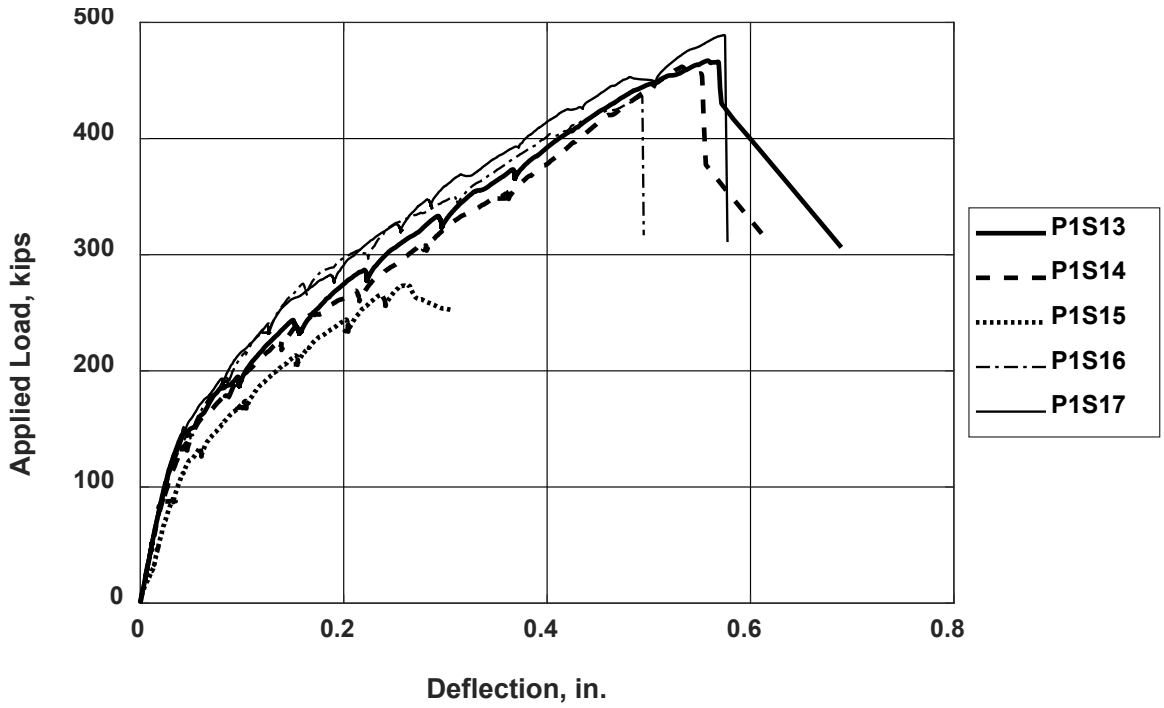

Figure 3.9: Applied load versus midspan deflection for specimens P1S13 through P1S17 (f_{ytm} = 88.0 ksi [607 MPa], h = 36 in. [910 mm], f_c' = 10 ksi [69 MPa]) [1 in. = 25.4 mm, 1 kip = 4.45 kN]

3.4 BEAM SHEAR STRENGTH

The shear strength (V_T) of each specimen is listed in Table 3.2. Except for specimens P2S11 and P2S12, V_T was calculated as half the sum of the maximum load applied to each specimen (P_{max}), the weight of the loading apparatus (fixtures), and a portion of the self-weight of the specimen. The total weight of the fixtures, which varied slightly among the specimens (Table 3.2), included the weight of the HP member, built-up channel beams, load cells, loading rods (either No. 20 or No. 14 [No. 64 or No. 43] threaded bars), nuts, and assorted plates, as described in Section 2.3.1. For most of Phases 2 and 3, the weight of the fixtures also included the weight of the jacks, which were moved from below the laboratory strong floor to the top of the loading apparatus in later tests. The portion of the specimen included in the calculation of self-weight is

Table 3.2: Measured and nominal shear strengths [a]

Specimen	P_{max}, kips	Fixture Weight, kips	Self-Weight, kips	V_T [b], kips	f_{yt}, ksi	f_{cm}, psi	V_c [c], kips	V_s [d], kips	V_n [e], kips	$\frac{V_T}{V_n}$	Norm. $\frac{V_{TH}}{V_{TS}}$ [f]
P1S1	275	5	7.1	144	69.8	4680	103	55	158	0.91	–
P1S2	273	5	7.1	143	69.8	4540	102	55	157	0.91	1.00
P1S3	288	5	7.1	150	69.8	4570	102	55	157	0.95	1.05
P1S4	350	5	7.1	181	69.8	4240	98.5	73.3	172	1.05	–
P1S5	354	5	7.1	183	69.8	4360	99.8	73.3	173	1.06	1.01
P1S6	336	5	7.1	174	69.8	4310	99.3	73.3	173	1.01	0.96
P1S7	290	5	7.1	151	85	4110	96.9	66.9	164	0.92	–
P1S8	373	5	7.1	193	85	4130	97.2	66.9	164	1.17	1.28
P1S9	307	5	7.1	160	85	5260	110	66.9	177	0.90	0.98
P1S10	385	5	7.1	199	85	4640	103	89.3	192	1.03	–
P1S11	394	4.4	7.1	203	85	4730	104	89.3	193	1.05	1.01
P1S12	363	4.4	7.1	187	85	4790	105	89.3	194	0.97	0.93
P1S13	468	5	7.1	240	85	11630	163	66.9	230	1.04	–
P1S14	462	5	7.1	237	85	11400	161	66.9	228	1.04	1.00
P1S15	276	5	7.1	144	85	12080	166	66.9	233	0.62	0.59
P1S16	437	4.4	7.1	224	85	9680	149	66.9	216	1.04	0.99
P1S17	490	4.4	7.1	251	85	9960	151	66.9	218	1.15	1.10
P2S1	200	4.4	0.71	103	86.2	9710	44.9	36	81	1.27	–
P2S2	172	4.4	0.71	88.6	86.2	9760	45	36	81.1	1.09	0.86
P2S3	243	4.4	1.6	125	86.2	10080	69.9	36.7	107	1.17	–
P2S4	217	4.4	1.6	112	86.2	9760	68.8	36.7	105	1.06	0.91
P2S5	361	6	13.2	190	83.5	5630	159	66.8	225	0.84	–
P2S6	415	6	13.2	217	83.5	5780	161	66.8	227	0.95	1.13
P2S7	755	4.4	13.2	386	82.7	9530	205	145	350	1.10	–
P2S8	765	4.4	13.2	391	82.7	10410	214	145	359	1.09	0.99
P2S9	697	5.4	13.2	358	83.5	10440	216	134	349	1.02	–
P2S10 [g]	771	5.4	13.2	395	83.5	11090	222	134	356	1.11	1.08
P2S11 [g, h]	484	6.1	11.7	502	83.5	9750	209	134	342	1.47	–
P2S12 [g, h]	481	6.1	11.7	498	83.5	9750	209	134	342	1.46	0.99
P3S1	673	6.2	13	346	66.3	4600	189	110	300	1.15	–
P3S2	530	6.2	13	275	66.3	4360	184	110	295	0.93	0.81
P3S3	470	6.2	13	245	84.5	4040	178	105	283	0.86	–
P3S4	505	6.2	13	262	84.5	4040	178	105	283	0.93	1.07
P3S5	359	6	7.2	186	84.5	5000	109	67.6	176	1.06	–
P3S6	337	6	7.2	175	84.5	4810	107	67.6	174	1.01	0.95
P3S7	405	6.1	7.2	209	84.5	5060	109	67.6	177	1.18	–
P3S8	443	6.1	7.2	228	84.5	5050	109	67.6	177	1.29	1.09
P3S9 [g]	263	6.1	7.2	138	84.5	4370	102	67.6	169	0.82	–
P3S10 [g]	283	6.1	7.2	148	84.5	4800	106	67.6	174	0.85	1.04

[a] 1 kip = 4.45 kN, 1 ksi = 6.9 MPa, 1 psi = 6.9 kPa

[b] Shear strength, calculated as half the sum of maximum applied load, loading frame weight, and contributing specimen self-weight (Figure 3.10). See Tables 2.1 through 2.3 for steel quantities and specimen dimensions

[c] Nominal contribution of concrete to shear strength, $2\sqrt{f_{cm}}b_w d$;

[d] Nominal contribution of transverse reinforcement to shear strength, $A_v f_{yt} d/s$; [e] Sum of V_c and V_s;

[f] Ratio of the measured shear strength for specimens reinforced for shear with headed bars (V_{TH}) to specimens reinforced for shear with stirrups or cross ties (V_{TS}) with V_{TH} and V_{TS} normalized to (divided by) V_n for specimen;

[g] Yielding of longitudinal reinforcement limited specimen strength

[h] Alternative loading system (Section 2.3.1.1) was used

highlighted in Figure 3.10. Except for specimens P2S11 and P2S12, this was the portion of the specimen located between the assumed potential failure surfaces on either side of midspan. For this calculation, it was assumed that failure occurred along a plane inclined 45 degrees from horizontal and located midway between the loading point and each support, as illustrated in Figure 3.10a (this approach is the simpler of two methods used by Reineck et al. 2013). The specimen self-weight included in V_T was thus calculated as $a_v bh \times 150\,\mathrm{lb/ft^3}$, $[a_v bh \times 2400\,\mathrm{kg/m^3}]$ where a_v is the shear span, b is the beam width, and h is the total beam depth.

The calculation of V_T was slightly different for specimens P2S11 and P2S12 because they were tested with an alternate loading system (Section 2.3.1.1). For these specimens, V_T was calculated as the sum of the maximum applied load (P_{max}), the weight of the fixtures, and the self-weight of the portion of the specimen shaded in Figure 3.10b.

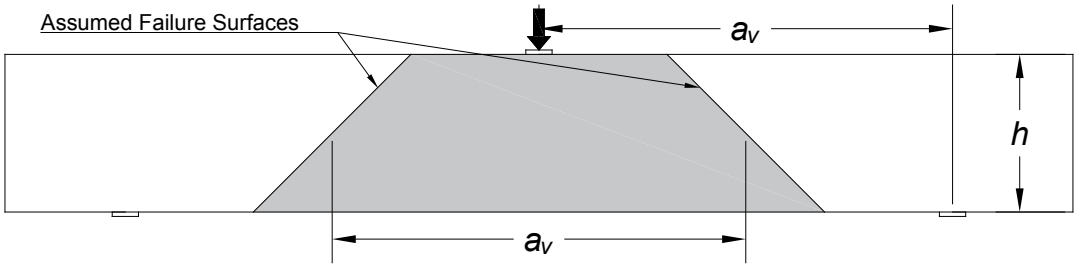

(a) Basic loading system (Section 2.3.1)

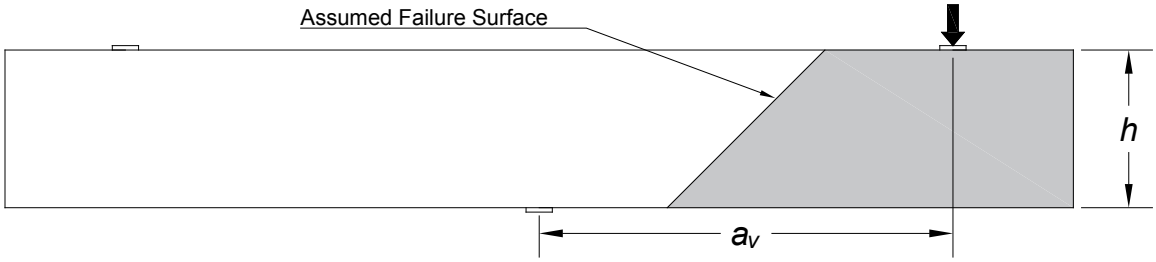

(b) Alternative loading system for specimens P2S11 and P2S12 (Section 2.3.1.1)

Figure 3.10: Assumed failure surfaces and self-weight considered in shear strength (shaded)

Table 3.2 also lists the nominal shear strength (V_n) of each specimen, calculated following the expressions in ACI 318-14, as the sum of the shear strength attributed to the concrete (V_c) and transverse reinforcement (V_s) (Eq. (3.1) through (3.3)) using the measured concrete compressive

strength (f_{cm}) and transverse reinforcement yield strengths (f_{ytm}) with nominal cross-sectional dimensions.

$$V_n = V_c + V_s \tag{3.1}$$

$$V_c = 2\sqrt{f_{cm}}b_w d \tag{3.2}$$

$$V_s = A_v f_{yt} d/s \tag{3.3}$$

where b_w = width of web, d = effective depth, and s = spacing of transverse reinforcement. In this study, the width of the web (b_w) equals the width of the beam (b).

The ratio of measured to nominal shear strength (V_T/V_n is shown in the next to last column of Table 3.2 for each specimen and in Figures 3.11 through 3.13 for the specimens in Phases 1 through 3, respectively. Omitting specimen P1S15, which had exceptionally low strength (V_T/V_n = 0.62; discussed in Section 3.3), the average value of V_T/V_n is 1.05, with maximum and minimum values of 1.47 and 0.82, respectively, a standard deviation of 0.150, and a coefficient of variation (COV) of 0.143. Further omitting specimens P2S10 through P2S12, P3S9, and P3S10, which exhibited longitudinal bar yielding before the peak load, the average is 1.04, with maximum and minimum values of 1.29 and 0.84, respectively, a standard deviation of 0.110 and a coefficient of variation (COV) of 0.106. In spite of exhibiting longitudinal bar yielding before reaching peak load, specimens P2S10 through P2S12 exceeded the nominal shear strength based on Eq. (3.3), with values of V_T/V_n between 1.11 and 1.47. Specimens P3S9 and P3S10, which were designed to yield in flexure, had values of V_T/V_n of 0.82 and 0.85, respectively.

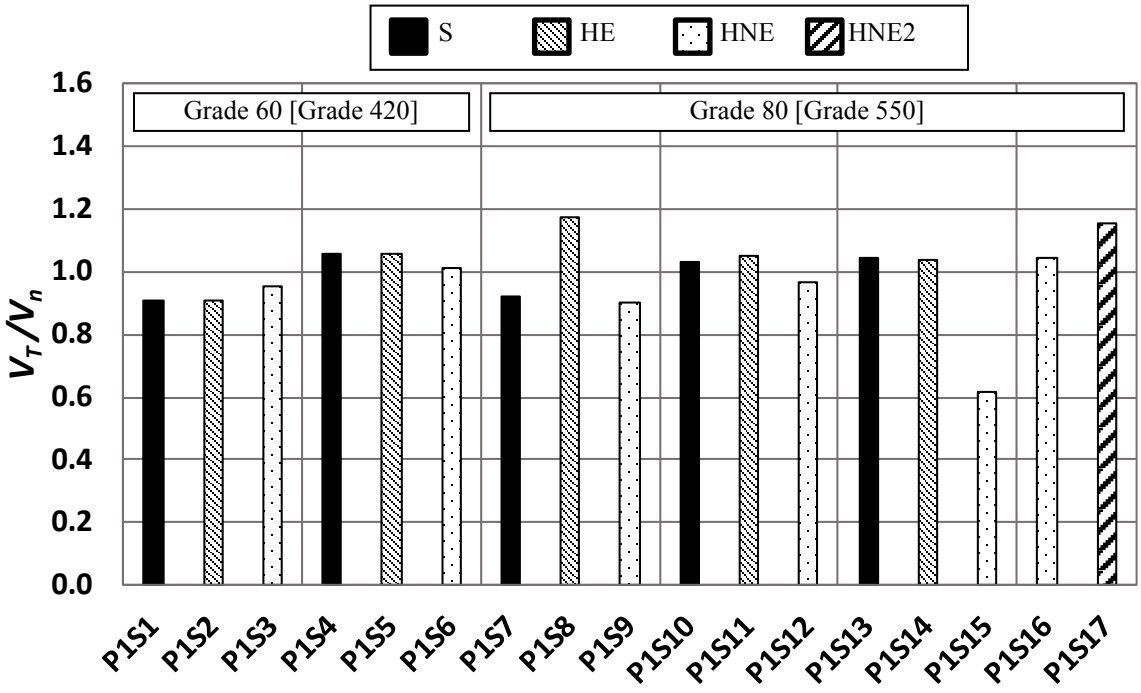

Figure 3.11: Ratio of measured to nominal shear strength for Phase 1 specimens

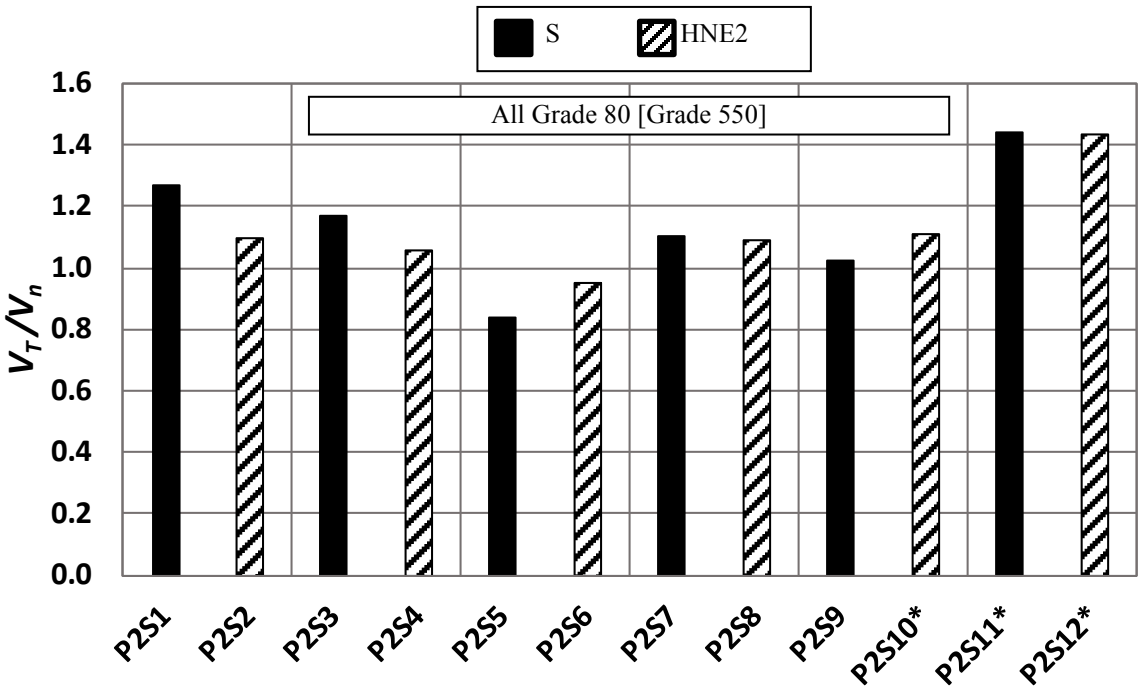

* Exhibited longitudinal bar yielding before peak load

Figure 3.12: Ratio of measured to nominal shear strength for Phase 2 specimens

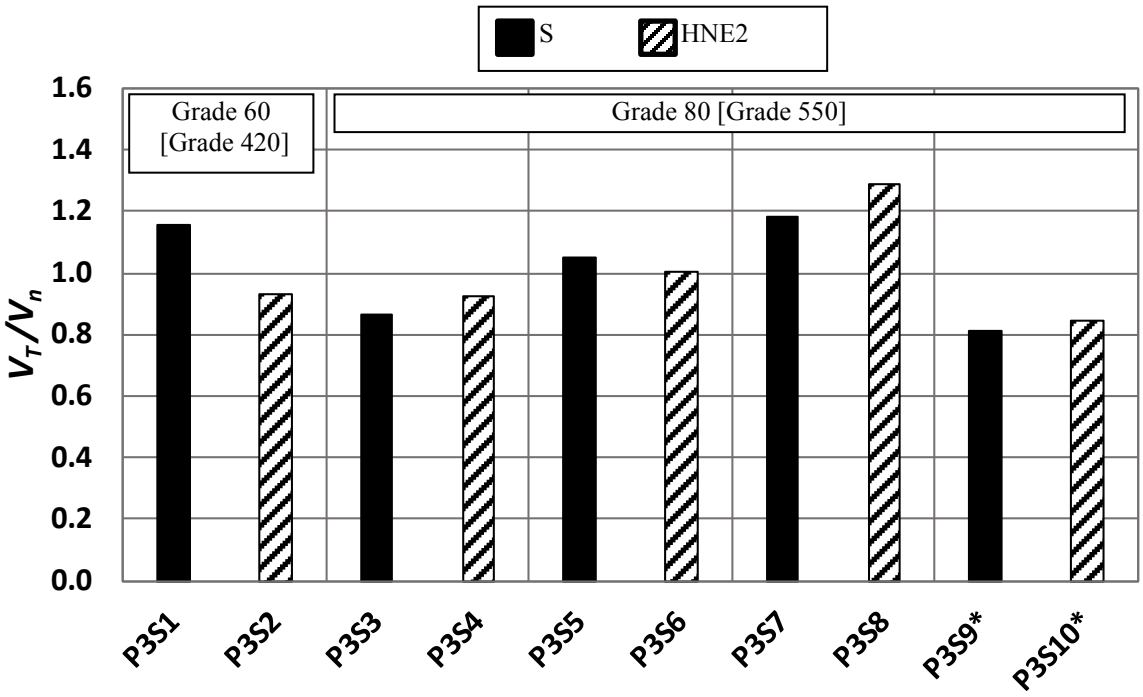

* Exhibited longitudinal bar yielding before peak load

Figure 3.13: Ratio of measured to nominal shear strength for Phase 3 specimens

3.4.1 Transverse reinforcement

Excluding specimens P1S15, P2S10 through P2S12, P3S9, and P3S10, of the remaining 33 specimens, 11 had VT/Vn less than 1.0 (six of 16 specimens in Phase 1, two of nine specimens in Phase 2, and three of eight specimens in Phase 3). Although all specimens had areas of transverse reinforcement exceeding the minimum area (Av,min) required by ACI 318-14 (Eq. 3.4), low strengths relative to the nominal strength (Vn) calculated using in Eq. (3.3) correlated with values of the product of the transverse reinforcement ratio and the measured transverse reinforcement yield strength ρtfytm below 80 psi [550 kPa].

$$\frac{A_{v,\min}}{b_w s} f_{yt} = \rho_{t,\min} f_{yt} = \max\left(50 \text{ psi},\ 0.75\sqrt{f_c'} \text{ psi}\right) \tag{3.4}$$

Figure 3.14 shows the values of V_T/V_n for the specimens in this study with the results presented for values of $\rho_t f_{ytm}$ < 80 psi and values of $\rho_t f_{ytm}$ > 80 psi. The individual results are presented from left to right in order of increasing $\rho_t f_{ytm}$. The values of $\rho_t f_{ytm}$ are given in Tables 2.1 through 2.3.

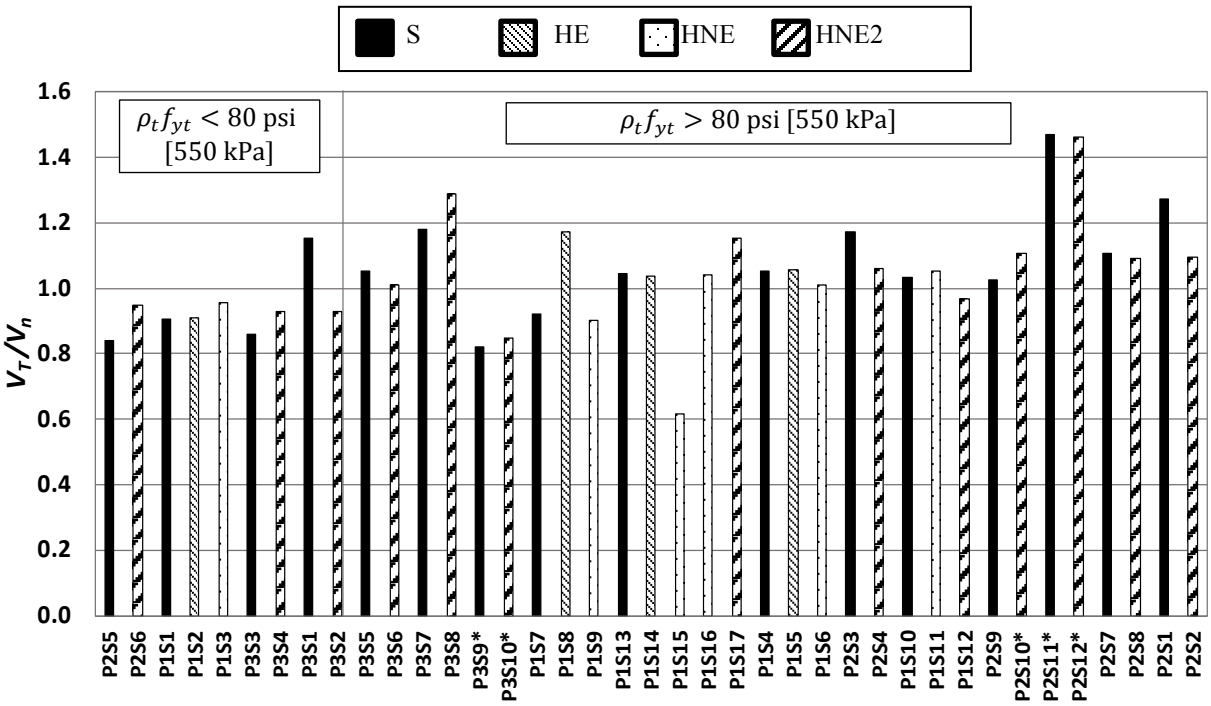

* Exhibited longitudinal bar yielding before peak load

Figure 3.14: Ratio of measured to nominal shear strength for all specimens

Not including specimens P1S15, P3S9, and P3S10, 11 specimens had V_T/V_n less than 1.0. Of the 11, eight had $\rho_t f_{ytm}$ less than 80 psi [550 kPa], two had $80 \leq \rho_t f_{ytm} < 90$ psi [$550 \leq \rho_t f_{ytm} <$ 620 kPa], and one had $\rho_t f_{ytm}$ greater than 90 psi [620 kPa], indicating a correlation between low $\rho_t f_{ytm}$ and low V_T/V_n. Furthermore, eight of the nine specimens (88.9%) with $\rho_t f_{ytm}$ less than 80 psi [550 kPa] had V_T/V_n less than 1.0, whereas only two of the eleven specimens (18.2%) with $80 \leq \rho_t f_{ytm} < 90$ psi [$550 \leq \rho_t f_{ytm} < 620$ kPa] and one of the sixteen specimens (6.3%) with $\rho_t f_{ytm} > 90$ psi [620 kPa] had V_T/V_n less than 1.0. The mean V_T/V_n was 0.94, with a standard deviation of 0.088, for specimens with $\rho_t f_{ytm} < 80$ psi [550 kPa] compared to mean V_T/V_n of 1.10, with a standard deviation of 0.136, for specimens with $\rho_t f_{ytm} > 80$ psi [550 kPa]. Student's t-test is used within this report to determine if differences between two sets of data (populations) are statistically significant, with $p \leq 0.05$ considered statistically significant. For the current comparison, $p =$ 0.0018 and the difference is clearly statistically significant.

3.4.2 Transverse Reinforcement Anchorage Details

The results in Table 3.2 and Figures 3.11 through 3.13 serve as a basis for comparisons between groups of specimens that isolate the effect of specific variables on shear strength. A key goal of this study is to establish the effectiveness of headed bars as shear reinforcement. This can be done by comparing the shear strength of specimens containing headed bars as transverse reinforcement (V_{TH}) with the shear strength of similar specimens containing stirrups (V_{TS}). The last column in Table 3.2 contains the ratios V_{TH}/V_{TS}. The values of V_{TH} and V_{TS} are normalized to the nominal shear strengths (V_n) calculated using Eq. (3.3) to limit the effects on the comparison of differences in concrete compressive strength, which did vary for specimens within the same group. Excluding specimen P1S15, the values of V_{TH}/V_{TS} shown in Table 3.2 range from 0.81 to 1.28, with an average of 1.01, a standard deviation of 0.098, and a COV of 0.097, indicating that headed bars are equivalent to stirrups as shear reinforcement. The one caveat involves the failure mode observed for specimen P1S15 and described in Section 3.2.1 – headed bars must be positioned so as not to result in splitting of the members. The successful performance of detail HNE2 indicates that a key requirement is the provision of adequate side cover. Providing adequate side cover will not be an issue for headed bars used as shear reinforcement in walls or mat foundations, a principal application in nuclear power plants.

3.4.3 Grade of Reinforcement

The study included eight specimens with Grade 60 [Grade 420] transverse reinforcement and 31 specimens with Grade 80 [Grade 550] transverse reinforcement. The mean value of V_T/V_n for the specimens with Grade 60 [Grade 420] transverse reinforcement is 1.00, with a standard deviation of 0.086 and a COV of 0.086. Not including specimen P1S15, the mean, standard deviation, and COV for the specimens with Grade 80 [Grade 550] transverse reinforcement are 1.06, 0.161 and 0.151. Removing in addition the four specimens in which the longitudinal reinforcement yielded prior to the peak load (P2S11, P2S12, P3S9, and P3S10), the mean, standard deviation, and COV for the specimens with Grade 80 [Grade 550] transverse reinforcement are 1.05, 0.114 and 0.108. These results show that for the specimens in the current study, there is no negative effect of reinforcement grade on V_T/V_n, indicating that members with the same value of

$\rho_t f_{yt}$ would be expected to have the same shear strength for both Grade 60 and Grade 80 [Grade 420 and Grade 550] transverse reinforcement. These observations match those of Sumpter et al. (2009), Munikrishna et al. (2011), and Lee et al. (2011), as described in Section 1.2.2.

3.4.4 Compression Reinforcement

Another variable, compression reinforcement, showed effects on V_T/V_n that were significant. Looking first at compression reinforcement, the effect of increasing the compression reinforcement ratio (ρ') from 0.05 to 1.42% on failure mode was illustrated in Figure 3.4. Specimens P1S7 and P1S9 with $\rho' = 0.05$ had respective values of V_T/V_n of 0.92 and 0.90 while specimens P3S5 and P3S6 with $\rho' = 1.42\%$ had respective values of V_T/V_n 1.06 and 1.01. The increase in V_T/V_n coincident with an increase in ρ' from 0.05 to 1.42% for this small set of beams is statistically significant ($p = 0.047$).

3.5 CRACK WIDTHS

At each pause in loading, cracks were traced with a permanent marker and the widths of the most prominent inclined cracks were measured and recorded. Recorded crack widths are listed in Appendix G for all specimens. The maximum crack width measured at each pause in loading is also plotted in Appendix G versus the percent of nominal strength and the percent of measured strength. For reference, each figure includes a horizontal line that crosses the ordinate (crack width) axis at 0.016 in. [0.40 mm], the crack width used by the ACI Building Code before 1999 as the basis for serviceability requirements for flexure. As described in Section 1.2.2.1, the 0.016-in. [0.40-mm] crack width represents the *most probable* maximum flexural crack width expected in conventionally proportioned members, a value that was exceeded in 31 to 98% of groups of specimens considered (Lutz and Gergely 1968). Thus, a crack width of 0.016-in. [0.40-mm] should most appropriately serve as a guide, not an upper limit, when evaluating the effects of various parameters on the serviceability of members in shear.

It is generally understood that inclined crack widths are affected by the transverse reinforcement ratio. This is shown in Figure 3.15, which compares the maximum inclined crack

width with the shear force for specimens P1S1 through P1S12 (P1S6 and P1S9 omitted for lack of data). The five beams with the largest crack widths (specimens P1S1, P1S2, P1S3, P1S7, and P1S8) had a transverse reinforcement ratio ($\rho_t = A_v/b_w s$) of 0.10%. The other five specimens, which had a transverse reinforcement ratio of 0.14%, had narrower cracks at the same loads.

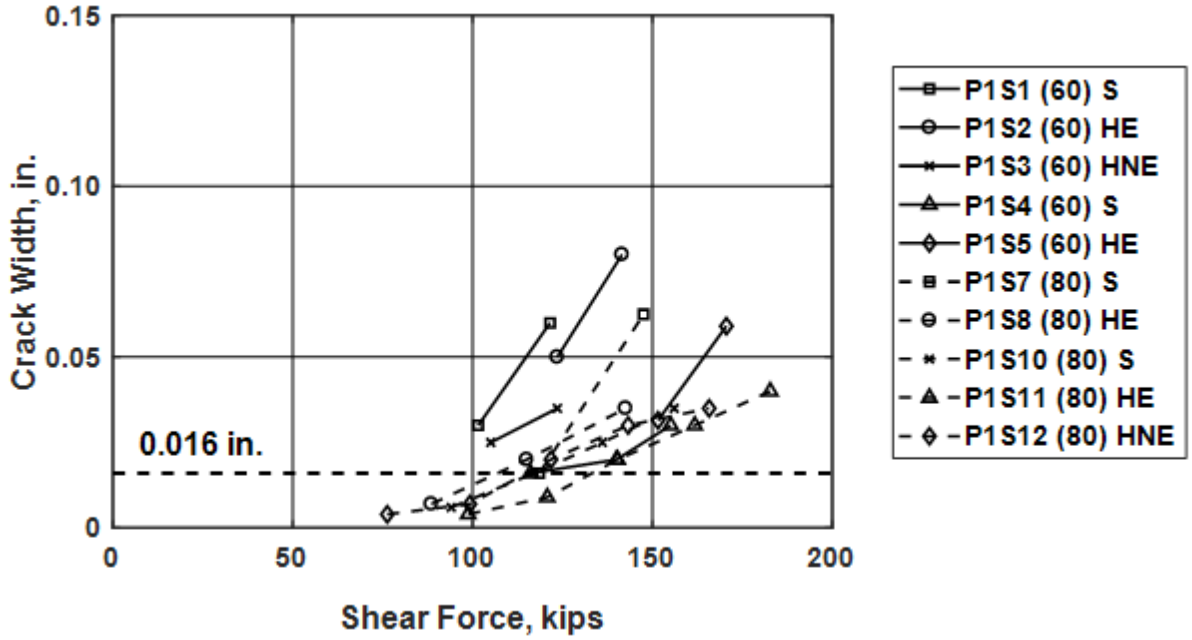

Figure 3.15: Maximum crack width versus shear force, specimens P1S1 through P1S12 (P1S6 and P1S9 omitted for lack of data) [1 in. = 25.4 mm, 1 kip = 4.45 kN]

It is expected, therefore, that reductions in transverse reinforcement ratio associated with use of higher-grade transverse reinforcement will result in wider inclined cracks. To examine the extent to which this was true, the maximum crack width measured at each pause in loading is plotted versus percent of nominal strength in Figures 3.16 and 3.17 for selected specimens; a value of 60% of the nominal strength is often used for comparison because it approximates the working load on a structure in service. Figure 3.16 shows results for four specimens in Phase 1 (all with total depth h = 36 in. [910 mm], effective depth d = 31.5 in. [800 mm], and width b = 24 in. [610 mm]), P1S4 and P1S5 (Grade 60 [Grade 420]) and specimens P1S7 and P1S8 (Grade 80 [Grade 550]), that had similar values of $\rho_t f_{ytm}$ (96.9 psi [669 kPa] for P1S4 and P1S5, and 88.5 psi [610 kPa] for P1S7 and P1S8) but had different values of transverse reinforcement grade and spacing.

As shown in Figure 3.16, crack width increased slightly as transverse reinforcement grade increased from Grade 60 to 80 [Grade 420 to 550], especially at loads greater than 70% of nominal strength. None of the specimens exhibited inclined cracks greater than 0.016 in. [0.40 mm] until the load exceeded approximately 65% of nominal strength. Regardless of grade, the inclined crack widths were less than the most probable maximum flexural crack width near service-level loads (taken as 60% of V_n).

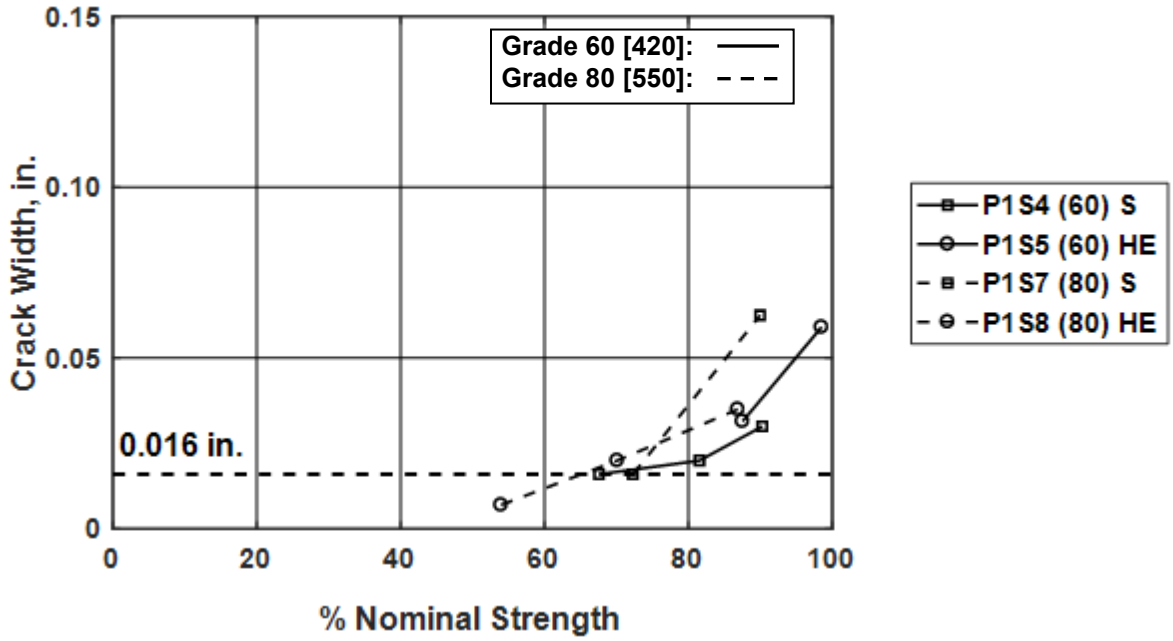

Figure 3.16: Maximum crack width versus percent of nominal strength: specimens with Grade 60 and 80 [Grade 420 and 550] transverse reinforcement in Phase 1 [1 in. = 25.4 mm]

The results in Figure 3.17 for specimens P3S1 through P3S4 show a larger difference between specimens with Grade 60 and 80 [Grade 420 and 550] transverse reinforcement. The specimens were similar (total depth h = 36 in. [910 mm], effective depth d = 33.25 in. [845 mm], width b = 42 in. [1070 mm], $\rho_t f_{ytm}$ = 78.9 and 75.4 psi [544 and 520 kPa] for Grades 60 and 80 [Grades 420 and 550], respectively), except for transverse reinforcement grade and area of the transverse reinforcement. Figure 3.17 shows that specimens P3S1 and P3S2 (Grade 60) had markedly narrower cracks than specimens P3S3 and P3S4 (Grade 80). The largest inclined crack width in specimens P3S3 and P3S4 (Grade 80) exceeded 0.016 in. between approximately 40 and

50% of the nominal strength, whereas the largest inclined cracks in specimens P3S1 and P3S2 (Grade 60) did not exceed 0.016 in. until reaching loads greater than 60% of the nominal strength.

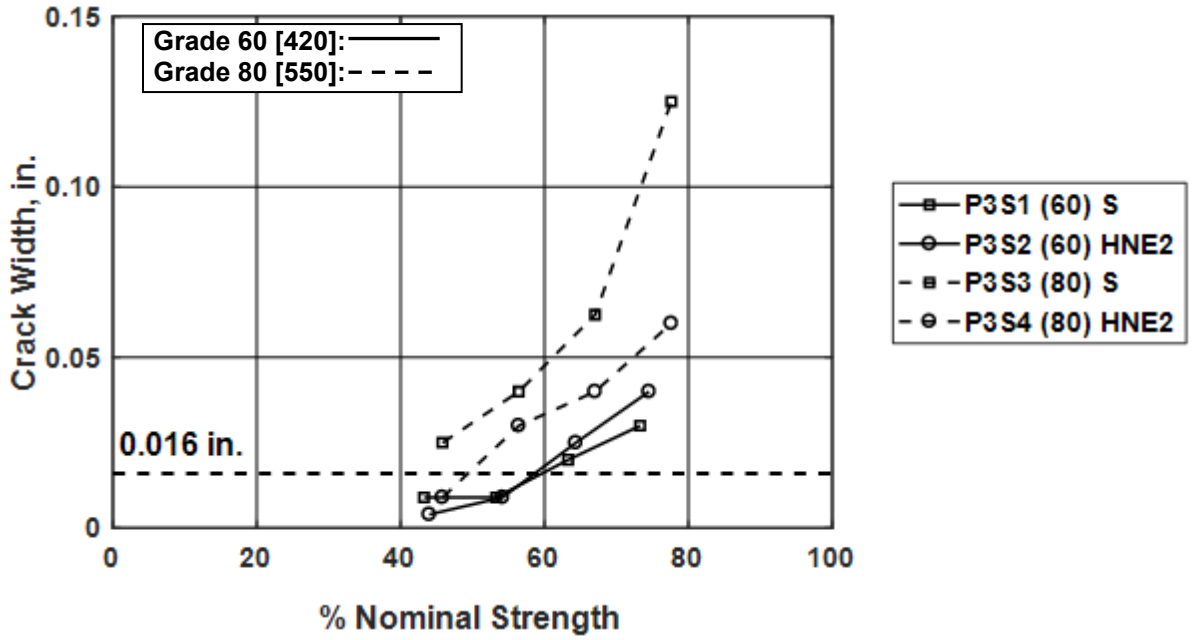

Figure 3.17: Maximum crack width versus percent of nominal strength: specimens with Grade 60 and 80 [Grade 420 and 550] transverse reinforcement in Phase [1 in. = 25.4 mm]

In Figures 3.16 and 3.17, specimens with Grade 80 [Grade 550] transverse reinforcement exhibited wider cracks than specimens with Grade 60 [Grade 420] transverse reinforcement (at 60 and 70% of nominal strength, crack widths in beams with Grade 80 [Grade 550] transverse reinforcement were 1.0 to 2.6 times greater, respectively, than the largest cracks in beams with Grade 60 [Grade 420] reinforcement). The crack widths are relatively close to the reference value of 0.016 in. for loads between 40 and 50% of the nominal strength.

To put the increase in crack width associated with the use of Grade 80 [Grade 550] transverse reinforcement in context, differences in crack width associated with ranges of total section depth h and concrete compressive strength f_{cm} expected in practice are worth evaluation. Figure 3.18 shows inclined crack width versus percent of nominal strength for specimens P2S1 through P2S4, P2S9, and P2S10. These specimens were similar (b = 24 in. [610 mm], Grade 80 [Grade 550] reinforcement, $\rho_t f_{ytm}$ = 158, 105, and 127 psi [1090, 725, 876 kPa] for P2S1/P2S2,

P2S3/P2S4, and P2S9/P2S10, respectively), except for *h*, with values of 12, 18, and 48 in. [310, 460, and 1220 mm]. Crack widths for the specimens with *h* of 12 or 18 in. [310 or 460 mm] were less than 0.016 in. [0.40 mm] at all load levels for which measurements were taken. The specimens with *h* of 48 in. [1220 mm] had crack widths exceeding 0.016 in. [0.40 in.] at 60% of the nominal strength that were approximately 4.9 times greater than in shallower beams. This is a larger relative difference in crack width than between specimens with Grade 60 and 80 [Grades 420 and 550] transverse reinforcement (1.0 to 2.6 times greater).

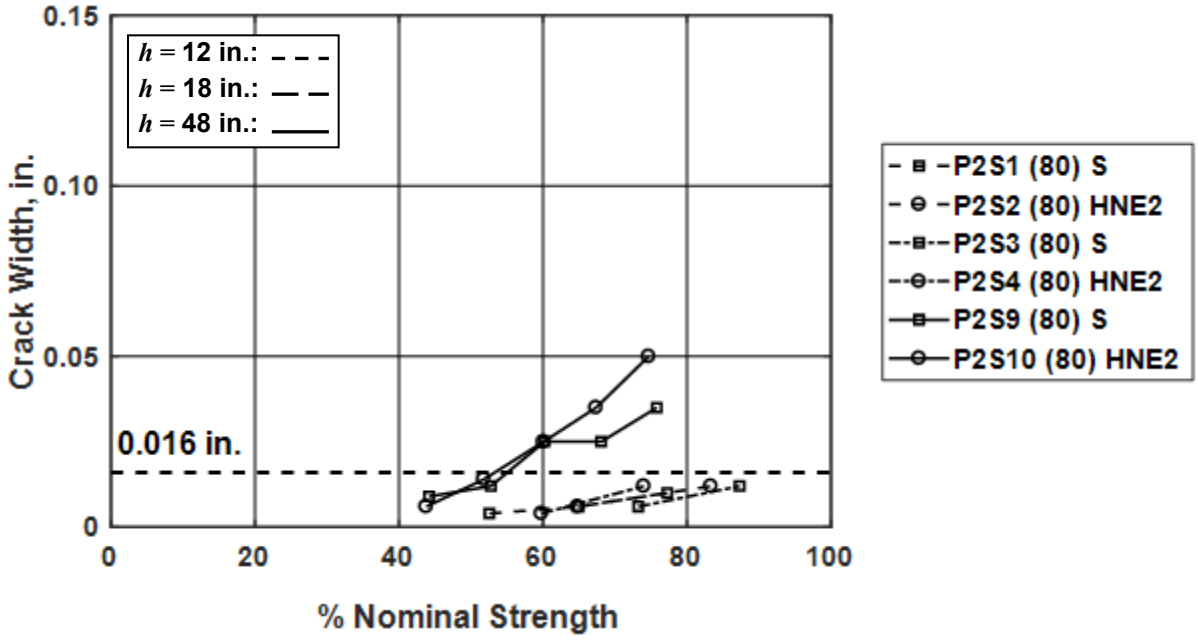

Figure 3.18: Maximum crack width versus percent of nominal strength: specimens with *h* = 12, 18, and 48 in. [1 in. = 25.4 mm]

Because increased beam depth is associated with increased crack width, crack widths reported in this study from tests of 36 and 48 in. [910 and 1220 mm] deep specimens are likely to be greater than those reported by others investigating the use of high strength transverse reinforcement (Sumpter et al. 2009, Munikrishna et al. 2011, Lee et al. 2011), who based their findings on tests of beams with depths of 14 to 28 in. [305 to 710 mm], as described in Section 1.2.2.1. It must, however, be noted that the specimens with *h* of 48 in. [1220 mm] are not representative of beams in practice because beams with overall depths greater than 36 in.[910 mm]

are required by ACI 318-14 to have skin reinforcement that will tend to reduce inclined crack widths. As explained in Section 2, skin reinforcement was not used for the 48-in. [1220 mm] deep beams because they were designed to represent walls and foundations, which do not have skin reinforcement.

Figure 3.19 shows crack width versus percent of nominal strength for specimens in Phase 1 that were similar except for f_{cm}. The figure includes specimens P1S7 and P1S8 (f_{cm} = 4110 and 4130 psi [28.4 and 28.5 MPa]) and specimens P1S13, P1S14, P1S16, and P1S17 (f_{cm} = 11630, 11400, 9680, and 9960 psi, [80.2, 78.7, 66.8, and 68.7 MPa] respectively). These specimens had the same overall and effective depths (h = 36 in. [910 mm], d = 31.5 in. [800 mm]), $\rho_t f_{ytm}$ (88.5 psi [610 kPa]), and calculated longitudinal reinforcement strain ε_{long} at nominal shear strength (0.0017). Two of the four specimens with the higher f_{cm} had the widest cracks throughout the test, and at loads greater than approximately 70% of nominal strength, all four specimens with the higher strength concrete had larger crack widths than either of the specimens with lower strength concrete. Four out of six specimens exhibited crack widths below 0.016 in. [0.40 mm] at 60 percent of the nominal strength. Neglecting specimen P1S13, which had comparatively wide cracks, the specimens with the higher f_{cm} had cracks that ranged from 0.6 to 4 times wider at 60% of nominal strength than the widest crack observed on a specimen with f_{cm} of 4110 or 4130 psi [28.4 or 28.5 MPa]. Including specimen P1S13, two for the four specimens designed for f'_c of 10,000 psi [69 MPa] had wider crack widths and two had narrower crack widths that the two specimens designed for f'_c of 4,000 psi [28 MPa], suggesting that concrete compressive strength has little effect on crack width. Interestingly, the relative changes in crack widths observed in this comparison are greater than those observed in Figure 3.16 and similar to those observed in Figure 3.17 for changes in transverse reinforcement grade from 60 to 80 [420 to 550]. Overall, the results therefore indicate that use of Grade 80 [Grade 550] transverse reinforcement causes a smaller change in crack width than other parameters, such as beam depth, that are accepted in practice.

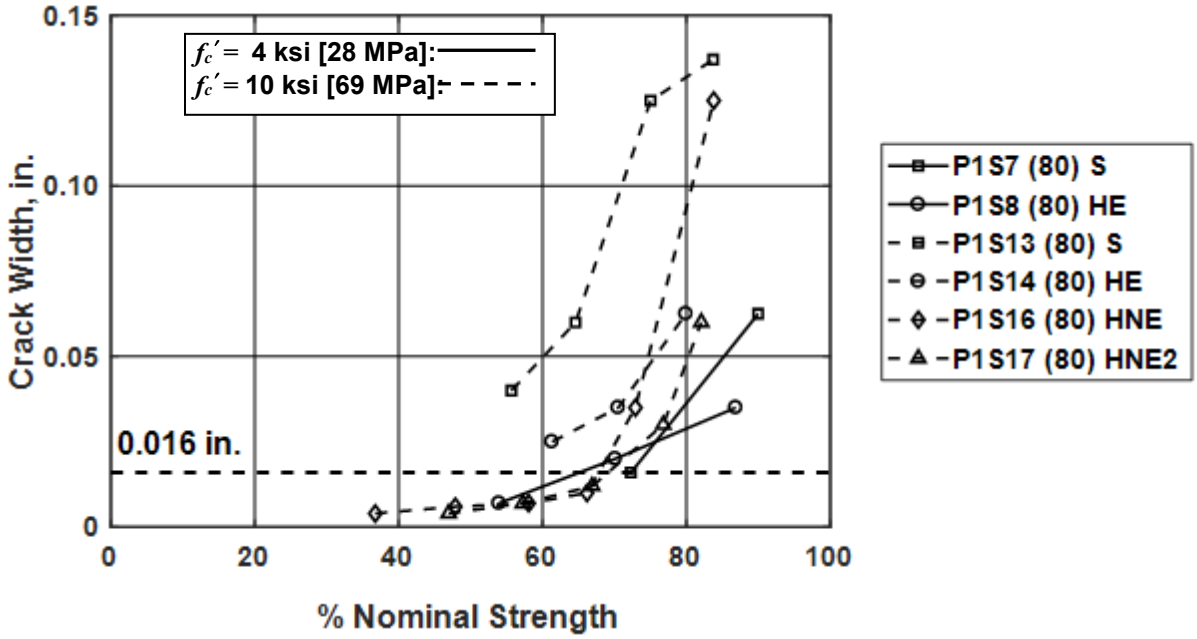

Figure 3.19: Maximum crack width versus percent of nominal strength: Specimens with f'_c = 4 and 10 ksi [28 and 69 MPa]. Listed in order of members with largest to smallest crack width. [1 in. = 25.4 mm]

3.6 REINFORCEMENT STRAINS

The reinforcement in each specimen was instrumented with 17 or 21 gauges at the locations shown in Figure 2.9. The recorded strains are plotted versus time in Appendix H for all specimens. For each specimen, three plots are shown: longitudinal reinforcement strain versus time, transverse reinforcement strain versus time, and strain versus time for six selected gauges (on either longitudinal or transverse reinforcement). For the third figure, a plot of load versus time was also included on a secondary vertical axis to allow for easy identification of the load associated with changes in strain. A sample set of plots is shown in this section for specimen P1S3, which contained Grade 60 [Grade 420] HNE transverse reinforcement spaced at $d/2$ and f_{cm} = 4570 psi [31.5 MPa].

Figure 3.20 shows that the strain in the longitudinal reinforcement increased step-wise with time as the load was monotonically increased in increments and then held constant to allow for marking cracks and photographing the specimens. For the first approximately 1400 seconds of the test, the measured strain was highest at midspan (LGM), somewhat lower at a distance d from midspan (LG10-d and LG11-d), and lowest at a distance $2d$ from midspan (LG9-2d and LG12-

2d). Figure 3.20 shows that after 1400 seconds, the strains recorded with LGM, LG10-d, and LG11-d were approximately equal. This change in behavior coincided with the development of pronounced inclined cracking throughout the middle third of the specimen. At approximately 2400 seconds, the strains in the gauges (except LG12-2d) dropped suddenly as the specimen failed in shear. At failure, the strain recorded with LG12-2d increased suddenly to near the yield strain of the longitudinal reinforcement (based on tensile test results plotted in Appendix D) because the failure surface intercepted the longitudinal reinforcement near the location of LG12-2d.

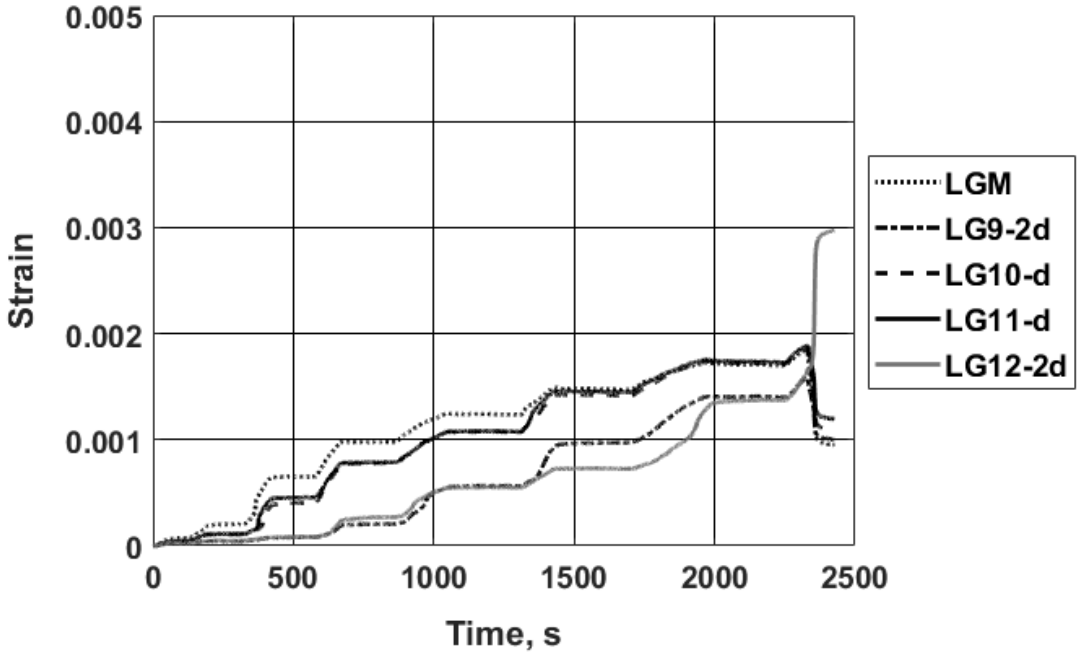

Figure 3.20: Longitudinal reinforcing bar strain: specimen P1S3

The results in Figure 3.20 show that the peak longitudinal reinforcement strains prior to failure were approximately 0.0018, near to the 0.0016 intended in design (Table 2.1). Like specimen P1S3, all but five specimens exhibited shear failures prior to yielding of the longitudinal reinforcement. The five exceptions were specimens P2S10, P2S11, P2S12, P3S9, and P3S10. These specimens exhibited yielding of the longitudinal reinforcement prior to exhibiting a brittle failure along an inclined failure surface consistent with a shear failure mode. Specimens P2S10, P2S11, and P2S12 exhibited longitudinal reinforcement yielding late in the test, before failing in shear at imposed shear forces that were 11, 47, and 46% greater than the nominal shear strength

calculated using measured material properties. Specimens P3S9 and P3S10 were somewhat different because they were designed to yield in flexure prior to failing in shear. Flexural yielding limited the strength of these specimens to 82 and 85% of the nominal beam shear strength.

Figure 3.21 shows transverse reinforcement strain versus time for specimen P1S3. The strain recorded with SG1M and SG8M, each located near mid-depth on a headed transverse bar located approximately 2*d* from midspan, increased more rapidly than the strain at the other strain gauge locations. The yield strain (approximately 0.0024 based on tension tests reported in Appendix D) was exceeded when the applied load exceeded approximately 75% of the peak strength of the specimen, which occurred at approximately 1400 seconds into the test. None of the other gauges recorded strains exceeding the yield strain until the specimen failed at approximately 2400 seconds. The strain recorded with both SG6M and SG8M increased significantly at failure, which is consistent with the failure surface intersecting those transverse bars (as shown in Appendix E).

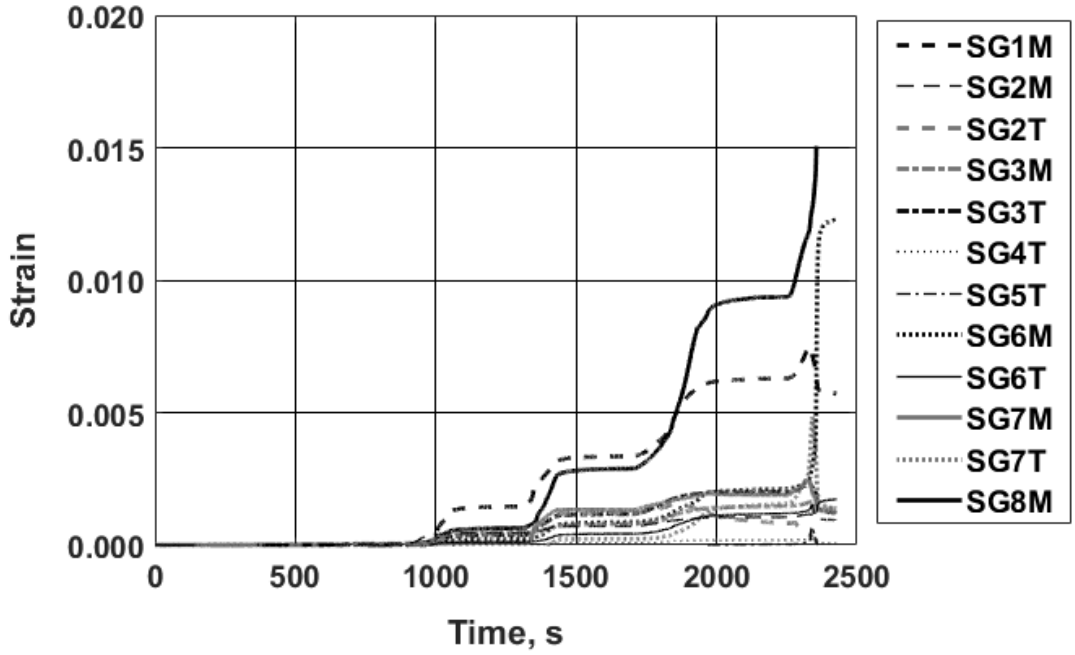

Figure 3.21: Transverse reinforcing bar strain: specimen P1S3

Yielding of the transverse reinforcement in specimen P1S3 prior to failure was typical of specimens in this study. With only five exceptions (specimens P1S15, P2S1, P2S2, P1S11, and

P2S12), at least one instrumented transverse reinforcing bar exhibited strains greater than the yield strain (defined based on tensile tests of bar samples reported in Appendix D) prior to failure. Yielding of transverse reinforcement frequently occurred between 60 and 90% of peak load. The five exceptions are discussed below:

- Specimen P1S15: The transverse reinforcement gauges nearest to the failure surface recorded strains that were below 0.0005 throughout the test. This indicates that the transverse reinforcement was not engaged, which is consistent with the observations after testing that the concrete may have split away from the sides of the specimen in a plane defined by the transverse reinforcement prior to failure (Section 3.2.1).
- Specimens P2S1 and P2S2: Although not certain, the lack of transverse reinforcement yielding prior to failure of specimens P2S1 and P2S2 may be attributable to the shape of the failure crack (Figure 3.22), which could have allowed for direct strut action to provide a force path from the loading point to the supports that circumvented the transverse reinforcement.
- Specimens P2S11 and P2S12: The lack of documented transverse reinforcement yielding is almost certainly due to instrumentation failures. The transverse reinforcement gauges were not functioning in the test of P2S11 and only the gauges near the middle support of specimen P2S12 were functioning. Given the over-strength of these specimens (Section 3.4), it is reasonable to expect that transverse reinforcement did yield prior to failure, consistent with other specimens.

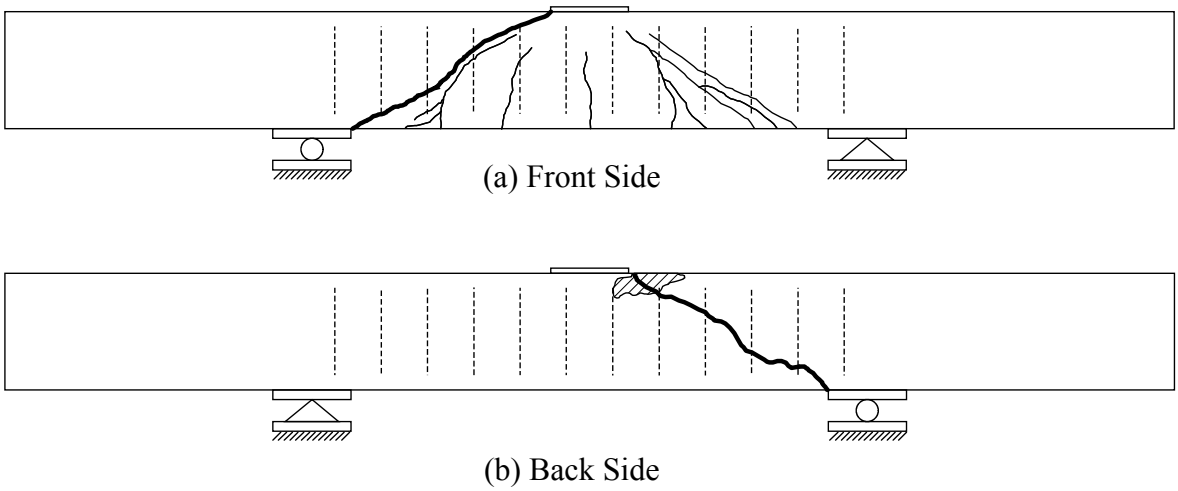

(a) Front Side

(b) Back Side

Figure 3.22: Damage to specimen P2S1 (h = 12 in. [310 mm], f_{ytm} = 86.2 ksi [595 MPa], f_{cm} = 9710 psi [67.0 MPa], S detail)

Figure 3.23 shows strain versus time for six gauges selected from among both the longitudinal and transverse gauges. Load versus time is also shown. The figure allows for a direct comparison between the longitudinal and transverse strains and the load. Whereas the longitudinal reinforcement strains increased somewhat proportionally to the load beginning early in the test, the transverse reinforcement strains did not begin to increase until the load was already near half of the failure load (approximately 1000 seconds into the test) when they were crossed by shear cracks. Shortly thereafter, at around 1400 seconds into the test, the transverse reinforcement strains increased to beyond the yield strain at two locations (gauges SG6M and SG8M). This yielding is consistent with the initiation of pronounced inclined cracking and coincided with the shift in longitudinal strain behavior evident in Figure 3.20 (LG10-d, LGM, and LG11-d began to exhibit similar strains). Figure 3.23 shows that, at failure, the strains recorded with gauges SG6M and SG8M increased suddenly to greater than 0.01 as the failure crack developed near to those gauges. At failure, strains recorded at other gauge locations decreased due to the decrease in load on the specimen. The results plotted in Figure 3.23 also clearly show that recorded longitudinal bar strains did not exceed the yield strain prior to specimen failure.

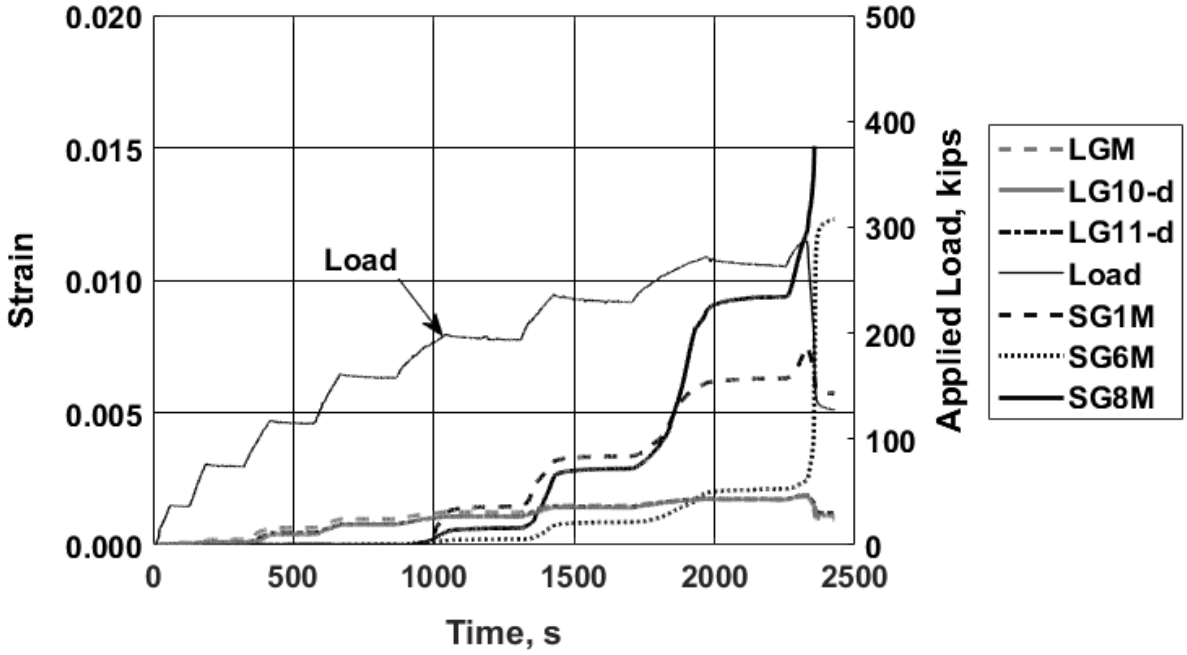

Figure 3.23: Strain recorded with selected gauges and load versus time: specimen P1S3 [1 kip = 4.45 kN]

Finally, strain gauge results can be used to assess whether transverse reinforcing bars with different anchorage types were similarly engaged in resisting shear when anchored within the flexural tension zone. Results from the Phase 3 tests are used here because they had four strain gauges mounted on transverse reinforcement near the bottom of the bars that were therefore within the flexural tension zone (the specimens in Phases 1 and 2 did not have gauges at these locations). In seven of the ten Phase 3 specimens (see Figures H.94, H.97, H.103, H.106, H.109, H.112, and H.118), strains consistent with yielding were recorded near the bottom of the transverse bars, including at loads as low as 40% of the peak specimen strength (P3S1). The only exceptions to this were specimens P3S3, P3S8, and P3S10, which include specimens with both S and HNE2 details. The headed transverse bars and crossties were therefore similarly effective at developing the yield strength of the transverse reinforcing bar when terminated within the flexural tension zone.

3.7 TRANSVERSE REINFORCEMENT ANCHORAGE LENGTHS

The crack maps discussed in Section 3.2 can be used to identify the number of stirrups intersected by the failure surface and the anchorage length available for each of the intersected stirrups (Appendix I). For example, Figure 3.24 shows that the failure surface of specimen P1S1 intersected three stirrup legs on both the front and back sides. It also shows, however, that two of those six stirrup legs had a relatively short anchorage length, where anchorage length is measured from the failure surface to the extreme outer end of the bar for stirrups and to the inside (bearing) face of the head for headed transverse bars. For either anchorage type, the reported anchorage length is the shorter of the lengths measured to the top and bottom of the beam.

The minimum length necessary to anchor a transverse reinforcing bar, represented by a multiple of the bar diameter (xd_b), can be indirectly assessed by calculating the strength of each specimen based on the number of legs of reinforcement that cross the failure surface (n_{legs}) while adjusting the value of n_{legs} based on the anchorage length (xd_b) above or below the failure surface. This was done for each specimen by assuming that that the shear strength could be expressed as the sum of the shear strength attributable to the concrete (V_c), as represented by Eq. (3.2), and the shear strength attributable to the transverse reinforcement ($V_{s,\text{legs}}$), represented by Eq. (3.5).

$$V_{s,\text{legs}} = A_b f_{ytm} n_{\text{legs}} \tag{3.5}$$

where $A_b f_{ytm}$ is the product of the transverse reinforcement area of an individual bar A_b and the measured yield stress f_{ytm}, and n_{legs} is the number of adequately anchored individual legs of transverse reinforcement intercepted by the failure surface determined from the crack maps in Appendix E. For Eq. (3.5), an adequately anchored leg is defined as one with an anchorage length not less than xd_b, where x was varied in the analysis to determine the best value of xd_b, and thus x. For instance, for specimen P1S1, which had No. 4 [No. 13] transverse reinforcement and back side anchorage lengths of 0.5, 6, and 12.6 in. [13, 152, and 320 mm] (see Appendix I), two stirrup legs would be considered adequately anchored for $1 < x \leq 12$.

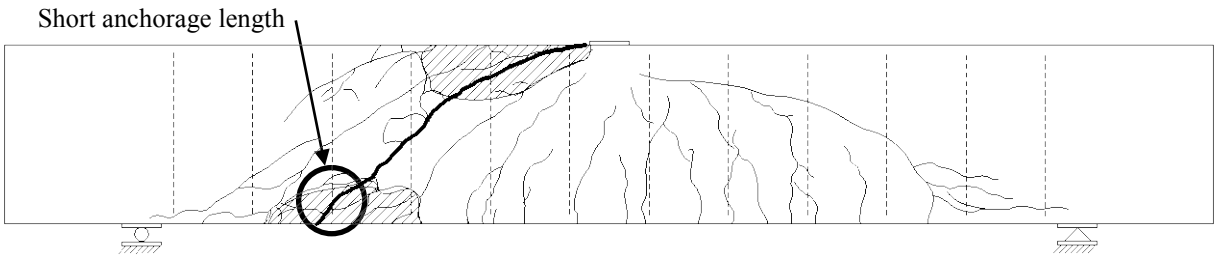

(a) Front side

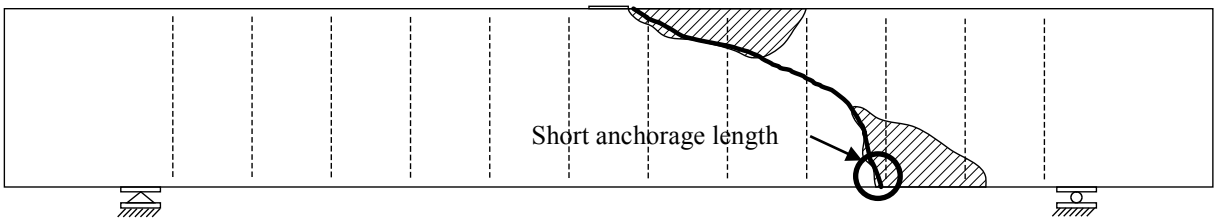

(b) Back side

Figure 3.24: Damage to specimen P1S1

The effect of anchorage length on the contribution of transverse reinforcement to shear strength was examined by comparing the values of the measured shear strength of each specimen (V_T) with $V_{n,\text{legs}}$, where $V_{n,\,legs} = V_c + V_{s,\,legs}$. Nine specimens were omitted from this analysis due to missing anchorage length data (specimen P2S3), atypical behavior (specimen P1S15), a failure mechanism that may not have engaged the transverse reinforcement (P2S1 and P2S2, described in Section 3.6), or longitudinal reinforcement yielding prior to failure (specimens P2S10 through P2S12, P2S9, and P3S10). As shown in Figure 3.25, the mean value of $V_T/V_{n,\text{legs}}$ increases from 0.83 to 1.13 as x increases from 0 to 15. The mean, however, may not be the best value to use for establishing x because V_c, as expressed in Eq. (3.1), does not reflect all aspects that affect the concrete contribution to shear strength (for example, shear-span to depth ratio, flexural reinforcement ratio, size effect). A better measure of the role of anchorage is perhaps shown in Figure 3.26, where the coefficient of variation (COV) of $V_T/V_{n,\text{legs}}$ is compared with x. For $0 \le x \le 15$, COV of $V_T/V_{n,\text{legs}}$ was between 0.124 and 0.154, with a minimum of 0.124 at $x = 5$.

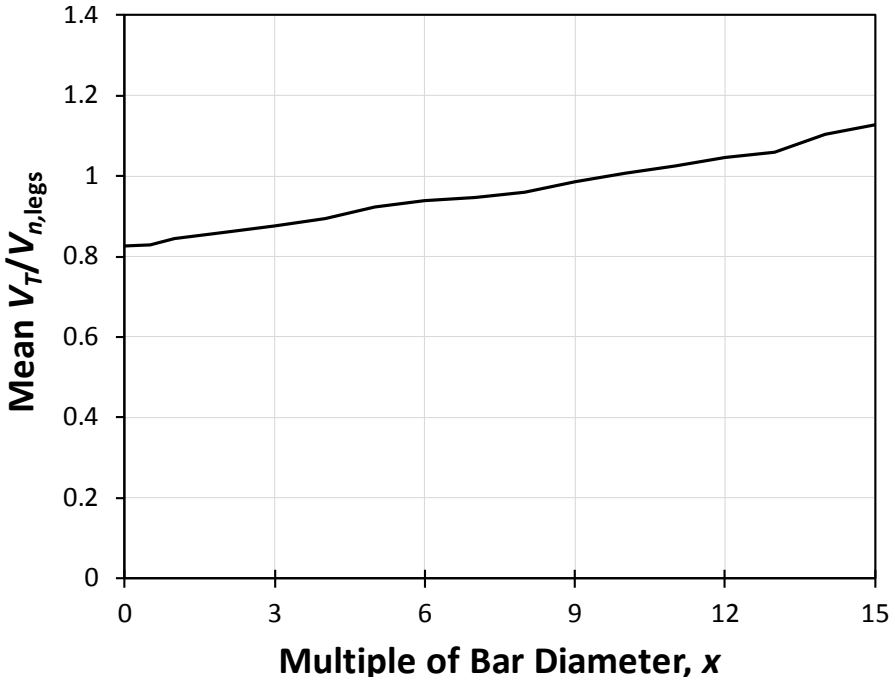

Figure 3.25: Mean of $V_T/V_{n,\text{legs}}$ versus multiple of bar diameter x, where xd_b is the minimum length necessary to anchor a transverse reinforcing bar

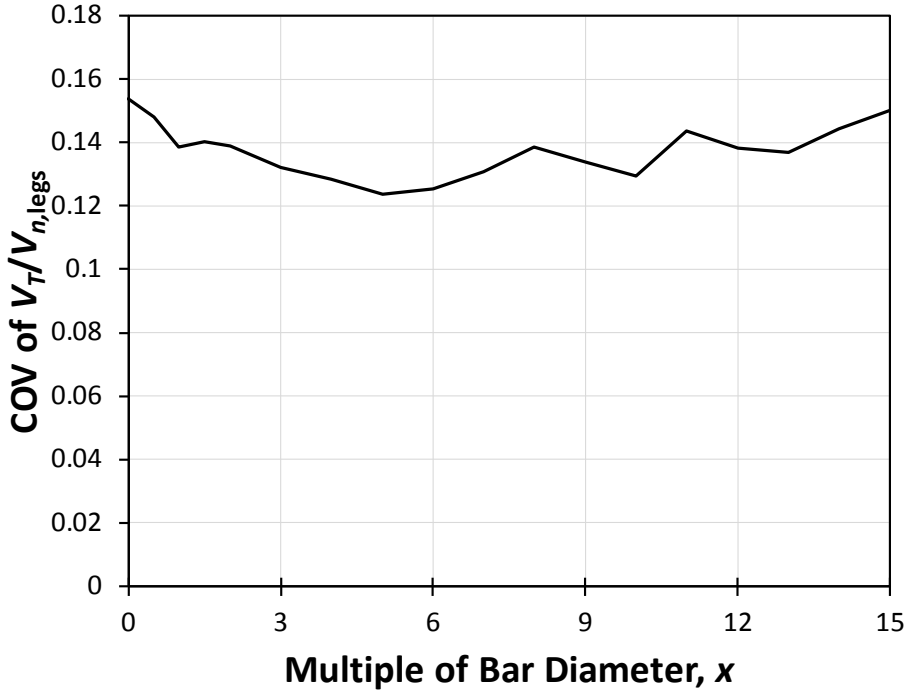

Figure 3.26: COV of $V_T/V_{n,\text{legs}}$ versus multiple of bar diameter x, where xd_b is the minimum length necessary to anchor a transverse reinforcing bar

A question that can be addressed by investigating $V_T/V_{n,\text{legs}}$ using the outcome of the analysis shown in Figure 3.26 is whether stirrups and headed transverse bars are similarly effective at developing the strength of transverse reinforcement. Groups of specimens with S, HE, HNE, and HNE2 anchorage details were compared in terms of $V_T/V_{n,\text{legs}}$ calculated with $x = 5$. The mean values of $V_T/V_{n,\text{legs}}$ for beams with S, HE, HNE, and HNE2 anchorage details were 0.852, 0.982, 0.979, and 0.939, implying that headed transverse bars may have been more effectively anchored at the critical section than stirrups with equal anchorage length, but the differences between these groups are not statistically significant based on Student's t-test (for example, $p = 0.10$, 0.066, and 0.17 for S specimens compared with similar HE, HNE, and HNE2 specimens, respectively).

Another pertinent question that can be addressed is whether the low strengths of beams with $\rho_t f_{ytm} < 80$ psi [550 kPa] are attributable to failure surfaces circumventing widely spaced transverse reinforcement. Because $V_{n,\text{legs}}$ ostensibly accounts for the number of engaged transverse bars crossed by the failure surface, groups of specimens with $\rho_t f_{ytm} < 80$ psi [550 kPa] and specimens with $\rho_t f_{ytm} > 80$ psi [550 kPa] were compared based on $V_T/V_{n,\text{legs}}$. Differences in $V_T/V_{n,\text{legs}}$ between specimens with $\rho_t f_{ytm} < 80$ psi [550 kPa] and specimens with $\rho_t f_{ytm} > 80$ psi [550 kPa] were again statistically significant ($p = 0.011$), although marginally less so than comparisons with V_T/V_n in Section 3.4 ($p = 0.0018$). The Student's t-test output is slightly sensitive to x, with p varying between 0.0024 and 0.011 for $0 \le x \le 6$. Regardless of the value of x selected, the high degree of significance of the correlation between low $V_T/V_{n,\text{legs}}$ values and $\rho_t f_{ytm} < 80$ psi indicates that the low strengths are likely attributable to $\rho_t f_{ytm} < 80$ psi [550 kPa] and not transverse reinforcement spacing.

3.8 RECOMMENDATIONS

Results are reported for 39 tests of beams designed to fail in shear. The tests were primarily designed to investigate the use of high strength (Grade 80) and headed bars as shear reinforcement. Key findings are summarized below:

Grade 80 [Grade 550] Transverse Reinforcement

It is recommended that Grade 80 [Grade 550] steel be permitted for use as transverse reinforcement for shear. Increasing the transverse reinforcement grade from Grade 60 [Grade 420] to Grade 80 [Grade 550] had no discernable effect on the crack patterns, load-deflection behavior, or shear strength. The only notable difference in behavior was a difference in inclined crack width. At 60 to 70% of nominal strength, maximum crack widths in beams with Grade 80 [Grade 550] transverse reinforcement were similar to or greater than the largest cracks in beams with Grade 60 [Grade 420] transverse reinforcement. These differences, however, were smaller than differences in crack width associated with increases in overall beam depth h, with h in the range of 12 to 48 in. [310 to 1220 mm]. The results, therefore, indicate that inclined crack widths will not represent a serviceability problem when Grade 80 [Grade 550] reinforcement is used.

Headed Transverse Reinforcement

It is recommended that headed transverse reinforcement be permitted as an alternative to stirrups and crossties for use as shear reinforcement in beams, foundations, and walls when used in a manner similar to that used in the specimens tested in this study. No. 6 [No. 19] and smaller headed bars are effective as shear reinforcement if the headed transverse bars are located away from the side faces of the member, similar to the HNE2 detail, and are enclosed by not less than one longitudinal bar with a clear cover to the transverse reinforcement of six bar diameters. In the current study, the minimum cover was 4.25 in. [110 mm] for No. 4 and No. 6 [No. 13 and No. 19] bars, representing clear covers of 8.5 and $5.7d_b$, respectively. No. 4 [No. 13] and smaller headed transverse reinforcement is not required to engage longitudinal reinforcement to be effective. Compared to beams with stirrups, beams with No. 4 [No. 13] headed transverse bars that either engaged or did not engage the longitudinal reinforcement had no discernable difference in overall behavior in terms of load versus deflection or crack widths, with the exception of beams with the HNE anchorage detail, which consisted of headed transverse bars placed near ($4d_b$) to the outside faces of the beam and not engaging longitudinal reinforcement exhibited somewhat different crack patterns than similar specimens with different transverse reinforcement anchorage details, and one specimen, specimen P1S15, failed in an unexpected manner at low strength.

Specimen P1S15 notwithstanding, there was no statistically significant difference in the ratio of measured to nominal shear strength V_T/V_n (with V_n calculated in accordance with ACI 318-14) between specimens with stirrups and headed transverse bars. Both stirrups and headed transverse bars exhibited strains consistent with yielding near the bottom of the bar within the flexural tension zone, indicating that tensile stresses orthogonal to the bar axis did not compromise the effectiveness of either hooked or headed anchorages for transverse bars.

Low Transverse Reinforcement Index ($\rho_t f_{ytm}$)

It is recommended that the value of minimum shear reinforcement required by ACI 318-14 be reevaluated. Although all specimens had transverse reinforcement areas exceeding the minimum (Eq. (3.4)), which ranged from 50 to 75 psi [345 to 520 kPa] for this study, low shear strengths relative to the nominal strength based on the provisions of ACI 318-14 strongly correlated with the lowest values of $\rho_t f_{ytm}$ used in this study. Of the nine specimens with $\rho_t f_{ytm}$ less than 80 psi [550 kPa], eight (89%) had ratios of measured-to-nominal shear strength V_T/V_n (with V_n calculated in accordance with ACI 318-14) less than 1.0. Differences in V_T/V_n between groups of specimens with $\rho_t f_{ytm} < 80$ psi [550 kPa] and with $\rho_t f_{ytm} > 80$ psi [550 kPa] were statistically significant ($p = 0.0018$). This was also true after nominal strength was modified to account for the number of transverse bars intercepted by the failure surface ($p = 0.011$).

Headed deformed bars serving as confining reinforcement for development of reinforcement

An issue beyond the scope of this study is the role of headed bars used as transverse reinforcement in providing confinement to longitudinal bars that are developed or spliced. The key concern is the potential for splitting cracks to pass around the heads of the confining reinforcement, as illustrated in Figure 3.27. Based on the lack of data, it is recommended that headed deformed bars used as shear reinforcement not be considered as contributing to confinement when calculating development or splice lengths unless there is sufficient space between the plane defined by the bearing face of the head and the plane defined by the center of the reinforcement being developed.

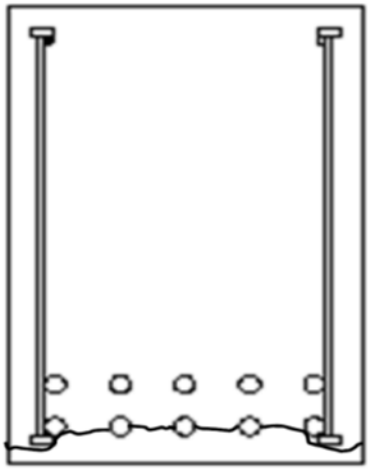

Figure 3.27: Splitting cracks not intercepted by headed deformed bars serving as transverse reinforcement.

CHAPTER 4: CODE PROVISIONS

4.1 GENERAL

The work described in this report supports changes to the ACI Building Code that will permit Grade 80 [Grade 550] deformed reinforcing bars and headed deformed bars to be used as shear reinforcement. Similar changes should be considered for adoption in ACI 349 and ACI 359. Tests were performed on members with total depths between 12 and 48 in. [310 and 1220 mm]. To ensure adequate anchorage, the lowest depth, 12 in. [310 mm], is used as the lower limit for members in which headed bars may be used as shear reinforcement. Placement inside at least one longitudinal bar with a minimum clear side cover to the shear reinforcement of six headed bar diameters is required for members where headed shear reinforcement does not engage the longitudinal reinforcement.

For simplicity, the proposed provisions are presented for ACI 318 in in.-lb units; equivalent provisions in SI units would be applicable for ACI 318M.

4.2 PROPOSED CODE PROVISIONS

This section lists proposed changes to the ACI Building Code and Commentary that are based on the reported test results. The section numbers are those that appear in ACI 318-14. Code changes are indicated using underline and ~~strikeout~~:

CHAPTER 8—TWO-WAY SLABS

8.4—Required strength

8.4.4 Factored two-way shear

8.4.4.1 Critical section

8.4.4.1.2 Slabs reinforced with stirrups, ~~or~~ headed shear stud reinforcement, or headed deformed bars shall be evaluated for two-way shear at critical sections in accordance with 22.6.4.2.

8.7—Reinforcement detailing

8.7.8 Shear reinforcement – headed deformed bars

8.7.8.1 Headed deformed bars are permitted as shear reinforcement in two-way slabs with a total depth not less than 12 in.

8.7.8.2 Headed deformed bar anchorage shall be in accordance with 25.7.2.

8.7.8.3 The spacing requirements of 8.7.6.3 for stirrups shall apply for headed deformed bars.

R8.7.8 Shear reinforcement – headed deformed bars

R8.7.8.1 The minimum total depth of 12 in. is based on the lower limit used in tests evaluating headed deformed bars as shear reinforcement.

CHAPTER 9—BEAMS

9.7—Reinforcement detailing

9.7.6 Transverse reinforcement

9.7.6.2 *Shear*

9.7.6.2.1 If required, shear reinforcement shall be provided using stirrups, hoops, ~~or~~ longitudinal bent bars, or headed deformed bars.

CHAPTER 20—STEEL REINFORCEMENT PROPERTIES, DURABILITY, AND EMBEDMENTS

20.2—Nonprestressed bars and wires

20.2.2 Design Properties

20.2.2.4 Types of nonprestressed bars and wires to be specified for particular structural applications shall be in accordance with Table 20.2.2.4a for deformed reinforcement and Table 20.2.2.4b for plain reinforcement.

Table 20.2.2.4a—Nonprestressed deformed reinforcement

Usage	Application	Maximum value of f_y or f_{yt} permitted for design calculations, psi.	Applicable ASTM specification			
			Deformed bars	Deformed wires	Welded wire reinforcement	Welded deformed bar mats
Flexure; axial force; and shrinkage and temperature	Special seismic systems	60,000	Refer to 20.2.2.5	Not permitted	Not permitted	Not permitted
	Other	80,000	A615, A706, A955, A996	A1064, A1022	A1064, A1022	A184[1]
Lateral support of longitudinal bars; or concrete confinement	Special seismic systems	100,000	A615, A706, A955, A996, A1035	A1064, A1022	A1064[2], A1022[2]	Not permitted
	Spirals	100,000	A706, A955, A996, A1035	A1064, A1022	Not permitted	Not permitted
	Other	80,000	A615, A706, A955, A996	A1064, A1022	A1064, A1022	Not permitted
Shear	Special seismic systems	60,000	A615, A706, A955, A996	A1064, A1022	A1064[2], A1022[2]	Not permitted
	Spirals	60,000	A615, A706, A955, A996	A1064, A1022	Not permitted	Not permitted
	Shear friction	60,000	A615, A706, A955, A996	A1064, A1022	A1064, A1022	Not permitted
	Stirrups, ties, hoops, headed deformed bars	60,000	A615, A706, A955, A996	Not permitted	A1064 and A1022 welded plain wire	Not permitted
		80,000	~~Not permitted~~ A615, A706, A955, A996	Not permitted	A1064 and A1022 welded deformed wire	Not permitted
Torsion	Longitudinal and transverse	60,000	A615, A706, A955, A996	A1064, A1022	A1064, A1022	Not permitted

[1]Welded deformed bar mats shall be permitted to be assembled using A615 or A706 deformed bars.
[2]ASTM A1064 and A1022 are not permitted in special seismic systems where the weld is required to resist stresses in response to confinement, lateral support of longitudinal bars, shear, or other actions.

CHAPTER 22—SECTIONAL STRENGTH

22.5—One-way shear strength

22.5.10 One-way shear reinforcement

22.5.10.5 One-way shear strength provided by transverse reinforcement

22.5.10.5.1 In nonprestressed and prestressed members, shear reinforcement satisfying (a), (b), or (c) shall be permitted:

(a) Stirrups, ties, ~~or~~ hoops, or headed deformed bars perpendicular to longitudinal axis of member

(b) Welded wire reinforcement with wires located perpendicular to longitudinal axis of member

(c) Spiral reinforcement

22.5.10.5.2 Headed deformed bars shall be permitted to be used as one-way shear reinforcement where ***h*** is not less than 12 in.

Renumber subsequent sections.

22.6—Two-way shear strength

R22.6—Two-way shear strength

Factored shear stress in two-way members due to shear and moment transfer is calculated in accordance with the requirements of 8.4.4. Section 22.6 provides requirements for determining nominal shear strength, either without shear reinforcement or with shear reinforcement in the form of stirrups, headed shear studs, headed deformed bars, or shearheads. Factored shear demand and strength are calculated in terms of stress, permitting superposition of effects from direct shear and moment transfer.

22.6.1 *General*

22.6.1.7 For two-way members reinforced with single- or multiple-leg stirrups or headed deformed bars, v_s shall be calculated in accordance with 22.6.7.

22.6.4 Critical sections for two-way members

22.6.4.2 For two-way members reinforced with headed shear reinforcement, headed deformed bars, or single- or multi-leg stirrups, a critical section with perimeter b_o located $d/2$ beyond the outermost peripheral line of shear reinforcement shall also be considered. The shape of this critical section shall be a polygon selected to minimize b_o.

22.6.7 Two-way shear strength provided by single- or multiple-leg stirrups or headed deformed bars

22.6.7.2 Headed deformed bars shall be permitted to be used as shear reinforcement in slabs and footings satisfying (a) and (b):

(a) ***h*** is at least 12 in.

(b) ***d*** is at least $16d_b$, where d_b is the diameter of the headed deformed bars

22.6.7.23 For two-way members with stirrups or headed deformed bars, v_s shall be calculated by:

$$v_s = \frac{A_v f_{yt}}{b_o s} \tag{22.6.7.2}$$

where A_v is the sum of the area of all legs of reinforcement on one peripheral line that is geometrically similar to the perimeter of the column section, and s is the spacing of the peripheral lines of shear reinforcement in the direction perpendicular to the column face.

CHAPTER 25—REINFORCEMENT DETAILS

25.4—Development of reinforcement

25.4.2 Development of deformed bars and deformed wires in tension

25.4.2.2 Headed deformed bars shall not be considered as contributing to transverse reinforcement A_{tr} in the calculation of K_{tr} in 25.4.2.3.

R25.4.2.2 The limitation on including headed deformed bars in the calculation of K_{tr} is based on the potential that the splitting crack accompanying bond failure may not be intercepted by the transverse headed bars, as shown in Fig. R25.4.2.2.

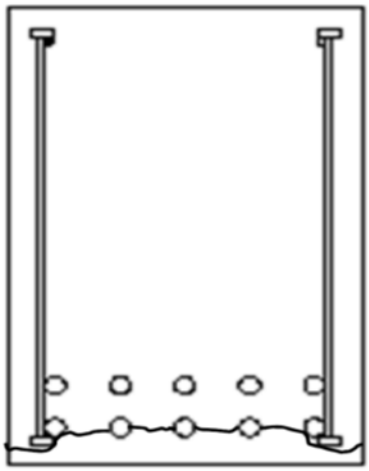

Fig. R25.4.2.2—Splitting cracks not intercepted by headed deformed bars serving as transverse reinforcement.

Renumber subsequent sections.

25.7—Transverse reinforcement

25.7.2 Headed deformed bars

25.7.2.1 Headed deformed bars with heads at both ends shall extend as close to the compression and tension surfaces of the member as cover requirements and proximity of other reinforcement permits. Where used as shear reinforcement, the bearing face of the head near the tension surface shall not be less than a distance ***d*** from the extreme compression fiber.

25.7.2.2 Headed deformed bars used as shear reinforcement shall consist of a straight length of headed deformed bar, with a head conforming to the requirements of 20.2.1.6 attached to both ends.

25.7.2.3 Headed deformed bars shall be anchored in accordance with (a) or (b):

(a) For No. 4 and smaller bars, engage the heads with the longitudinal reinforcement

(b) For No. 6 and smaller bars, locate the headed deformed bars inside at least one longitudinal bar with clear concrete side cover to the shear reinforcement of at least $\mathbf{6}\boldsymbol{d_b}$, where $\boldsymbol{d_b}$ is the nominal diameter of the shear reinforcement

25.7.2.4 Headed deformed bars larger than No. 6 shall not be used as shear reinforcement

R25.7.2 Headed deformed bars

R25.7.2.1 As with stirrups, headed bars used as shear reinforcement should be extended as close as practicable to the compression face of the member. Tests show that heads can provide adequate anchorage if the bars are anchored as required in 25.7.2.3.

R25.7.2.3 Tests demonstrate that headed deformed bars provide shear strength equal to that of stirrups if No. 4 and smaller headed bars engage longitudinal reinforcement with the bearing face of the head in contact with a longitudinal bar or if No. 6 and smaller headed bars are placed inside longitudinal reinforcement with side cover to the headed bar of at least six bar diameters.

Renumber subsequent sections.

CHAPTER 5: SUMMARY AND CONCLUSIONS

5.1 SUMMARY

This project focused on determining whether headed deformed bars can used in reinforced concrete members in place of stirrups as shear reinforcement as well as whether shear reinforcement with yield strengths up to 80 ksi [550 MPa] can be used without problems related to either strength or serviceability with the goal of improving the economy and ease of construction of nuclear power plants, as well as conventional buildings, both in the U.S, and internationally. Thirty-nine beams with a shear span-to-depth ratio of 3 were tested. Shear reinforcement consisted of Grade 60 and Grade 80 [Grade 420 and 550] No. 3, No. 4, and No. 6 [No. 10, No. 13, and No. 19] headed deformed bars and stirrups spaced between one-quarter and one-half of the member effective depth. For direct comparisons, Grade 60 and Grade 80 [Grade 420 and Grade 550] shear reinforcement was designed to provide approximately the same contribution to shear strength ($\rho_t f_{ytm}$ = product of measured yield strength and bar area divided by product of beam width and reinforcement spacing). For each set of test parameters, the shear strength of members reinforced with U stirrups and crossties was compared with the strength of matching specimens reinforced with headed bars as shear reinforcement. Within each group of specimens, the stirrups and headed bars of the same grade were fabricated from the same heat of steel. Stirrups were anchored around longitudinal bars, as required by ACI 318-14. Headed bars were anchored using one of three details: (1) engaged with longitudinal bars, that is, with the bearing face of the head in contact with a longitudinal bar; (2) not engaged with longitudinal reinforcement, with the headed bar outside of the longitudinal reinforcement and close to the side of the member; and (3) not engaged with longitudinal reinforcement, with the headed bar inside of the longitudinal reinforcement and at least 4 in. [100 mm] from the side of the member. Member depths of 12, 18, 36, and 48 in. [310, 460, 910, and 1220 mm] were used in conjunction with widths of 24 and 42 in. [610 and 1070 mm]. Test specimens included singly-reinforced members, representing beams, and doubly-reinforced members, representing walls and mat foundations. Modifications to ACI 318-14 are proposed.

5.2 CONCLUSIONS

The following conclusions are based on the test results and analyses presented in the report.

1. Adequately anchored headed deformed bars provide shear strengths that are equivalent to hooked stirrups. Furthermore, strain measurements taken near the anchorage points of the shear reinforcement indicate both types of anchorage are capable of developing yield strains in the reinforcement.
2. Headed bars used as shear reinforcement are adequately anchored when placed (1) in direct contact between the bearing face of the head with longitudinal reinforcement for No. 4 [No. 13] or smaller bars or (2) inside at least one longitudinal bar and providing side concrete cover to the headed bar of at least six headed bar diameters for No. 6 [No. 19] or smaller bars. Placing headed bars outside of longitudinal reinforcement and close to the side of a member may result in reduced shear strength.
3. Grade 80 [Grade 550] shear reinforcement provides the same strength and similar serviceability as Grade 60 [Grade 420] shear reinforcement.
4. Low strengths relative to the nominal strength calculated using the provisions of ACI 318-14 occurred for specimens with $\rho_t f_{ytm}$ below 80 psi [550 kPa]. This finding indicates that the value of the minimum shear reinforcement prescribed in ACI 318-14 should be reevaluated.
5. Shear crack widths increase with beam depth.

REFERENCES

ACI Committee 318, 2014, *Building Code Requirements for Structural Concrete (ACI 318-14) and Commentary (ACI 318R-14)*, American Concrete Institute, Farmington Hills, MI, 519 pp.

ACI Committee 349, 2013, *Code Requirements for Nuclear Safety-Related Concrete Structures (ACI 349-13) and Commentary*, American Concrete Institute, Farmington Hills, MI, 196 pp.

ACI Committee 359, 2013, *Code for Concrete Containments (ACI 359-13)*, Section III, Division 2, ASME Boiler and Pressure Vessel Code, American Society of Mechanical Engineers, New York.

ASTM A370, 2017. "Standard Test Methods and Definitions for Mechanical Testing of Steel Products," (ASTM A370/A370M-17), ASTM International, West Conshohocken, Pennsylvania, 8 pp.

ASTM A970, 2016. "Standard Specification for Headed Steel Bars for Concrete Reinforcement," (ASTM A970/A970M-16), ASTM International, West Conshohocken, Pennsylvania, 9 pp.

ASTM A1044, 2015. "Standard Specification for Steel Stud Assemblies for Shear Reinforcement of Concrete," (ASTM A1044/A1044M-15), ASTM International, West Conshohocken, Pennsylvania, 5 pp.

ASTM C39, 2017. "Standard Test Method for Compressive Strength of Cylindrical Concrete Specimens," (ASTM C39/C39M-17b), ASTM International, West Conshohocken, Pennsylvania, 8 pp.

ASTM C138, 2017. "Standard Test Method for Density (Unit Weight), Yield, and Air Content (Gravimetric) of Concrete," (ASTM C138/C138M-17a), ASTM International, West Conshohocken, Pennsylvania, 6 pp.

ASTM C143, 2015. "Standard Test Method for Slump of Hydraulic-Cement Concrete," (ASTM C143/C143M-15a), ASTM International, West Conshohocken, Pennsylvania, 4 pp.

ASTM C231, 2017. "Standard Test Method for Air Content of Freshly Mixed Concrete by the Pressure Method," (ASTM C231/C231M-17a), ASTM International, West Conshohocken, Pennsylvania, 10 pp.

ASTM C1064, 2017. "Standard Test Method for Temperature of Freshly Mixed Hydraulic-Cement Concrete," (ASTM C1064/C1064M-17), ASTM International, West Conshohocken, Pennsylvania, 3 pp.

Collins, M. P., and Kuchma, D., 1999, "How Safe Are Our Large, Lightly Reinforced Concrete Beams, Slabs, and Footings?" *ACI Structural Journal*, Vol. 96, No. 4, July-Aug., pp. 482-491.

Darwin, D., Dolan, C., and Nilson, A., 2016, *Design of Concrete Structures*, 15th edition. McGraw Hill, New York, 786 pp.

Dyken, T. and Kepp, B., 1988, "Properties of T-Headed Reinforcing Bars in High Strength Concrete," *Nordic Concrete Research*, Vol. 7, No. 4, pp. 41-51.

Gayed, R. B. and Ghali, A., 2004, "Double-Head Studs as Shear Reinforcement in Concrete I-Beams," *ACI Structural Journal*, Vol. 101, No. 4, July-Aug., pp. 549-557.

Jaeger, T. and Marti, P., 2009, "Reinforced Concrete Slab Shear Prediction Competition: Experiments," *ACI Structural Journal*, Vol. 106, No. 3, pp. 300-308.

Kani, G. N. J., 1967, "How Safe Are Our Large Reinforced Concrete Beams?" *Journal of the American Concrete Institute*, Vol. 64, No. 3, Mar., pp. 128-141.

Kim, Y. H., Yoon, Y. S., Cook, W. D., and Mitchell, D., 2004, "Repeated Loading Tests of Concrete Walls Containing Headed Shear Reinforcement," *Journal of Structural Engineering*, ASCE, Vol. 130, No. 8, Aug., pp. 1233-1241.

Kuo, W. W., Hsu, T. T. C., and Hwang, S. J., 2014, "Shear Strength of Reinforced Concrete Beams" *ACI Structural Journal*, Vol. 111, No. 4, July-Aug., pp. 809-818.

Lee, J., Choi, I., and Kim, S., 2011, "Behavior of Concrete Beams Reinforced with ASTM A1035 Grade 100 Stirrups under Shear," *ACI Structural Journal*, Vol. 108, No. 1, Jan.-Feb., pp. 620-629.

Loov, R. E., 2002, "Shear Design of Uniformly Loaded Beams," *Proceedings of the Sixth International Conference on Short and Medium Span Bridges*, Vancouver, BC, Canada, pp. 515-522.

Lubell, A. S., Bentz, E. C., and Collins, M. P., 2009, "Headed Shear Reinforcement Assemblies for One-Way Shear," *ACI Structural Journal*, Vol. 106, No. 6, Nov.-Dec. pp. 878-886.

Lutz, L., and Gergely, P., 1968, "Maximum Crack Width in Reinforced Concrete Flexural Members," *ACI Special Publication* 20, Jan., pp. 87-117.

Marzouk, H. and Jiang, D., 1997, "Experimental Investigation on Shear Enhancement Types for High-Strength Concrete Plates," *ACI Structural Journal*, Vol. 94, No. 1, pp. 49-58.

Monteleone, V., 1993, "Headed Shear Reinforcement in Shell Elements Under Reversed Cyclic Loading" (Masters Degree Thesis), University of Toronto, Canada, 267 pp.

Munikrishna, A., Hosny, A., Rizkalla, S., and Zia, P., 2011, "Shear Behavior of Reinforced Concrete Beams with High-Strength Stirrups," *ACI Structural Journal*, Vol. 108, No. 5, Sep.-Oct., pp. 34-41.

Reineck, K.-H., Bentz, E. C., Fitik, B., Kuchma, D. A., and Bayrak, O., 2013, "ACI-DAfStb Database of Shear Tests on Slender Reinforced Concrete Beams without Stirrups," *ACI Structural Journal*, Vol. 110, No. 5, Sep.-Oct., pp. 867-875.

Sherwood, E., Lubell, A., Bentz, E., and Collins, M., 2006, "One-Way Shear Strength of Thick Slabs and Wide Beams," *ACI Structural Journal*, Vol. 103, No. 6, Nov.-Dec., pp. 794-802.

Sumpter M., Rizkalla, S., and Zia, P., 2009, "Behavior of High-Performance Steel as Shear Reinforcement for Concrete Beams," *ACI Structural Journal*, Vol. 106, No. 2, Mar.-Apr., pp. 171-177.

Taub, J., and Neville, A. M., 1960a, "Resistance to Shear of Reinforced Concrete Beams Part 1– Beams without Web Reinforcement," *Journal of the American Concrete Institute*, Vol. 57, No. 11, Nov, pp. 193-220.

Taub, J., and Neville, A. M., 1960b, "Resistance to Shear of Reinforced Concrete Beams Part 2– Beams with Vertical Stirrups," *Journal of the American Concrete Institute*, Vol. 57, No. 12, Dec., pp. 315-336.

Tompos, E. J., and Frosch, R. J., 2002, "Influence of Beam Size, Longitudinal Reinforcement, and Stirrup Effectiveness on Concrete Shear Strength," *ACI Structural Journal*, Vol. 99, No. 5, Sep.-Oct., pp. 559-567.

Yang, J. M., Min, K. H., Shin, H. O., and Yoon, Y. S., 2010, "The Use of T-Headed Bars in High-Strength Concrete Members," *Fracture Mechanics of Concrete and Concrete Structures – High Performance, Fiber Reinforced Concrete, Special Loadings, and Structural Applications*, B. H. Oh (ed.), Korea Concrete Institute, pp. 1328-1334.

Yang, Y., 2015, "Shear Strength and Behavior of Reinforced Concrete Structures with T-Headed Bars in Safety-Related Nuclear Facilities" (Doctoral Thesis), Purdue University, West Lafayette, Indiana, 251 pp.

Yoshida, Y., 2000, "Shear Reinforcement for Large Lightly Reinforced Concrete Members" (Masters Degree Thesis), University of Toronto, Canada, 160 pp.

Zheng, L., 1989, "Shear Tests to Investigate Stirrup Spacing Limits" (Masters Degree Thesis), University of Toronto, Canada, 177 pp.

APPENDIX A: NOTATION AND CONVERSION FACTORS

The following is the notation used throughout the text of this report. Where applicable, it is in accordance with ACI 318-14.

a_v Shear span, distance from the center of the concentrated load to the center of the support, in.

A_b Area of an individual reinforcing bar, in.^{2}

A_{brg} Bearing area of head, in.^{2}

A_s Area of longitudinal tension reinforcement, in.^{2}

A'_s Area of longitudinal compression reinforcement, in.^{2}

A_v Area of shear reinforcement within spacing s, in.^{2}

$A_{v,min}$ Minimum area of shear reinforcement within spacing s, in.^{2}

b_w Web width of a beam, in.

b Width of compression face of member, equal to b_w, in.

d Distance from top of beam to centroid of tension reinforcement, in.

d' Distance from top of beam to centroid of compression reinforcement, in.

Δ_{max} Deflection corresponding to maximum applied load, in.

ε_{long} Strain of the longitudinal tension reinforcement

f'_c Specified concrete compressive strength, ksi

f_{cm} Measured average compressive strength of concrete, from testing three, 6 × 12 in. steel-formed concrete cylinders, ksi

f_v Stress applied to transverse reinforcing bar, ksi

f_y Yield strength of longitudinal tension reinforcement, ksi

f_{yt} Yield strength of transverse reinforcement, ksi

h Total specimen depth, in.

λ Reduction factor applied to mechanical properties of lightweight concrete

ℓ_T Measured total length of specimen, in.

M_u Factored moment at section, kip-in.

n Total number of stirrups/headed bars intercepted by a crack

n_{legs} Total number of effective legs of transverse reinforcement intercepted by the failure surface

ϕ Strength reduction factor

s Spacing of transverse reinforcement, center-to-center, in.

V_c Nominal shear strength attributed to concrete, kips

V_{cz} Shear force from uncracked concrete compression zone, contribution to V_c, kips

V_d Shear force from dowel action, contribution to V_c, kips

V_i Shear force from aggregate interlock, contribution to V_c, kips

V_s Nominal shear strength attributed to transverse reinforcement, kips

$V_{s,legs}$ Nominal shear strength attributed to transverse reinforcement accounting for the number of legs of shear reinforcement intercepted by the failure surface, kips

V_n Nominal shear strength (V_c+V_s), kips

$V_{n,legs}$ Nominal shear strength (V_c+$V_{s,legs}$) accounting for the number of legs of shear reinforcement intercepted by the failure surface, kips

V_T Tested shear strength, kips

V_u Factored shear force at section, kips

P_{max} Maximum applied load, kips

ρ Tension reinforcement ratio, A_s/bd

ρ' Compression reinforcement ratio, A'_s/bd

ρ_t Transverse reinforcement ratio, $A_v/b_w s$

ρ_w Tension reinforcement ratio within the beam web, $A_s/b_w d$

For the interested reader, the following table includes more information about the conversions used and can be utilized to provide increased precision for converting between units.

Table A.1: Conversion Factors

in.-lb	**SI Equivalent**
Length	
1 in.	25.4 mm
Area	
1 in^2	6.45×10^{-4} m^2
Solid Volume	
1 ft^3	2.83×10^{-2} m^2
1 yd^3	0.765 m^3
Liquid Volume	
1 oz	29.6 mL
Force	
1 lb	4.45 N
1 kip (kilopound)	4.45 kN
Stress	
1 psi	6.89 kPa
1 ksi	6.89 MPa
Unit Weight	
1 lb/ft^3	16.0 kg/m^3
1 lb/yd^3	0.593 kg/m^3
Yield Strength (Reinforcing Steel)	
60,000 psi (Grade 60)	420 MPa (Grade 420)
75,000 psi (Grade 75)	520 MPa (Grade 520)
80,000 psi (Grade 80)	550 MPa (Grade 550)
100,000 psi (Grade 100)	690 MPa (Grade 690)
120,000 psi (Grade 120)	830 MPa (Grade 830)

Table A.2: Equivalent Bar Sizes

in.-lb	**SI**
No. 3	No. 10
No. 4	No. 13
No. 5	No. 16
No. 6	No. 19
No. 7	No. 22
No. 8	No. 25
No. 9	No. 29
No. 10	No. 32
No. 11	No. 36
No. 14	No. 43
No. 18	No. 57

APPENDIX B: SPECIMEN DETAILS: CROSS-SECTIONS, ELEVATIONS, AND AS-BUILT DIMENSIONS

Drawings with nominal dimensions are provided for specimens from Phases 1, 2, and 3 in Figures B.1 through B.6, B.7 through B.15, and B.16 through B.22, respectively. The as-built specimen dimensions (height, width, and length) for specimens from Phases 1, 2, and 3 are provided in Tables B.1 through B.3, respectively. As-built height was measured on one side of the specimen at three locations (midspan and near supports) and averaged. As-built width was measured on the bottom of the specimen at three locations (midspan and near the supports) and averaged. As-built length was measured at mid-height on one side of the specimen.

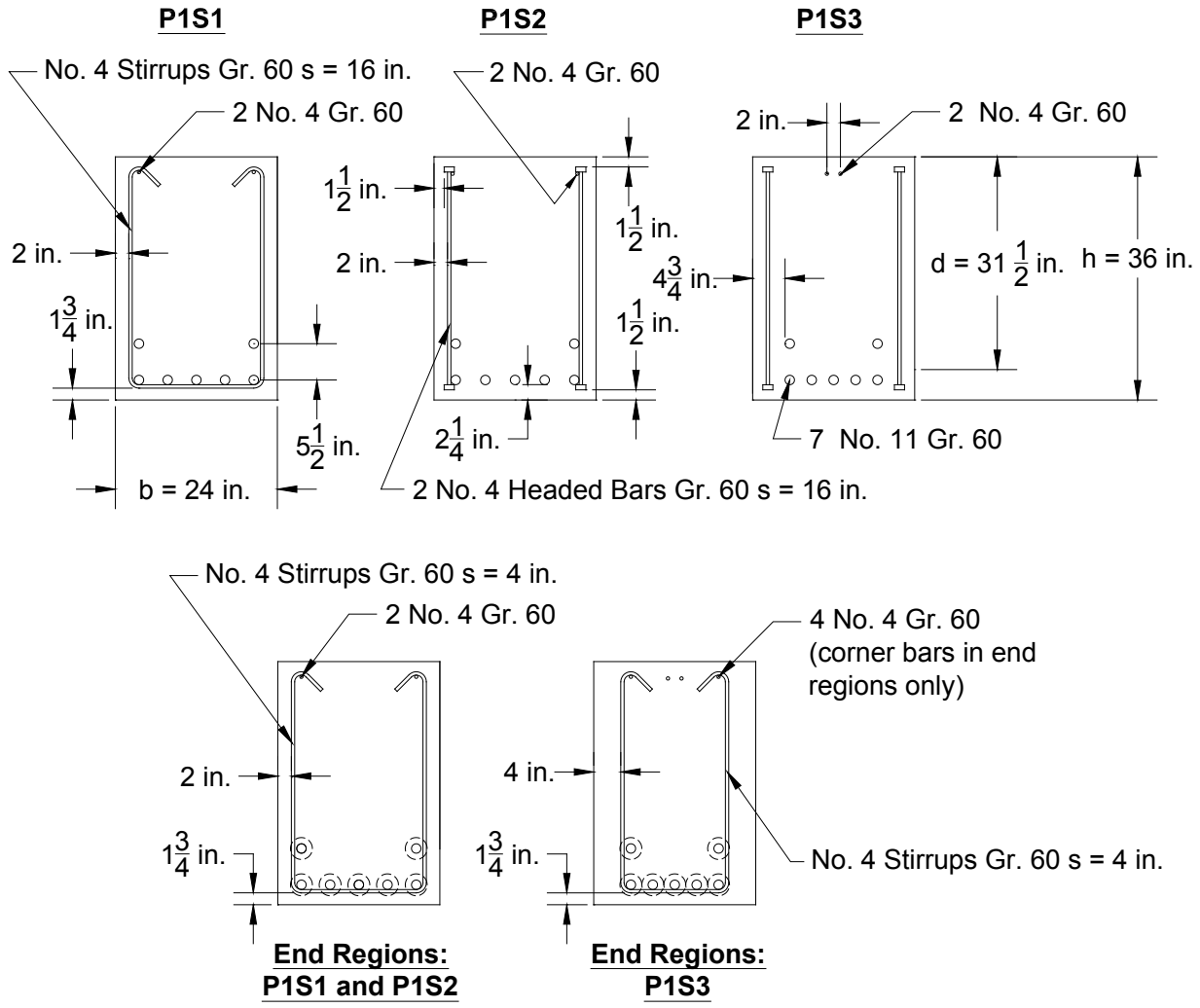

Figure B.1: Cross-sections of P1S1 through P1S3 [1 ksi = 6.9 MPa, 1 in. = 25.4 mm]

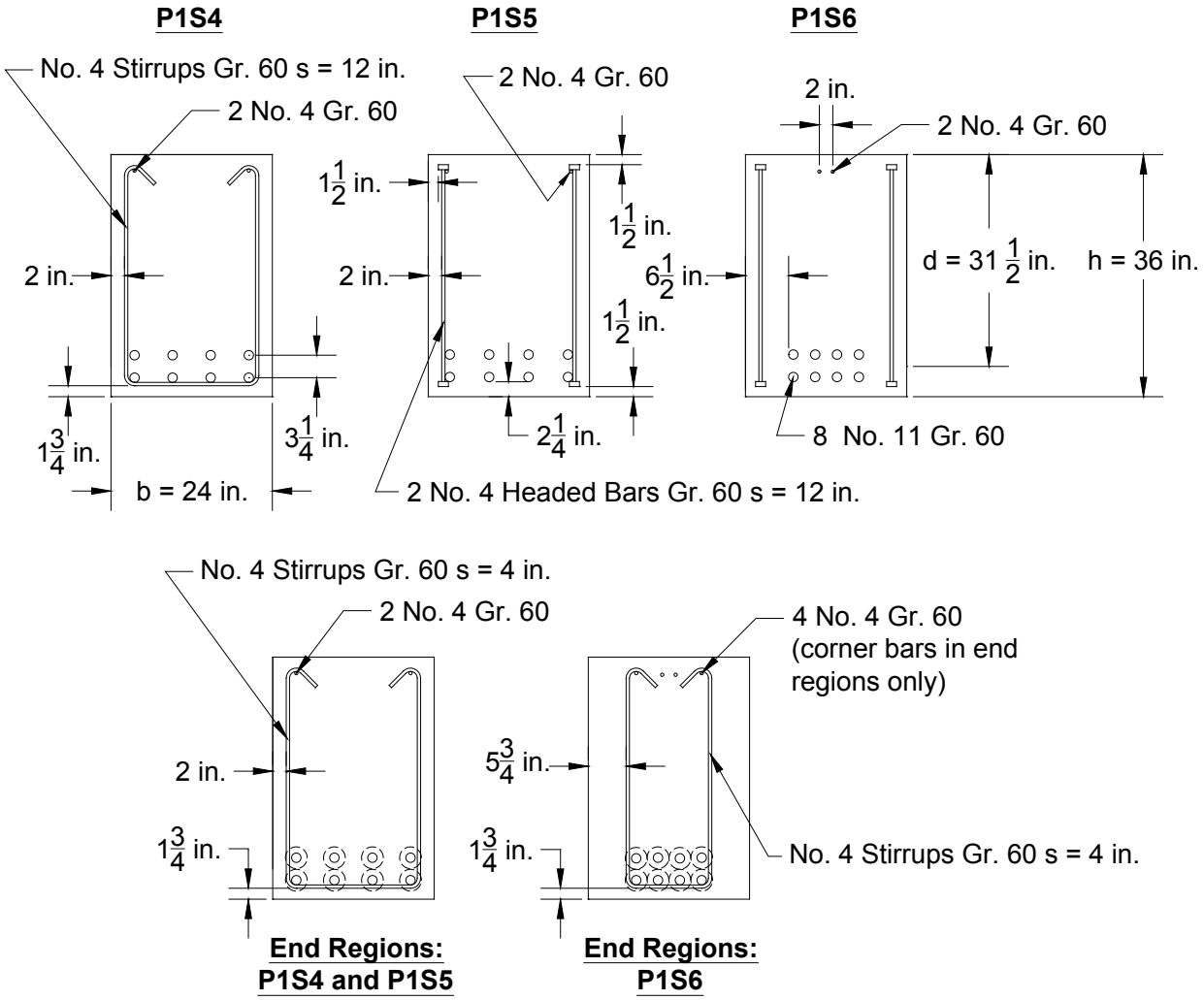

Figure B.2: Cross-sections of P1S4 through P1S6 [1 ksi = 6.9 MPa, 1 in. = 25.4 mm]

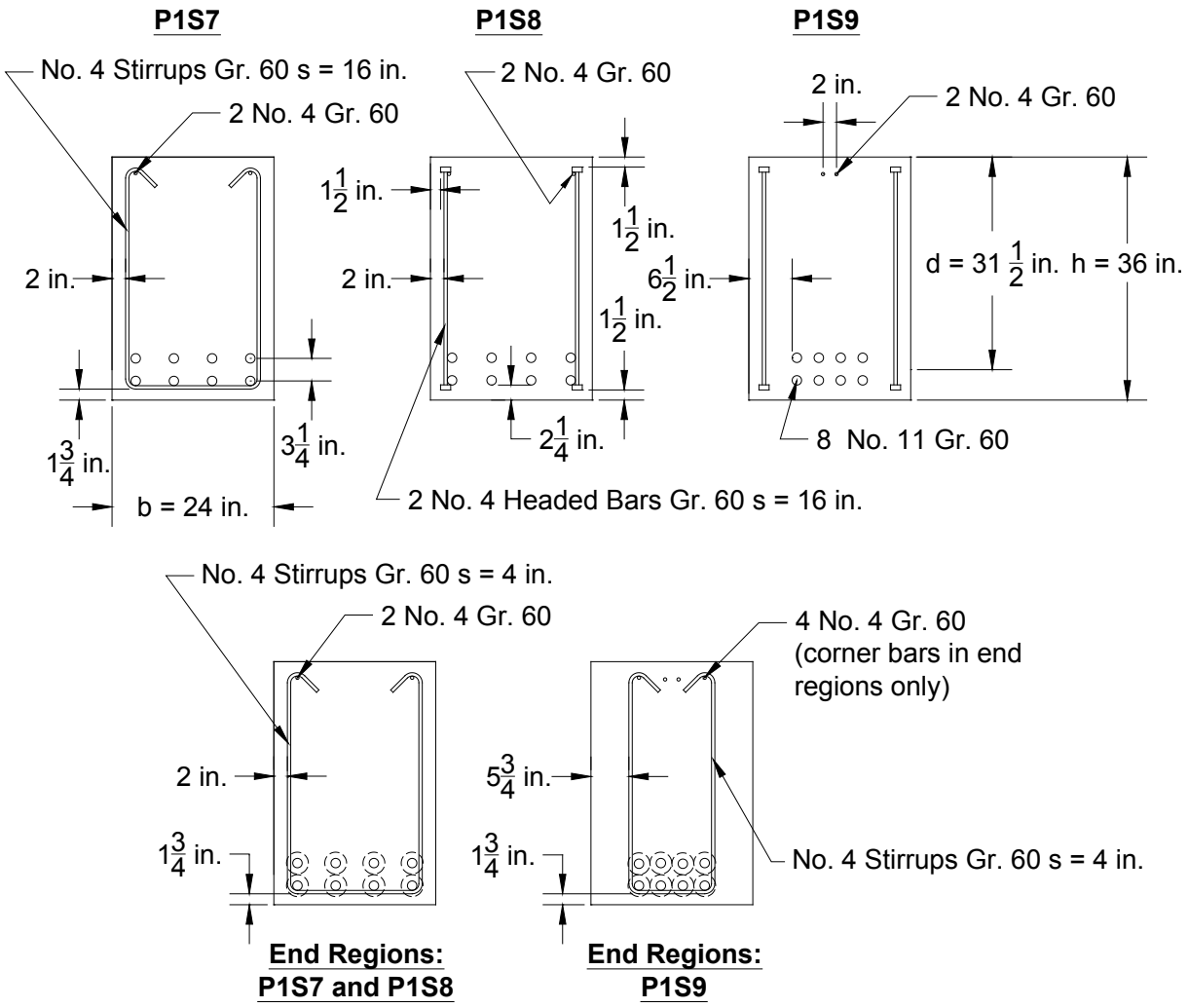

Figure B.3: Cross-sections of P1S7 through P1S9 [1 ksi = 6.9 MPa, 1 in. = 25.4 mm]

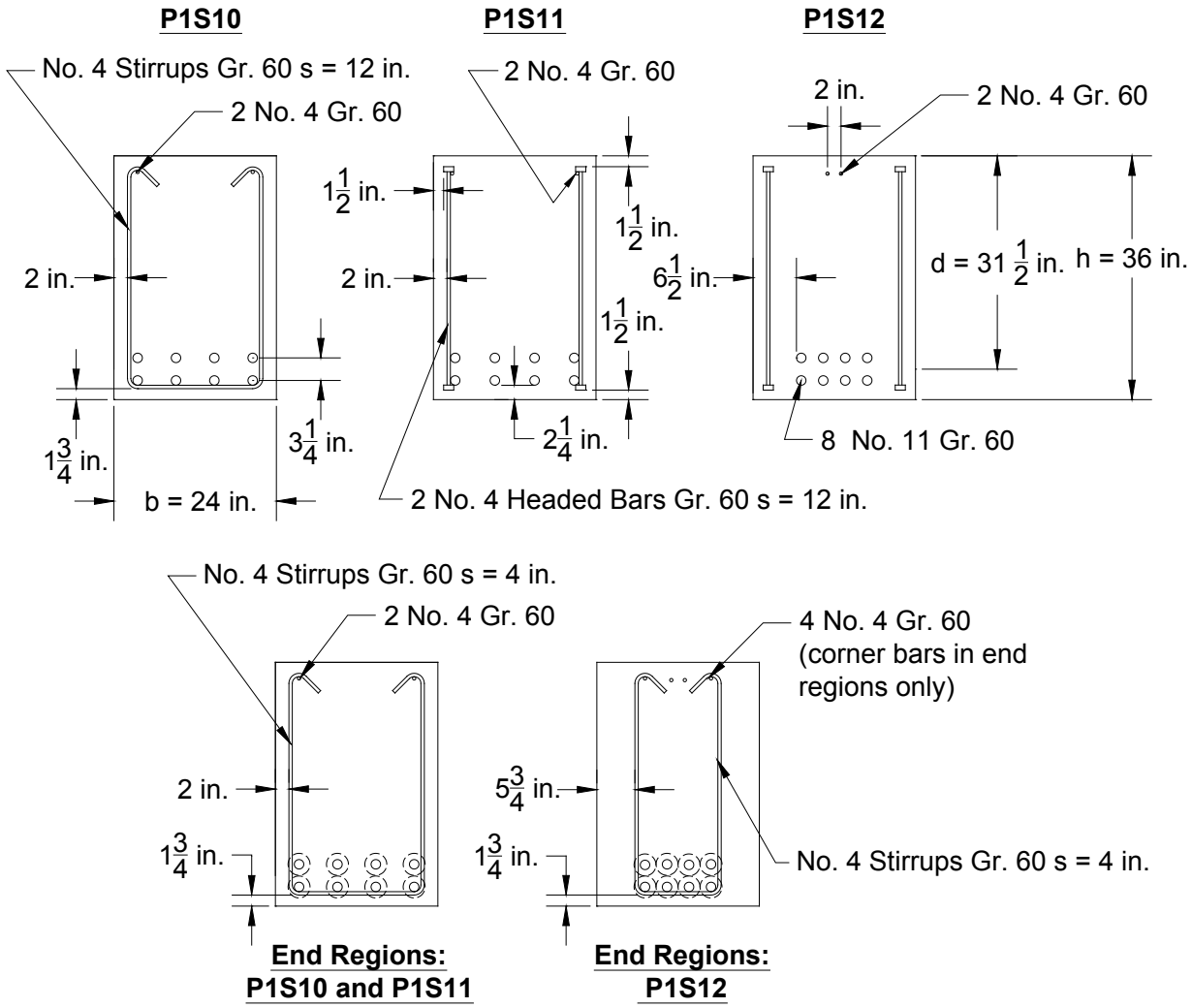

Figure B.4: Cross-sections of P1S10 through P1S12 [1 ksi = 6.9 MPa, 1 in. = 25.4 mm]

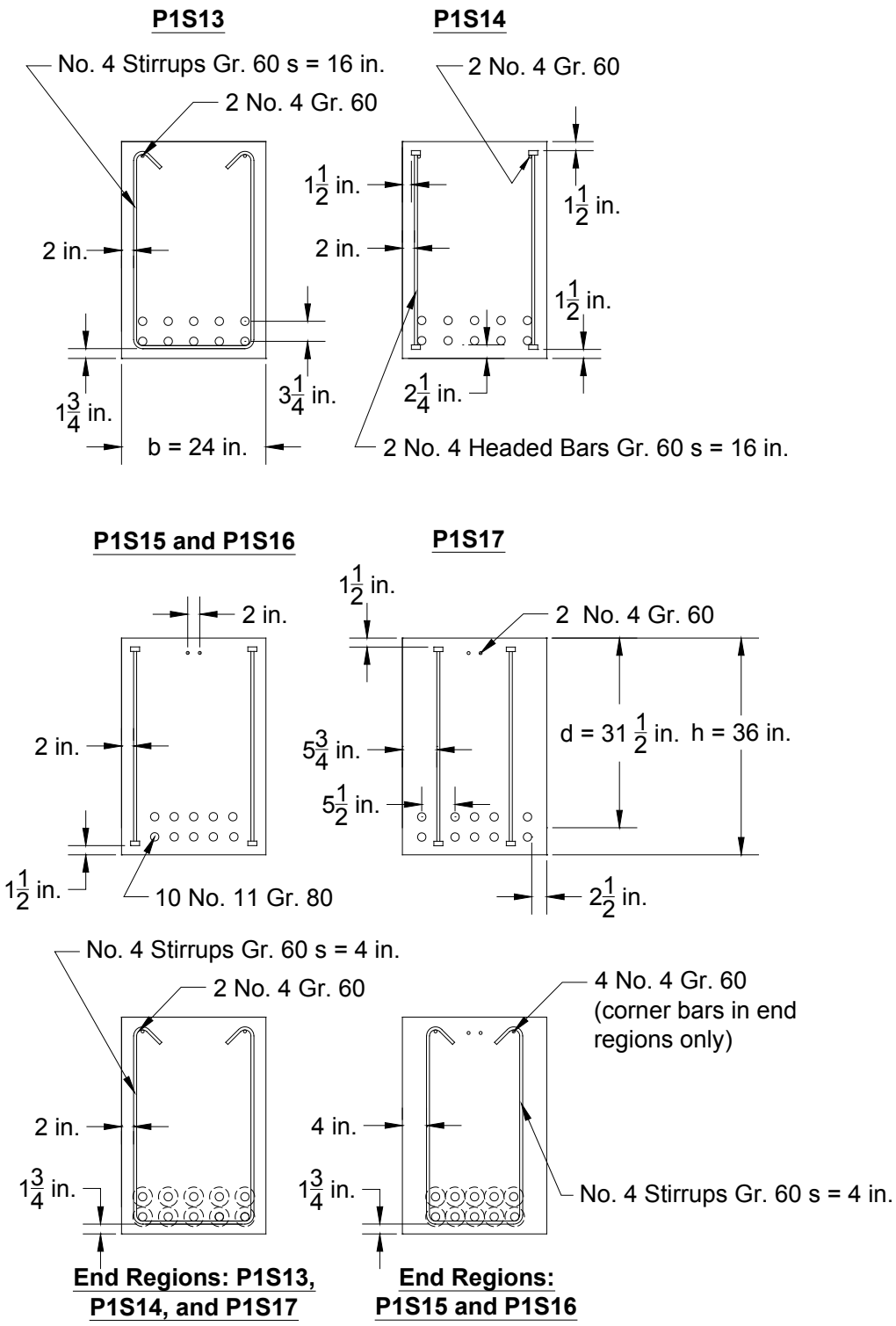

Figure B.5: Cross-sections of P1S13 through P1S17 [1 ksi = 6.9 MPa, 1 in. = 25.4 mm]

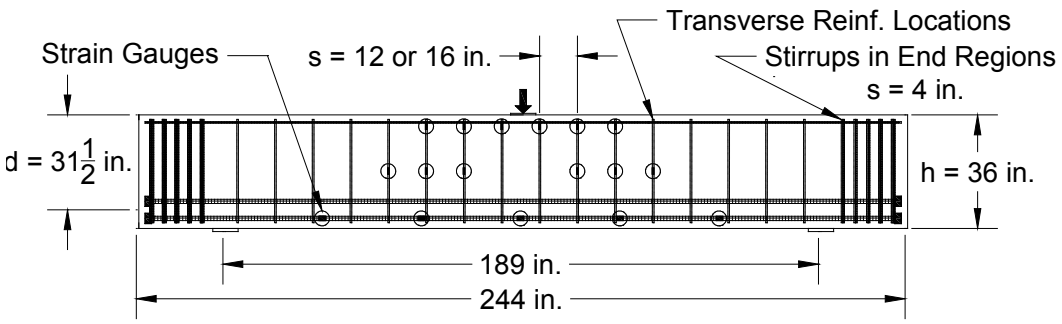

Figure B.6: Elevation of P1S1 through P1S17 [1 ksi = 6.9 MPa, 1 in. = 25.4 mm]

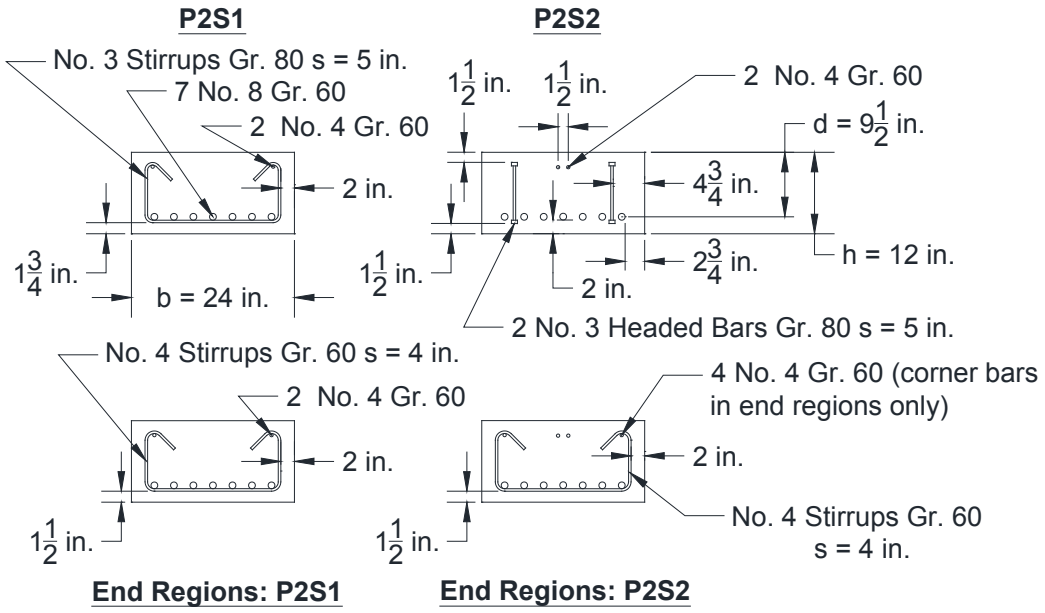

Figure B.7: Cross-sections of P2S1 and P2S2 [1 ksi = 6.9 MPa, 1 in. = 25.4 mm]

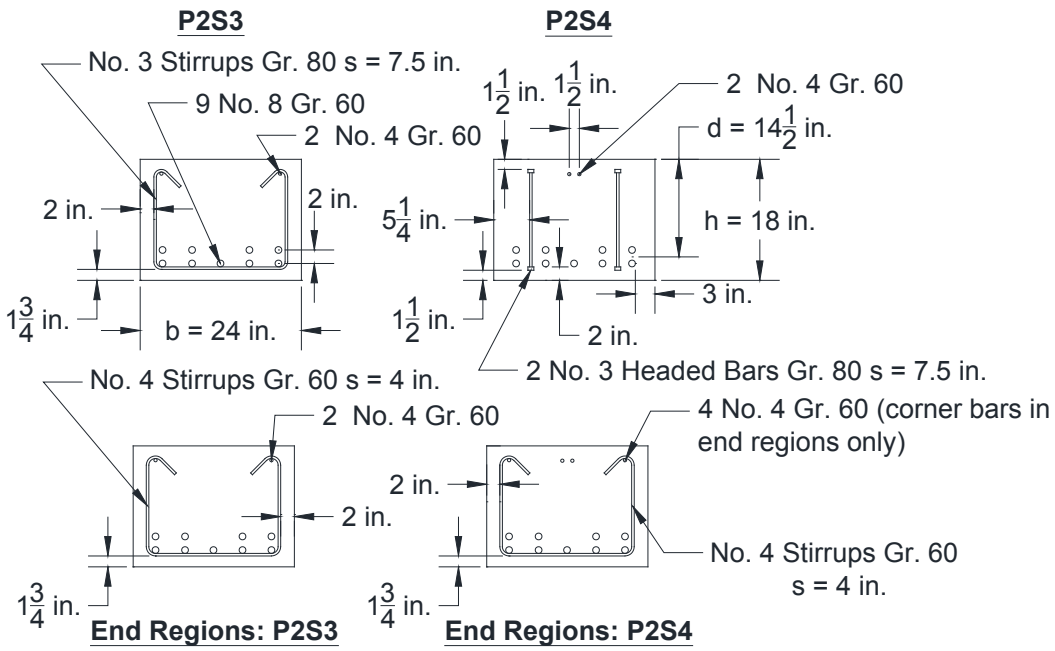

Figure B.8: Cross-sections of P2S3 and P2S4 [1 ksi = 6.9 MPa, 1 in. = 25.4 mm]

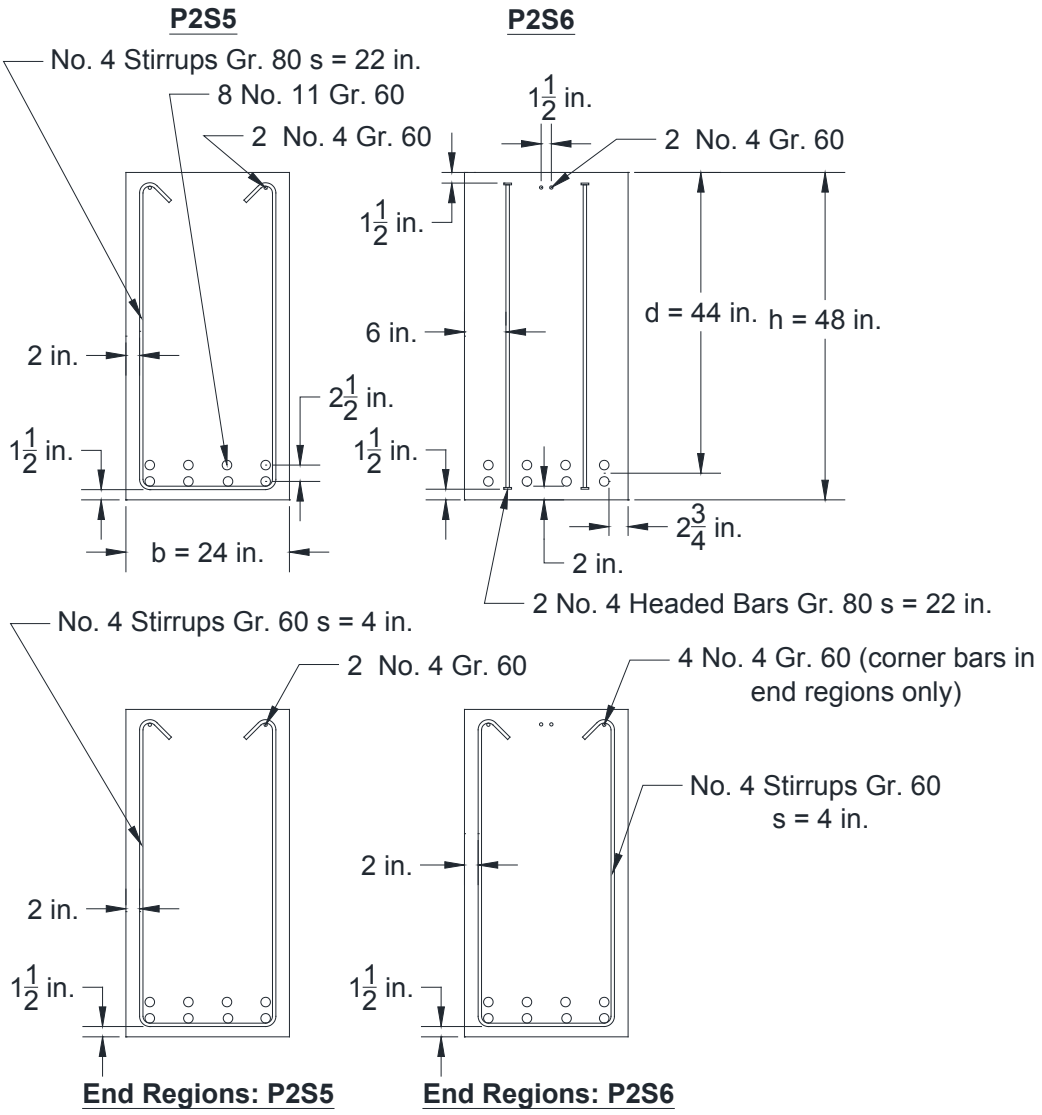

Figure B.9: Cross-sections of P2S5 and P2S6 [1 ksi = 6.9 MPa, 1 in. = 25.4 mm]

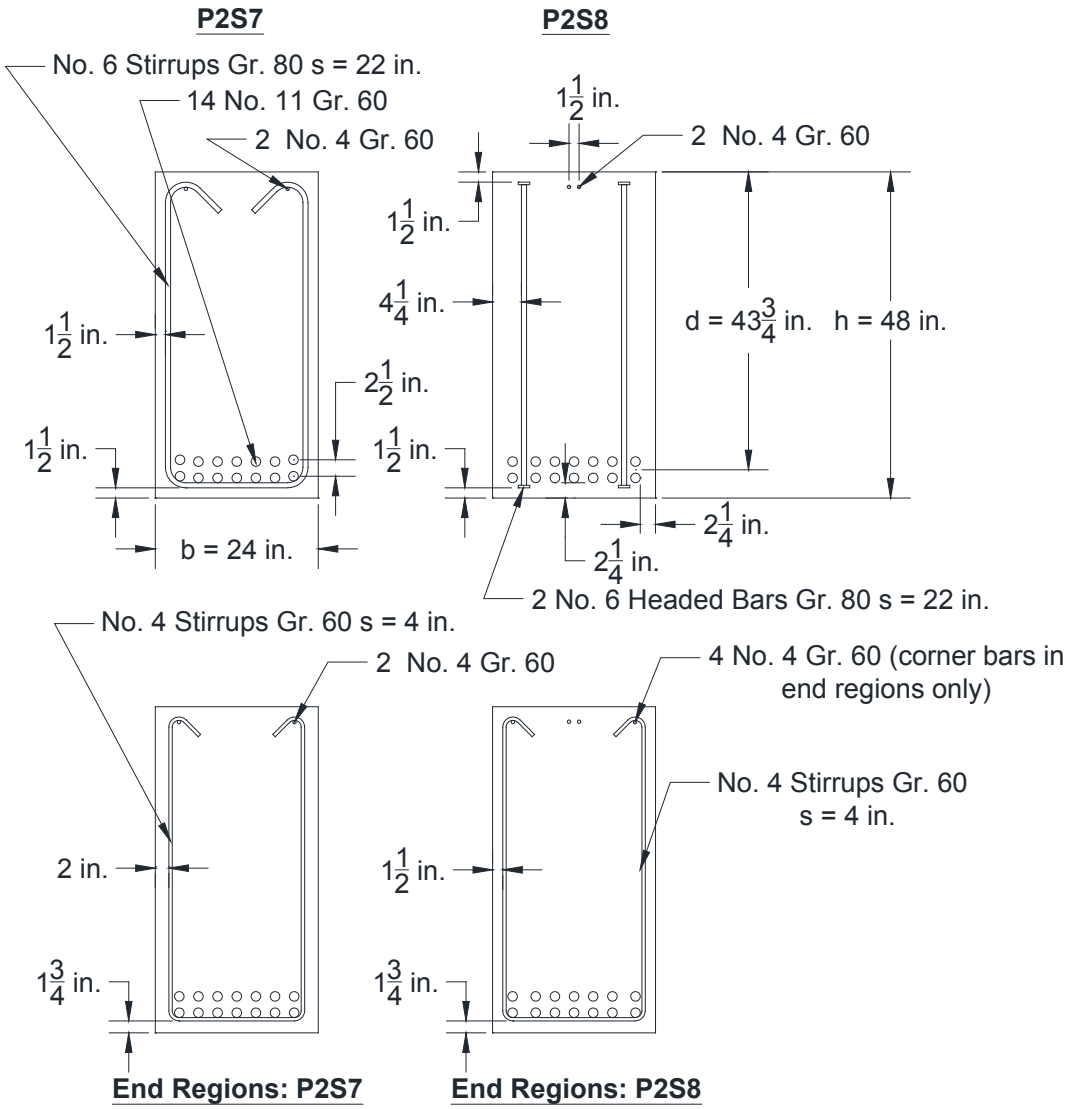

Figure B.10: Cross-sections of P2S7 and P2S8 [1 ksi = 6.9 MPa, 1 in. = 25.4 mm]

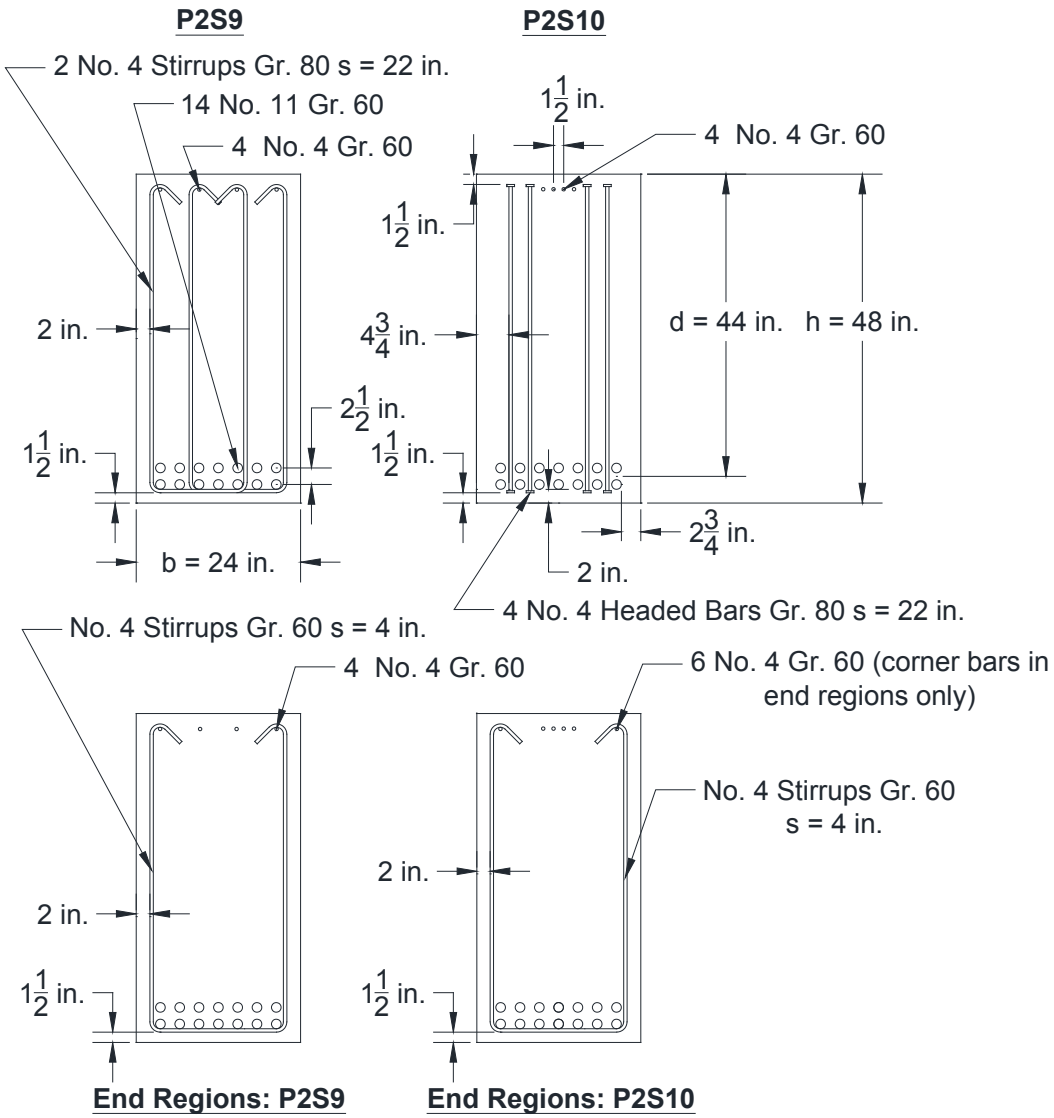

Figure B.11: Cross-sections of P2S9 and P2S10 [1 ksi = 6.9 MPa, 1 in. = 25.4 mm]

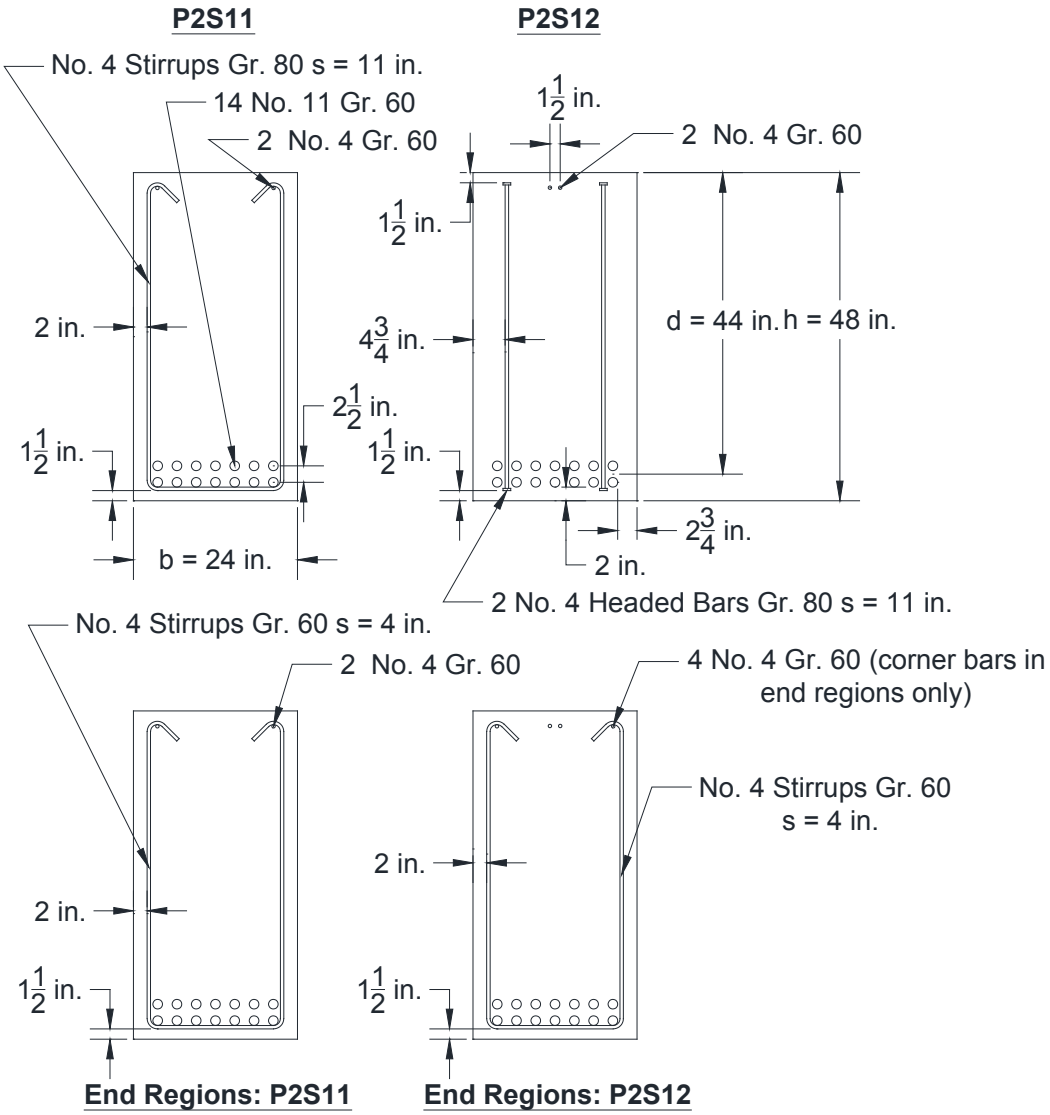

Figure B.12: Cross-sections of P2S11 and P2S12 [1 ksi = 6.9 MPa, 1 in. = 25.4 mm]

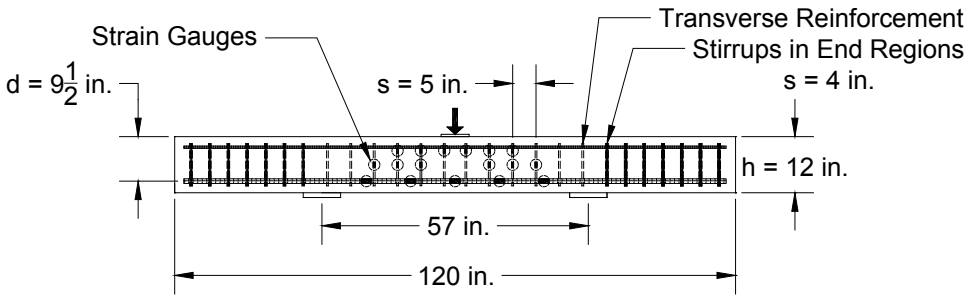

Figure B.13: Elevation of P2S1 and P2S2 [1 ksi = 6.9 MPa, 1 in. = 25.4 mm]

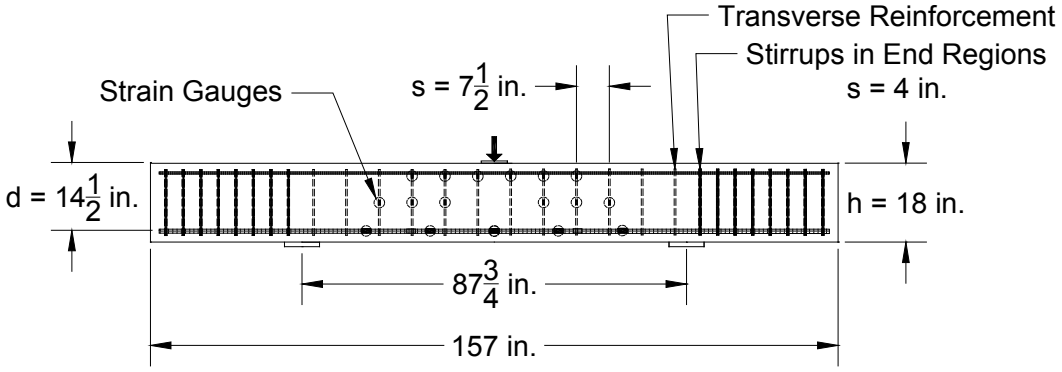

Figure B.14: Elevation of P2S3 and P2S4 [1 ksi = 6.9 MPa, 1 in. = 25.4 mm]

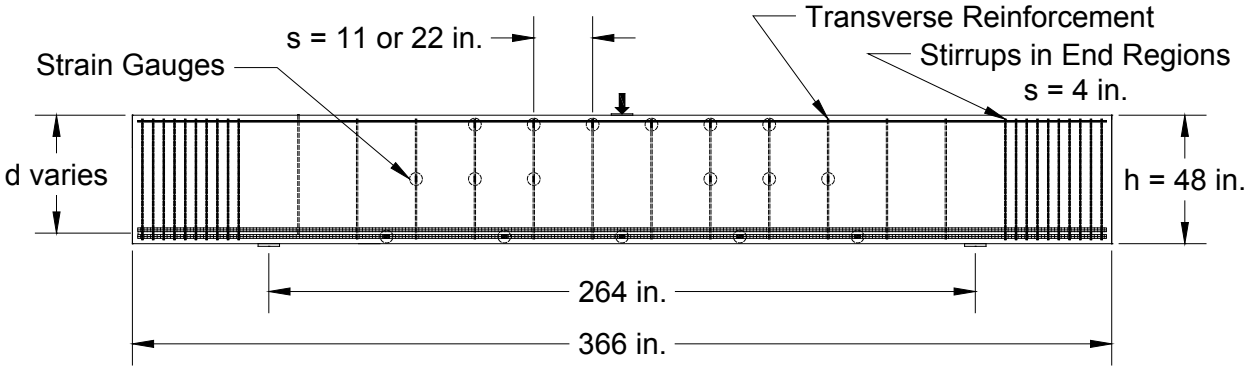

Figure B.15: Elevation of P2S5 through P2S12 [1 ksi = 6.9 MPa, 1 in. = 25.4 mm]

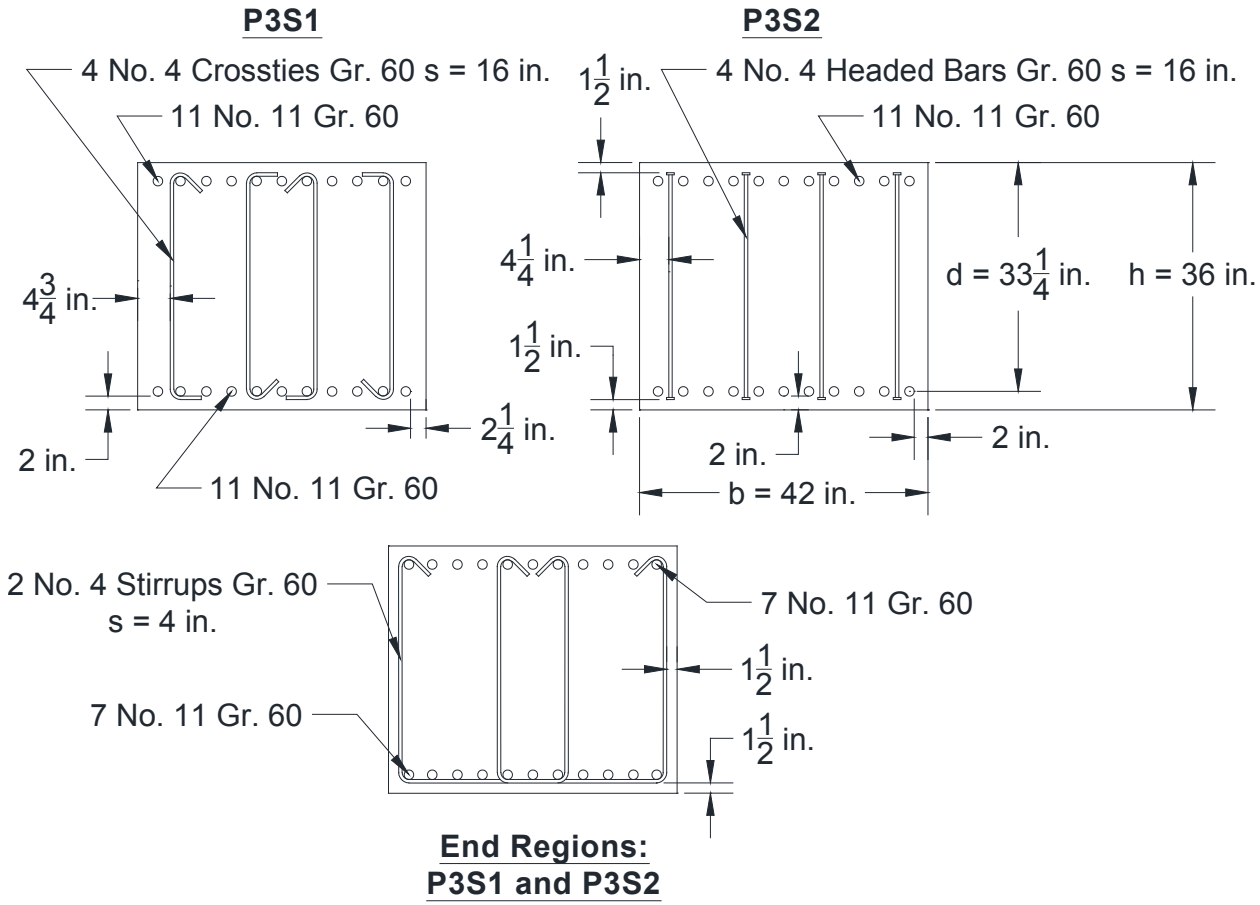

Figure B.16: Cross-sections of P3S1 and P3S2 [1 ksi = 6.9 MPa, 1 in. = 25.4 mm]

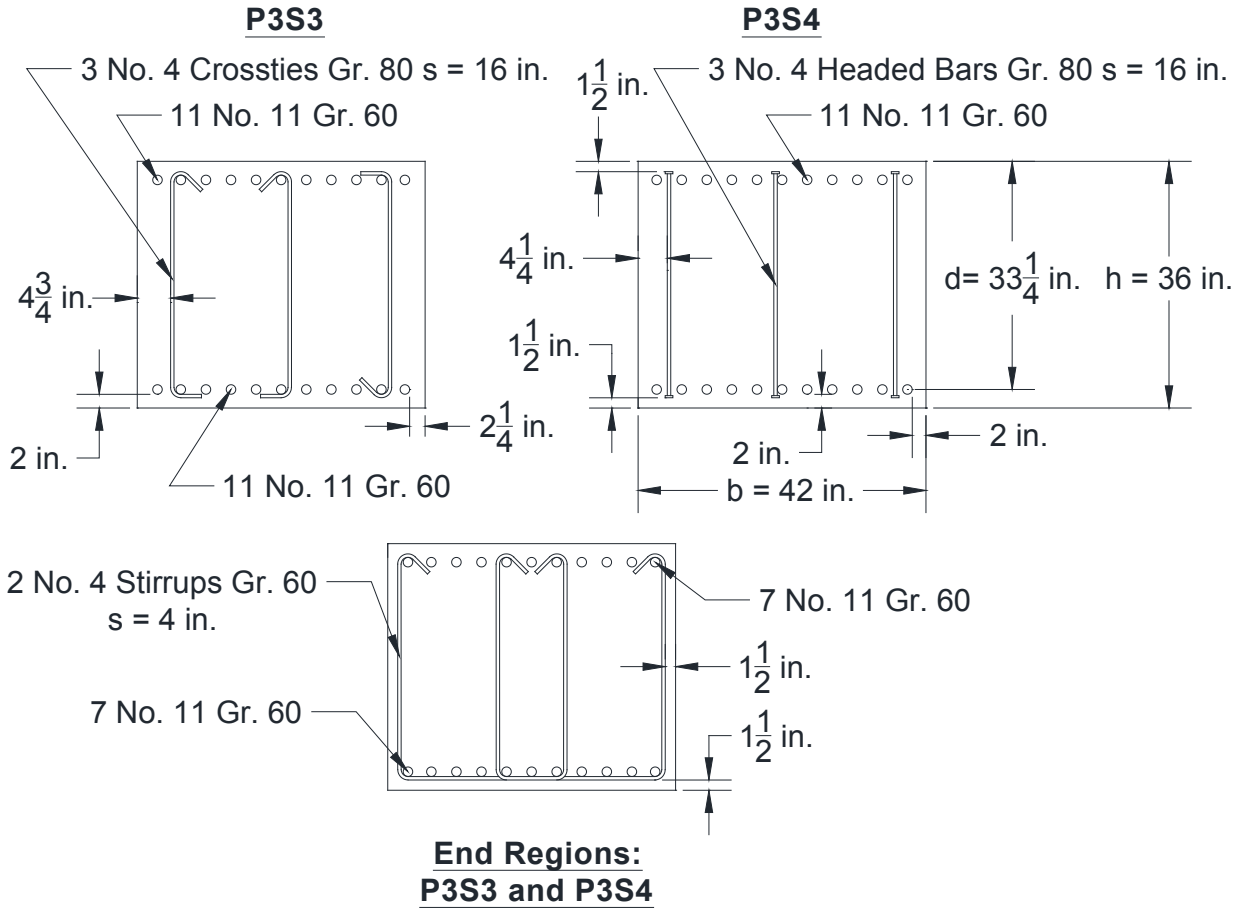

Figure B.17: Cross-sections of P3S3 and P3S4 [1 ksi = 6.9 MPa, 1 in. = 25.4 mm]

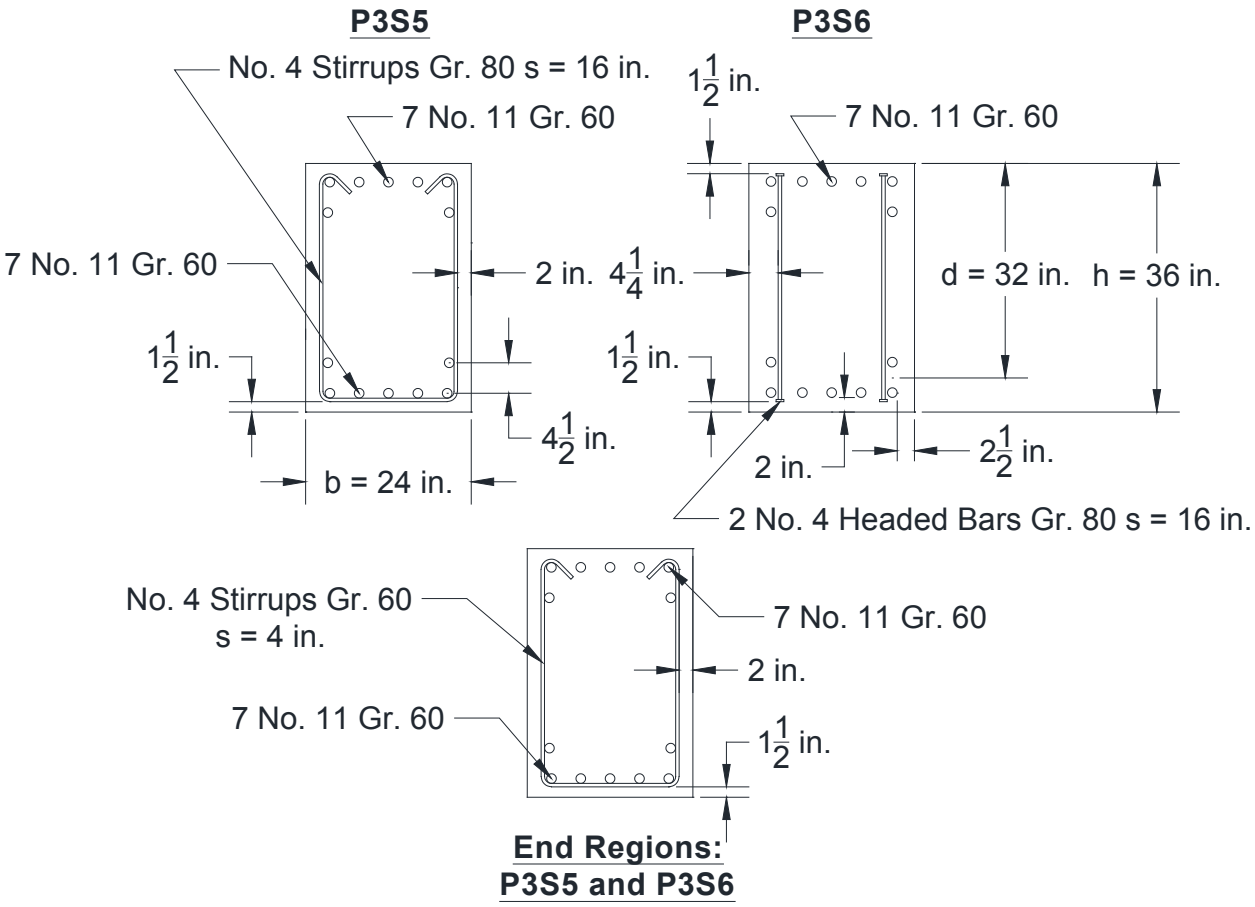

Figure B.18: Cross-sections of P3S5 and P3S6 [1 ksi = 6.9 MPa, 1 in. = 25.4 mm]

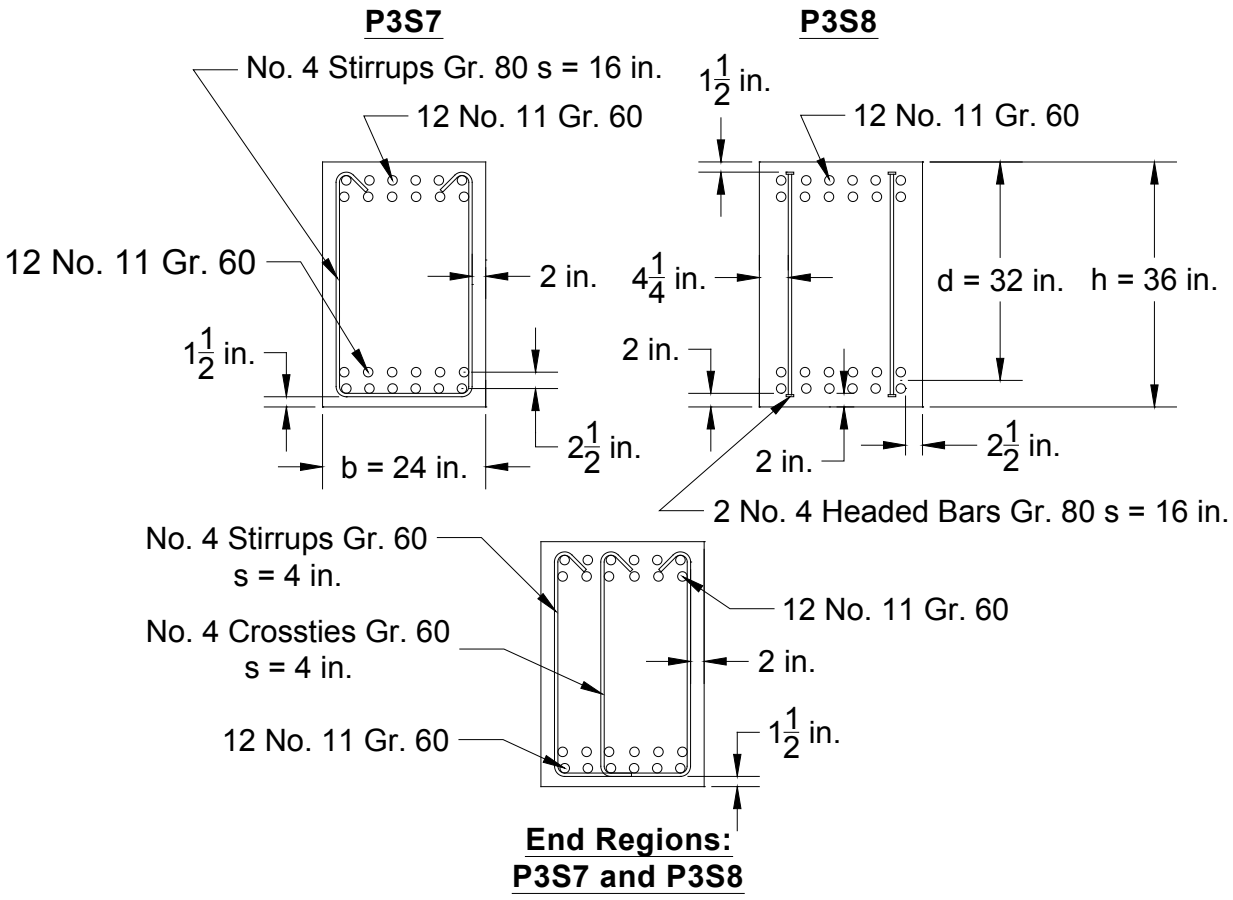

Figure B.19: Cross-sections of P3S7 and P3S8 [1 ksi = 6.9 MPa, 1 in. = 25.4 mm]

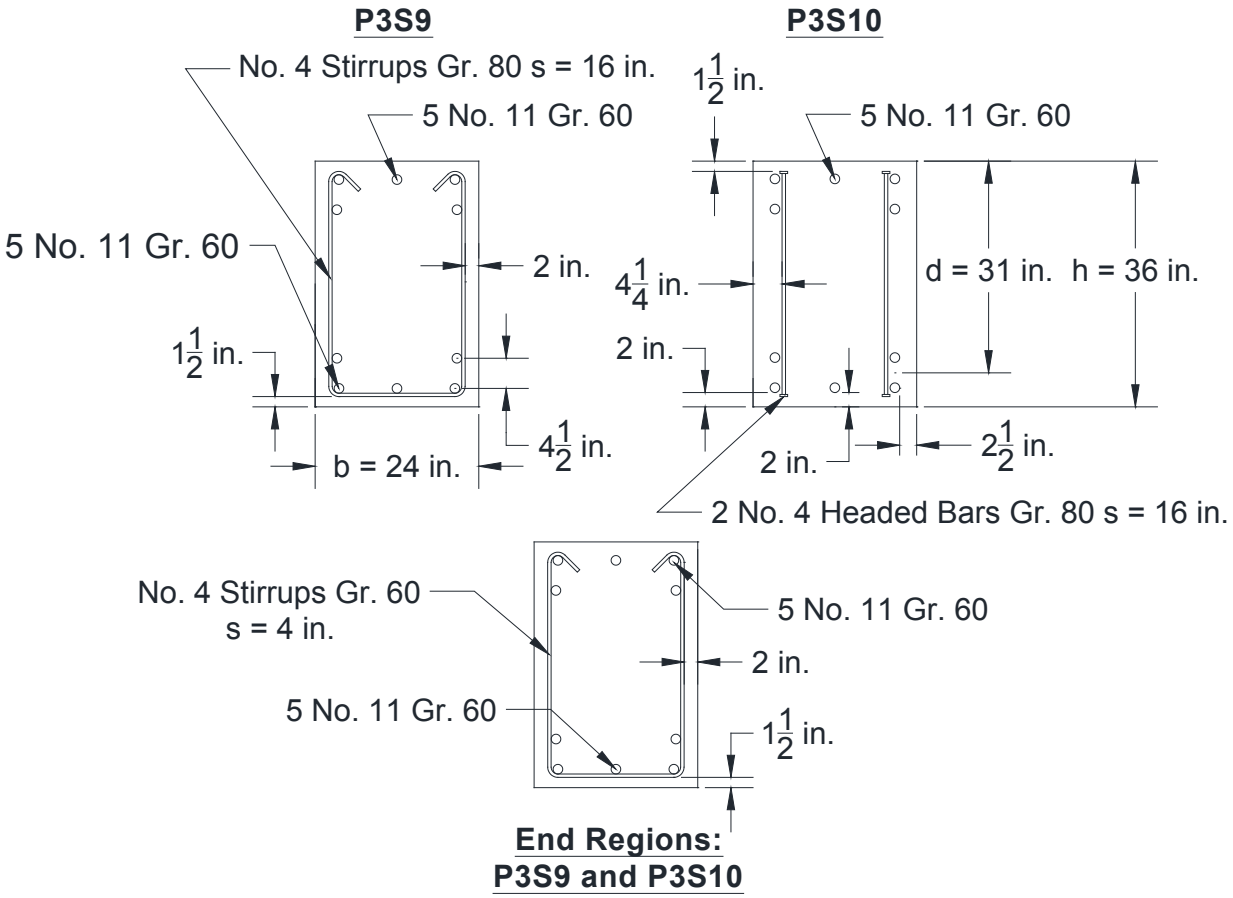

Figure B.20: Cross-sections of P3S9 and P3S10 [1 ksi = 6.9 MPa, 1 in. = 25.4 mm]

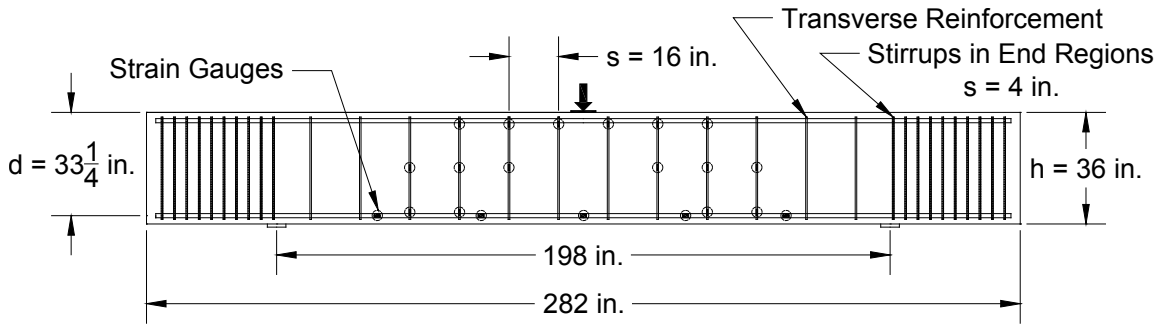

Figure B.21: Elevation of P3S1 through P3S4 [1 ksi = 6.9 MPa, 1 in. = 25.4 mm]

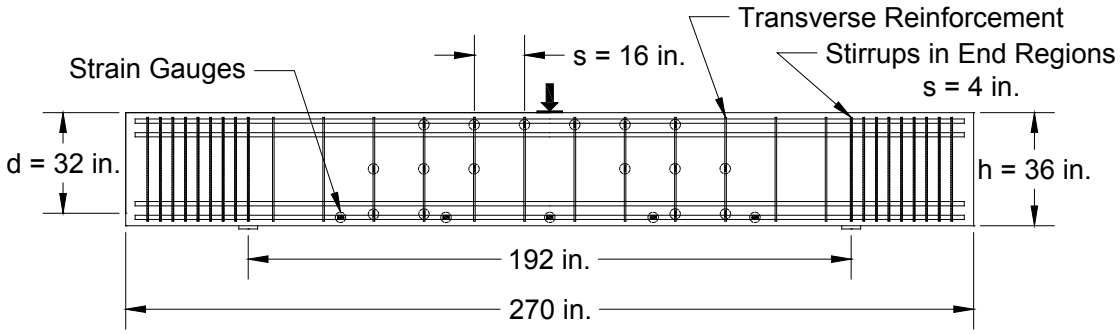

Figure B.22: Elevation P3S5 through P3S10 [1 ksi = 6.9 MPa, 1 in. = 25.4 mm]

Table B.1: As-built dimensions for specimens in Phase 1[a]

Specimen	Specimen Parameters			
	Head / Hook Detail [b]	***h*, in. (mm)**	***b*, in. (mm)**	**Length, in. (mm)**
P1S1	S	36.5 (925)	24.5 (620)	245.0 (6225)
P1S2	HE	36.5 (925)	24.0 (610)	246.0 (6250)
P1S3	HNE	36.5 (925)	24.5 (620)	245.5(6260)
P1S4	S	36.5 (925)	24.5 (620)	246.0 (6250)
P1S5	HE	36.75 (935)	24.0 (610)	245.5 (6235)
P1S6	HNE	36.0 (915)	24.25 (615)	245.5 (6235)
P1S7	S	36.5 (925)	24.5 (620)	245.75 (6240)
P1S8	HE	36.5 (925)	24.5 (620)	245.75 (6240)
P1S9	HNE	36.5 (925)	24.0 (610)	246.0 (6250)
P1S10	S	36.5 (925)	24.5 (620)	246.0 (6250)
P1S11	HE	36.5 (925)	24.5 (620)	246.5 (6260)
P1S12	HNE	36.5 (925)	24.5 (620)	245.5 (6235)
P1S13	S	36.0 (915)	24.0 (610)	246.0 (6250)
P1S14	HE	36.5 (925)	24.5 (620)	245.5 (6235)
P1S15	HNE	36.5 (925)	24.5 (620)	246.0 (6250)
P1S16	HNE	36.5 (925)	24.5 (620)	246.5 (6260)
P1S17	HNE2	36.5 (925)	24.5 (620)	246.5 (6260)

[a] All measurements rounded to 1/4-inch [5-mm] increments

[b] See Figure 2.1

Table B.2: As-built dimensions for specimens in Phase 2[a]

Specimen	Specimen Parameters			
	Head / Hook Detail [b]	***h*, in. (mm)**	***b*, in. (mm)**	**Length, in. (mm)**
P2S1	S	12.0 (305)	24.25 (615)	121.0 (3075)
P2S2	HNE2	12.0 (305)	24.0 (610)	121.0 (3075)
P2S3	S	18.0 (450)	24.0 (610)	156.0 (3960)
P2S4	HNE2	18.0 (450)	24.5 (620)	156.0 (3960)
P2S5	S	48.25 (1225)	24.5 (620)	365.0 (9270)
P2S6	HNE2	48.25 (1225)	24.5 (620)	366.0 (9295)
P2S7	S	48.0 (1220)	24.25 (615)	365.0 (9270)
P2S8	HNE2	48.25 (1225)	24.25 (615)	368.0 (9345)
P2S9	S	48.0 (1220)	24.25 (615)	367.0 (9320)
P2S10	HNE2	48.0 (1220)	24.25 (615)	365.0 (9270)
P2S11	S	48.0 (1220)	24.0 (610)	367.0 (9320)
P2S12	HNE2	48.5 (1230)	24.25 (615)	366.0 (9295)

[a] All measurements rounded to 1/4-inch [5-mm] increments

[b] See Figure 2.1

Table B.3: As-built dimensions for specimens in Phase 3[a]

Specimen	Specimen Parameters			
	Head / Hook Detail [b]	***h*, in.**	***b*, in.**	**Length, in.**
P3S1	S	36.25 (920)	42.0 (1065)	282.0 (7165)
P3S2	HNE2	36.25 (920)	42.0 (1065)	282.0 (7165)
P3S3	S	36.0 (915)	42.5 (1080)	282.5 (7175)
P3S4	HNE2	36.75 (935)	42.0 (1065)	282.5 (7175)
P3S5	S	36.0 (915)	24.0 (610)	270.0 (6860)
P3S6	HNE2	36.0 (915)	24.25 (615)	270.0 (6860)
P3S7	S	36.25 (920)	24.5 (620)	270.5 (6870)
P3S8	HNE2	36.25 (920)	24.5 (620)	270.5 (6870)
P3S9	S	36.25 (920)	24.0 (610)	270.5 (6870)
P3S10	HNE2	36.25 (920)	24.75 (630)	270.0 (6860)

[a] All measurements rounded to 1/4-inch [5-mm] increments

[b] See Figure 2.1

APPENDIX C: PLASTIC CONCRETE PROPERTIES

Tables C.1 through C.3 list the plastic properties of the concrete used in this study. The unit weight, slump, air content, and temperature were determined in accordance with ASTM C138, C143, C231, and C1064, respectively.

Table C.1: Plastic concrete properties for specimens from Phase 1

Specimen	Truck No.	Unit Weight, lb/ft^3 (kg/m^3)	Slump, in. (mm)	Air Content, % [a]	Concrete Temperature, °F (°C)
P1S1, P1S2 & P1S3	1	150.0 (2403)	10.00 (255)	-	73 (23)
	2	148.0 (2371)	10.50 (265)	-	73 (23)
P1S5 & P1S6	1	145.6 (2332)	8.75 (220)	-	78 (25.5)
	2	147.4 (2361)	9.25 (235)	-	78 (25.5)
P1S4, P1S7 & P1S8	1	146.2 (2342)	8.50 (215)	-	65 (18.5)
	2	146.8 (2351)	9.00 (230)	-	65 (18.5)
P1S9	1	148.0 (2371)	8.00 (205)	-	68 (20)
	2	147.0 (2355)	7.00 (180)	-	68 (20)
P1S10, P1S11 & P1S12	1	148.3 (2375)	7.00 (180)	-	56 (13.5)
	2	146.6 (2348)	7.00 (180)	-	55 (13)
P1S13, P1S14 & P1S15	1	- [b]	9.00 (230)	-	60 (15.5)
	2	- [b]	9.00 (230)	-	62 (16.5)
P1S16 & P1S17	1	149.0 (2387)	8.50 (215)	-	58 (14)

[a] Air content not measured
[b] Unit weight not measured

Table C.2: Plastic concrete properties for specimens from Phase 2

Specimen	Truck No.	Unit Weight, lb/ft^3 (kg/m^3)	Slump, in. (mm)	Air Content, %	Concrete Temperature, °F (°C)
P2S1 & P2S2	1	- [a]	6.00 (150)	0.7	64 (18)
P2S3 & P2S4	1	- [a]	6.00 (150)	0.7	64 (18)
P2S5 & P2S6	1	148.0 (2371)	9.00 (230)	0.8	72 (22)
	2	148.0 (2371)	8.75 (220)	0.9	72 (22)
	3	151.2 (2422)	8.00 (205)	0.6	75 (24)
P2S7 & P2S8	1	- [a]	10.00 (255)	0.5	84 (29)
	2	- [a]	9.75 (250)	0.9	83 (28.5)
	3	152.1 (2436)	9.50 (240)	1.1	85 (29.5)
P2S9 & P2S10	1	148.2 (2374)	6.25 (160)	1.1	80 (26.5)
	2	148.2 (2374)	9.00 (230)	0.8	86 (30)
	3	148.2 (2374)	9.75 (250)	0.8	86 (30)
P2S11 & P2S12	1	151.8 (2432)	8.00 (205)	1.0	69 (20.5)
	2	152.2 (2438)	8.00 (205)	0.9	69 (20.5)
	3	151.8 (2432)	8.00 (205)	1.0	73 (23)

[a] Unit weight not measured

Table C.3: Plastic concrete properties for specimens from Phase 3

Specimen	Truck No.	Unit Weight, lb/ft^3 (kg/m^3)	Slump, in. (mm)	Air Content, %	Concrete Temperature, °F (°C)
P3S1 & P3S2	1	147.6 (2364)	8.50 (215)	0.6	80 (26.5)
	2	148.6 (2380)	8.50 (215)	0.8	81 (27)
P3S3 & P3S4	1	148.9 (2385)	9.00 (230)	1.0	60 (15.5)
	2	148.3 (2375)	9.75 (250)	1.0	65 (18.5)
	3	146.9 (2353)	9.50 (240)	1.2	63 (17)
P3S5 & P3S6	1	148.0 (2371)	7.00 (180)	0.8	62 (16.5)
	2	151.6 (2428)	9.00 (230)	0.6	67 (19.5)
P3S7 & P3S8	1	147.8 (2367)	8.25 (210)	1.2	77 (25)
	2	148.7 (2382)	9.00 (230)	1.0	76 (24.5)
P3S9 & P3S10	1	148.9 (2385)	9.50 (240)	0.7	70 (21)
	2	150.1 (2404)	9.50 (240)	0.3	70 (21)

APPENDIX D: MEASURED STRESS VERSUS STRAIN FOR STEEL REINFORCEMENT

For each bar size and grade used in this study, two samples were tested in tension in accordance with ASTM A370. Strain was measured over an 8-in. [200-mm] gauge length using the optical tracking system described in Section 2.3.2.2. Figures D.1 through D.26 show plots of the recorded stress versus strain for each bar sample that was tested. Below each figure three parameters are listed: the nominal cross-sectional area of the bar, the average strain rate during testing (determined based on the recorded data), and the yield stress of the bar determined with the 0.2% offset method. Figures D.1 and D.2 are repeated as D.5 and D.6 and again as D.15 and D.16 because the Grade 60 [Grade 420] No. 4 [No. 13] bars used as longitudinal bars in Phases 1 and 2 were from the same heat as the Grade 60 [Grade 420] No. 4 [No. 13] bars used as transverse reinforcement in some specimens of Phase 1.

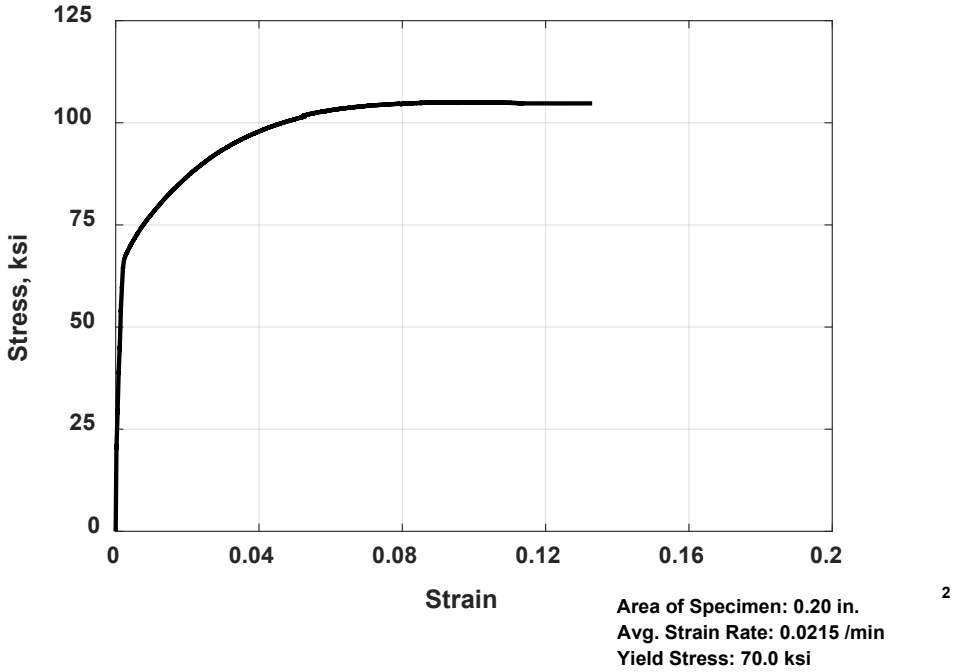

Figure D.1: Stress versus strain for No. 4 [No 13] transverse reinforcing bar (Grade 60 [Grade 420], Sample 1, Phase 1) [1 in.^{2} = 0.000645 m^2, 1 ksi = 6.9 MPa]

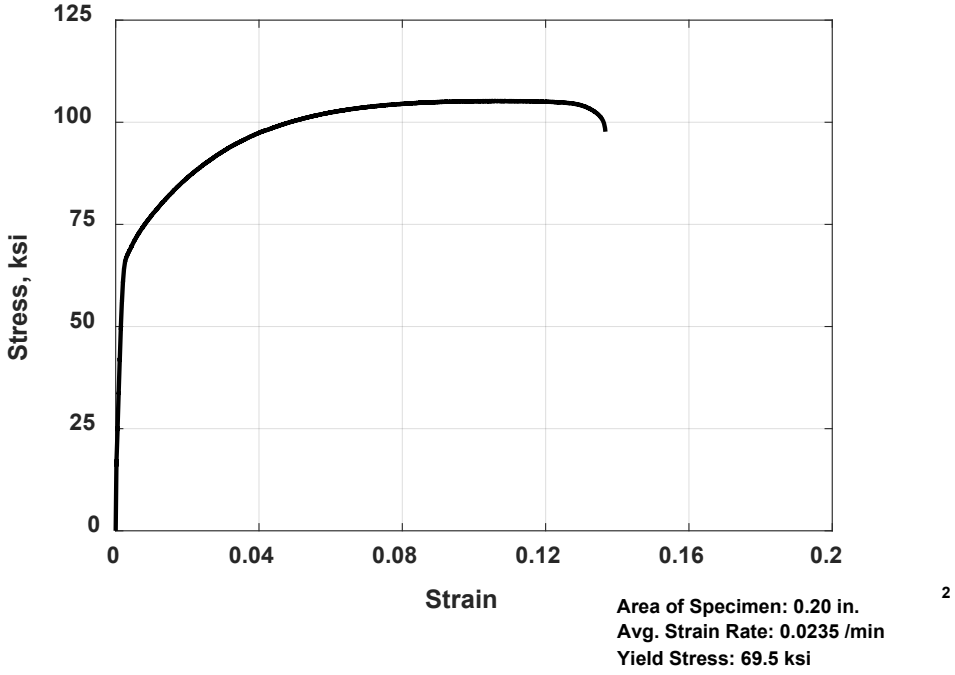

Figure D.2: Stress versus strain for No. 4 [No. 13] transverse reinforcing bar (Grade 60 [Grade 420], Sample 2, Phase 1) [1 in.^{2} = 0.000645 m^2, 1 ksi = 6.9 MPa]

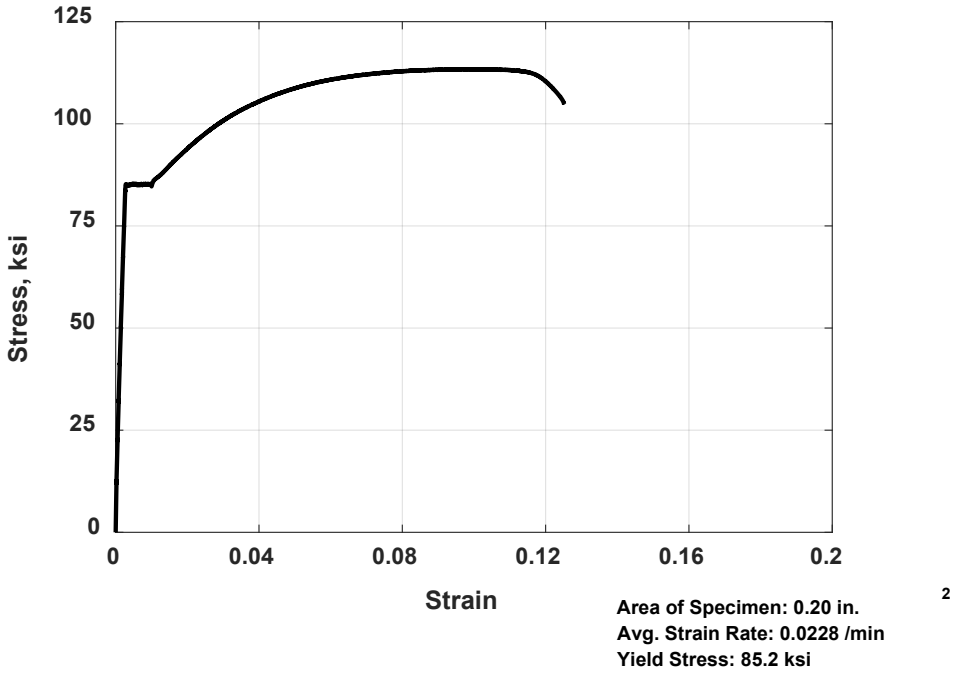

Figure D.3: Stress versus strain for No. 4 [No. 13] transverse reinforcing bar (Grade 80 [Grade 550], Sample 1, Phase 1) [1 in.^{2} = 0.000645 m^2, 1 ksi = 6.9 MPa]

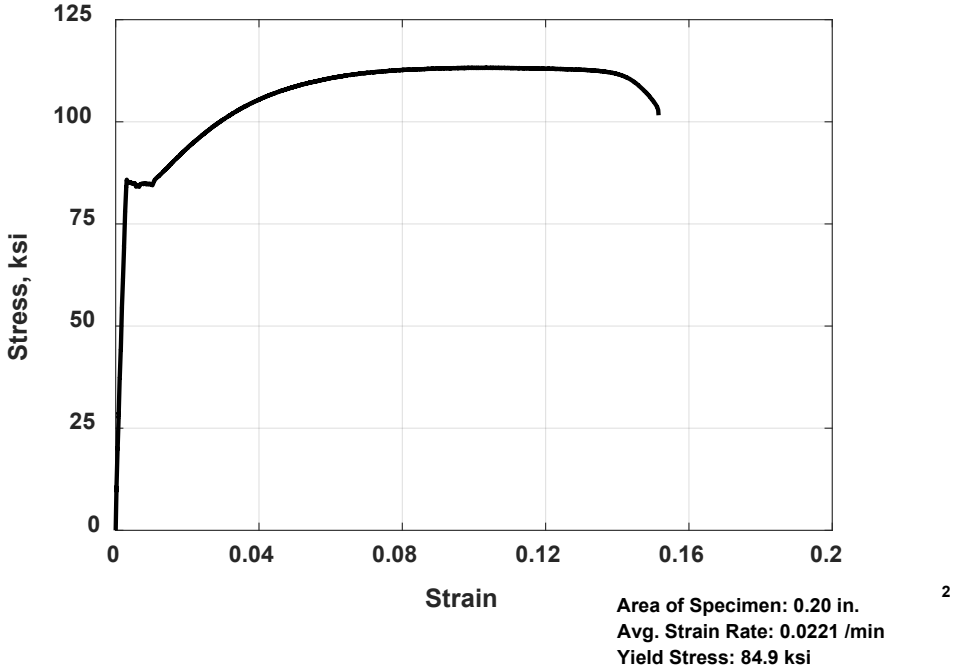

Figure D.4: Stress versus strain for No. 4 [No. 13] transverse reinforcing bar (Grade 80 [Grade 550], Sample 2, Phase 1) [1 in.^{2} = 0.000645 m^2, 1 ksi = 6.9 MPa]

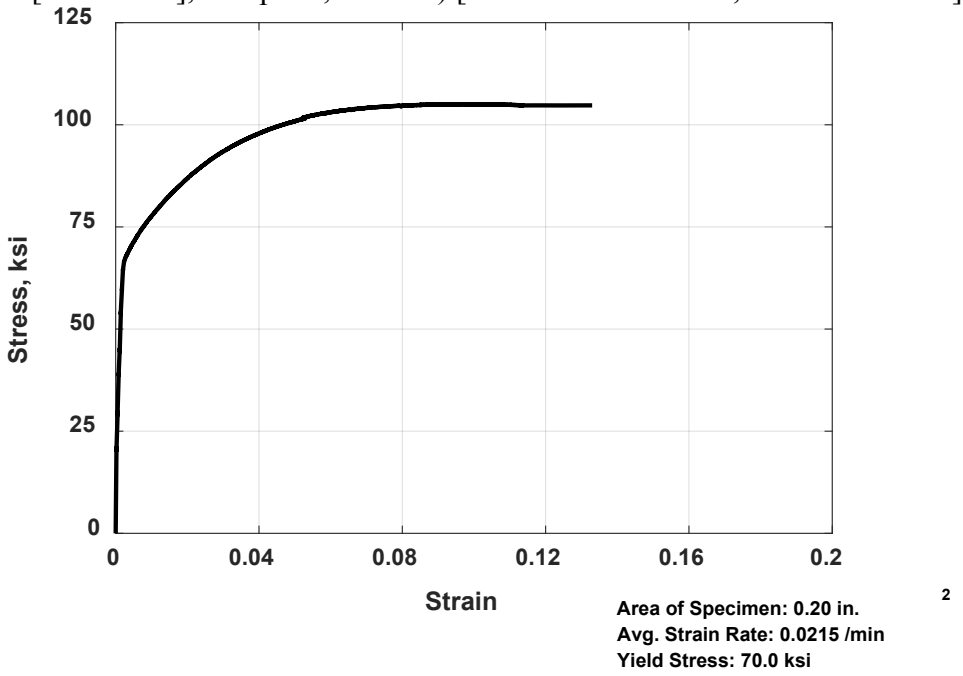

Figure D.5: Stress versus strain for No. 4 [No. 13] longitudinal reinforcing bar (Grade 60 [Grade 420], Sample 1, Phase 1) [1 in.^{2} = 0.000645 m^2, 1 ksi = 6.9 MPa]

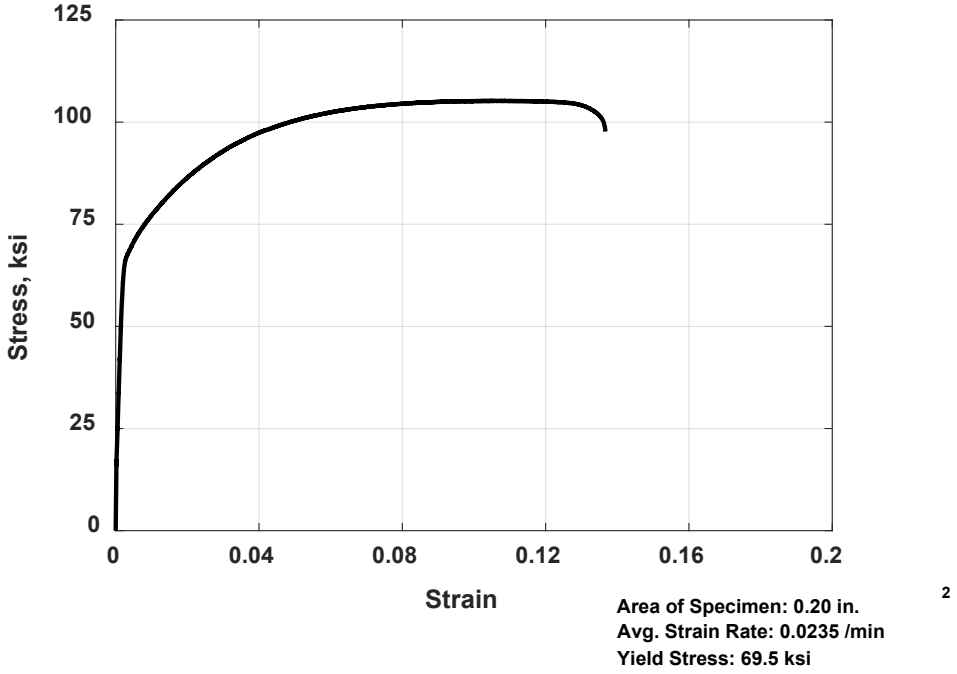

Figure D.6: Stress versus strain for No. 4 [No. 13] longitudinal reinforcing bar (Grade 60 [Grade 420], Sample 2, Phase 1) [1 in.^{2} = 0.000645 m^2, 1 ksi = 6.9 MPa]

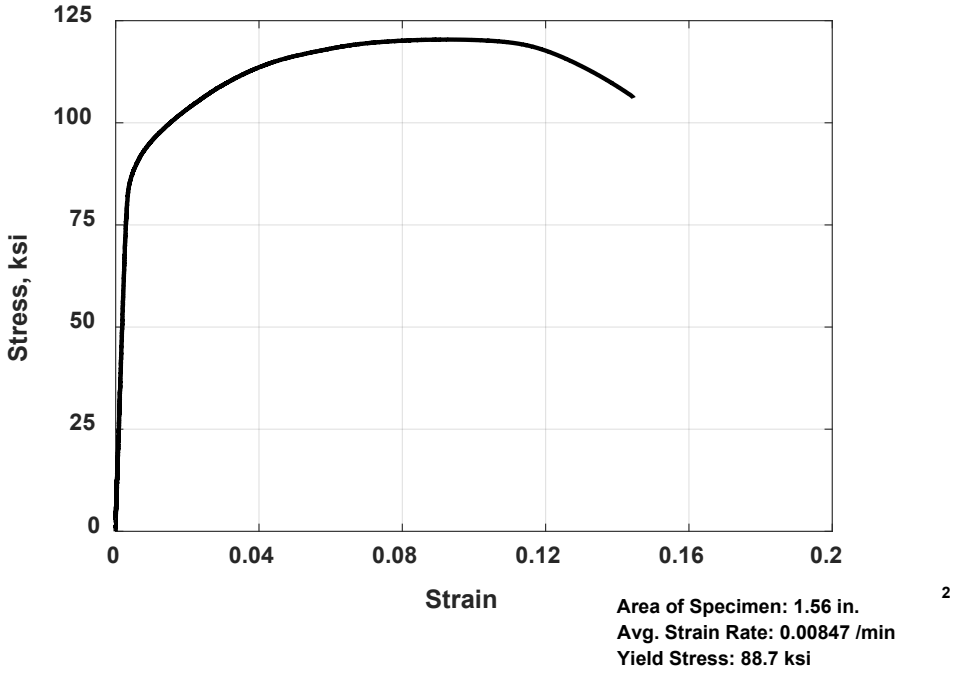

Figure D.7: Stress versus strain for No. 11 [No. 36] longitudinal reinforcing bar (Grade 80 [Grade 550], Sample 1, Phase 1) [1 in.^{2} = 0.000645 m^2, 1 ksi = 6.9 MPa]

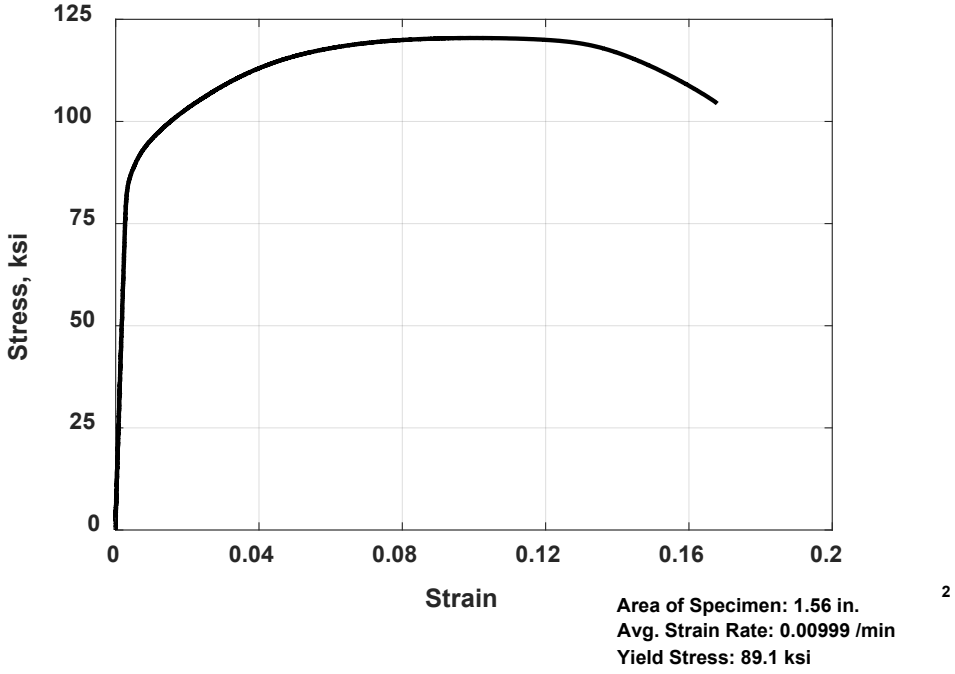

Figure D.8: Stress versus strain for No. 11 [No. 36] longitudinal reinforcing bar (Grade 80 [Grade 550], Sample 2, Phase 1) [1 in.^{2} = 0.000645 m^2, 1 ksi = 6.9 MPa]

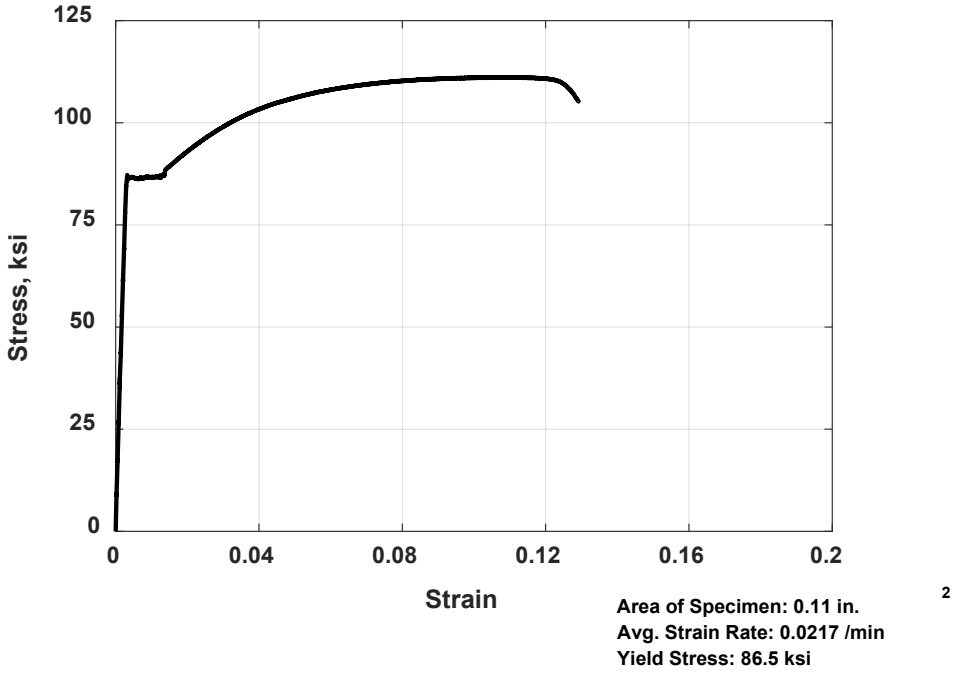

Figure D.9: Stress versus strain for No. 3 [No. 10] transverse reinforcing bar (Grade 80 [Grade 550], Sample 1, Phase 2) [1 in.^{2} = 0.000645 m^2, 1 ksi = 6.9 MPa]

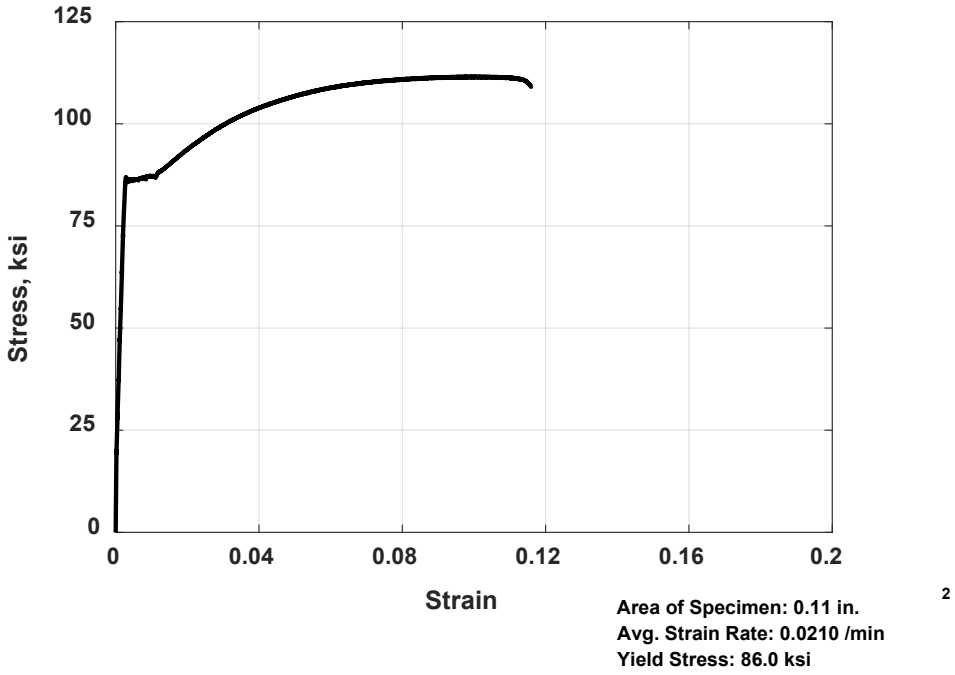

Figure D.10: Stress versus strain for No. 3 [No. 10] transverse reinforcing bar (Grade 80 [Grade 550], Sample 2, Phase 2) [1 in.^{2} = 0.000645 m^2, 1 ksi = 6.9 MPa]

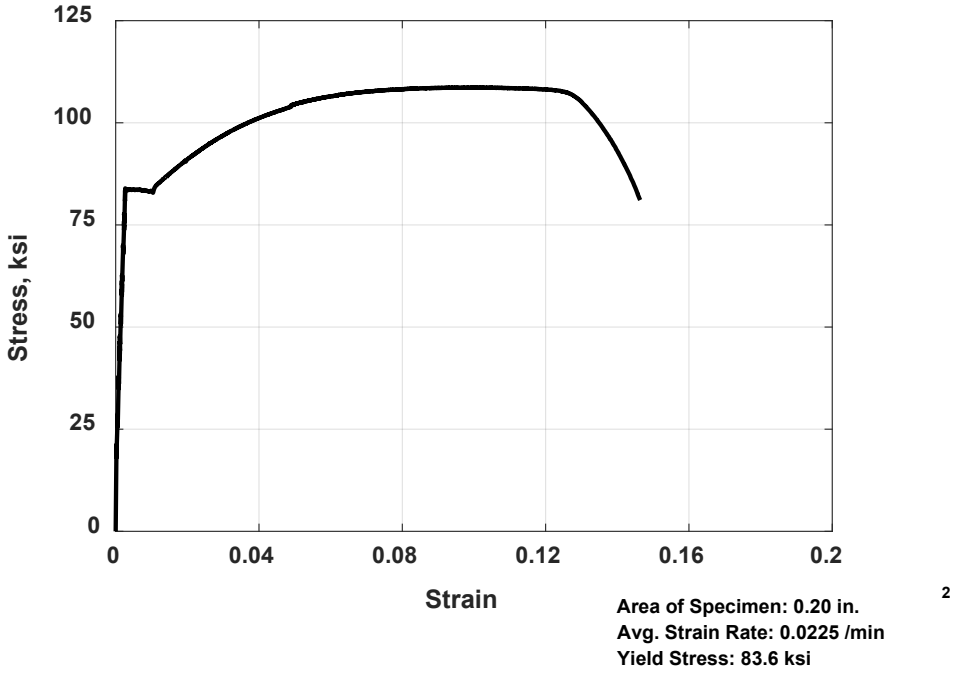

Figure D.11: Stress versus strain for No. 4 [No. 13] transverse reinforcing bar (Grade 80 [Grade 550], Sample 1, Phase 2) [1 in.^{2} = 0.000645 m^2, 1 ksi = 6.9 MPa]

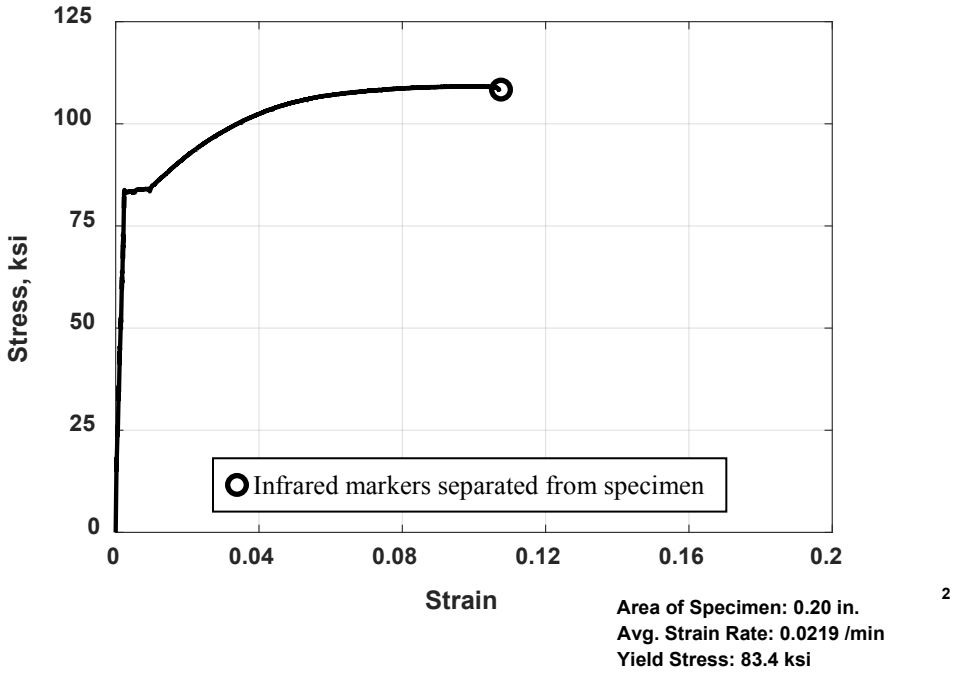

Figure D.12: Stress versus strain for No. 4 [No. 13] transverse reinforcing bar (Grade 80 [Grade 550], Sample 2, Phase 2) [1 in.^{2} = 0.000645 m^2, 1 ksi = 6.9 MPa]

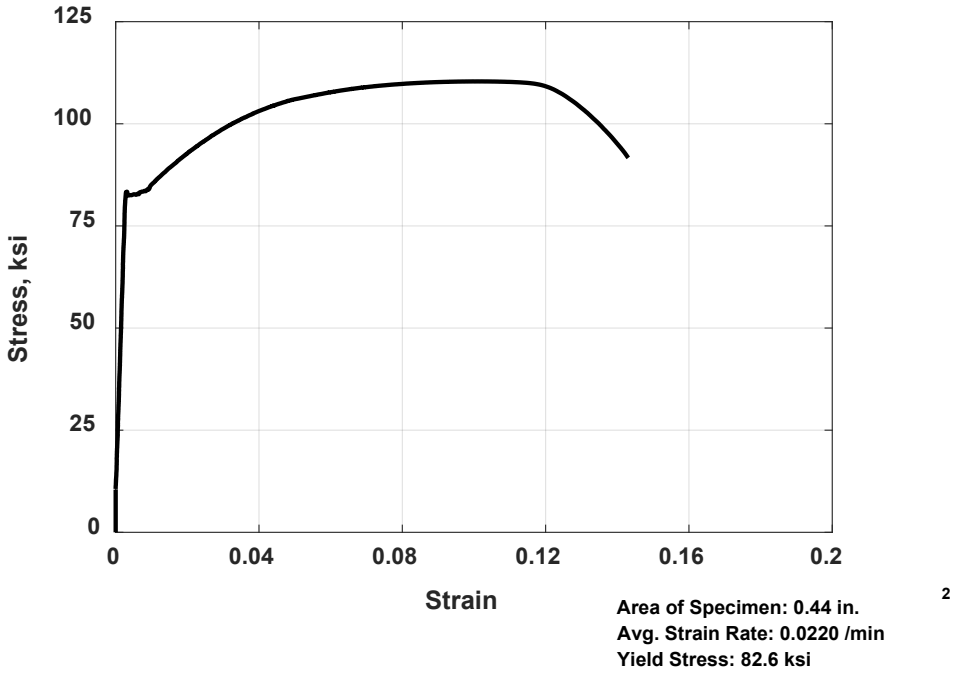

Figure D.13: Stress versus strain for No. 6 [No. 19] transverse reinforcing bar (Grade 80 [Grade 550], Sample 1, Phase 2) [1 in.^{2} = 0.000645 m^2, 1 ksi = 6.9 MPa]

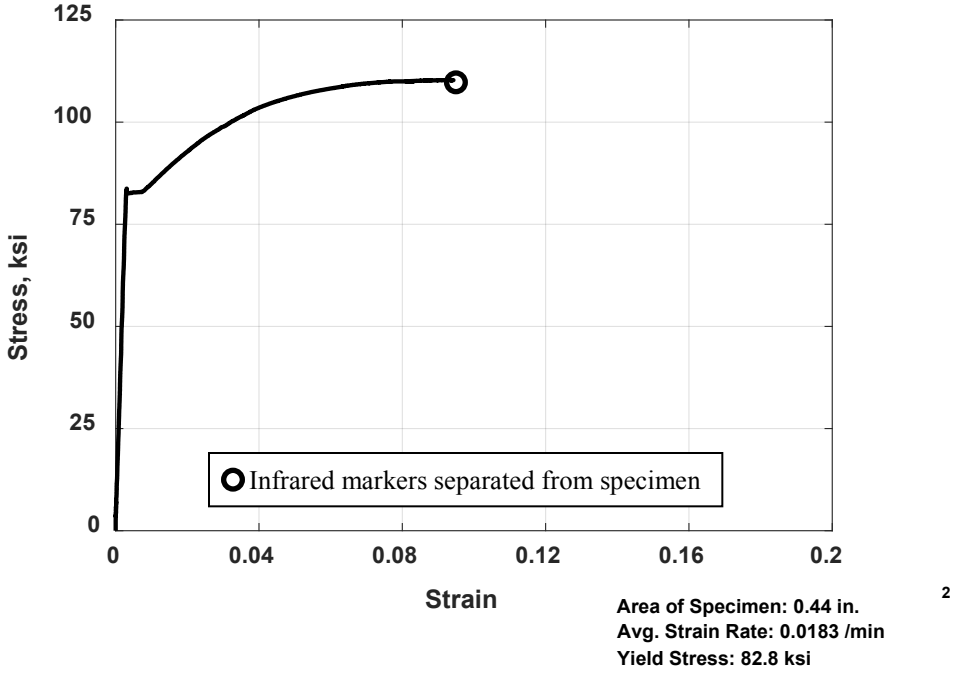

Figure D.14: Stress versus strain for No. 6 [No. 19] transverse reinforcing bar (Grade 80 [Grade 550], Sample 2, Phase 2) [1 in.^{2} = 0.000645 m^2, 1 ksi = 6.9 MPa]

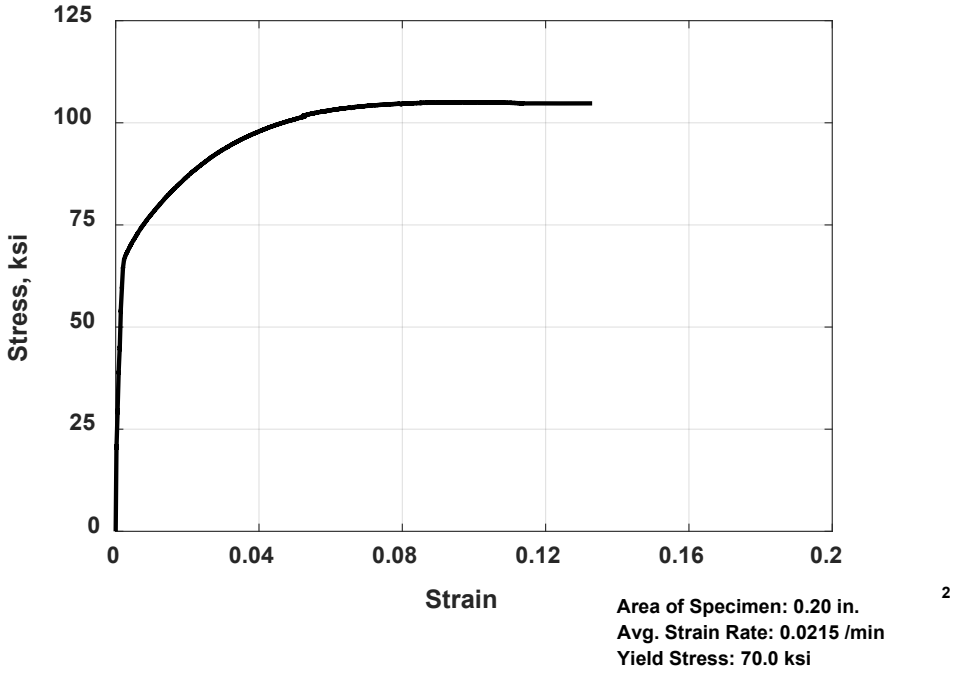

Figure D.15: Stress versus strain for No. 4 [No. 13] longitudinal reinforcing bar (Grade 60 [Grade 420], Sample 1, Phase 2) [1 in.^{2} = 0.000645 m^2, 1 ksi = 6.9 MPa]

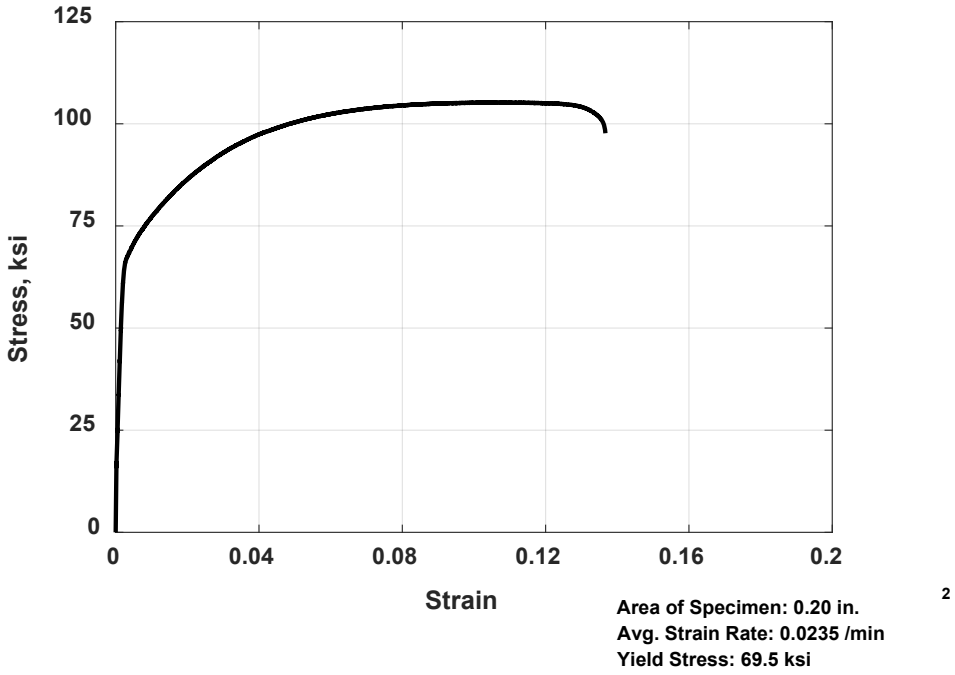

Figure D.16: Stress versus strain for No. 4 [No. 13] longitudinal reinforcing bar (Grade 60 [Grade 420], Sample 2, Phase 2) [1 in.^{2} = 0.000645 m^2, 1 ksi = 6.9 MPa]

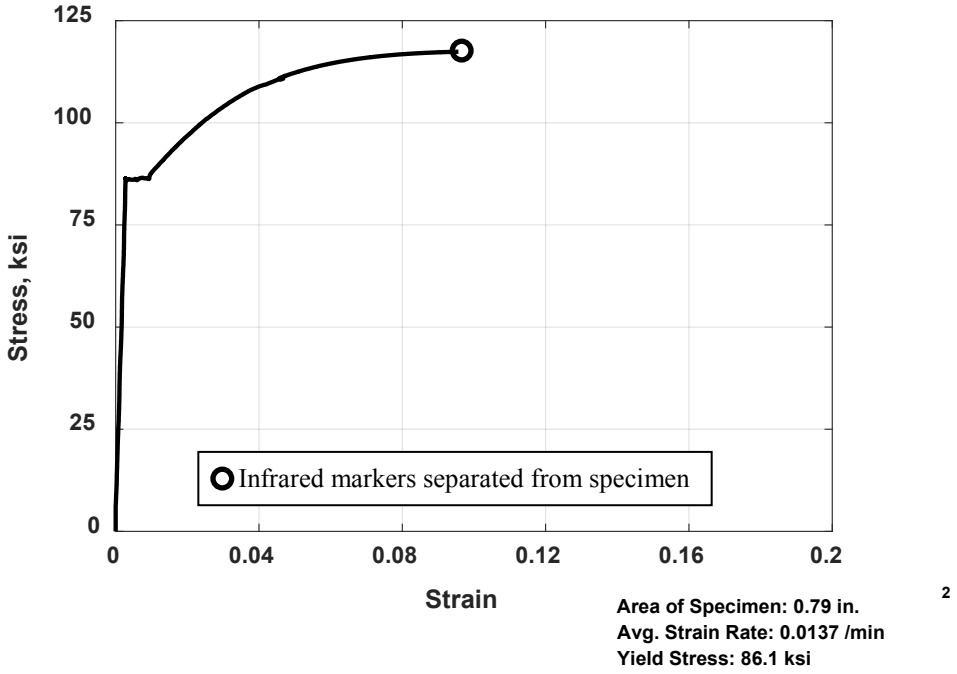

Figure D.17: Stress versus strain for No. 8 [No. 25] longitudinal reinforcing bar (Grade 80 [Grade 550], Sample 1, Phase 2) [1 in.^{2} = 0.000645 m^2, 1 ksi = 6.9 MPa]

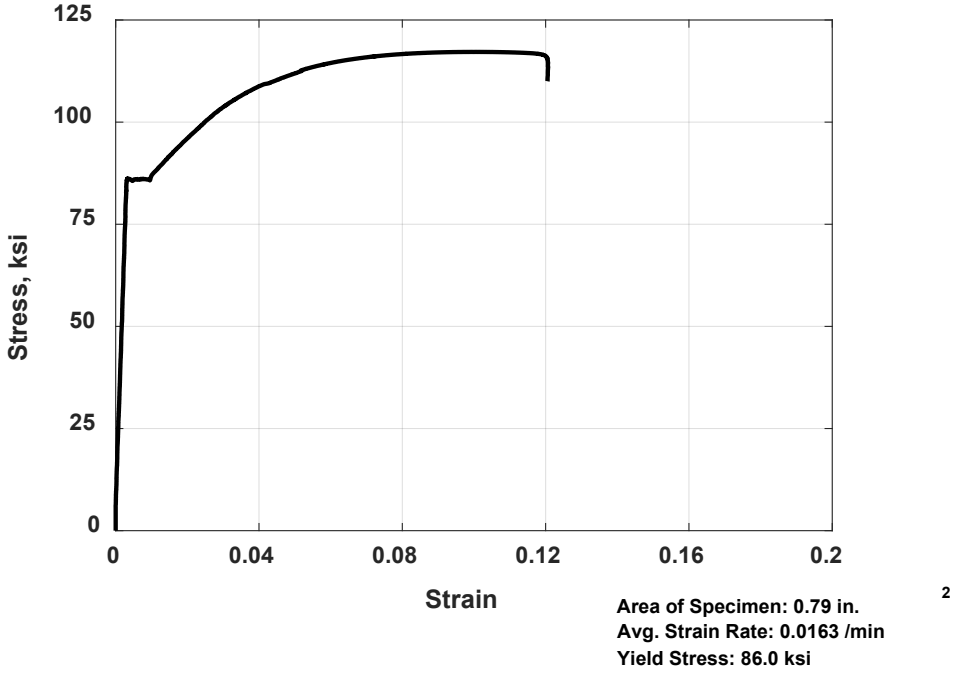

Figure D.18: Stress versus strain for No. 8 [No. 25] longitudinal reinforcing bar (Grade 80 [Grade 550], Sample 2, Phase 2) [1 in.^{2} = 0.000645 m^2, 1 ksi = 6.9 MPa]

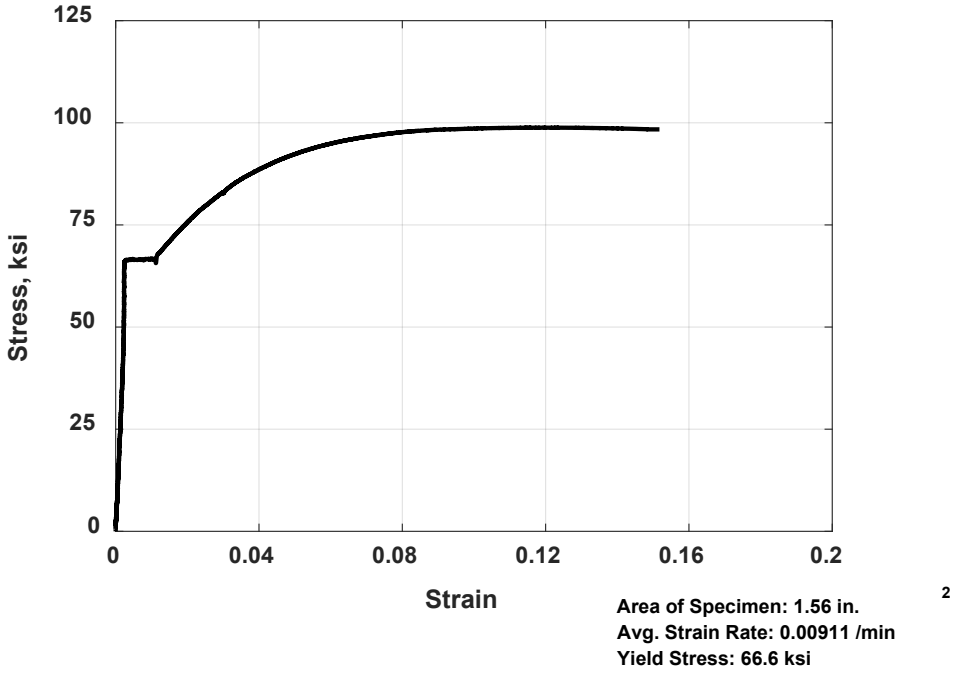

Figure D.19: Stress versus strain for No. 11 [No. 36] longitudinal reinforcing bar (Grade 60 [Grade 420], Sample 1, Phase 2) [1 in.^{2} = 0.000645 m^2, 1 ksi = 6.9 MPa]

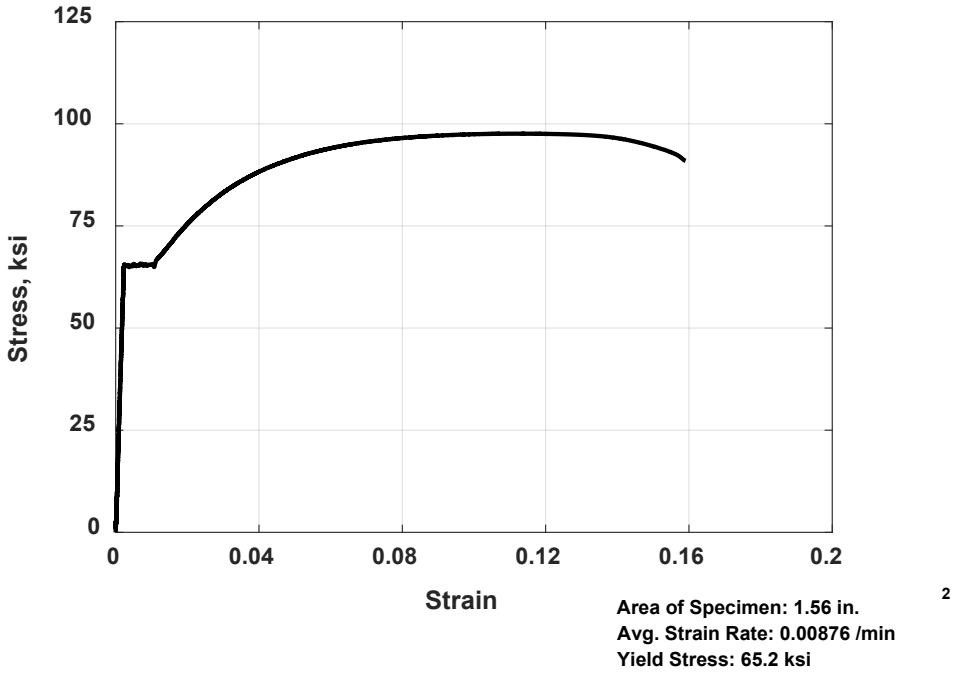

Figure D.20: Stress versus strain for No. 11 [No. 36] longitudinal reinforcing bar (Grade 60 [Grade 420], Sample 2, Phase 2) [1 in.^{2} = 0.000645 m^2, 1 ksi = 6.9 MPa]

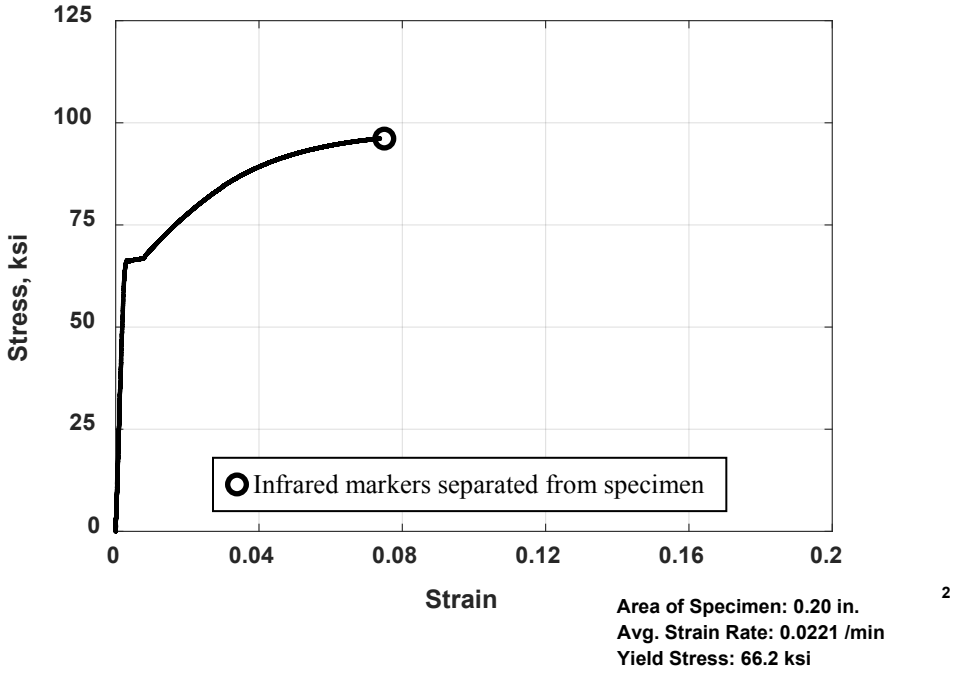

Figure D.21: Stress versus strain for No. 4 [No. 13] transverse reinforcing bar (Grade 60 [Grade 420], Sample 1, Phase 3) [1 in.^{2} = 0.000645 m^2, 1 ksi = 6.9 MPa]

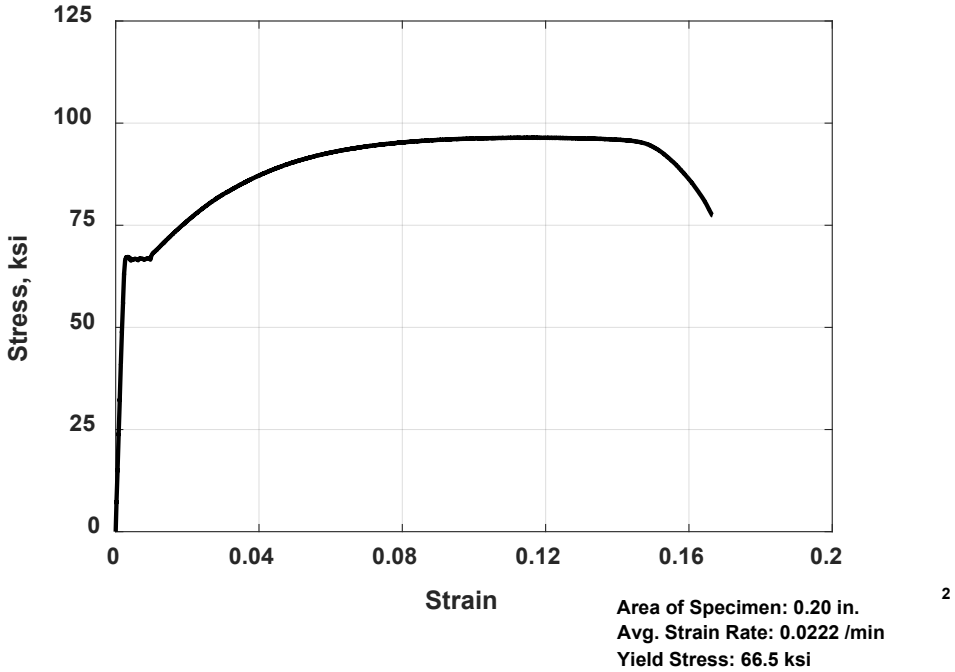

Figure D.22: Stress versus strain for No. 4 [No. 13] ransverse reinforcing bar (Grade 60 [Grade 420], Sample 2, Phase 3) [1 in.^{2} = 0.000645 m^2, 1 ksi = 6.9 MPa]

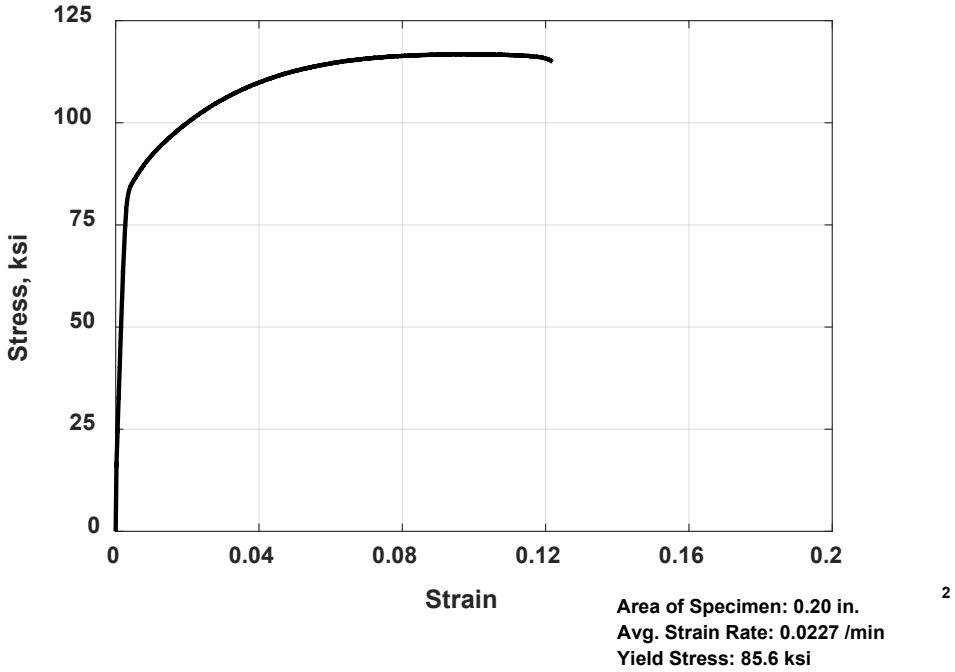

Figure D.23: Stress versus strain for No. 4 [No. 13] transverse reinforcing bar (Grade 80 [Grade 550], Sample 1, Phase 3) [1 in.^{2} = 0.000645 m^2, 1 ksi = 6.9 MPa]

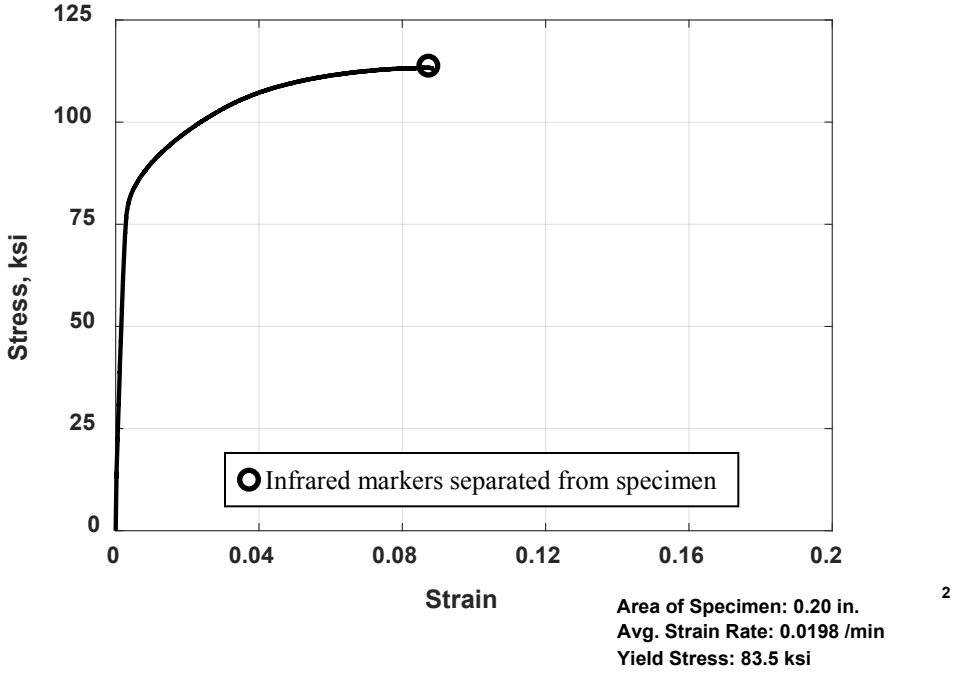

Figure D.24: Stress versus strain for No. 4 [No. 13] transverse reinforcing bar (Grade 80 [Grade 550], Sample 2, Phase 3) [1 in.^{2} = 0.000645 m^2, 1 ksi = 6.9 MPa]

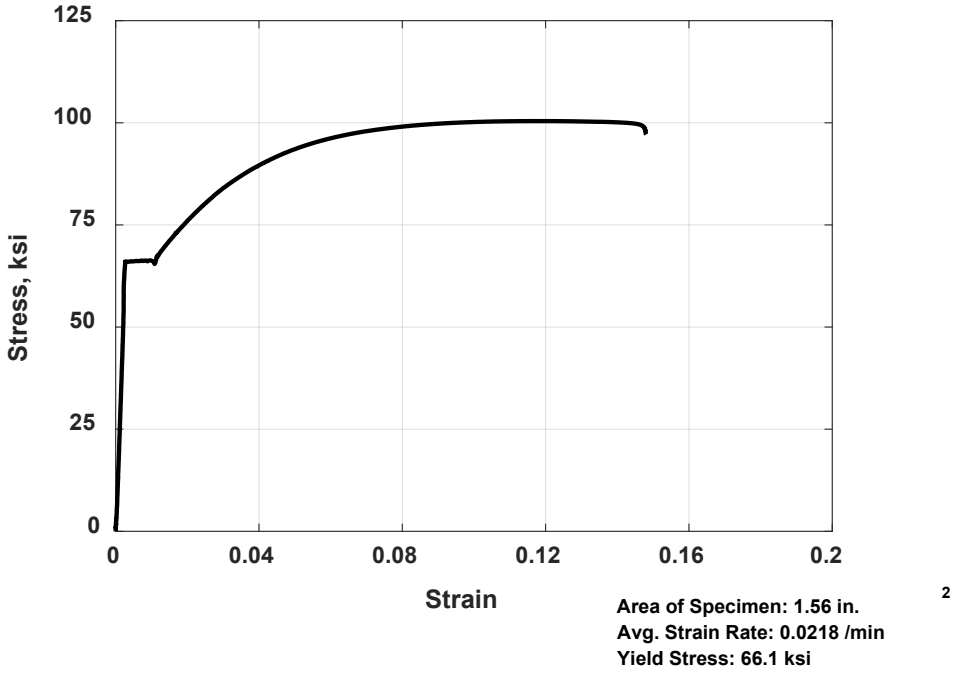

Figure D.25: Stress versus strain for No. 11 [No. 36] longitudinal reinforcing bar (Grade 60 [Grade 420], Sample 2, Phase 3) [1 in.^{2} = 0.000645 m^2, 1 ksi = 6.9 MPa]

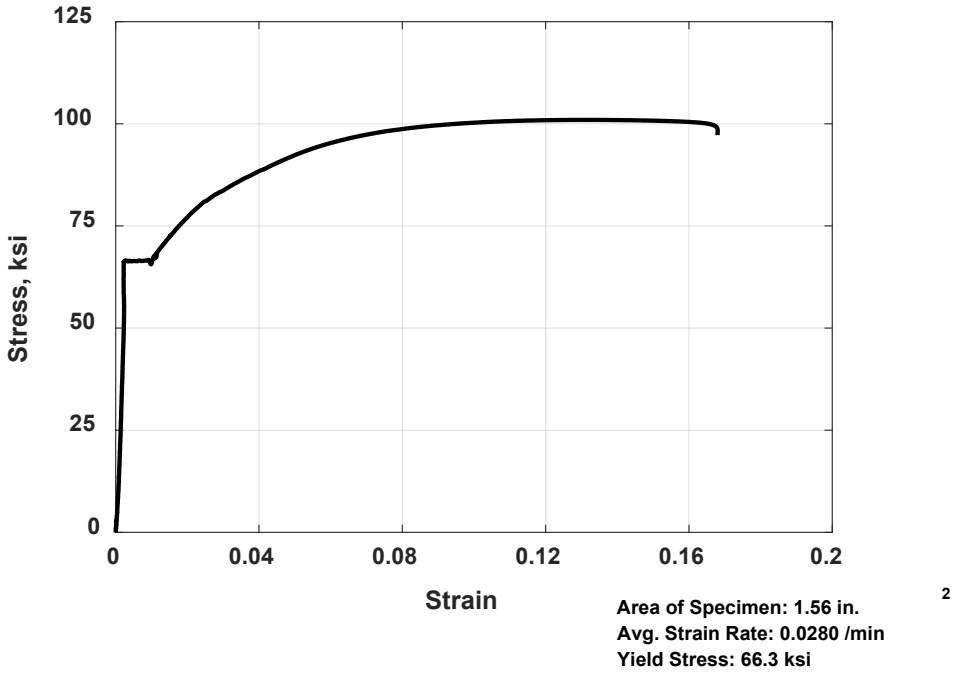

Figure D.26: Stress versus strain for No. 11 [No. 36] longitudinal reinforcing bar (Grade 60 [Grade 420], Sample 2, Phase 3) [1 $in.^2$ = 0.000645 m^2, 1 ksi = 6.9 MPa]

APPENDIX E: OBSERVED CRACKING AND DAMAGE

The following figures show the location and extent of cracking and damage at failure for each specimen in this study. To create the figures, photos taken just before and after failure were overlaid onto line representations of the specimens and cracks and damage were traced. Two diagrams are provided for each specimen: (a) shows the front side of the beam, where cracking was documented during testing, and (b) shows the back side. Data from the back side is limited, as optical tracking was conducted on the back side of the specimen, and documenting cracking would have interfered with these measurements. All figures show the failure surface, regions were concrete spalling occurred, and the nominal location of transverse reinforcement. Figures representing the front side of the specimens also include the locations of cracks. All figures in this appendix use the legend shown in Figure E.1. For simplicity, end reinforcement and bar heads have been omitted from all figures.

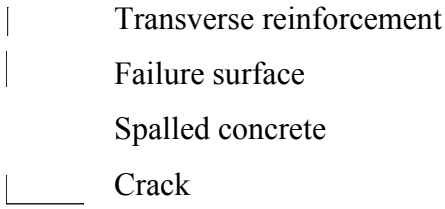

Figure E.1: Legend for crack maps

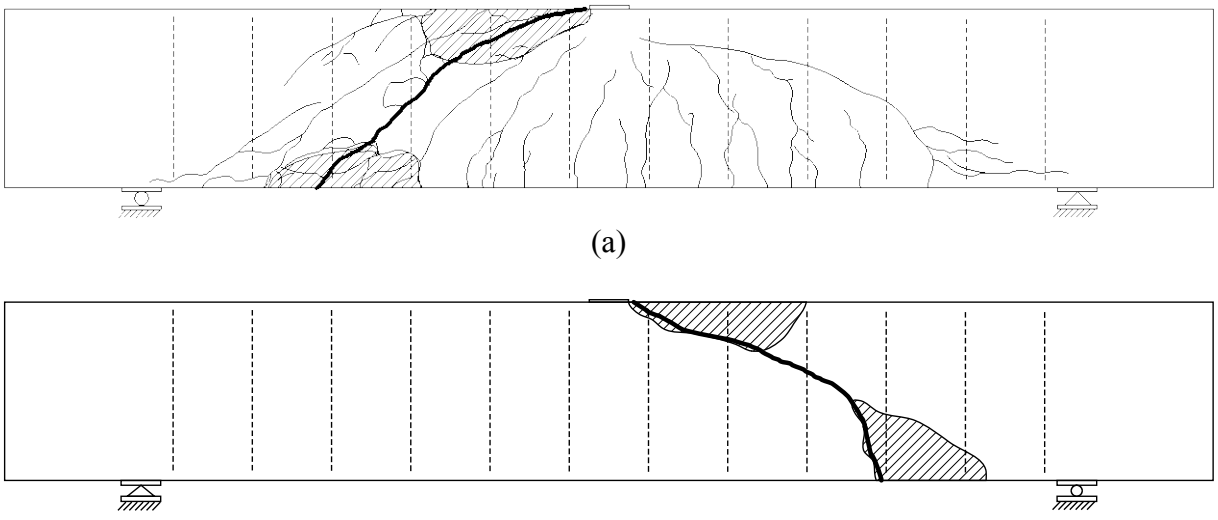

(a)

(b)

Figure E.2: Observed damage in specimen P1S1, (a) front side, (b) back side

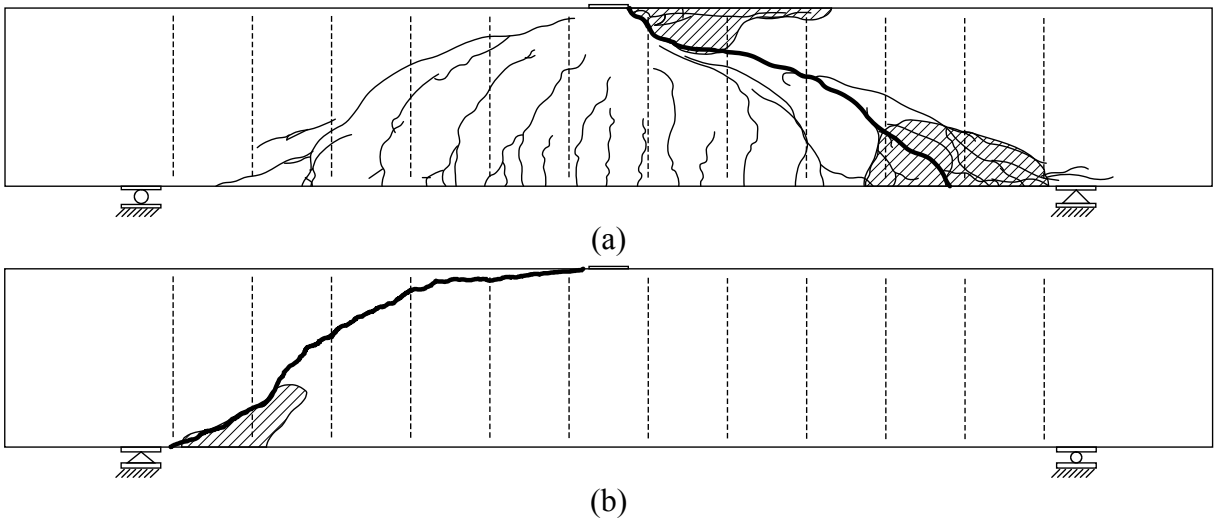

(a)

(b)

Figure E.3: Observed damage in specimen P1S2, (a) front side, (b) back side

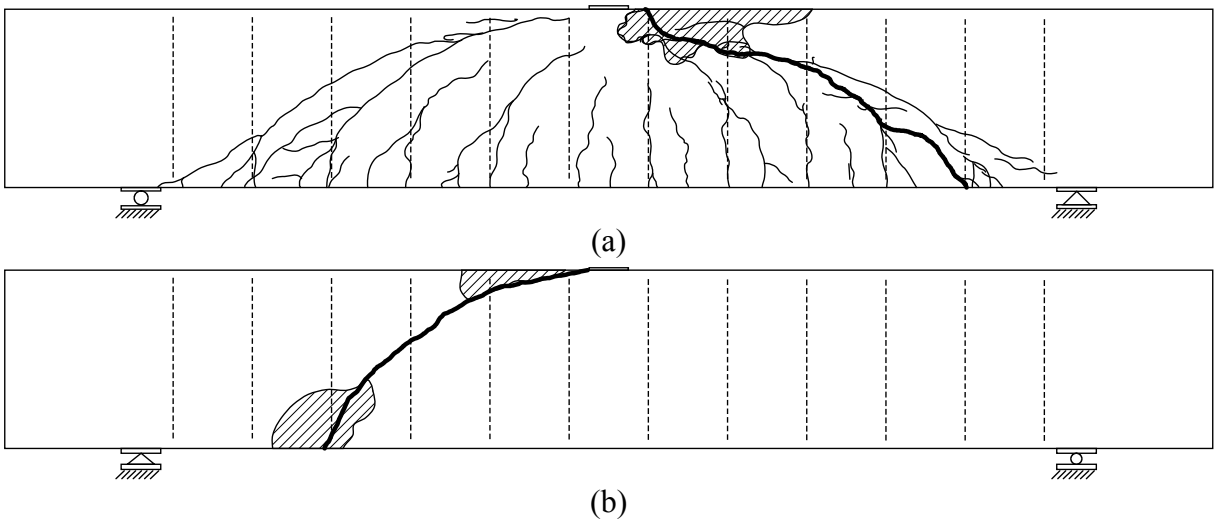

(a)

(b)

Figure E.4: Observed damage in specimen P1S3, (a) front side, (b) back side

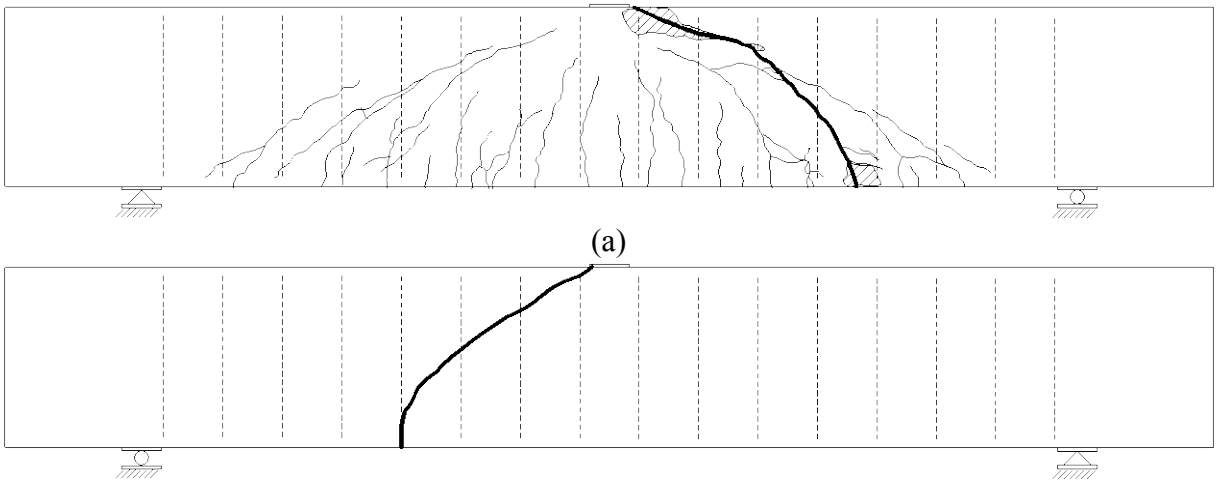

(a)

(b)

Figure E.5: Observed damage in specimen P1S4, (a) front side, (b) back side

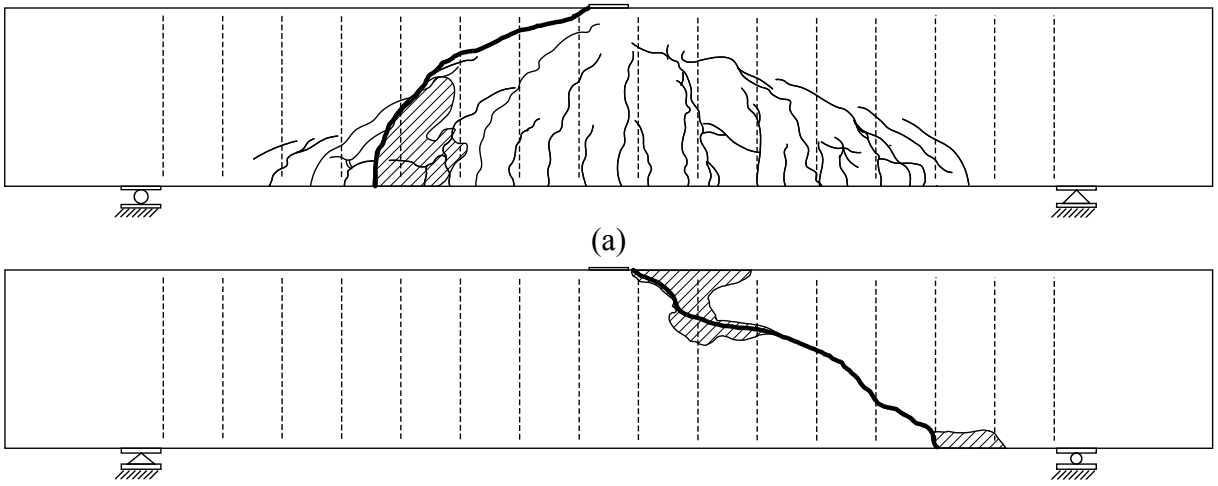

(a)

(b)

Figure E.6: Observed damage in specimen P1S5, (a) front side, (b) back side

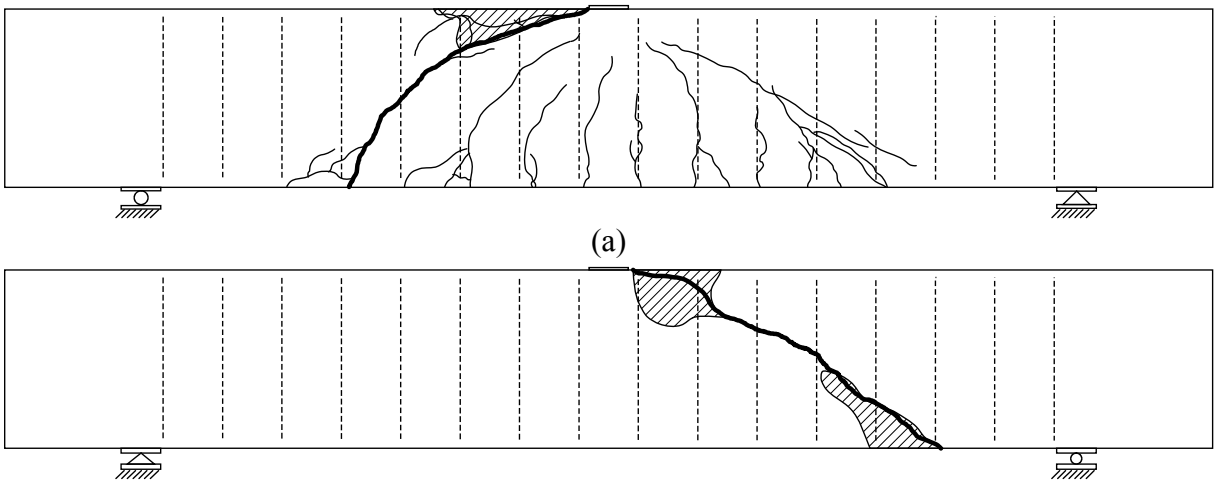

(a)

(b)

Figure E.7: Observed damage in specimen P1S6, (a) front side, (b) back side

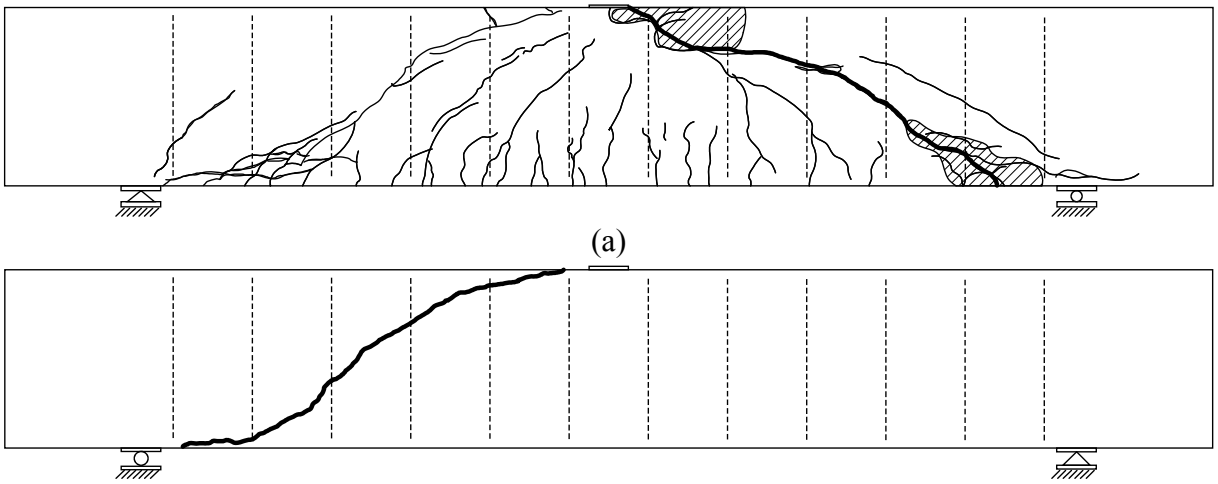

(a)

(b)

Figure E.8: Observed damage in specimen P1S7, (a) front side, (b) back side

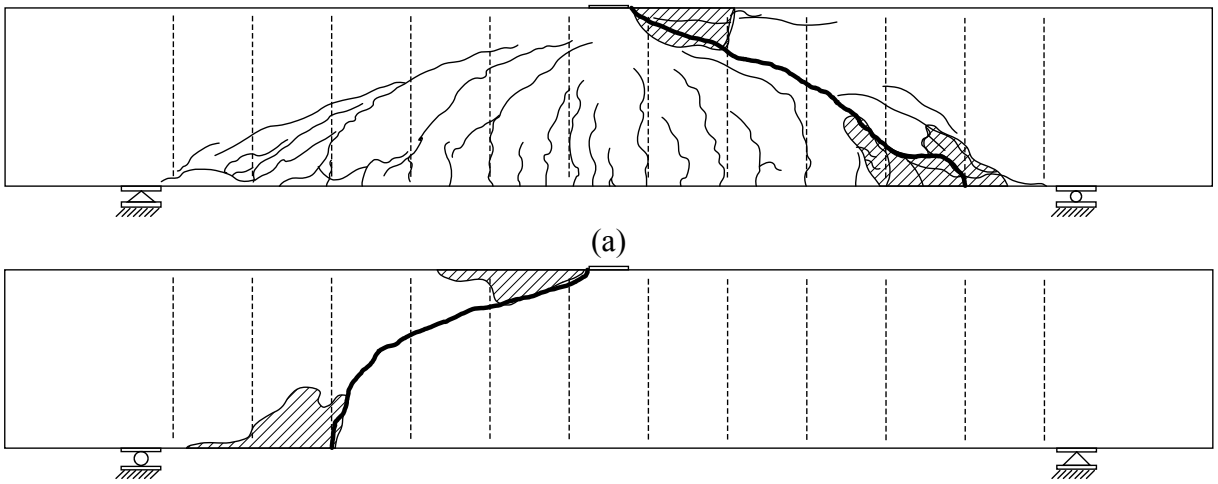

(a)

(b)

Figure E.9: Observed damage in specimen P1S8, (a) front side, (b) back side

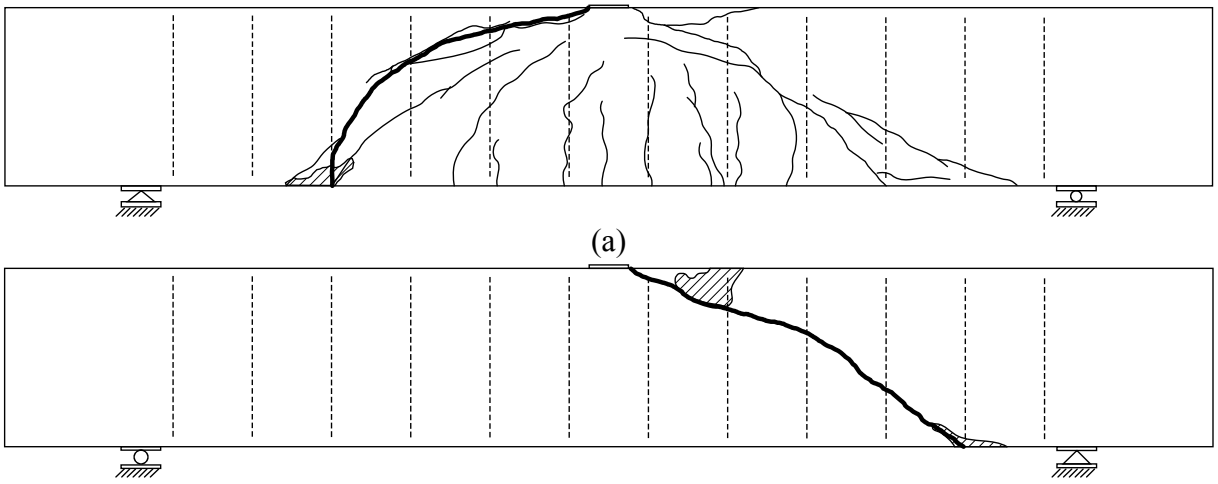

(a)

(b)

Figure E.10: Observed damage in specimen P1S9, (a) front side, (b) back side

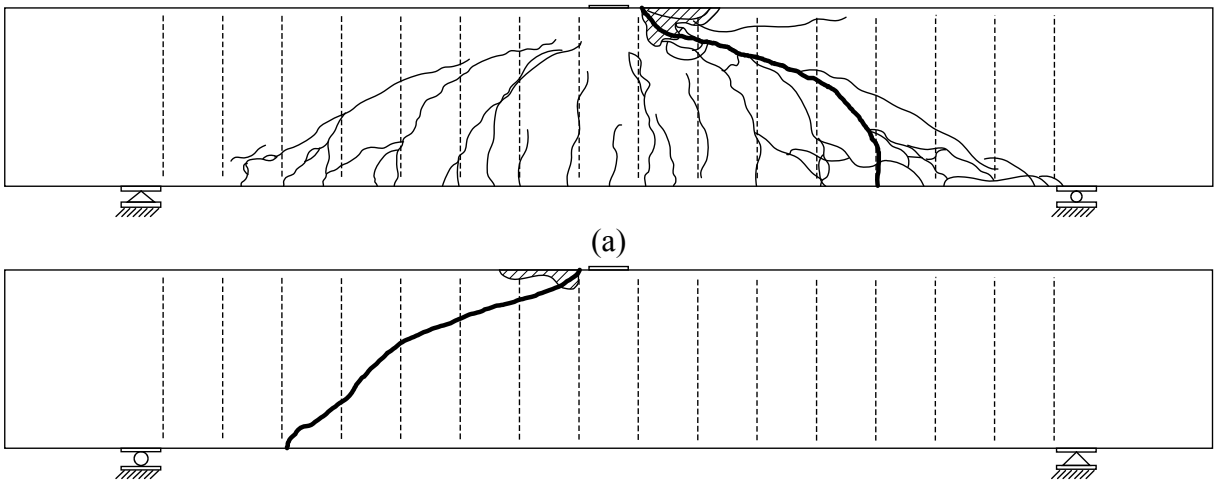

(a)

(b)

Figure E.11: Observed damage in specimen P1S10, (a) front side, (b) back side

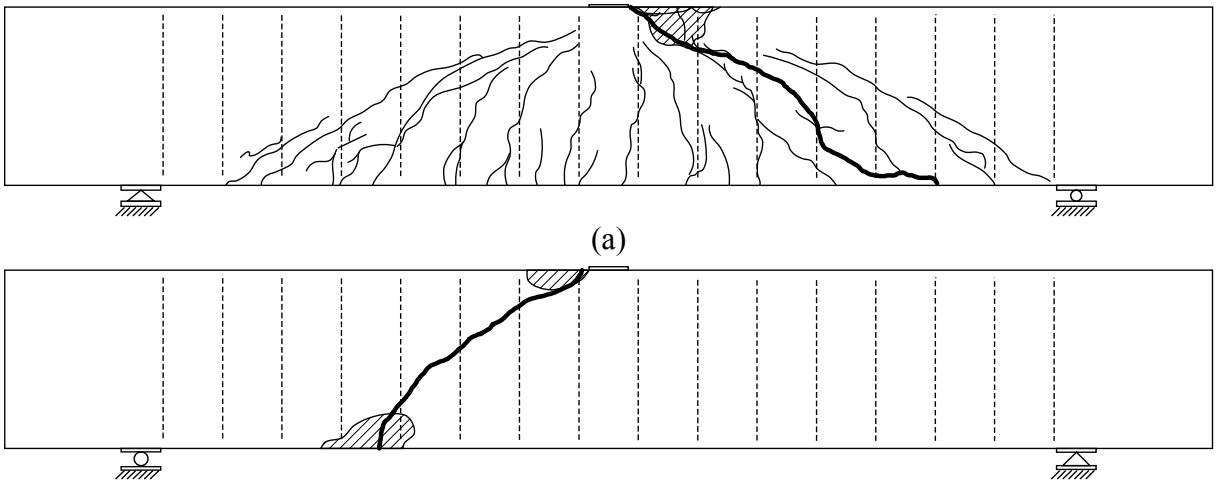

(a)

(b)

Figure E.12: Observed damage in specimen P1S11, (a) front side, (b) back side

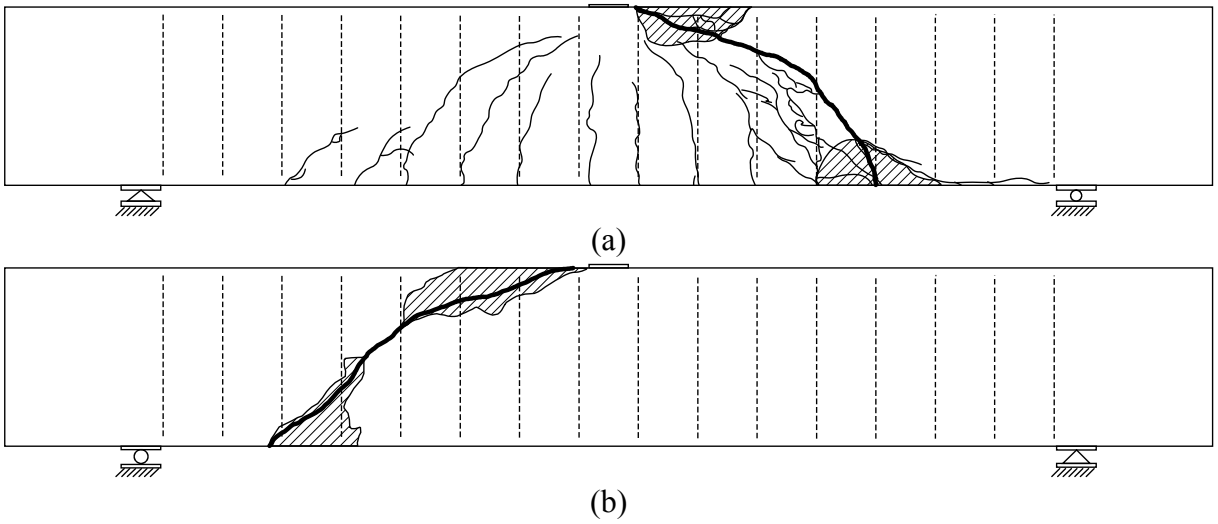

(a)

(b)

Figure E.13: Observed damage in specimen P1S12, (a) front side, (b) back side

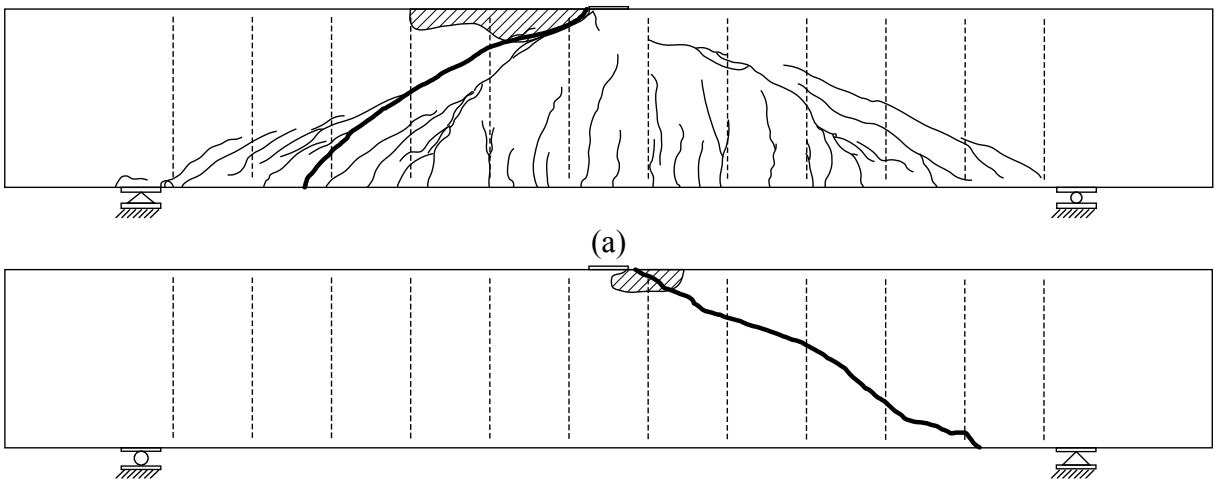

(a)

(b)

Figure E.14: Observed damage in specimen P1S13, (a) front side, (b) back side

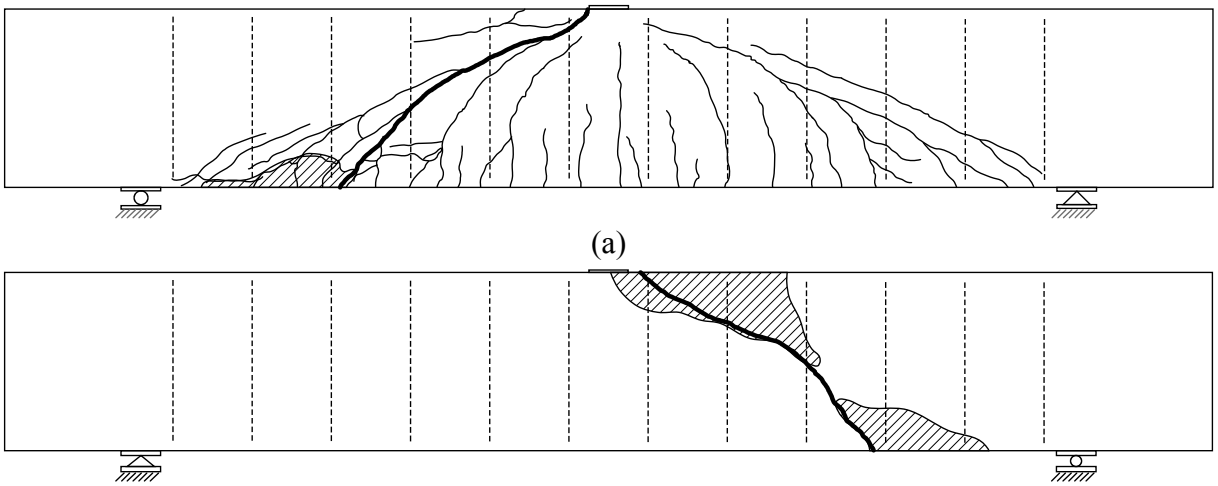

(a)

(b)

Figure E.15: Observed damage in specimen P1S14, (a) front side, (b) back side

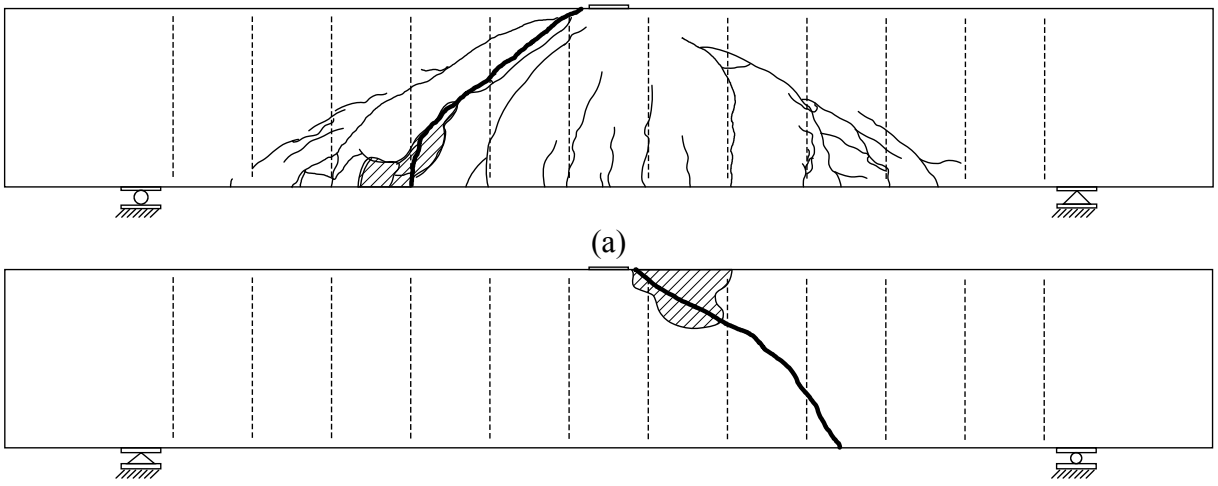

(a)

(b)

Figure E.16: Observed damage in specimen P1S15, (a) front side, (b) back side

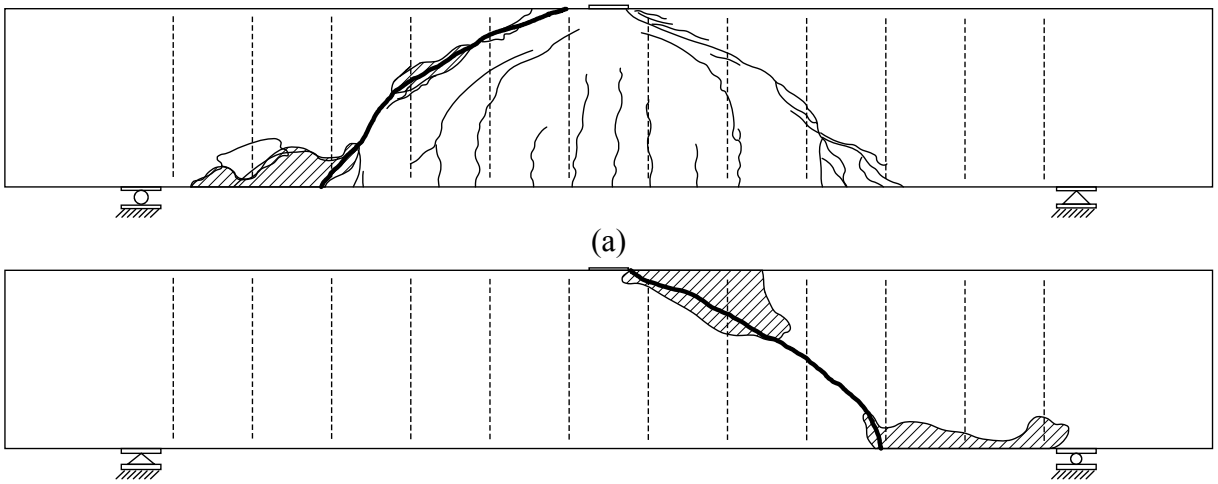

(a)

(b)

Figure E.17: Observed damage in specimen P1S16, (a) front side, (b) back side

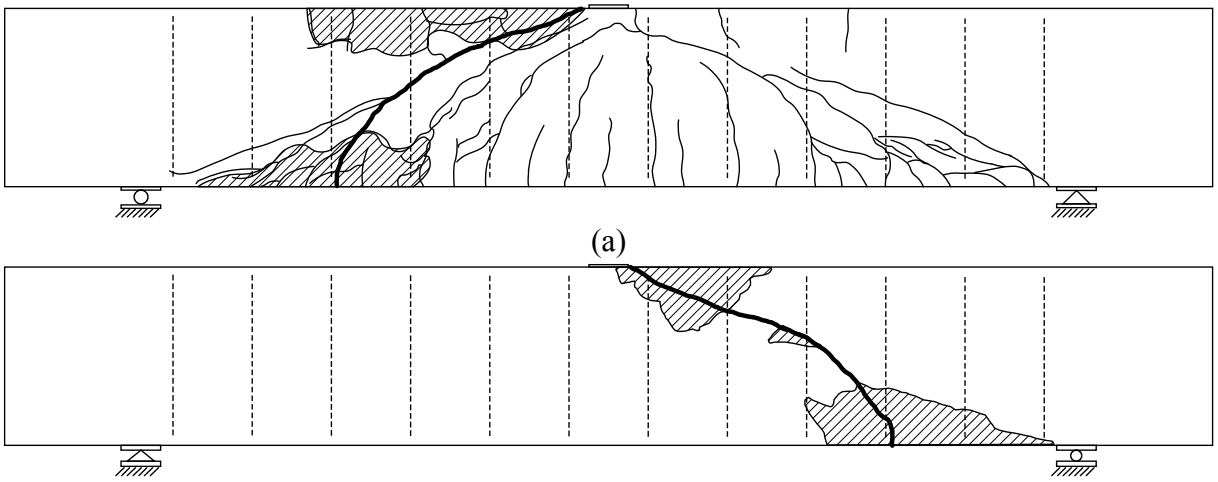

(a)

(b)

Figure E.18: Observed damage in specimen P1S17, (a) front side, (b) back side

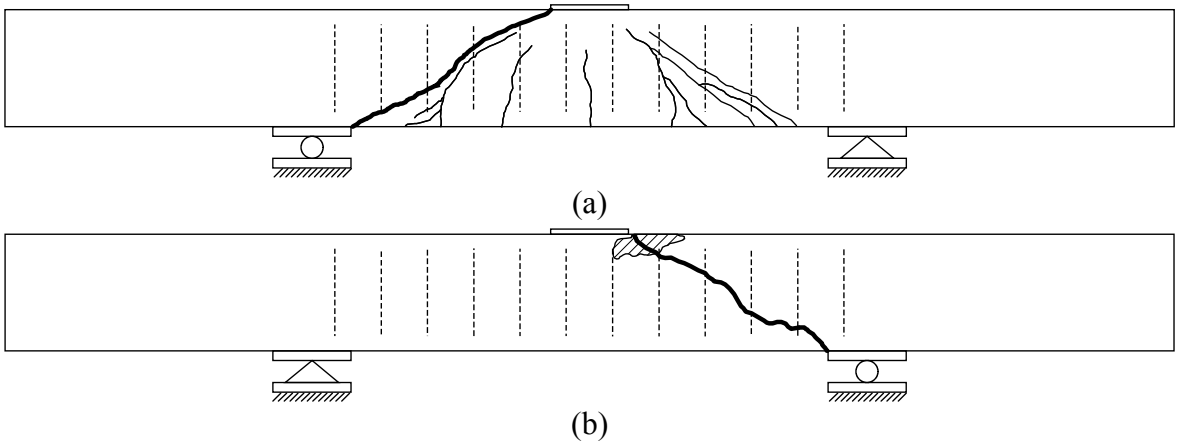

Figure E.19: Observed damage in specimen P2S1, (a) front side, (b) back side

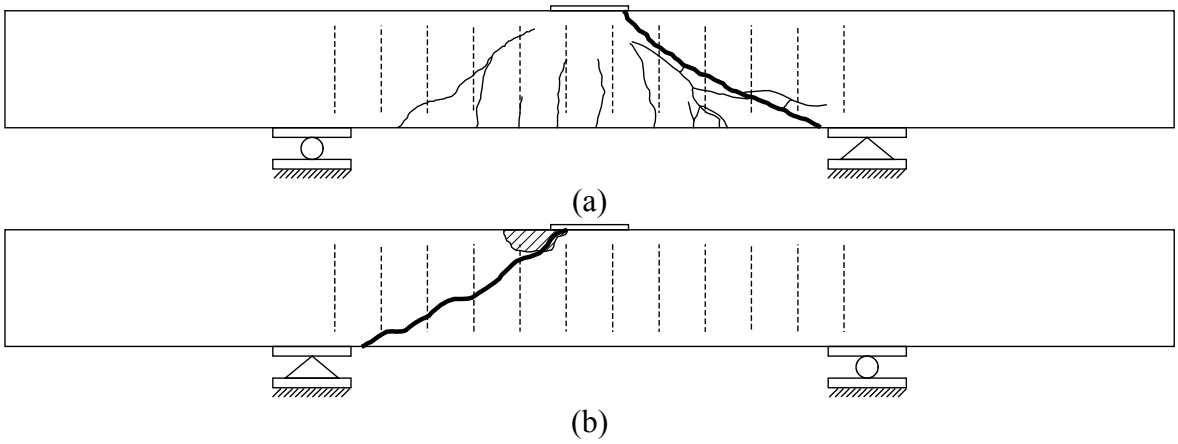

Figure E.20: Observed damage in specimen P2S2, (a) front side, (b) back side

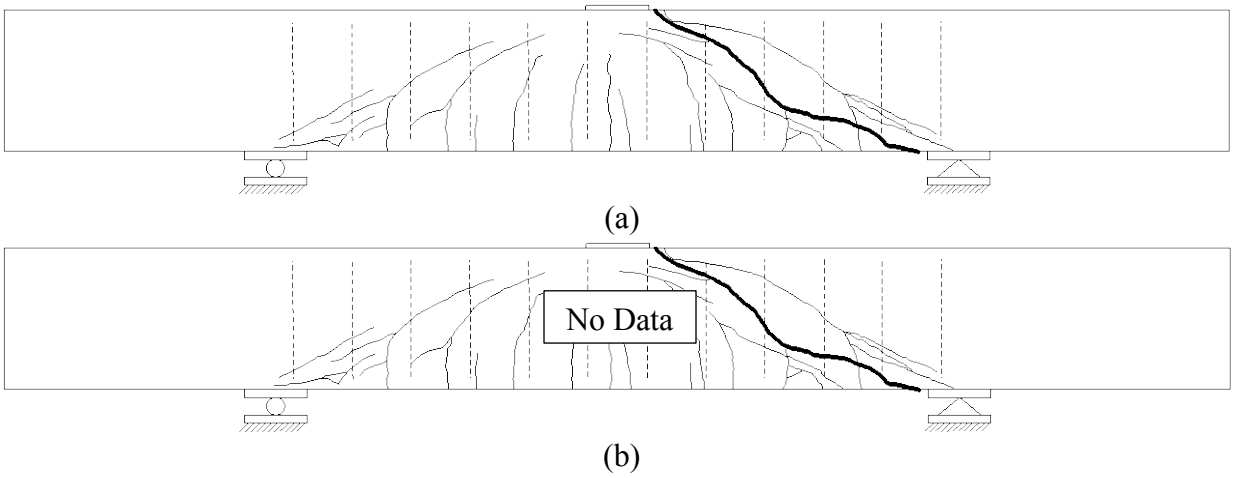

Figure E.21: Observed damage in specimen P2S3, (a) front side, (b) back side

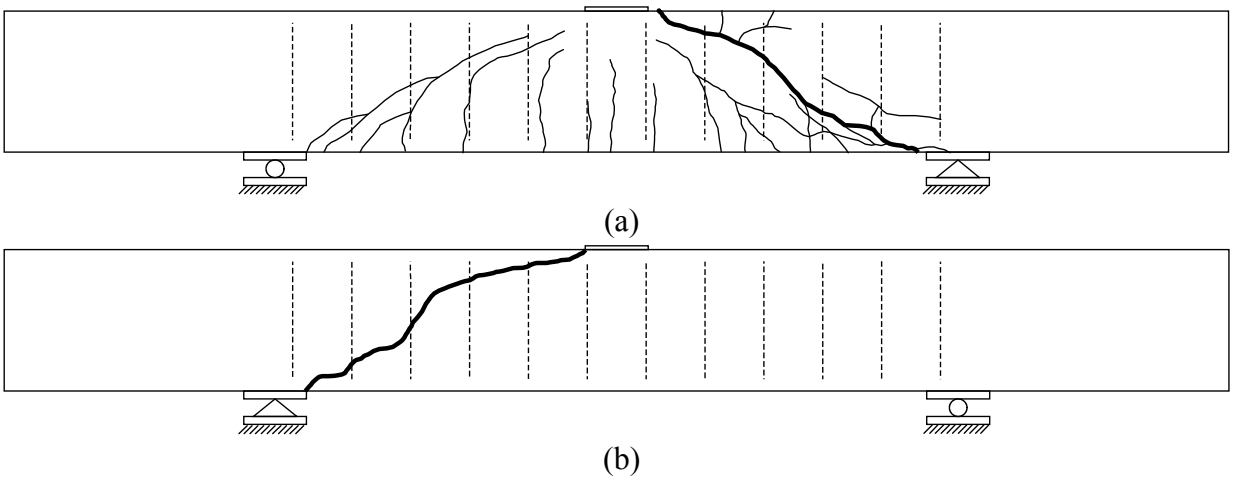

Figure E.22: Observed damage in specimen P2S4, (a) front side, (b) back side

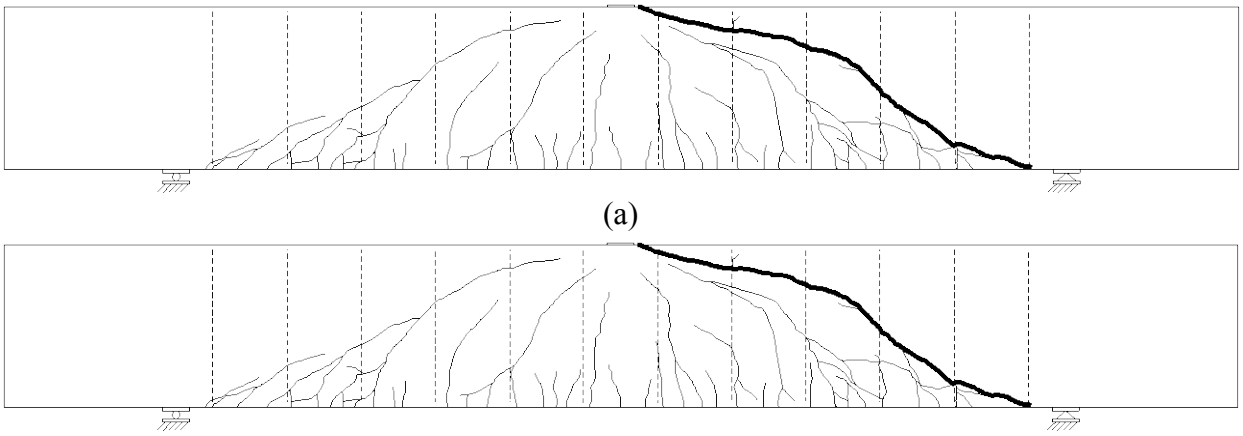

(a)

(b)

Figure E.23: Observed damage in specimen P2S5, (a) front side, (b) back side

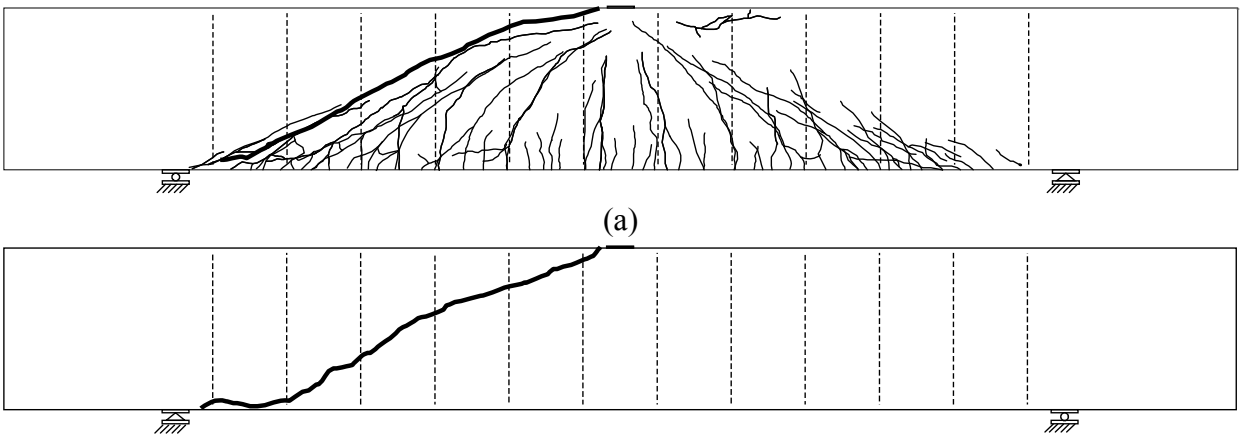

(a)

(b)

Figure E.24: Observed damage in specimen P2S6, (a) front side, (b) back side

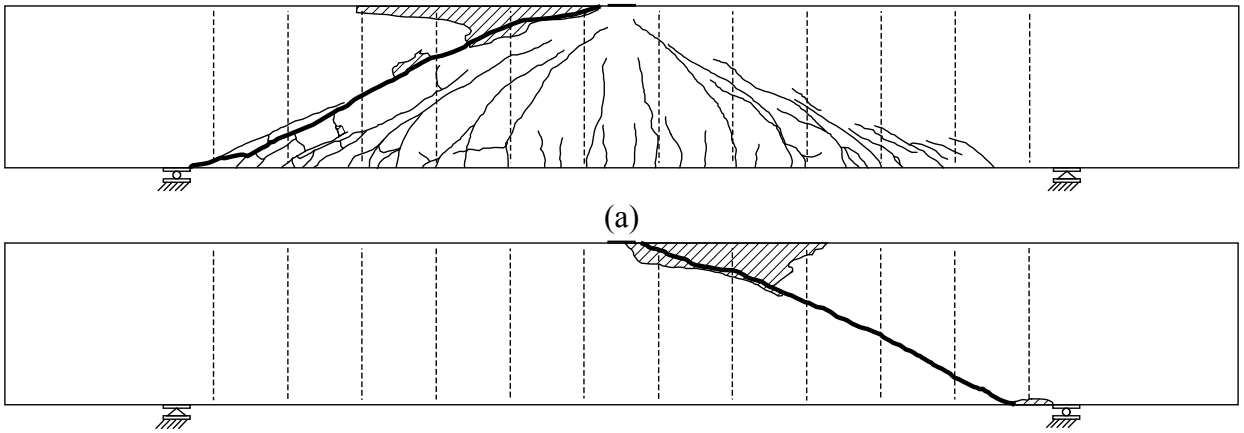

(a)

(b)

Figure E.25: Observed damage in specimen P2S7, (a) front side, (b) back side

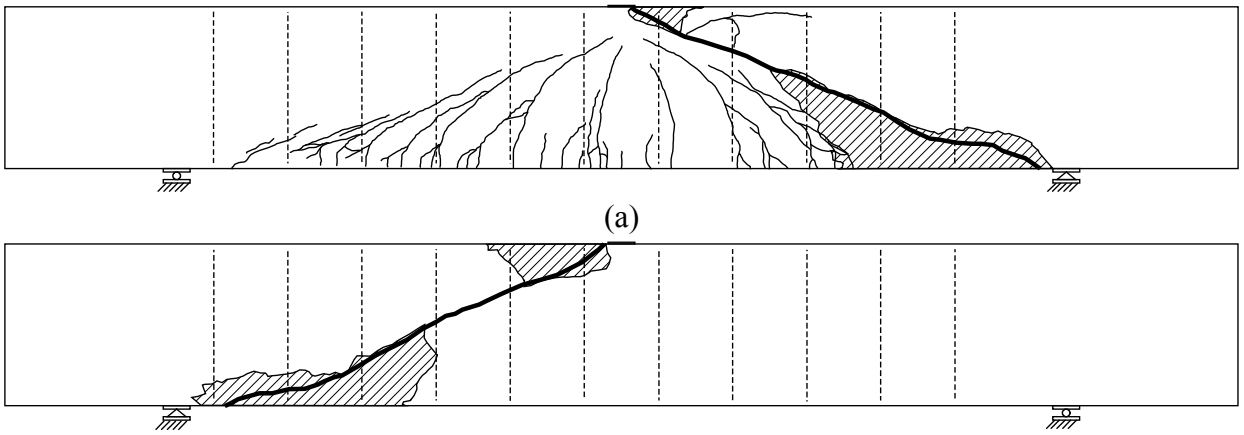

(a)

(b)

Figure E.26: Observed damage in specimen P2S8, (a) front side, (b) back side

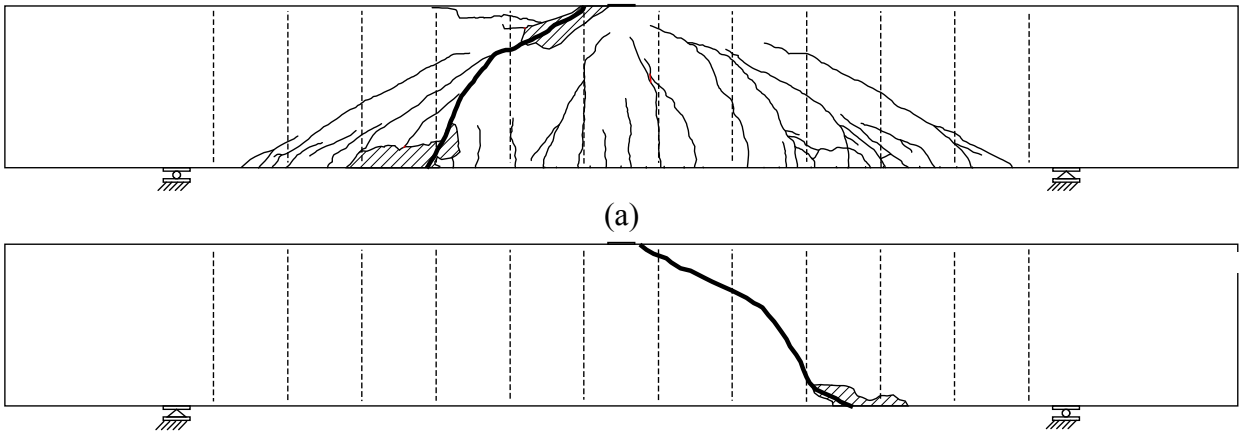

(a)

(b)

Figure E.27: Observed damage in specimen P2S9, (a) front side, (b) back side

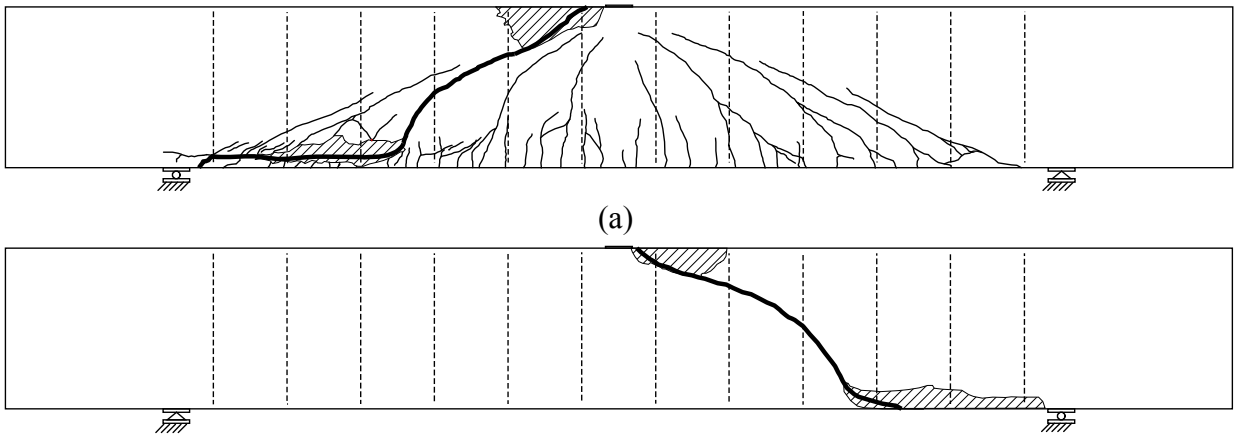

(a)

(b)

Figure E.28: Observed damage in specimen P2S10, (a) front side, (b) back side

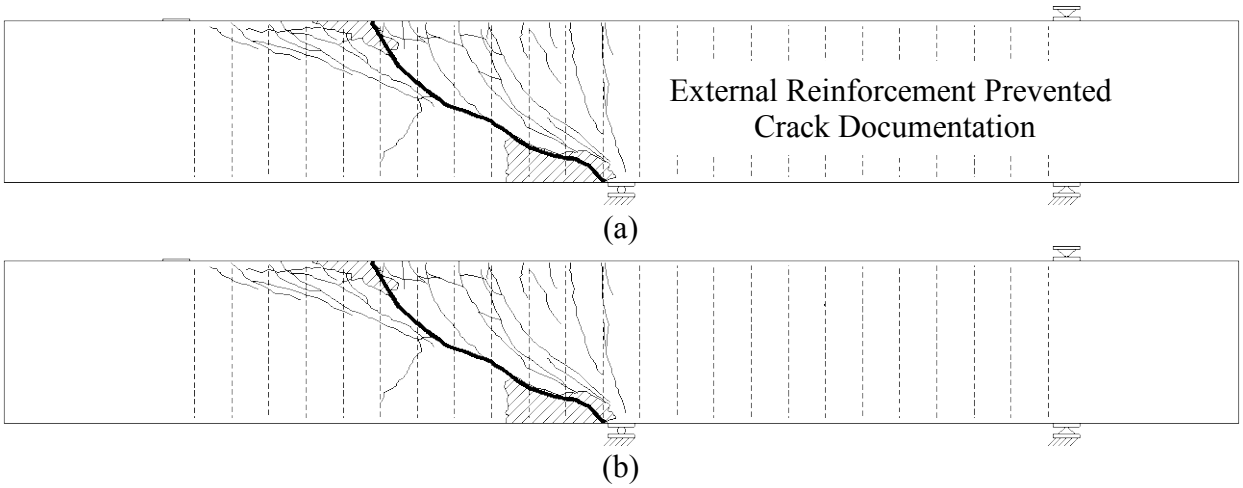

Figure E.29: Observed damage in specimen P2S11, (a) front side, (b) back side

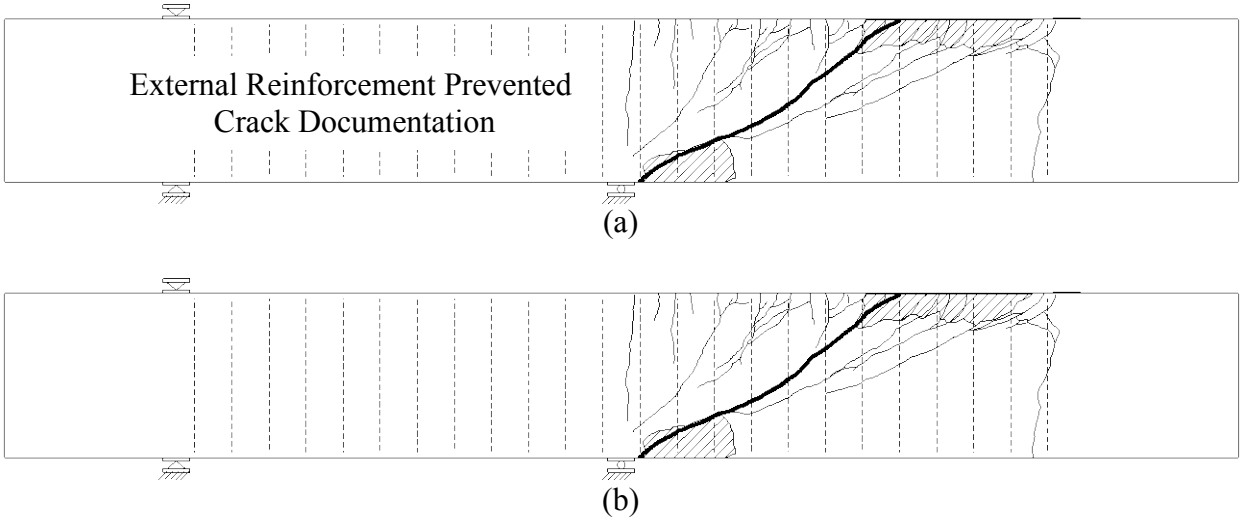

Figure E.30: Observed damage in specimen P2S12, (a) front side, (b) back side

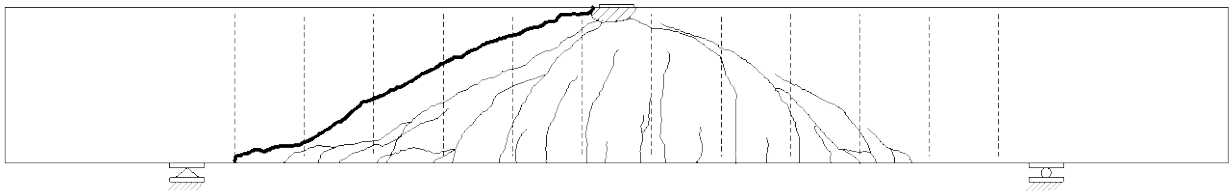

(a)

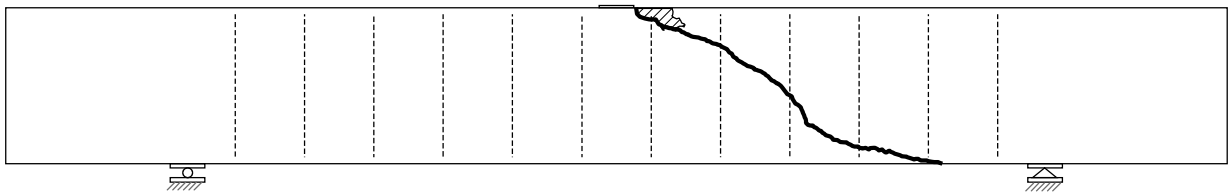

(b)

Figure E.31: Observed damage in specimen P3S1, (a) front side, (b) back side

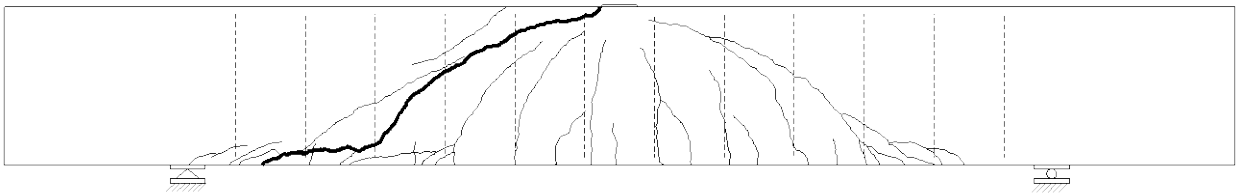

(a)

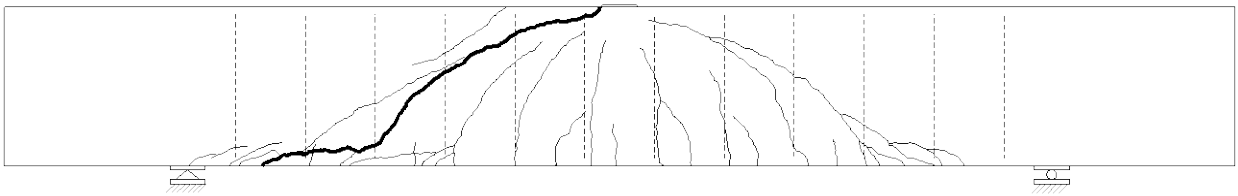

(b)

Figure E.32: Observed damage in specimen P3S2, (a) front side, (b) back side

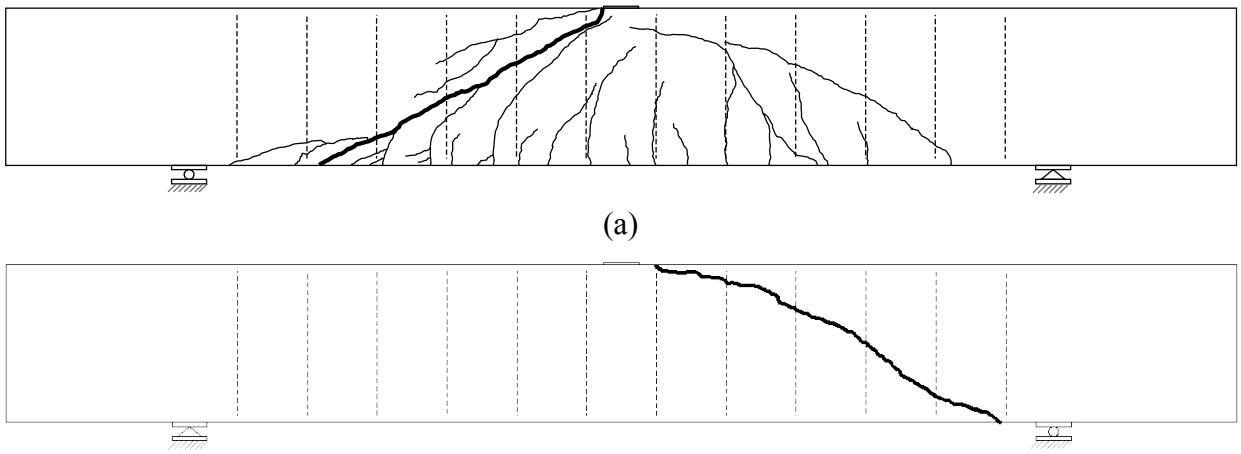

(a)

(b)

Figure E.33: Observed damage in specimen P3S3, (a) front side, (b) back side

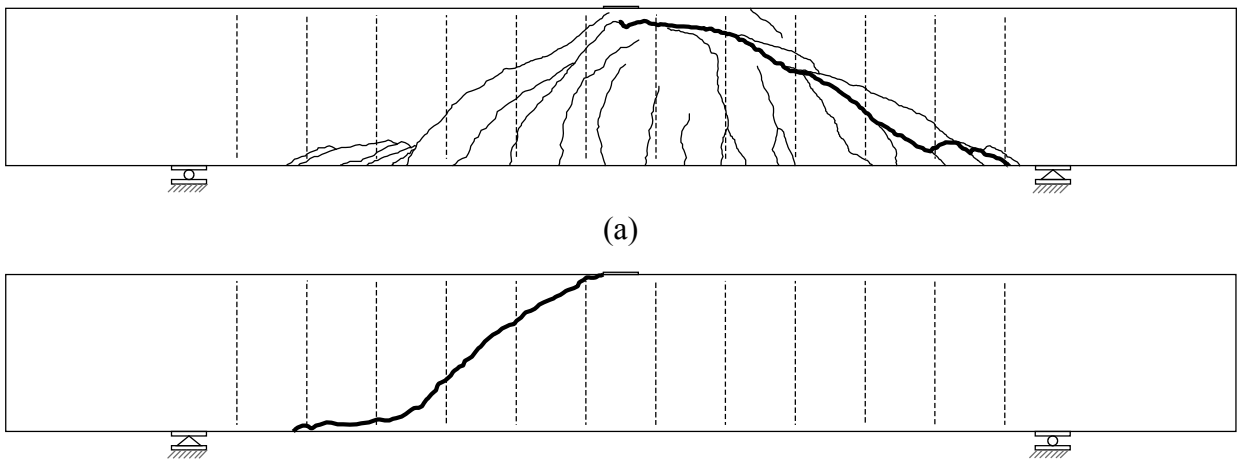

(a)

(b)

Figure E.34: Observed damage in specimen P3S4, (a) front side, (b) back side

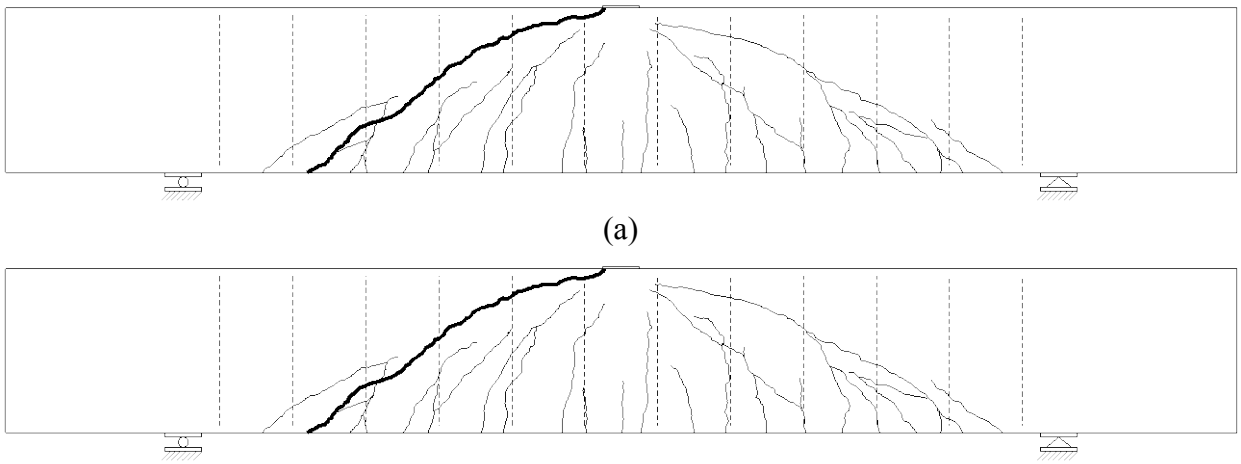

(a)

(b)

Figure E.35: Observed damage in specimen P3S5, (a) front side, (b) back side

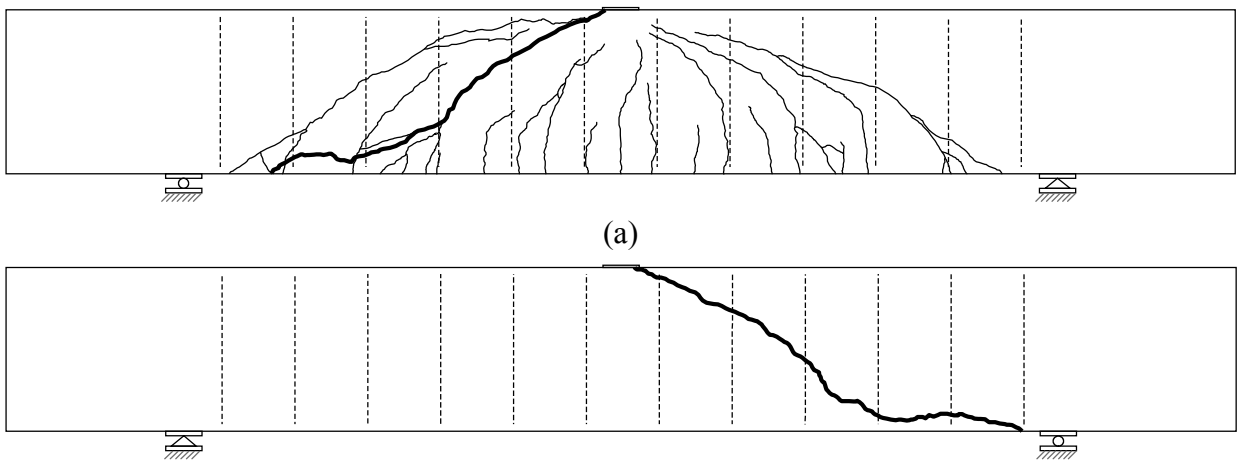

(a)

(b)

Figure E.36: Observed damage in specimen P3S6, (a) front side, (b) back side

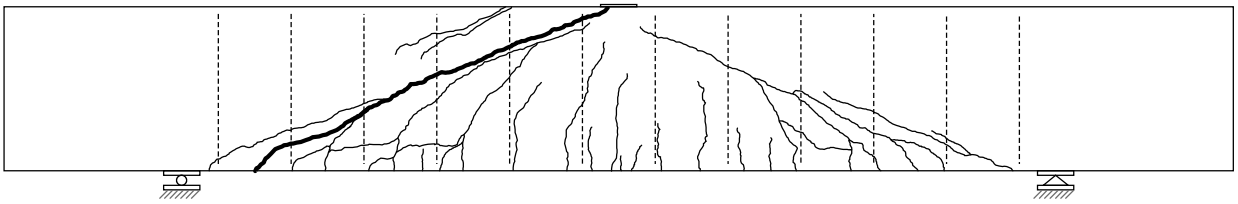

(a)

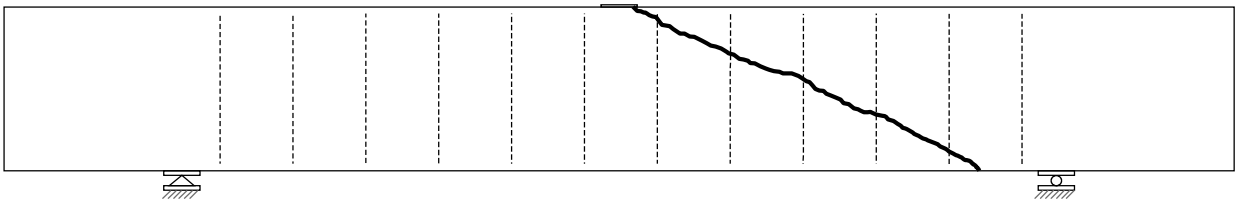

(b)

Figure E.37: Observed damage in specimen P3S7, (a) front side, (b) back side

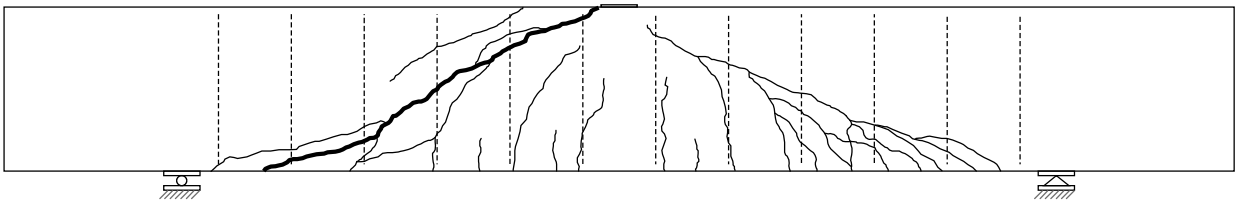

(a)

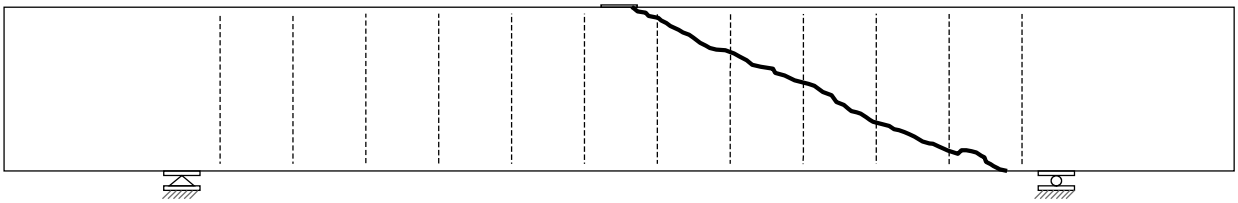

(b)

Figure E.38: Observed damage in specimen P3S8, (a) front side, (b) back side

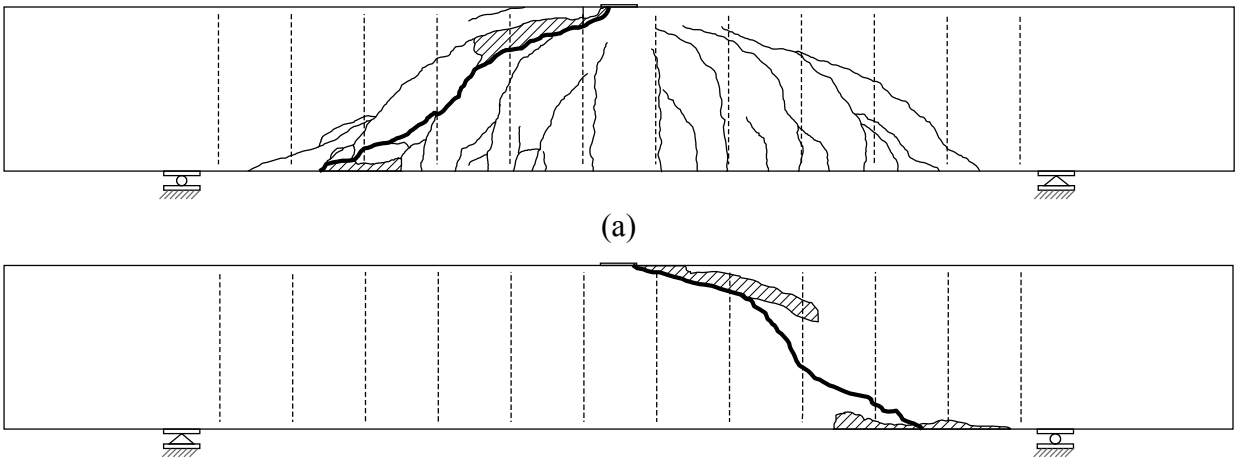

(a)

(b)

Figure E.39: Observed damage in specimen P3S9, (a) front side, (b) back side

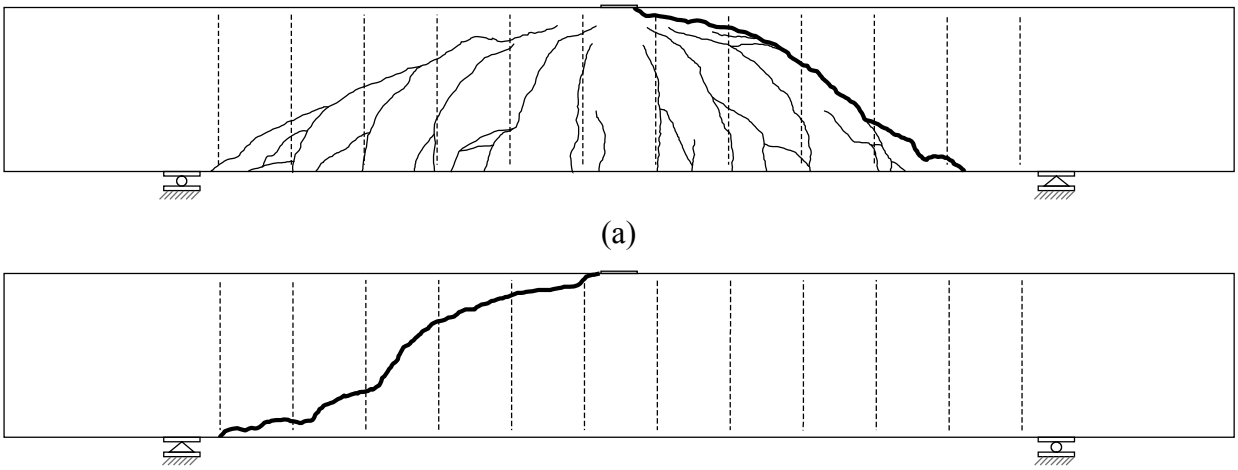

(a)

(b)

Figure E.40: Observed damage in specimen P3S10, (a) front side, (b) back side

APPENDIX F: Applied Load versus Deflection

This appendix includes plots of applied load versus deflection for all specimens. The applied load represents the total force applied to each specimen (the sum of the four load cell outputs) but not the weight of the loading apparatus or the portion of specimen self-weight contributing to shear. The deflection was calculated as the vertical displacement of the optical tracking markers located at midspan (column J in Figure 2.10) minus the average vertical displacement of markers located directly over the supports (SM1 and SM2 in Figure 2.10). Where either SM1 or SM2 was not available, data from the available marker was assumed to represent the displacement of the specimen over the support at both ends of the specimen (specimens where this was done are identified in the captions of the following figures). Calculation of deflection was more involved for specimens P2S11 and P2S12 because a different loading system was used (Figure 2.8). To facilitate comparisons between the deflections of specimens P2S11 and P2S12 and those of other specimens, the measured tip deflection under the applied load was modified to account for vertical movement at the roller support and rotation of the specimen with respect to the roller support, shown in Figure F-1, using Eq. (F.1). The value calculated with Eq. (F.1) is equivalent to the centerline deflection of a center loaded simply supported beam.

$$\text{Deflection} = \Delta_{\text{load}} - \Delta_{\text{roller}} - a\theta_{\text{roller}} \tag{F.1}$$

where Δ_{load} is the displacement (positive down) measured under the point of load application, Δ_{roller} is the displacement of the specimen over the roller support (positive down), a is the shear span (132 in. [4.67 m] for specimens P2S11 and P2S12), and θ_{roller} is the rotation of the specimen directly over the roller in radians (measured using the optical tracking markers over the roller, positive clockwise in Figure F-1).

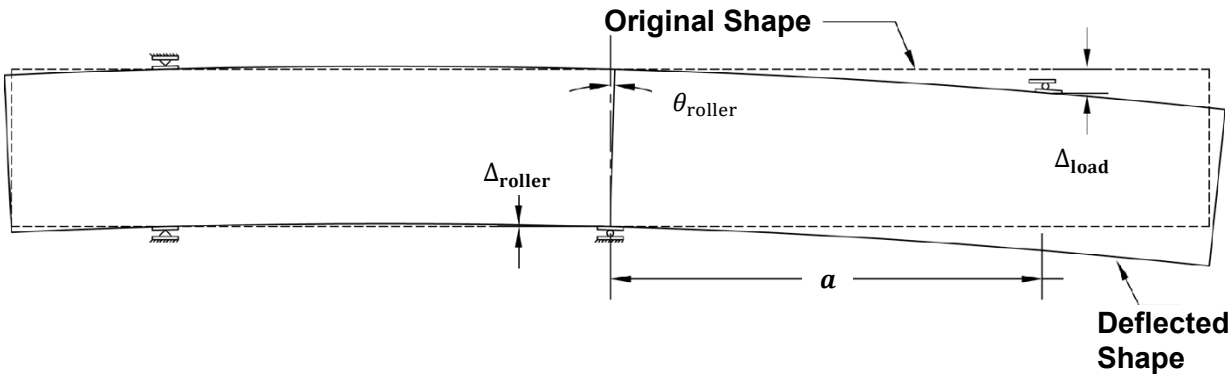

Figure F.1: Schematic of deflected shape for specimens P2S11 and P2S12 with variables used to calculate deflection

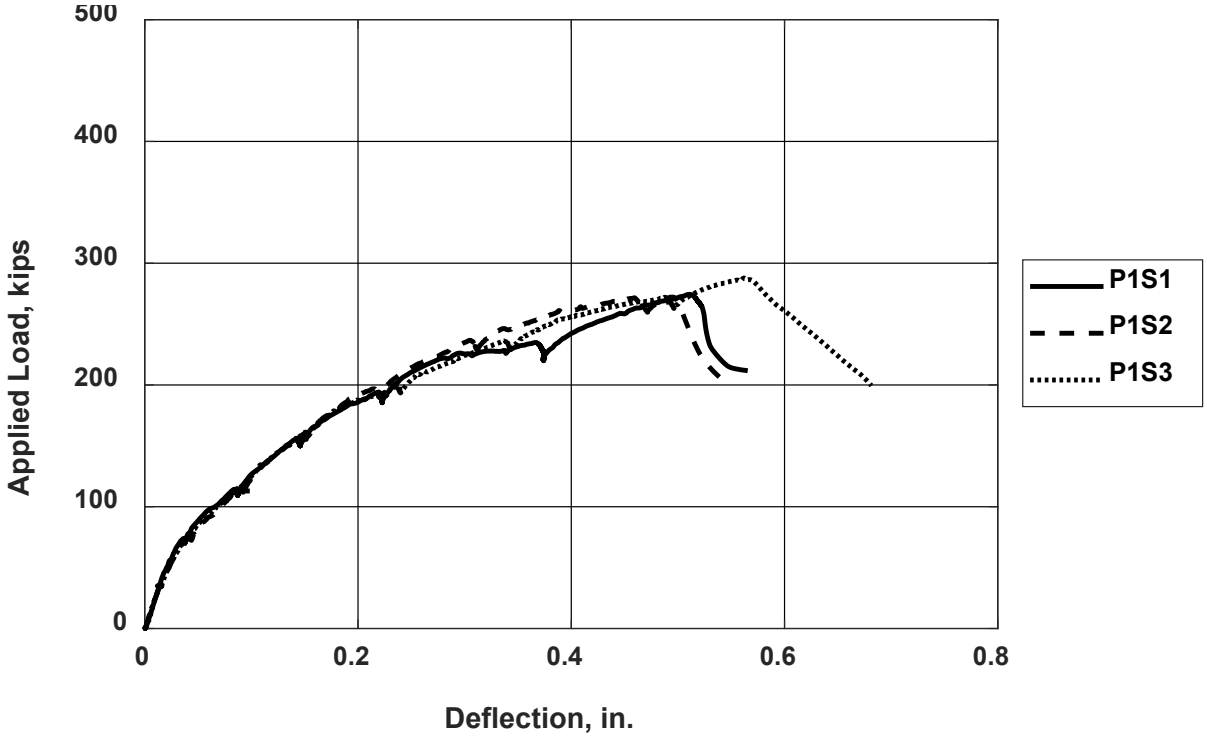

Figure F.2: Load versus deflection for specimens P1S1 through P1S3 [1 kip = 4.45 kN, 1 in. = 25.4 mm]

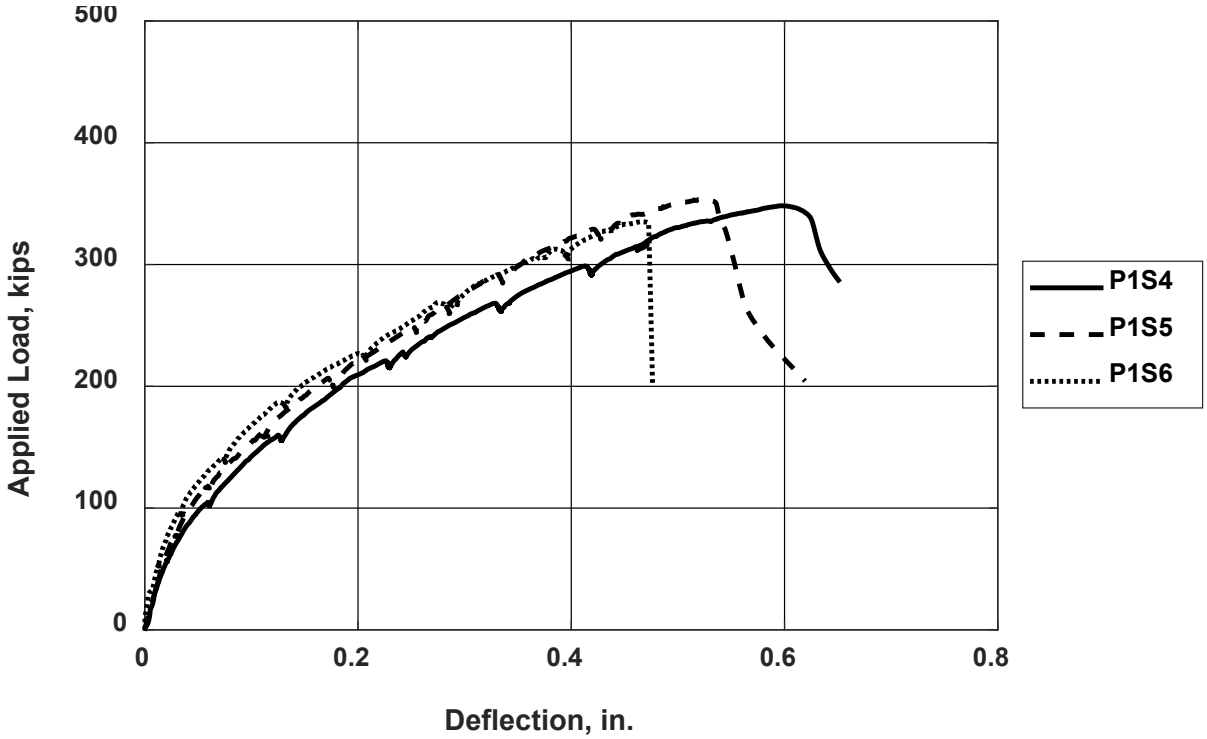

Figure F.3: Load versus deflection for specimens P1S4 through P1S6 [1 kip = 4.45 kN, 1 in. = 25.4 mm]

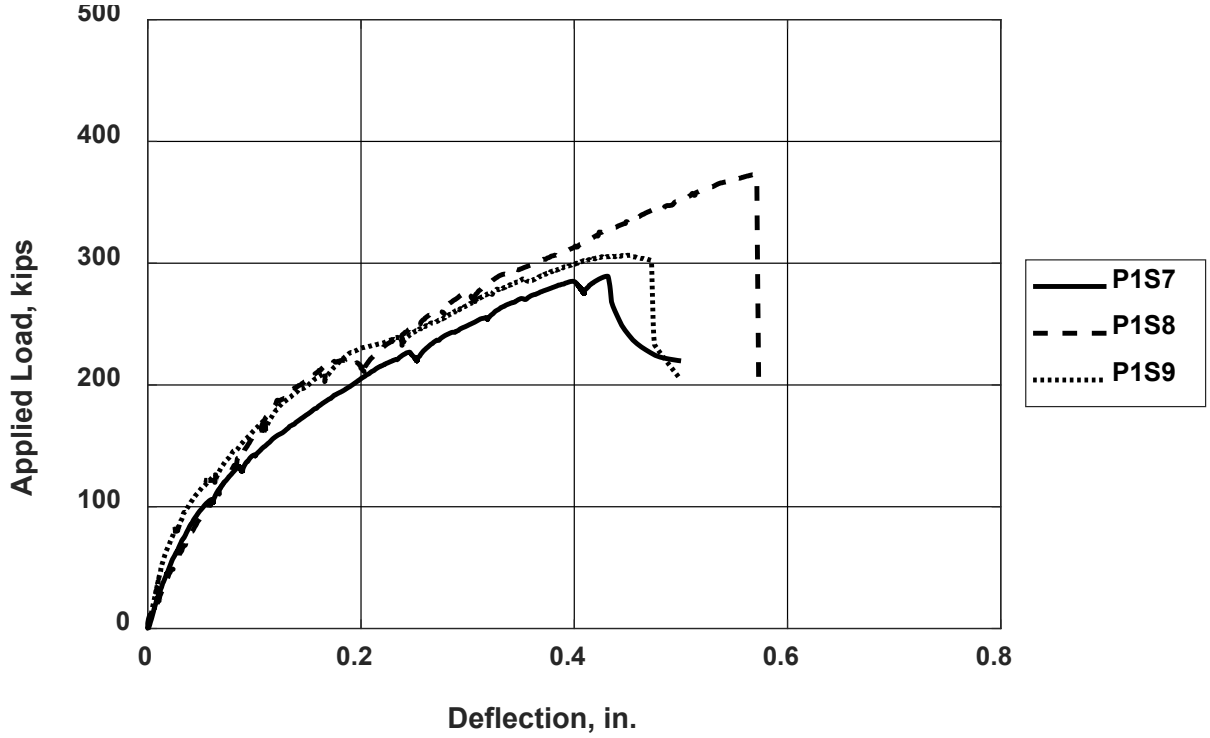

Figure F.4: Load versus deflection for specimens P1S7 through P1S9 [1 kip = 4.45 kN, 1 in. = 25.4 mm]

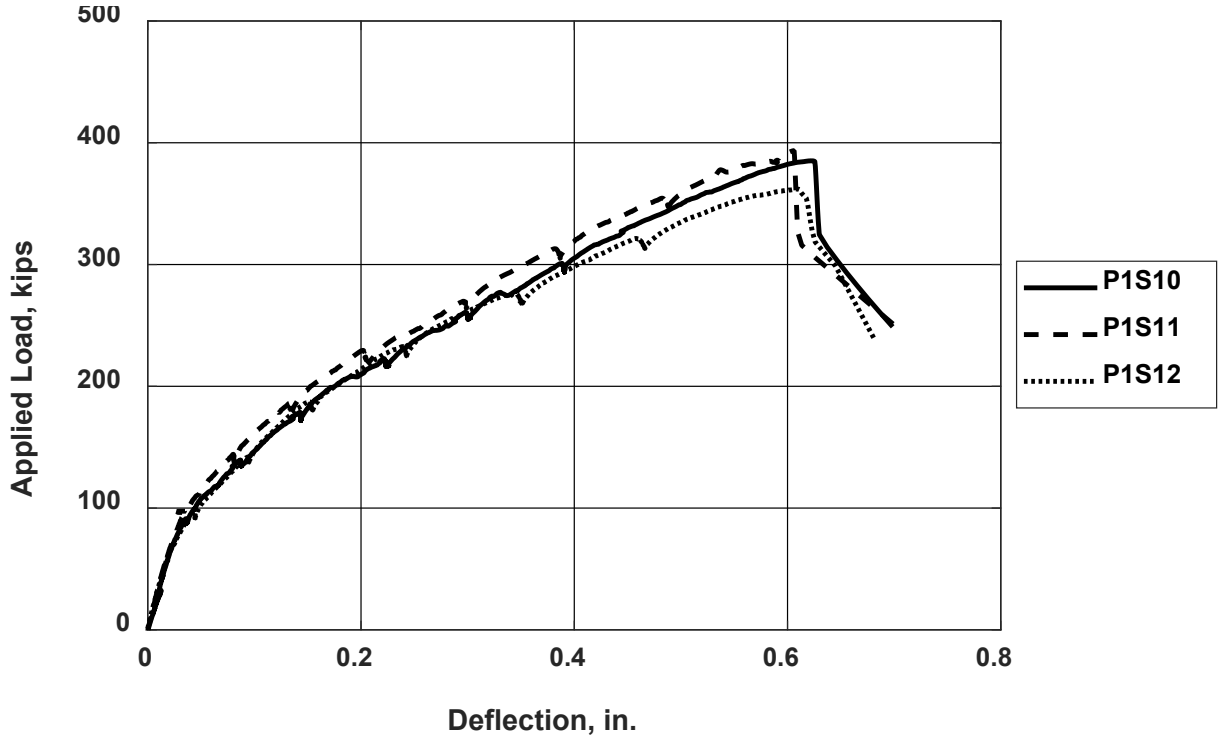

Figure F.5: Load versus deflection for specimens P1S10 through P1S12 [1 kip = 4.45 kN, 1 in. = 25.4 mm]

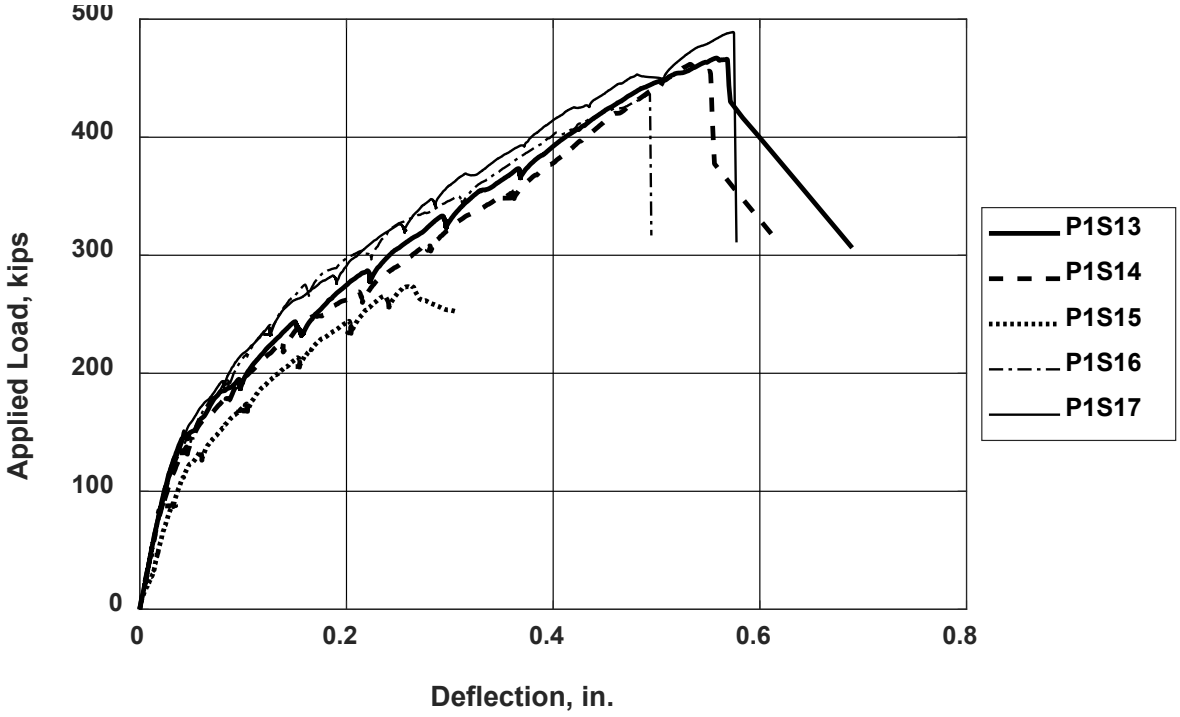

Figure F.6: Load versus deflection for specimens P1S13 through P1S17 [1 kip = 4.45 kN, 1 in. = 25.4 mm]

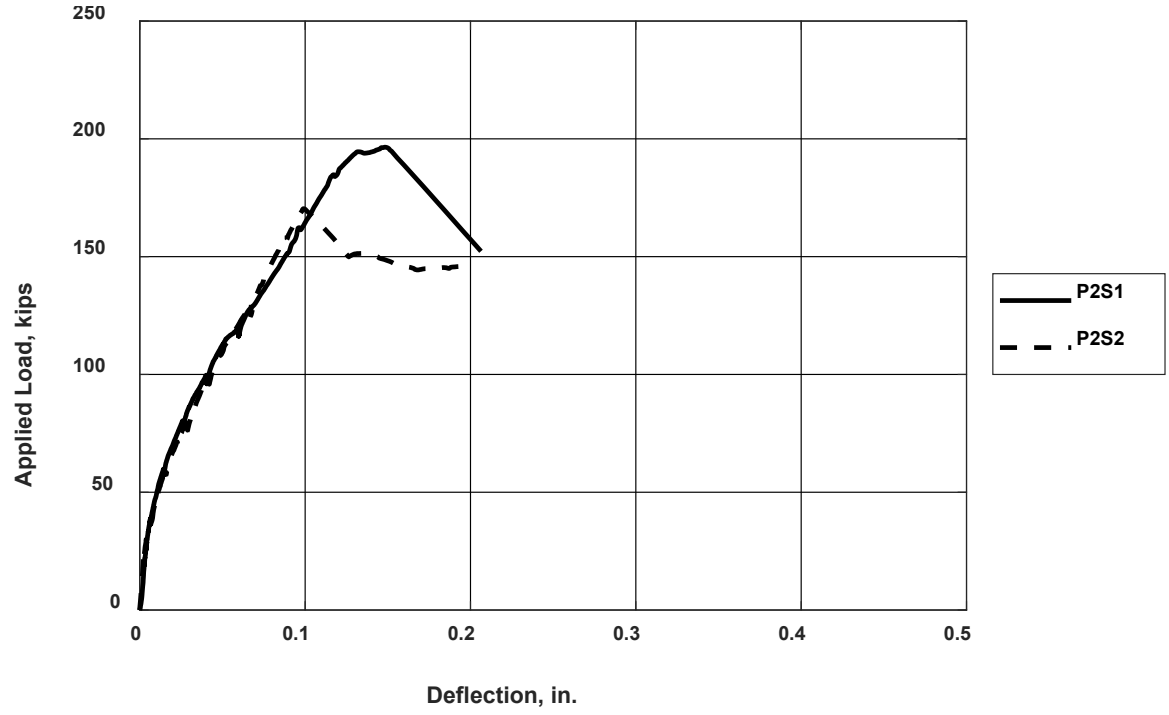

Figure F.7: Load versus deflection for specimens P2S1 and P2S2 (SM1 and SM2 were both missing for both specimens; the average vertical displacement of markers A1 and B1 was used to represent beam settlement at supports) [1 kip = 4.45 kN, 1 in. = 25.4 mm]

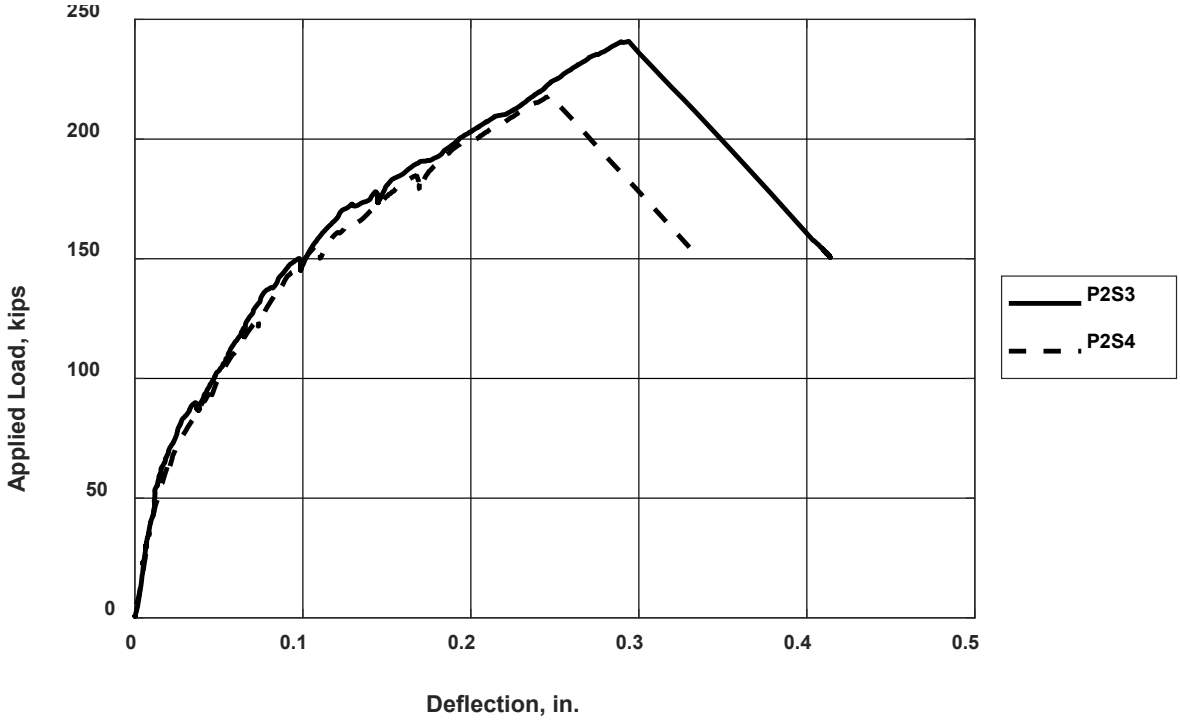

Figure F.8: Load versus deflection for specimens P2S3 and P2S4 (SM2 was missing for both specimens; SM1 data were used to represent beam settlement at supports) [1 kip = 4.45 kN, 1 in. = 25.4 mm]

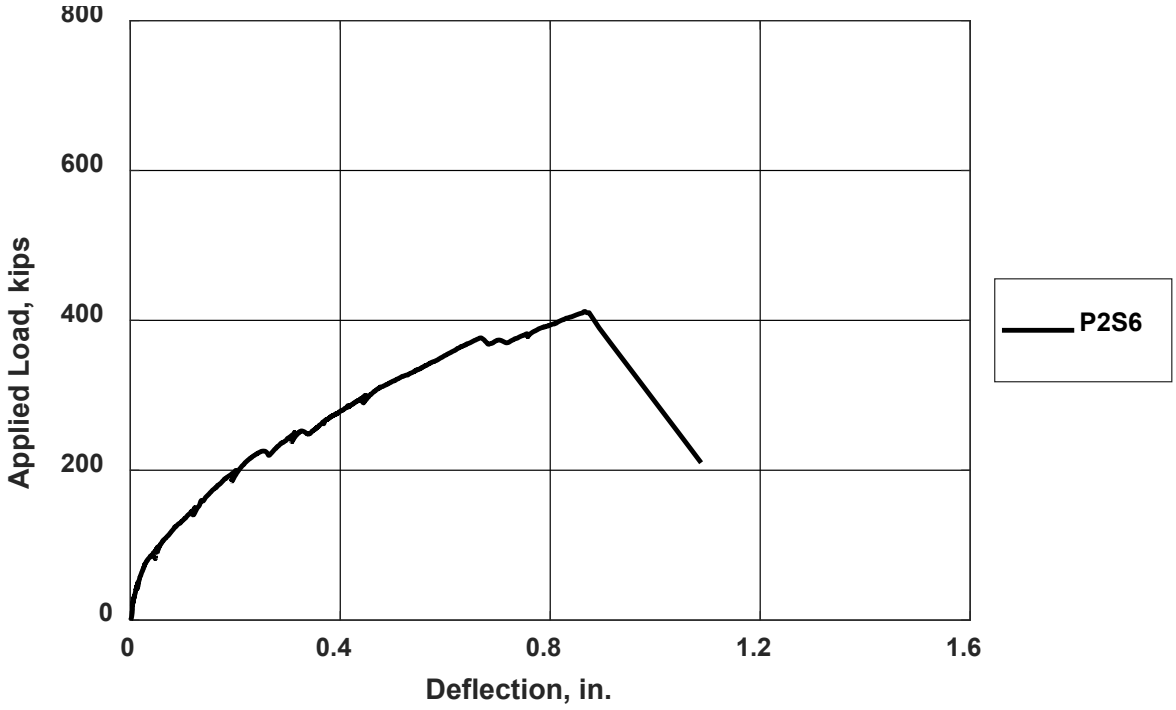

Figure F.9: Load versus deflection for specimen P2S6 (deflection data not obtained for specimen P2S5) [1 kip = 4.45 kN, 1 in. = 25.4 mm]

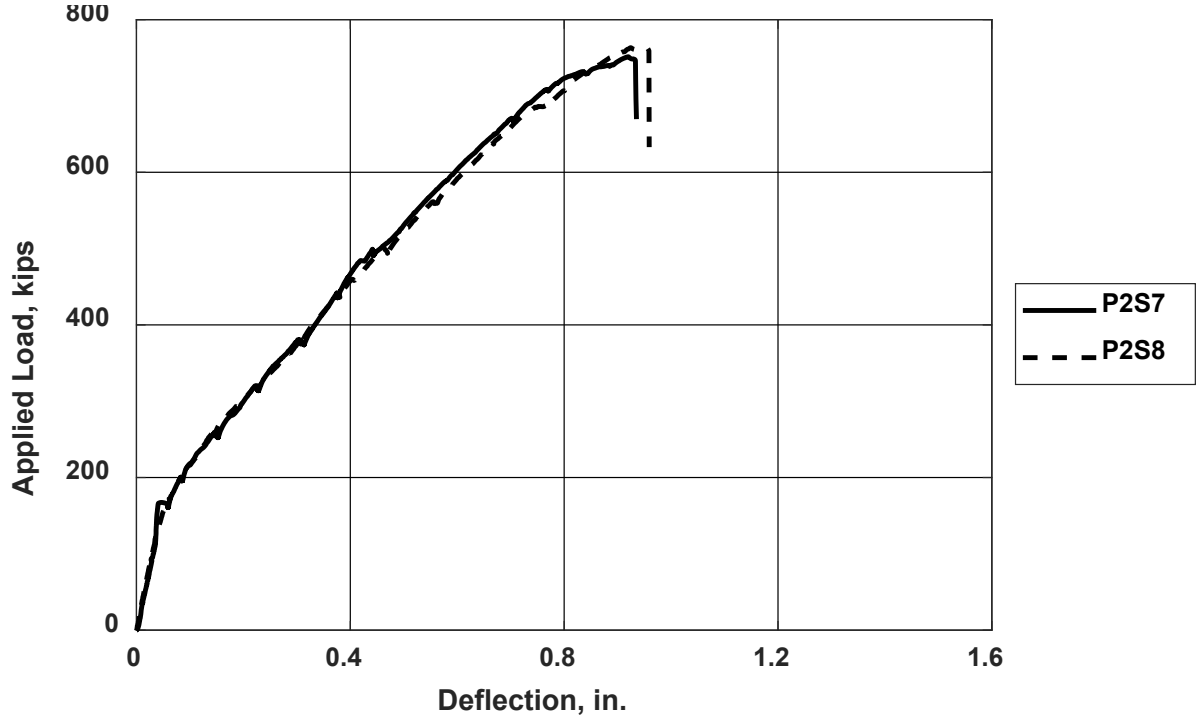

Figure F.10: Load versus deflection for specimens P2S7 and P2S8 [1 kip = 4.45 kN, 1 in. = 25.4 mm]

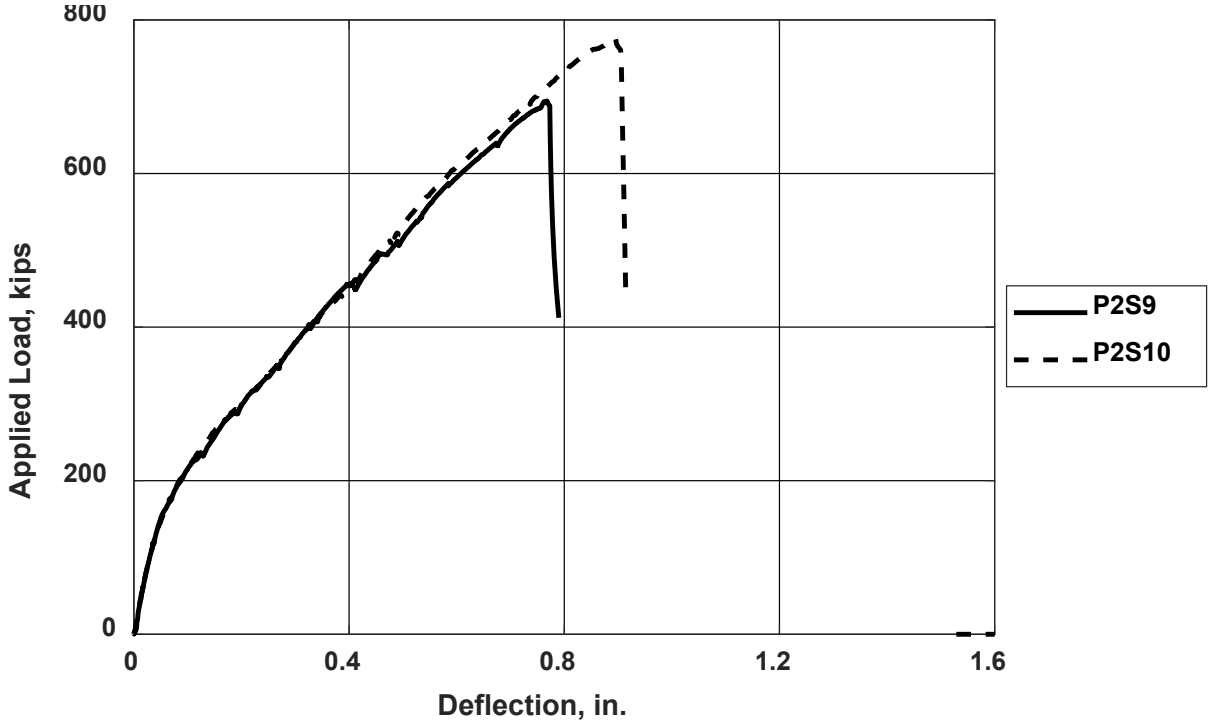

Figure F.11: Load versus deflection for specimens P2S9 and P2S10 [1 kip = 4.45 kN, 1 in. = 25.4 mm]

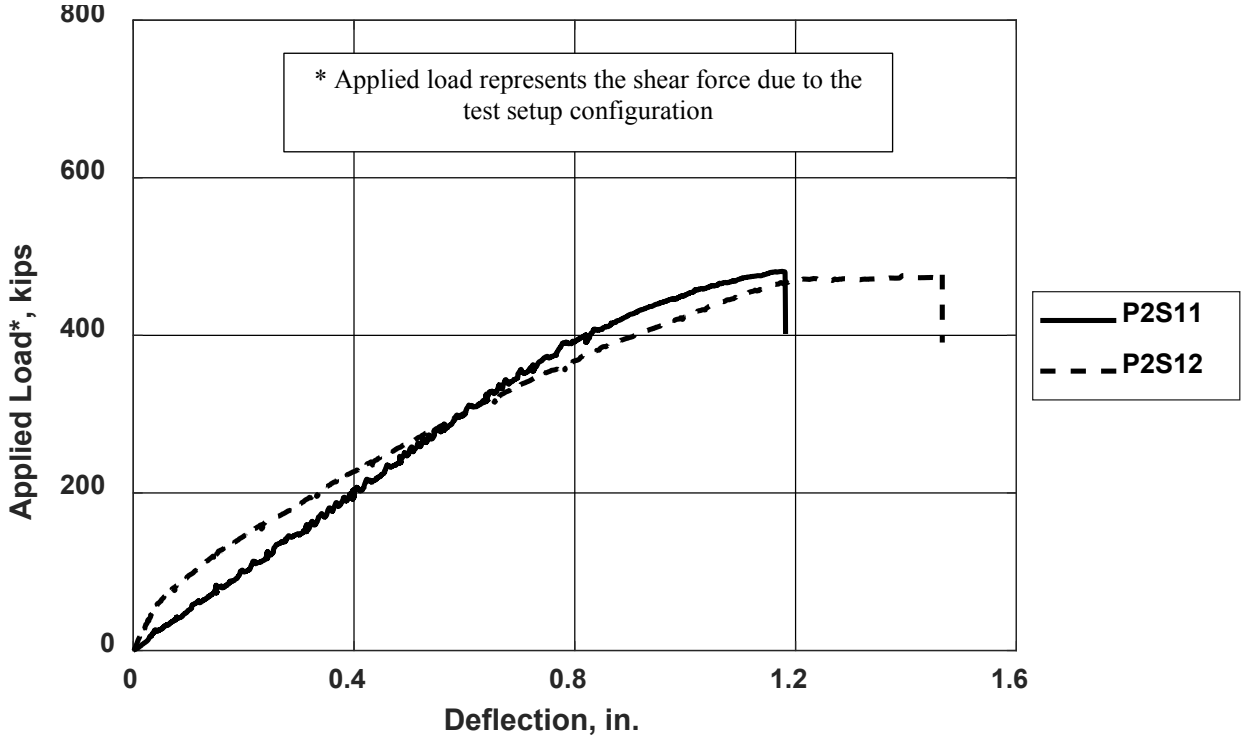

Figure F.12: Load versus deflection for specimens P2S11 and P2S12 [1 kip = 4.45 kN, 1 in. = 25.4 mm]

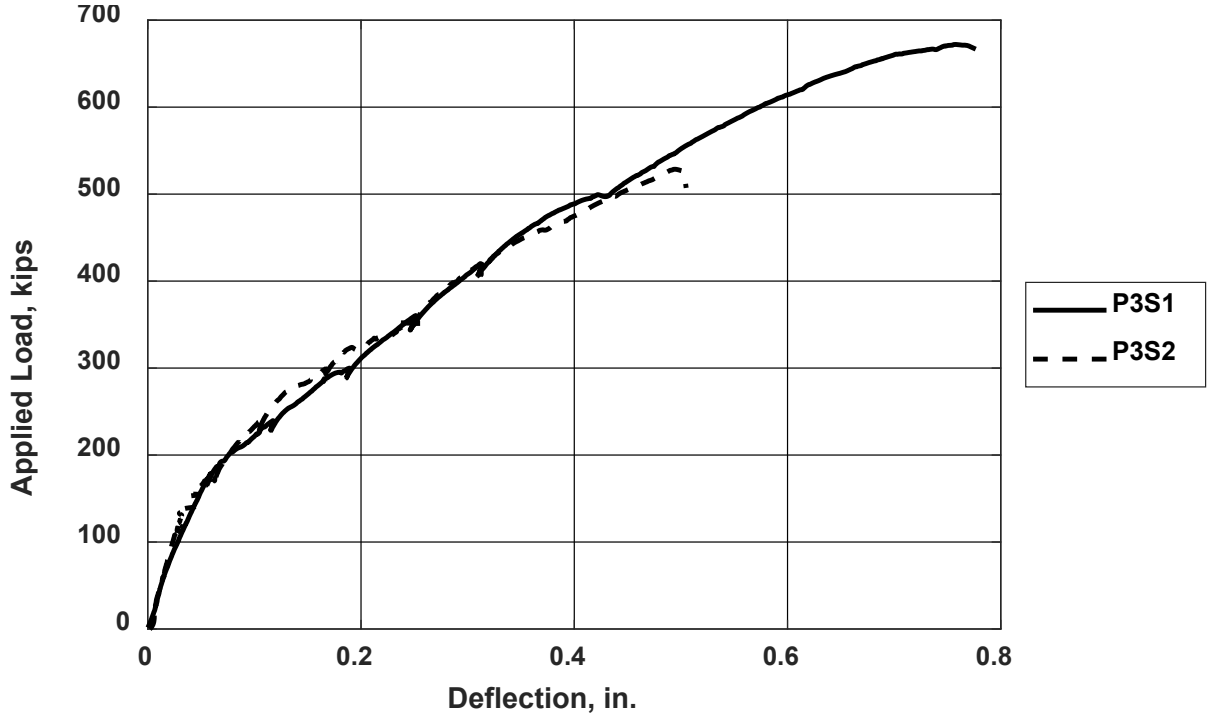

Figure F.13: Load versus deflection for specimens P3S1 and P3S2 [1 kip = 4.45 kN, 1 in. = 25.4 mm]

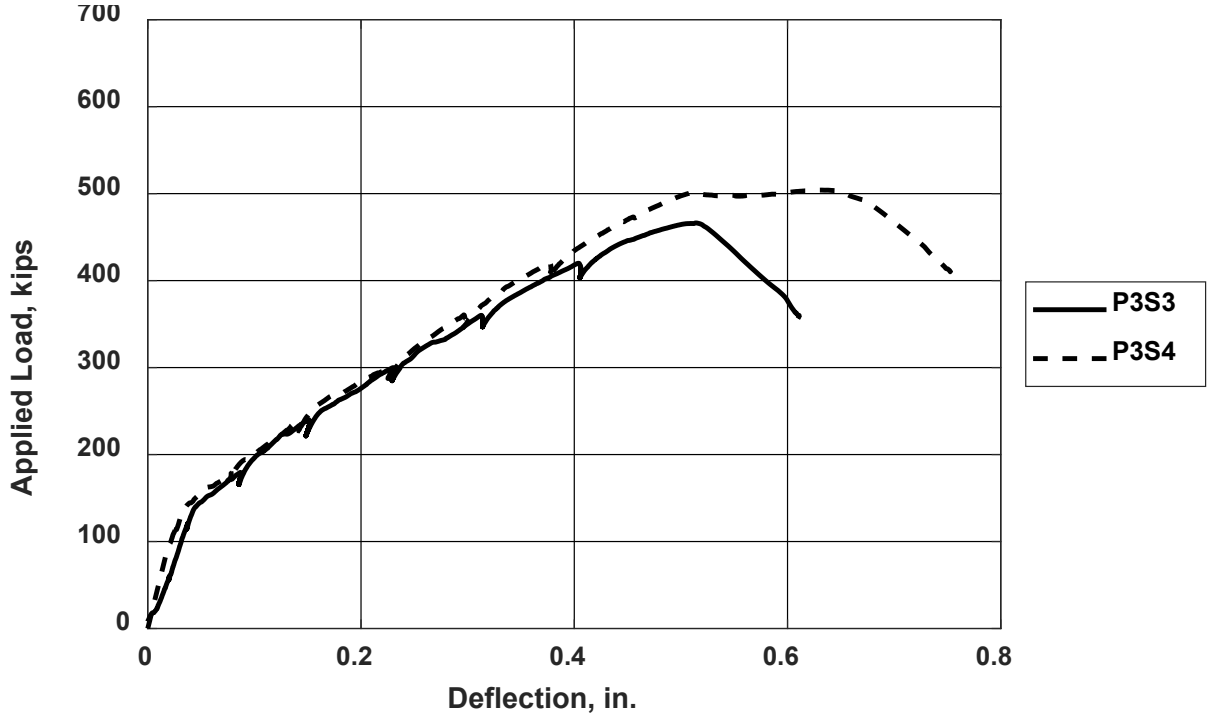

Figure F.14: Load versus deflection for specimens P3S3 and P3S4 [1 kip = 4.45 kN, 1 in. = 25.4 mm]

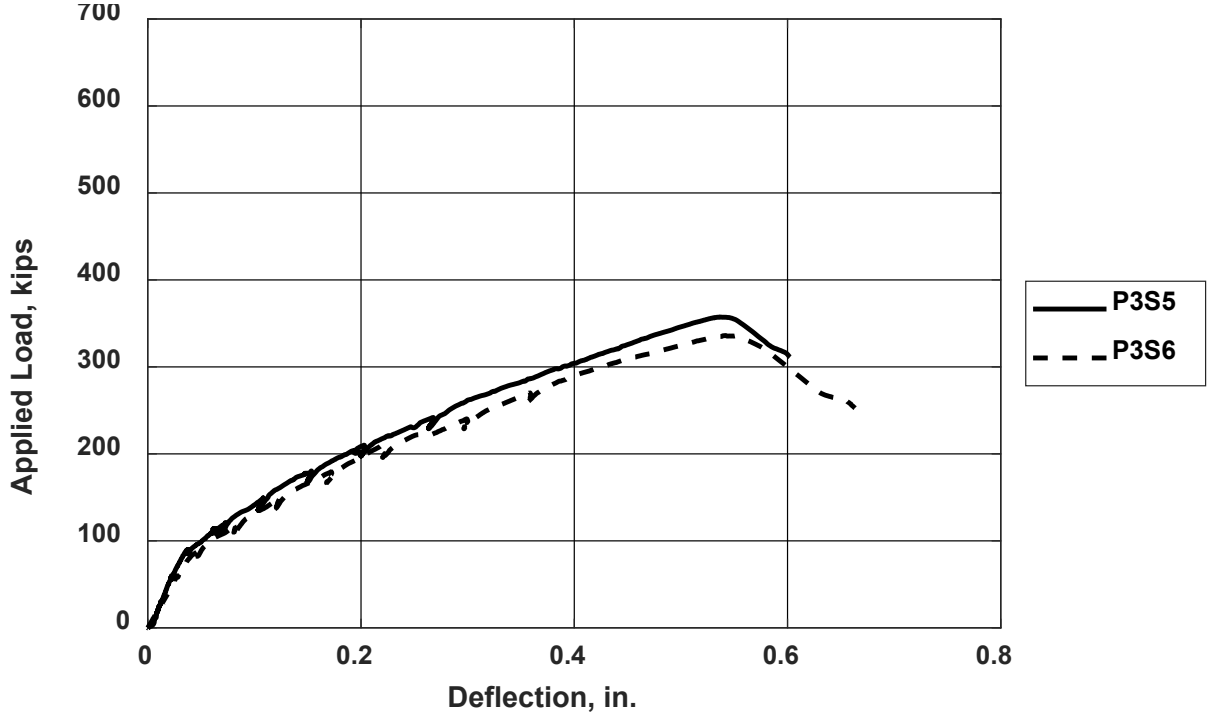

Figure F.15: Load versus deflection for specimens P3S5 and P3S6 [1 kip = 4.45 kN, 1 in. = 25.4 mm]

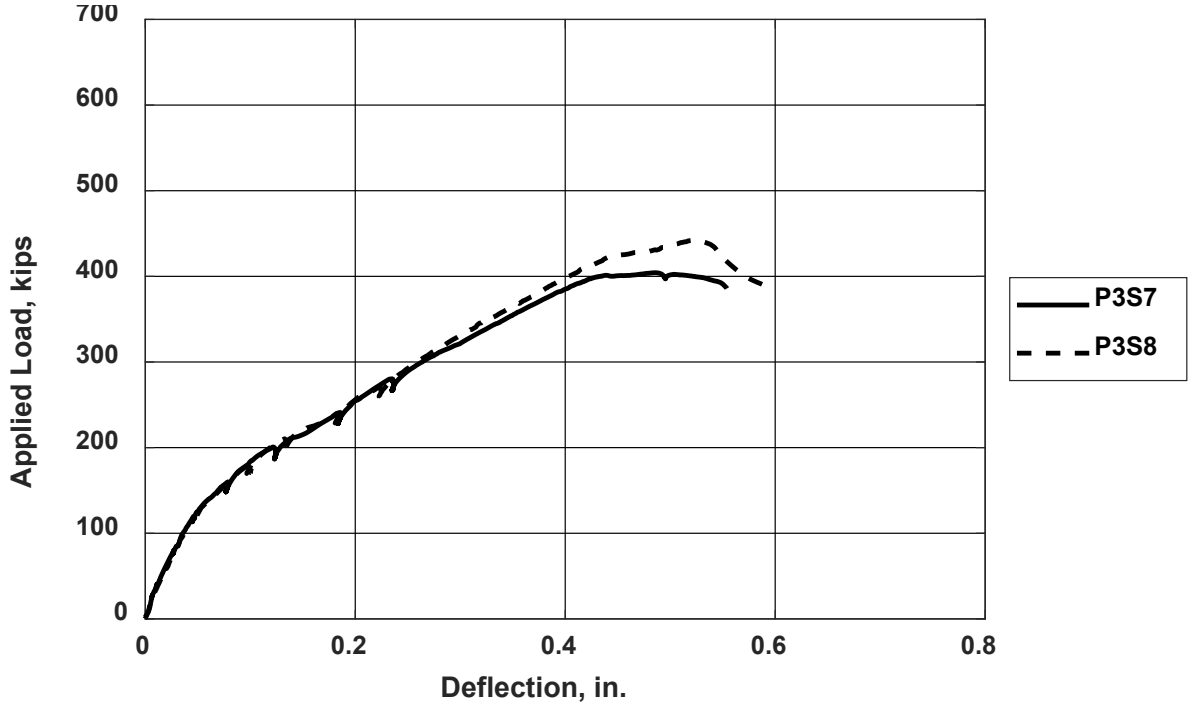

Figure F.16: Load versus deflection for specimens P3S7 and P3S8 [1 kip = 4.45 kN, 1 in. = 25.4 mm]

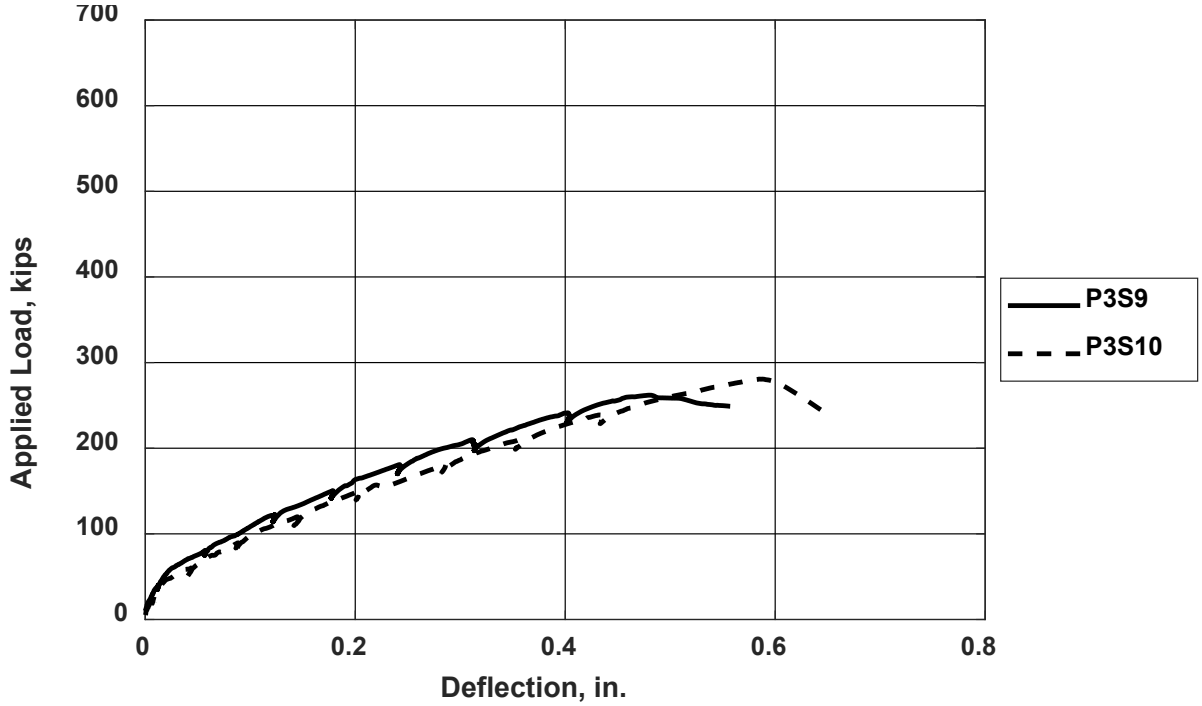

Figure F.17: Load versus deflection for specimens P3S9 and P3S10 (SM1 was missing for specimen P3S9; SM2 data were used to represent beam settlement at supports) [1 kip = 4.45 kN, 1 in. = 25.4 mm]

APPENDIX G: MEASURED CRACK WIDTHS

The tables in this Appendix list the widths of selected cracks and the shear force in the specimen at the time of crack width measurement, along with the nominal and measured strengths of the specimens. Cracks were measured with crack comparators during pauses in the loading at semi-regular intervals up to approximately 80% of the nominal beam strength. At each pause, the widths of several cracks were measured; only the widths of inclined cracks are reported.

Figures are provided that show measured crack width versus percent of measured strength and versus percent of nominal strength. Measured strength refers to the maximum shear force imposed on each specimen (including self-weight of the specimen and loading apparatus). Nominal strength refers to the lesser of the force associated with nominal beam shear strength or the force associated with nominal beam flexural strength, with each calculated using measured material properties (nominal strength was controlled by flexure for two specimens: P3S9 and P3S10). In three cases, the longitudinal bars yielded prior to the shear failure even though the calculated strength was controlled by shear. These specimens are identified in the figure captions. An experimental error prevented the recording of crack widths for Specimens P1S6 and P1S9.

A horizontal reference line was superimposed over the crack width data in each figure that crosses the vertical axis at 0.016 in., the crack width used by the ACI Building Code before 1999 as the basis for serviceability requirements for flexure. The limit of 0.016 in. [0.40 mm] for crack width was based on an equation proposed by Gergely and Lutz (1968) for the “most probable maximum crack width,” a value that Gergely and Lutz showed was exceeded by 31 to 98 percent of experimentally measured crack widths reported in the studies used to develop the equation.

Table G.1: Shear force and crack widths for Phase 1 specimens

Specimen	Nom. Str, kips (kN)	Meas. Str V_T [a], kips (kN)	Shear Force[a], kips (kN)	Measured Inclined Crack Width CW, in. [b] (Crack I.D.)						Max. CW, in. (mm)
				(1)	(2)	(3)	(4)	(5)	(6)	
P1S1	158 (703)	144 (641)	102 (454) 122 (543)	0.030 0.060						0.030 (0.76) 0.060 (1.52)
P1S2	157 (699)	143 (636)	124 (552) 142 (632)	0.050 0.080						0.050 (1.27) 0.080 (2.03)
P1S3	157 (699)	150 (668)	105 (467) 124 (552)	0.025 0.035						0.025 (0.64) 0.035 (0.89)
P1S4	172 (765)	181 (805)	116 (516) 140 (623) 155 (690)	0.010 0.020 0.030	0.010 0.016 0.020	0.012 0.016 0.016	0.016 0.020 0.030			0.016 (0.40) 0.020 (0.51) 0.030 (0.76)
P1S5	173 (770)	183 (814)	152 (676) 171 (761)	0.030 0.060						0.030 (0.76) 0.060 (1.52)
P1S6	No Data Available									
P1S7	164 (730)	151 (672)	119 (530) 148 (659)	0.012 0.025	0.012 0.020	0.016 0.063	 0.035	 0.016		0.016 (0.40) 0.063 (1.60)
P1S8	164 (730)	193 (859)	89 (396) 115 (512) 143 (636)	0.007 0.010 0.020	 0.016 0.035	 0.020 0.030				0.007 (0.18) 0.020 (0.51) 0.035 (0.89)
P1S9	No Data Available									
P1S10	192 (854)	199 (886)	94 (418) 117 (521) 136 (605) 156 (694)	0.006 0.010 0.016 0.020	0.004 0.006 0.009 0.010	 0.009 0.020 0.030	 0.016 0.025 0.035			0.006 (0.15) 0.016 (0.40) 0.025 (0.64) 0.035 (0.89)
P1S11	193 (859)	203 (903)	99 (441) 121 (538) 140 (623) 162 (721) 183 (814)	0.004 0.006 0.009 0.012 0.030	0.004 0.009 0.012 0.020 0.025	 0.009 0.020 0.025 0.030	 0.006 0.006 0.006 0.006	 0.016 0.030 0.040		0.004 (0.10) 0.009 (0.23) 0.020 (0.51) 0.030 (0.76) 0.040 (1.02)
P1S12	194 (863)	187 (832)	76 (338) 99 (441) 122 (543) 143 (636) 166 (739)	0.004 0.007 0.010 0.012 0.016	 0.020 0.030 0.035	 0.004 0.006 0.006 0.007	 0.016 0.020 0.025			0.004 (0.10) 0.007 (0.18) 0.020 (0.51) 0.030 (0.76) 0.035 (0.89)
P1S13	230 (1024)	240 (1068)	128 (570) 149 (663) 173 (770) 193 (859)	0.040 0.060 0.125 0.137	0.009 0.020 0.030 0.035	 0.010 0.012 0.012	 0.020 0.025	 0.020		0.040 (1.02) 0.060 (1.52) 0.125 (3.18) 0.137 (3.48)
P1S14	228 (1015)	237 (1055)	140 (623) 161 (716) 183 (814)	0.020 0.035 0.063	0.025 0.035 0.045	 0.030 0.035				0.025 (0.64) 0.035 (0.89) 0.063 (1.60)

[a] Accounts for the applied load, loading frame weight, and contributing specimen self-weight (Section 3.3.1)
[b] 1 in. = 25.4 mm

Table G.1 Cont.: Shear force and crack widths for Phase 1 specimens

Specimen	Nom. Str, kips (kN)	Meas. Str V_T [a], kips (kN)	Shear Force[a], kips (kN)	Measured Inclined Crack Width CW, in. [b] (Crack I.D.)						Max. CW, in. (mm)
				(1)	(2)	(3)	(4)	(5)	(6)	
P1S15	233 (1037)	144 (641)	93 (414)	0.007						0.007 (0.18)
			112 (498)	0.016	0.010	0.004				0.016 (0.40)
			127 (565)	0.030	0.020	0.010				0.030 (0.76)
			138 (614)	0.050	0.035	0.010				0.050 (1.27)
P1S16	216 (961)	224 (997)	79 (352)	0.004	0.004					0.004 (0.10)
			103 (458)	0.006	0.006					0.006 (0.15)
			125 (556)	0.007	0.007					0.007 (0.18)
			143 (636)	0.009	0.007	0.010				0.010 (0.25)
			157 (699)	0.010	0.007	0.016	0.020	0.035		0.035 (0.88)
			181 (805)	0.012	0.007	0.020	0.125	0.125		0.125 (3.18)
P1S17	218 (970)	251 (1117)	102 (454)	0.004						0.004 (0.10)
			125 (556)	0.007	0.004					0.007 (0.18)
			146 (650)	0.010	0.012	0.009				0.012 (0.30)
			167 (743)	0.012	0.016	0.020	0.030	0.025		0.030 (0.76)
			179 (797)	0.012	0.025	0.040	0.060	0.035		0.060 (1.52)

[a] Accounts for the applied load, loading frame weight, and contributing specimen self-weight (Section 3.3.1)

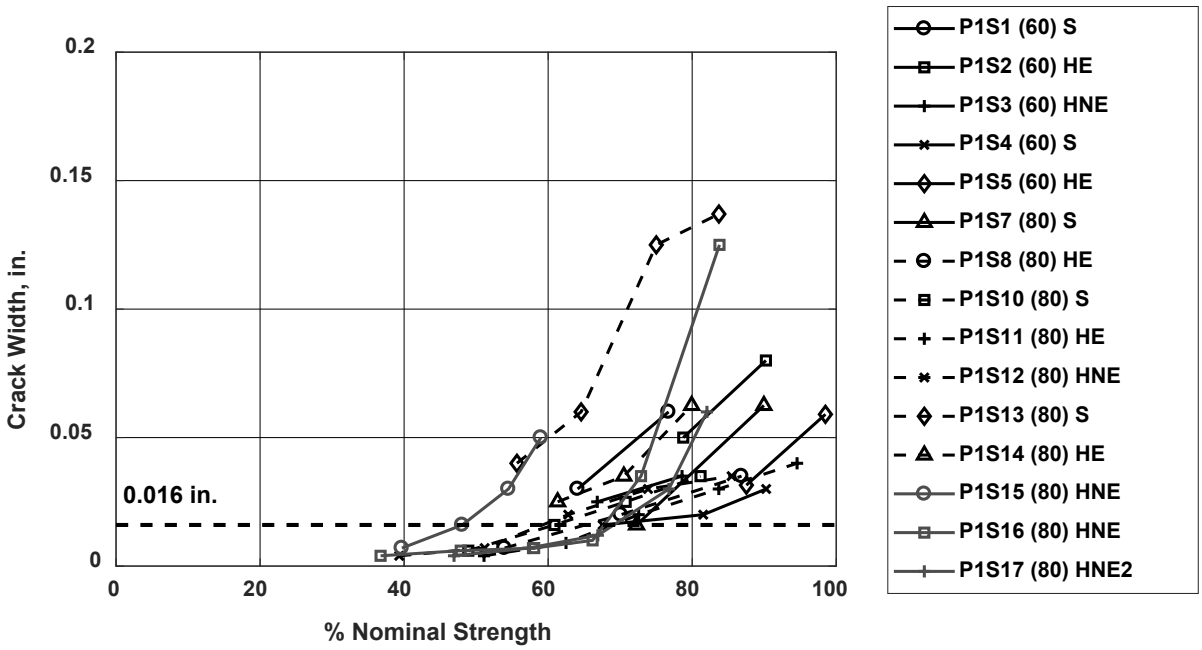

Figure G.1: Crack width versus percent of nominal strength: Phase 1 specimens [1 in. = 25.4 mm]

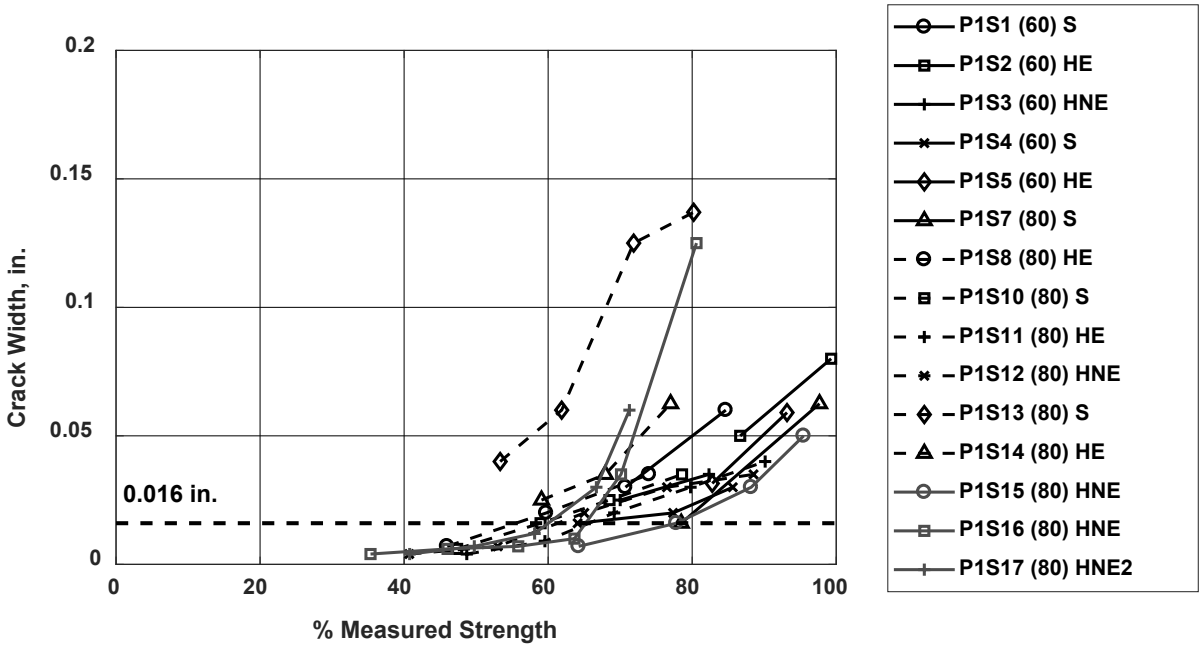

Figure G.2: Crack width versus percent of measured strength: Phase 1 specimens [1 in. = 25.4 mm]

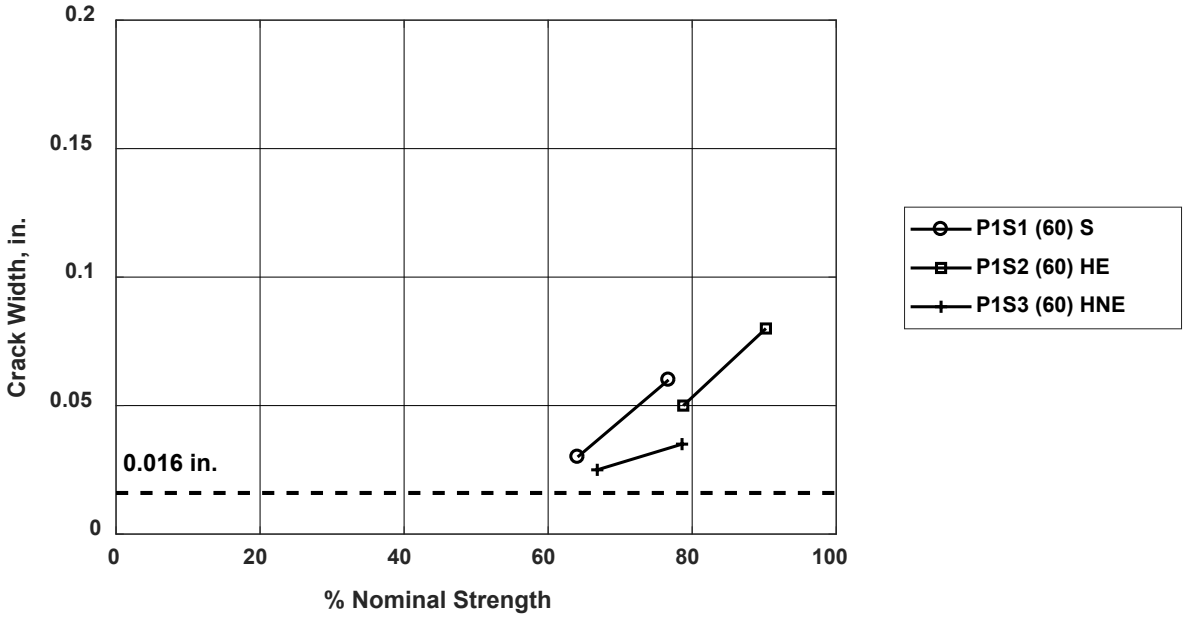

Figure G.3: Crack width versus percent of nominal strength: specimens P1S1 through P1S3 [1 in. = 25.4 mm]

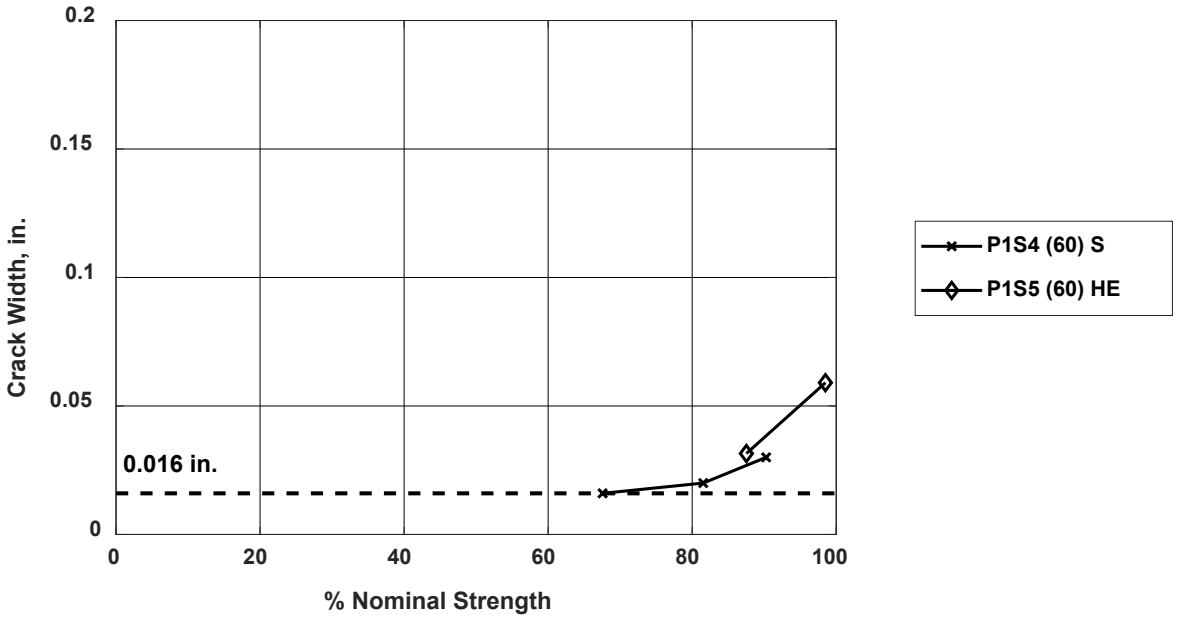

Figure G.4: Crack width versus percent of nominal strength: specimens P1S4 and P1S5 [1 in. = 25.4 mm]

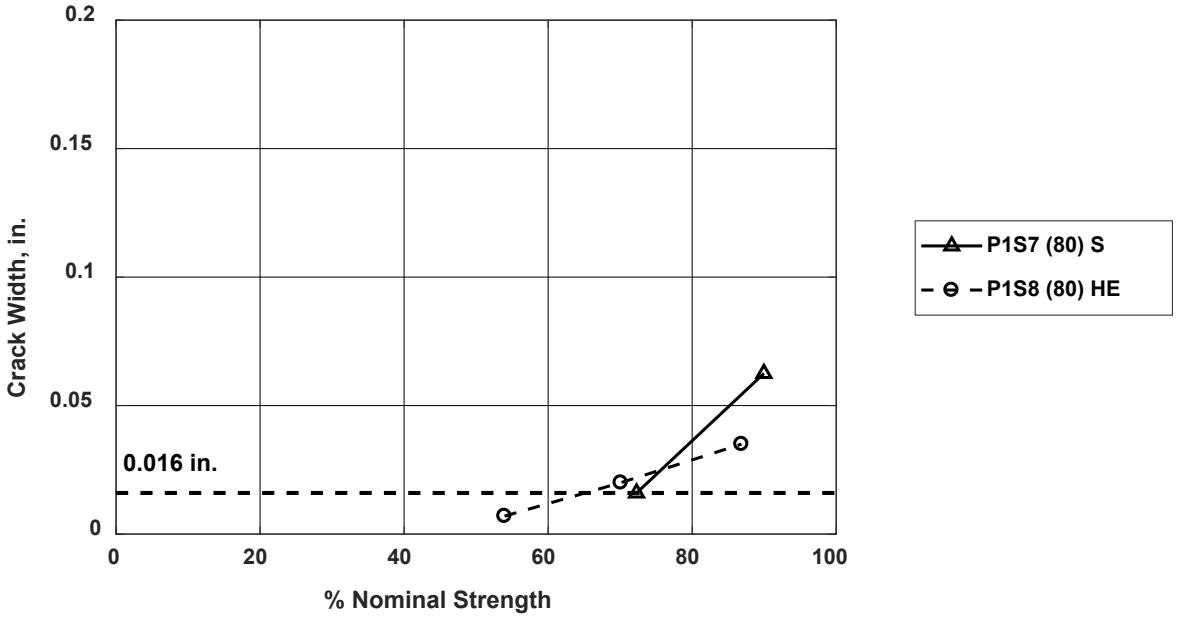

Figure G.5: Crack width versus percent of nominal strength: specimens P1S7 and P1S8 [1 in. = 25.4 mm]

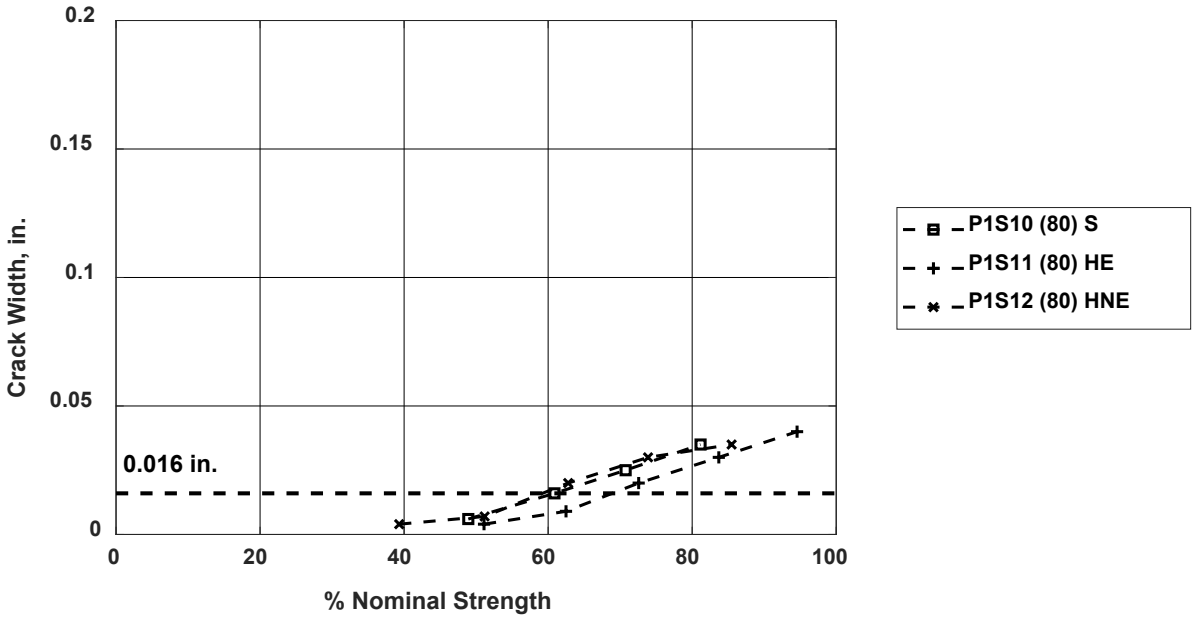

Figure G.6: Crack width versus percent of nominal strength: specimens P1S10 through P1S12 [1 in. = 25.4 mm]

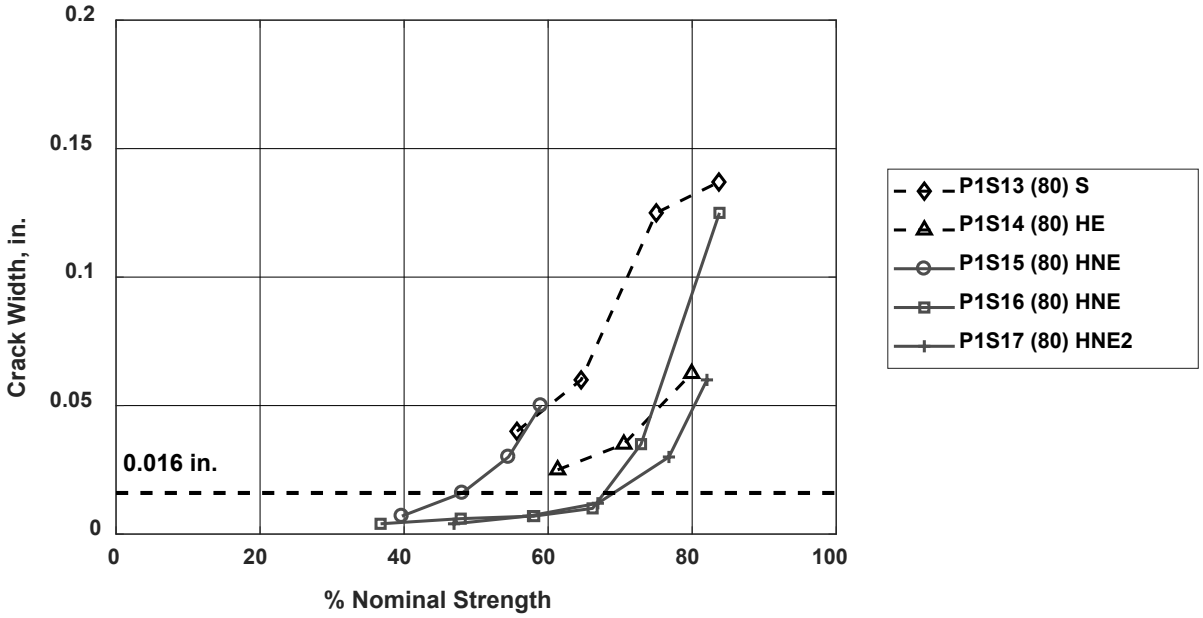

Figure G.7: Crack width versus percent of nominal strength: specimens P1S13 through P1S17 [1 in. = 25.4 mm]

Table G.2: Shear force and crack widths for Phase 2 specimens

Specimen	Nom. Str, kips (kN)	Meas. Str V_T [a], kips (kN)	Shear Force[a], kips (kN)	Measured Inclined Crack Width CW, in. [b] (Crack I.D.)						Max. CW, in. (mm)
				(1)	(2)	(3)	(4)	(5)	(6)	
P2S1	81 (360)	103 (458)	43 (191)	0.004						0.004 (0.10)
			53 (236)	0.006						0.006 (0.15)
			63 (280)	0.009	0.010					0.010 (0.25)
P2S2	81 (360)	89 (396)	53 (236)	0.006	0.004					0.006 (0.15)
			68 (303)	0.012	0.004					0.012 (0.30)
P2S3	107 (476)	125 (556)	78 (347)	0.006						0.006 (0.15)
			93 (414)	0.012	0.012	0.012				0.012 (0.30)
P2S4	105 (467)	112 (498)	63 (280)	0.004						0.004 (0.10)
			78 (347)	0.012	0.004					0.012 (0.30)
P2S5	225 (1001)	190 (846)	85 (378)	0.004	0.004					0.004 (0.10)
			110 (490)	0.007	0.007	0.006				0.007 (0.18)
			135 (601)	0.012	0.012	0.025	0.006			0.025 (0.64)
			160 (712)	0.020	0.009	0.025	0.030			0.030 (0.76)
P2S6	227 (1010)	217 (966)	85 (378)	0.004	0.006					0.006 (0.15)
			110 (490)	0.006	0.009	0.007	0.004			0.009 (0.23)
			135 (601)	0.007	0.012	0.016	0.009	0.020	0.009	0.020 (0.51)
			160 (712)	0.007	0.030	0.050	0.007	0.060	0.030	0.060 (1.52)
P2S7	350 (1558)	386 (1718)	169 (752)	0.009						0.009 (0.23)
			199 (886)	0.025	0.006					0.025 (0.64)
			229 (1019)	0.030	0.012					0.030 (0.76)
			259 (1153)	0.035	0.025					0.035 (0.89)
P1S8	359 (1598)	391 (1740)	169 (752)	0.009	0.010					0.010 (0.25)
			199 (886)	0.020	0.016					0.020 (0.51)
			229 (1019)	0.020	0.030					0.030 (0.76)
			259 (1153)	0.025	0.035					0.035 (0.89)
			289 (1286)	0.025	0.035					0.035 (0.89)
P2S9	349 (1553)	358 (1593)	154 (685)	0.009	0.009	0.007				0.009 (0.23)
			184 (819)	0.010	0.012	0.012	0.012			0.012 (0.30)
			210 (935)	0.020	0.025	0.020	0.020			0.025 (0.64)
			238 (1059)	0.025	0.025	0.020	0.025	0.016		0.025 (0.64)
			265 (1179)	0.030	0.030	0.035	0.035	0.025	0.016	0.035 (0.89)
P2S10	356 (1584)	395 (1758)	156 (694)	0.005	0.006					0.006 (0.15)
			184 (819)	0.012	0.014	0.009	0.009			0.014 (0.36)
			214 (952)	0.020	0.025	0.010	0.020			0.025 (0.64)
			240 (1068)	0.030	0.035	0.030	0.025			0.035 (0.89)
			266 (1184)	0.035	0.050	0.030	0.035			0.050 (1.27)
P2S11	342 (1552)	502 (2234)	84 (374)	0.004						0.004 (0.10)
			95 (423)	0.007	0.006					0.007 (0.18)
			111 (494)	0.007	0.007	0.020				0.020 (0.51)
			127 (565)	0.012	0.009	0.025				0.025 (0.64)
			153 (681)	0.016	0.010	0.060				0.060 (1.52)
			169 (752)	0.040	0.010	0.125				0.125 (3.18)

[a] Accounts for the applied load, loading frame weight, and contributing specimen self-weight (Section 3.3.1)

[b] 1 in. = 25.4 mm

Table G-2 cont.: Shear force and crack widths for Phase 2 specimens

Specimen	Nom. Str, kips (kN)	Meas. Str V_T [a], kips (kN)	Shear Force[a], kips (kN)	Measured Inclined Crack Width CW, in. [b] (Crack I.D.)						Max. CW, in. (mm)
				(1)	(2)	(3)	(4)	(5)	(6)	
P2S12	342 (1552)	498 (2216)	89 (396)	0.016						0.016 (0.40)
			109 (485)	0.020	0.009					0.020 (0.51)
			129 (574)	0.030	0.020					0.030 (0.76)
			149 (663)	0.035	0.040	0.040				0.040 (1.02)
			169 (752)	0.040	0.050	0.016				0.050 (1.27)

[a] Accounts for the applied load, loading frame weight, and contributing specimen self-weight (Section 3.3.1)
[b] 1 in. = 25.4 mm

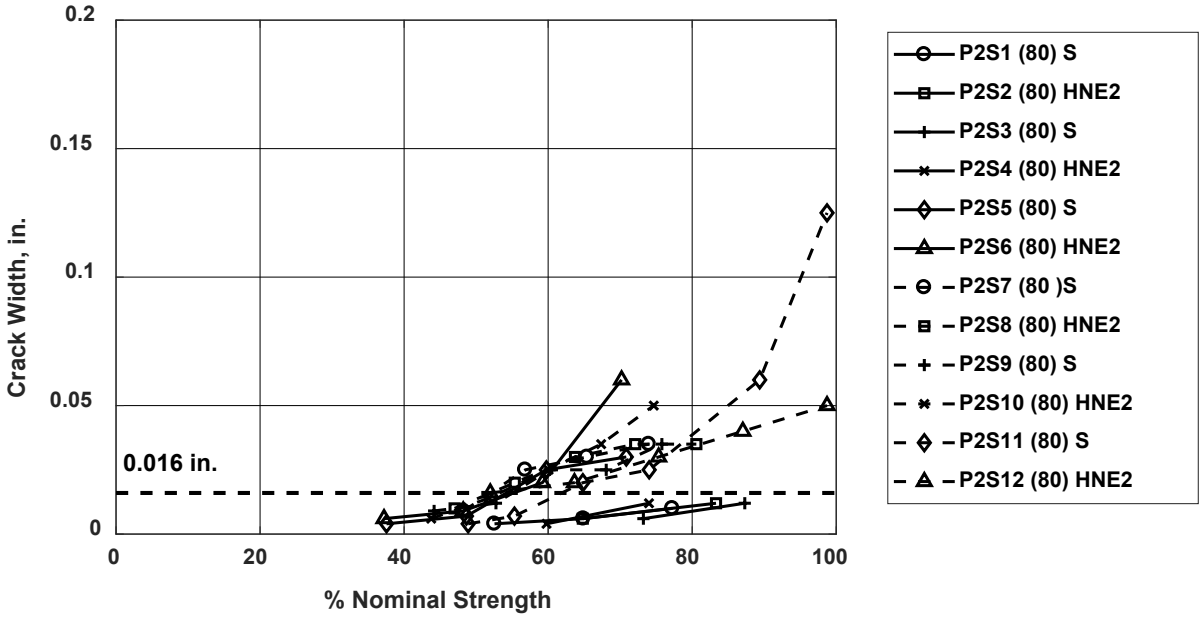

Figure G.8: Crack width versus percent of nominal strength: Phase 2 specimens (longitudinal reinforcement yielded in specimens P2S10 through P2S12 before shear failure) [1 in. = 25.4 mm]

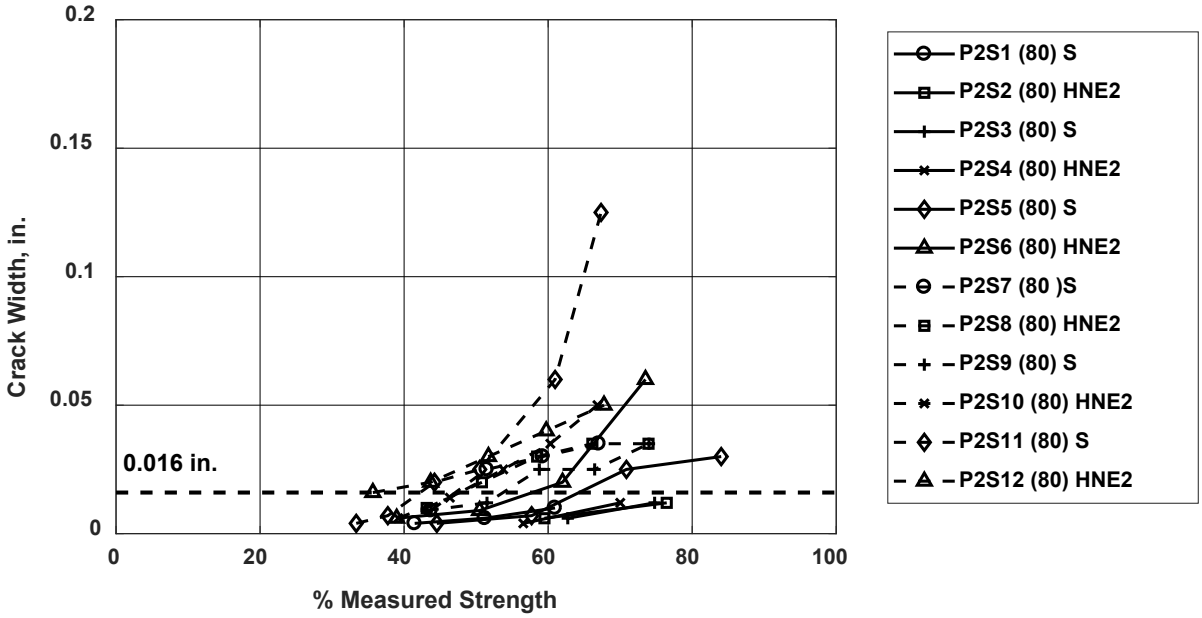

Figure G.9: Crack width versus percent of measured strength: Phase 2 specimens (longitudinal reinforcement yielded in specimens P2S10 through P2S12 before shear failure) [1 in. = 25.4 mm]

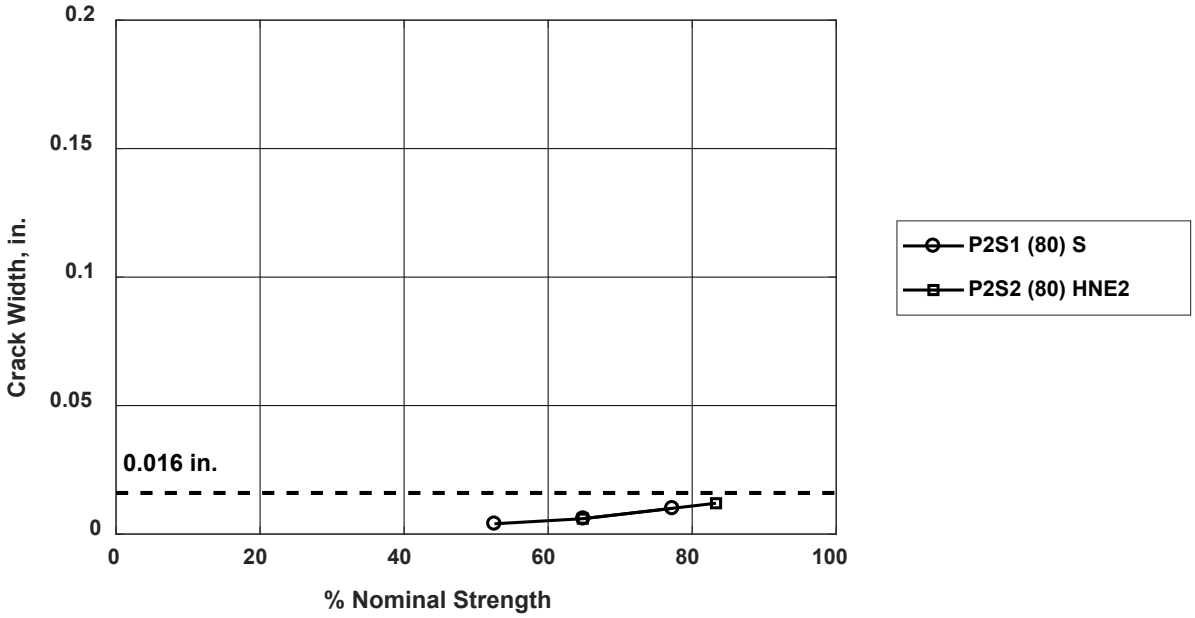

Figure G.10: Crack width versus percent of nominal strength: specimens P2S1 and P2S2 [1 in. = 25.4 mm]

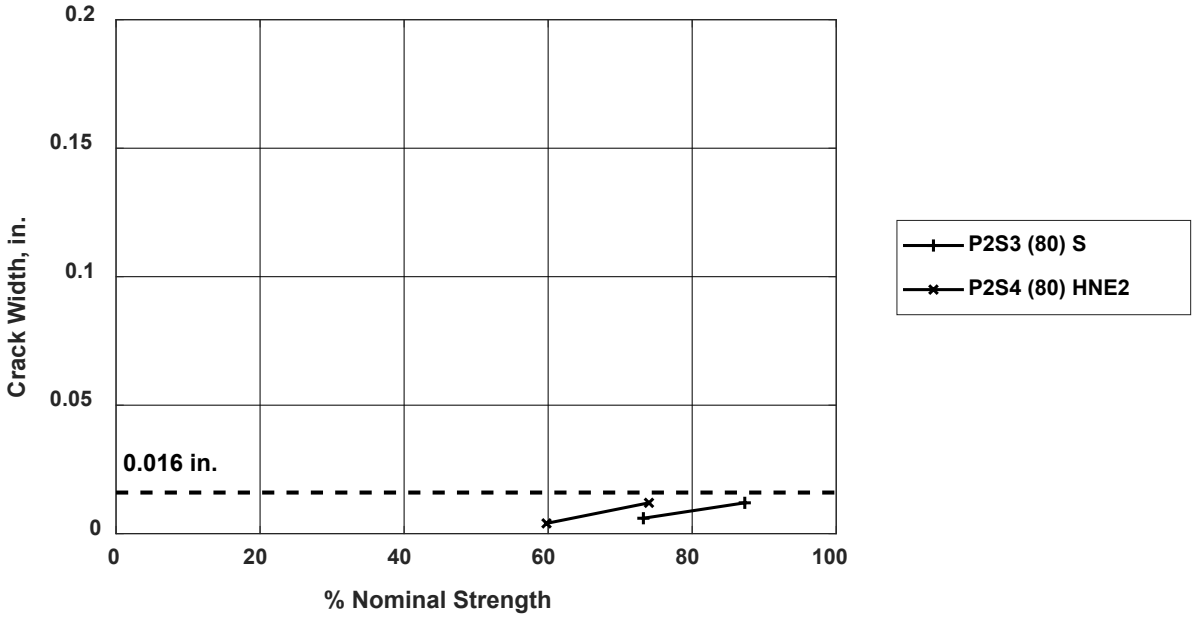

Figure G.11: Crack width versus percent of nominal strength: specimens P2S3 and P2S4 [1 in. = 25.4 mm]

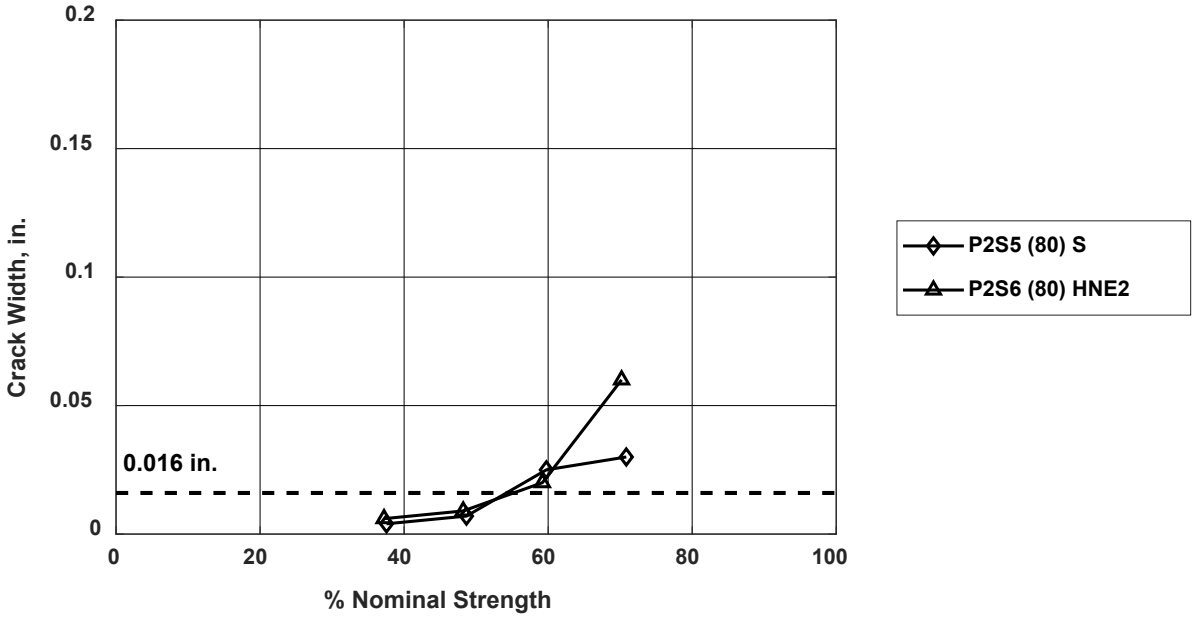

Figure G.12: Crack width versus percent of nominal strength: specimens P2S5 and P2S6 [1 in. = 25.4 mm]

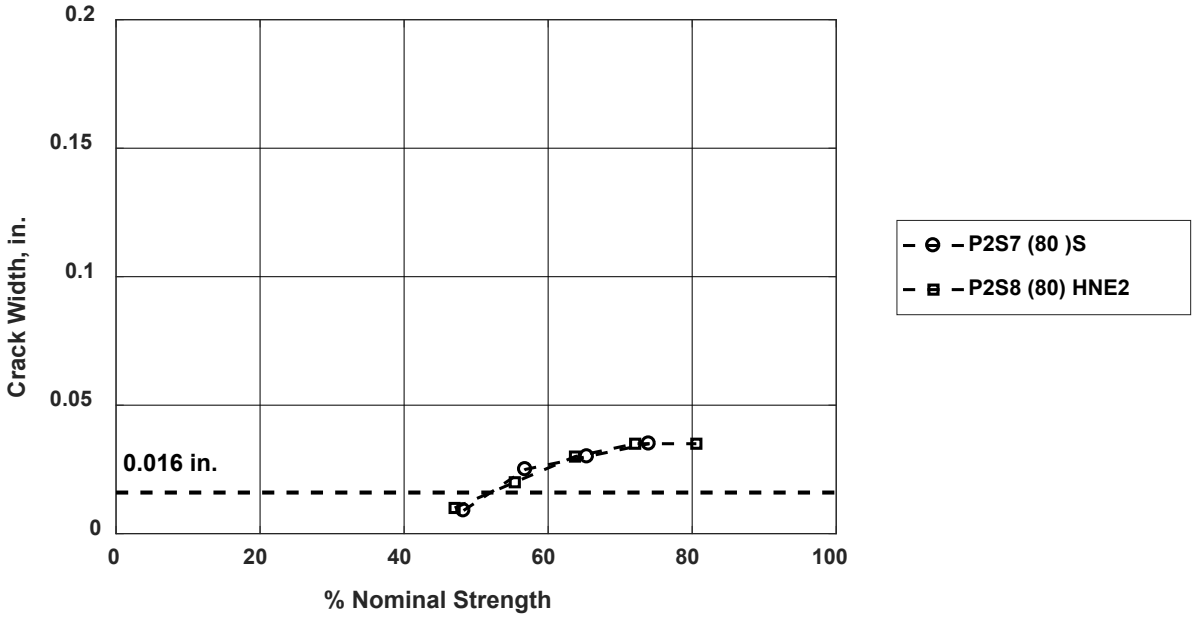

Figure G.13: Crack width versus percent of nominal strength: specimens P2S7 and P2S8 [1 in. = 25.4 mm]

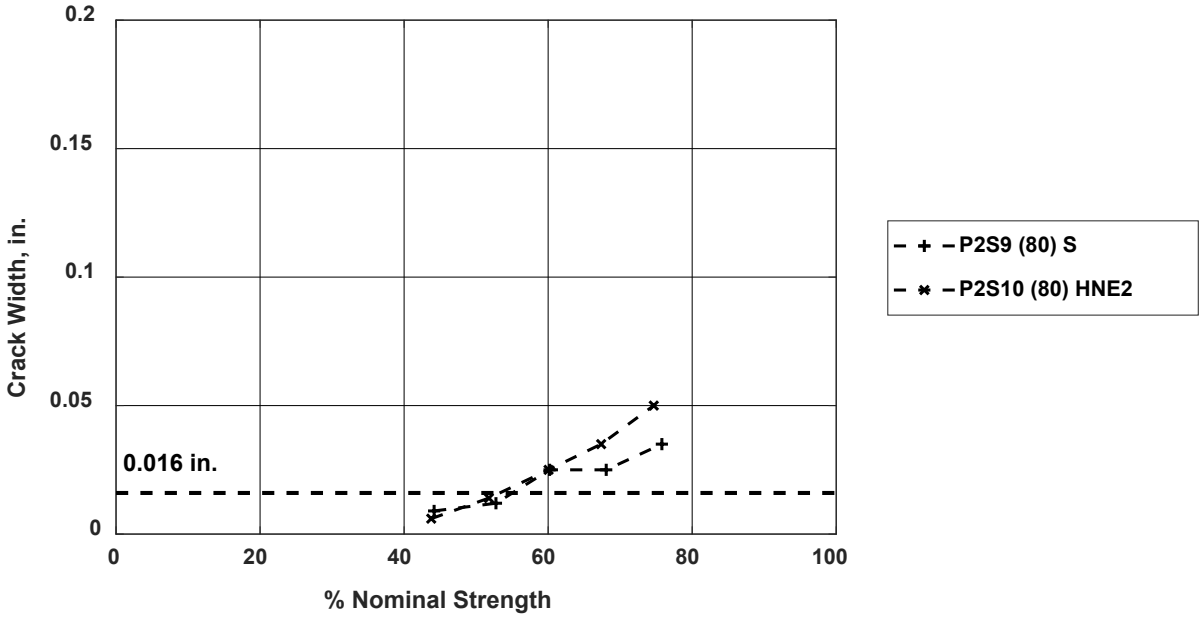

Figure G.14: Crack width versus percent of nominal strength: specimens P2S9 and P2S10 (longitudinal reinforcement yielded in specimen P2S10 before shear failure) [1 in. = 25.4 mm]

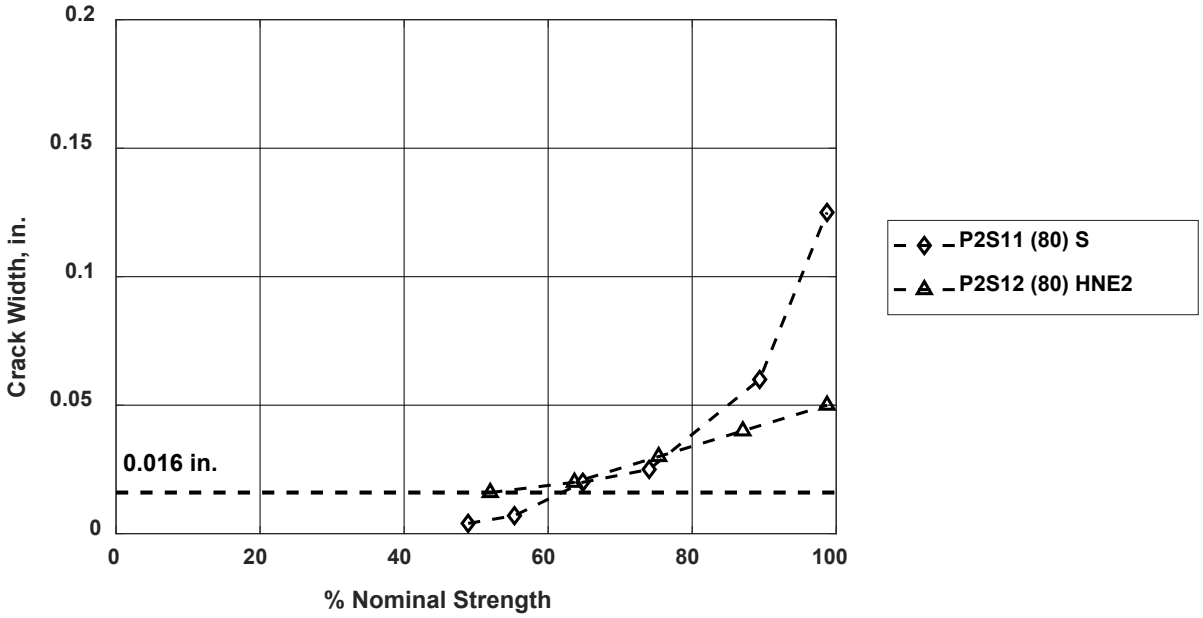

Figure G.15: Crack width versus percent of nominal strength: specimens P2S11 and P2S12 (longitudinal reinforcement yielded in specimens P2S11 and P2S12 before shear failure) [1 in. = 25.4 mm]

Table G.3: Shear force and crack widths for Phase 3 specimens

Specimen	Nom. Str, kips (kN)	Meas. Str V_T [a], kips (kN)	Shear Force[a], kips (kN)	Measured Inclined Crack Width CW, in. [b] (Crack I.D.)						Max. CW, in. (mm)
				(1)	(2)	(3)	(4)	(5)	(6)	
P3S1	300 (1335)	346 (1540)	130 (579)	0.009	0.004					0.009 (0.23)
			160 (712)	0.009	0.004					0.009 (0.23)
			190 (846)	0.009	0.004	0.009	0.020			0.020 (0.51)
			220 (979)	0.007	0.004	0.020	0.030			0.030 (0.76)
P3S2	295 (1313)	275 (1224)	130 (579)	0.004	0.004					0.004 (0.10)
			160 (712)	0.006	0.009	0.004	0.006			0.009 (0.23)
			190 (846)	0.007	0.012	0.025	0.020			0.025 (0.64)
			220 (979)	0.010	0.016	0.040	0.020			0.040 (1.02)
P3S3	283 (1259)	245 (1090)	130 (579)	0.007		0.025				0.025 (0.64)
			160 (712)	0.007	0.004	0.040	0.006			0.040 (1.02)
			190 (846)	0.009	0.012	0.063	0.025			0.063 (1.60)
			220 (979)	0.012	0.012	0.125	0.060			0.125 (3.18)
P3S4	283 (1259)	262 (1166)	130 (579)	0.004	0.009		0.007			0.009 (0.23)
			160 (712)	0.009	0.016	0.004	0.030			0.030 (0.76)
			190 (846)	0.009	0.020	0.016	0.040			0.040 (1.02)
			220 (979)	0.012	0.025	0.040	0.060			0.060 (1.52)
P3S5	176 (783)	186 (828)	97 (432)	0.007	0.006					0.007 (0.18)
			112 (498)	0.009	0.010	0.006				0.010 (0.25)
			127 (565)	0.010	0.016	0.025				0.025 (0.64)
P3S6	174 (774)	175 (779)	82 (365)	0.006						0.006 (0.15)
			97 (432)	0.009	0.004					0.009 (0.23)
			112 (498)	0.020	0.012		0.006			0.020 (0.51)
			127 (565)	0.025	0.012	0.035	0.020			0.035 (0.89)
			142 (632)	0.035	0.025	0.050	0.025			0.050 (1.27)
P3S7	177 (788)	209 (930)	107 (476)	0.007	0.006					0.007 (0.18)
			127 (565)	0.010	0.016	0.020	0.006	0.009		0.020 (0.51)
			147 (654)	0.009	0.025	0.035	0.016	0.010		0.035 (0.89)
P3S8	177 (788)	228 (1015)	97 (432)	0.009		0.009				0.009 (0.23)
			112 (498)	0.010	0.004	0.009				0.010 (0.25)
			127 (565)	0.010	0.006	0.009	0.012	0.040		0.040 (1.02)
			142 (632)	0.012	0.006	0.010	0.030	0.060		0.060 (1.52)
P3S9	165 (734) [c]	138 (614)	67 (298)	0.006						0.006 (0.15)
			82 (365)	0.009	0.004					0.009 (0.23)
			97 (432)	0.010	0.009	0.012	0.007			0.012 (0.30)
			112 (498)	0.009	0.012	0.030	0.020			0.030 (0.76)
			127 (565)	0.009	0.012	0.040	0.016			0.040 (1.02)
P3S10	164 (730) [c]	148 (659)	67 (298)	0.006	0.007					0.007 (0.18)
			82 (365)	0.009	0.007	0.010	0.009			0.010 (0.25)
			97 (432)	0.010	0.009	0.012	0.020			0.020 (0.51)
			112 (498)	0.012	0.007	0.012	0.030			0.030 (0.76)
			127 (565)	0.016	0.007	0.012	0.050			0.050 (1.27)

[a] Accounts for the applied load, loading frame weight, and contributing specimen self-weight (Section 3.3.1)

[b] 1 in. = 25.4 mm

[c] Beam nominal flexural strength divided by shear span a_v

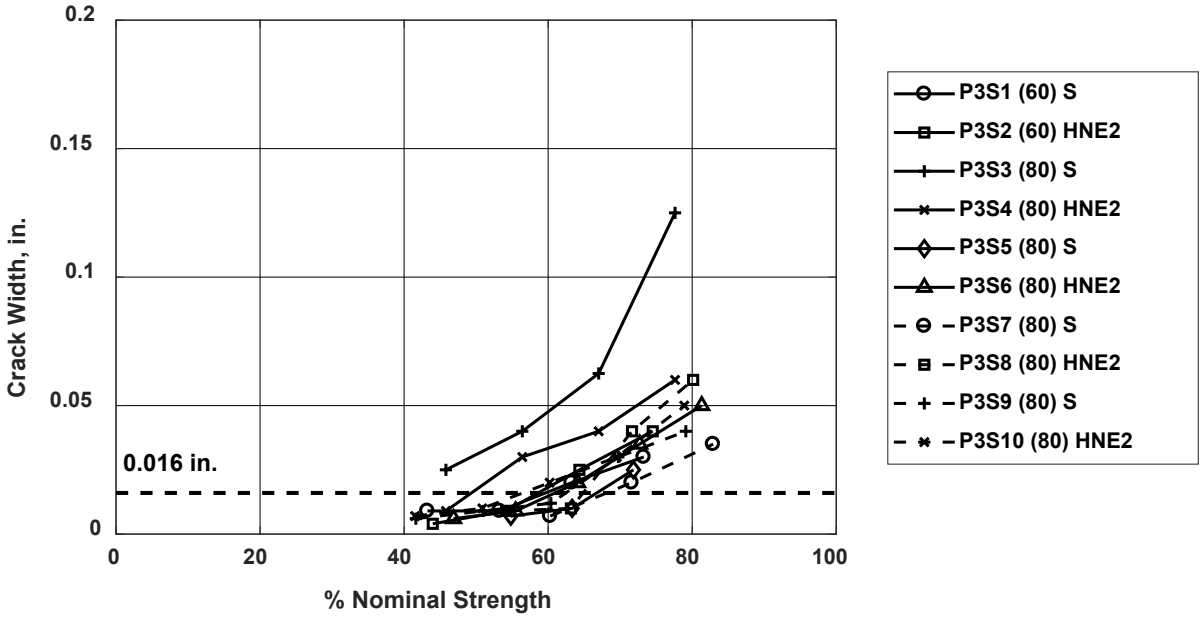

Figure G.16: Crack width versus percent of nominal strength: Phase 3 specimens (longitudinal reinforcement yielded in specimens P3S9 and P3S10 before shear failure) [1 in. = 25.4 mm]

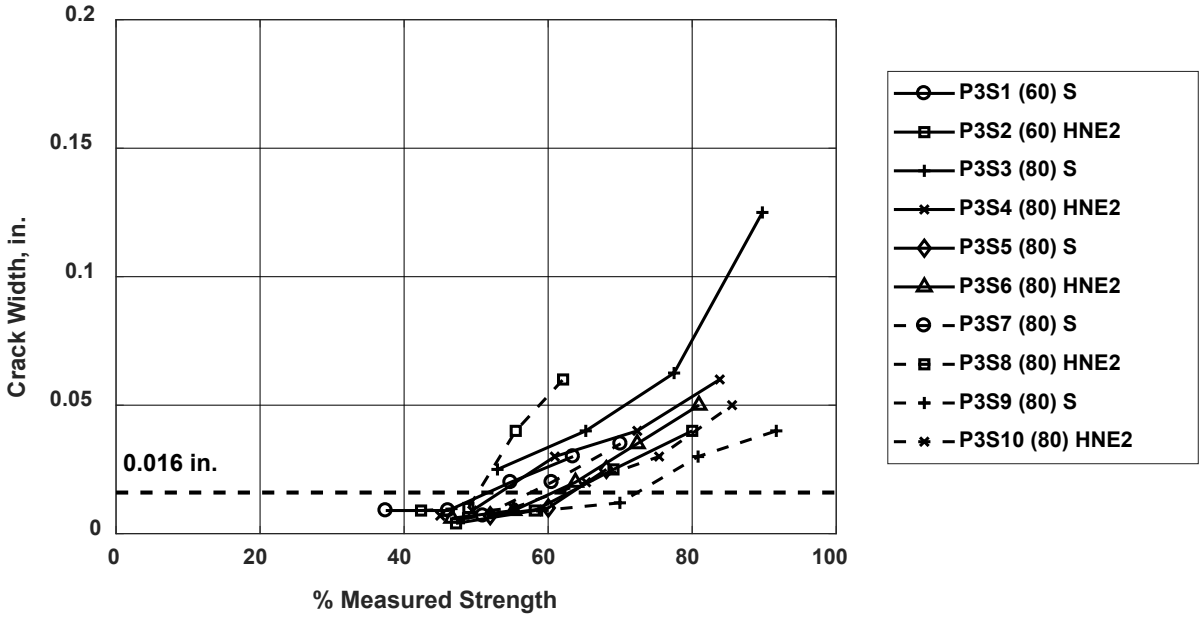

Figure G.17: Crack width versus percent of measured strength: Phase 3 specimens (longitudinal reinforcement yielded in specimens P3S9 and P3S10 before shear failure) [1 in. = 25.4 mm]

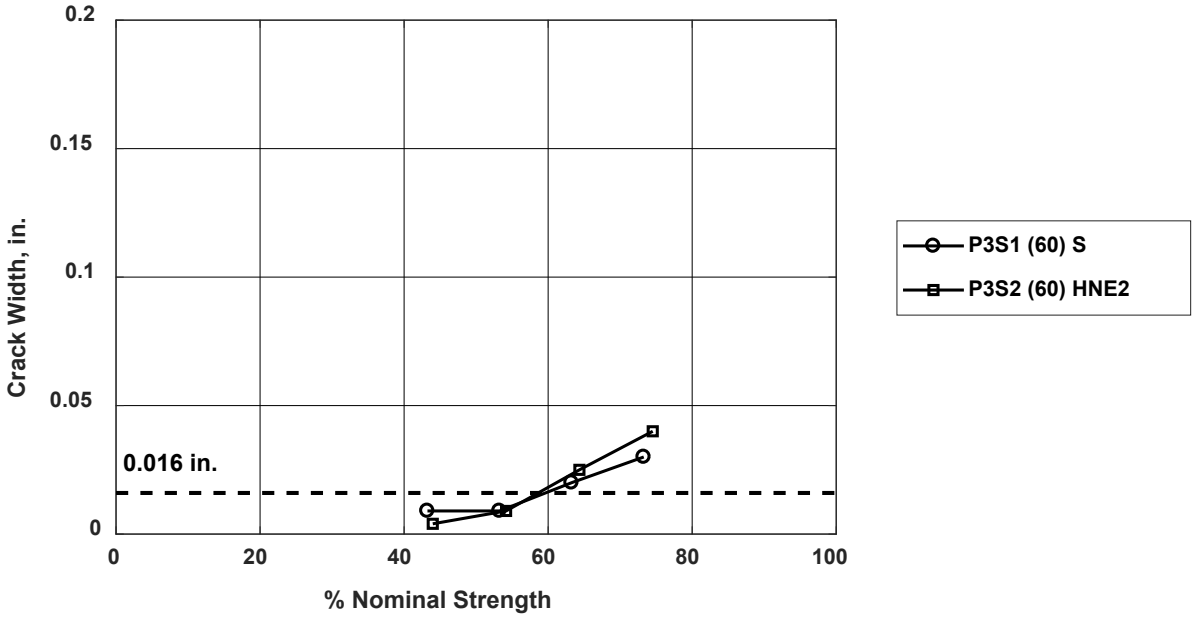

Figure G.18: Crack width versus percent of nominal strength: specimens P3S1 and P3S2 [1 in. = 25.4 mm]

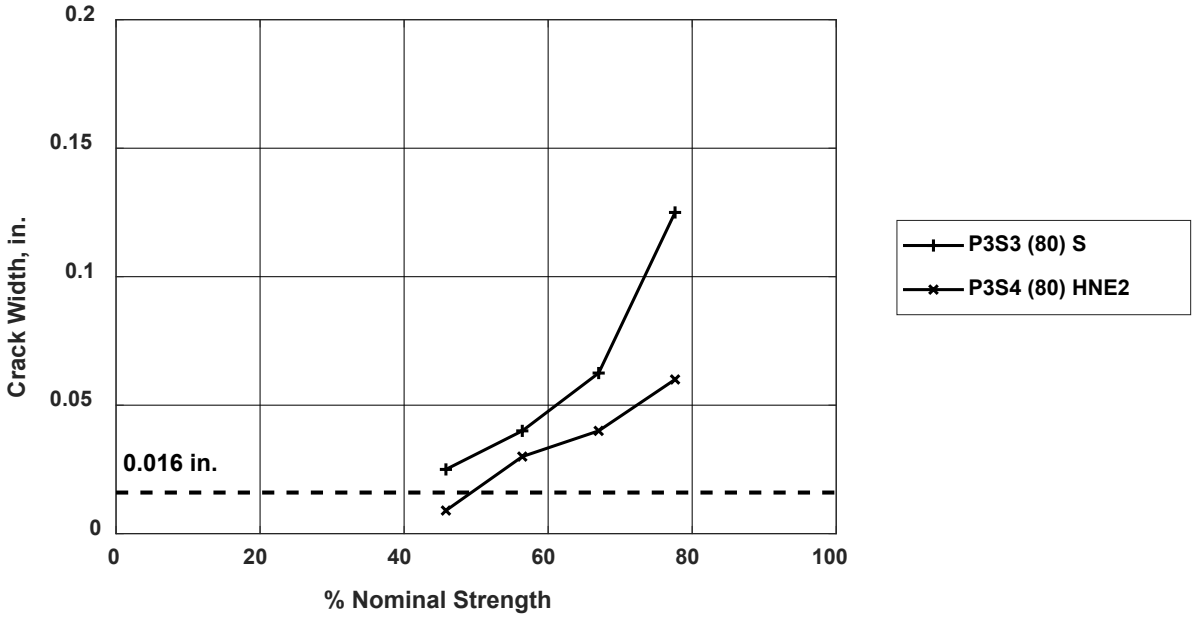

Figure G.19: Crack width versus percent of nominal strength: specimens P3S3 and P3S4 [1 in. = 25.4 mm]

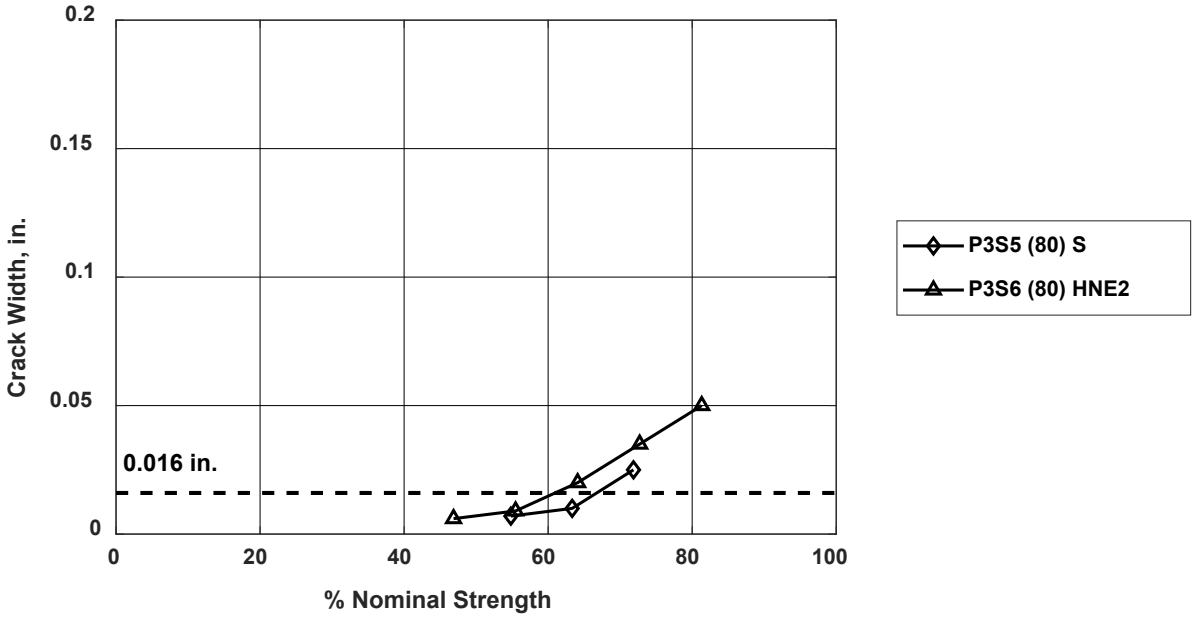

Figure G.20: Crack width versus percent of nominal strength: specimens P3S5 and P3S6 [1 in. = 25.4 mm]

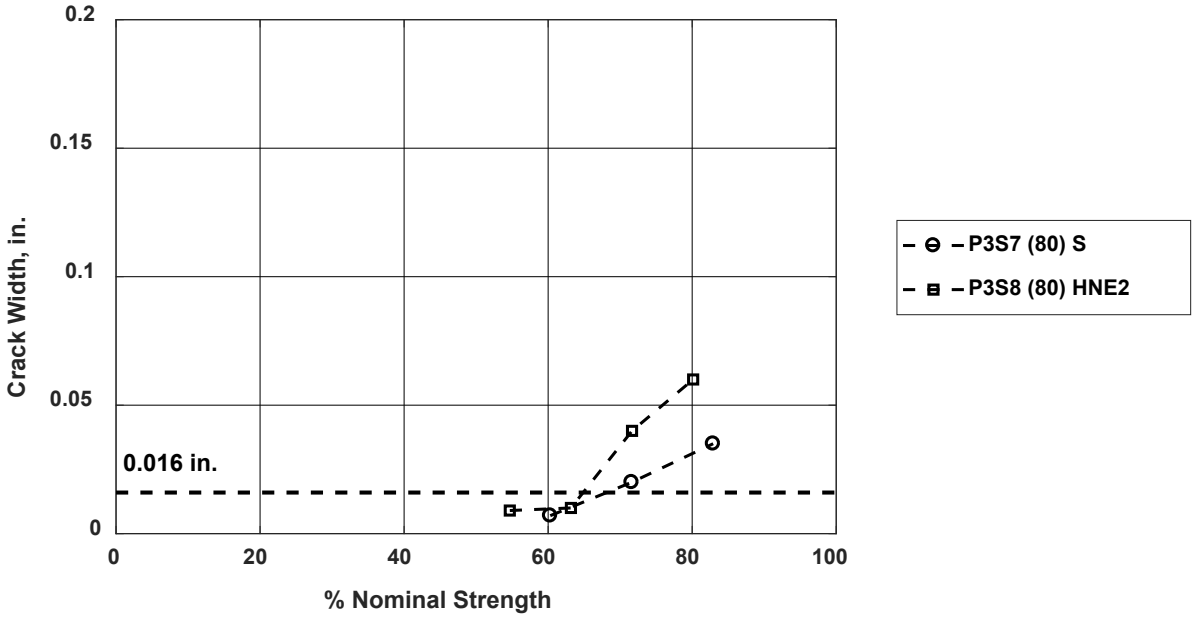

Figure G.21: Crack width versus percent of nominal strength: specimens P3S7 and P3S8 [1 in. = 25.4 mm]

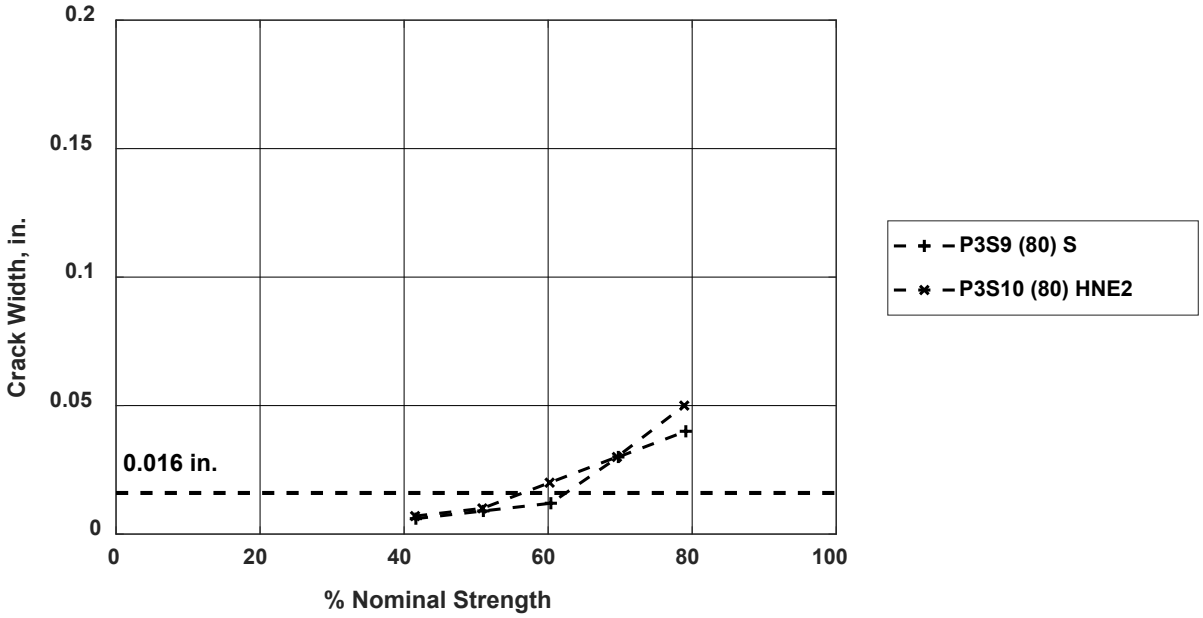

Figure G.22: Crack width versus percent of nominal strength: specimens P3S9 and P3S10 (longitudinal reinforcement yielded in specimens P3S9 and P3S10 before shear failure) [1 in. = 25.4 mm]

APPENDIX H: RECORDED STRAIN

Appendix H contains plots of recorded strain versus time for all specimens. Strain was recorded using 120-ohm foil-type strain gauges located on the transverse and longitudinal reinforcement. Specimens in Phases 1 and 2 had 17 strain gauges and specimens in Phase 3 had 21 strain gauges. The locations of strain gauges for specimens in each phase are shown in diagrams that precede the results.

For each specimen there are three plots: strain from gauges on the longitudinal reinforcement versus time, strain from gauges on the transverse reinforcement versus time, and strain versus time for six gauges selected from the first two plots. The latter plot also includes the recorded load for reference on a secondary axis. This plot can be used to determine the applied load at which changes in recorded strain occurred (such as, identifying what applied load was associated with transverse reinforcement yielding). There is no data collected from the strain gauges mounted on the longitudinal reinforcement for Specimens P1S16, P1S17, or P2S11, as the strain gauges were damaged at some point during fabrication or movement of the beam.

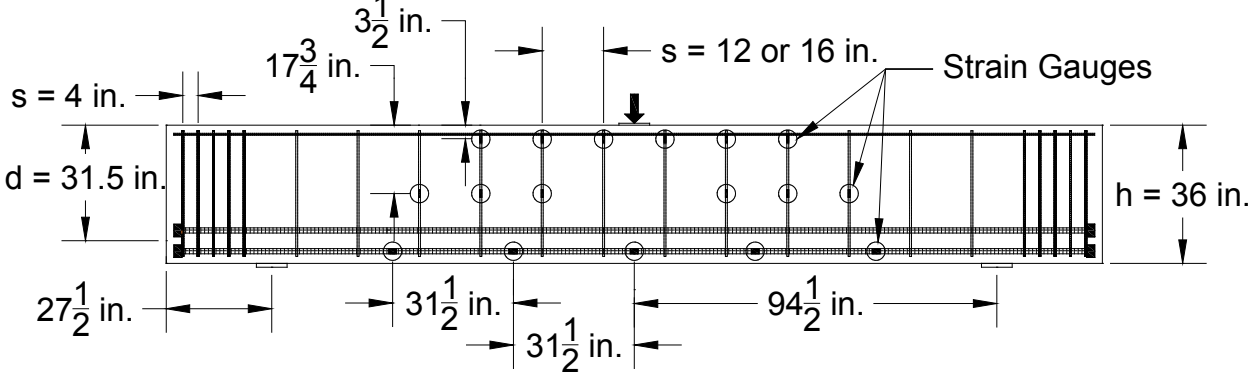

(a)

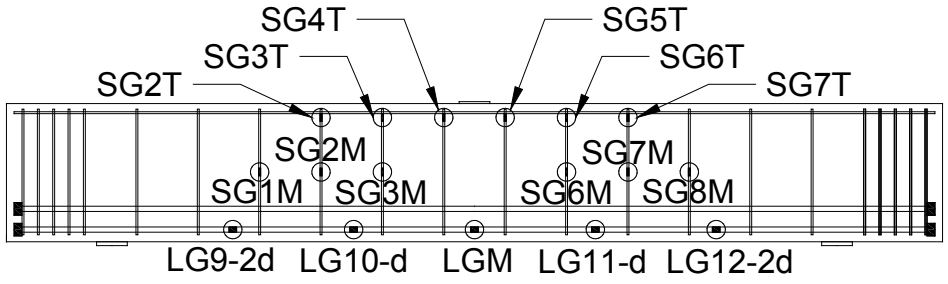

(b)

Figure H.1: Phase 1 specimens: Strain gauge (a) locations and (b) naming convention [1 in. = 25.4 mm]

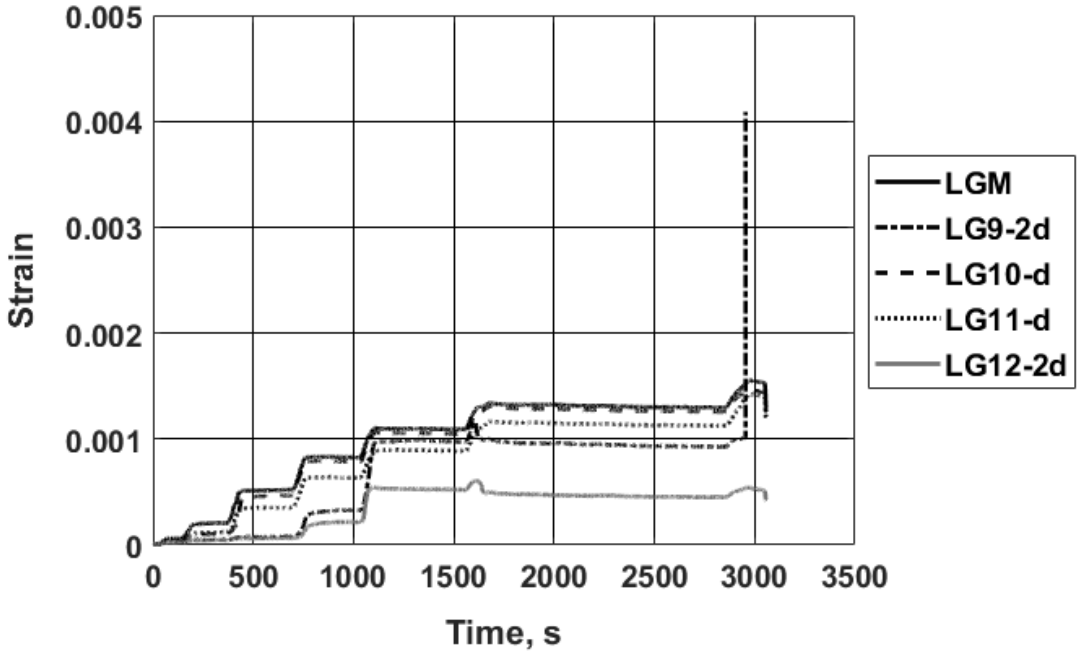

Figure H.2: Longitudinal reinforcing bar strain: specimen P1S1

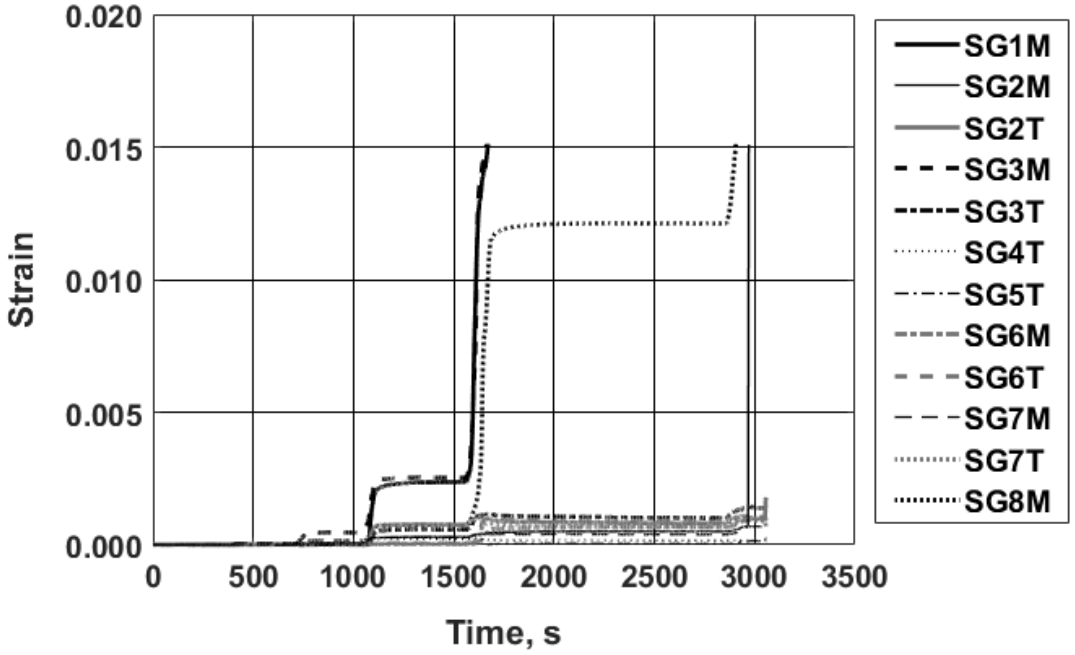

Figure H.3: Transverse reinforcing bar strain: specimen P1S1

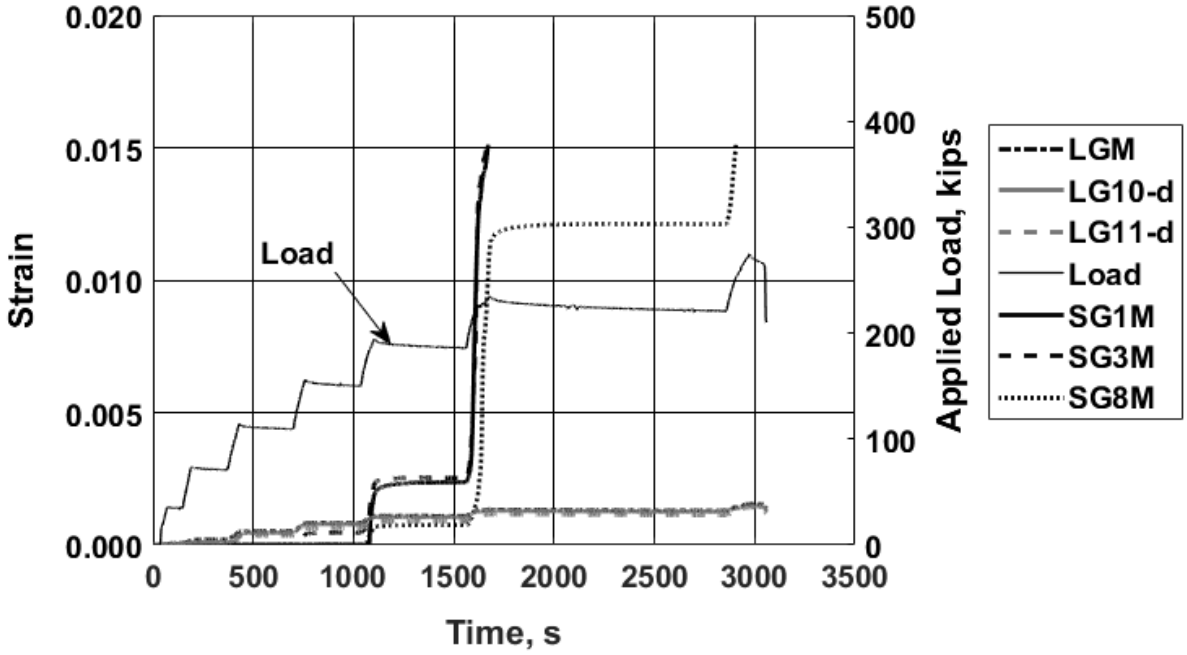

Figure H.4: Strain recorded with selected gauges and load versus time: specimen P1S1 [1 kip = 4.45 kN]

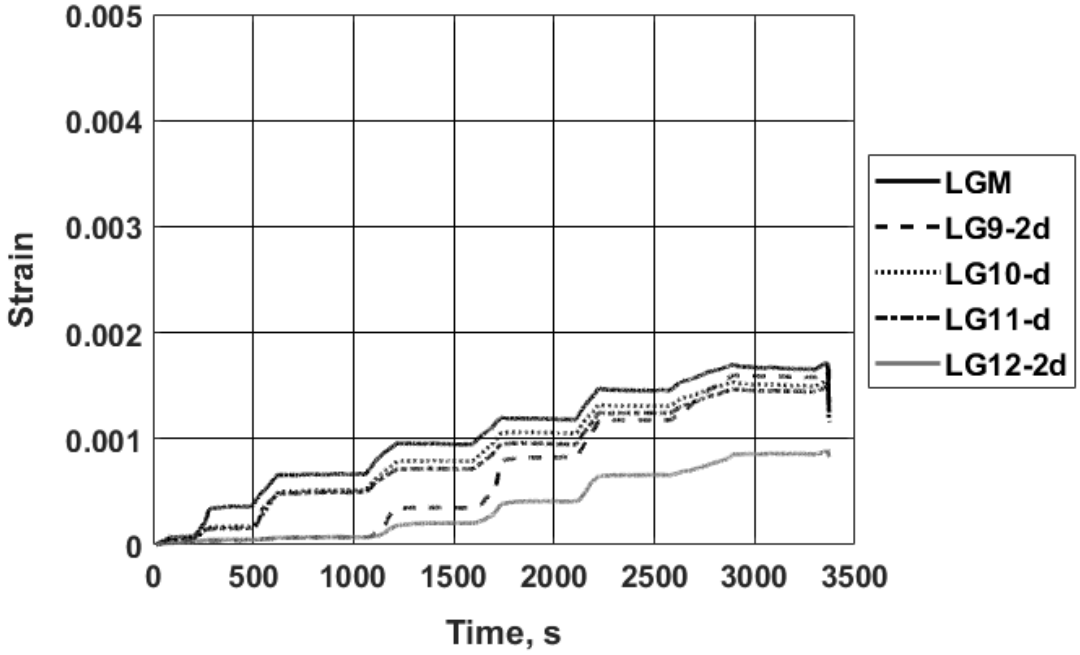

Figure H.5: Longitudinal reinforcing bar strain: specimen P1S2

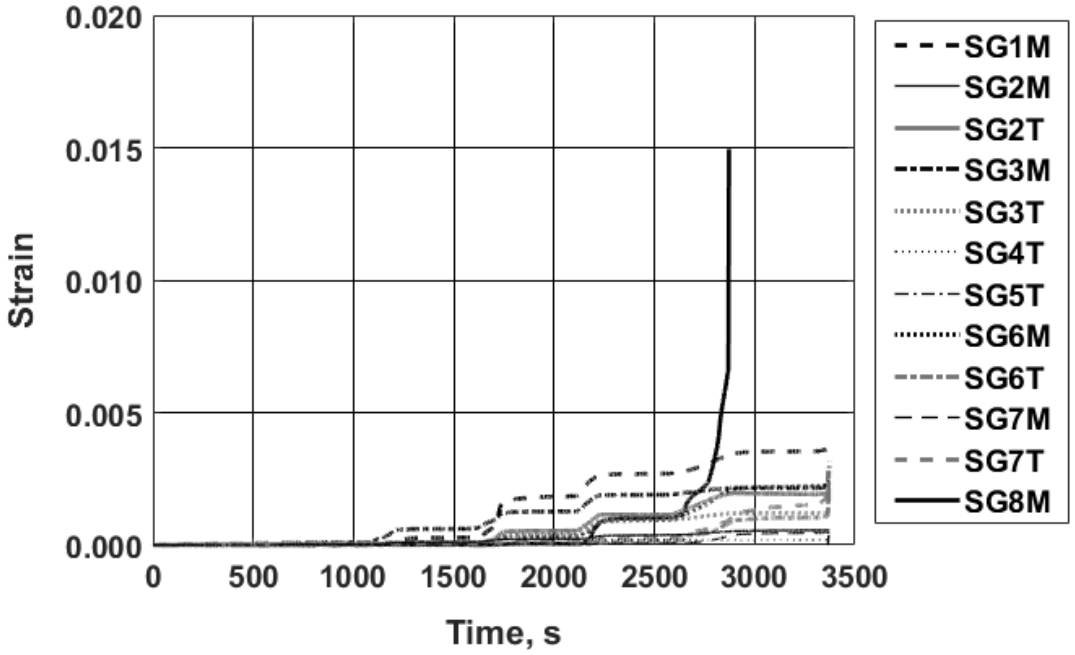

Figure H.6: Transverse reinforcing bar strain: specimen P1S2

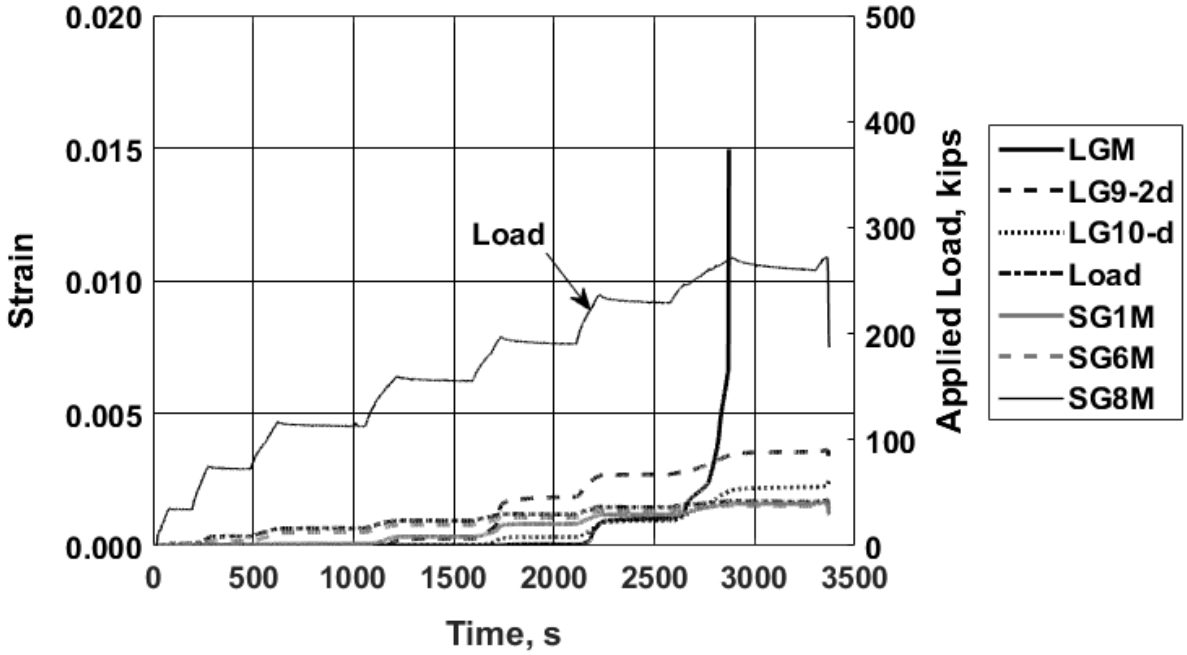

Figure H.7: Strain recorded with selected gauges and load versus time: specimen P1S2 [1 kip = 4.45 kN]

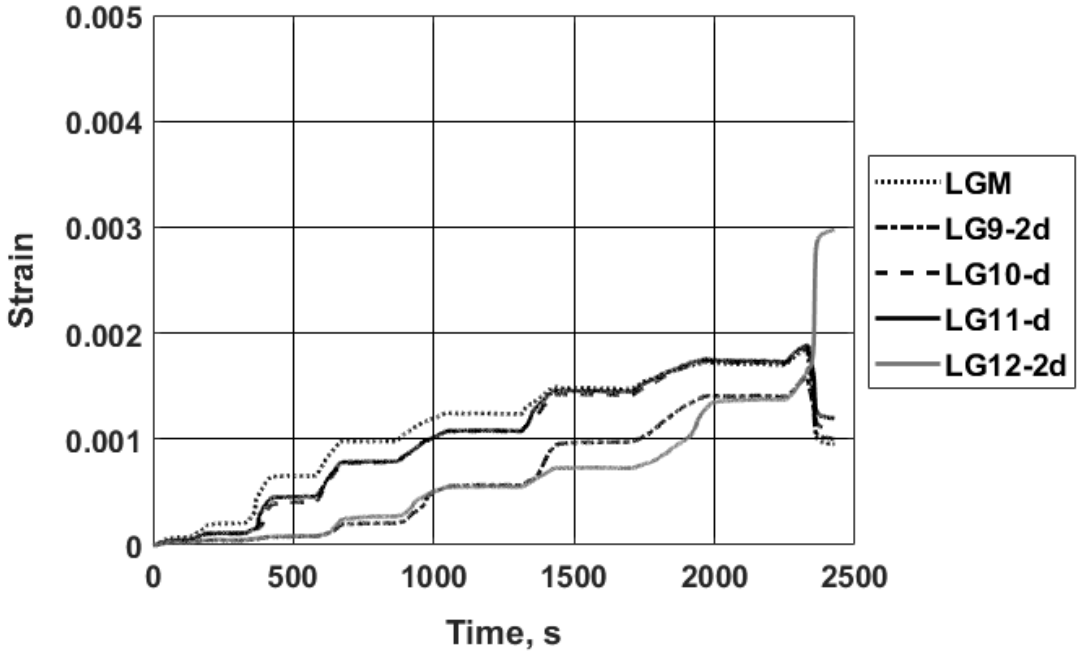

Figure H.8: Longitudinal reinforcing bar strain: specimen P1S3

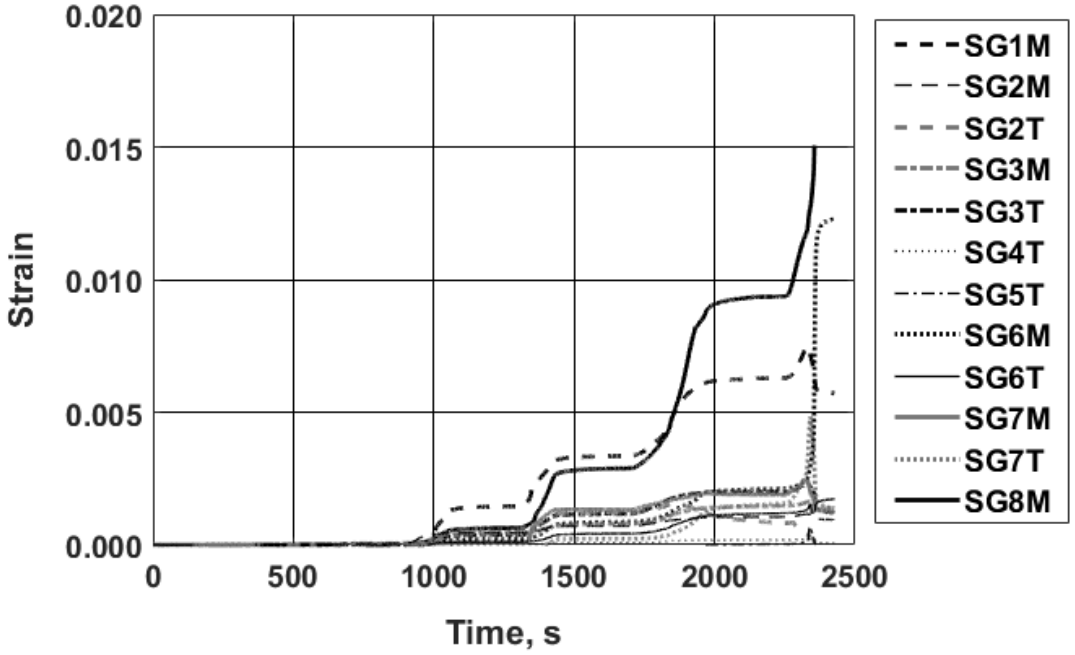

Figure H.9: Transverse reinforcing bar strain: specimen P1S3

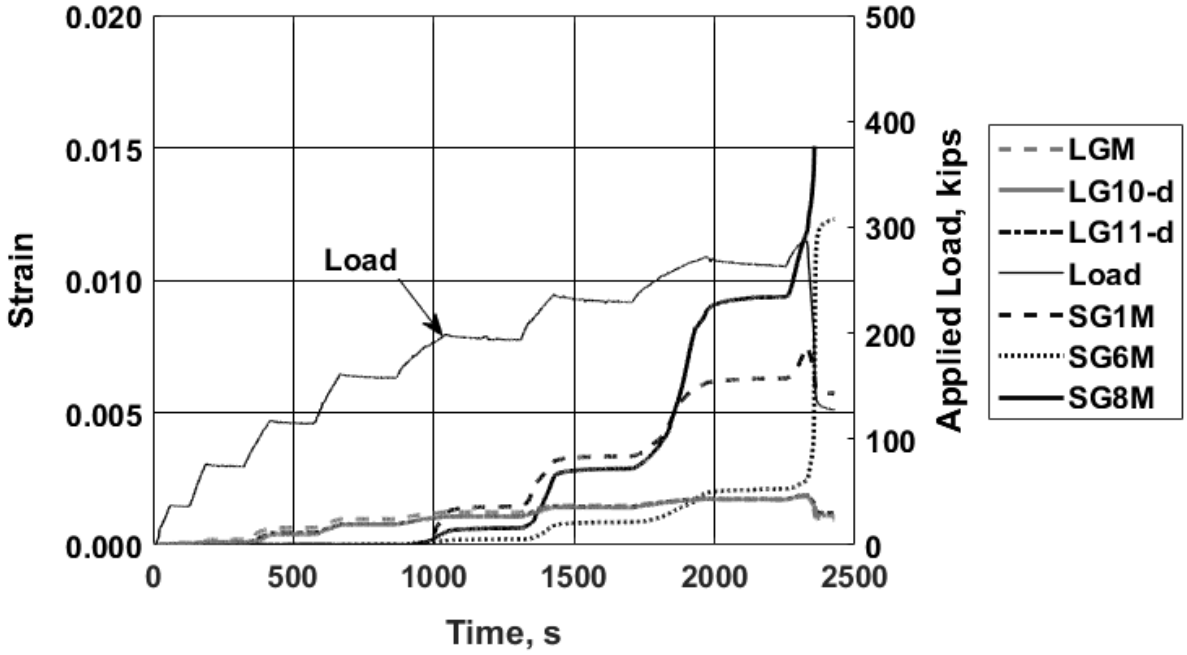

Figure H.10: Strain recorded with selected gauges and load versus time: specimen P1S3 [1 kip = 4.45 kN]

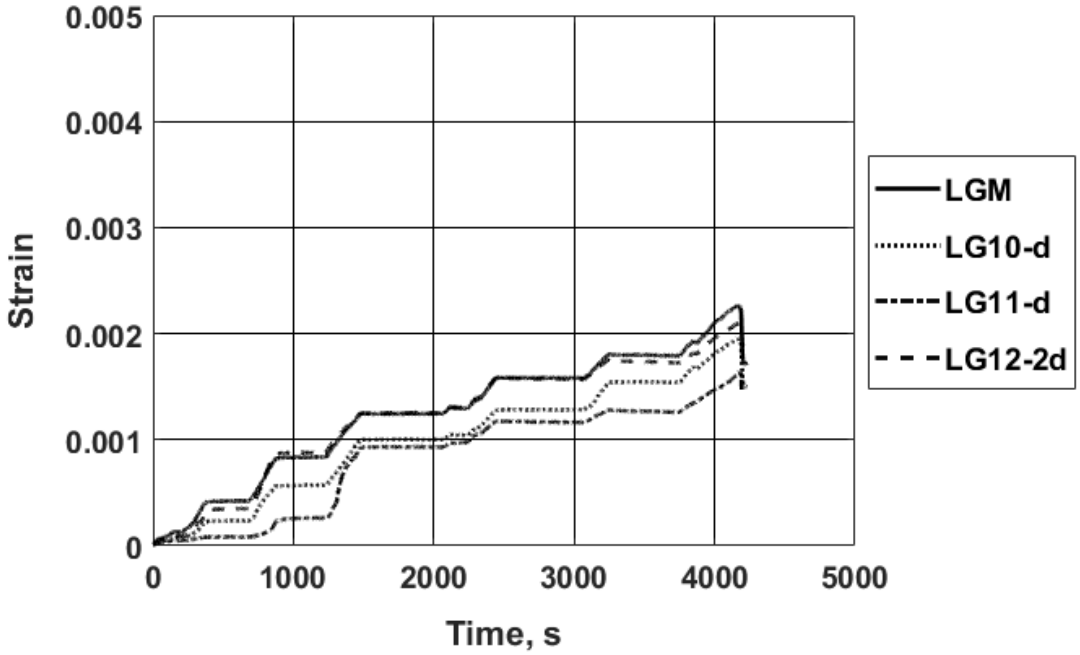

Figure H.11: Longitudinal reinforcing bar strain: specimen P1S4

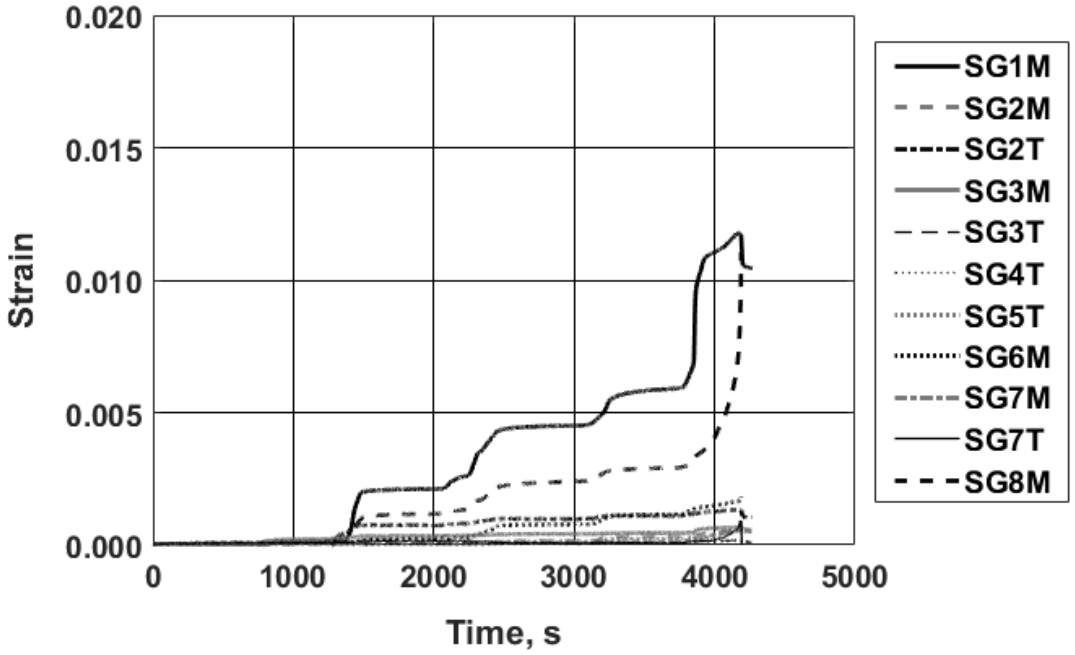

Figure H.12: Transverse reinforcing bar strain: specimen P1S4

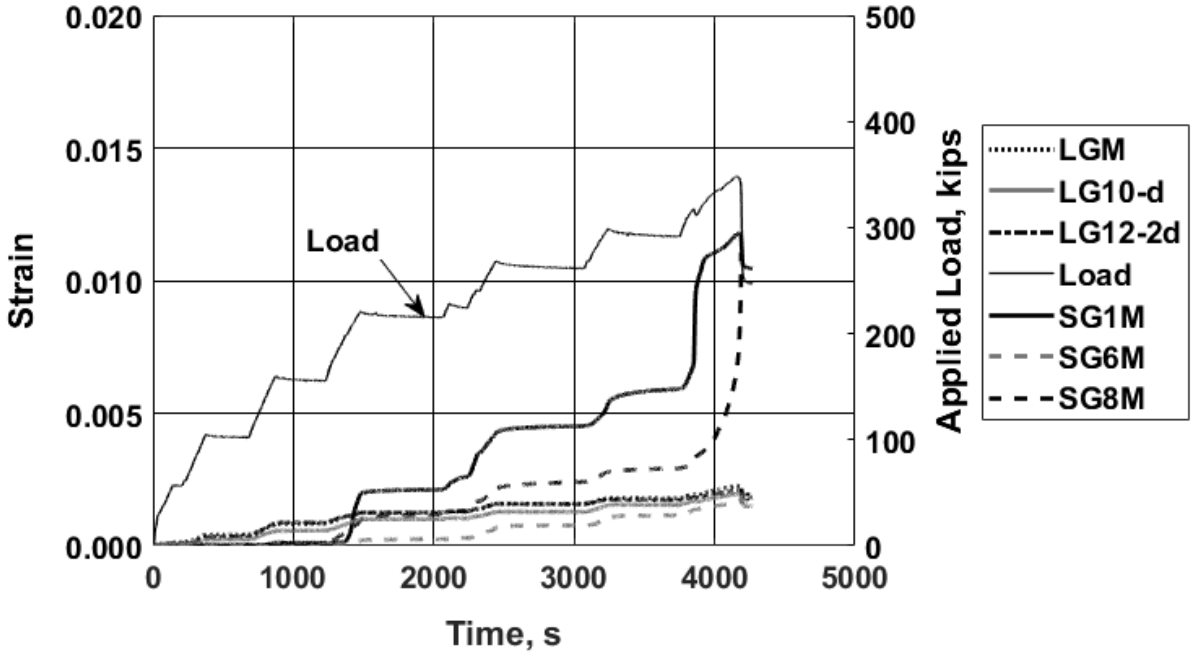

Figure H.13: Strain recorded with selected gauges and load versus time: specimen P1S4 [1 kip = 4.45 kN]

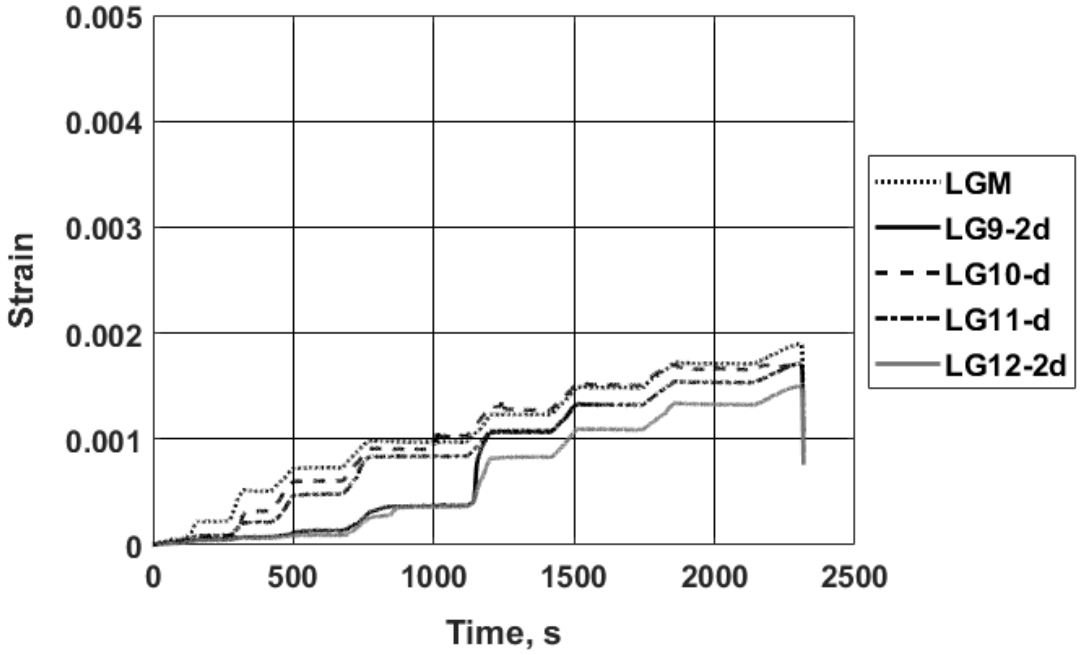

Figure H.14: Longitudinal reinforcing bar strain: specimen P1S5

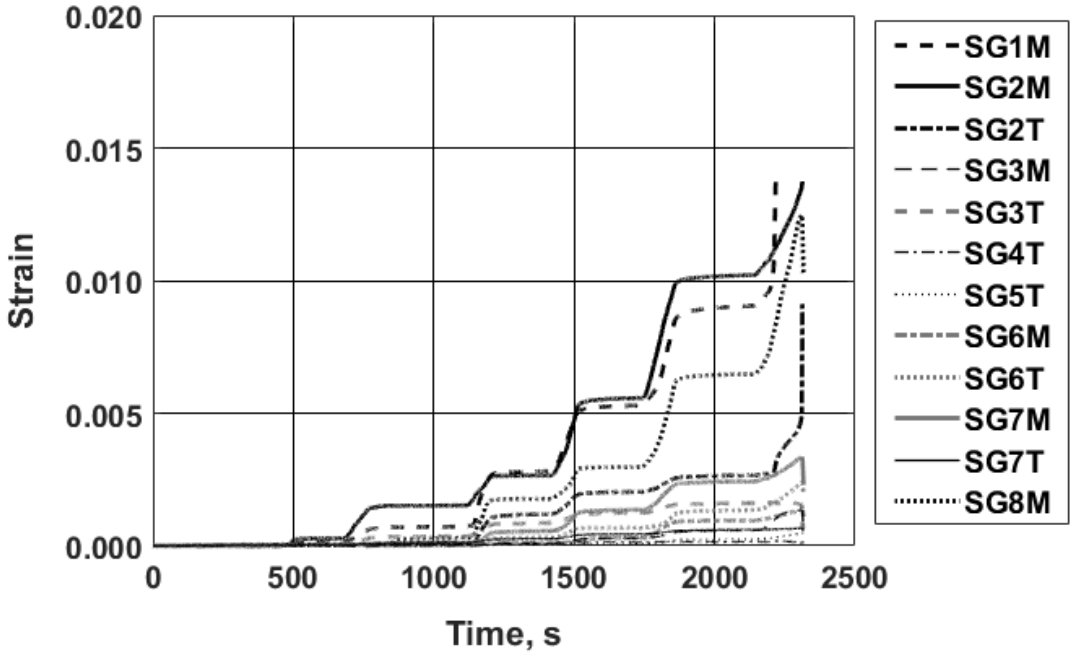

Figure H.15: Transverse reinforcing bar strain: specimen P1S5

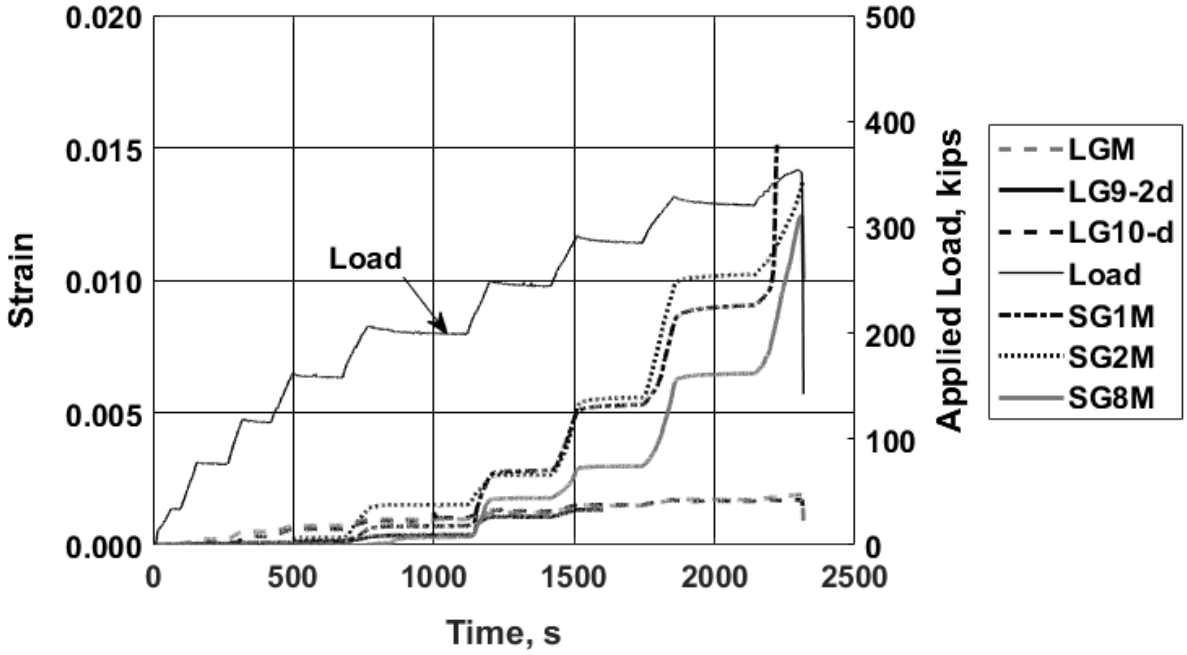

Figure H.16: Strain recorded with selected gauges and load versus time: specimen P1S5 [1 kip = 4.45 kN]

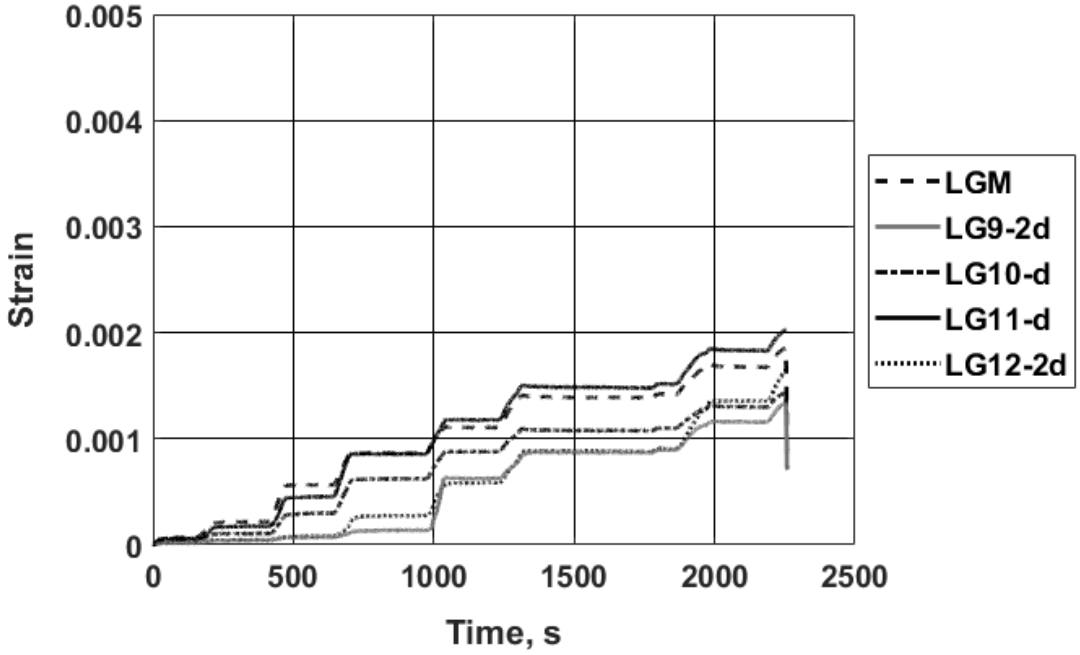

Figure H.17: Longitudinal reinforcing bar strain: specimen P1S6

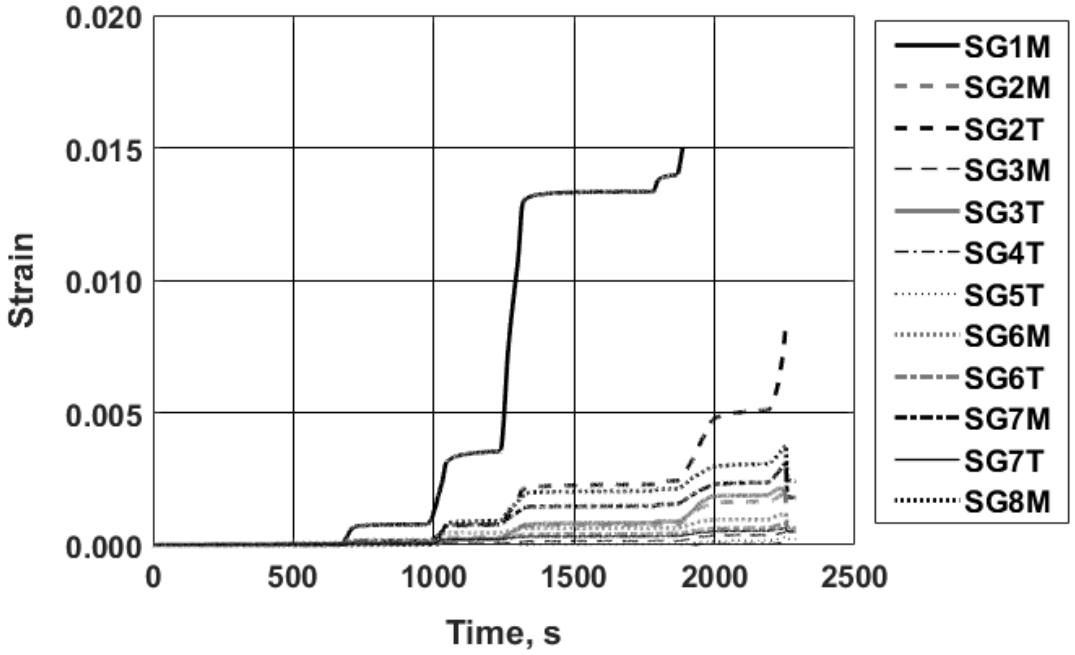

Figure H.18: Transverse reinforcing bar strain: specimen P1S6

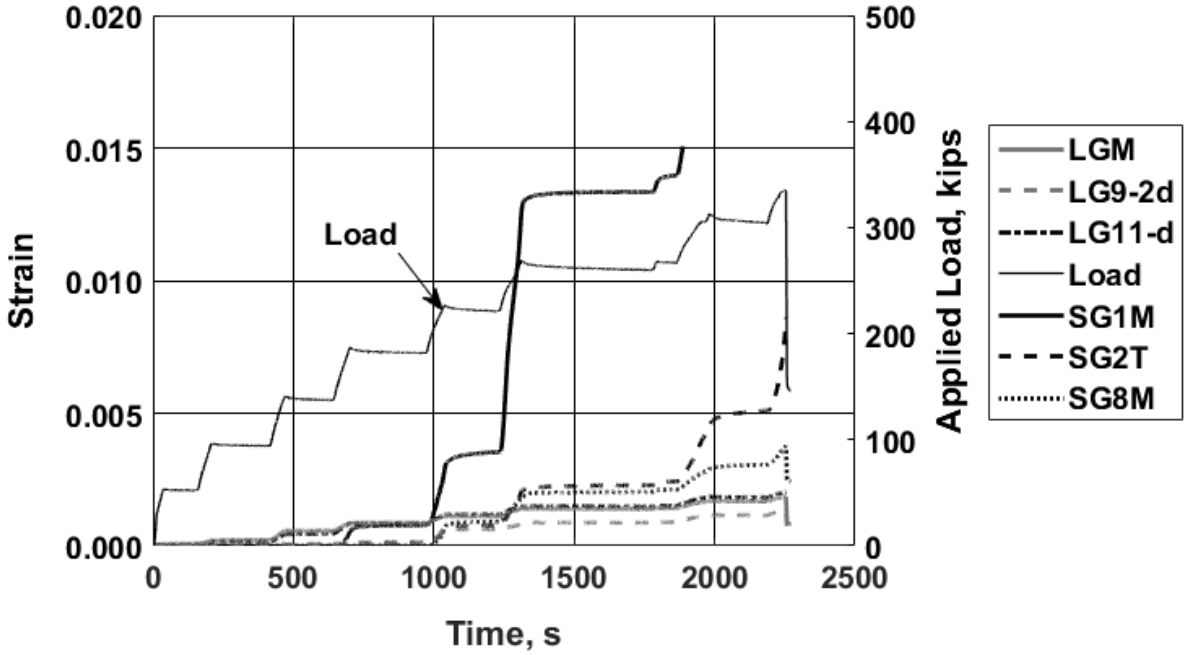

Figure H.19: Strain recorded with selected gauges and load versus time: specimen P1S6 [1 kip = 4.45 kN]

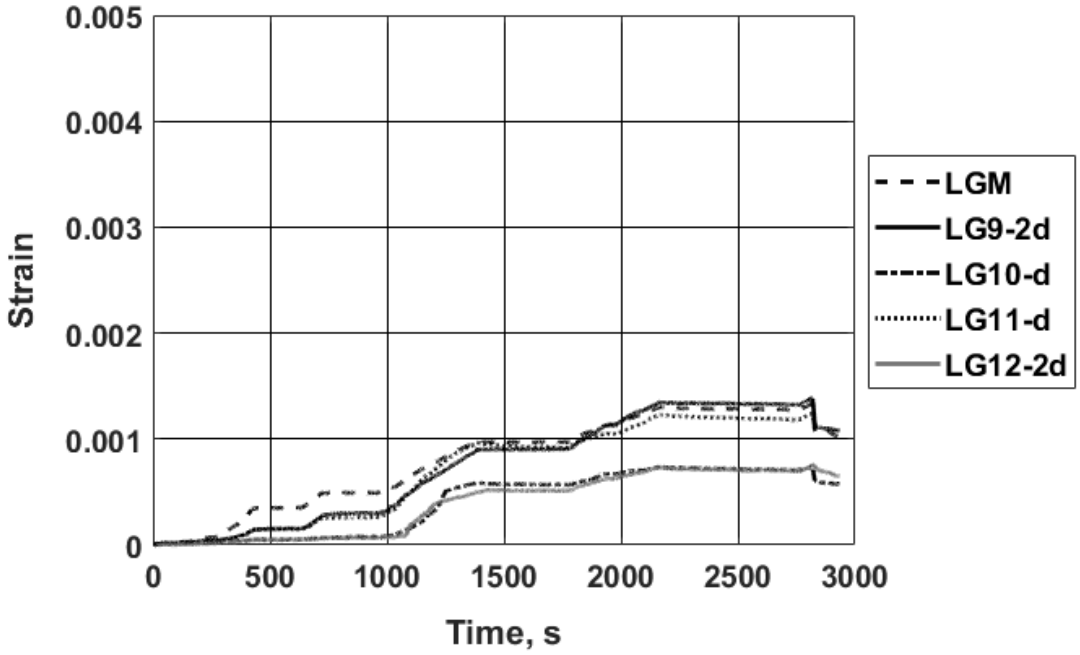

Figure H.20: Longitudinal reinforcing bar strain: specimen P1S7

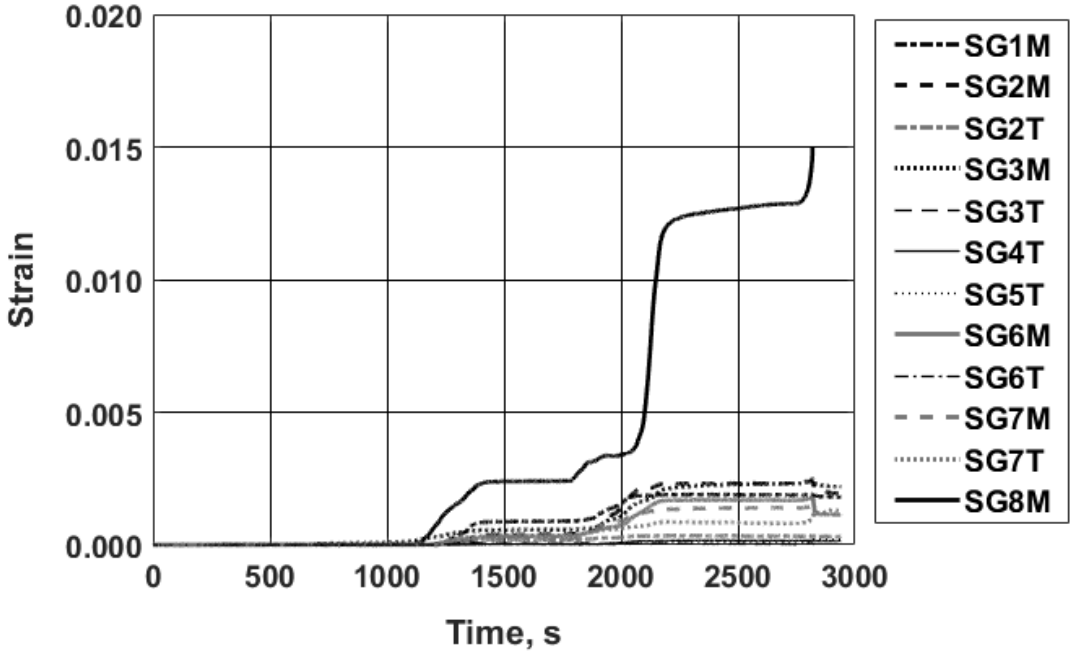

Figure H.21: Transverse reinforcing bar strain: specimen P1S7

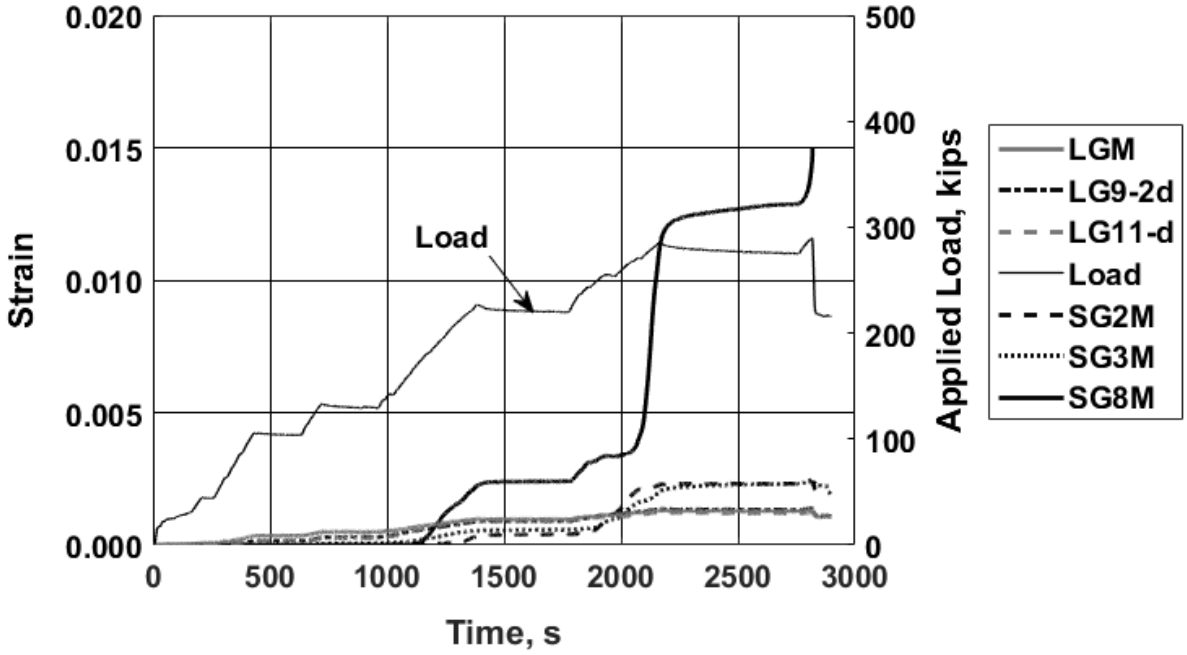

Figure H.22: Strain recorded with selected gauges and load versus time: specimen P1S7 [1 kip = 4.45 kN]

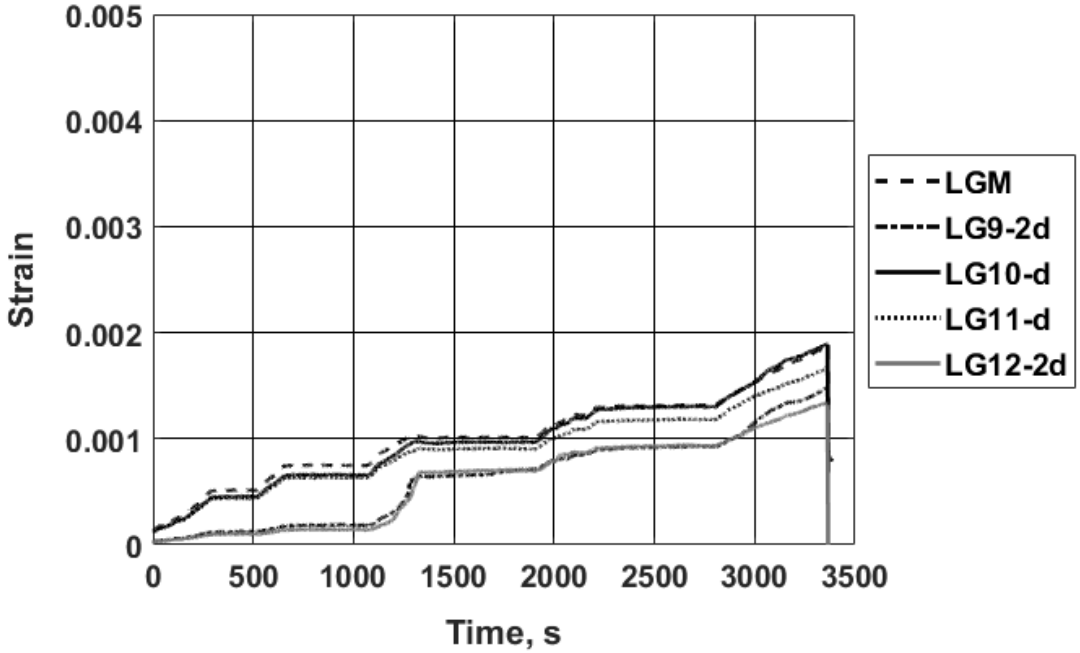

Figure H.23: Longitudinal reinforcing bar strain: specimen P1S8

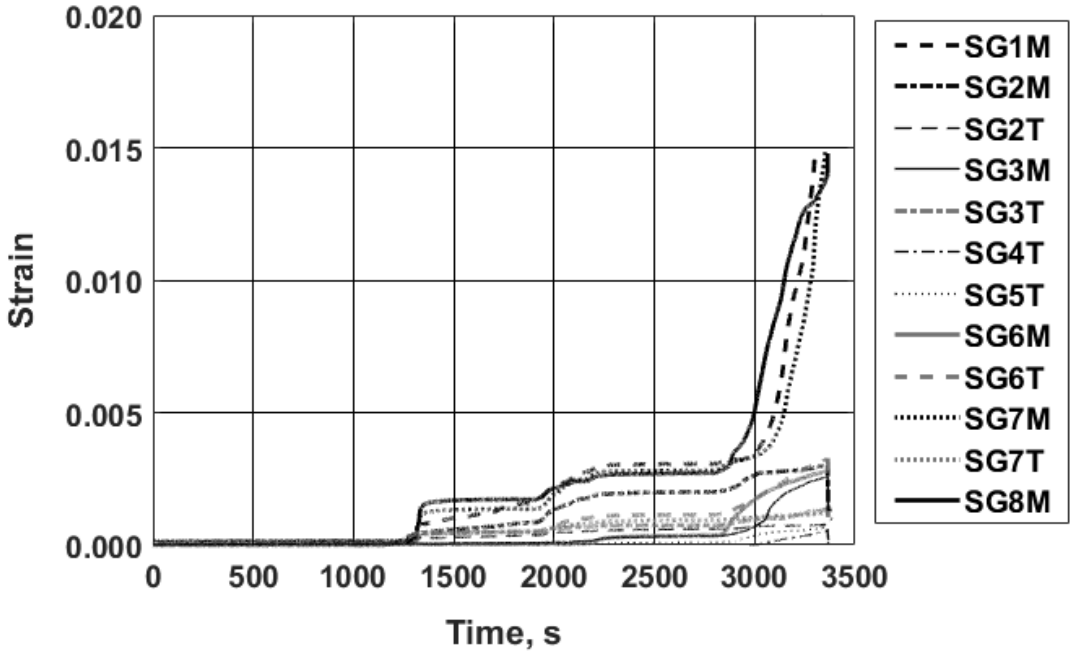

Figure H.24: Transverse reinforcing bar strain: specimen P1S8

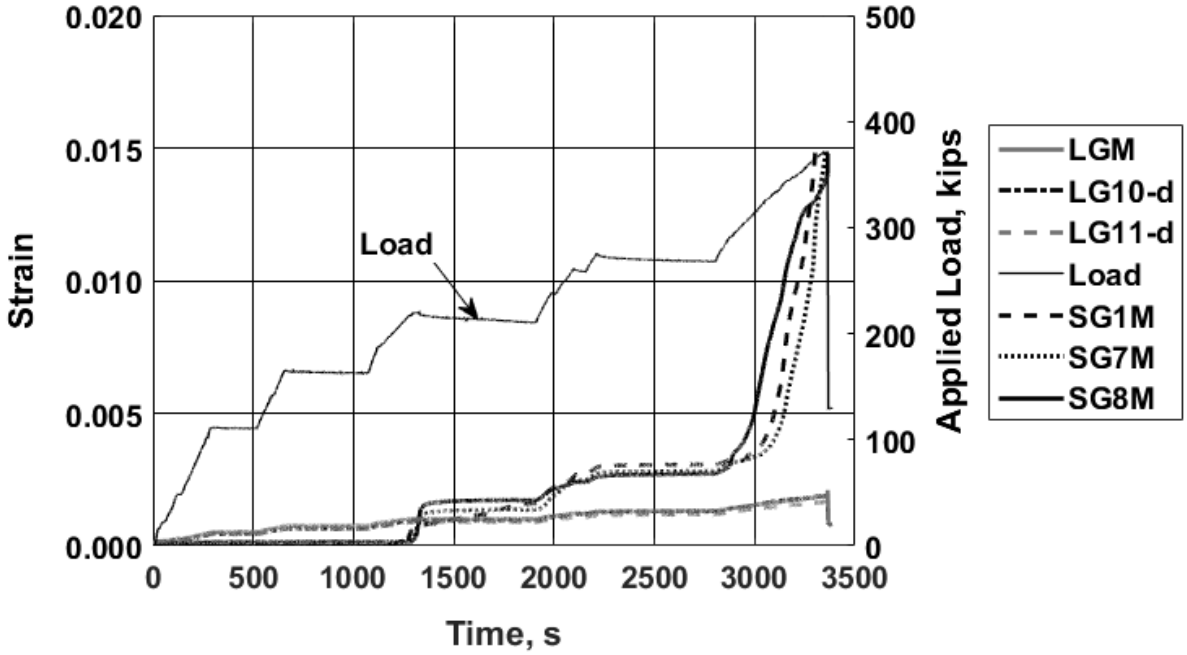

Figure H.25: Strain recorded with selected gauges and load versus time: specimen P1S8 [1 kip = 4.45 kN]

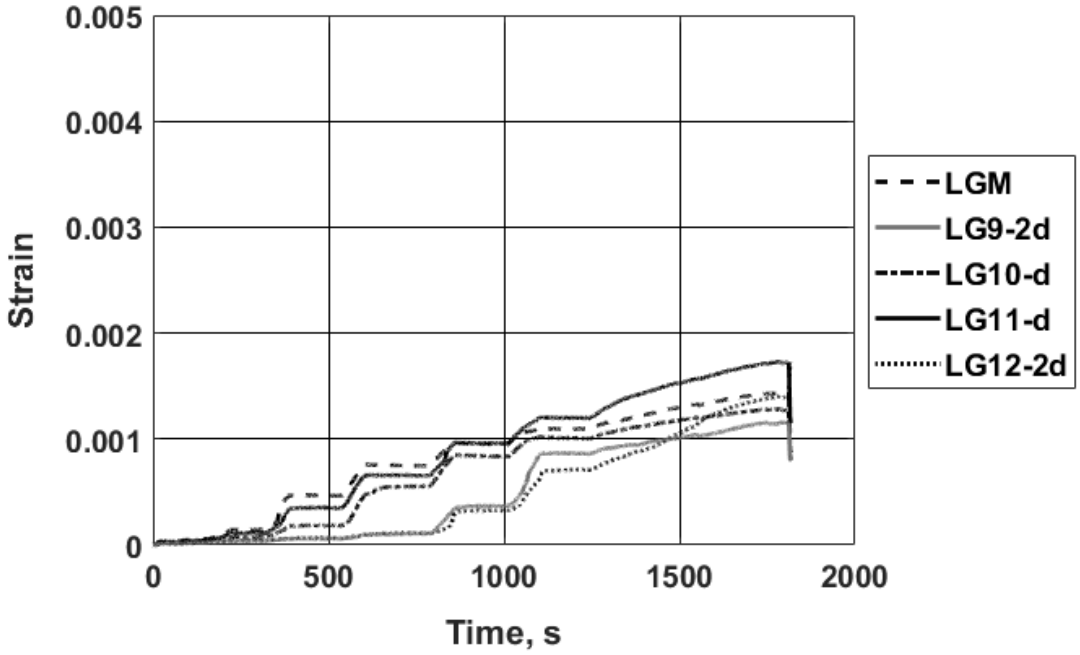

Figure H.26: Longitudinal reinforcing bar strain: specimen P1S9

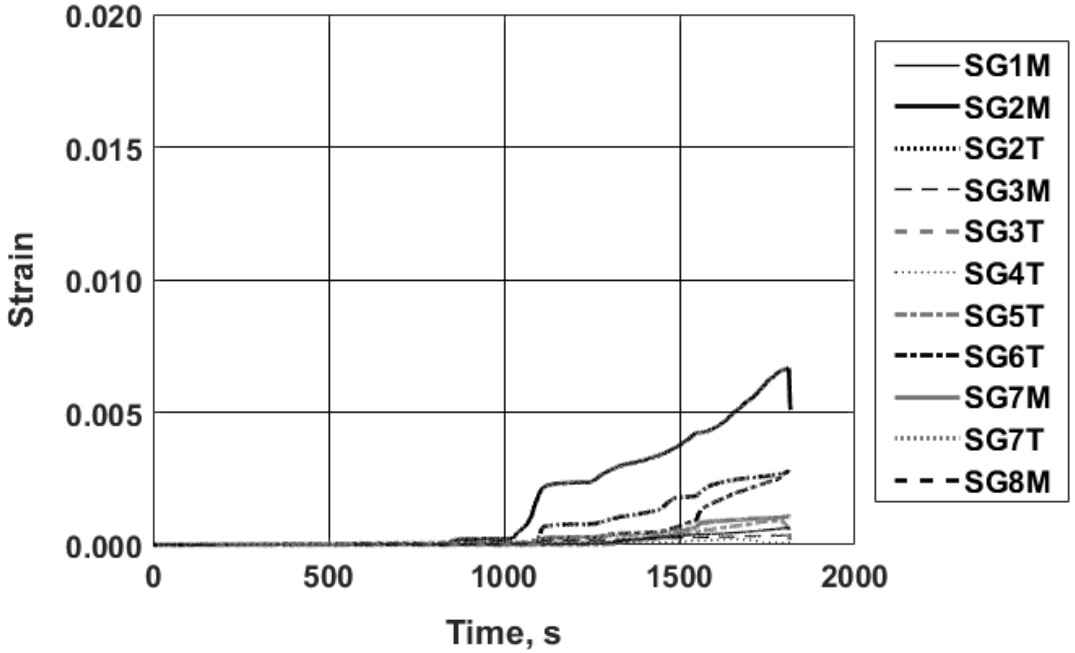

Figure H.27: Transverse reinforcing bar strain: specimen P1S9

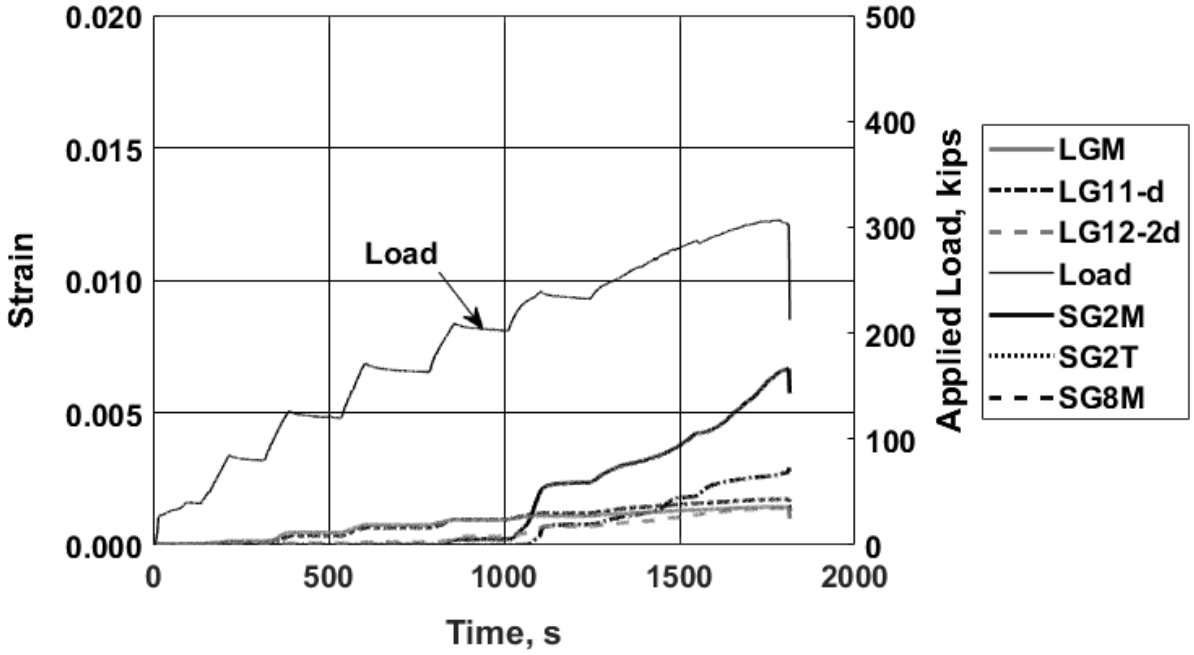

Figure H.28: Strain recorded with selected gauges and load versus time: specimen P1S9 [1 kip = 4.45 kN]

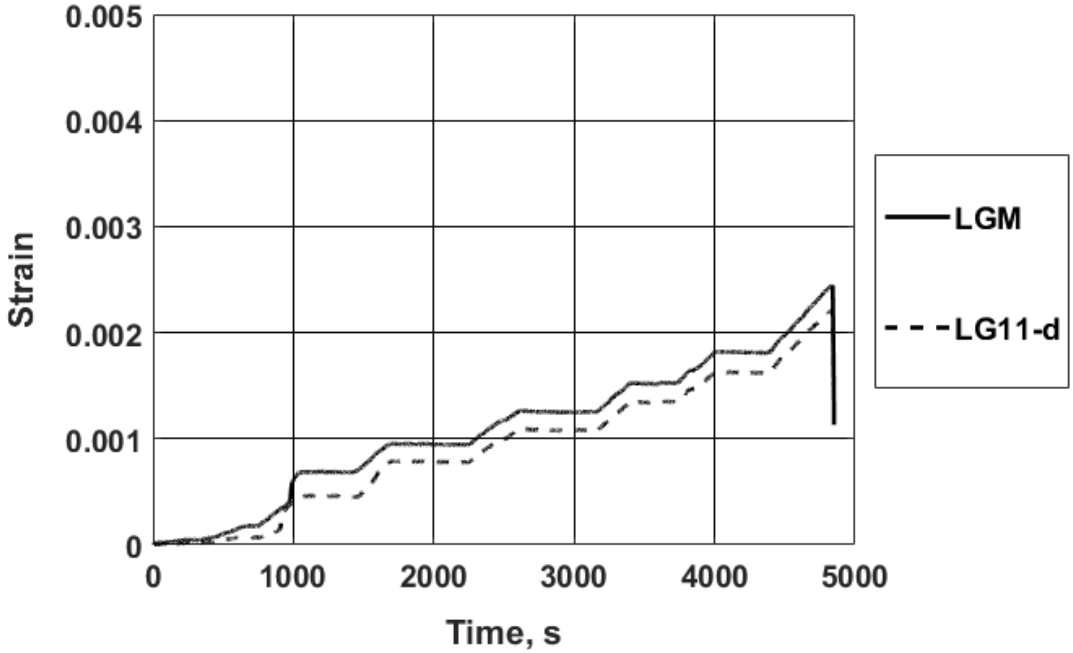

Figure H.29: Longitudinal reinforcing bar strain: specimen P1S10

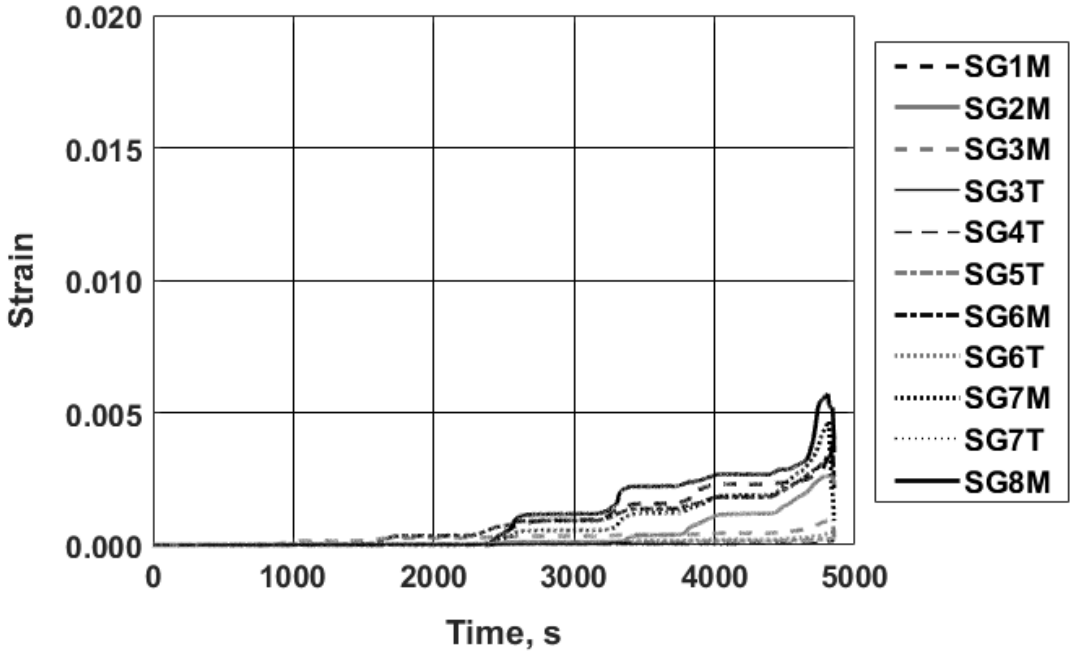

Figure H.30: Transverse reinforcing bar strain: specimen P1S10

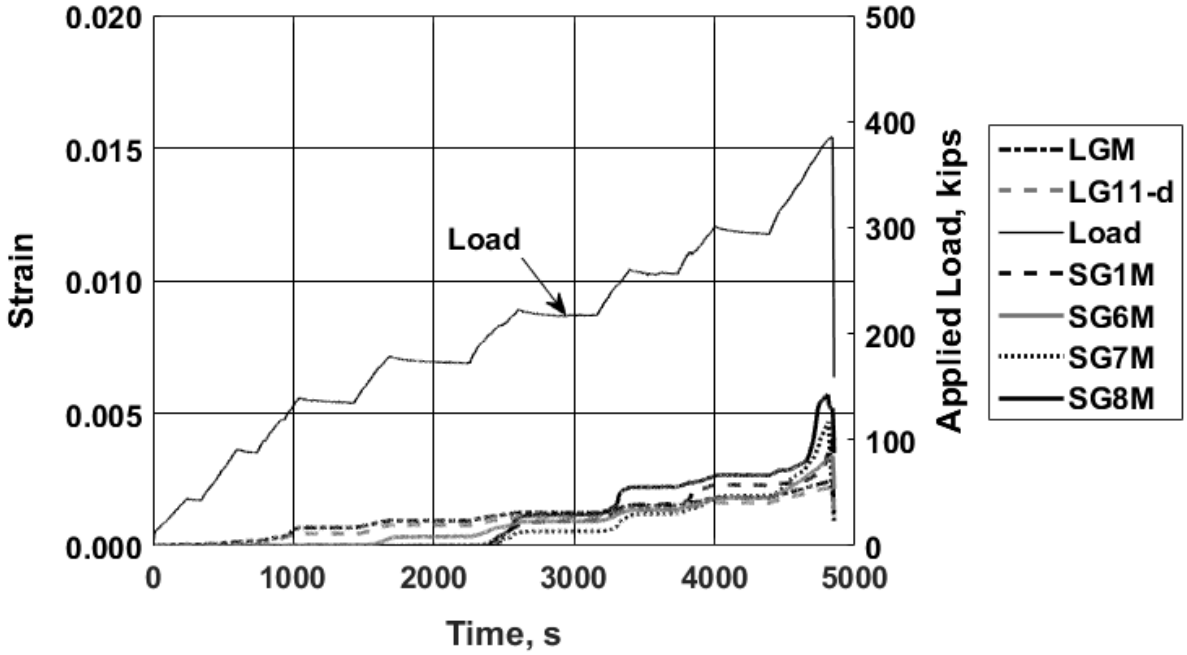

Figure H.31: Strain recorded with selected gauges and load versus time: specimen P1S10 [1 kip = 4.45 kN]

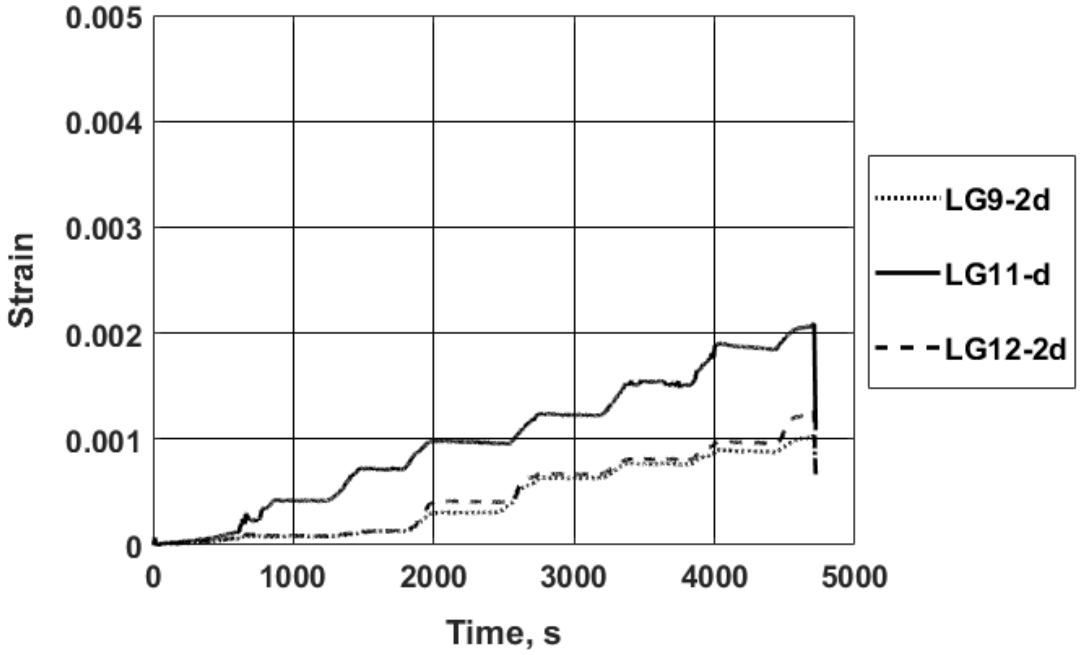

Figure H.32: Longitudinal reinforcing bar strain: specimen P1S11

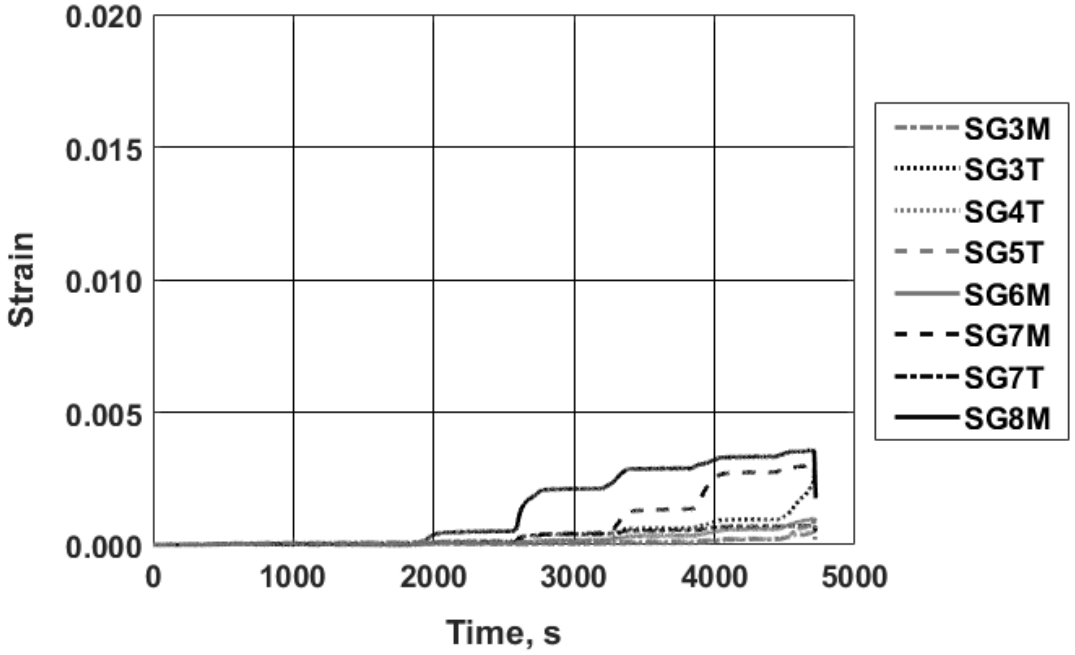

Figure H.33: Transverse reinforcing bar strain: specimen P1S11

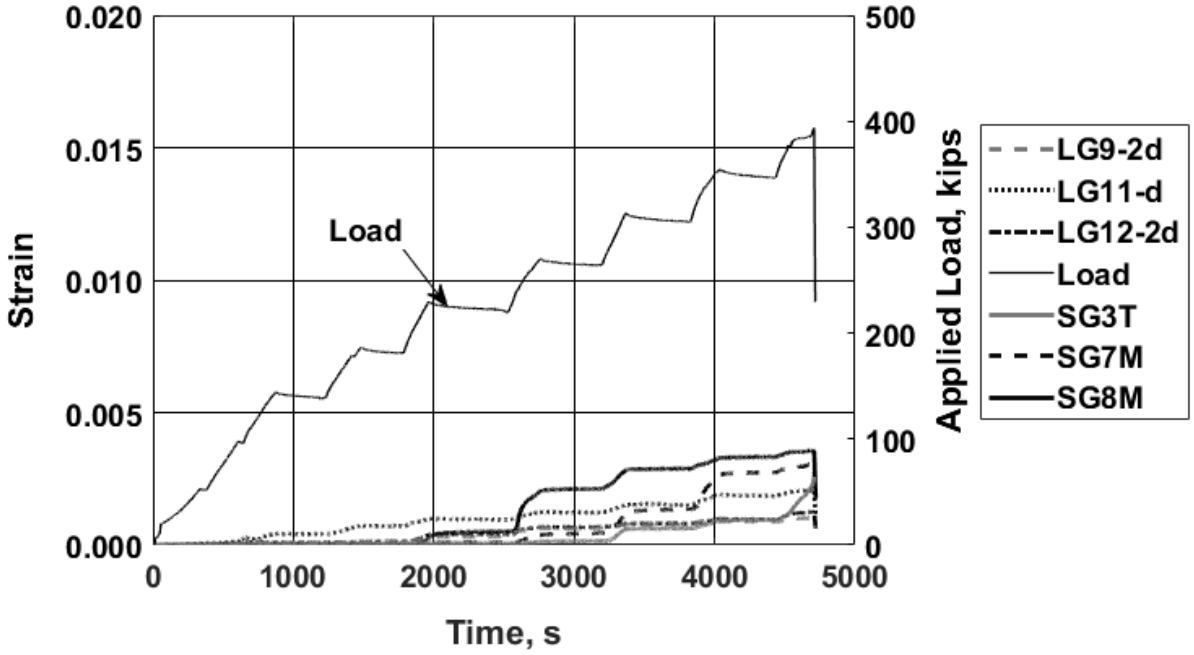

Figure H.34: Strain recorded with selected gauges and load versus time: specimen P1S11 [1 kip = 4.45 kN]

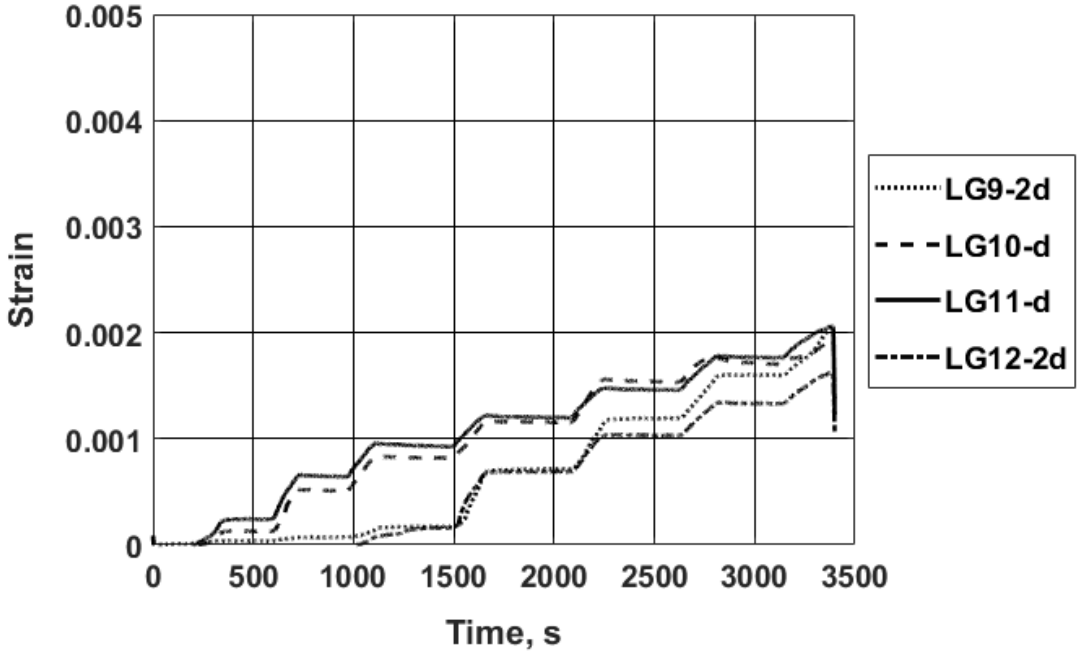

Figure H.35: Longitudinal reinforcing bar strain: specimen P1S12

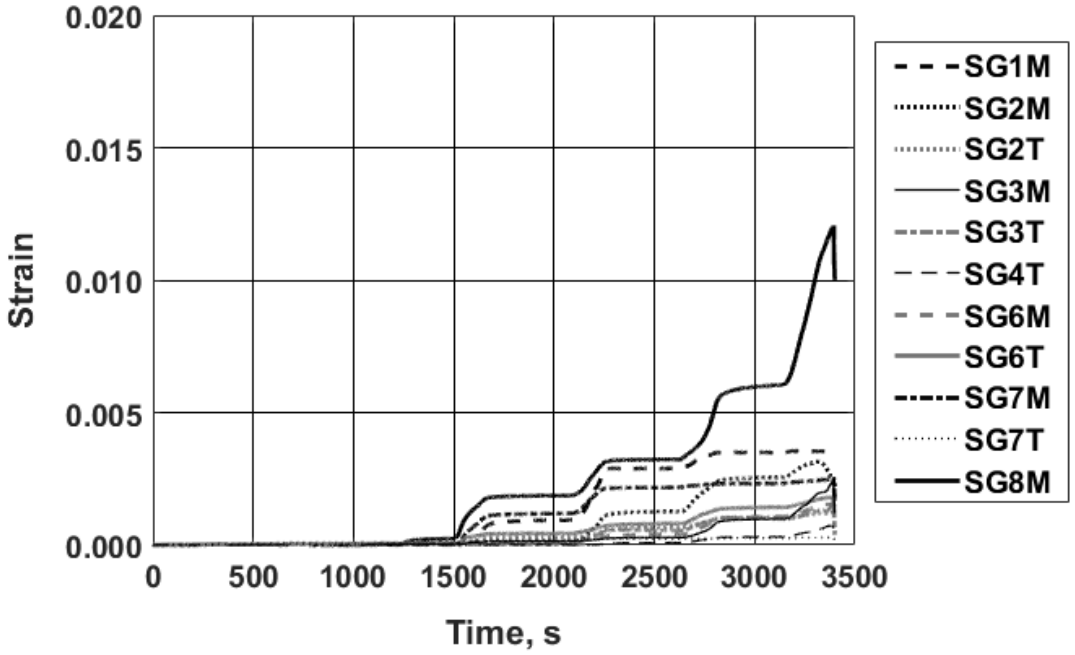

Figure H.36: Transverse reinforcing bar strain: specimen P1S12

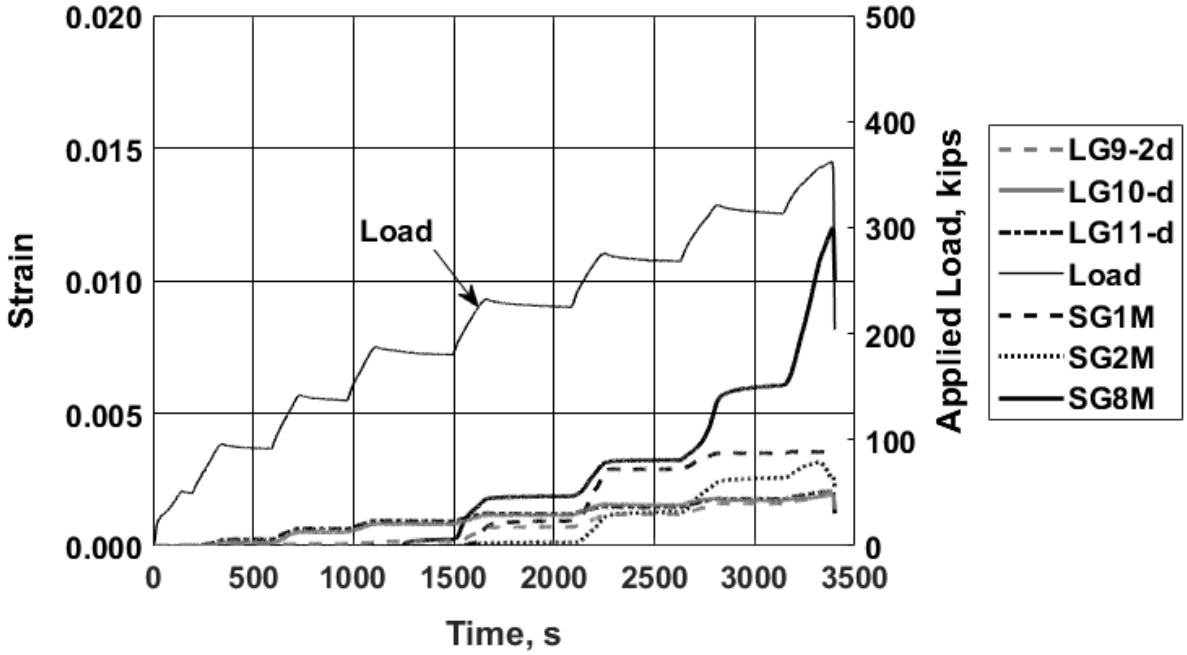

Figure H.37: Strain recorded with selected gauges and load versus time: specimen P1S12 [1 kip = 4.45 kN]

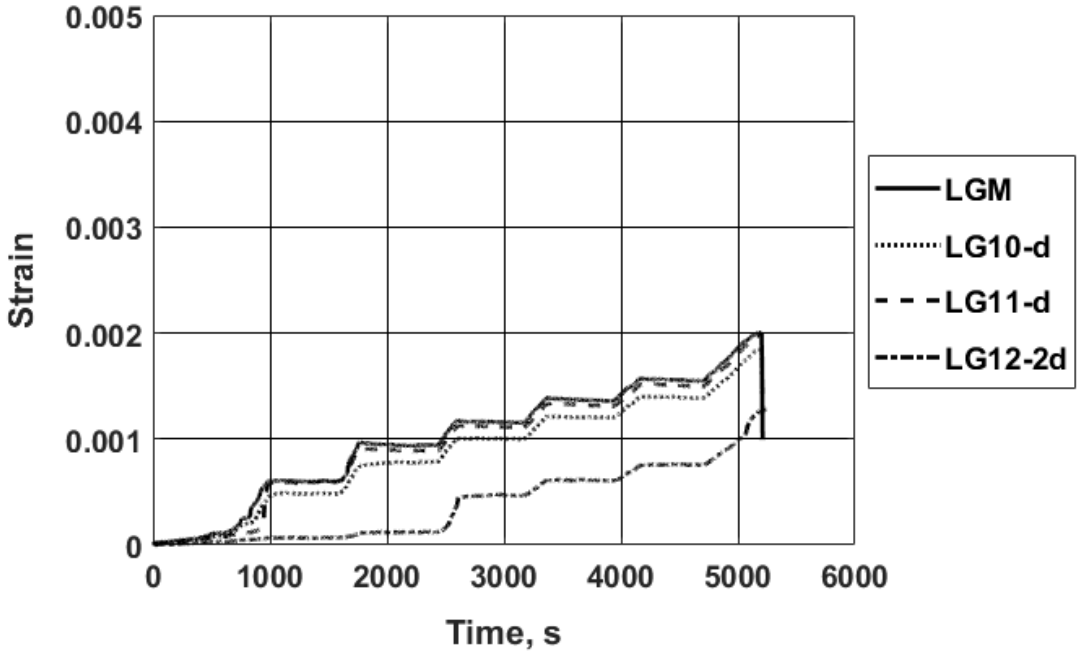

Figure H.38: Longitudinal reinforcing bar strain: specimen P1S13

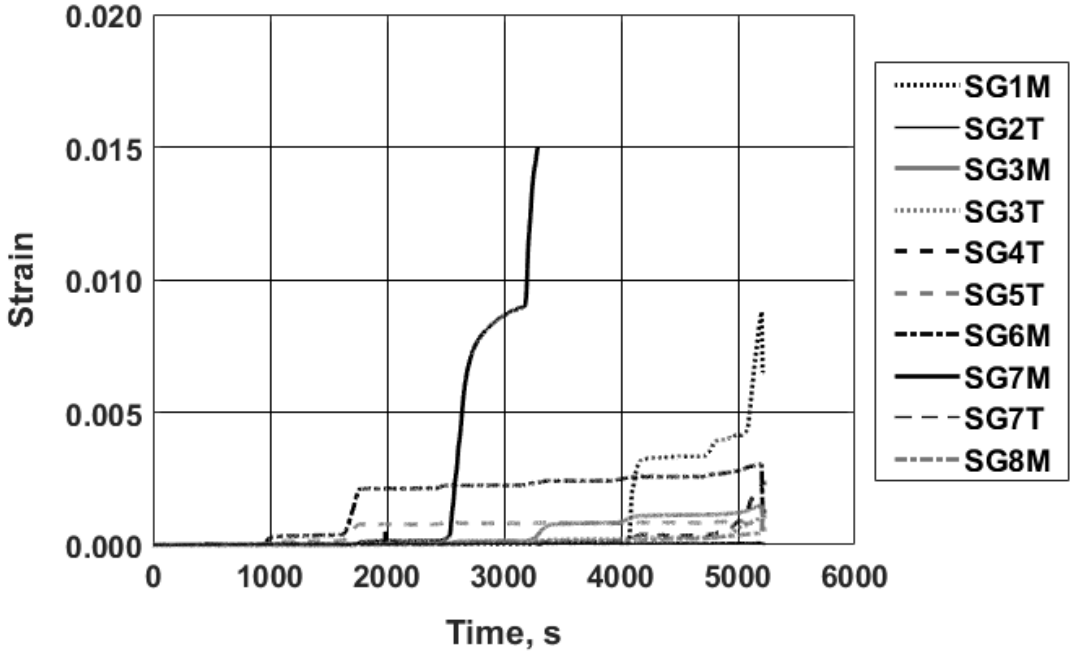

Figure H.39: Transverse reinforcing bar strain: specimen P1S13

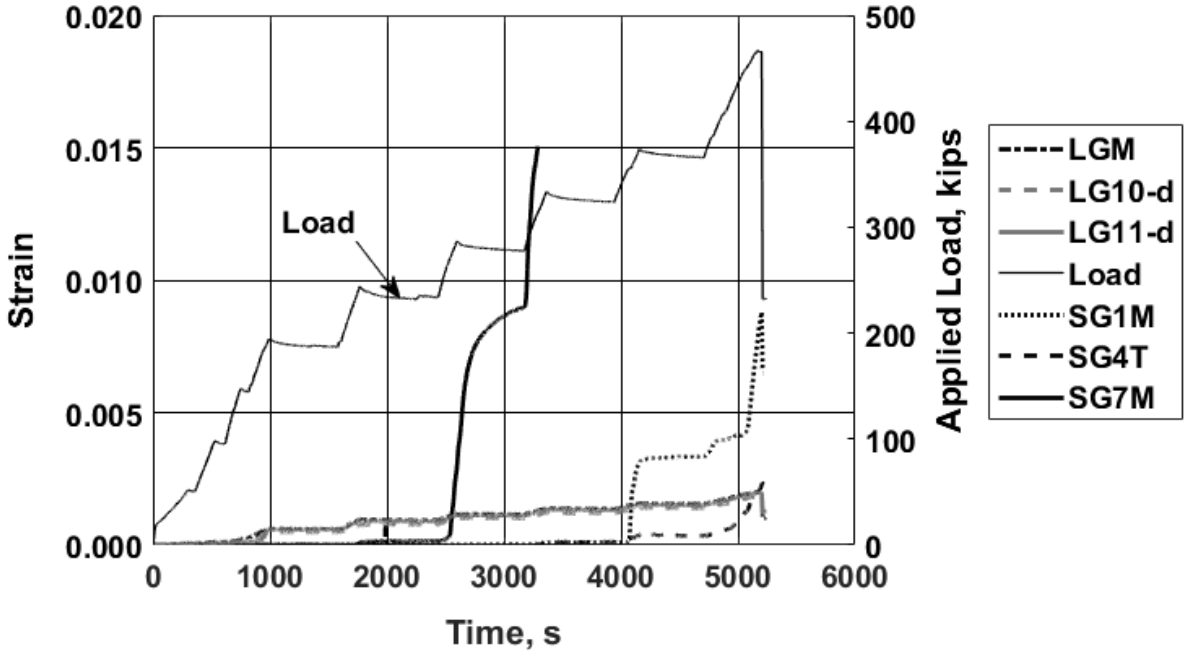

Figure H.40: Strain recorded with selected gauges and load versus time: specimen P1S13 [1 kip = 4.45 kN]

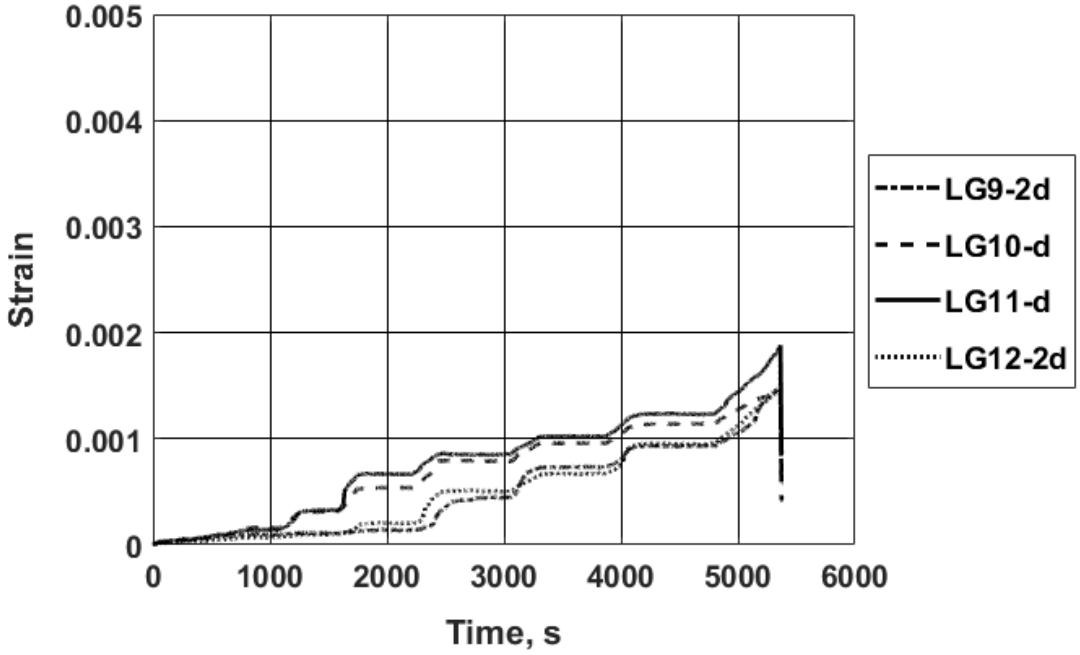

Figure H.41: Longitudinal reinforcing bar strain: specimen P1S14

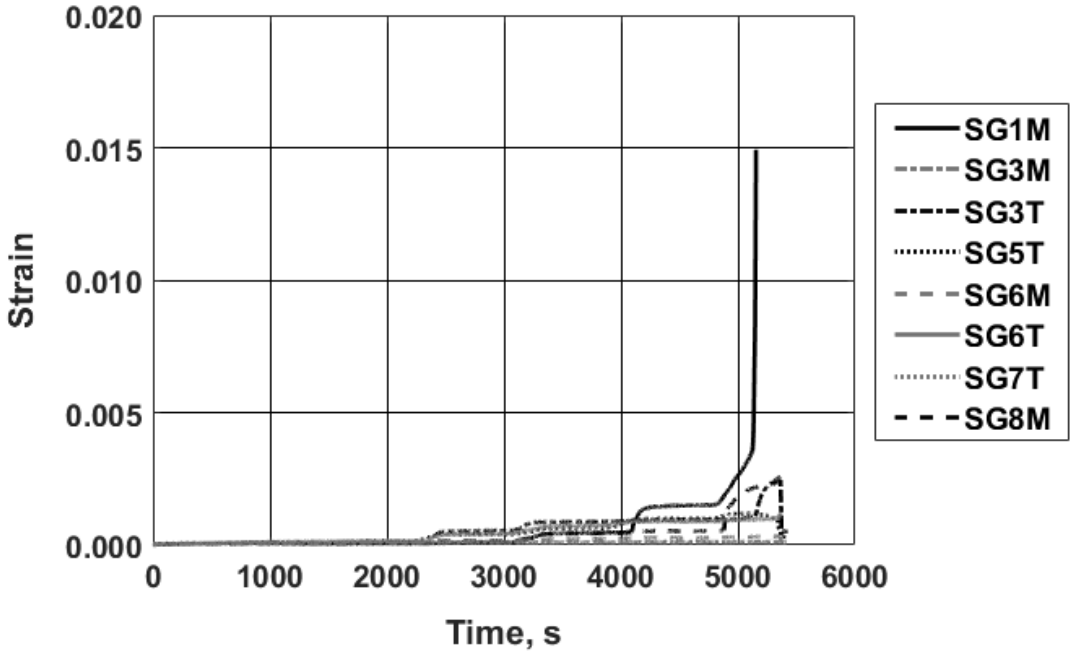

Figure H.42: Transverse reinforcing bar strain: specimen P1S14

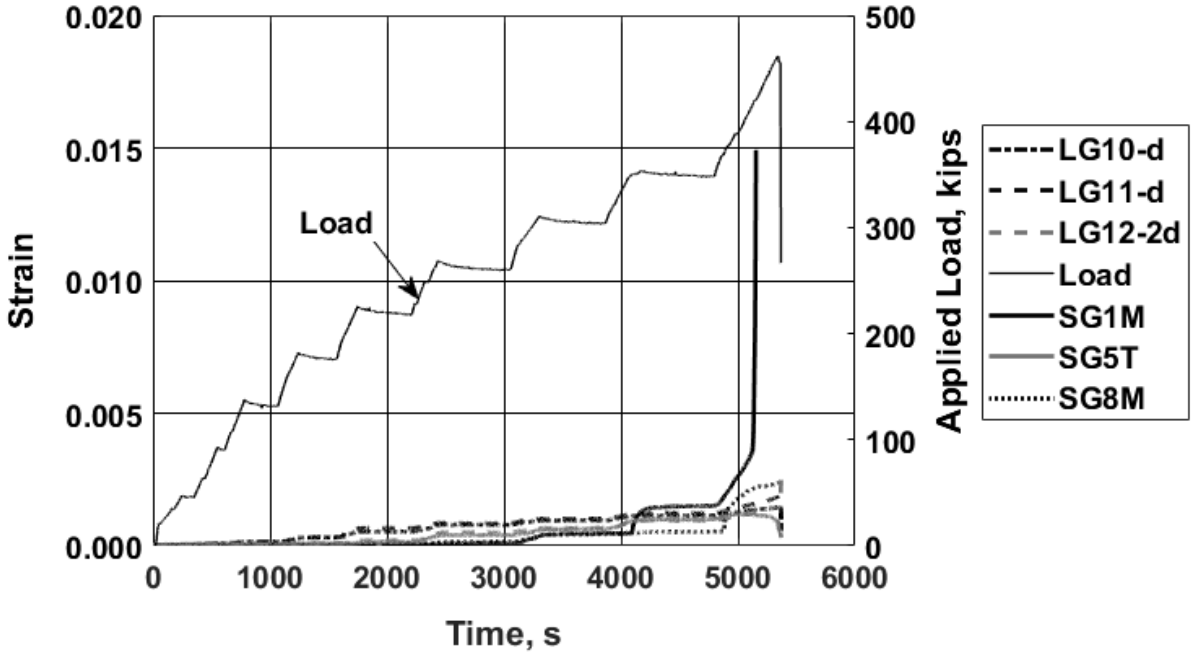

Figure H.43: Strain recorded with selected gauges and load versus time: specimen P1S14 [1 kip = 4.45 kN]

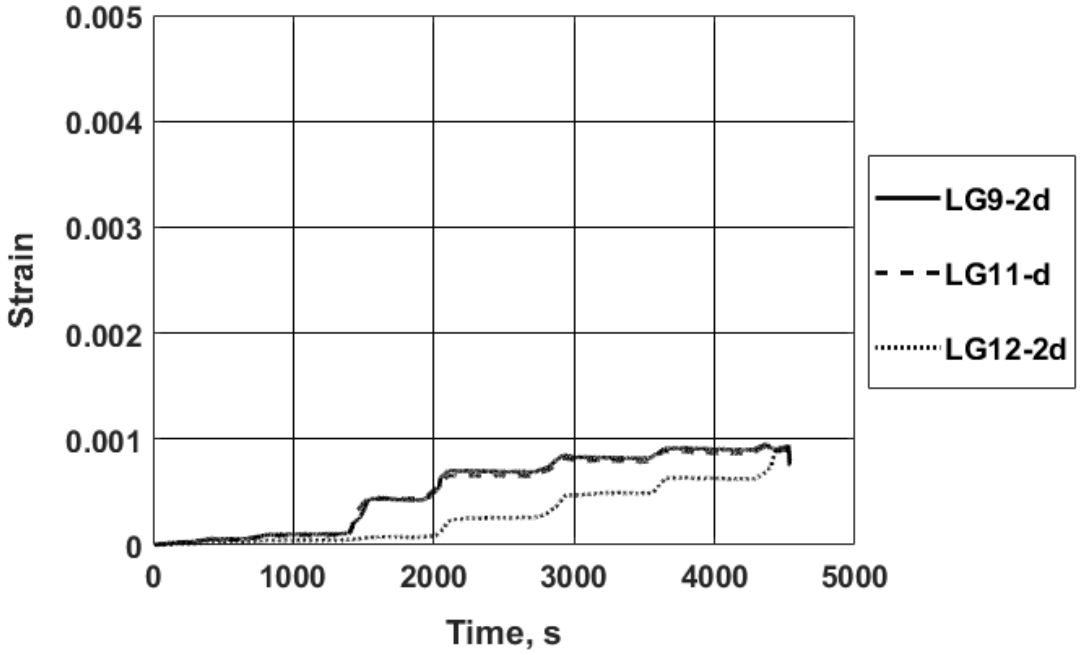

Figure H.44: Longitudinal reinforcing bar strain: specimen P1S15

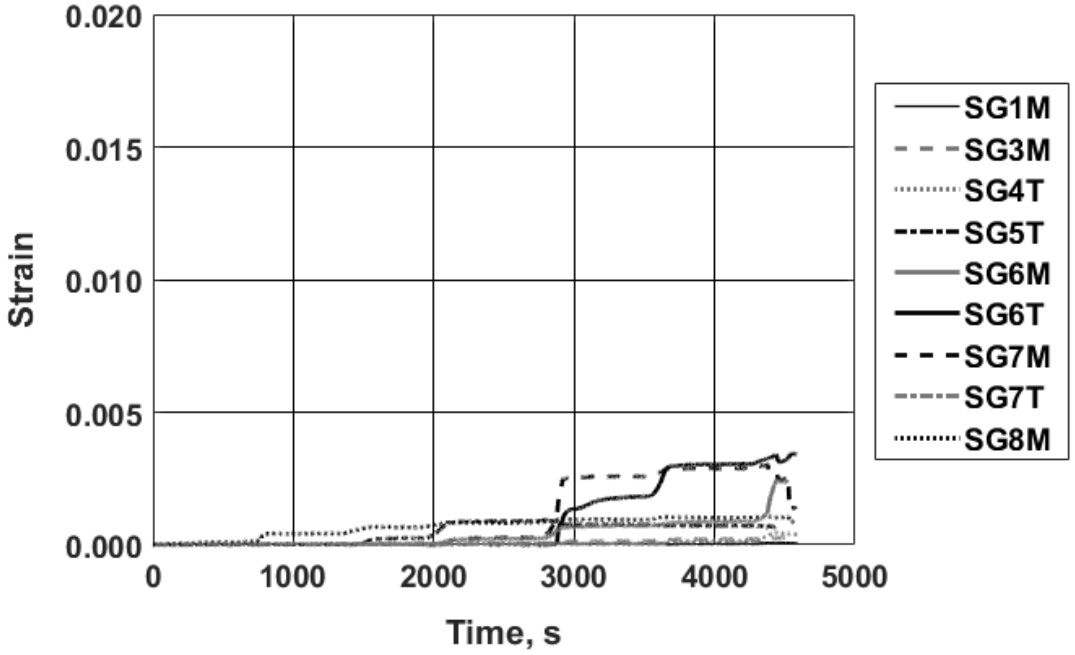

Figure H.45: Transverse reinforcing bar strain: specimen P1S15

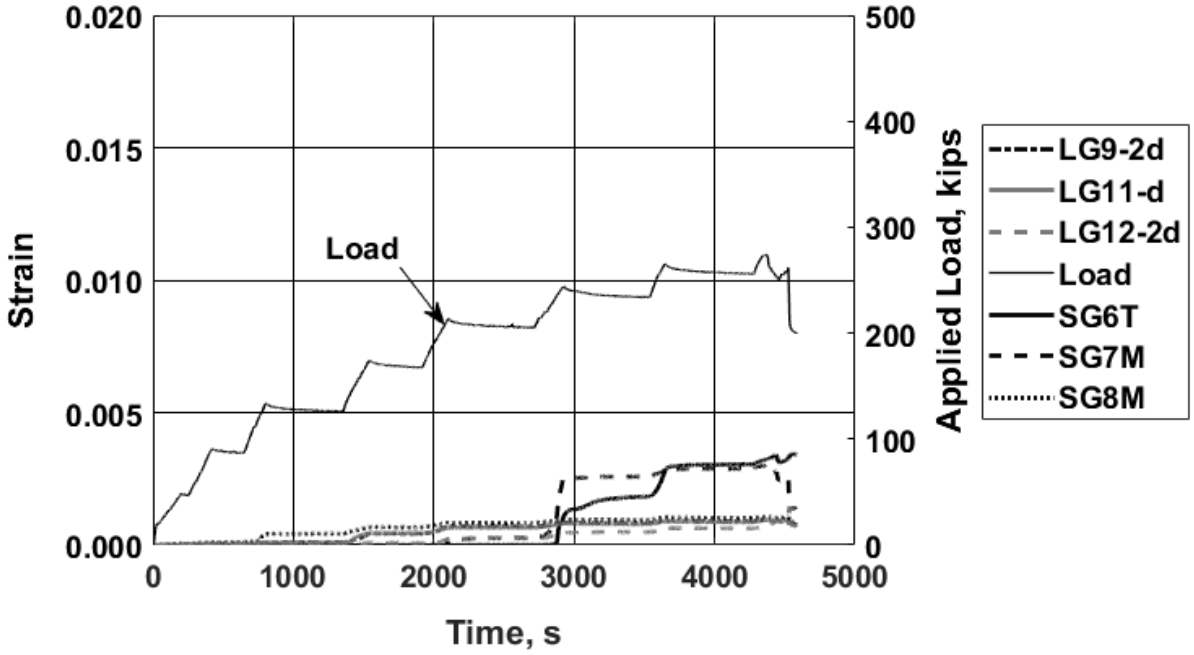

Figure H.46: Strain recorded with selected gauges and load versus time: specimen P1S15 [1 kip = 4.45 kN]

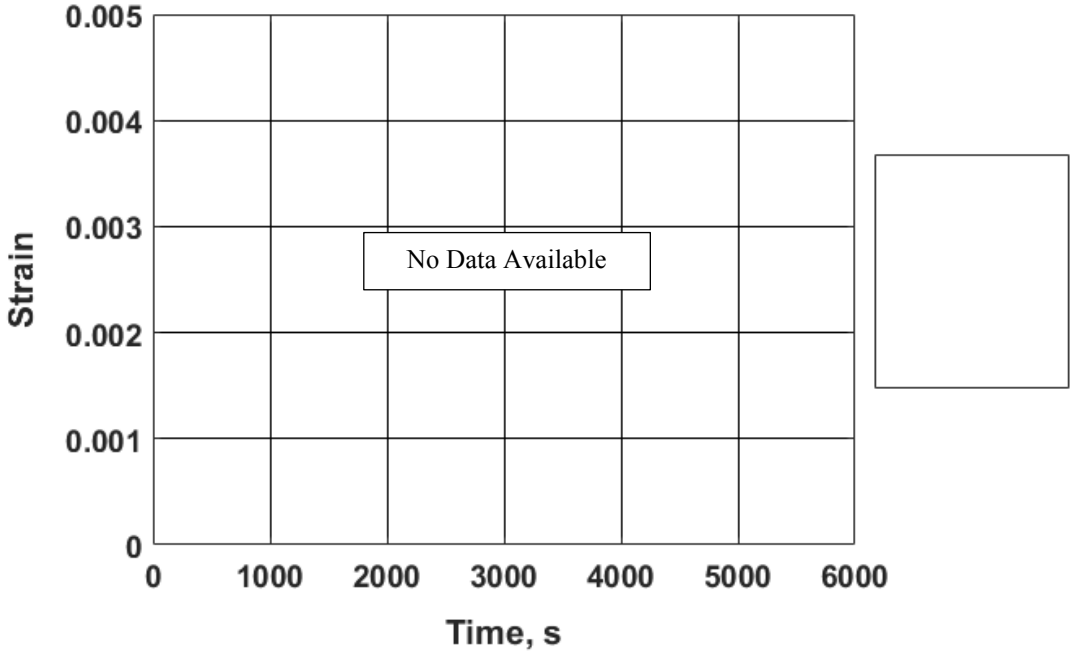

Figure H.47: Longitudinal reinforcing bar strain: specimen P1S16

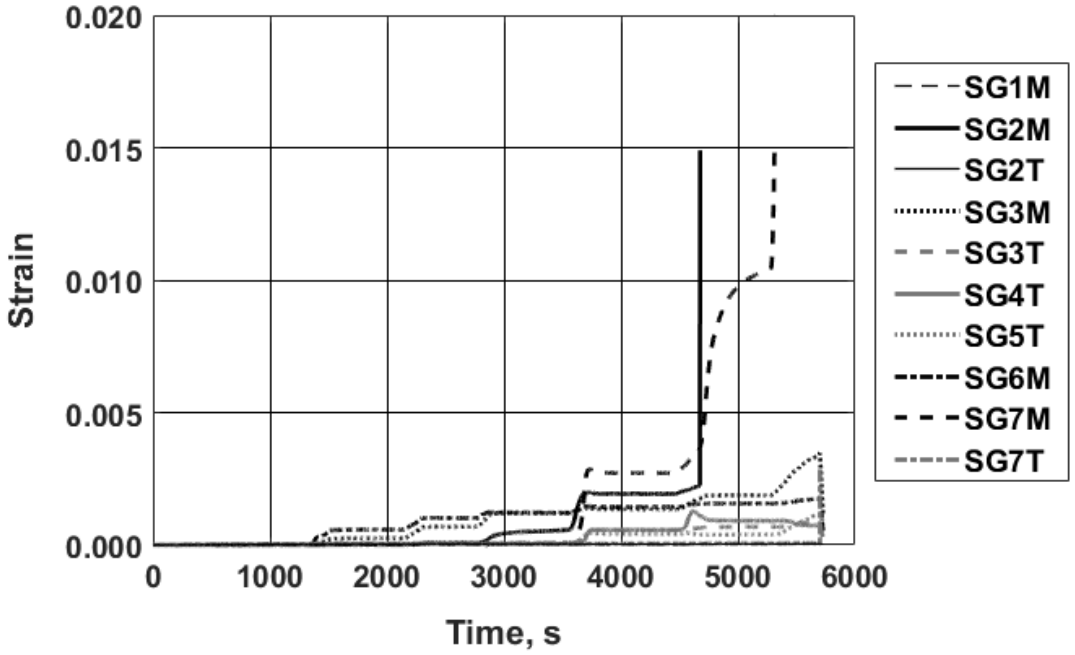

Figure H.48: Transverse reinforcing bar strain: specimen P1S16

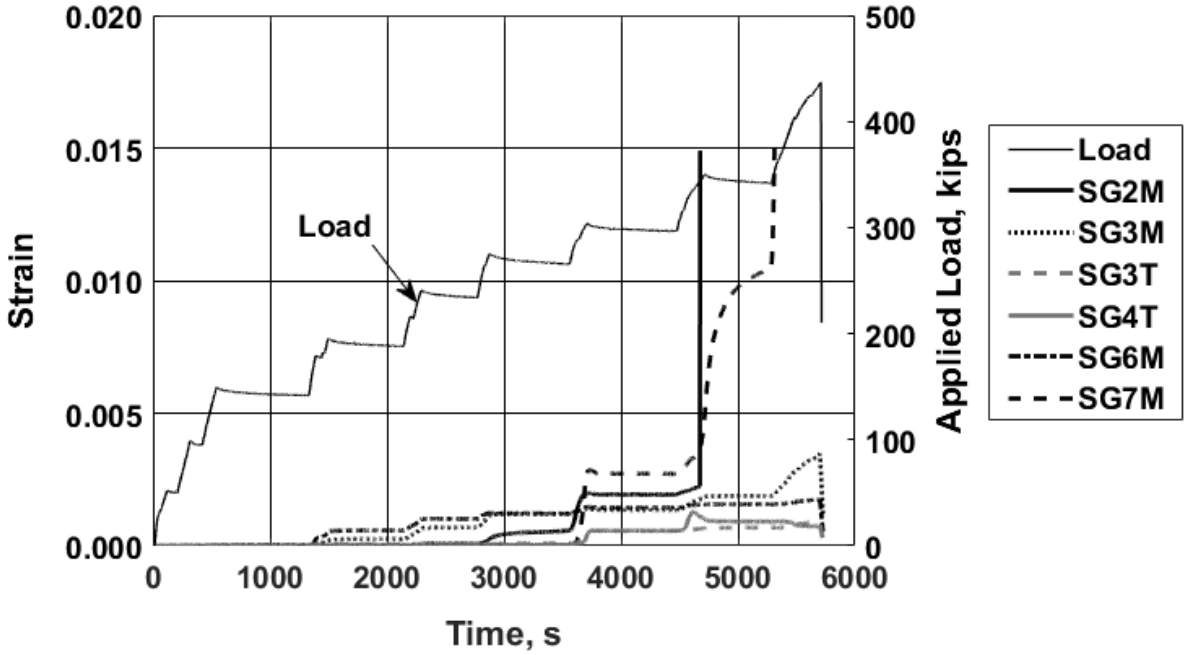

Figure H.49: Strain recorded with selected gauges and load versus time: specimen P1S16 [1 kip = 4.45 kN]

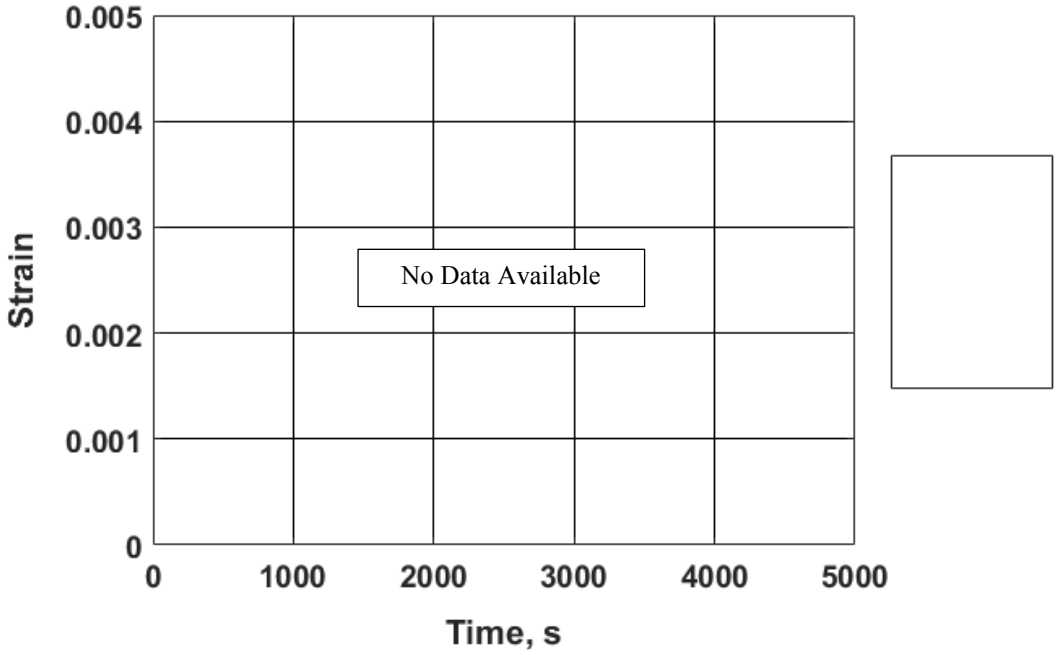

Figure H.50: Longitudinal reinforcing bar strain: specimen P1S17

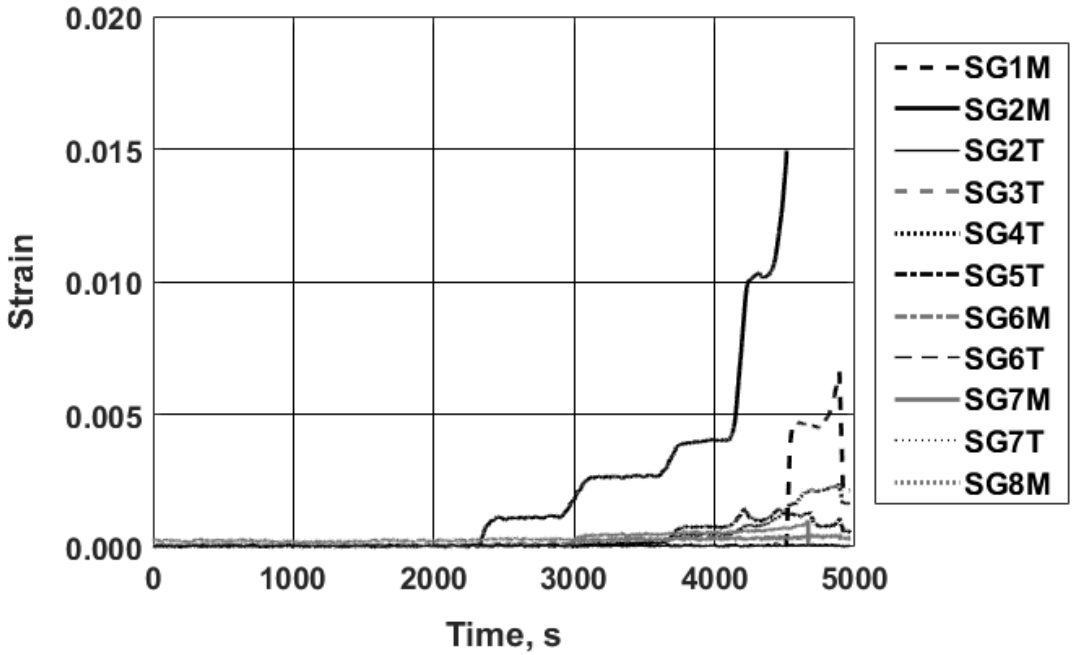

Figure H.51: Transverse reinforcing bar strain: specimen P1S17

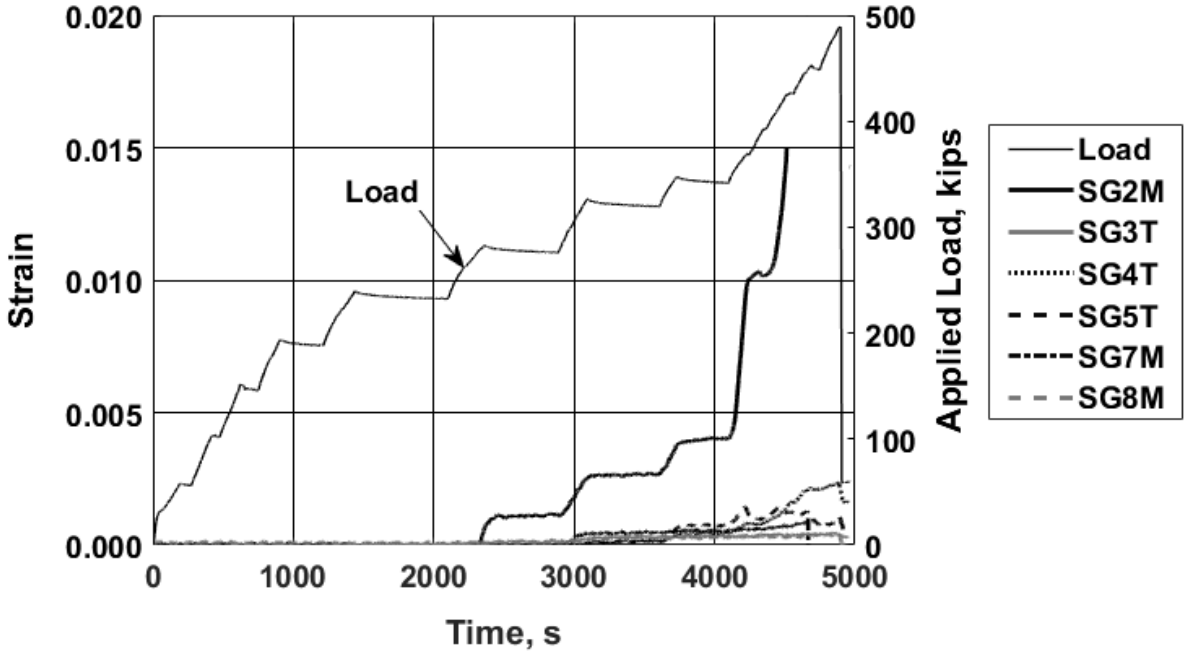

Figure H.52: Strain recorded with selected gauges and load versus time: specimen P1S17 [1 kip = 4.45 kN]

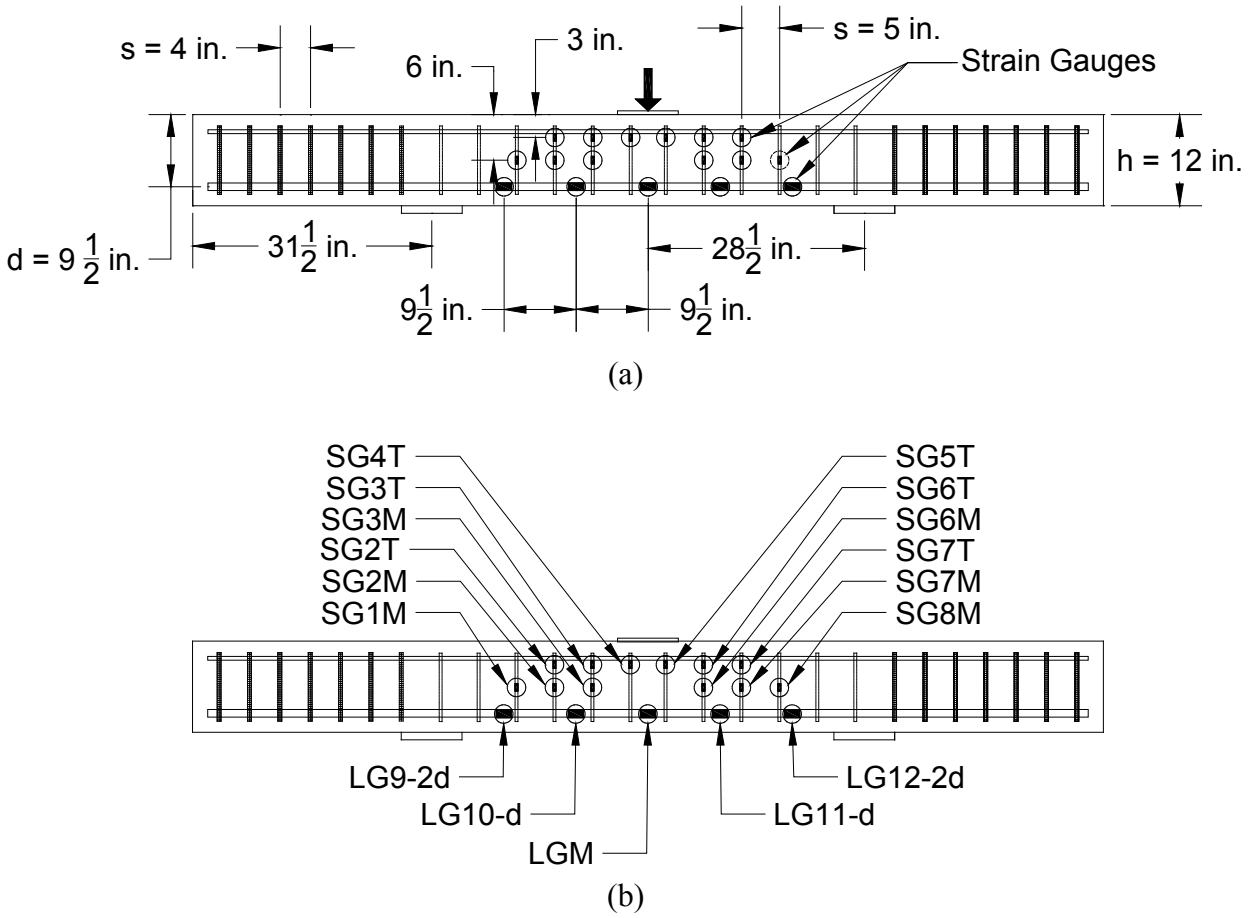

Figure H.53: Specimens P2S1 and P2S2: Strain gauge (a) locations and (b) naming convention [1 in. = 25.4 mm]

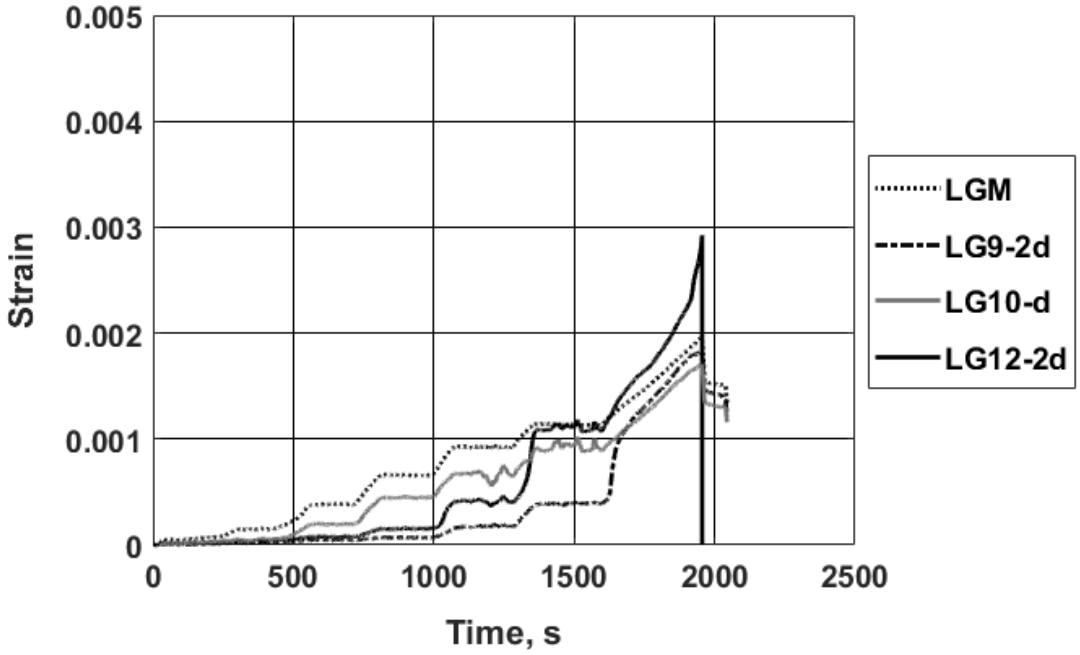

Figure H.54: Longitudinal reinforcing bar strain: specimen P2S1

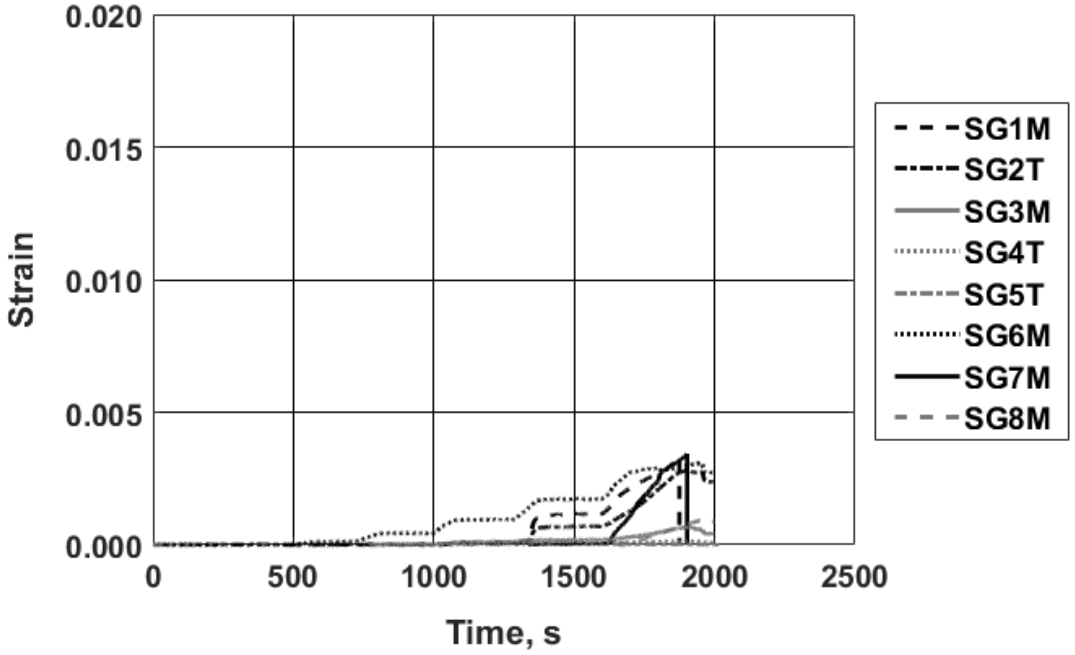

Figure H.55: Transverse reinforcing bar strain: specimen P2S1

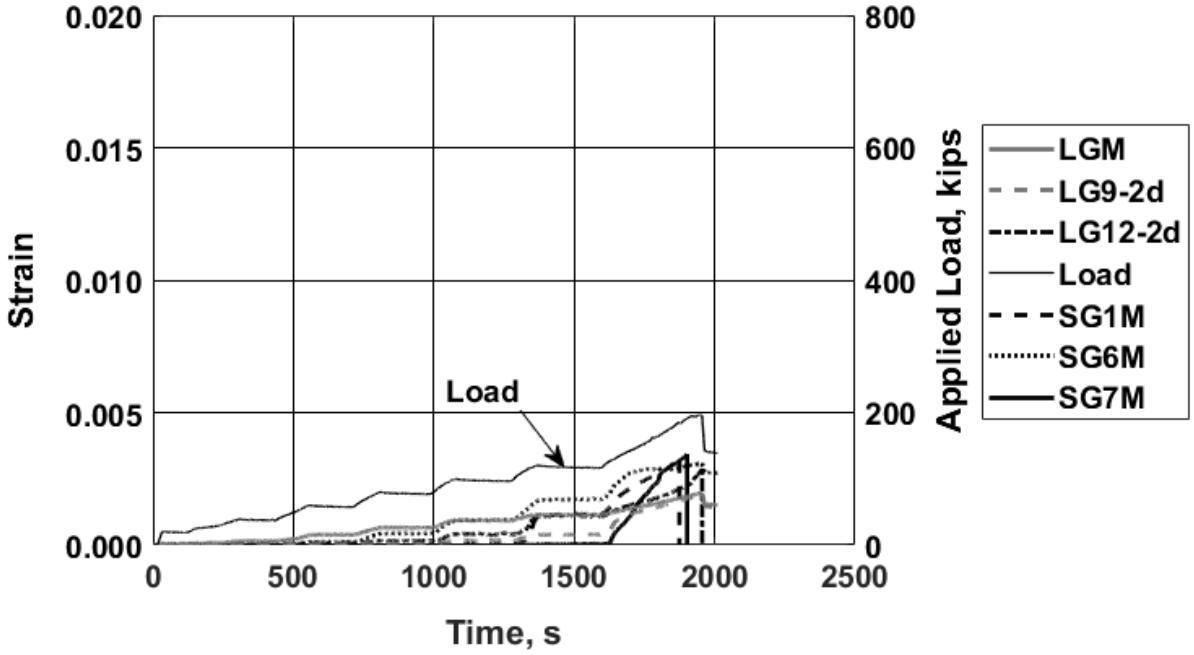

Figure H.56: Strain recorded with selected gauges and load versus time: specimen P2S1 [1 kip = 4.45 kN]

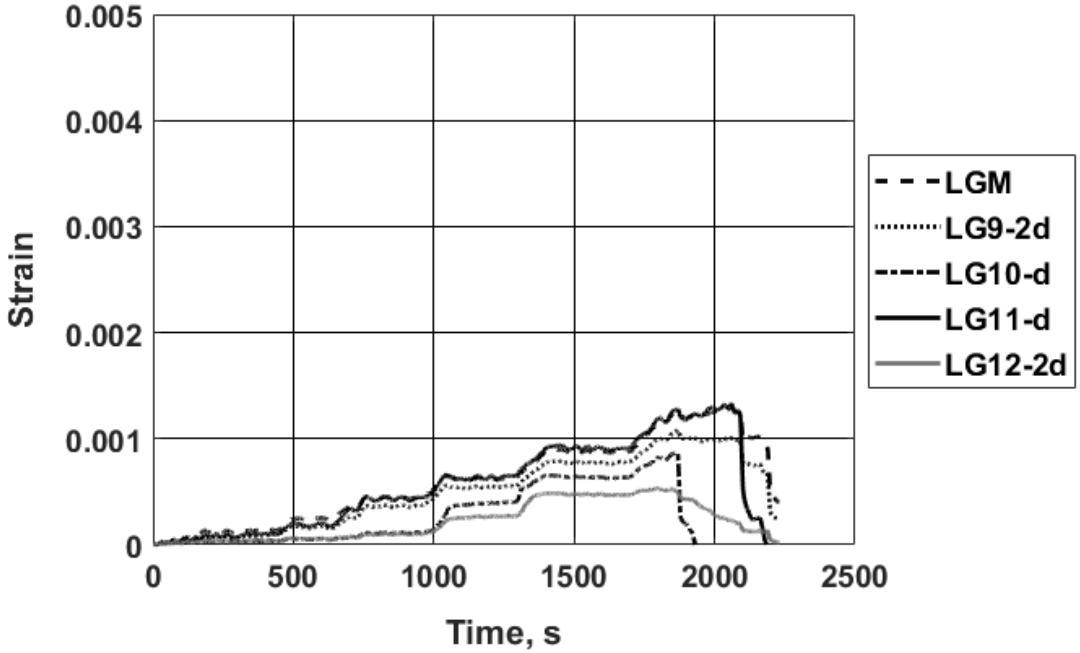

Figure H.57: Longitudinal reinforcing bar strain: specimen P2S2

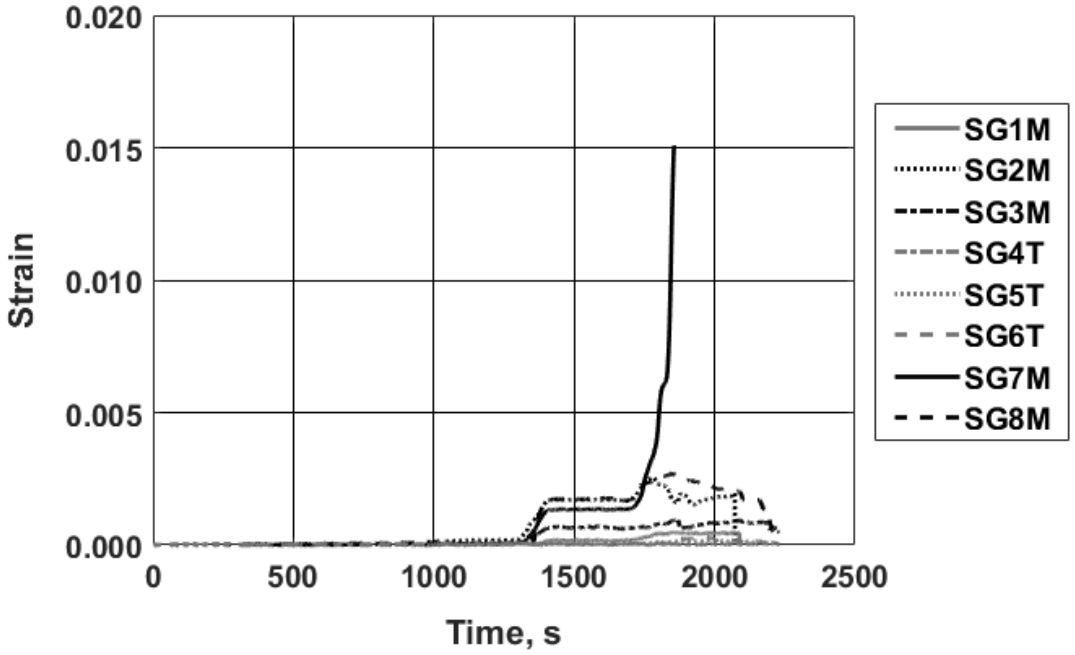

Figure H.58: Transverse reinforcing bar strain: specimen P2S2

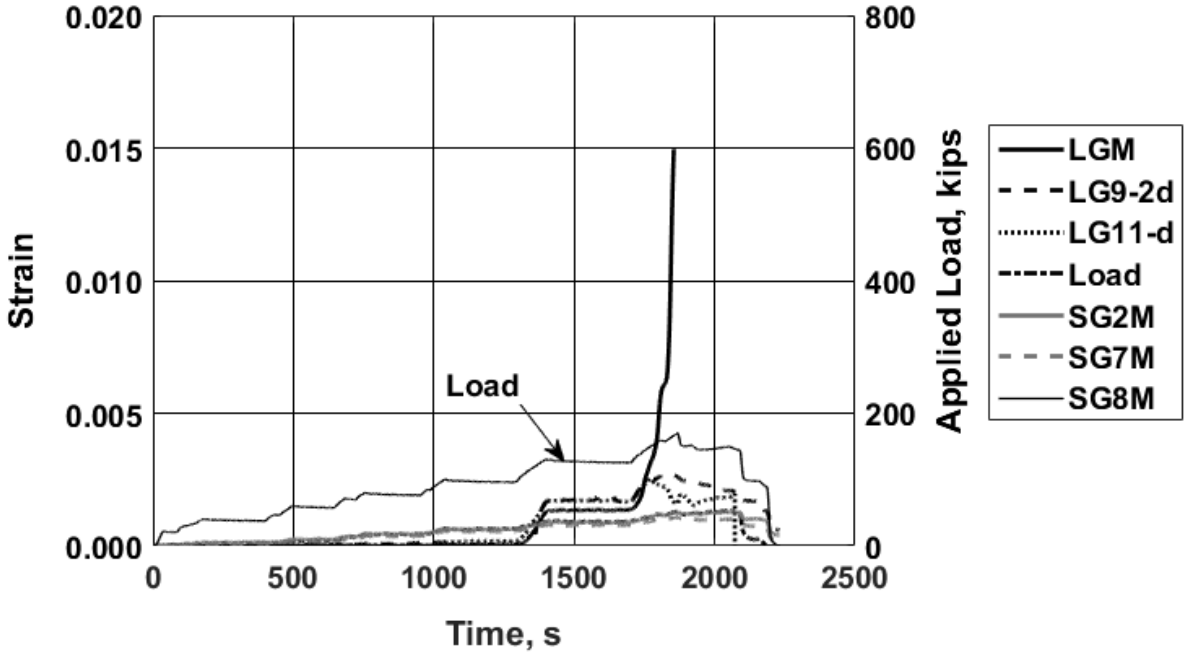

Figure H.59: Strain recorded with selected gauges and load versus time: specimen P2S2 [1 kip = 4.45 kN]

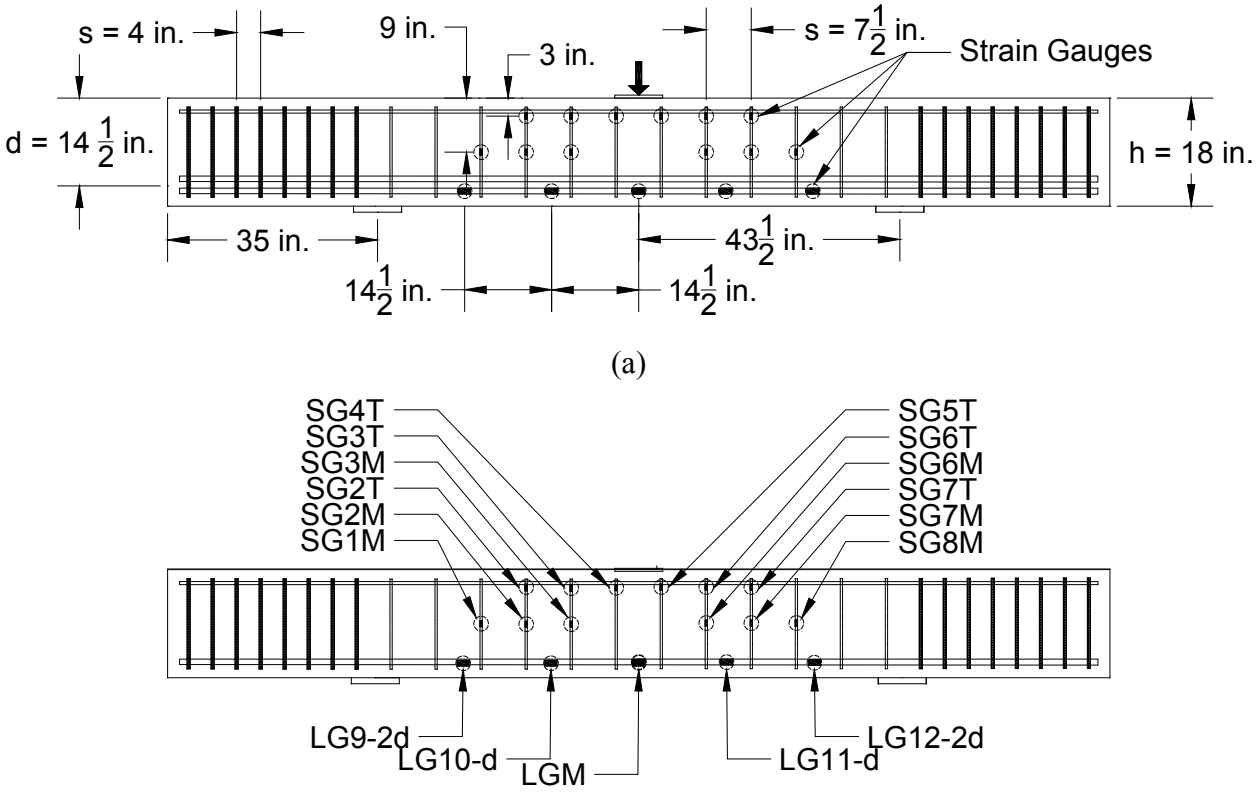

Figure H.60: Specimens P2S3 and P2S4: Strain gauge (a) locations and (b) naming convention [1 in. = 25.4 mm]

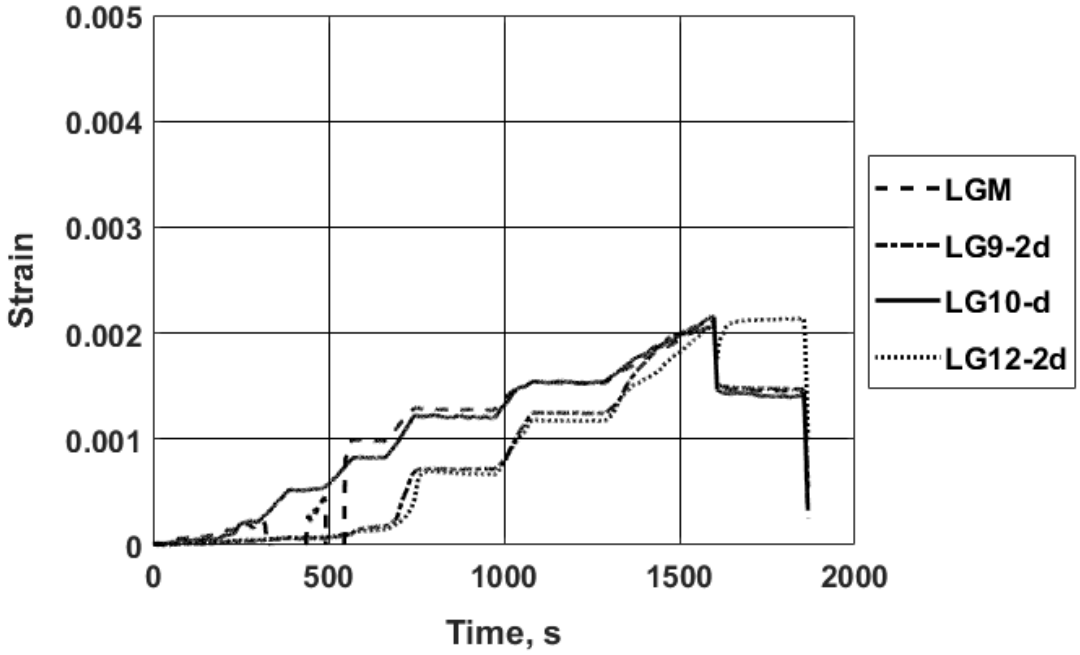

Figure H.61: Longitudinal reinforcing bar strain: specimen P2S3

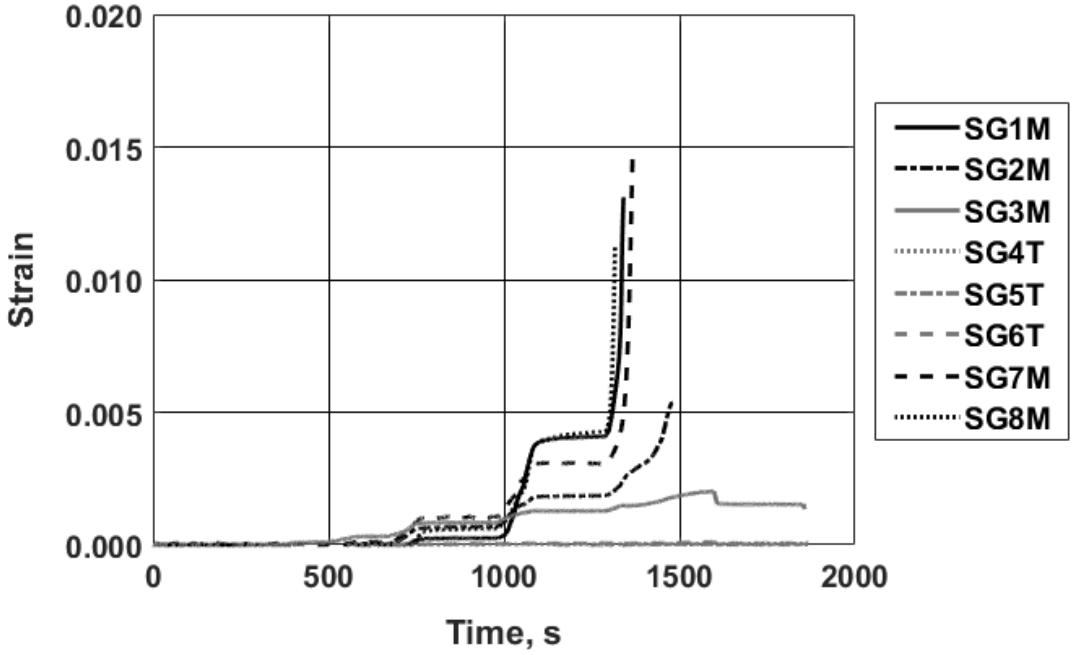

Figure H.62: Transverse reinforcing bar strain: specimen P2S3

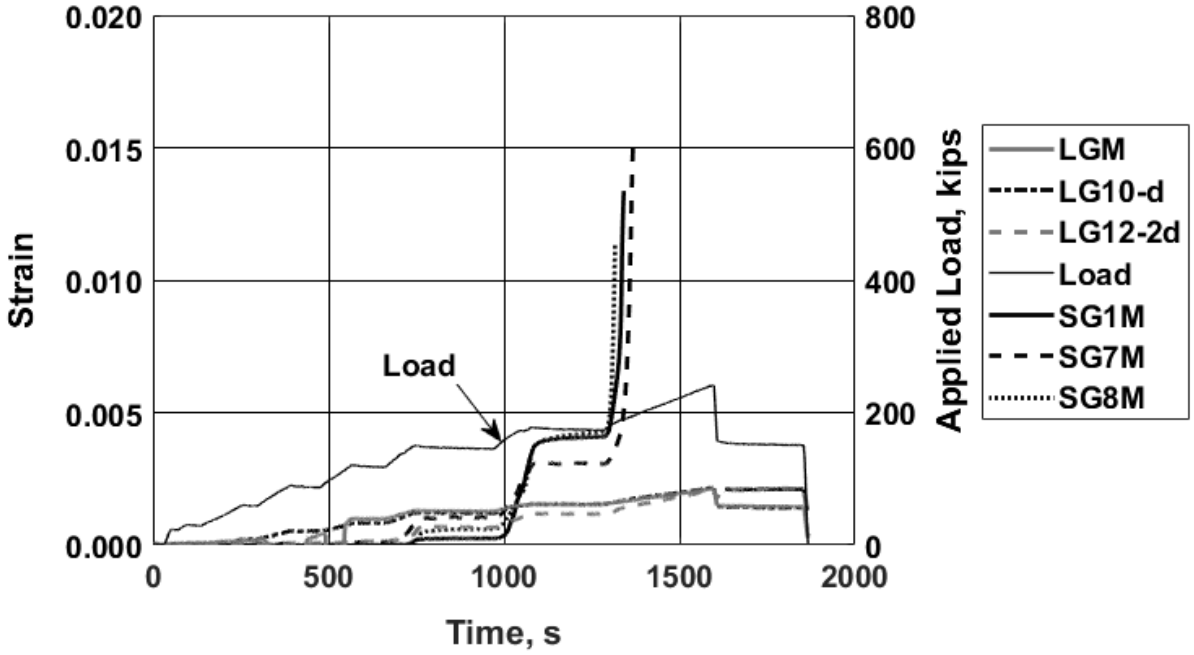

Figure H.63: Strain recorded with selected gauges and load versus time: specimen P2S3 [1 kip = 4.45 kN]

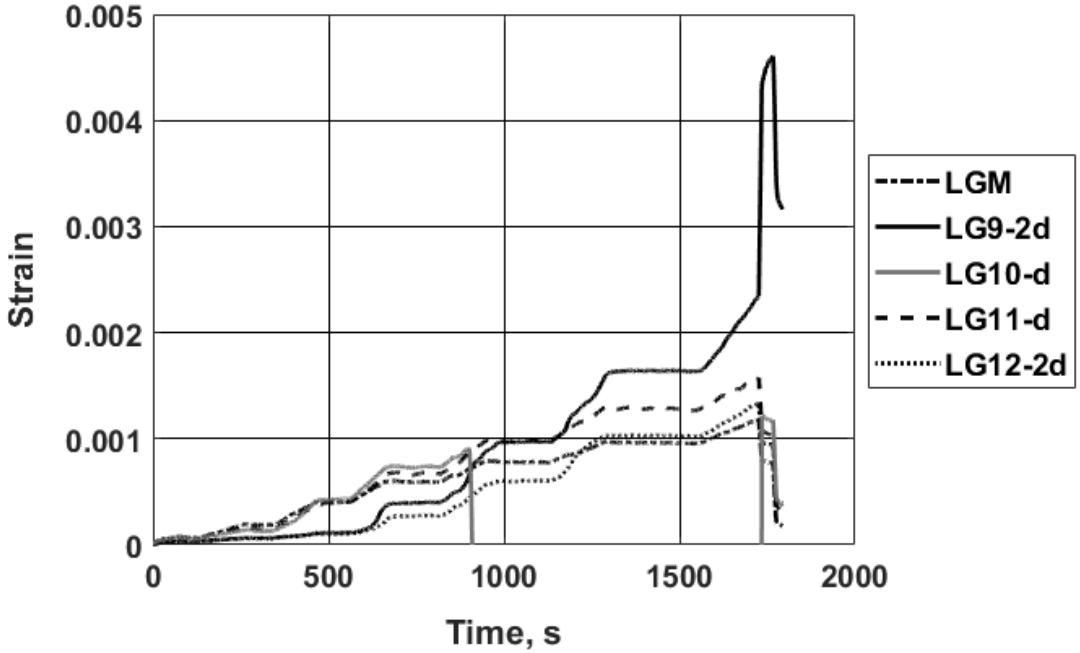

Figure H.64: Longitudinal reinforcing bar strain: specimen P2S4

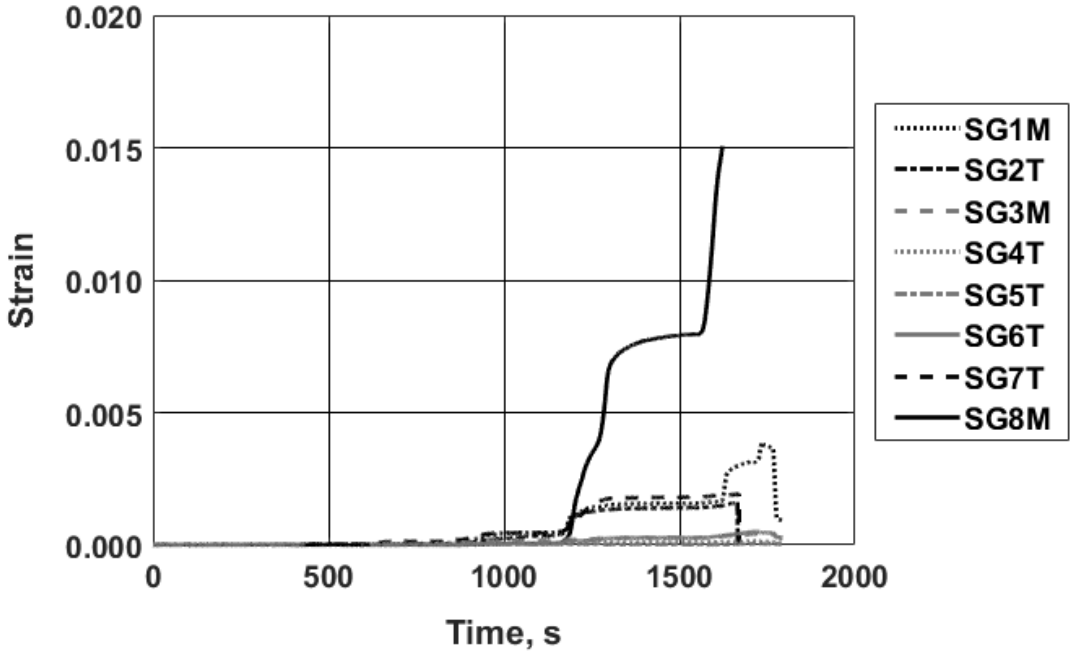

Figure H.65: Transverse reinforcing bar strain: specimen P2S4

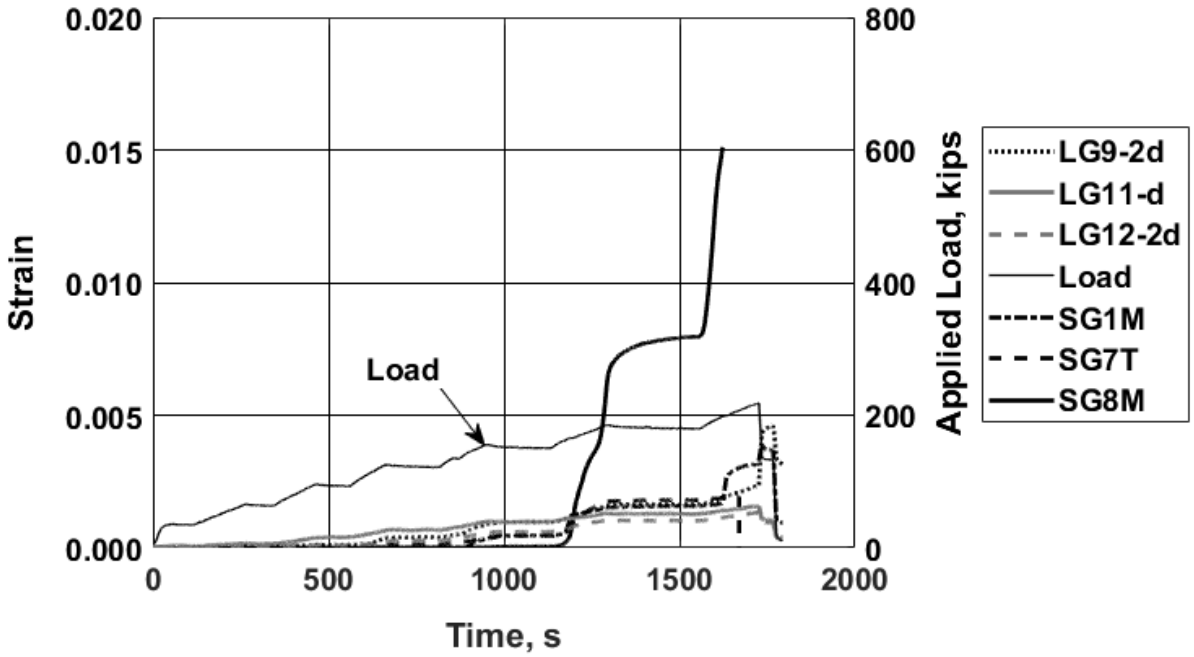

Figure H.66: Strain recorded with selected gauges and load versus time: specimen P2S4 [1 kip = 4.45 kN]

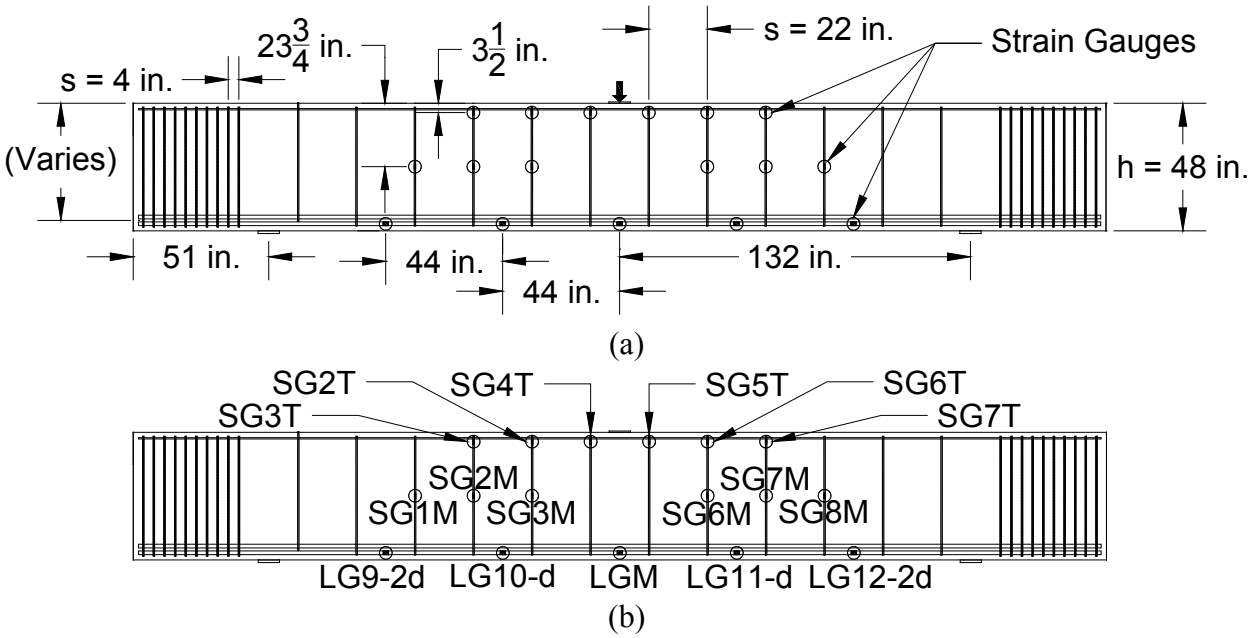

Figure H.67: Specimens P2S5 through P2S10: Strain gauge (a) locations and (b) naming convention [1 in. = 25.4 mm]

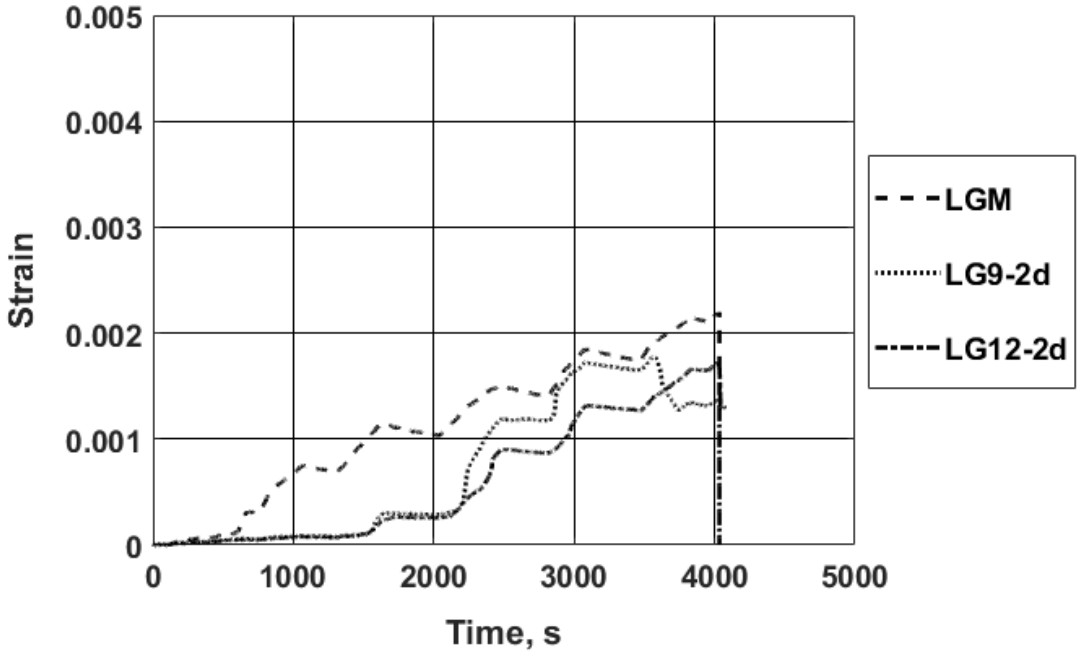

Figure H.68: Longitudinal reinforcing bar strain: specimen P2S5

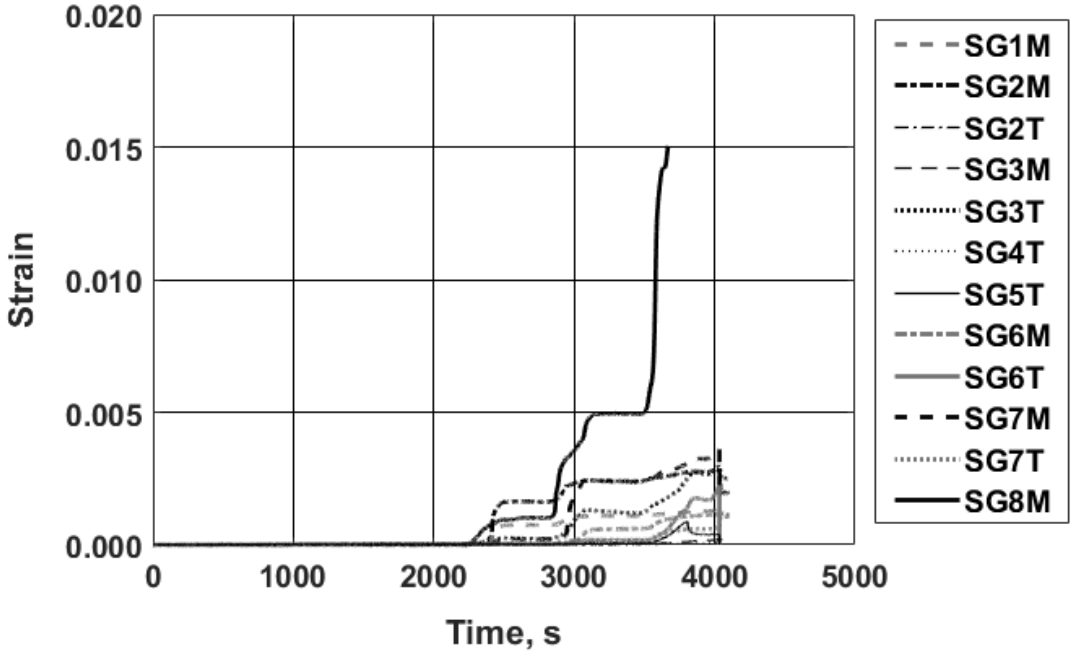

Figure H.69: Transverse reinforcing bar strain: specimen P2S5

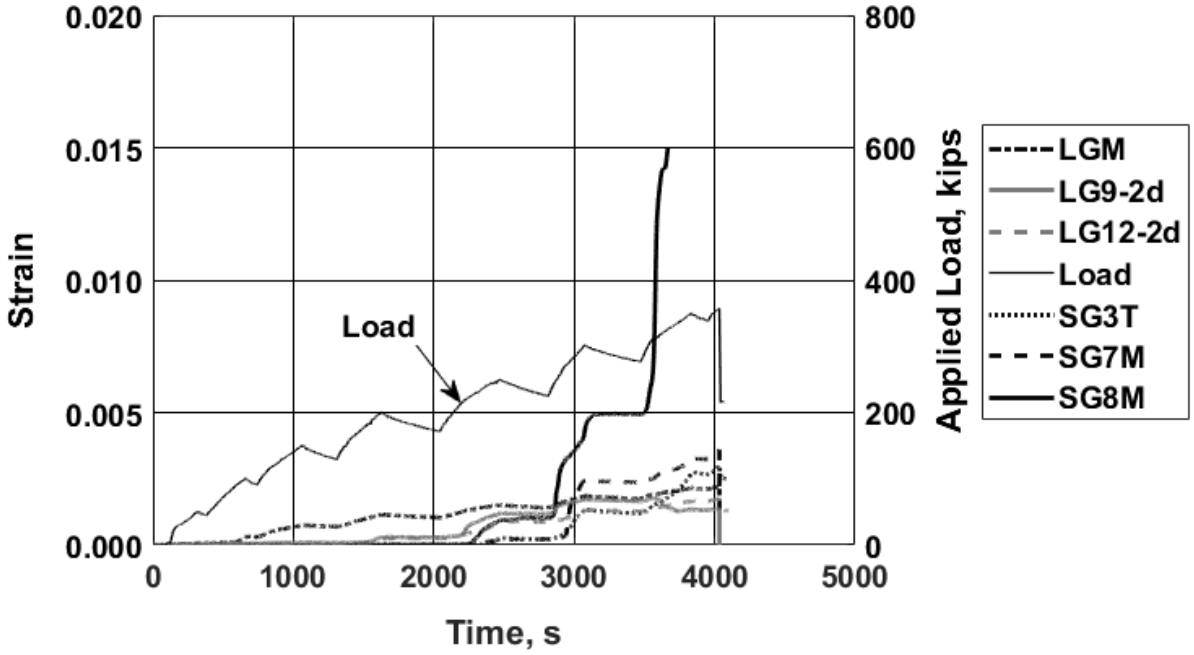

Figure H.70: Strain recorded with selected gauges and load versus time: specimen P2S5 [1 kip = 4.45 kN]

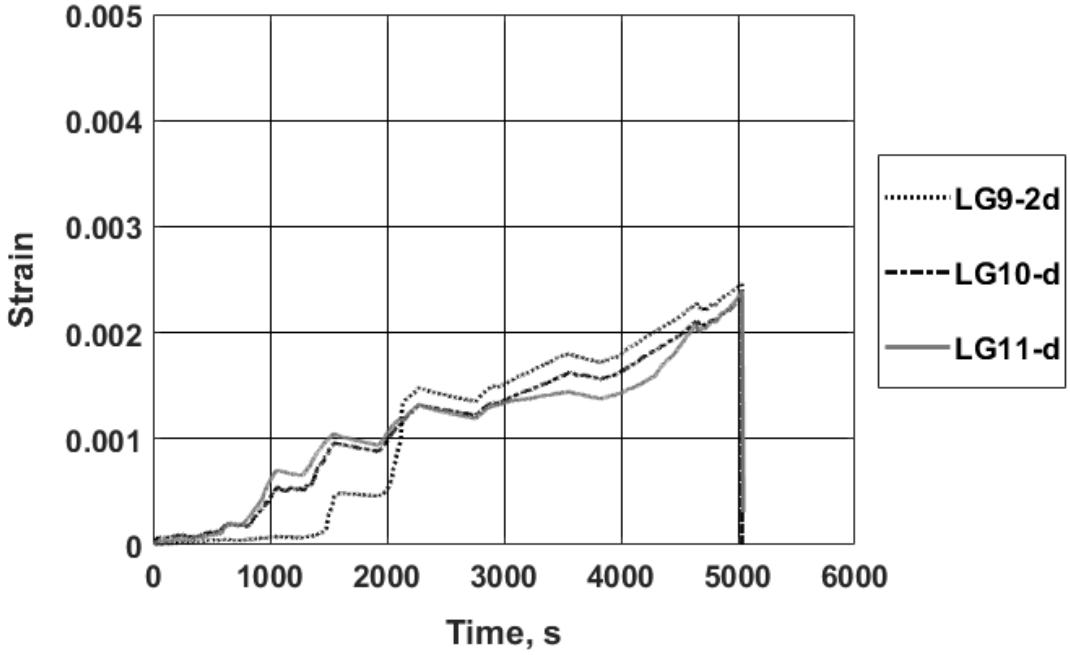

Figure H.71: Longitudinal reinforcing bar strain: specimen P2S6

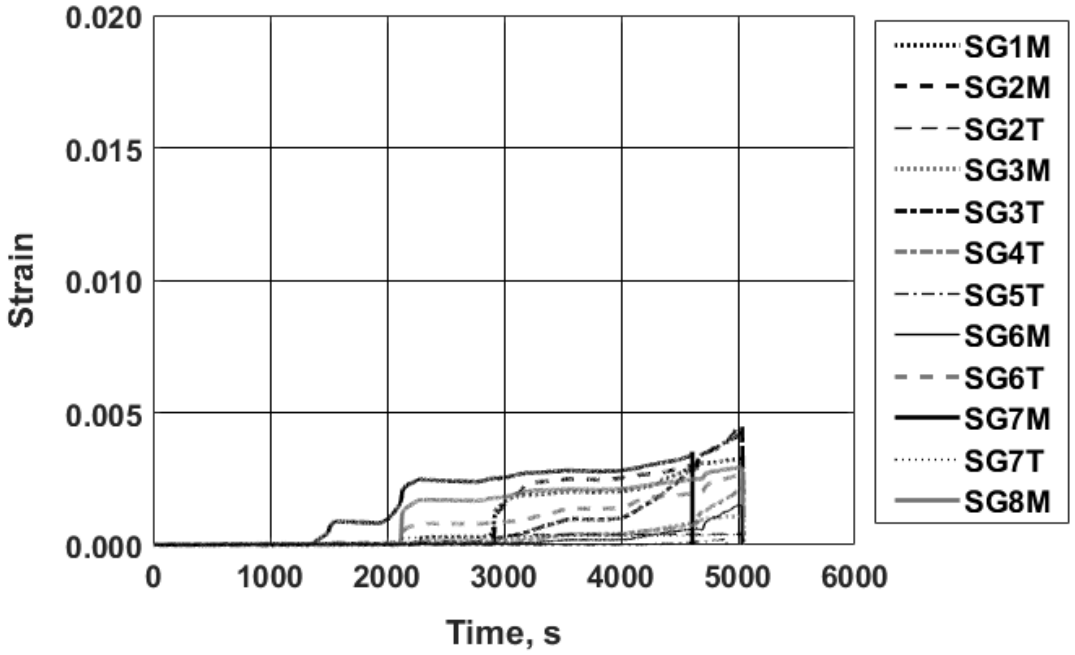

Figure H.72: Transverse reinforcing bar strain: specimen P2S6

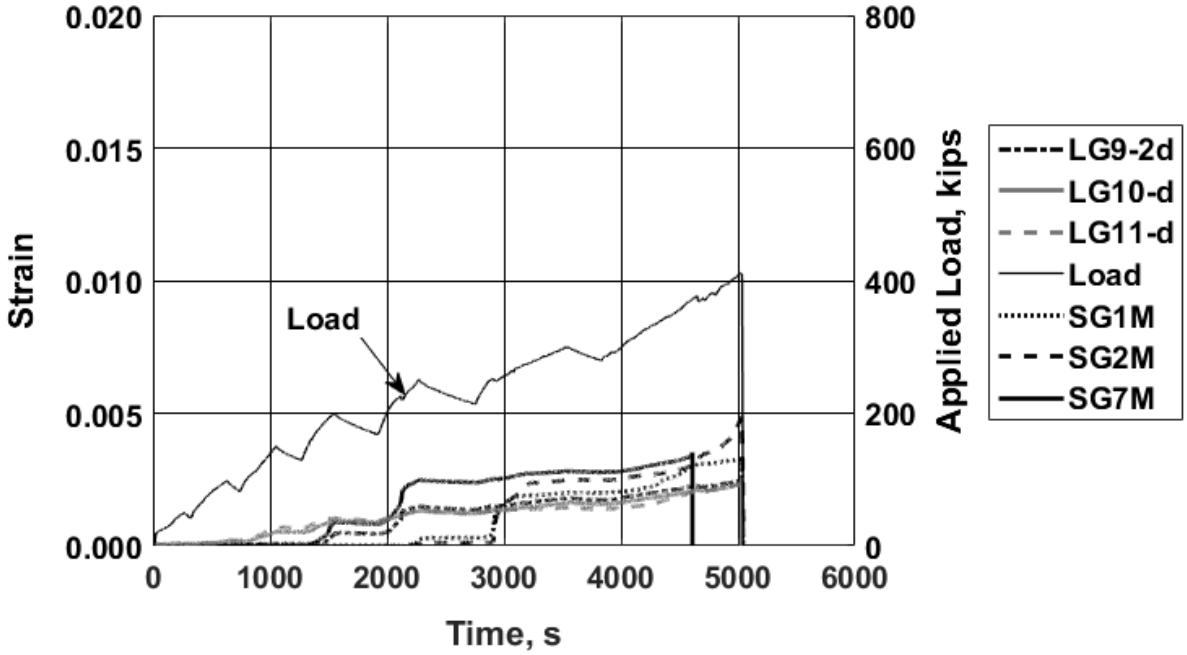

Figure H.73: Strain recorded with selected gauges and load versus time: specimen P2S6 [1 kip = 4.45 kN]

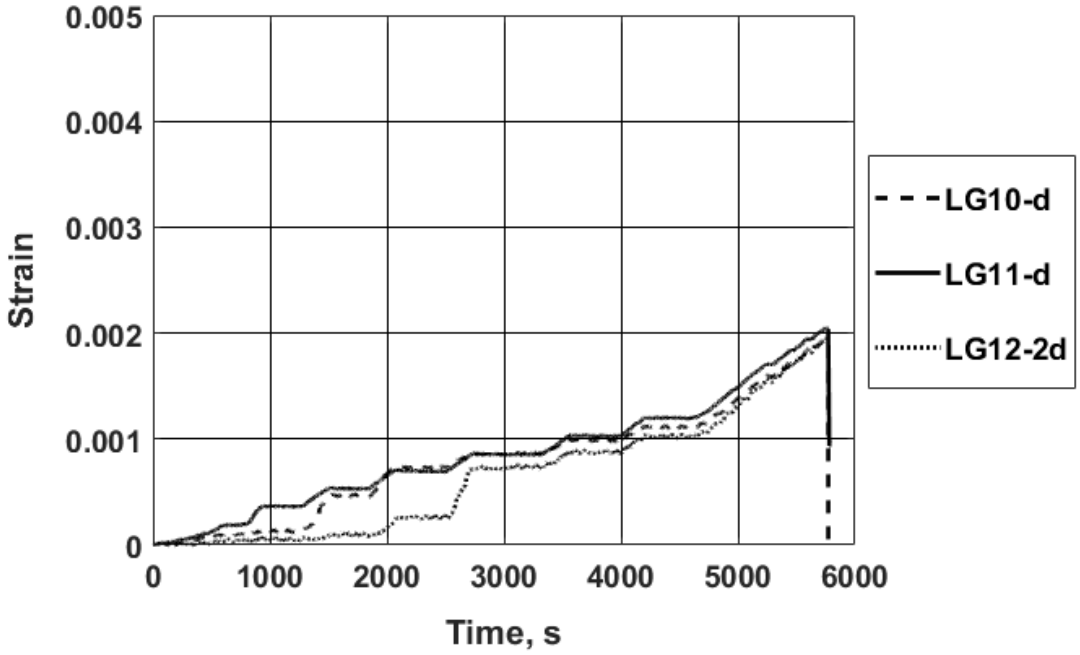

Figure H.74: Longitudinal reinforcing bar strain: specimen P2S7

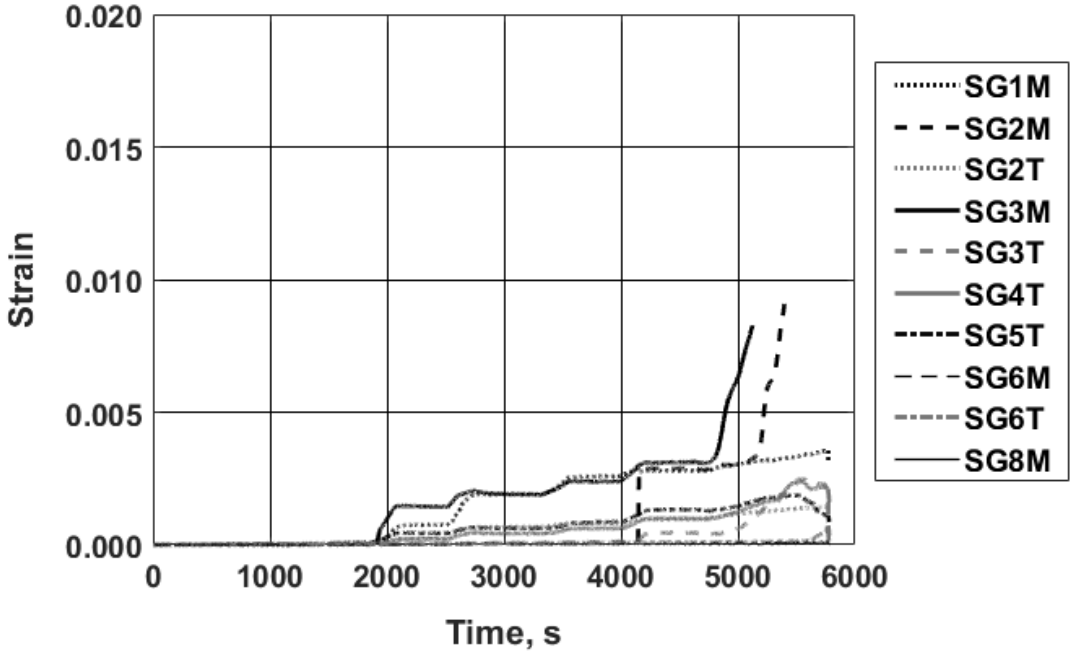

Figure H.75: Transverse reinforcing bar strain: specimen P2S7

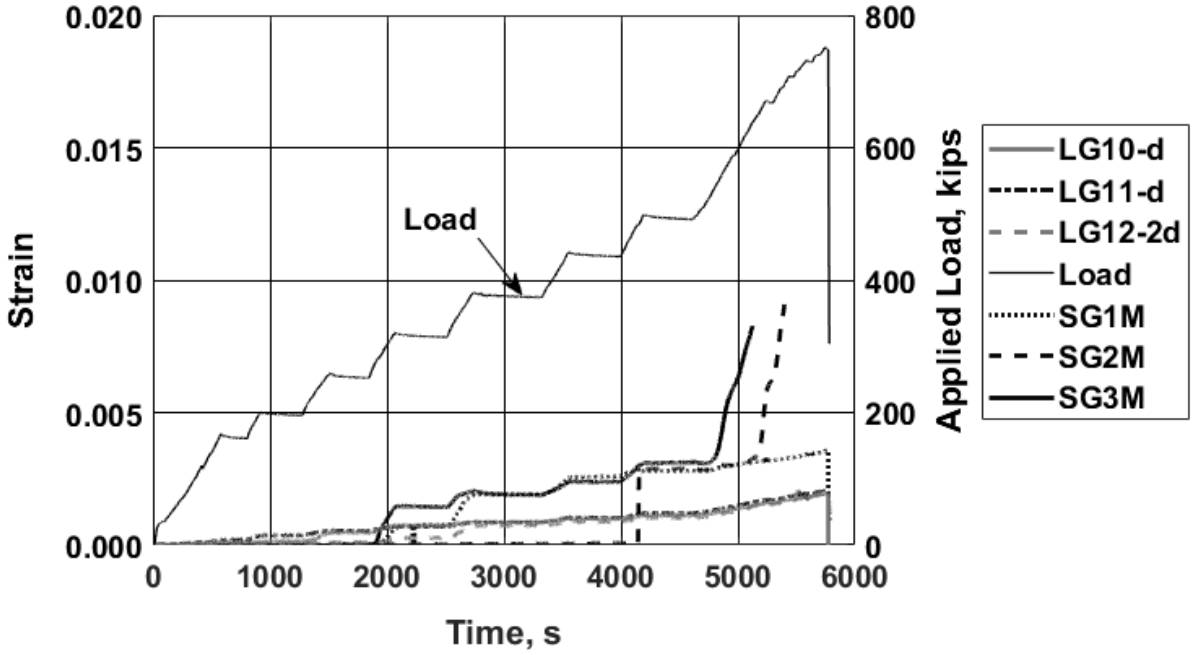

Figure H.76: Strain recorded with selected gauges and load versus time: specimen P2S7[1 kip = 4.45 kN]

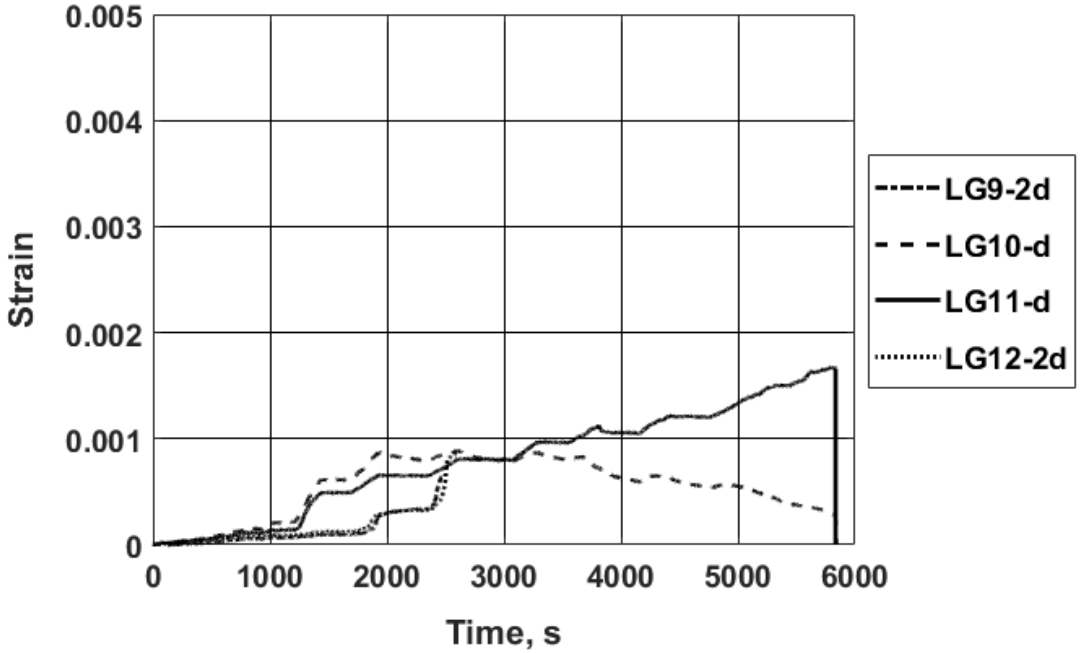

Figure H.77: Longitudinal reinforcing bar strain: specimen P2S8

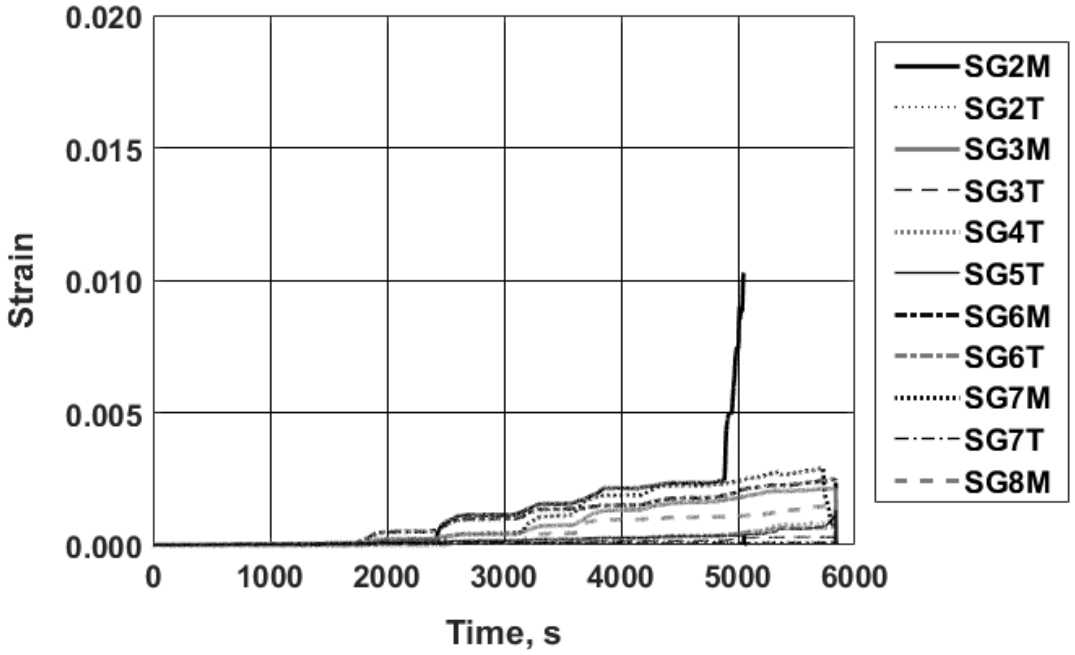

Figure H.78: Transverse reinforcing bar strain: specimen P2S8

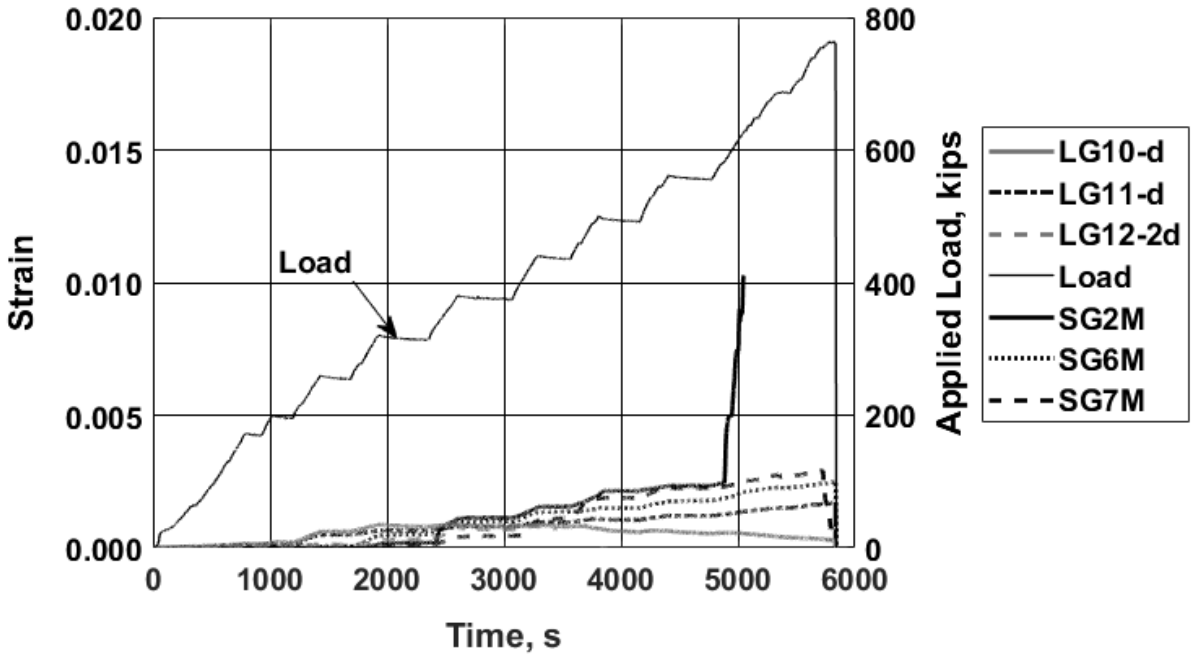

Figure H.79: Strain recorded with selected gauges and load versus time: specimen P2S8 [1 kip = 4.45 kN]

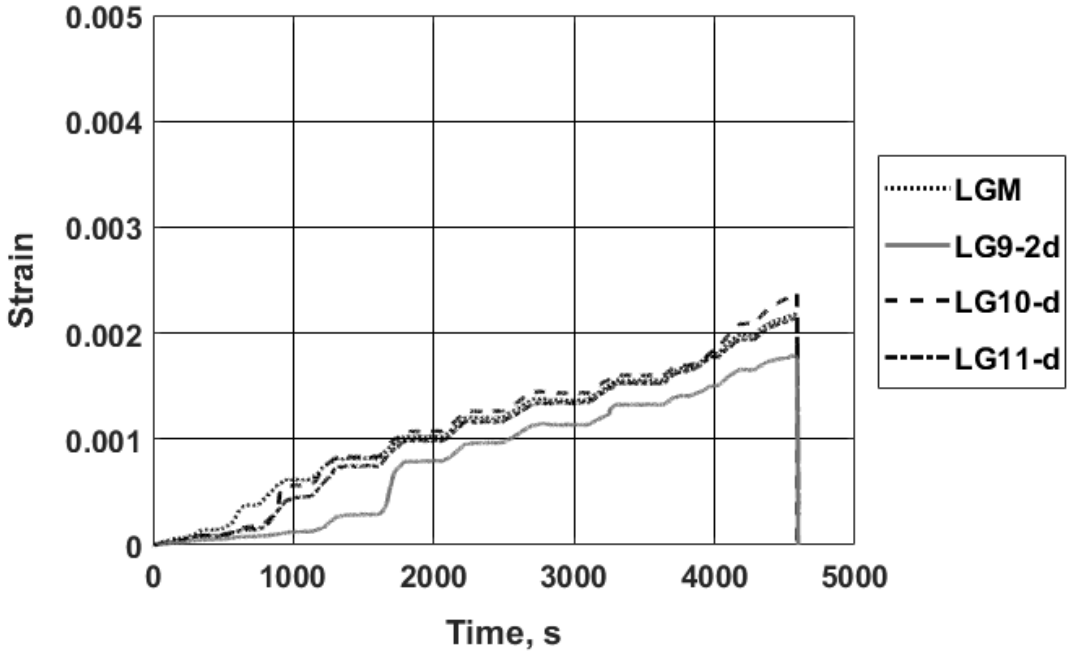

Figure H.80: Longitudinal reinforcing bar strain: specimen P2S9

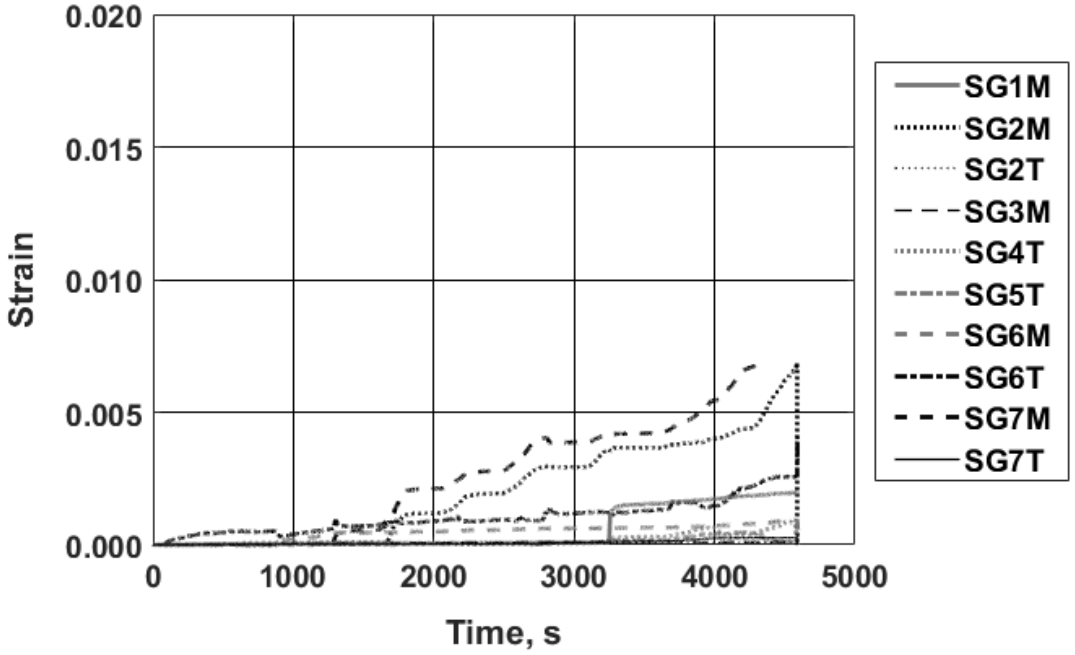

Figure H.81: Transverse reinforcing bar strain: specimen P2S9

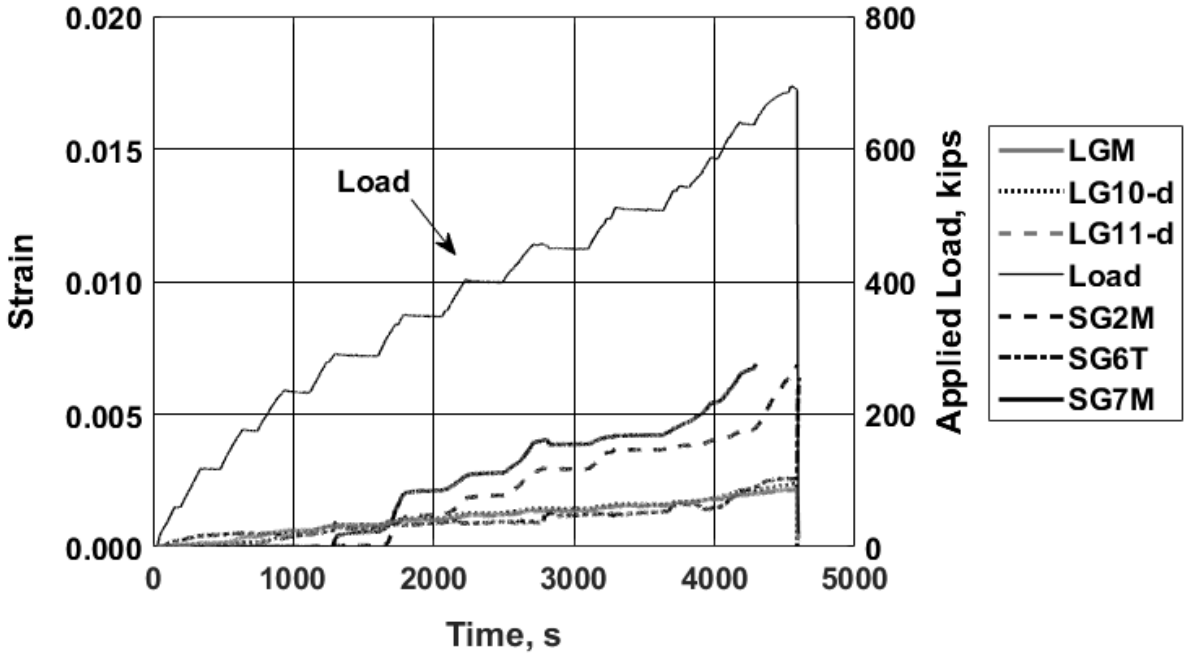

Figure H.82: Strain recorded with selected gauges and load versus time: specimen P2S9 [1 kip = 4.45 kN]

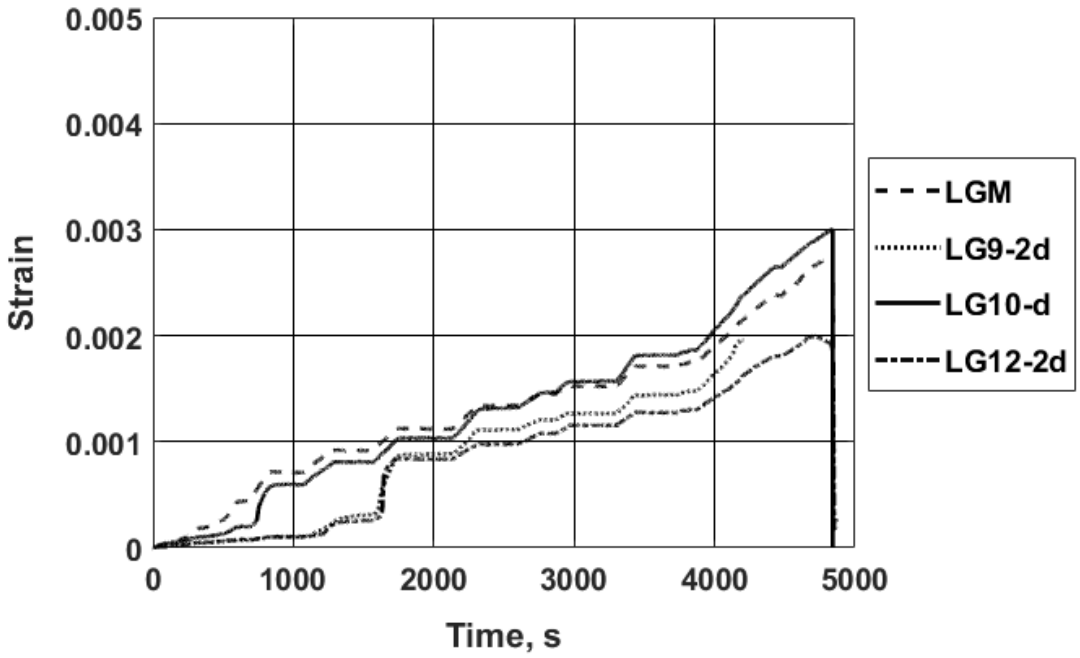

Figure H.83: Longitudinal reinforcing bar strain: specimen P2S10

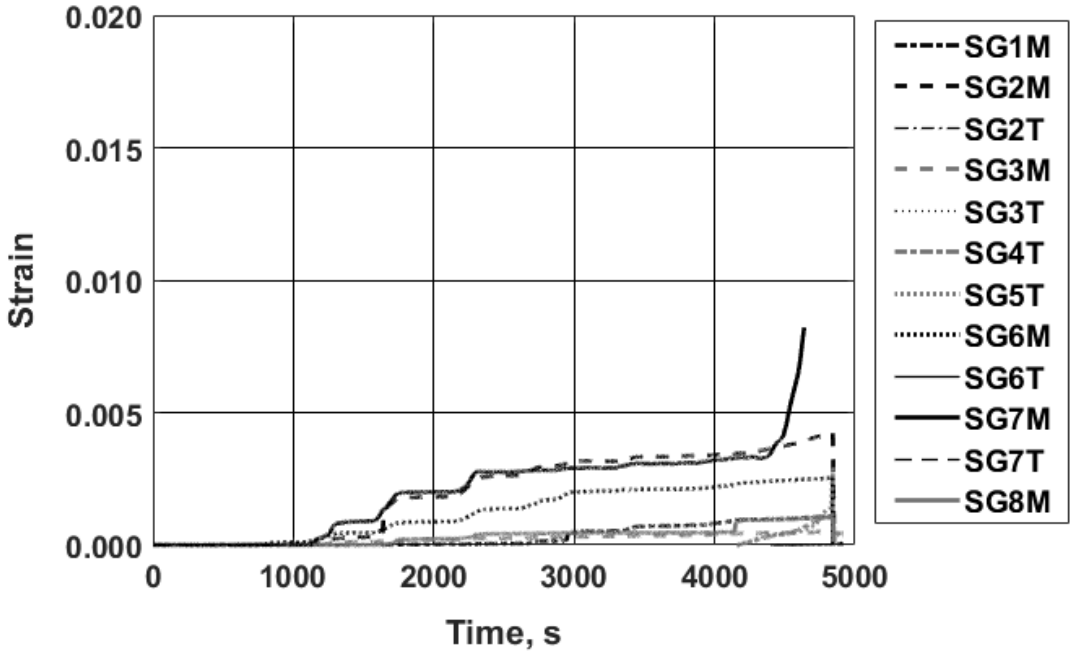

Figure H.84: Transverse reinforcing bar strain: specimen P2S10

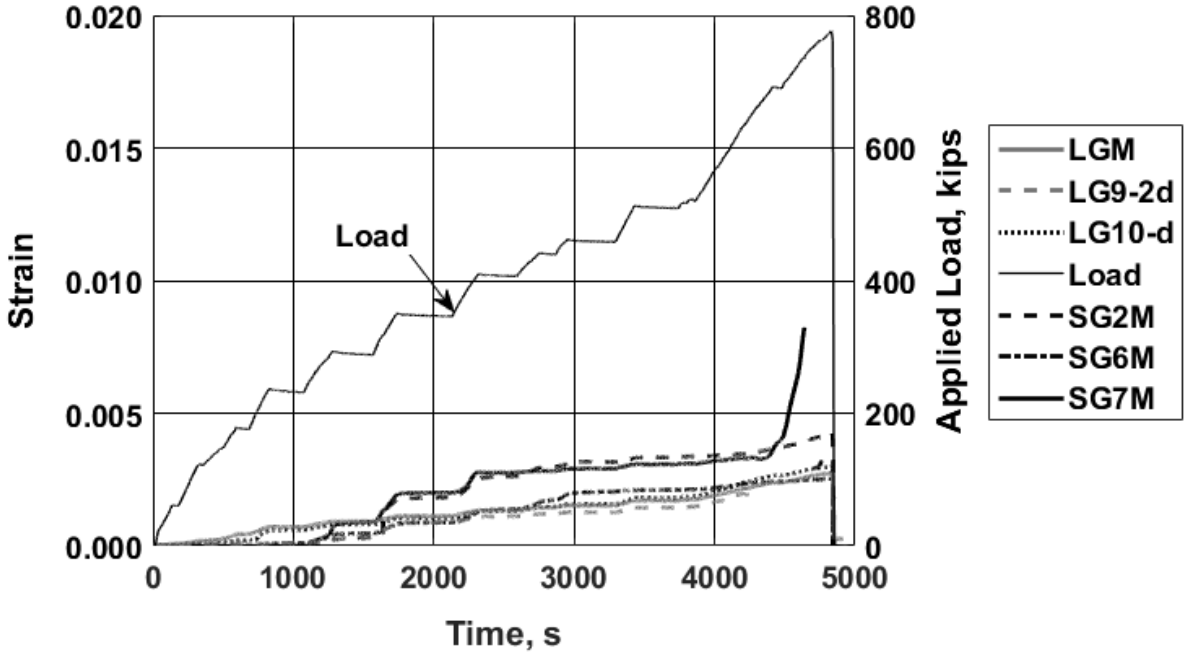

Figure H.85: Strain recorded with selected gauges and load versus time: specimen P2S10 [1 kip = 4.45 kN]

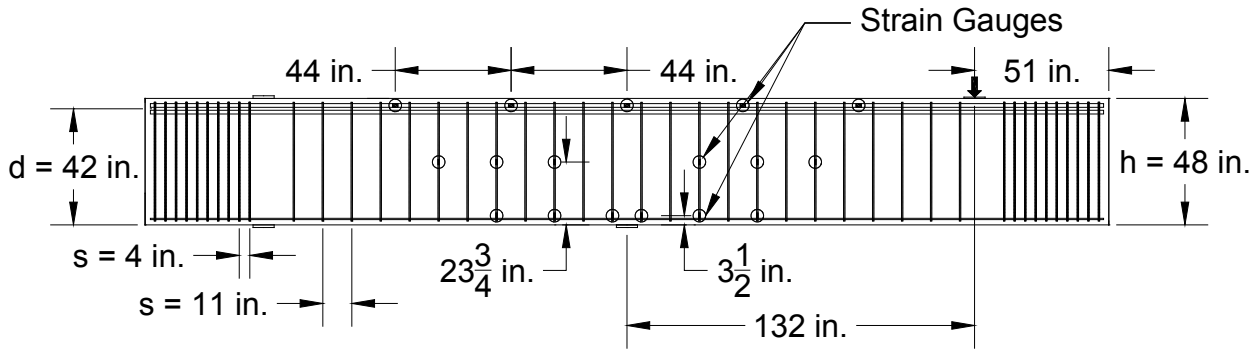

(a)

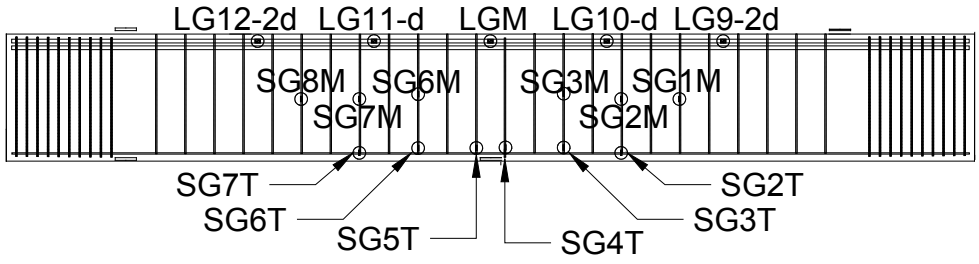

(b)

Figure H.86: Specimens P2S11 and P2S12: Strain gauge (a) locations and (b) naming convention [1 in. = 25.4 mm]

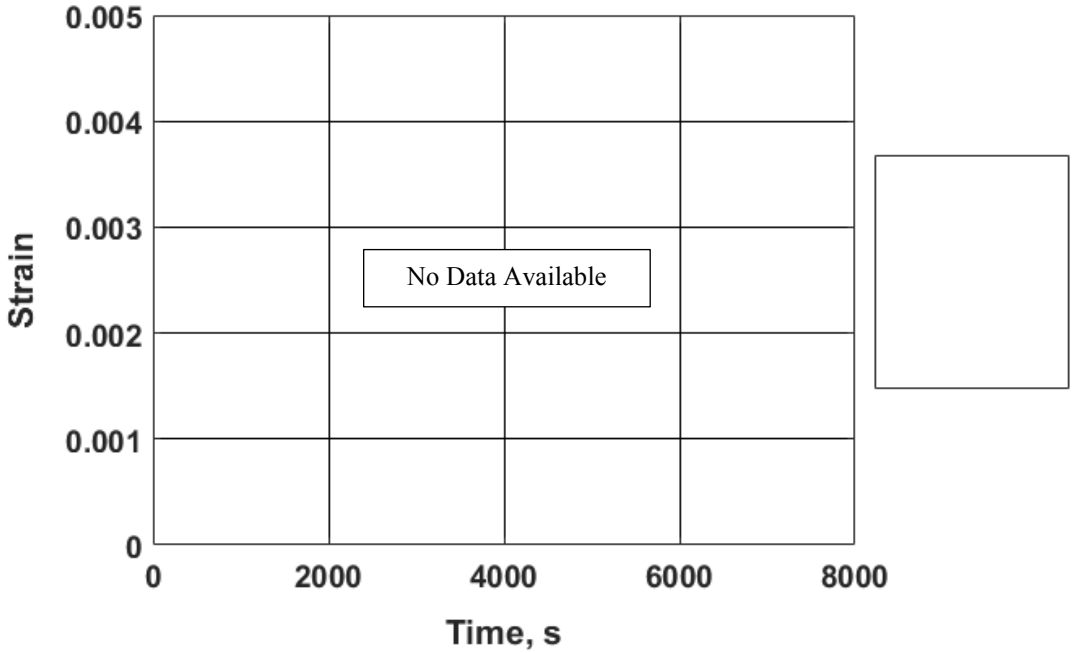

Figure H.87: Longitudinal reinforcing bar strain: specimen P2S11

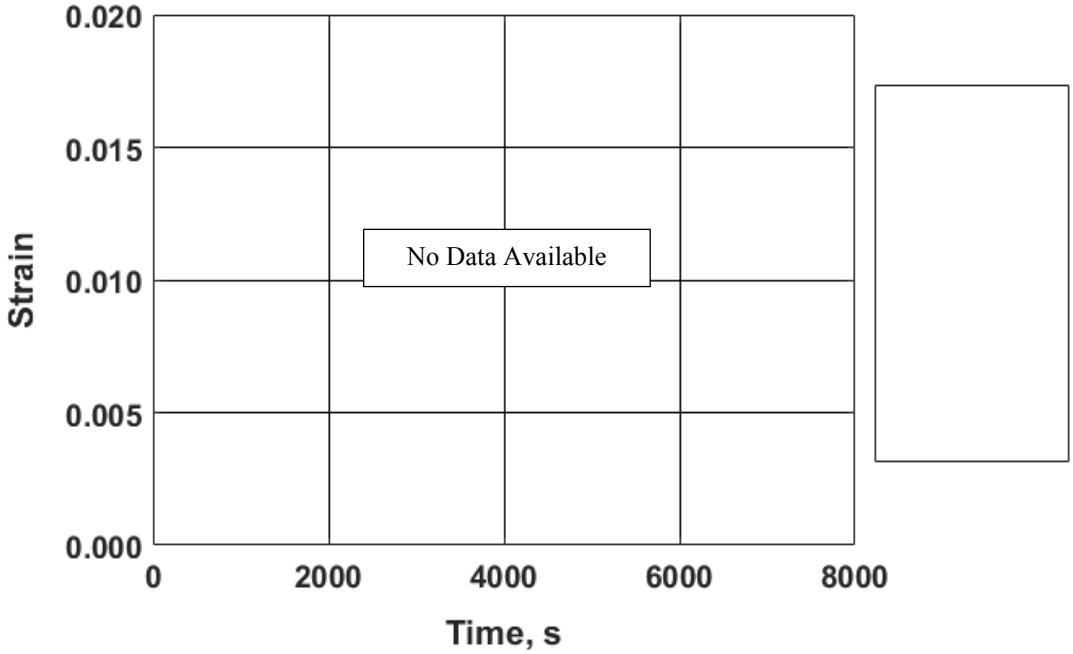

Figure H.88: Transverse reinforcing bar strain: specimen P2S11

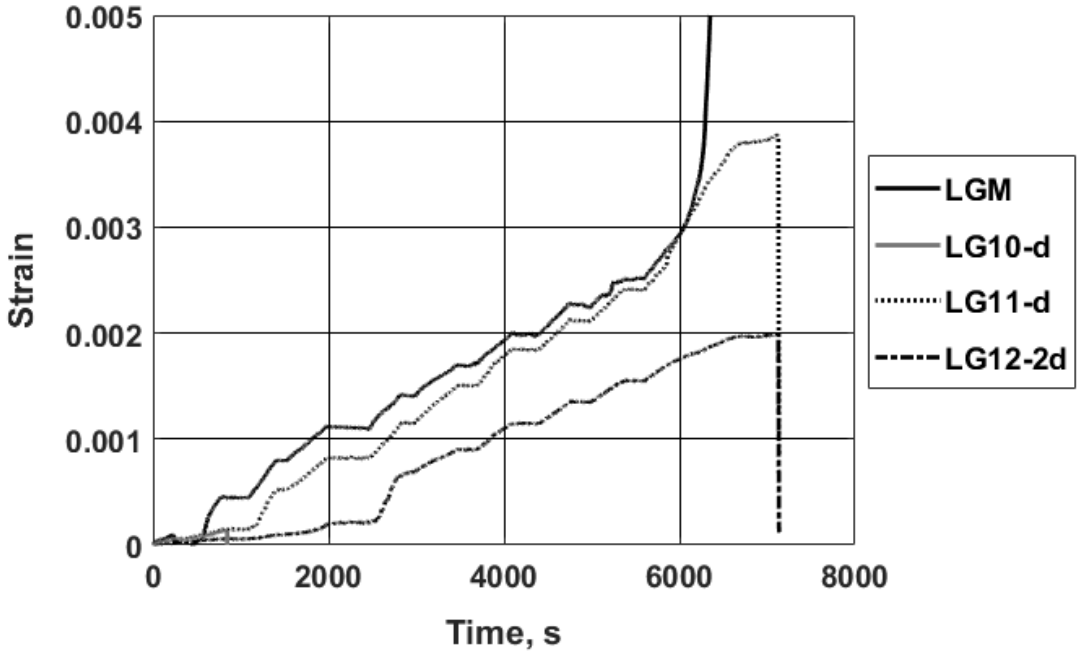

Figure H.89: Longitudinal reinforcing bar strain: specimen P2S12

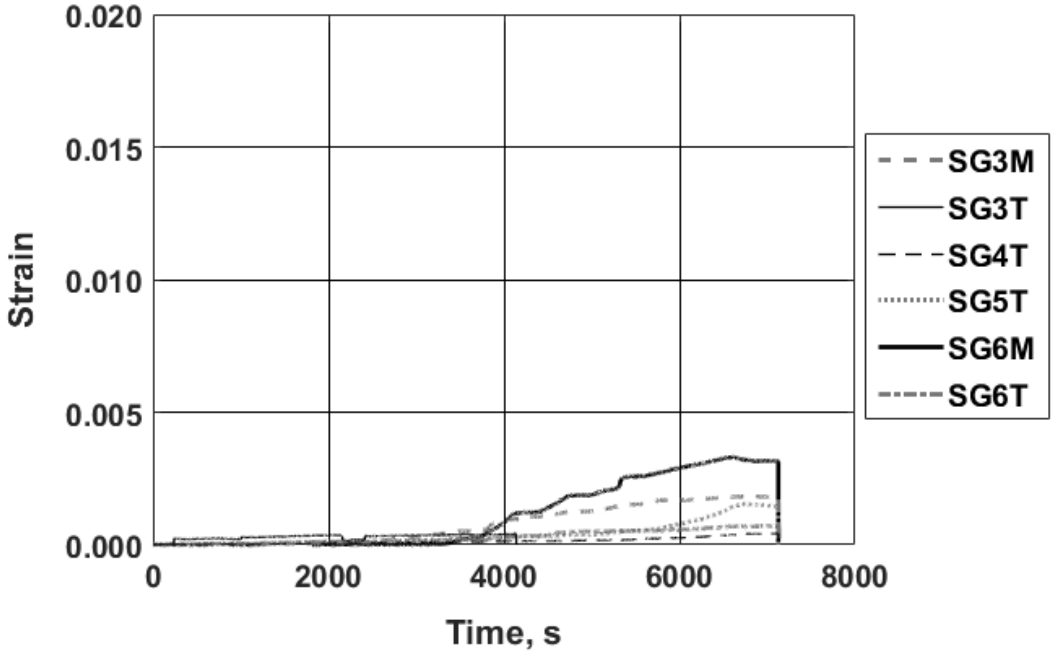

Figure H.90: Transverse reinforcing bar strain: specimen P2S12

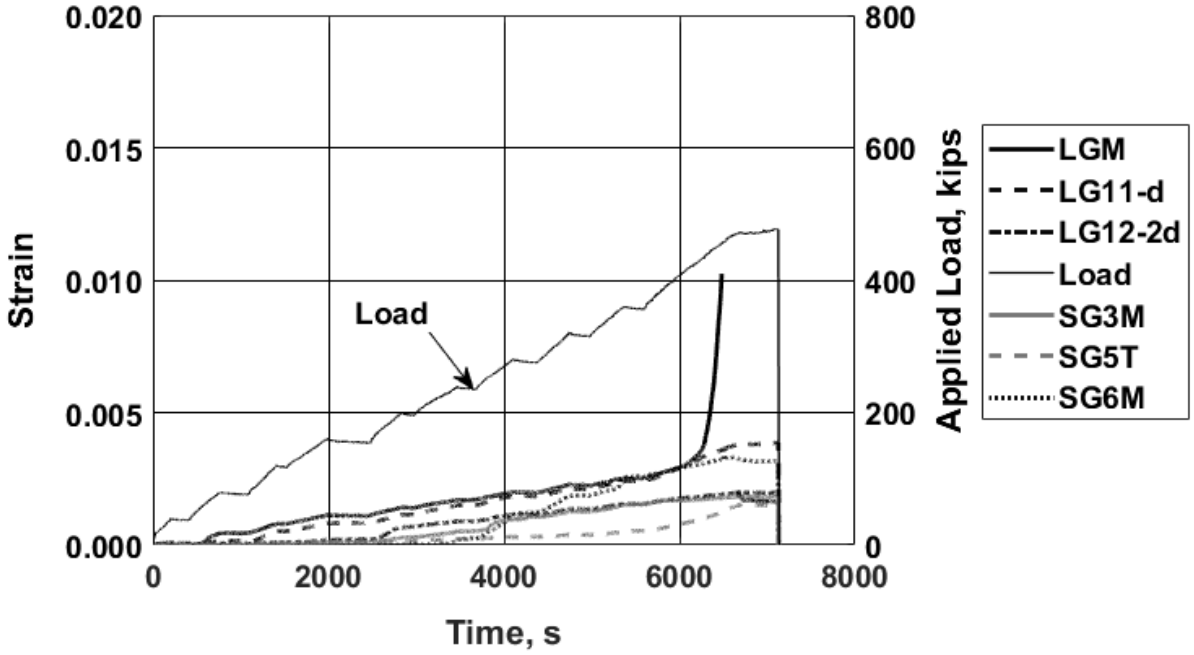

Figure H.91: Strain recorded with selected gauges and load versus time: specimen P2S12 [1 kip = 4.45 kN]

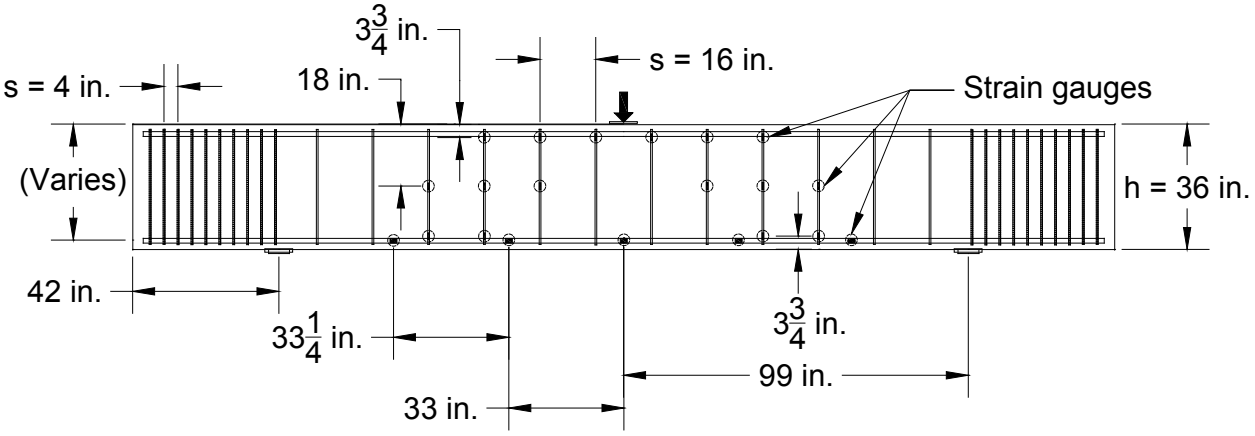

(a)

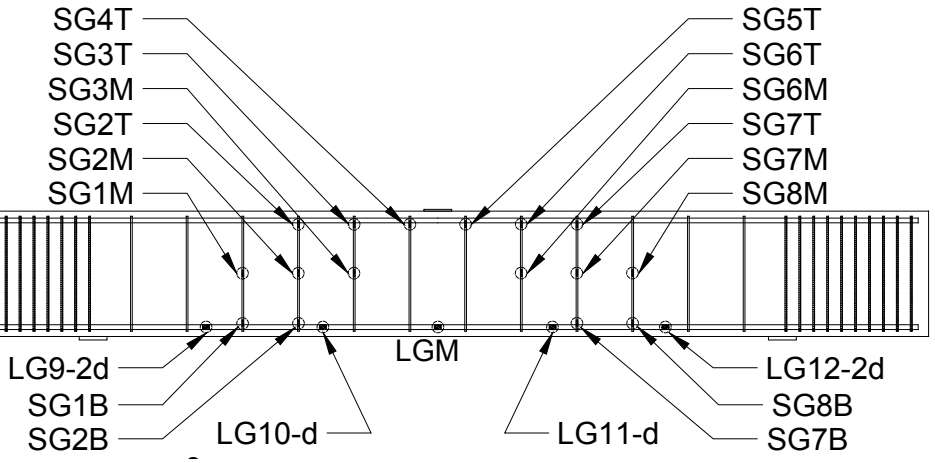

(b)

Figure H.92: Phase 3 specimens: Strain gauge (a) locations and (b) naming convention [1 in. = 25.4 mm]

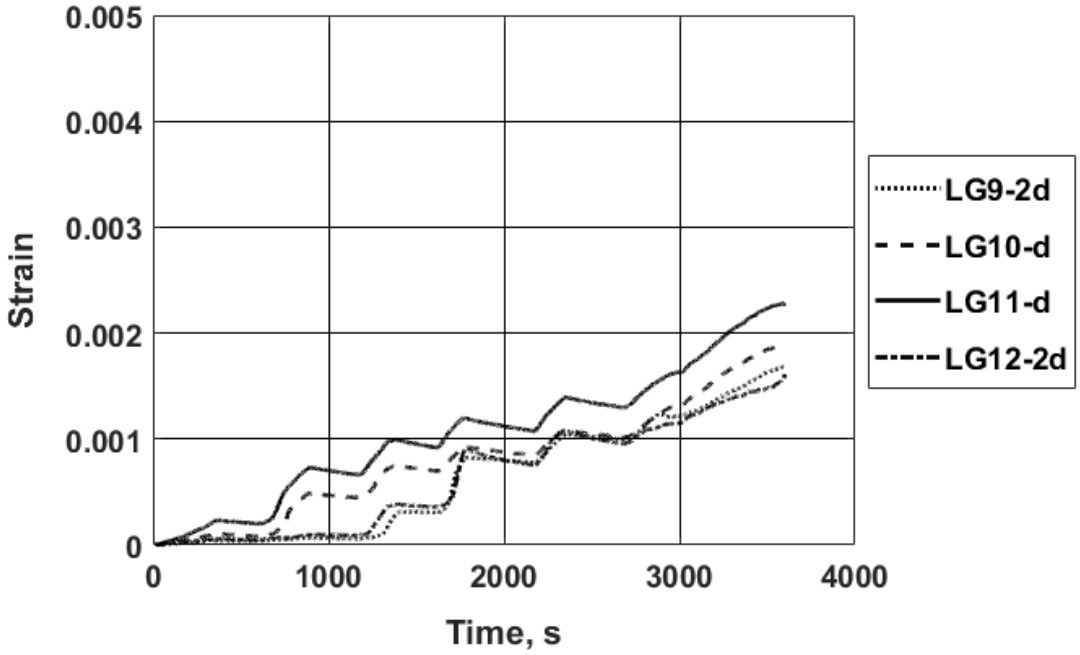

Figure H.93: Longitudinal reinforcing bar strain: specimen P3S1

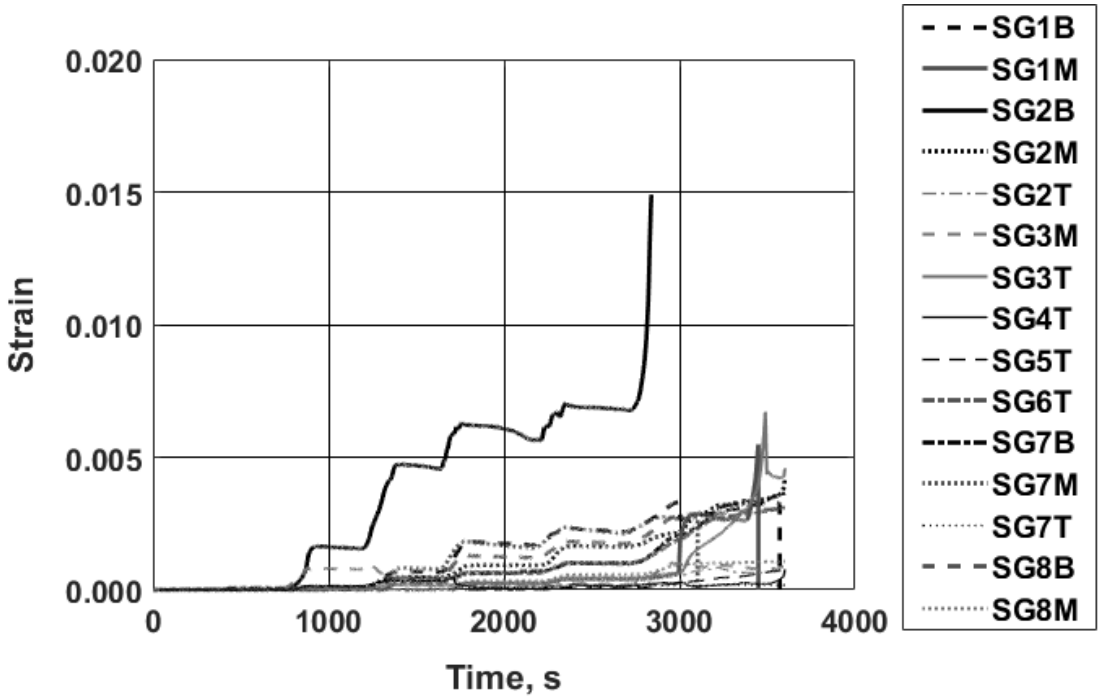

Figure H.94: Transverse reinforcing bar strain: specimen P3S1

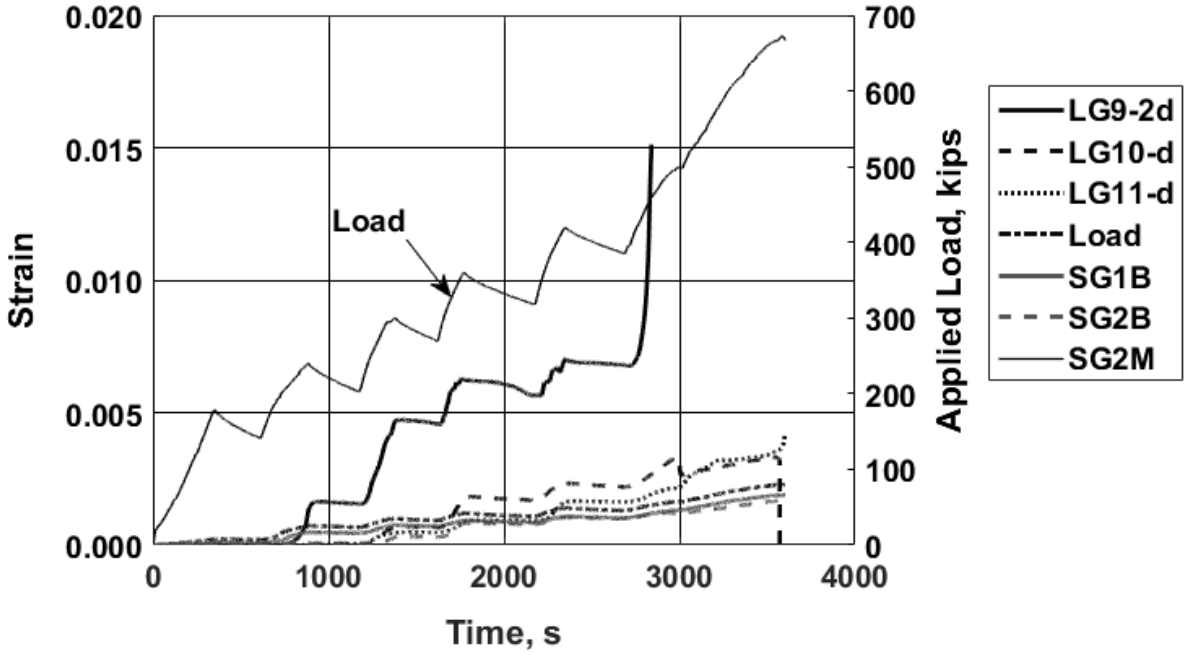

Figure H.95: Strain recorded with selected gauges and load versus time: specimen P3S1[1 kip = 4.45 kN]

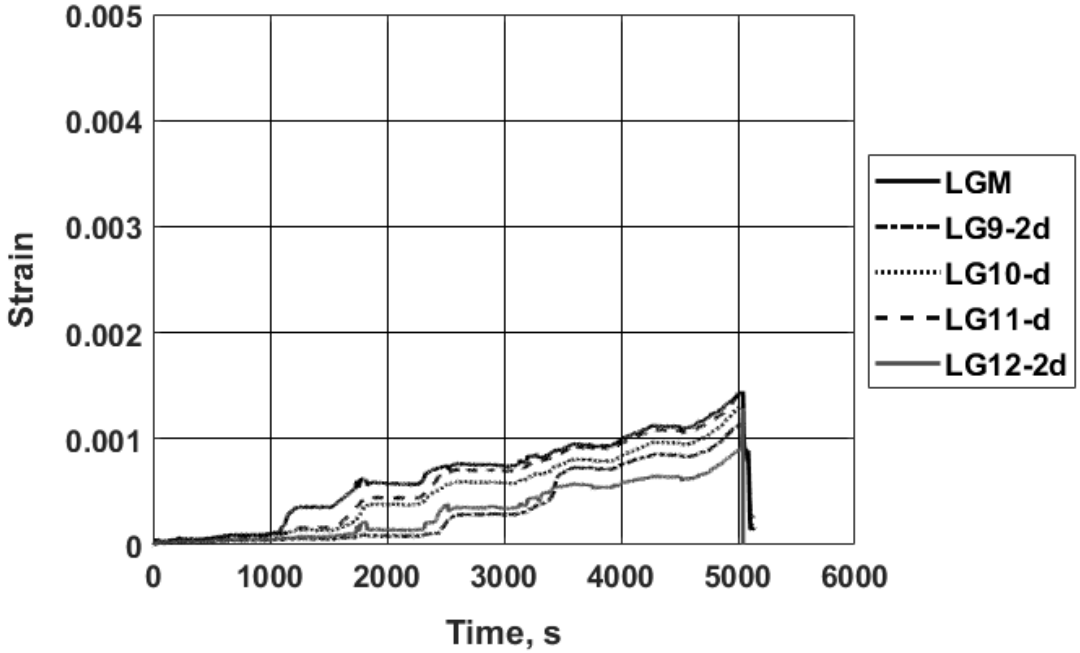

Figure H.96: Longitudinal reinforcing bar strain: specimen P3S2

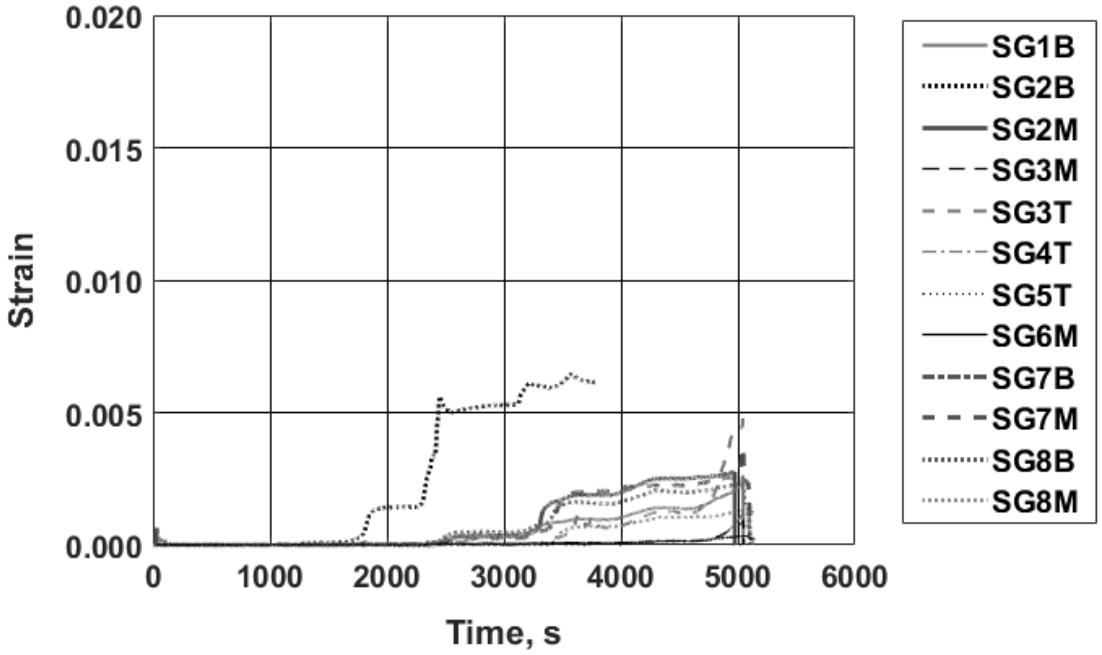

Figure H.97: Transverse reinforcing bar strain: specimen P3S2

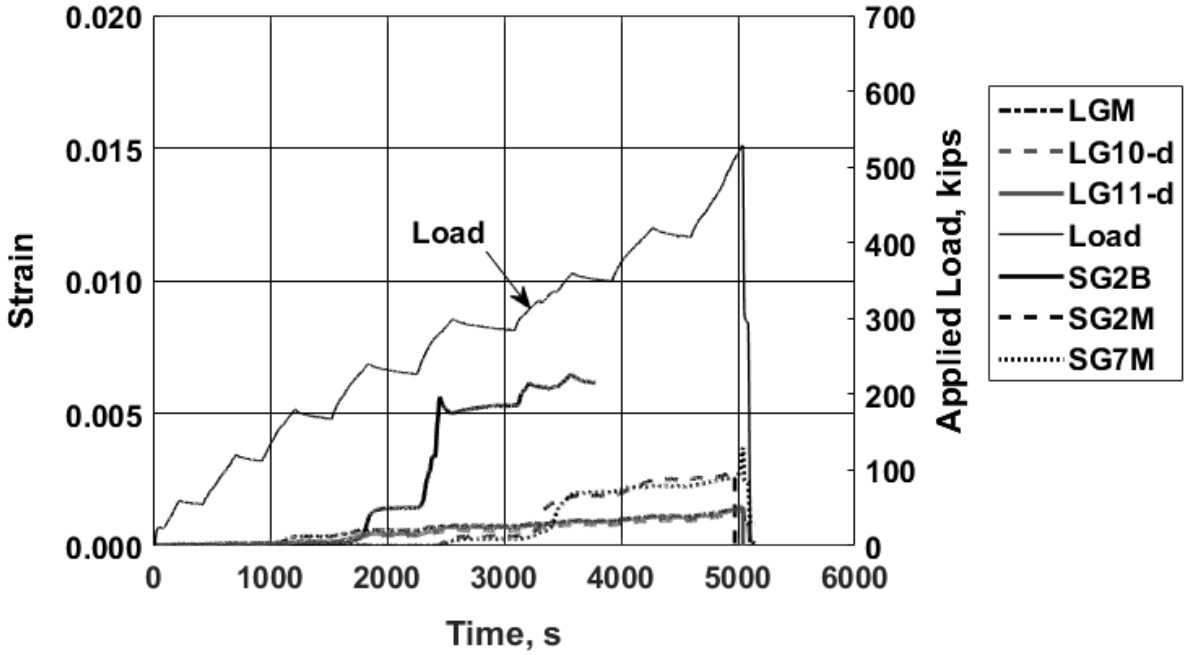

Figure H.98: Strain recorded with selected gauges and load versus time: specimen P3S2 [1 kip = 4.45 kN]

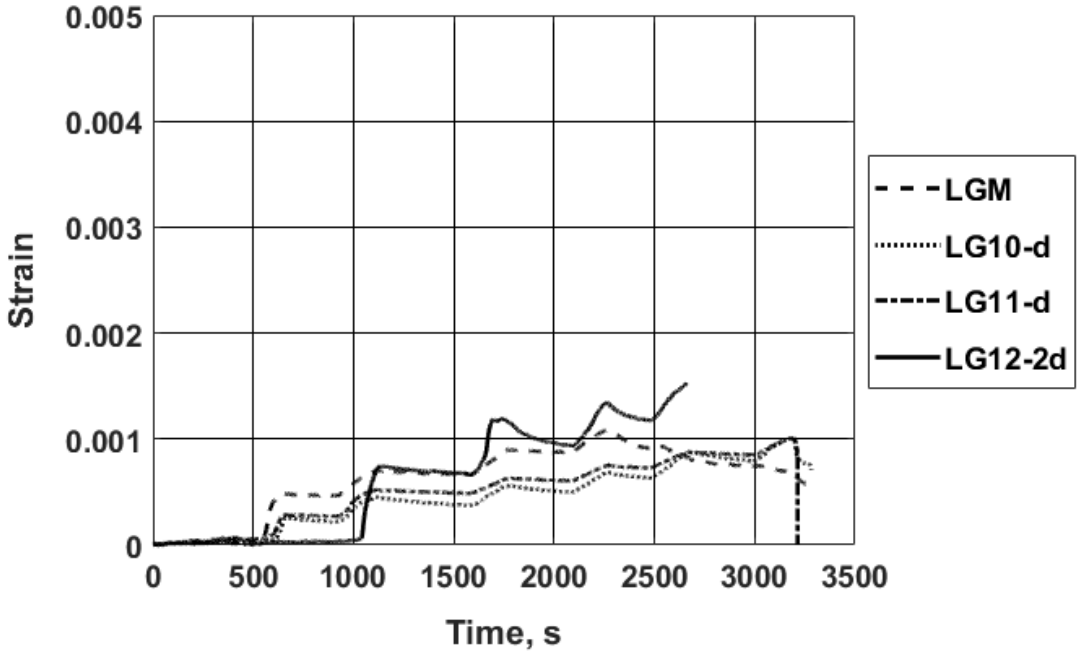

Figure H.99: Longitudinal reinforcing bar strain: specimen P3S3

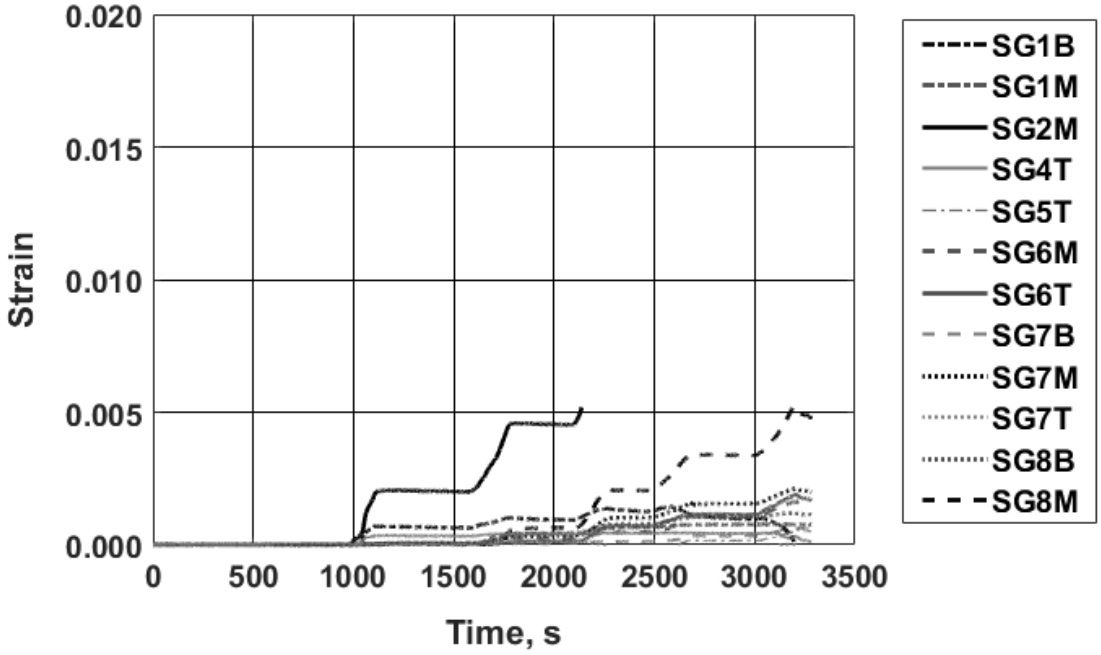

Figure H.100: Transverse reinforcing bar strain: specimen P3S3

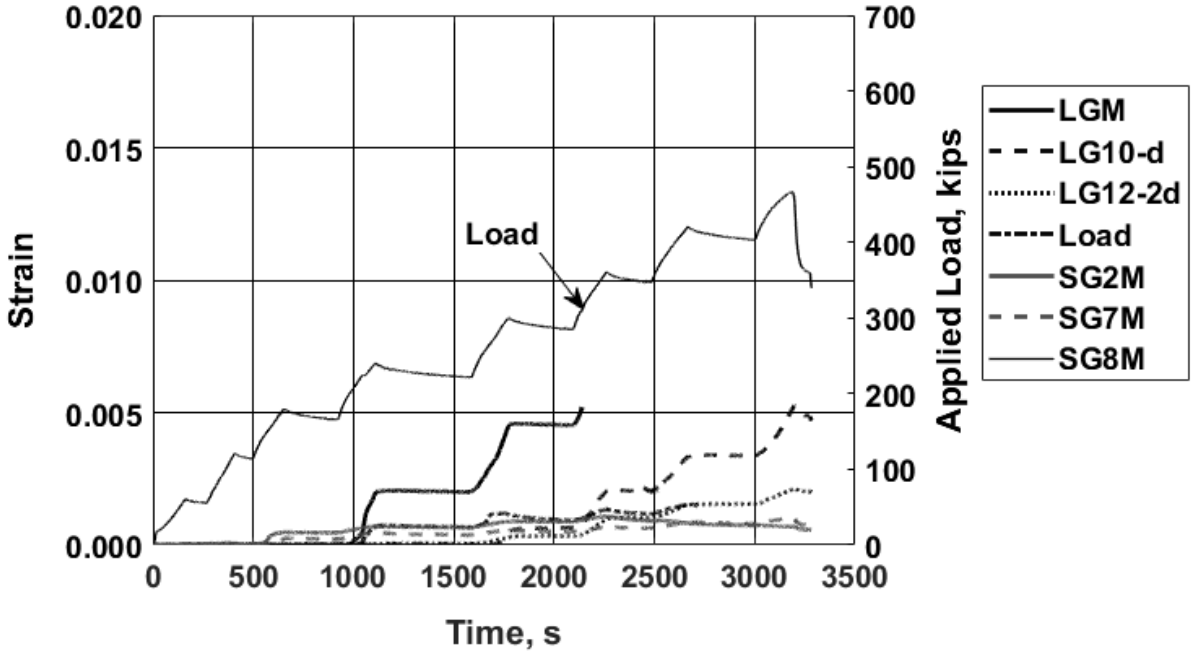

Figure H.101: Strain recorded with selected gauges and load versus time: specimen P3S3 [1 kip = 4.45 kN]

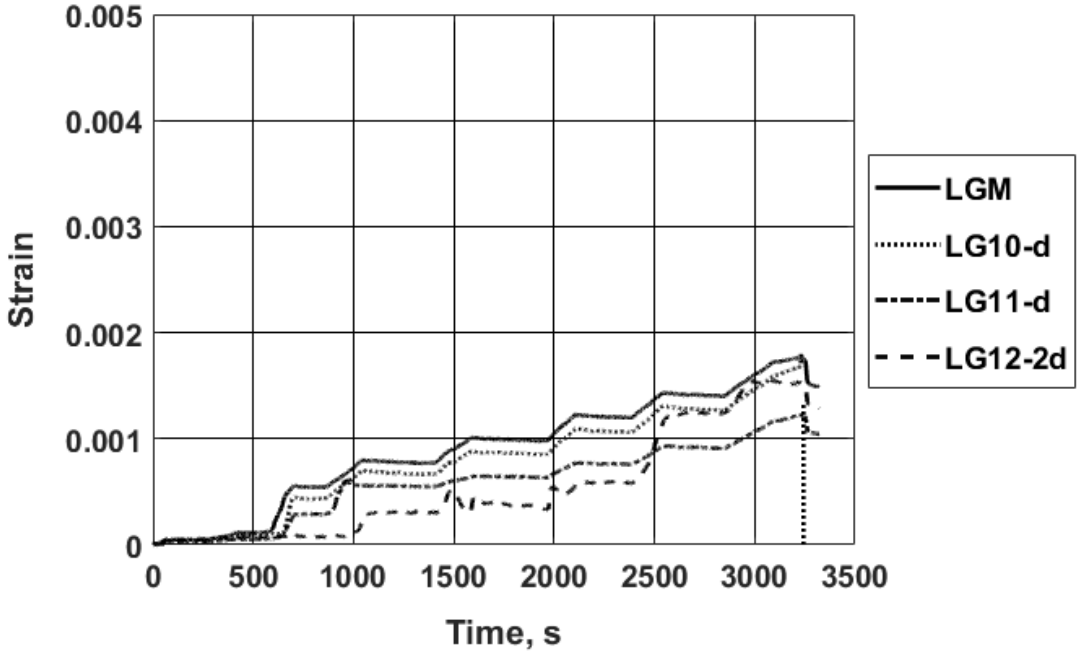

Figure H.102: Longitudinal reinforcing bar strain: specimen P3S4

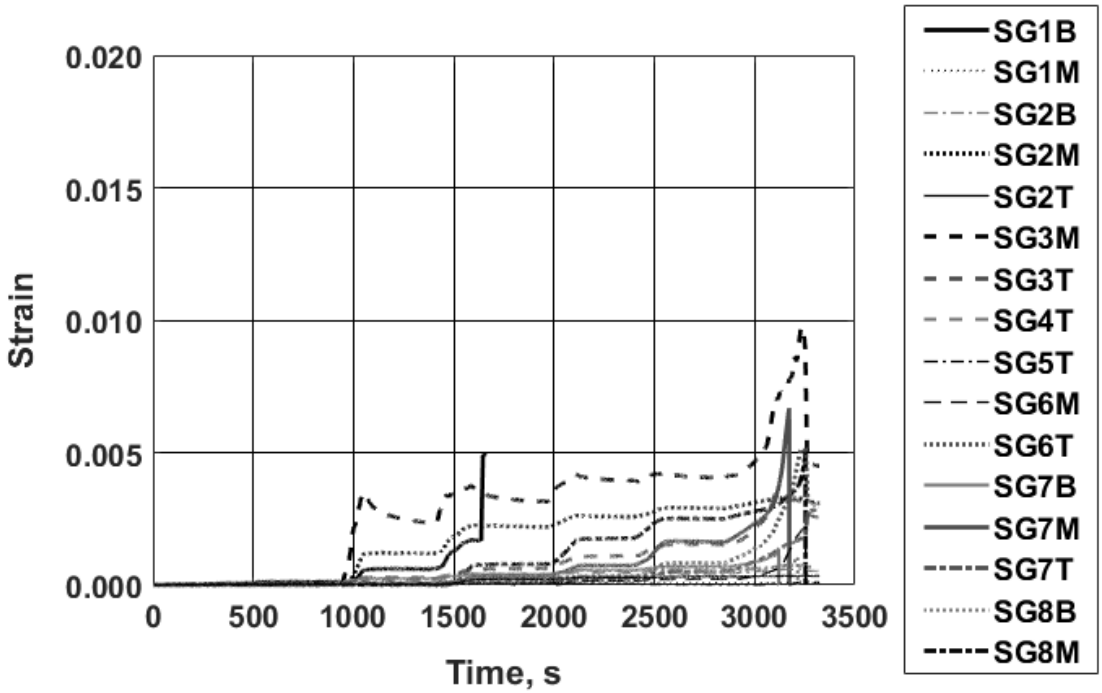

Figure H.103: Transverse reinforcing bar strain: specimen P3S4

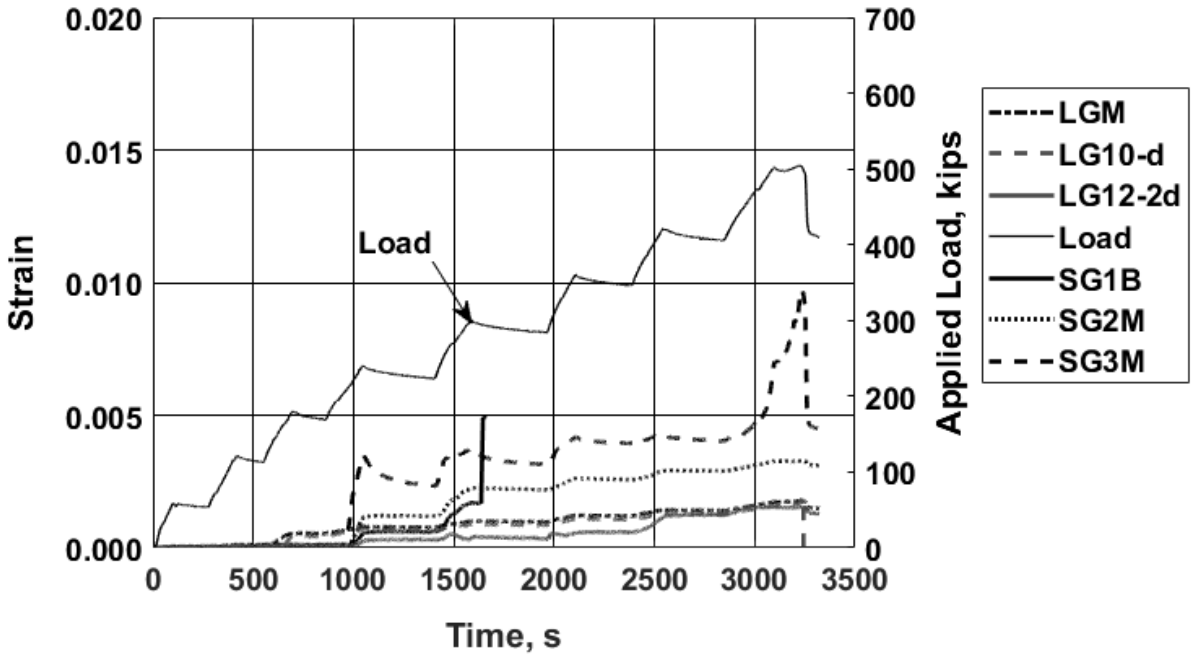

Figure H.104: Strain recorded with selected gauges and load versus time: specimen P3S4 [1 kip = 4.45 kN]

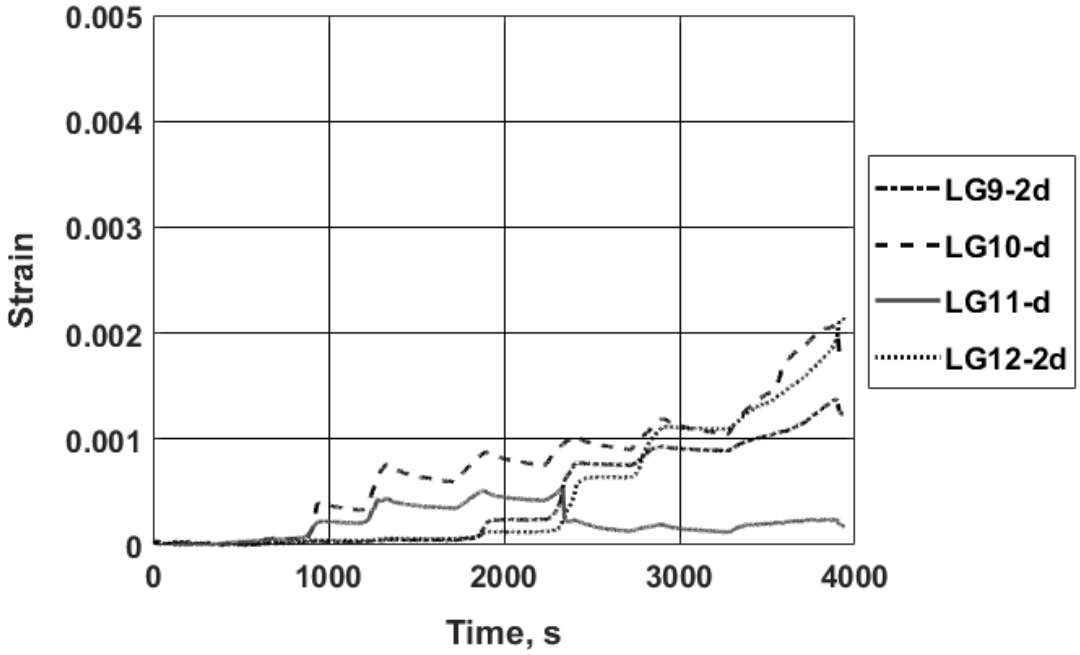

Figure H.105: Longitudinal reinforcing bar strain: specimen P3S5

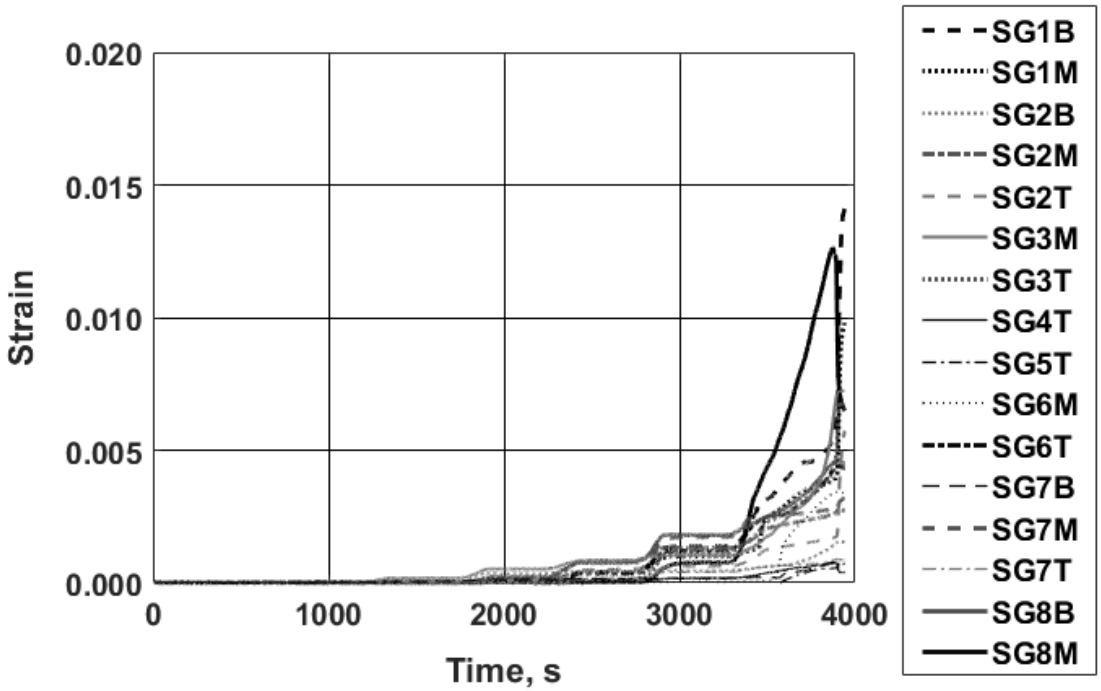

Figure H.106: Transverse reinforcing bar strain: specimen P3S5

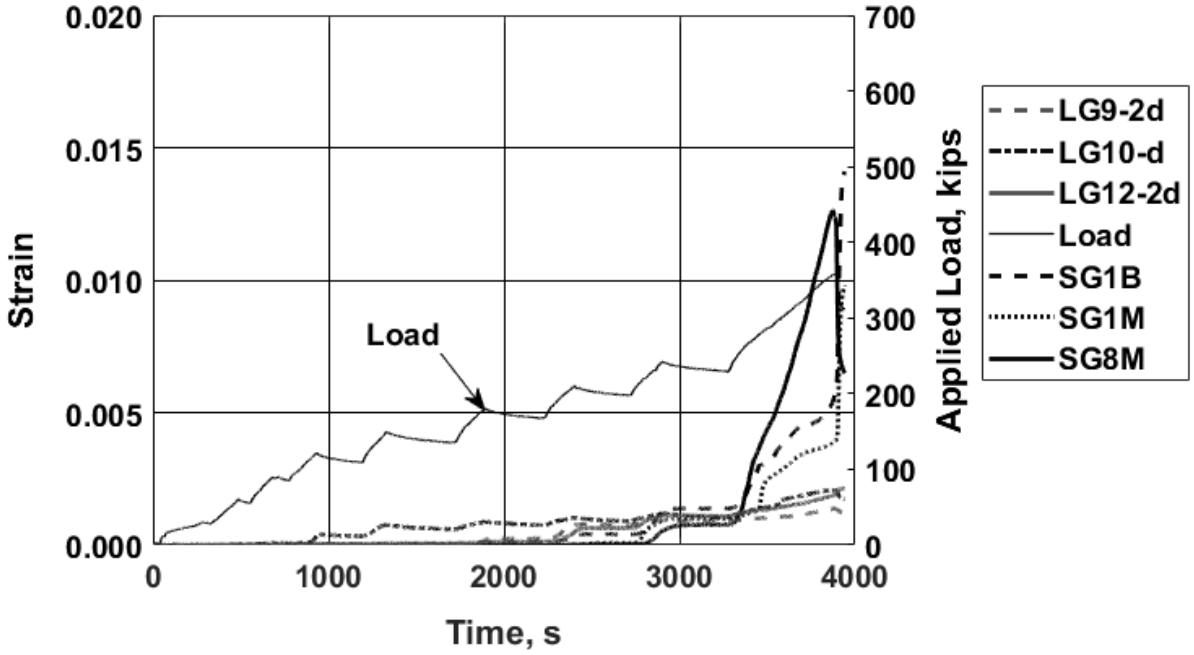

Figure H.107: Strain recorded with selected gauges and load versus time: specimen P3S5 [1 kip = 4.45 kN]

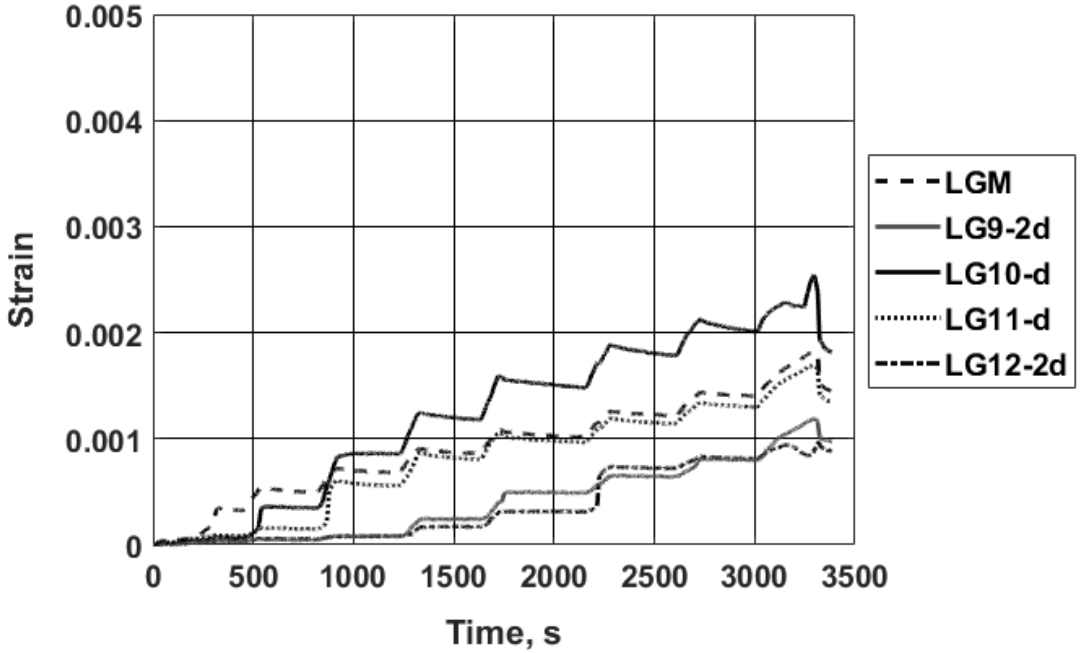

Figure H.108: Longitudinal reinforcing bar strain: specimen P3S6

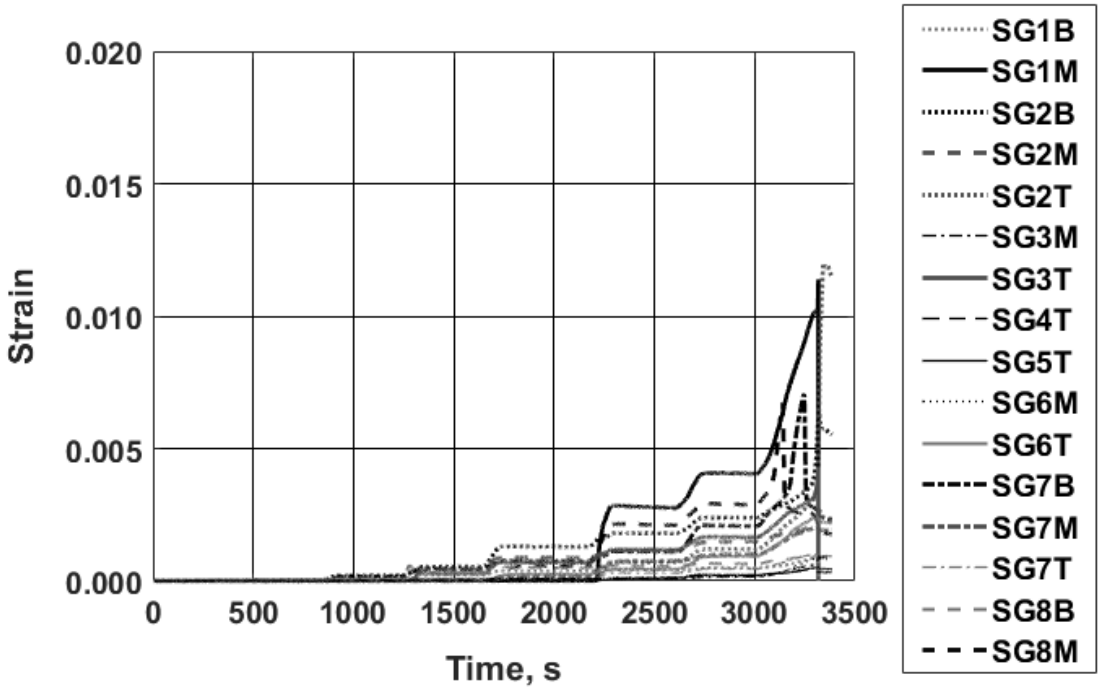

Figure H.109: Transverse reinforcing bar strain: specimen P3S6

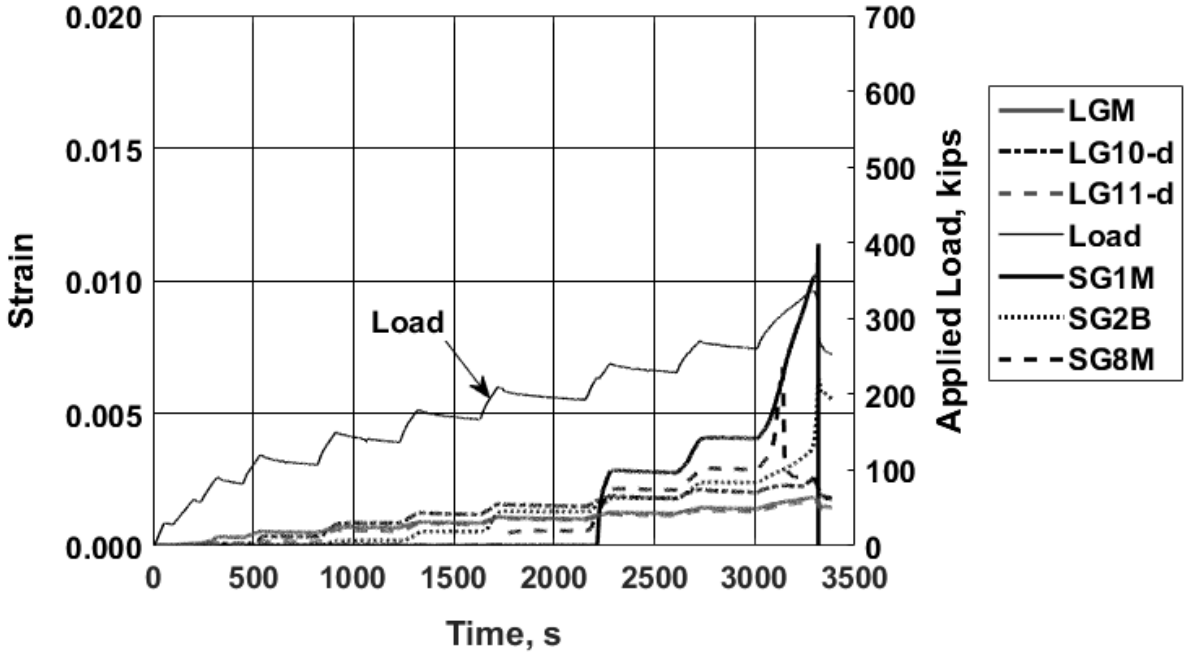

Figure H.110: Strain recorded with selected gauges and load versus time: specimen P3S6 [1 kip = 4.45 kN]

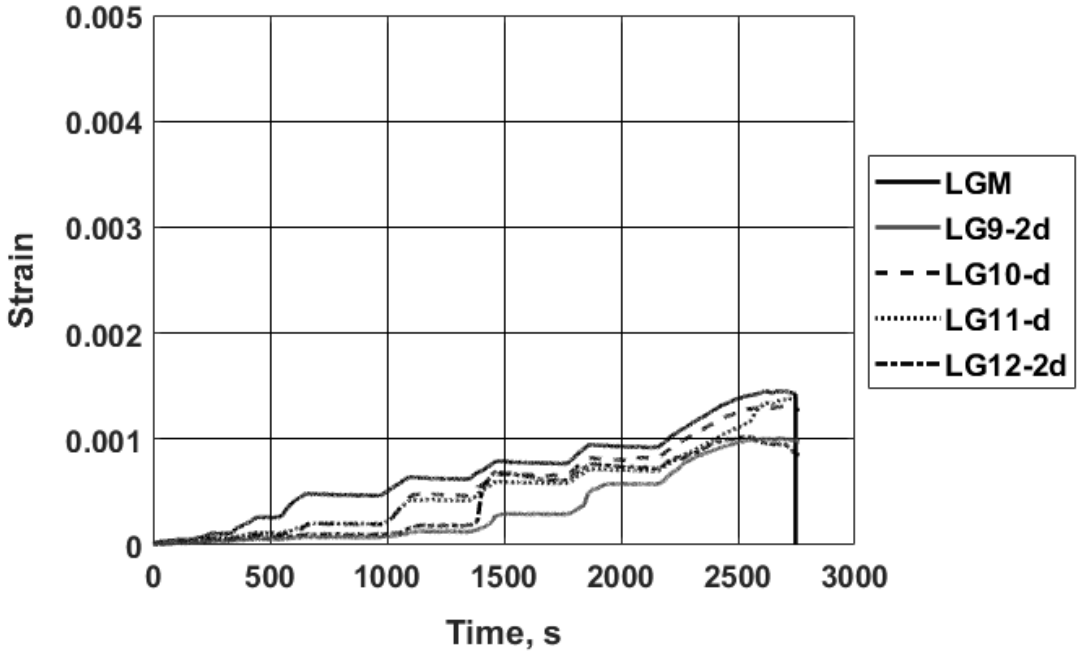

Figure H.111: Longitudinal reinforcing bar strain: specimen P3S7

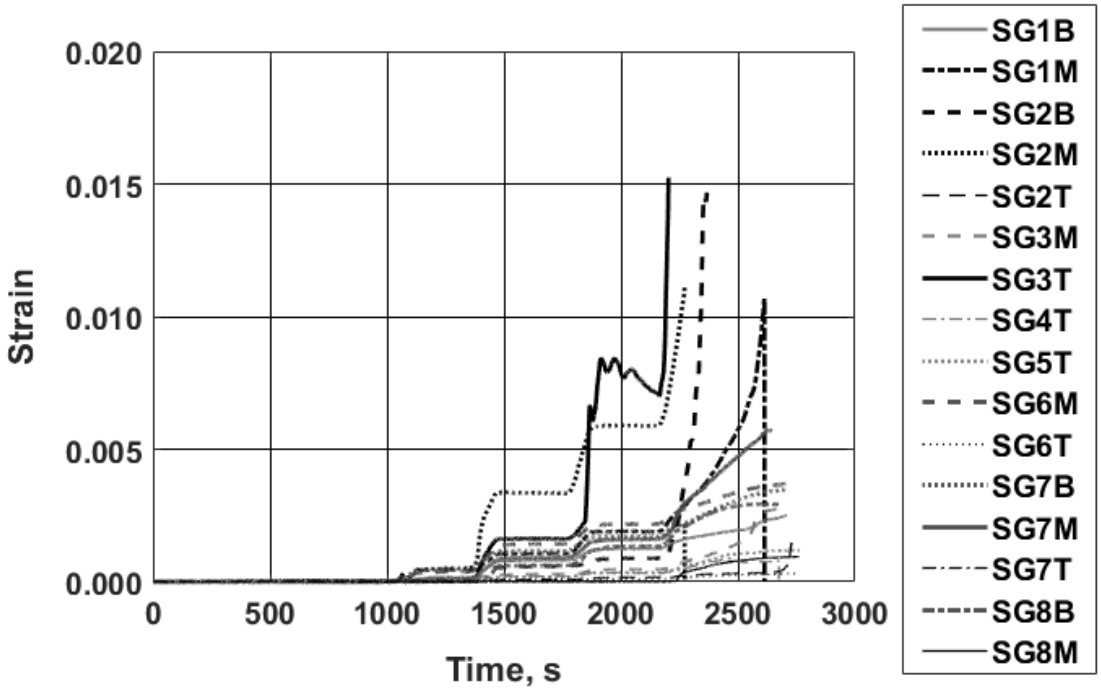

Figure H.112: Transverse reinforcing bar strain: specimen P3S7

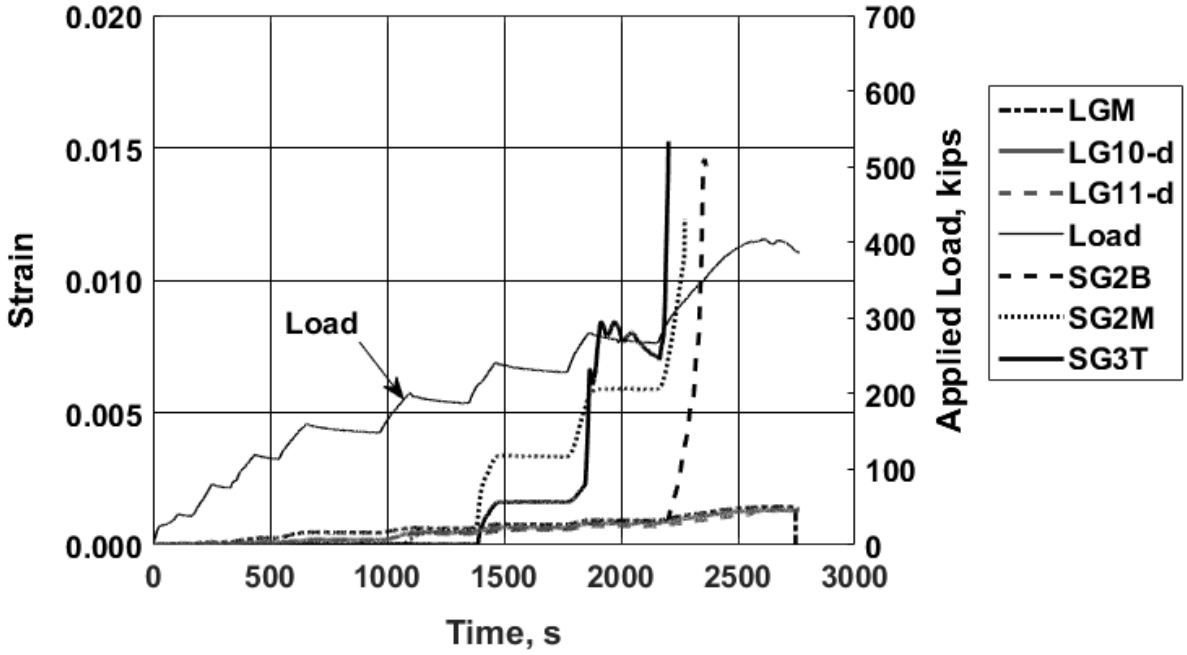

Figure H.113: Strain recorded with selected gauges and load versus time: specimen P3S7 [1 kip = 4.45 kN]

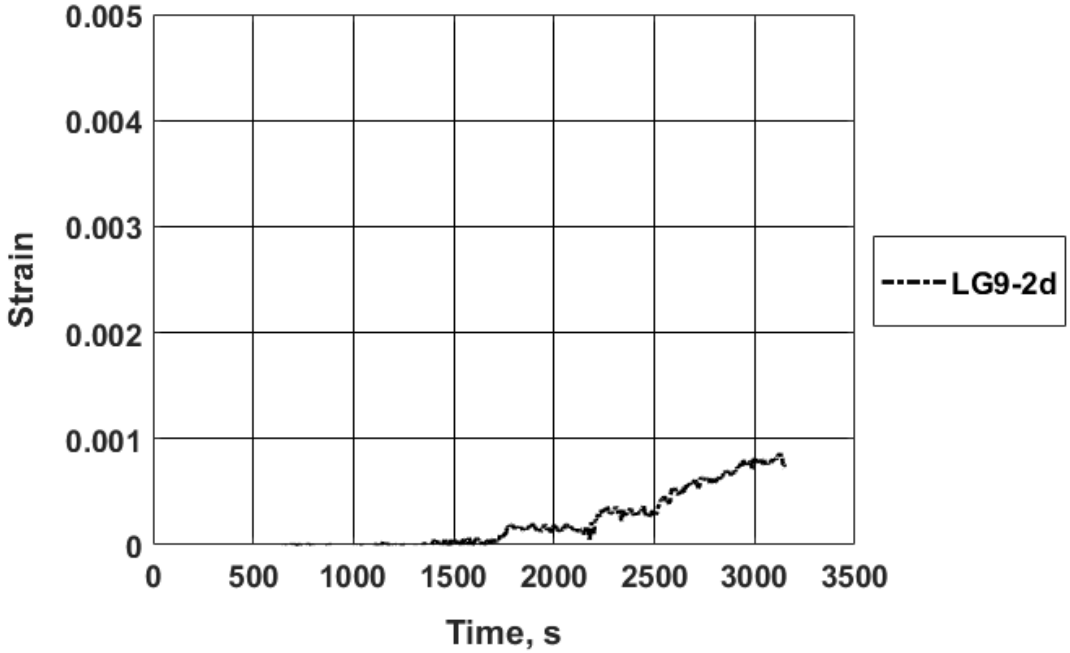

Figure H.114: Longitudinal reinforcing bar strain: specimen P3S8

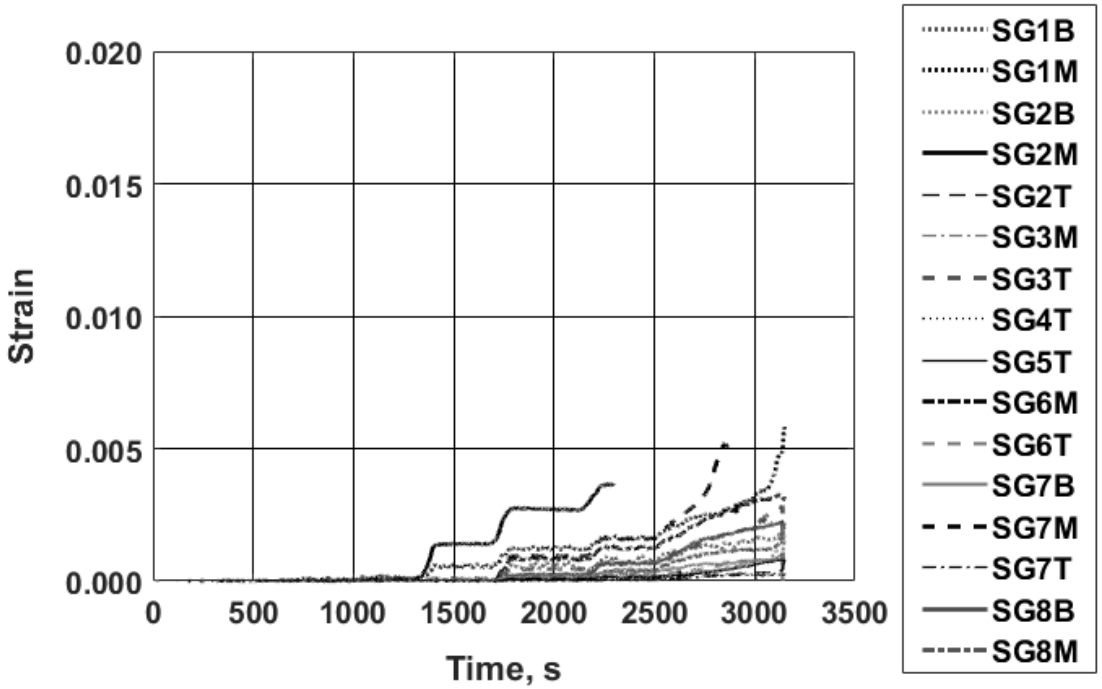

Figure H.115: Transverse reinforcing bar strain: specimen P3S8

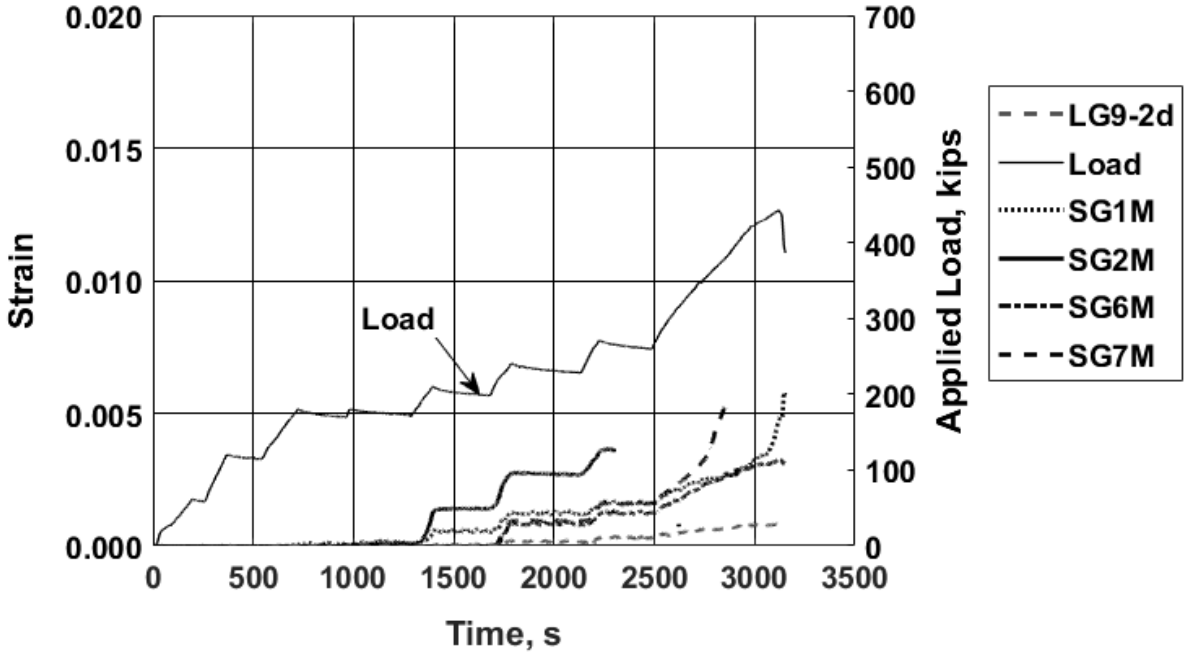

Figure H.116: Strain recorded with selected gauges and load versus time: specimen P3S8 [1 kip = 4.45 kN]

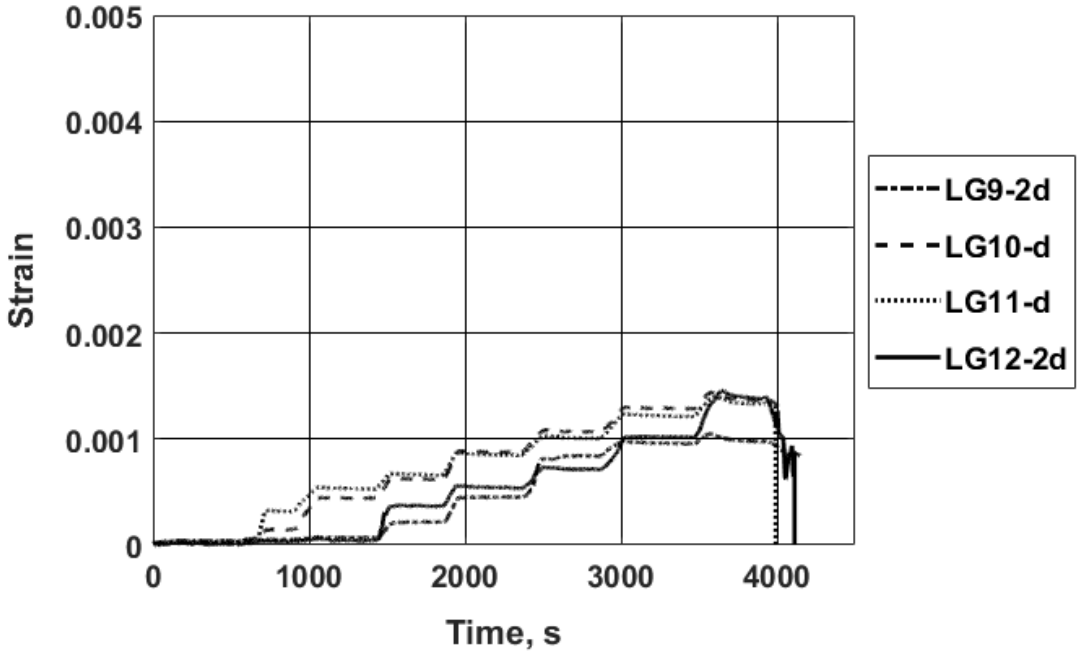

Figure H.117: Longitudinal reinforcing bar strain: specimen P3S9

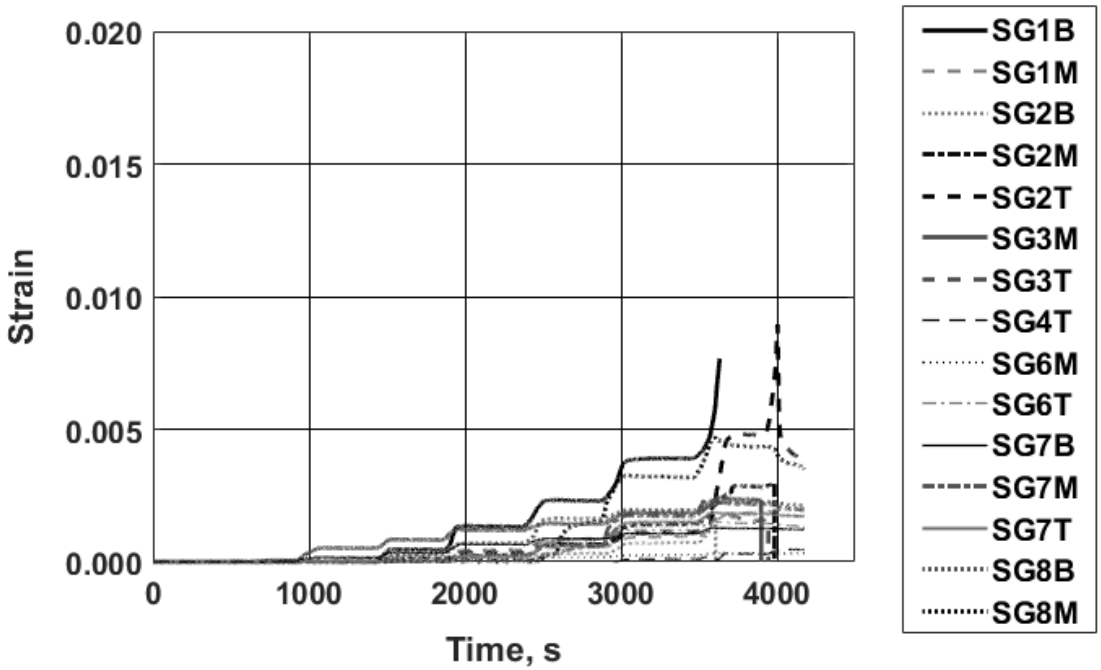

Figure H.118: Transverse reinforcing bar strain: specimen P3S9

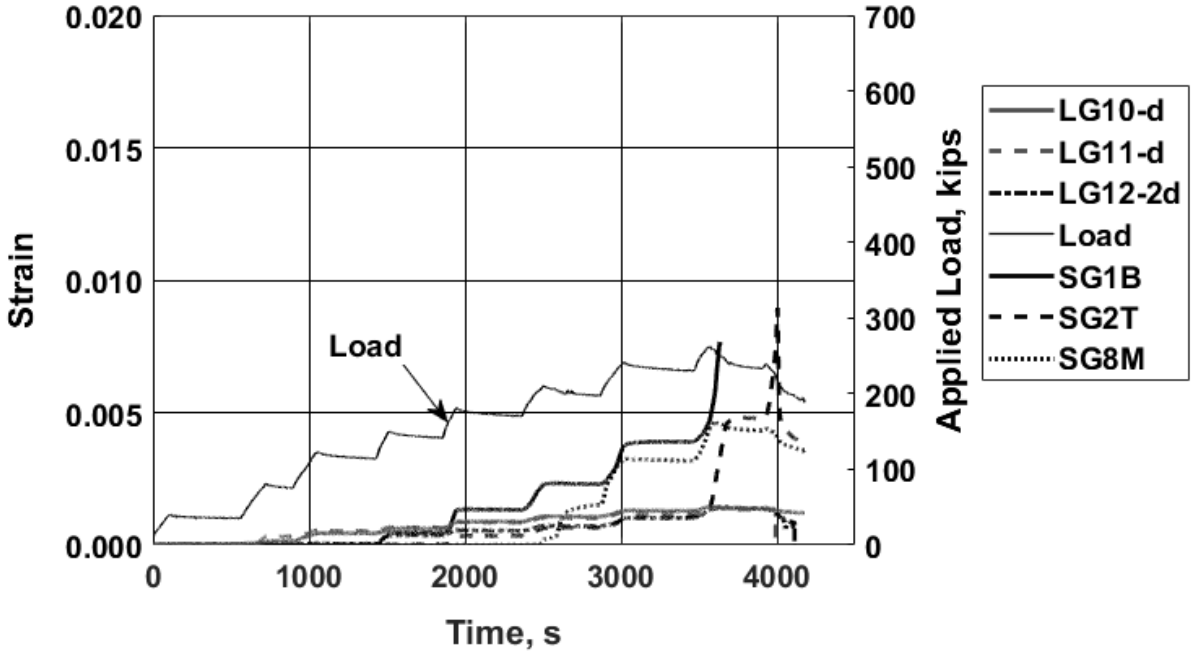

Figure H.119: Strain recorded with selected gauges and load versus time: specimen P3S9 [1 kip = 4.45 kN]

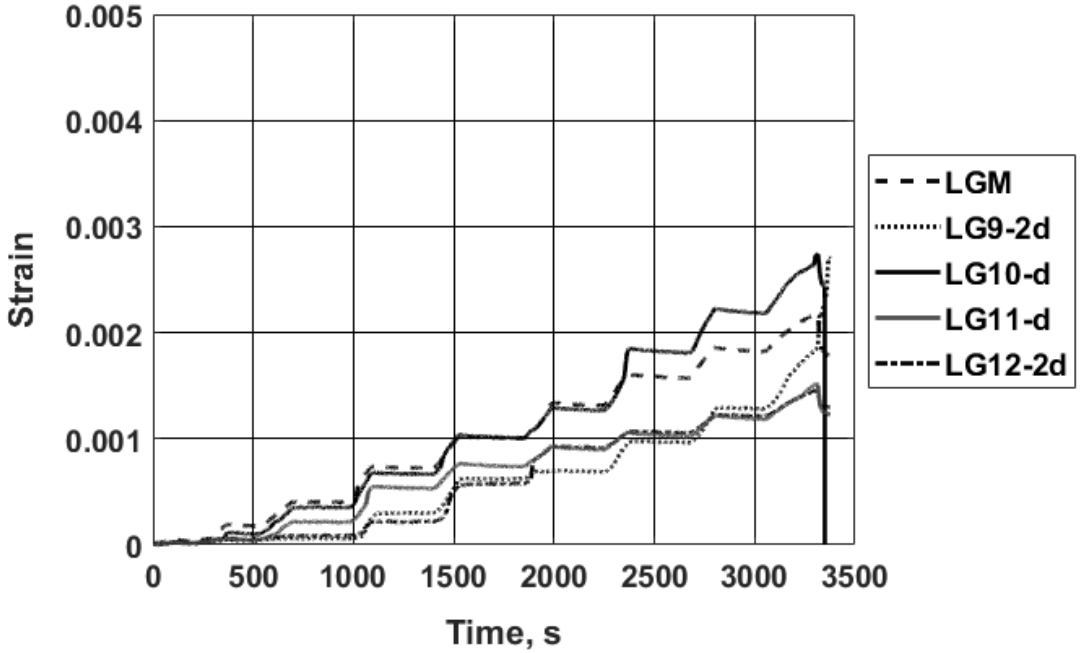

Figure H.120: Longitudinal reinforcing bar strain: specimen P3S10

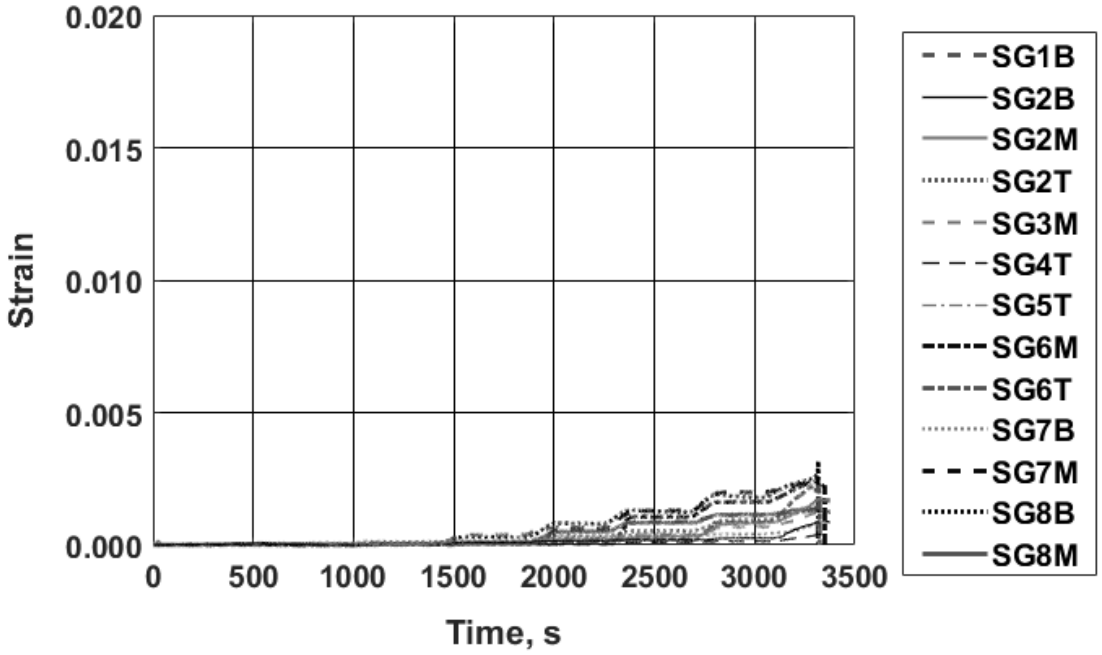

Figure H.121: Transverse reinforcing bar strain: specimen P3S10

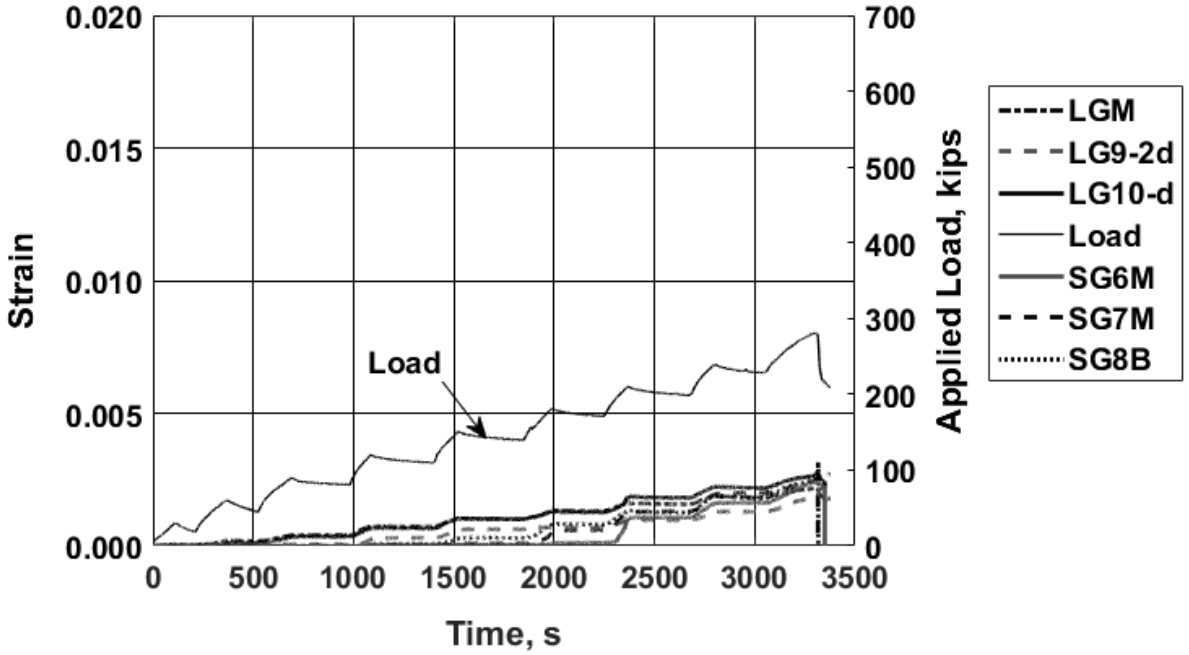

Figure H.122: Strain recorded with selected gauges and load versus time: specimen P3S10 [1 kip = 4.45 kN]

APPENDIX I: ANCHORAGE LENGTHS

Appendix I contains tables listing the transverse reinforcement anchorage lengths for each specimen, determined after the transverse reinforcement was intercepted by the failure surface. This information is useful for determining the total amount of transverse reinforcement that was effective in resisting the opening of an inclined crack. If the crack crossed near the end of a transverse reinforcing bar, it is unlikely that the bar was able to develop its yield strength in the short anchorage length on one side of the crack. Transverse reinforcement anchorage length was determined by measuring the distance from the centerline of the failure surface shown in the crack maps (Appendix E) to the location of the nearest end of the transverse reinforcement, taken as the edge of the specimen minus the nominal concrete cover and transverse reinforcement head thickness (where applicable). For each specimen (excluding specimens P2S11 and P2S12), the nominal locations of the transverse reinforcement were numbered starting from the first transverse reinforcing bar on either side of midspan to the last transverse reinforcing bar within the supports as shown in Figure I-1a. For specimens P2S11 and P2S12, the nominal locations of the transverse reinforcement were numbered starting from the first transverse reinforcing bar after the midspan support to the last transverse reinforcing bar before the loading plate, as shown in Figure I-1b. The anchorage length for each transverse reinforcing bar crossing the failure surface is shown in Tables I.1 through I.4. Bars not crossing the failure surface have no anchorage length listed.

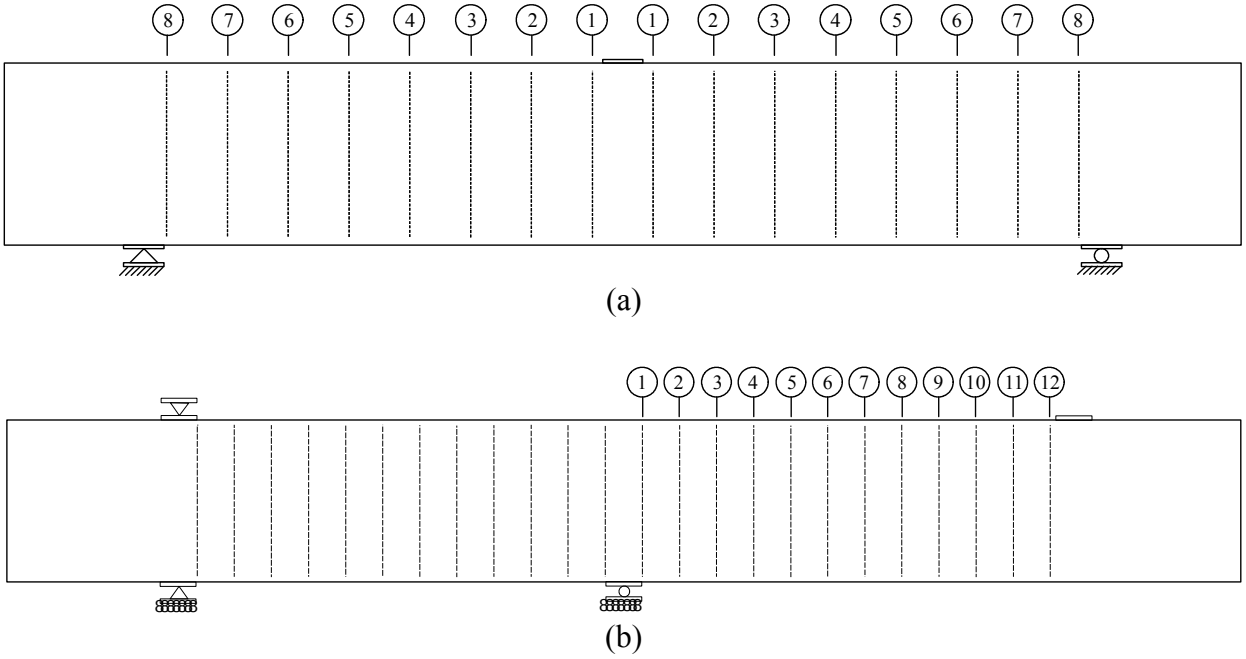

Figure I.1: Transverse reinforcement ID for: (a) all specimens (excluding P2S11 and P2S12) (b) specimens P2S11 and P2S12

Table I.1: Transverse reinforcement anchorage lengths for Phase 1 specimens

Specimen	Anchorage length for each transverse reinforcement ID, in., (mm)											
	1		2		3		4		5		6	
	Front	Back	Front	Back	Front	Back	Front	Back	Front	Back	Front	Back
P1S1	-	0.5	4.9	6.0	16.0	12.6	2.4	-	-	-	-	-
	-	(12.7)	(125)	(152)	(406)	(320)	(61.0)	-	-	-	-	-
P1S2	1.2	0.1	6.6	2.1	11.6	11.3	8.7	5.6	-	-	-	-
	(30.5)	(2.5)	(168)	(53.3)	(295)	(287)	(221)	(142)	-	-	-	-
P1S3	-	-	6.5	2.0	9.6	12.0	10.0	0.3	-	-	-	-
	-	-	(165)	(50.8)	(244)	(305)	(254)	(7.6)	-	-	-	-
P1S4	-	-	3.7	7.1	8.1	15.0	13.4	5.2	-	-	-	-
	-	-	(94.0)	(180)	(206)	(381)	(340)	(132)	-	-	-	-
P1S5	-	-	2.3	7.4	7.0	9.8	13.1	14.0	-	7.4	-	-
	-	-	(58.4)	(188)	(178)	(249)	(333)	(356)	-	(188)	-	-
P1S6	-	-	1.9	1.4	6.2	9.8	15.5	14.8	-	6.9	-	-
	-	-	(48.3)	(35.6)	(158)	(249)	(394)	(376)	-	(175)	-	-
P1S7	0.2	-	6.8	1.6	10.1	9.2	15.2	12.1	4.8	0.6	-	0.3
	(5.1)	-	(173)	(40.6)	(257)	(234)	(386)	(307)	(122)	(15.2)	-	(7.6)
P1S8	0.4	0.7	6.6	5.2	13.1	10.9	5.9	-	-	-	-	-
	(10.2)	(17.8)	(168)	(132)	(333)	(277)	(150)	-	-	-	-	-
P1S9	-	-	2.4	6.0	8.5	10.8	-	9.2	-	-	-	-
	-	-	(61.0)	(152)	(216)	(274)	-	(234)	-	-	-	-
P1S10	-	-	5.0	4.5	8.5	8.2	13.1	13.2	7.0	7.8	-	-
	-	-	(127)	(114)	(216)	(208)	(333)	(335)	(178)	(198)	-	-
P1S11	-	-	6.3	4.9	10.3	13.5	10.5	6.9	-	-	-	-
	-	-	(160)	(125)	(262)	(343)	(267)	(175)	-	-	-	-
P1S12	-	-	2.5	1.1	6.7	4.4	13.7	9.8	-	9.4	-	0.4
	-	-	(63.5)	(27.9)	(170)	(112)	(348)	(249)	-	(239)	-	(10.2)
P1S13	1.6	-	6.2	8.2	15.2	13.7	5.7	7.7	-	1.5	-	-
	(40.6)	-	(158)	(208)	(386)	(348)	(145)	(196)	-	(38.1)	-	-
P1S14	1.7	-	7.6	7.8	13.8	15.4	-	-	-	-	-	-
	(43.2)	-	(193)	(198)	(351)	(391)	-	-	-	-	-	-
P1S15	-	-	11.6	8.8	-	8.7	-	-	-	-	-	-
	-	-	(295)	(224)	-	(221)	-	-	-	-	-	-
P1S16	-	-	3.0	6.6	12.3	15.6	0.6	-	-	-	-	-
	-	-	(76.2)	(168)	(312)	(396)	(15.2)	-	-	-	-	-
P1S17	-	-	4.3	6.6	13.0	12.0	-	3.2	-	-	-	-
	-	-	(109)	(168)	(330)	(305)	-	(81.3)	-	-	-	-

Table I.2: Transverse reinforcement anchorage lengths for Phase 2 specimens (excluding specimens P2S11 and P2S12)

Specimen	Anchorage length for each transverse reinforcement ID, in., (mm)									
	1		2		3		4		5	
	Front	Back	Front	Back	Front	Back	Front	Back	Front	Back
P2S1	-	-	-	0.7	2.4	2.5	2.3	2.4	-	0.8
	-	-	-	(17.8)	(61.0)	(63.5)	(58.4)	(61.0)	-	(20.3)
P2S2	-	-	1.7	1.1	3.4	3.1	1.1	1.0	-	-
	-	-	(43.2)	(27.9)	(86.4)	(78.7)	(27.9)	(25.4)	-	-
P2S3[a]	0.3	-	2.1	-	6.7	-	2.9	-	-	-
	(7.6)	-	(53.3)	-	(170)	-	(73.7)	-	-	-
P2S4	-	-	0.8	-	3.9	1.9	3.0	6.2	-	1.5
	-	-	(20.3)	-	(99.1)	(48.3)	(76.2)	(158)	-	(38.1)
P2S5	0.6	-	5.5	2.2	10.4	7.0	21.7	17.7	5.7	9.3
	(15.2)	-	(140)	(55.9)	(264)	(178)	(551)	(450)	(145)	(236)
P2S6	0.5	1.9	9.2	9.8	18.3	17.7	14.0	13.9	3.1	0.9
	(12.7)	(48.3)	(234)	(249)	(465)	(450)	(356)	(353)	(78.7)	(22.9)
P2S7	-	2.0	4.0	6.6	13.5	16.1	19.9	19.4	8.3	6.5
	-	(50.8)	(102)	(168)	(343)	(409)	(506)	(493)	(211)	(165)
P2S8	2.5	3.1	11.2	11.7	19.9	21.2	15.0	10.5	5.9	3.0
	(63.5)	(78.7)	(285)	(297)	(506)	(539)	(381)	(267)	(150)	(76.2)
P2S9	-	3.3	11.4	12.3	3.0	7.1	-	-	-	-
	-	(83.8)	(290)	(312)	(76.2)	(180)	-	-	-	-
P2S10	-	2.6	12.4	9.6	20.6	21.6	1.5	0.3	-	-
	-	(66.0)	(315)	(244)	(523)	(549)	(38.1)	(7.6)	-	-

[a] No data available for back side of specimen P2S3

Table I.3: Transverse reinforcement anchorage lengths for specimens P2S11 and P2S12

Specimen	Anchorage length for each transverse reinforcement ID, in., (mm)											
	1		2		3		4		5		6	
	Front	Back	Front	Back	Front	Back	Front	Back	Front	Back	Front	Back
P2S11	-	-	5.7	3.7	9.1	6.5	16.7	11.6	20.6	15.9	16.9	22
	-	-	(145)	(94.0)	(231)	(165)	(424)	(295)	(523)	(404)	(429)	(559)
P2S12	-	-	5.9	3.4	10.2	7.7	14.7	11.8	20.6	16.3	14	20.9
	-	-	(150)	(86.4)	(260)	(196)	(373)	(300)	(523)	(414)	(356)	(531)

Table I.3 (cont.): Transverse reinforcement anchorage lengths for specimens P2S11 and P2S12

Specimen	Anchorage length for each transverse reinforcement ID, in., (mm)									
	7		8		9		10		11	
	Front	Back	Front	Back	Front	Back	Front	Back	Front	Back
P2S11	3.2	13.3	-	2.8	-	-	-	-	-	-
	(81.3)	(338)	-	(71.1)	-	-	-	-	-	-
P2S12	5.6	17.5	0.5	11	-	4.2	-	2.7	-	1.5
	(142)	(445)	(12.7)	(279)	-	(107)	-	(68.6)	-	(38.1)

Table I.4: Transverse reinforcement anchorage lengths for Phase 3 specimens

Specimen	Anchorage length for each transverse reinforcement ID, in., (mm)									
	1		2		3		4		5	
	Front	Back	Front	Back	Front	Back	Front	Back	Front	Back
P3S1	-	0.9	5.4	7.9	12.0	13.5	12.9	2.1	-	-
	-	(22.9)	(137)	(201)	(305)	(343)	(328)	(53.3)	-	-
P3S2	-	-	4.8	4.4	13.4	11.8	2.5	2.1	-	1.2
	-	-	(122)	(112)	(340)	(300)	(63.5)	(53.3)	-	(30.5)
P3S3	0.5	-	12.0	2.7	13.5	9.2	5.0	15.7	-	4.3
	(12.7)	-	(305)	(68.6)	(343)	(234)	(127)	(399)	-	(109)
P3S4	-	-	4.4	8.8	13.4	10.2	10.3	0.8	-	-
	-	-	(112)	(224)	(340)	(259)	(262)	(20.3)	-	-
P3S5	-	1.0	4.2	5.2	13.4	12.6	8.9	12.2	-	-
	-	(25.4)	(107)	(132)	(340)	(320)	(226)	(310)	-	-
P3S6	-	0.4	9.0	8.1	8.8	13.9	2.3	1.5	-	-
	-	(10.2)	(229)	(206)	(224)	(353)	(58.4)	(38.1)	-	-
P3S7	-	-	7.0	8.8	13.5	14.1	3.8	10.5	4.5	2.8
	-	-	(178)	(224)	(343)	(358)	(96.5)	(267)	(114)	(71.1)
P3S8	-	-	7.5	8.1	16.3	14.9	4.8	8.6	-	2.5
	-	-	(191)	(206)	(414)	(379)	(122)	(218)	-	(63.5)
P3S9	2.1	-	3.3	4.2	9.8	12.0	8.5	4.9	-	-
	(53.3)	-	(83.8)	(107)	(249)	(305)	(216)	(125)	-	-
P3S10	-	-	2.9	3.3	10.5	8.8	8.6	8.2	-	-
	-	-	(73.7)	(83.8)	(267)	(224)	(218)	(208)	-	-